The Radiation Chemistry of Polysaccharides

Edited by:
Saphwan Al-Assaf
Xavier Coqueret
Khairul Zaman Haji Mohd Dahlan
Murat Sen
Piotr Ulanski

IAEA
International Atomic Energy Agency

THE RADIATION CHEMISTRY OF POLYSACCHARIDES

The following States are Members of the International Atomic Energy Agency:

AFGHANISTAN
ALBANIA
ALGERIA
ANGOLA
ANTIGUA AND BARBUDA
ARGENTINA
ARMENIA
AUSTRALIA
AUSTRIA
AZERBAIJAN
BAHAMAS
BAHRAIN
BANGLADESH
BARBADOS
BELARUS
BELGIUM
BELIZE
BENIN
BOLIVIA, PLURINATIONAL STATE OF
BOSNIA AND HERZEGOVINA
BOTSWANA
BRAZIL
BRUNEI DARUSSALAM
BULGARIA
BURKINA FASO
BURUNDI
CAMBODIA
CAMEROON
CANADA
CENTRAL AFRICAN REPUBLIC
CHAD
CHILE
CHINA
COLOMBIA
CONGO
COSTA RICA
CÔTE D'IVOIRE
CROATIA
CUBA
CYPRUS
CZECH REPUBLIC
DEMOCRATIC REPUBLIC OF THE CONGO
DENMARK
DJIBOUTI
DOMINICA
DOMINICAN REPUBLIC
ECUADOR
EGYPT
EL SALVADOR
ERITREA
ESTONIA
ETHIOPIA
FIJI
FINLAND
FRANCE
GABON
GEORGIA
GERMANY
GHANA
GREECE
GUATEMALA
GUYANA
HAITI
HOLY SEE
HONDURAS
HUNGARY
ICELAND
INDIA
INDONESIA
IRAN, ISLAMIC REPUBLIC OF
IRAQ
IRELAND
ISRAEL
ITALY
JAMAICA
JAPAN
JORDAN
KAZAKHSTAN
KENYA
KOREA, REPUBLIC OF
KUWAIT
KYRGYZSTAN
LAO PEOPLE'S DEMOCRATIC REPUBLIC
LATVIA
LEBANON
LESOTHO
LIBERIA
LIBYA
LIECHTENSTEIN
LITHUANIA
LUXEMBOURG
MADAGASCAR
MALAWI
MALAYSIA
MALI
MALTA
MARSHALL ISLANDS
MAURITANIA
MAURITIUS
MEXICO
MONACO
MONGOLIA
MONTENEGRO
MOROCCO
MOZAMBIQUE
MYANMAR
NAMIBIA
NEPAL
NETHERLANDS
NEW ZEALAND
NICARAGUA
NIGER
NIGERIA
NORWAY
OMAN
PAKISTAN
PALAU
PANAMA
PAPUA NEW GUINEA
PARAGUAY
PERU
PHILIPPINES
POLAND
PORTUGAL
QATAR
REPUBLIC OF MOLDOVA
ROMANIA
RUSSIAN FEDERATION
RWANDA
SAN MARINO
SAUDI ARABIA
SENEGAL
SERBIA
SEYCHELLES
SIERRA LEONE
SINGAPORE
SLOVAKIA
SLOVENIA
SOUTH AFRICA
SPAIN
SRI LANKA
SUDAN
SWAZILAND
SWEDEN
SWITZERLAND
SYRIAN ARAB REPUBLIC
TAJIKISTAN
THAILAND
THE FORMER YUGOSLAV REPUBLIC OF MACEDONIA
TOGO
TRINIDAD AND TOBAGO
TUNISIA
TURKEY
TURKMENISTAN
UGANDA
UKRAINE
UNITED ARAB EMIRATES
UNITED KINGDOM OF GREAT BRITAIN AND NORTHERN IRELAND
UNITED REPUBLIC OF TANZANIA
UNITED STATES OF AMERICA
URUGUAY
UZBEKISTAN
VANUATU
VENEZUELA, BOLIVARIAN REPUBLIC OF
VIET NAM
YEMEN
ZAMBIA
ZIMBABWE

The Agency's Statute was approved on 23 October 1956 by the Conference on the Statute of the IAEA held at United Nations Headquarters, New York; it entered into force on 29 July 1957. The Headquarters of the Agency are situated in Vienna. Its principal objective is "to accelerate and enlarge the contribution of atomic energy to peace, health and prosperity throughout the world''.

THE RADIATION CHEMISTRY OF POLYSACCHARIDES

EDITED BY:
SAPHWAN AL-ASSAF
XAVIER COQUERET
KHAIRUL ZAMAN HAJI MOHD DAHLAN
MURAT SEN
PIOTR ULANSKI

INTERNATIONAL ATOMIC ENERGY AGENCY
VIENNA, 2016

COPYRIGHT NOTICE

Marketing and Sales Unit, Publishing Section
International Atomic Energy Agency
Vienna International Centre
PO Box 100
1400 Vienna, Austria
fax: +43 1 2600 29302
tel.: +43 1 2600 22417
email: sales.publications@iaea.org
http://www.iaea.org/books

Printed by the IAEA in Austria
December 2016
STI/PUB/1731

IAEA Library Cataloguing in Publication Data

Names: International Atomic Energy Agency.
Title: The radiation chemistry of polysaccharides / International Atomic Energy Agency.
Description: Vienna : International Atomic Energy Agency, 2016. | Includes bibliographical references.
Identifiers: IAEAL 16-01075 | ISBN 978–92–0–101516–7 (paperback : alk. paper)
Subjects: LCSH: Polysaccharides. | Polymers — Effect of radiation on. | Radiation chemistry.
Classification: UDC 543.635.25:544.54 | STI/PUB/1731

FOREWORD

Radiation processing offers a clean and additive-free method for the preparation of value-added novel materials based on renewable, non-toxic and biodegradable natural polymers and natural polymer waste. Past research has shown that, depending on the irradiation conditions, natural polysaccharides (alginate, chitin, chitosan, carrageeneans, carboxyl methyl cellulose, etc.) can be either degraded or cross-linked by radiation. This paved the way for the development of many successful applications, some of which have been commercialized for use in agriculture, healthcare and environmental protection.

This publication provides information to help to disseminate knowledge and encourage researchers from different fields (radiation chemists, plant biologists, agricultural engineers, food safety specialists, medical doctors, etc.) to liaise and develop a variety of products from natural materials using environmentally friendly radiation technology. It complements previous efforts of the IAEA, such as consultants meetings and technical meetings, as well as a coordinated research project (CRP) on the Development of Radiation Processed Products of Natural Polymers for Applications in Agriculture, Healthcare, Industry and Environment. The designation of the Malaysian Nuclear Agency (Nuclear Malaysia) as an IAEA Collaborating Centre on Radiation Processing of Natural Polymers in October 2006 also supported successful developments in this field.

This publication is a result of a collaborative effort by participants of this CRP, coordinated by five selected editors, who collected and edited the contributions, wrote several chapters and ensured the consistency of the usage of terms throughout this publication. Additional chapters initially prepared for an intended publication initiated by Nuclear Malaysia were also integrated into this publication. In this way, this publication covers basic aspects of the radiation chemistry of polysaccharides, methods for their full characterization, as well as examples of applications of radiation processed polysaccharides in healthcare, food and agriculture, as well as environmental applications.

The IAEA wishes to thank all participants for their valuable and timely contributions. In particular, efforts of the editors, X. Coqueret (France), H.M.D. Khairul Zaman (Malaysia), P. Ulanski (Poland), M. Sen (Turkey) and S. Al-Assaf (United Kingdom) are acknowledged. The IAEA officer responsible for this publication was A. Safrany of the Division of Physical and Chemical Sciences.

EDITORIAL NOTE

Guidance provided here, describing good practices, represents expert opinion but does not constitute recommendations made on the basis of a consensus of Member States.

This report does not address questions of responsibility, legal or otherwise, for acts or omissions on the part of any person.

Although great care has been taken to maintain the accuracy of information contained in this publication, neither the IAEA nor its Member States assume any responsibility for consequences which may arise from its use.

The use of particular designations of countries or territories does not imply any judgement by the publisher, the IAEA, as to the legal status of such countries or territories, of their authorities and institutions or of the delimitation of their boundaries.

The mention of names of specific companies or products (whether or not indicated as registered) does not imply any intention to infringe proprietary rights, nor should it be construed as an endorsement or recommendation on the part of the IAEA.

The authors are responsible for having obtained the necessary permission for the IAEA to reproduce, translate or use material from sources already protected by copyrights.

Material prepared by authors who are in contractual relation with governments is copyrighted by the IAEA, as publisher, only to the extent permitted by the appropriate national regulations.

This publication has been prepared from the original material as submitted by the authors. The views expressed do not necessarily reflect those of the IAEA, the governments of the nominating Member States or the nominating organizations.

The IAEA has no responsibility for the persistence or accuracy of URLs for external or third party Internet web sites referred to in this book and does not guarantee that any content on such web sites is, or will remain, accurate or appropriate.

CONTENTS

1. INTRODUCTION

1.1. BACKGROUND

Radiation processing offers a clean and additive-free method for the preparation of value-added novel materials based on renewable, non-toxic and biodegradable natural polymers. The results of research work in some Member States have shown that natural polysaccharides (alginates, chitin, chitosan and carrageeneans) can be either degraded or cross-linked by radiation, depending on the irradiation conditions. Consequently, many applications have been developed in the areas of agriculture, healthcare and environmental protection, and some of them have been successfully commercialized. These successes clearly indicate that the radiation processing of natural polymers has emerged as an exciting area where the unique characteristics of these polymeric materials can be exploited for a variety of practical applications.

Recognizing the potential benefits that radiation technology can offer for the processing of natural polymers into useful products, the IAEA has implemented a number of activities in response to Member State requests for technical cooperation projects and has held consultants meetings on the Technical, Economical and Environmental Advantages of Radiation Processing of Cellulose (2001), the Radiation Processing of Polysaccharides (2003; the results of the meeting were published as Ref. [1.1]), the Irradiation of Natural Resources for Marketable Products (2004), and the Radiation Processing of Natural Polymers for Development of Finished Products for Health Care, Agriculture and Environment (2007). The designation of the Malaysian Nuclear Agency (Nuclear Malaysia) as an IAEA Collaborating Centre on the Radiation Processing of Natural Polymers in October 2006 has successfully supported developments in this field.

Most recently, a coordinated research project (CRP) on the Development of Radiation Processed Products of Natural Polymers for Applications in Agriculture, Healthcare, Industry and Environment was successfully completed. This CRP began at the end of 2007 with the aim of harmonizing the procedures for both the evaluation methods for radiation modified natural polymers as well as the protocols for their field testing as plant elicitors. The first research coordination meeting was held in March 2008 in Vienna, and the meeting report was published as IAEA working material. The second research coordination meeting was held 12–16 October 2009 in Reims, France, and published as Ref. [1.2]. The third research coordination meeting of the CRP was held in Vienna, 27 June to 1 July 2011, where the accomplishments of this project were reviewed. The sixteen participating institutions produced considerable results. Guidelines to

produce radiation-degraded chitosan from shrimp, prawn and crab exoskeletons and squid pens were developed. It was reported at the meeting, and is described in this publication, that radiation-degraded low-molecular-weight alginate, carrageenan and chitosan, when applied under well-defined conditions, act to promote plant growth, protect plants from diseases and as a natural antioxidant for the preservation of food and related products. It was shown in numerous field tests that oligochitosan and oligoalginate promote the growth of tomato, lettuce, spinach, cabbage and pepper. Additionally, it was observed that oligochitosan may reduce the disease index by more than 50% compared with controls and hence may increase the productivity of rice by 10–20%. Using such natural, non-toxic, non-polluting and biodegradable products instead of chemical fertilizers on a large scale may result in significant environmental benefit. Furthermore, electron beam processing of sugarcane bagasse was shown to be a potentially beneficial and economical way of enhancing the enzymatic hydrolysis of cellulose when combined with thermal pretreatment for production of biofuel from non-food resources. Additionally, the suitability of radiation-cross-linked natural polymers for use in transparent, flexible, mechanically strong, biocompatible, effective and economical hydrogel dressings, super water adsorbents and various other products was demonstrated.

The IAEA, following the suggestions of the participants, decided that instead of publishing a Meeting Report, it would be more useful to issue a publication on the radiation chemistry of polysaccharides, and to include in it selected research findings of the participants of this CRP. This publication is therefore the result of a collaborative effort by participants of this CRP. Additional chapters prepared for an intended publication initiated by Nuclear Malaysia were also integrated into this publication.

1.2. OBJECTIVES

The objective of this publication is to provide basic information and to disseminate knowledge to encourage researchers from different fields (radiation chemists, plant biologists, agricultural engineers, food safety specialists, medical doctors, etc.) to liaise and to develop a variety of products from natural materials using radiation technology.

1.3. SCOPE

The publication includes basic information on polysaccharides, a class of natural or bio-sourced polymers that are non-toxic and renewable; it discusses their

origin, structure and properties. The publication introduces the reader to the radiation chemistry of polymers and gives examples of products developed from radiation modified polysaccharides. Guidance provided here, describing good practices, represents expert opinion but does not constitute recommendations made on the basis of a consensus of Member States.

1.4. STRUCTURE

This publication is structured as follows. Chapter 2 introduces polysaccharides, describes their origin and methods for their extraction and purification, as well as their structure–property relations. Chapter 3 gives basic information on the radiation chemistry of polymers, starting with the interaction of ionizing radiation with matter, and ending with methods for studying radiation induced effects in polymers. Chapter 4 deals with the effects of ionizing radiation on polysaccharides, while Chapter 5 explains how structural parameters affect the radiation degradation of polysaccharides. Chapters 6 and 7 describe various analytical techniques that could be used for the characterization of polysaccharides, as well as for the investigation of the changes introduced by ionizing radiation. These general chapters are then followed by Chapters 8–16, which are devoted to various applications of radiation modified polysaccharides, from agricultural to medical and food packaging applications.

This publication uses a number of abbreviations. While they are introduced and explained in the text, a list of all abbreviations is provided at the end of the publication.

REFERENCES TO CHAPTER 1

[1.1] INTERNATIONAL ATOMIC ENERGY AGENCY, Radiation Processing of Polysaccharides, IAEA-TECDOC-1442, IAEA, Vienna (2004).

[1.2] INTERNATIONAL ATOMIC ENERGY AGENCY, Report of the 2nd RCM on "Development of radiation-processed products of natural polymers for application in agriculture, healthcare, industry and environment" (2010), http://www-naweb.iaea.org/napc/iachem/meetings/RCMs/RC-1091-2_report_complete.pdf

2. POLYSACCHARIDES: ORIGIN, SOURCE AND PROPERTIES

S. AL-ASSAF
Hydrocolloids Research Centre, Institute of Food Science and Innovation,
University of Chester,
Chester, United Kingdom

2.1. INTRODUCTION

Polysaccharides are natural polymers that can be extracted from various sources. They can be extracted from plant cell walls (such as pectin, cellulose and starch); from seeds (guar gum (GG), locust bean gum (LBG) and tara gum (TG)); from tubers or roots (konjac mannan); and from seaweed (alginate and agarm carrageenan). In some cases, the source is tree exudates (gum arabic (GA), ghatti gum and karaya gum) or animals (hyaluronan, chitosan and chondroitin sulphate). Some types of bacteria and fungi are also a source of polysaccharides (xanthan, gellan, wellan, dextran, pullulan and cellulose). In their natural environment, polysaccharides provide structural support, gelation, hydration and lubrication, and play a role in cell signalling. They are commonly referred to as hydrocolloids, particularly in the food industry, but this term also includes proteins. Owing to their remarkable properties, polysaccharides are currently used as thickening, stabilizing, gelling, film forming and emulsifying agents in various industrial sectors. Furthermore, the quest to understand how they function in their natural assembly, whether as part of a cell wall or in connective tissues, has led to their use as a source of dietary fibre, as a therapeutic agent to restore lubrication in diseased osteoarthritic joints, as plant growth promoters and in anti-ageing applications, among others; they may find many more applications in the future. This chapter will explore the origins, molecular structures and conformations of natural polymers, with an emphasis on functionality. Also, methods employed for the modification of polysaccharides to enhance their functionality or produce novel materials, as well as those using radiation processing, will be briefly mentioned.

2.2. STRUCTURE AND PROPERTIES OF POLYSACCHARIDES

Polysaccharides are composed of monosaccharides (sugar units) that are glycosidically linked. The most abundant monosaccharide in nature is D-glucose,

which is one of the main products of photosynthesis and is used by cells as their primary source of energy. If the glucose unit is linked with other similar units at the alpha position (i.e. α 1–4 D-glucose), the resultant polysaccharide will be amylose, which is one of the main constituents of starch. On the other hand, if the glucose units are linked in the beta position (β 1–4 D-glucose) the resultant polysaccharide is cellulose (see Fig. 2.1). The different stereochemical linkage leads to a different conformation and hence different physical properties such as the fact that starch is a weak powder and is water soluble while cellulose is characterized by its ability to form strong fibres and is insoluble. The composition may vary and a polysaccharide could be formed of two different monomers, as in the case of alginate.

Alginate is a linear copolymer of (1–4) linked β D-mannuronate (M) and β L-guluronate (G) residues. The residues are arranged in a blockwise pattern with G blocks and M blocks interspersed with alternating MG residue blocks [2.1]. The overall composition of M/G residues and their distribution patterns vary by seaweed species and subsequently determine their gelling strength.

Hyaluronan is an example of an AB type copolymer where the repeating units (glucuronic acid and N acetyl glucosamine) are equally repeated throughout the polymer [2.2]. The structure of the majority of polysaccharides is a mixture of various units, often made up from the same monomer unit as the backbone and linked with other sugar units with side chains of various lengths. The solubility is due to the presence of many hydroxyl groups and varies according to the monosaccharides present, and neutral polysaccharides are therefore less soluble compared to polyelectrolytes (whether charged or ionic). When dissolved in water, they adopt various conformations (spherical, random coil or rod-like) depending on the type of monosaccharides and their linkage (α or β) and ability to associate by intra and intermolecular interactions. This will in turn determine the degree to which they can affect the flow behaviour of the solution and thus determines their functionality in a given application. The degree of polymerization (molecular weight) is another factor that determines the physical properties of a polysaccharide. In the food industry, their ability to modify the flow properties of aqueous foodstuffs and their gelling ability is greatly utilized.

2.3. EXTRACTION AND PROCESSING

One of the first steps commonly employed in the extraction of polysaccharides is the careful selection of the raw materials and removal of impurities by washing with water. Pigments, waxes and oil, if present, are usually removed by the use of an organic solvent such as toluene, chloroform or

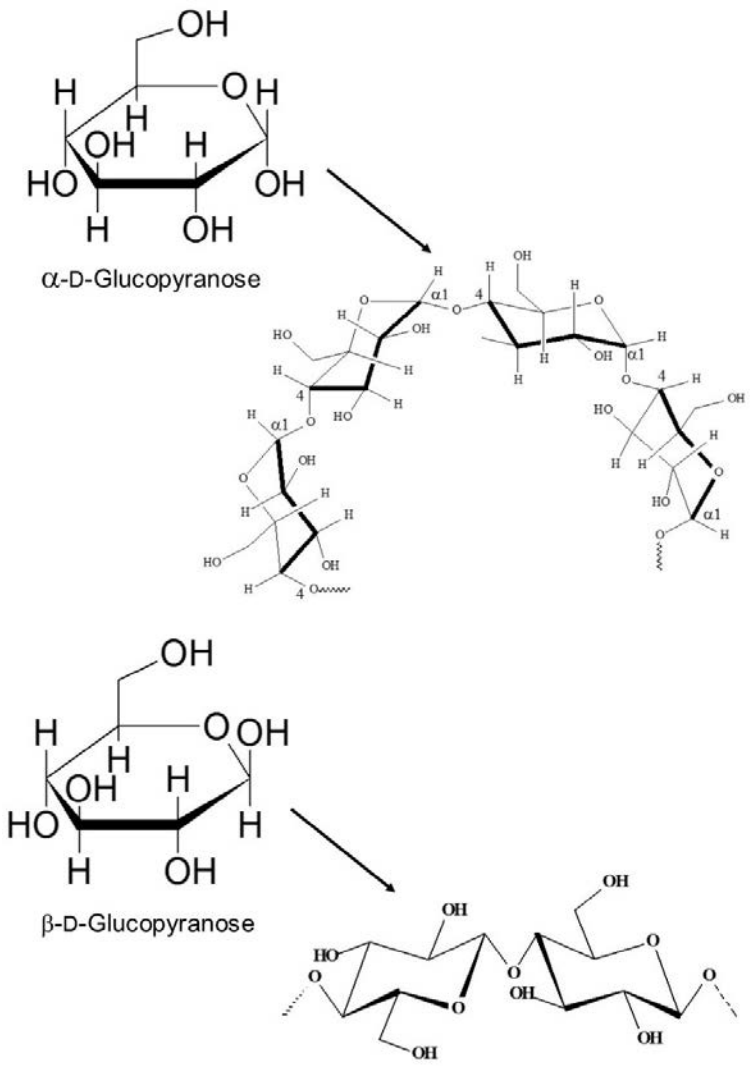

FIG. 2.1. (Above) structure of α D-glucopyranose and repeating units of amylose; (below) structure of β D-glucopyranose and repeating units of cellulose.

methanol. Subsequent steps could involve alkaline or acid extraction or extraction by heating and cooling, particularly for gelling polysaccharides.

The next step is the clarification of the extract by filtration and addition of monovalent salt (NaCl) in excess to exchange the multivalent counterions. Finally, purification is carried out by a precipitation step using a non-solvent

such as ethanol or isopropyl alcohol (in a water/alcohol ratio of ~1:1) [2.3, 2.4]. The slurry is then dried and milled for use.

Microbial polysaccharides can be commercially produced and extracted from a pure culture of a certain type of bacterium in a fermentation process where the uptake of oxygen is controlled throughout. The bacterium acts as an extremely efficient enzyme mini-factory converting >70% of the substrate (a monosaccharide such as D-glucose or a related monosaccharide) to a polymeric material [2.5]. At the final stage of fermentation, the broth is pasteurized to kill the bacteria, which are subsequently removed by centrifugation. The final slurry obtained by alcohol precipitation is then dried and milled.

Other examples of polysaccharides are tree exudates such as GA (Fig. 2.2). Gummosis is promoted when the tree is subjected to stress conditions such as heat, drought and insect attack [2.6]. Systematic wounding, called tapping, is used in the plantation of *Acacia senegal*. The timing and intensity of tapping influences gum yield [2.7, 2.8]. The gums are secreted as a sticky fluid and grow up to 1.5–7.5 cm in diameter. They gradually dry and harden on exposure to the atmosphere. Collectors harvest the partially dried gum, and as many as three collections at three week intervals from the same tree are possible. A yield of 0.5–2 kg is obtained per tree annually. The gum nodules can be further processed by mechanical kibbling, milling or spray drying.

FIG. 2.2. GA nodules obtained following the manual wounding of an acacia tree.

2.4. VISCOSITY

One of the main functionalities of polysaccharides is to increase the viscosity of aqueous solution. The states of solutions as a function of concentration are shown in Fig. 2.3. The solution is considered dilute if clusters contain no more than two molecules.

There is only a negligible probability of interaction among three molecules or particles. The semi-dilute region is where the molecules start to touch each other and its flow behaviour is controlled by the degree of chain overlapping. In molecular terms, the transition from the dilute to the concentrated region corresponds to the onset of coil overlap between the polymer chains and the critical concentration (c^*) at which it occurs; it therefore depends on the volume occupied by each molecule in isolation. At a concentration, c, above c^*, accommodation of the polymer coils within the available volume is possible only by the interpenetration of segments of neighbouring chains, so that molecular motions are no longer independent, and the chains form an entangled network. The relationship between viscosity and concentration can be generally described as shown in Fig. 2.4. At low polymer concentration, i.e. in a dilute region, the zero shear viscosity increases more or less linearly with increasing concentration. With a further increase in concentration, however, a point is reached at which the slope changes abruptly to a much higher value. The variation with concentration of the specific viscosity determined at a zero shear rate for polysaccharides was found to scale as slopes of 1.4 for dilute solutions and 3.3 following the onset of coil overlap between polymer chains [2.9]. Deviation from the value of 3.3 in this region has been taken as evidence for aggregation, otherwise called hyper-entanglement [2.10]. The zero shear specific viscosity, for polysaccharides, was found to be close to 10 mPa·s at c^*.

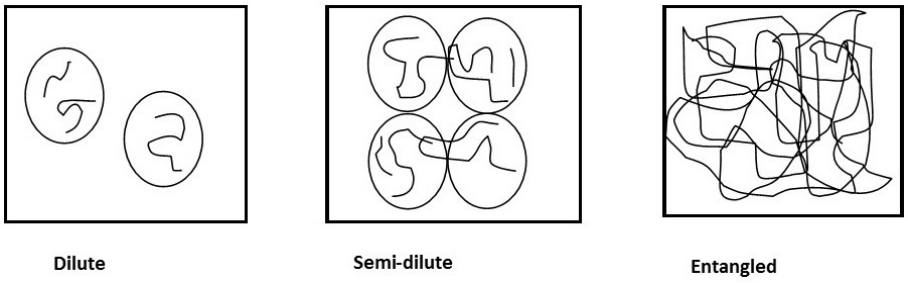

FIG. 2.3. States of solutions as a function of increasing concentration.

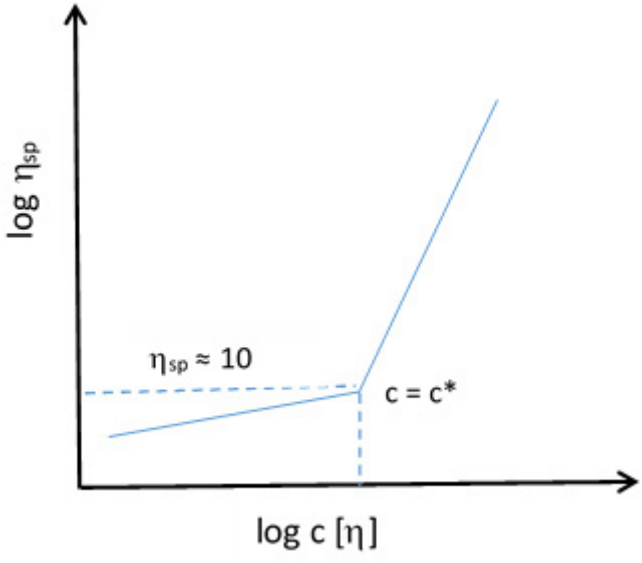

FIG. 2.4. Schematic illustration of zero shear rate specific viscosity dependence on concentration.

Morris et al. showed that the behaviour of random coil polysaccharides can be generalized by the use of a master plot to describe the effect of concentration (c) and molecular weight dependence on shear rate [2.11, 2.12]. For random coil polysaccharides with a wide polydispersity of chain length, the double log plots of viscosity against shear rate are identical in shape and differ only in their position relative to the two axes. The limiting viscosity number or intrinsic viscosity, $[\eta]$, is an index of the size of isolated polymer coils. For random coil solutions, the intrinsic viscosity varies with coil dimensions, according to the Flory-Fox equation.

$$[\eta] = \frac{\Phi 6^{3/2} R^3}{M} \tag{2.1}$$

where R is the radius of gyration, M is the molecular weight, and Φ is a constant (for a flexible random coil polymer, it has a value of 2.6×10^{26} kg^{-1}). If each coil is regarded as a sphere of radius R, the hydrodynamic volume is proportional to $[\eta]M$. Since the total number of coils is proportional to c/M, the degree of occupancy of space can be characterized by the dimensionless coil overlap parameter, $C[\eta]$. Polysaccharides have been shown to behave similarly with c^*, and the transition from the dilute to the concentrated regime occurs at a value of $C[\eta]$ that is close to 4, therefore, giving $c^* \sim 4/[\eta]$ [2.12]. Rinaudo subsequently proposed Eq. (2.2) to describe the zero shear viscosity of a polysaccharide

solution in the dilute and semi-dilute regions. Deviation from the master curve is taken as evidence of interchain interaction or aggregation [2.13].

$$\eta_{sp} = c[\eta](1 + k_1(c[\eta]) + k_2(c[\eta])^2 + k_3(c[\eta]^3) \quad (2.2)$$

where $k_1 = 0.4$, $k_2 = k_1/2!$ and $k_3 = k_1/3!$. The k_1 value represents the Huggins constant and is about 0.4 for many completely water soluble polysaccharides.

Rheological measurements have been used to gain a better understanding of the structure–property relationship of polysaccharides. Different rheological experiments such as oscillation, flow, creep and stress relaxation provide information about the microstructure, gelation behaviour, association, presence of junction zones and structural conformation of polysaccharides. Some of the common terms generally used in the rheological characterization of polysaccharide solutions or fluids are defined below [2.14, 2.15].

Newtonian fluids are those with a viscosity that does not change with changes in the shear rate, such as water and thin motor oil, whereas the viscosity of non-Newtonian fluids responds to changes in shear rate in a variety of ways. Non-Newtonian fluids are subcategorized as pseudoplastic fluids, dilatants and plastic fluids. Pseudoplastic fluids include paints, emulsions and dispersions and their viscosity decreases when the shear rate increases, a response that is known as shear thinning. Shear thinning ceases immediately when shear is removed. Dilatants exhibit the opposite behaviour, shear thickening, meaning that their viscosity increases with the shear rate, and are often fluids with high levels of deflocculated solids, for example, compounds used in confectionary, mixtures of corn starch and water, clay slurries and sand in water. Plastic fluids exhibit solid-like behaviour when they are static, but flow may be induced by the application of force. The amount of force needed to disrupt the structure of the fluid and thereby to induce flow is known as the yield value, and once flow begins, the behaviour of the fluid may be Newtonian, pseudoplastic or dilatant. Tomato ketchup is a plastic fluid [2.16].

There are two further categories of fluid behaviour, thixotropy and rheopexy, that describe how viscosity can change with time although the shear rate remains the same. Thixotropic fluids are a type of pseudoplastic fluid that decrease in viscosity over time under a constant shear rate, usually rapidly and then more gradually, and when the shear rate is removed, they require some time to recover their initial viscosity. Examples of thixotropic fluids are greases, heavy inks and paint. Rheopexic fluids exhibit increasing viscosity under a constant shear rate; examples are gypsum pastes and printing inks. Two different substances in combination may provide a stronger rheological effect than the addition of the rheological effects of both would suggest, a phenomenon known as synergism [2.16]. Strong synergies

are obtained upon combination of xanthan with galactomannans such as LBG, GG and TG, and glucomannans such as konjac gum.

Figure 2.5 shows the flow properties of selected polysaccharides, and Table 2.1 gives their main structural features and conformation in aqueous solution.

At 1 weight % (wt%) only xanthan gives the highest viscosity at a low shear rate and is thus preferred as a thickener or stabilizer for dispersed solids or emulsions. Its high shear thinning behaviour gives a low viscosity when subjected to mixing or pouring. It is relatively unaffected by ionic strength, pH (1–13), shear or temperature and is therefore used in products such as salad dressings.

Carboxymethyl cellulose (CMC) is cellulose that is chemically modified by replacing the hydroxyl group with a carboxymethyl (CM) group that makes it water soluble depending on the degree of substitution (DS). The water solubility characteristics of CMC depend not only on the DS, but also on the uniformity of the distribution of the substituent CM group on the polymer chain. A uniform distribution is described as blockiness. The uniformity of the substituent group also affects its flow behaviour.

When compared with another linear polysaccharide, such as hyaluronan, the main difference can be attributed to the molecular weight and hydrodynamic volume it can occupy. Generally, high weight average molecular weight ($\overline{M}_w$) polymers exhibit higher viscosity than low $\overline{M}_w$ ones. With increased $\overline{M}_w$, the shear rate at which shear thinning appears shifts to a lower value [2.18].

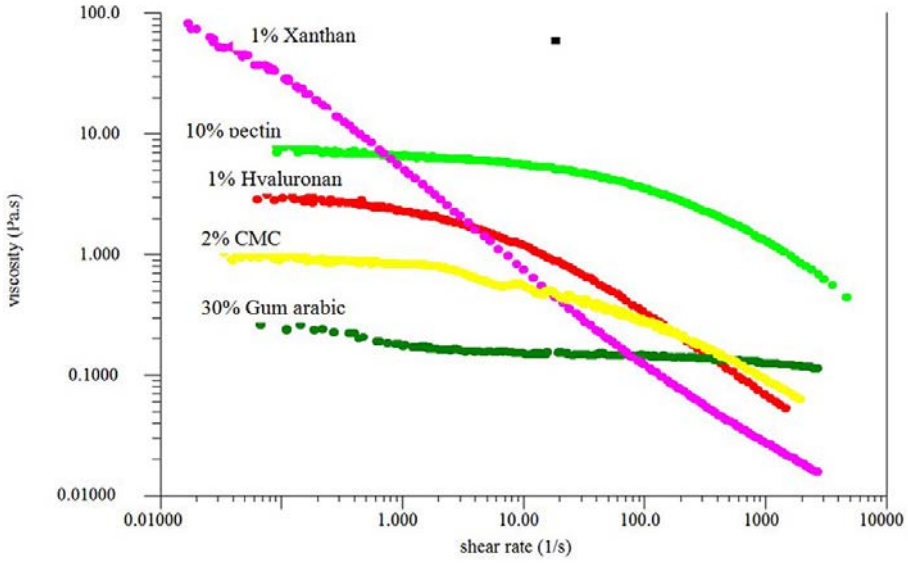

FIG. 2.5. Shear flow viscosity profile as a function of shear rates for selected polysaccharides dissolved in distilled water and determined using a controlled stress rheometer at 25°C [2.17].

TABLE 2.1. MAIN STRUCTURAL FEATURES AND CONFORMATION OF POLYSACCHARIDES SHOWN IN FIG. 2.5

Polysaccharide	Source	Structural features	Functional group, conformation, branching, etc.
Hyaluronan	Animal, bacterial	β 1–4 linked D-glucuronic acid linked to N-acetyal glycosamine	Anionic linear polymer with stiff random coil conformation
Xanthan	Microbial	Anhydroglucose unit with β 1,4 glucoside linkage and glucoronic acid and mannopyranose in side chains	Anionic polymer (pyruvate and acetate groups), very stiff double stranded helical, rod-like conformation
Carboxymethyl cellulose	Plant (cellulose derivative)	Anhydroglucose unit with β 1,4 glucosidic linkage	Anionic polymer (COO- group), linear polymer, coil conformation at high concentration
Gum arabic	Plant exudates	1, 3 linked β D galactose core with branching through 3 and 6 linked galactose and 3 linked arabinose	Anionic polymer (COO- group), highly branched
Pectin	Plant	Backbone consists of α (1–4) linked D-galacturonic acid units interrupted by (1–2) linked L-rhamnopyranosyl residue in adjacent or alternate positions, whereas the side chains consist mainly of D-galactose and L-arabinose	Anionic polymer (COO- group), smooth region and branch (hairy) region, random coil conformation

Another example of a slightly branched structure is found in pectin at 10 wt%. This can be clearly shown to have a Newtonian plateau where viscosity does not change with increasing shear rate. The plateau is due to the dynamic equilibrium between the molecules; although the deformation imposed in this region results in the breaking of entanglements between molecules, an equal number of new entanglements are formed, in the same or different places, and therefore the viscosity of the solution stays the same. Subsequently, the onset of shear rate dependence occurs when the rate of imposed deformation exceeds the rate of re-entanglements, leading to a decrease in viscosity with increasing shear rate. GA, owing to its highly branched structure, has the lowest viscosity of the polysaccharides shown in Fig. 2.5. Owing to its low viscosity, it can be dissolved up to 50 wt% to produce a solution of moderate viscosity.

In addition to concentration, conformation and hydrodynamic size, there are other factors that affect the viscosity–shear rate dependency of polysaccharides. Polysaccharides are in general polyelectrolyte (i.e. anionic, but with the exception of chitosan, which is cationic; see Table 2.1). In the absence of salt, intramolecular repulsion between charged sites within an individual chain can expand the volume of the molecule and give a higher viscosity. The addition of salts, which introduces counterions, can screen the electrostatic repulsion and shrink the molecule volume and hence reduce the viscosity [2.19]. On the other hand, there are some special cases where the addition of salt enhances the viscosity of a polysaccharide solution as it promotes interactions such as cross-linking, coordinating force or other specific interactions between polysaccharides and metal ions. Alginate and pectin (polyuronates) have the ability to bind divalent cations such as Ca^{2+} to form an egg box structure (Fig. 2.6), in which Ca^{2+} ions are embedded between two parallel chains through coordinating force [2.20]. The presence of metal ions also affects the gelling behaviour, microstructure and mechanical properties of gelling polysaccharides. For cold set gels such

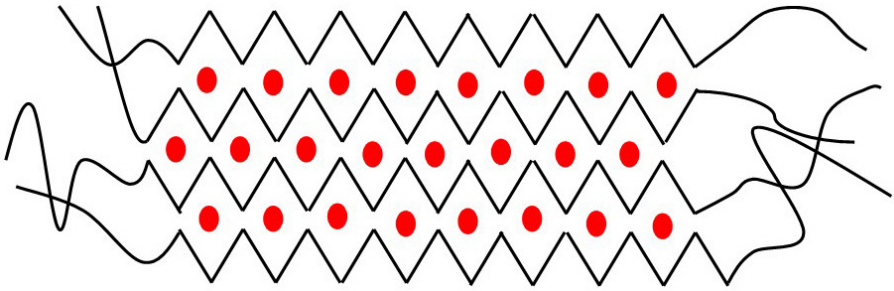

FIG. 2.6. Egg box model proposed for the interaction between polyuronates and Ca^{2+} ions (denoted as red circles between two polymeric chains).

as gellan [2.21] and carrageenan [2.22] where conformational transition drives gelation, the addition of metal ions stabilizes the ordered conformation and therefore influences gelling temperature and the resulting gel properties.

2.5. FINE TUNING OF STRUCTURE

There has been significant interest in refining methods of extraction, processing conditions and modification to obtain polysaccharides suitable for specific applications. For example, alginates from different algae or even from different tissues of the same plant can yield different glucuronic acid contents required for its gelling property. The stipe and holdfast in *Laminaria hyperborea*, an alage growing in very exposed coastal areas, have a high glucuronic acid content, which confers mechanical rigidity, whereas the leaves have an alginate characterized by a low glucuronic acid content, which confers a flexible texture [2.23].

Another example is pectin, which is widely used in the food industry as an emulsifier and stabilizer. It is commercially extracted from plant cell walls such as those of citrus fruits, tomatoes and apples. In the past, pectin has most often been used to make jams and jellies, but it has more recently been used as a stabilizer in fruit juice and acidic dairy drinks. Pectin can be classified into high methoxyl pectin (HM pectin) with a degree of esterification > 50% and low methoxyl pectin (LM pectin) with a degree of esterification < 50% [2.24, 2.25]. Both forms are capable of forming physical gels. LM pectin can form gels in the presence of calcium and other divalent ions or at acid pHs [2.26–2.28], while HM pectin forms gels at pH < 4.5 and in the presence of more than 55% sugar or a similar cosolute [2.29]. Figure 2.7 shows the main groups present on pectin chain molecules and how they contribute to its gelling property.

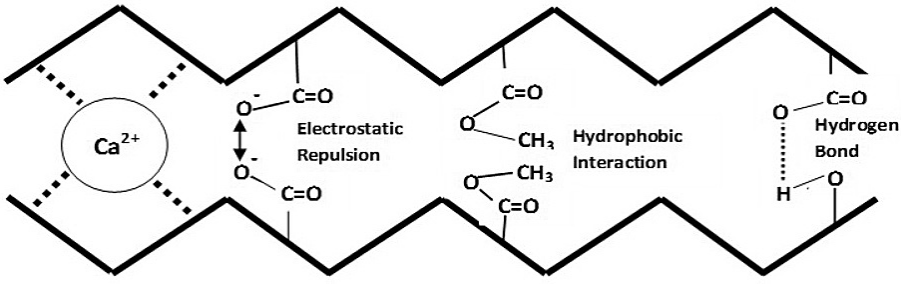

FIG. 2.7. The main groups present in pectin which confer its gelling properties.

These interactions are influenced by both intrinsic factors (molecular weight, distribution of methyl esters, side chains, degree of esterification) and extrinsic factors (pH, ionic strength, Ca concentration and temperature) [2.25, 2.28, 2.30–2.33]. The strength of pectin's gelling properties has received significant attention in order to refine the fine structure required for specific applications.

Irradiation is another method that has been used to modify polysaccharides. However, polysaccharides are generally degraded by the direct or indirect action of ionizing radiation. Both direct actions (irradiation in the solid state) and indirect actions (irradiation in aqueous solution) result in free-radical-induced scission of the glycosidic bonds in polysaccharide chains, which subsequently leads to a loss of viscosity and functionality [2.34–2.37]. Carrageenan has been the subject of many investigations to produce new materials with either a higher gelling strength [2.38, 2.39] or a lower molecular weight (oligomers) to be used as plant growth promoters [2.40, 2.41].

Carrageenans are widely utilized in the food industry owing to their excellent physical functional properties, such as their thickening, gelling and stabilizing abilities, and they have been used to improve the texture of cottage cheese, to control the viscosity and texture of puddings and dairy desserts, and as binders and stabilizers in the meat processing industry, for the manufacture of patties, sausages and low fat hamburgers. Carrageenans are also used in various non-food products, such as pharmaceutical, cosmetic, printing and textile formulations [2.42]. Carrageenans stabilize toothpaste preparations, absorb body fluids when used in wound dressings and interact with human carotene to improve the texture of skin and hair when used in hand lotions and shampoos. They have proved to be useful as tableting excipients owing to their good compatibility, high robustness and the persistent viscoelasticity of the tablet during compression.

Carrageenans are obtained from different species of *Rhodophyta: Gigartina, Chondrus crispus, Eucheuma* and *Hypnea*. These polysaccharides are traditionally split into six basic forms: iota (ι), kappa (κ), lambda (λ), mu (μ), nu (ν) and theta (θ) carrageenan [2.39]. Carrageenans belong to the family of hydrophilic linear sulphated galactans. They mainly consist of alternating 3 linked β D-galactopyranose (G units) and 4 linked α D-galactopyranose (D units) or 4 linked 3,6-anhydro α D-galactopyranose (DA units), which form the disaccharide repeating unit of carrageenans. The gelation of carrageenans, especially κ carrageenans, involves two separate and successive steps; coil to helix transition upon cooling and subsequent cation dependent aggregation between helices. The presence of a suitable cation, typically potassium or calcium, is an absolute requirement for gelation to proceed. For both ι and κ carrageenans, the alkali metal ions (Li^+, Na^+, K^+, Rb^+ and Cs^+) are all capable of inducing gelation, but K^+ and Rb^+ are considerably more effective than the

other ions in inducing gelation at much lower concentrations of both the cation and the carrageenan [2.43]. A novel radiation modification technique in the solid state in the presence of unsaturated alkyne gas has recently been reported [2.22]. These results demonstrate that by careful selection of absorbed dose it is possible to obtain a novel gelling material from κ carrageenan without the use of a gelling agent. The result is a hydrogel form of carrageenan produced in the absence of a gelling agent. A dose of around 5 kGy is preferred for modification, because at higher doses, the degradation induced reduces the proportion of hydrogel in the substance. The irradiation of carrageenan can produce 78% hydrogel with an almost fourfold improvement in viscosity compared with control. The proposed cross-linking mechanism using radiation modification in the solid state suggests that a three dimensional hydrogel structure is produced from superhelical rods that are responsible for the increase in viscosity, elasticity and mechanical properties as shown in Fig. 2.8 [2.22].

GA, a tree exudate, also exhibits inherent natural variations which have been attributed to factors such as location, age of tree, soil type, rainfall, time of picking, drying, storage and subsequent treatments. It contains three main fractions with different molecular weights and protein contents, namely: arabinogalactan protein, arabinogalactan and glycoprotein. By studying the mentioned factors and identifying structural characteristics, it has been possible to produce specific products with the defined molecular weights required for oil in water emulsion [2.44, 2.45]. Furthermore, the association of the proteinaceous components, an integral part of the structure, induced by maturation treatment (heating) resulted in a hydrogel form with greatly enhanced viscosity and water binding ability (Fig. 2.9). When the gum is matured, the protein associated with the lower molecular weight is transferred, leaving an increased concentration of the high molecular weight fraction. Gums such as gum ghatti and *Acacia kerensis* have been treated in this way and used in denture care [2.46].

Another area that has received considerable interest in recent years is the interaction between proteins and polysaccharides, which has been advanced to contribute to applications that control the texture of food formulations or increase emulsification performance and stability. Their applications in the food industry have been well reviewed [2.47–2.51]. Proteins carry positive charges at pH values below their isoelectric point (pI). Polysaccharides bearing carboxylic, phosphate or sulphate groups confer an anionic character. The interaction between positively charged proteins with anionic polysaccharides is highly dependent on factors such as pH, weight ratio, ionic strength and the charge density of the bio-polymers. Experimentally, this is achieved by acidification of a given protein/polysaccharide ratio and measurement of the pH, light scattering intensity and the zeta potential of the mixed solution to determine the phase diagram. For example, investigation revealed that soluble sodium caseinate / sugar beet

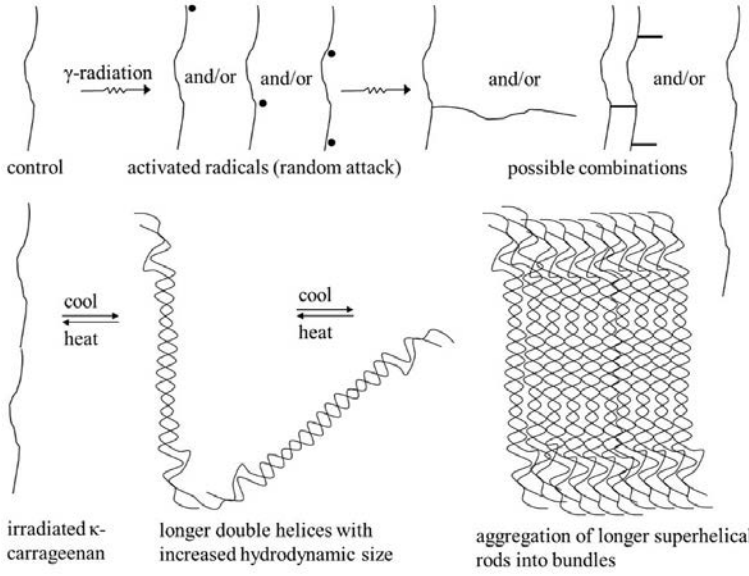

FIG. 2.8. Proposed cross-linking mechanism of κ carrageenan following irradiation in the solid state in the presence of unsaturated alkyne gas.

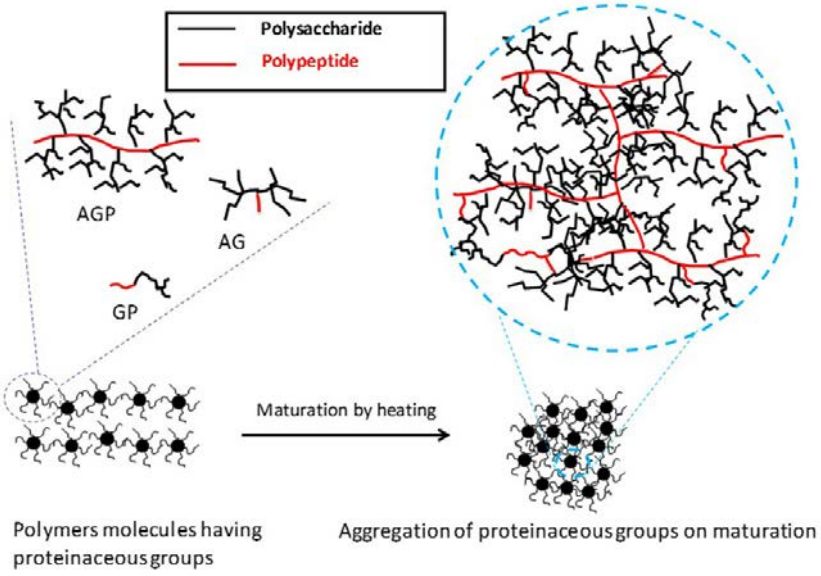

FIG. 2.9. Maturation of GA to induce aggregation of the proteinaceous part of molecules leading initially to higher molecular weight materials with enhanced functionality and subsequently to a highly aggregated hydrogel network.

pectin complexes first form on acidification, and then aggregate into insoluble complexes that disassociate into soluble polymers upon further decreasing the pH [2.52]. The critical pHs for the formation of soluble and insoluble complexes and the disappearance of insoluble complexes are designated as pH_c, pH_φ and pH_d, respectively. These critical pH values define four regions in the phase diagram whereby soluble complexes formed between sodium caseinate and sugar beet pectin can be identified. Subsequently, emulsions were prepared in these regions and a stable emulsion was obtained at a low sodium caseinate / sugar beet pectin ratio (0.3% sodium caseinate and 1.2% sugar beet pectin) at acidic pHs where the properties of the emulsion are controlled by both emulsifiers. Only under the condition described above was it possible to significantly to improve the stability of emulsions stabilized by sugar beet pectin, which is otherwise not possible.

The most recent work to fine-tune the physicochemical properties and/or biological activities of polysaccharides utilizes enzymatic modifications. By selecting specific enzymes to target and control the pattern of substitution (acetylation in chitosan [2.53], sulphonation in carrageenan [2.54] or methyl-esterification in pectin [2.55, 2.56]), the sequence of monosaccharide building blocks (alginate) or their glycosidic linkage type [2.57, 2.58], or the distribution patterns of acetylated and/or pyruvylated side chains in bacterial xanthan gums [2.59, 2.60], modifications can be achieved. The results demonstrate that it will be possible to produce specific products with defined structural characteristics following enzymatic modification.

REFERENCES TO CHAPTER 2

[2.1] FANG, Y.P., et al., Multiple steps and critical behaviors of the binding of calcium to alginate, J. Phys. Chem. B. **111** 10 (2007) 2456–2462.

[2.2] GUNNING, A.P., MORRIS, V.J., AL-ASSAF, S., PHILLIPS, G.O., Atomic force microscopic studies of hylan and hyaluronan, Carbohydr. Polym. **30** 1 (1996) 1–8.

[2.3] RINAUDO, M., "Polysaccharides", Kirk Othemer Encyclopedia of Chemical Technology, 5th edn, John Wiley & Sons, London (2006) 549–586.

[2.4] RINAUDO, M., "Advances in characterization of polysaccharides in aqueous solution and gel state", Polysaccharides: Structural Diversity and Functional Versatility (DUMITRU, S., Ed.), Marcel Dekker, New York (2005) 237–280.

[2.5] TOMBS, M.P., HARDINGS, S.E., An Introduction to Polysaccharide Biotechnology, Taylor & Francis, London (1998).

[2.6] JOSELEAU, J.P., ULLMANN, G., Biochemical evidence for the site of formation of gum arabic in *Acacia senegal*, Phytochem. **29** 11 (1990) 3401–3405.

[2.7] BALLAL, M.E., EL SIDDIG, E.A., ELFADL, M.A., LUUKKANEN, O., Gum arabic yield in differently managed *Acacia senegal* stands in western Sudan, Agrofor. Forum **63** (2005) 237–245.

[2.8] BALLAL, M.E., EL SIDDIG, E.A., ELFADL, M.A., LUUKKANEN, O., Relationship between environmental factors, tapping dates, tapping intensity and gum arabic yield of an *Acacia senegal* plantation in western Sudan, J. Arid Environ. **63** 2 (2005) 379–389.

[2.9] MORRIS, E.R., "Rheology of hydrocolloids", Gums and Stabilisers for the Food Industry (PHILLIPS, G.O., WILLIAMS, P.A., WEDLOCK, D.J., Eds), Oxford University Press, New York (1984) 57–78.

[2.10] AL-HADITHI, T.S.R., BARNES, H.A., WALTERS, K., The relationship between the linear (oscillatory) and nonlinear (steady-state) flow properties of a series of polymer and colloidal systems, Colloid. Polym. Sci. **270** 1 (1991) 40–46.

[2.11] MORRIS, E.R., Shear-thinning of 'random coil' polysaccharides: Characterization by two parameters from a simple linear plot, Carbohydr. Polym. **13** (1990) 85–96.

[2.12] MORRIS, E.R., CUTLER, A.N., ROSS-MURPHY, S.B., REES, D.A., Concentration and shear rate dependence of viscosity in random coil polysaccharide solutions, Carbohydr. Polym. **1** (1981) 5–21.

[2.13] RINAUDO, M., Relation between the molecular structure of some polysaccharides and original properties in sol and gel states, Food Hydrocoll. **15** 4–6 (2001) 433–440.

[2.14] BARNES, H.A., A Handbook of Elementary Rheology, University of Wales, Aberystwyth, UK (2000).

[2.15] STEFFE, J.F., Rheological Methods in Food Process Engineering, 2nd edn, Freeman Press, East Lansing, MI (1996).

[2.16] SHARMA, D.B.R., DHULDHOYA, N.C., MERCHANT, S.U., MERCHANT, S.U., Hydrocolloids: Efficient Rheology Control Additives (2007), http://www.techno-preneur.net/information-desk/sciencetechmagazine/2007/feb07/Hydrocolloids_efficient.pdf

[2.17] AL-ASSAF, S., PHILLIPS, G.O., Hydrocolloids: Structure function relationships, Food Sci. Tech **23** 3 (2009) 17–20.

[2.18] BARROW, M.S., BROWN, S.W.J., WILLIAMS, P.R., WILLIAMS, R.L., Rheology of dilute polymer solutions and engine lubricants in high deformation rate extensional flows produced by bubble collapse, J. Fluid. Eng. **126** 2 (2004) 162–169.

[2.19] WILLIAMS, P.A., PHILLIPS, G.O., "Introduction to food hydrocolloids", Handbook of Hydrocolloids (PHILLIPS, G.O., WILLIAMS, P.A., Eds), Woodhead Publishing, Cambridge (2004) 1–19.

[2.20] GRANT, G.T., MORRIS, E.R., REES, D.A., SMITH, P.J.C., THOM, D., Biological interactions: The egg box model, FEBS Lett. **32** (1973) 195–198.

[2.21] FUNAMI, T., et al., Molecular structures of gellan gum imaged with atomic force microscopy (AFM) in relation to the rheological behavior in aqueous systems in the presence of sodium chloride, Food Hydrocoll. **23** 2 (2009) 548–554.

[2.22] GULREZ, S., AL-ASSAF, S., PHILLIPS, G.O., "Characterisation and radiation modification of carrageenan in solid state", Radiation Processing Technology Applications (KHANDAL, R.K., Ed.), Shriram Institute for Industrial Research, New Delhi (2010) 525–538.

[2.23] DRAGET, K.I., "Alginate", Handbook of Hydrocolloids, 2nd edn (PHILLIPS, G.O., WILLIAMS, P.A., Eds), Woodhead Publishing, Cambridge (2009) 155–168.
[2.24] KJONIKSEN, A.L., HIORTH, M., NYSTROM, B., Association under shear flow in aqueous solutions of pectin, Eur. Polym. J. **41** 4 (2005) 761–770.
[2.25] STROM, A., Influence of pectin fine structure on the mechanical properties of calcium-pectin and acid-pectin gels, Biomacromolecules **8** 9 (2007) 2668–2674.
[2.26] CAPEL, F., NICOLAI, T., DURAND, D., BOULENGUER, P., LANGENDORFF, V., Calcium and acid induced gelation of (amidated) low methoxyl pectin, Food Hydrocoll. **20** 6 (2006) 901–907.
[2.27] GILSENAN, P.M., RICHARDSON, R.K., MORRIS, E.R., Thermally reversible acid-induced gelation of low-methoxy pectin, Carbohydr. Polym. **41** 4 (2000) 339–349.
[2.28] LOOTENS, D., et al., Influence of pH, Ca concentration, temperature and amidation on the gelation of low methoxyl pectin, Food Hydrocoll. **17** 3 (2003) 237–244.
[2.29] LOFGREN, C., et al., Effects of calcium, pH, and blockiness on kinetic rheological behavior and microstructure of HM pectin gels, Biomacromolecules **6** 2 (2005) 646–652.
[2.30] CAPEL, F., NICOLAI, T., DURAND, D., Influence of chain length and polymer concentration on the gelation of (amidated) low-methoxyl pectin induced by calcium, Biomacromolecules **6** 6 (2005) 2954–2960.
[2.31] CARDOSO, S.M., COIMBRA, M.A., DA SILVA, J.A.L., Temperature dependence of the formation and melting of pectin-Ca2+ networks: A rheological study, Food Hydrocoll. **17** 6 (2003) 801–807.
[2.32] FRAEYE, I., et al., Influence of intrinsic and extrinsic factors on rheology of pectin-calcium gels, Food Hydrocoll. **23** 8 (2009) 2069–2077.
[2.33] KJONIKSEN, A.L., HIORTH, M., NYSTROM, B., Temperature-induced association and gelation of aqueous solutions of pectin. A dynamic light scattering study, Eur. Polym. J. **40** 11 (2004) 2427–2435.
[2.34] AL-ASSAF, S., Rheological Properties and Free Radical Stability of Cross-linked Hyaluronan (Hylan), PhD Thesis, Univ. of Salford (1997).
[2.35] AL-ASSAF, S., HAWKINS, C.L., PARSONS, B.J., DAVIES, M.J., PHILLIPS, G.O., Identification of radicals from hyaluronan (hyaluronic acid) and cross-linked derivatives using electron paramagnetic resonance spectroscopy, Carbohydr. Polym. **38** 1 (1999) 17–22.
[2.36] AL-ASSAF, S., MEADOWS, J., PHILLIPS, G.O., WILLIAMS, P.A., The effects of hydroxyl radical attack on the rheological performance of hylan and hyaluronan, Biorheol. **36** 1–2 (1999) 55–56.
[2.37] AL-ASSAF, S., et al., The enhanced stability of the cross-linked hylan structure to hydroxyl (OH) radicals compared with the uncross-linked hyaluronan, Radiat. Phys. Chem. **46** 2 (1995) 207–217.
[2.38] ABAD, L.V., RELLEVE, L.S., ARANILLA, C.T., DELA ROSA, A.M., Properties of radiation synthesized PVP-kappa carrageenan hydrogel blends, Radiat. Phys. Chem. **68** 5 (2003) 901–908.
[2.39] CAMPO, V.L., KAWANO, D.F., DA SILVA, D.B., CARVALHO, I., Carrageenans: Biological properties, chemical modifications and structural analysis – A review, Carbohydr. Polym. **77** 2 (2009) 167–180.

[2.40] ABAD, L.V., et al., Radiolysis studies of aqueous [kappa]-carrageenan, Nucl. Instrum. Methods Phys. Res. Sect. B **268** 10 (2010) 1607–1612.
[2.41] RELLEVE, L., et al., Degradation of carrageenan by radiation, Polym. Degrad. Stability **87** 3 (2005) 403–410.
[2.42] IMESON, A.P., "Carrageenan", Handbook of Hydrocolloids (PHILLIPS, G.O., WILLIAMS, P.A., Eds), Woodhead Publishing, Cambridge (2000) 87–102.
[2.43] FUNAMI, T., et al., Influence of molecular structure imaged with atomic force microscopy on the rheological behavior of carrageenan aqueous systems in the presence or absence of cations, Food Hydrocoll. **21** 4 (2007) 617–629.
[2.44] AL-ASSAF, S., PHILLIPS, G.O., WILLIAMS, P.A., DU PLESSIS, T.A., Application of ionizing radiations to produce new polysaccharides and proteins with enhanced functionality, Nucl. Instrum. Meth. B **265** 1 (2007) 37–44.
[2.45] AOKI, H., et al., Characterization and properties of *Acacia senegal* (L.) willd. var. *Senegal* with enhanced properties (Acacia (*sen*) SUPER GUM™): Part 5. Factors affecting the emulsification of *Acacia senegal* and Acacia *(sen)* SUPER GUM ™, Food Hydrocoll. **21** 3 (2007) 353–358.
[2.46] AL-ASSAF, S., DICKSON, P.A., PHILLIPS, G.O., THOMPSON, C., TORRES, J.C., Compositions Comprising Polysaccharide Gums, Patent No. WO 2009016362 (A2), Feb. 2009, filed Jul. 2008, available on-line.
[2.47] DE KRUIF, C.G., TUINIER, R., Polysaccharide protein interactions, Food Hydrocoll. **15** 4–6 (2001) 555–564.
[2.48] DE KRUIF, C.G., WEINBRECK, F., DE VRIES, R., Complex coacervation of proteins and anionic polysaccharides, Curr. Opin. Colloid. Interface Sci. **9** 5 (2004) 340–349.
[2.49] TURGEON, S.L., BEAULIEU, M., SCHMITT, C., SANCHEZ, C., Protein-polysaccharide interactions: phase-ordering kinetics, thermodynamic and structural aspects, Curr. Opin. Colloid. Interface Sci. **8** 4–5 (2003) 401–414.
[2.50] TURGEON, S.L., SCHMITT, C., SANCHEZ, C., Protein-polysaccharide complexes and coacervates, Curr. Opin. Colloid. Interface. Sci. **12** 4–5 (2007) 166–178.
[2.51] YE, A.Q., Complexation between milk proteins and polysaccharides via electrostatic interaction: Principles and applications - a review, Int. J. Food Sci. Technol. **43** 3 (2008) 406–415.
[2.52] LI, X., FANG, Y., PHILLIPS, G.O., AL-ASSAF, S., Improved sugar beet pectin-stabilized emulsions through complexation with sodium caseinate, J. Arg. Food Chem. **61** 6 (2013) 1388–1396.
[2.53] HAMER, S.N., MOERSCHBACHER, B.M., KOLKENBROCK, S., Enzymatic sequencing of partially acetylated chitosan oligomers, Carbohydr. Res. **392** (2014) 16–20.
[2.54] PRÉCHOUX, A., HELBERT, W., Preparation and detailed NMR analyses of a series of oligo-α-carrageenans, Carbohydr. Polym. **101** (2014) 864–870.
[2.55] REMOROZA, C., et al., A *Bacillus licheniformis* pectin acetylesterase is specific for homogalacturonans acetylated at O-3, Carbohydr. Polym. **107** (2014) 85–93.
[2.56] REMOROZA, C., BROXTERMAN, S., GRUPPEN, H., SCHOLS, H.A., Two-step enzymatic fingerprinting of sugar beet pectin, Carbohydr. Polym. **108** (2014) 338–347.

[2.57] THOMAS, F., et al., Comparative characterization of two marine alginate lyases from *Zobellia galactanivorans* reveals distinct modes of action and exquisite adaptation to their natural substrate, J Biol. Chem. **288** 23 (2013) 23021–23037.

[2.58] HEHEMANN, J.-H., BORASTON, A.B., CZJZEK, M., A sweet new wave: Structures and mechanisms of enzymes that digest polysaccharides from marine algae, Curr. Opin. Struct. Biol. **28** (2014) 77–86.

[2.59] KOOL, M.M., GRUPPEN, H., SWORN, G., SCHOLS, H.A., Comparison of xanthans by the relative abundance of its six constituent repeating units, Carbohydr. Polym. **98** (2013) 914–921.

[2.60] KOOL, M.M., GRUPPEN, H., SWORN, G., SCHOLS, H.A., The influence of the six constituent xanthan repeating units on the order–disorder transition of xanthan, Carbohydr. Polym. **104** (2014) 94–100.

Chapter 3

INTRODUCTION TO THE RADIATION CHEMISTRY OF POLYMERS

X. COQUERET
University of Reims Champagne-Ardenne,
Reims, France

S. SABHARWAL
Radiation Technology Development Division,
Bhabha Atomic Research Centre,
Trombay, Mumbai, India

H.M.D. KHAIRUL ZAMAN
Radiation Processing Technology Division,
Malaysia Nuclear Agency,
Bangi, Malaysia

R. CZECHOWSKA-BISKUP, R.A. WACH, J.M. ROSIAK, P. ULANSKI
Institute of Applied Radiation Chemistry, Faculty of Chemistry,
Lodz University of Technology,
Lodz, Poland

S.K.H. GULREZ, S. AL-ASSAF
Hydrocolloids Research Centre, Institute of Food Science and Innovation,
University of Chester,
Chester, United Kingdom

3.1. INTRODUCTION

Ionizing radiation is a very efficient, versatile and clean tool for modifying polymers in general, and polysaccharides in particular. The advantages of using radiation include the possibility of processing materials in any physical form, at a convenient temperature (often at room temperature), typically with no need for any added initiators nor for other chemicals. Moreover, the treatment can be homogeneous, is easily conducted with high reliability, generates no waste and requires only a short processing time. High speed production and high

productivity is one of the important considerations for the industrial application of ionizing radiation, and in particular, the use of electron accelerators.

This chapter is intended as a brief general introduction to the radiation chemistry of polymers, illustrated by a few representative examples. The interaction of high energy radiation with organic monomers and polymers induces various chemical transformations of increasing importance from both a scientific and a technological standpoint. Cross-linking and scission in polymers and networks, polymerization of pure and blended monomers, grafting onto synthetic and natural polymers as well as the chemical activation of organic materials by oxidation can be induced by irradiation under soft conditions. After more than fifty years of complementary basic and application orientated research, an improved understanding of the radiation chemistry of polymers has been found to lead to many applications of current technological, economical and societal interest. A better understanding of the primary events and subsequent chemical reactions mediated by ionic or free radical intermediates has led to an increasing number of industrial processes that include food, drug and medical device sterilization, cross-linking of thermoplastics and elastomers, grafting polymerization, surface patterning for micro or nanotechnologies and curing of coatings and composites.

3.2. IONIZING RADIATION

Radiation chemistry deals with the study of chemical changes induced by high energy charged particles or electromagnetic radiation, which is termed ionizing radiation, with energy in the range of 10^2–10^7 eV. Radiation–matter interaction can cause the ionization and excitation of molecules and atoms within the substrate by various possible pathways, resulting in the formation of a variety of reactive species. Ionizing radiation is almost completely absorbed by the electronic structure of the absorber and is therefore a very effective and efficient method for generating reactive species that can initiate chemical reactions. The basic modes of interaction between ionizing radiation and atoms or molecules are non-specific and thus non-selective in nature. As a comparison, chemical processing requires the use of chemicals that will always leave residues that need to be removed from the system. Another alternative technology uses enzymes, which are expensive; their availability is limited and it is difficult to control the enzymatic process. However, the choice of the processing technology also depends on the characteristics of the material that needs to be processed.

3.3. RADIATION SOURCES

Radiation processing has been extensively used in industry since the 1950s. The main sources of radiation used in radiation chemistry and technology are electron beams generated from electron accelerators, and gamma radiation from radioactive sources, mainly ^{60}Co, although ^{137}Cs is used in small units for research purposes. Both types of radiation are used for a variety of applications such as the curing of thin layer coatings, the cross-linking of polymeric products, the modification of polymer compounds by grafting, coupling and chain scissioning, as well as sterilizing medical items. Table 3.1 lists the main advantages and disadvantages of using gamma ray sources and electron accelerators.

TABLE 3.1. ADVANTAGES AND DISADVANTAGES OF GAMMA RAY SOURCES AND ELECTRON ACCELERATORS FOR RADIATION PROCESSING

Source type	Gamma sources	Electron accelerators
Advantages	High penetration (uniform dose, possibility to irradiate large objects or boxes) Easy operation Relatively low operation costs	Safety of operation (beam off — radiation off) No radioactive waste High dose rate means a high throughput
Disadvantages	Necessity to replace the sources to keep activity at the desired level High safety requirements on-site and during transport of sources Problems and costs with utilization of the sources Radiation cannot be ‘switched off’	Low penetration depth of electron beam (large objects cannot be irradiated, smaller items can only be irradiated in flat boxes)

Electron accelerators can be designed to provide a wide range of energy, typically from 80 keV to 10 MeV. The penetration depth of the electron beam depends on the electron energy. The thickness and density of the products will determine the type of energy of the electron accelerator required to perform the process. Energies below 1 MeV are used mainly for surface treatment, while electrons with energy of a few MeV ($E > 2$ MeV) can penetrate more than 1 cm into a material exhibiting a density corresponding to water.

Electron accelerators come in a variety of types. Van de Graaff machines are known for their reliability and relative simplicity of design, although their beam power is limited, and the electron energy typically does not exceed 3 MeV. Linear accelerators using microwave energy to speed up electrons to a few MeV, or even above 10 MeV, have been most widely applied in pilot scale and industrial irradiation. Recently, more compact accelerators of a comparable energy but with a significantly higher output have been designed, where electrons pass through the circular cavity of the accelerator multiple times before being driven to the target. An example, the Rhodotron, is shown in Fig. 3.1.

Owing to a smaller interaction cross-section with matter, gamma radiation is much more penetrating; it is mainly used for the sterilization of medical products and the irradiation of food items that are bulky and packed with high density products. A diagram of a simple research scale gamma irradiator is shown in Fig. 3.2, while Fig. 3.3 shows a medium sized, dry storage panoramic irradiation system that may be used for technology development or small scale industrial irradiation. A design for a large scale irradiation facility based on isotope sources is presented in Fig. 3.4.

(a)

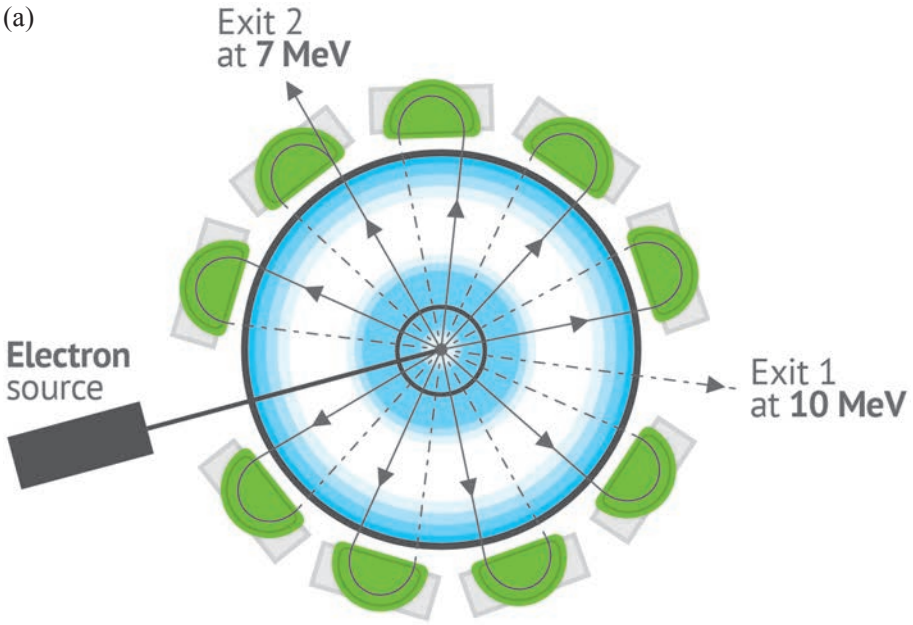

FIG. 3.1. The IBA Rhodotron is an electron beam accelerator able to generate beam energies of up to 10 MeV and a beam power of up to 560 kW. (a) The Rhodotron's operating principle: The electron source generates electrons which are accelerated multiple times through the cavity; when the desired energy is reached, the beam of electrons is extracted from the cavity. (b) External view. (Images courtesy of IBA.)

(b)

FIG. 3.1. (Cont.) The IBA Rhodotron is an electron beam accelerator able to generate beam energies of up to 10 MeV and a beam power of up to 560 kW. (a) The Rhodotron's operating principle: The electron source generates electrons which are accelerated multiple times through the cavity; when the desired energy is reached, the beam of electrons is extracted from the cavity. (b) External view. (Images courtesy of IBA.)

At the time of writing, there were more than 200 industrial gamma irradiation units around the world, 85% of which were being utilized for sterilization purposes. On the other hand, more than 1400 electron accelerator units were in operation for research and/or industrial processing in 2012 for polymer modification only [3.1, 3.2].

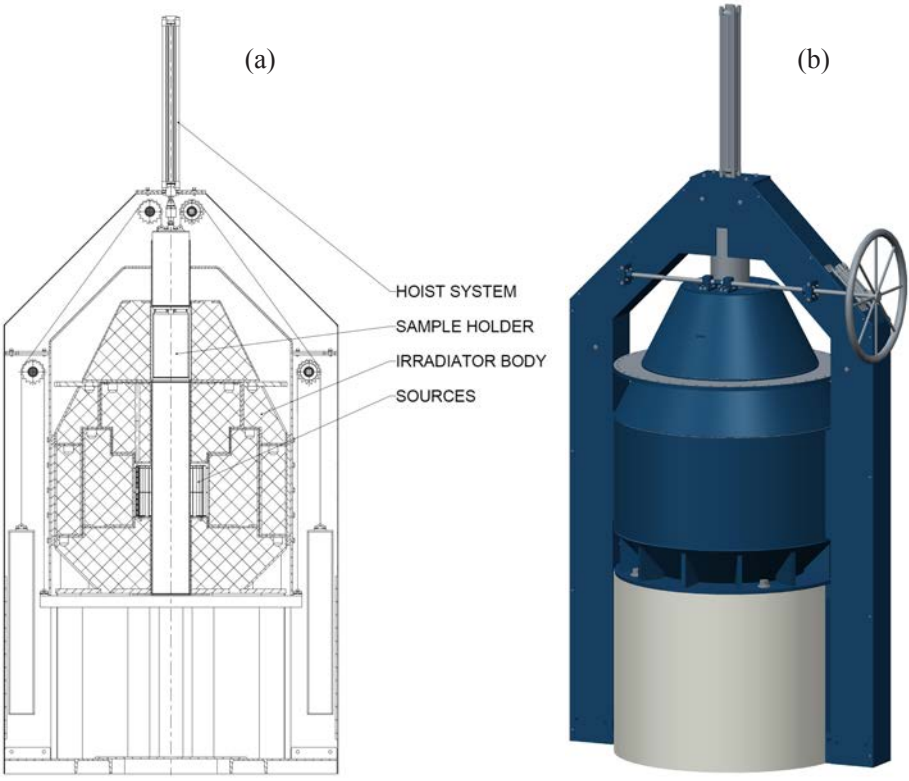

FIG. 3.2. Diagram of a laboratory scale gamma irradiator, with gamma sources located at a fixed position within the shield and a moving column containing the sample holder: (a) Cross-section and (b) external view. (Images courtesy of Izotop, Hungary.)

A new, emerging technique exploits the possibility of converting electron beams into X rays. Although no radioactive isotope is involved, the conversion results in high energy electromagnetic radiation that is highly penetrating, comparable in terms of physical nature and penetrating power to conventional gamma rays. In this technique, an electron beam hits a target which emits X rays by bremsstrahlung, which in turn are orientated by design towards the material to be modified or sterilized. An example is shown in Fig. 3.5. Although the energetic efficiency of the conversion process is relatively low, the method is claimed to be attractive because it combines the advantages of electron accelerators and gamma sources while eliminating the main disadvantages of both, i.e. low penetration depth of the electron beam (EB) and the use of radioactive isotopes.

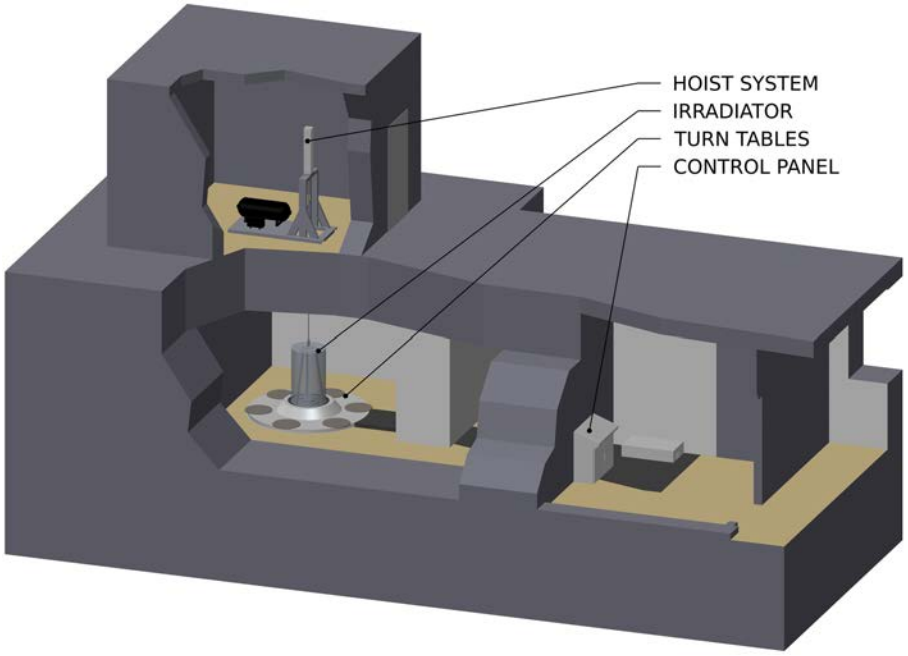

FIG. 3.3. Diagram of a panorama type, dry storage gamma irradiator, with gamma sources located in a column which is pulled up from the shield to irradiate the goods located in the irradiation chamber (for instance, on the turntables located around the irradiator). (Image courtesy of Izotop, Hungary.)

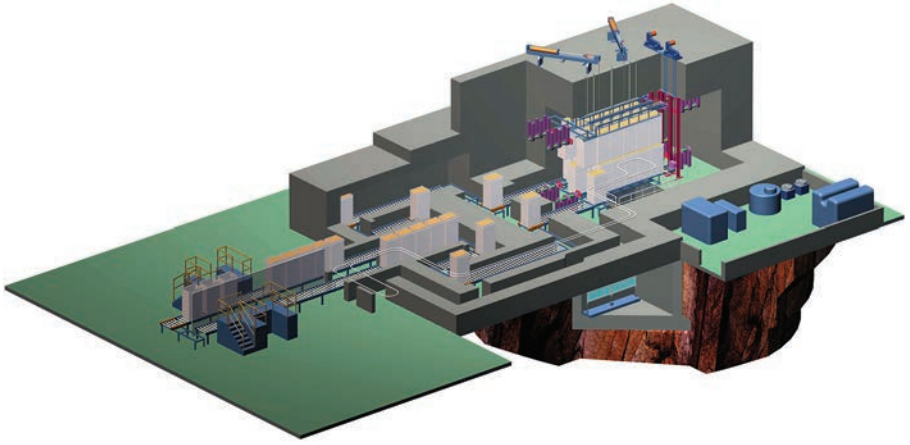

FIG. 3.4. Diagram of a large scale gamma irradiation facility. (Image courtesy of Nordion, Canada.)

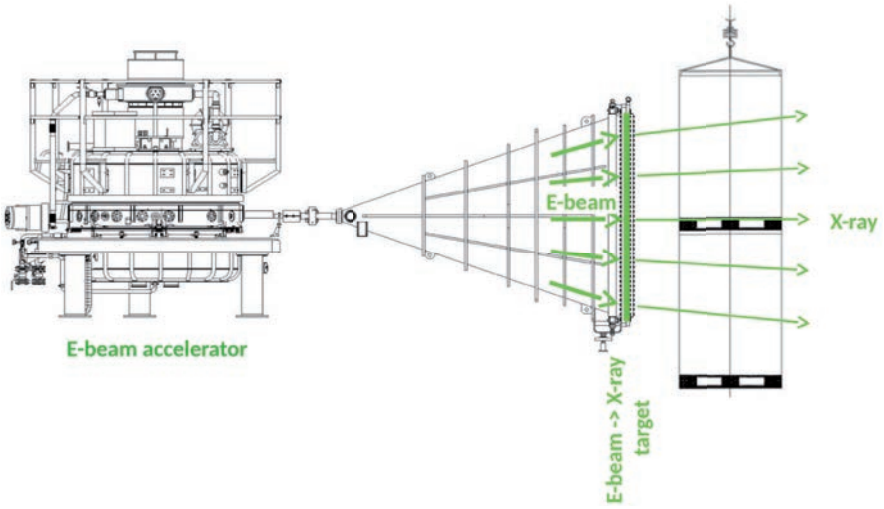

FIG. 3.5. High power X ray generator. An EB accelerator generates a beam of electrons which is directed towards an X ray target. The X ray target converts the beam of electrons into highly penetrating X rays. (Image courtesy of IBA.)

It should be stressed that, owing to high investment costs, establishing a new irradiation facility is not always the most cost effective way of employing radiation technology in industry, especially for production on a small scale, such as during the introduction of new products or the performance of pilot scale tests. In many countries, industrial scale irradiation facilities act as service centres that provide irradiation on demand, on a commercial basis.

Currently, about 30 000 particle accelerators are operated world-wide, for applications in medicine, industry, security, defence and basic science. The market for medical and industrial accelerators currently exceeds US $3.5 billion dollars a year, and it is growing at more than ten per cent annually. All digital electronics now depend on particle beams for ion implantation, creating a US $1.5 billion annual market for ion beam accelerators. However, if one includes all the products that are processed, treated or inspected by particle beams, the total collective annual value is more than US $500 billion [3.3].

3.4. INTERACTION OF IONIZING RADIATION WITH MATTER

A thorough knowledge of the processes by which high energy radiation interacts with matter is a prerequisite for understanding radiation-chemical effects, as it is the absorbed energy which finally results in the observed chemical changes. The extent and process of energy absorption depends on the nature of

the radiation as well as that of the material. The high energy radiation commonly used in industry to process material is ≤10.0 MeV, at which level the energy of the radiation is not sufficient to induce changes in the nucleus of the atoms that could result in the formation of a radioisotope. The important parameters are energy, mass and charge of the radiation, and the atomic number or electron density of the material [3.4]. The mechanism of interaction of (i) electromagnetic radiation such as gamma radiation and (ii) charged particles such as electrons, which are of relevance to radiation processing and radiation-chemical studies, are briefly explained below.

3.4.1. Interaction of gamma radiation with matter

High energy penetrating electromagnetic radiation that arises from the decay of atomic nuclei is termed γ rays. The γ rays emitted by radioactive isotopes are mono-energetic and possess at least one discrete energy. For example, ^{60}Co emits γ photons of energy 1.332 MeV and 1.173 MeV. For a narrow beam, the intensity of gamma radiation transmitted through an absorbing material (Fig. 3.6) decays exponentially as a function of the distance, as indicated by Eq. (3.1).

$$I = I_0(\exp(-\mu x)) \tag{3.1}$$

where I_0 is the incident radiation intensity, x is the thickness of material penetrated by radiation, and μ is the linear attenuation coefficient. The attenuation coefficient is the sum of a number of partial coefficients representing different processes occurring inside the absorber. These are: (i) the photoelectric effect, (ii) Compton scattering, (iii) pair production, (iv) coherent scattering and (v) photo-nuclear reactions (Fig. 3.7). The relative importance of each process depends on the photon energy and on the atomic number of the absorbing material. Whereas coherent scattering is of importance for low energy photons (<0.1 MeV), photo-nuclear reactions are possible with photons of energies in the range of 2–8 MeV for low atomic number (Z) materials, and in the region of 7–20 MeV for high Z materials. Thus, for gamma radiation emitted by ^{60}Co or ^{137}Cs sources, only the first three interaction processes are operating. Depending on the incident photon energy, the photon flux is attenuated and the total linear attenuation coefficient (μ) is given by Eq. (3.2).

$$\mu = \tau + \sigma + \kappa \tag{3.2}$$

where τ, σ and κ are the linear attenuation coefficients in units of cm^{-1} for the photoelectric effect, Compton scattering and positron electron pair production, respectively.

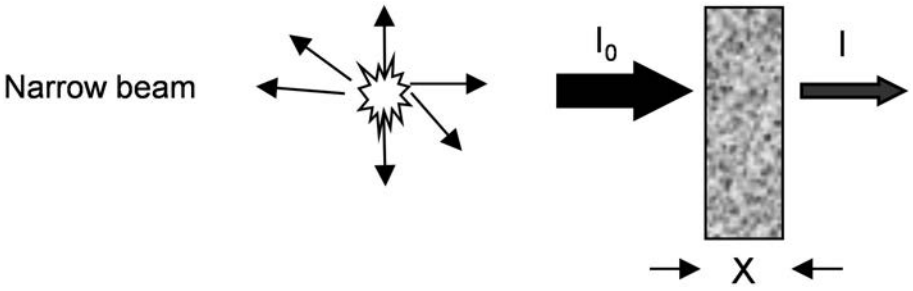

FIG. 3.6. Absorption of a narrow beam of gamma rays by an absorber layer of thickness x.

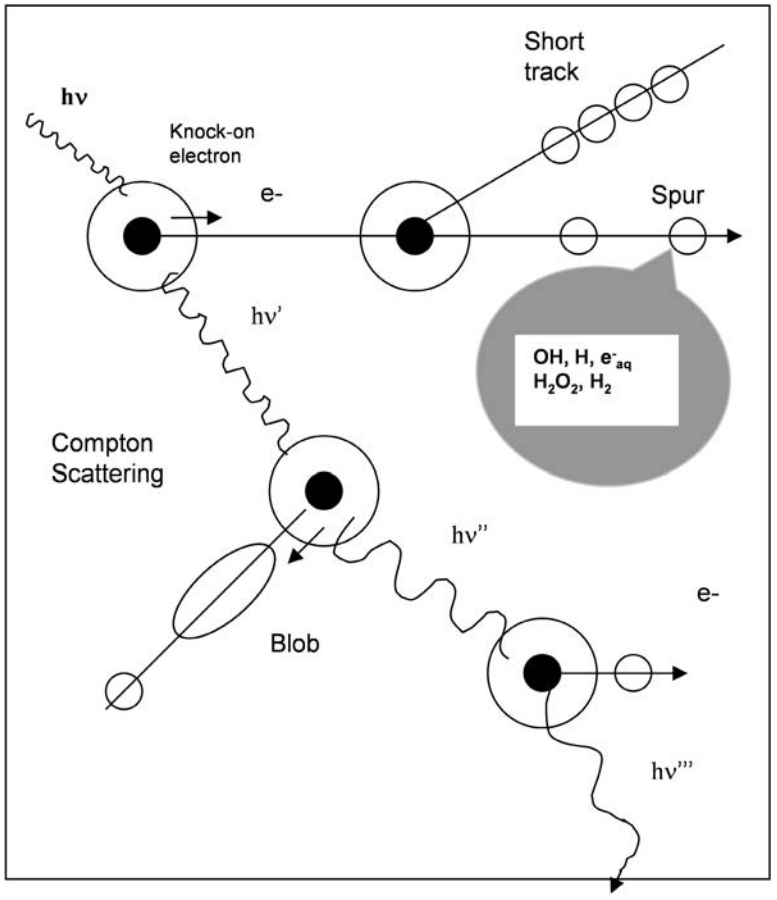

FIG. 3.7. Excitation and ionization processes by gamma rays. Adapted from Ref. [3.5].

3.4.2. Interaction of electrons with matter

In the case of accelerated electrons, the most important processes by which the charged particles interact with matter are (i) elastic scattering, (ii) inelastic collisions and (iii) emission of electromagnetic radiation. The relative importance of each process depends mainly upon the energy of the electrons, and to a smaller extent, on the *Z* value of the stopping material. High energy electrons are relativistic charged particles. Passing close to the nucleus of an atom, they are decelerated and radiate energy in the form of electromagnetic radiation such as X rays (bremsstrahlung).

Another type of radiation known as Cherenkov or Vavilov–Cherenkov radiation is the electromagnetic radiation emitted when a charged particle (such as an electron) passes through a dielectric medium at a speed greater than the phase velocity of light in that medium. The charged particles polarize the molecules of that medium, which then rapidly turn back to their ground state, emitting radiation of a blue colour in the process, as shown in Fig. 3.8.

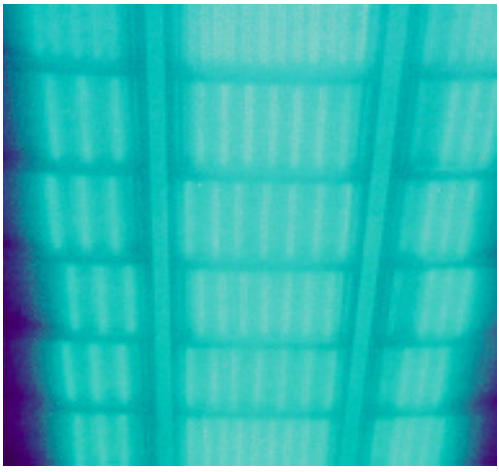

FIG. 3.8. Cerenkov radiation emitted by a ^{60}Co source in water.

Radiation emission is the predominant process taking place in the matter at high electron energies and for high *Z* materials, whereas elastic and inelastic scattering predominates at low electron energies. Elastic scattering occurs when the electrons passing close to the nucleus of an atom are deflected by its electrostatic field. Inelastic scattering occurs when electrons interact with the electrostatic field of atomic electrons so that the atomic electrons are either raised to a higher energy level (excitation) or are ejected from the atom (ionization).

Inelastic scattering is the only process that generates excited or ionized species in the absorber material and results in significant chemical or biological change. The incident primary electrons are gradually slowed down and cascades of secondary and tertiary electrons are produced. The overall absorption of ionizing radiation by matter results in the formation of tracks of excited and ionized species.

3.4.3. Depth–dose profiles for gamma and electron radiation

When a beam of radiation interacts with the substrate, the secondary electron radiation builds up to generate a maximum of energy deposition at a distance below the impinging surface related to the maximum range of secondary electrons. The dose then falls off as the primary beam is attenuated. The depth–dose distribution curves for electrons and γ rays in water show maxima for energy absorbed per unit volume element shifted to a larger distance from the surface as the energy of the photon or electron increases. The γ rays emitted by ^{60}Co that have an average energy of 1.25 MeV show a maximum depth dose at 0.5 cm from the surface. For 0.5 MeV and 3.0 MeV electrons, the maximum is located at 1 mm and 4.5 mm from the surface, respectively. Typical depth–dose curves for the irradiation of water by electromagnetic radiation and by electron irradiation are shown in Fig. 3.9, in parts (a) and (b) respectively.

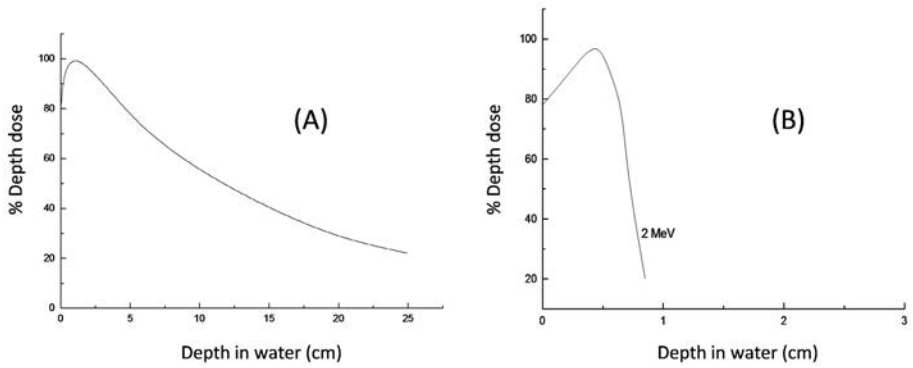

FIG. 3.9. (a) Per cent depth–dose curve for the irradiation of water by ^{60}Co γ radiation; (b) Depth–dose curve for 2 MeV electrons in water.

3.4.4. Radiation dosimetry and parameters for the quantification of chemical effects induced by radiation

Management of the physical, chemical or biological changes produced by ionizing radiation necessitates knowledge of the amount of energy absorbed per

unit mass of the absorber and of the distribution of the absorbed energy in the absorbing material. Radiation dosimetry encompasses the methodologies and tools for the determination of these quantities.

Absorbed dose: The absorbed dose is the amount of energy absorbed from the radiation beam per unit mass of the irradiated material. Absorbed dose is a measure of that part of the energy that, when transferred to the irradiated material, induces the formation of ions and excited molecules. The SI unit for absorbed dose is joules per kilogram (J/kg), known as gray (symbol Gy). The previously used units were rad (1 rad = 0.01 Gy).

Absorbed dose rate: The absorbed dose rate is the absorbed dose per unit of time, for example, Gy/s.

Radiation-chemical yield: Traditionally, radiation-chemical yields have been reported in terms of G values, where G(A) represents the number of events or chemical species of type A formed per 100 eV of energy absorbed [3.6]. In SI units, the radiation-chemical yield, G, is defined as the change in moles of events or of chemical species formed or decomposed by an energy absorption of 1 J [3.7]. G values reported in terms of number of species formed per 100 eV are converted into SI units using the following relationship (3.3).

$$G\,(\text{mol/J}) = 1.036 \times 10^{-7}\, G\,(1/100\text{eV}) \tag{3.3}$$

Primary and secondary dosimeters: Dosimeters can be classified into two categories: primary dosimeters and secondary dosimeters. Primary dosimeters utilize a physical measurement such as temperature rise in a calorimeter, ionization produced in a gas or the charge carried by a beam of charged particles of known energy [3.8, 3.9]. Secondary dosimeters are those dosimeters whose response to radiation has to be calibrated against a primary dosimeter. These include Fricke dosimeters, solutions of various dyes, clear as well as red perspex dosimeters, cellulose acetate and other thermoplastic films, and alanine dosimeters [3.10]. The choice of a dosimeter for a particular application depends on many factors including (i) the state of the system, (ii) the dose range to be monitored and (iii) the nature of the radiation. Changes of absorbance in the ultraviolet visible (UV-Vis) domain can be easily measured from radiochromic films. However, alanine dosimeters that are based on quantitative electron spin resonance measurements have the advantage of a higher stability for free radicals generated by irradiation, as well as a lower dependence on temperature, humidity and dose rate [3.11].

Low dose dosimetry (Fricke dosimeter): Doses up to a few hundred Gy are typically used in research and only exceptionally in radiation processing. There are many dosimetric systems available for this dose range, the classical example being the chemical Fricke dosimeter. It is based on radiation induced oxidation of

ferrous ions to ferric ions in acidic aqueous solutions [3.12, 3.13]. The standard Fricke dosimeter consists of an aerated solution of 1×10^{-3} mol dm^{-3} ferrous ammonium sulphate, 1×10^{-3} mol dm^{-3} NaCl dissolved in 0.4 mol dm^{-3} sulphuric acid (pH = 0.46) [3.14]. The yield of Fe^{3+} ions produced is determined by absorption spectrophotometry employing the Lambert–Beer law ($\Delta A = \Delta\varepsilon\ c\ l$) at 304 nm with $\varepsilon(Fe^{3+}) = 220.5 \pm 0.3$ m^2/mol and $\varepsilon(Fe^{2+}) = 0.1$ m^2/mol at 25°C. The $G(Fe^{3+}) \times \varepsilon$ value accepted for electron and photon radiation in the range (1–30) MeV is 352×10^6 m$^2 \cdot$kg$^{-1} \cdot$Gy^{-1} at 25°C [3.10]. The Fricke dosimeter can be used to accurately determine doses only up to 400 Gy because of oxygen depletion in the system. Using oxygenated solutions, this limit can be enhanced to 2 kGy. The Fricke dosimeter is independent of dose rate between $(0.2–2) \times 10^6$ Gy/s. A modified version of the Fricke dosimeter, sometimes referred to as a super Fricke dosimeter, containing 10^{-2} mol dm^{-3} ferrous ions, which are oxygenated but without any sodium chloride, is dose rate independent up to absorbed dose rates of the order of 10^8 Gy/s. The upper limit of absorbed dose that can be measured using a super Fricke dosimeter is 2 kGy.

The Fe^{3+} generates a blue colour that can be quantified through a spectrophotometer [3.15] by plotting the absorbance at 304 nm for solutions irradiated for different periods of time. The colorimetric dose response for the solution is linear up to 400 Gy while complete oxidation takes place at a dose of about 700 Gy. The chemical reactions involved in Fricke dosimetry are detailed below:

$$H^\bullet + O_2 \rightarrow HO_2^\bullet$$
$$HO_2^\bullet + Fe^{2+} \rightarrow HO_2^- + Fe^{3+}$$
$$HO_2^- + H^+ \rightarrow H_2O_2$$
$$HO^\bullet + Fe^{2+} \rightarrow HO^- + Fe^{3+}$$
$$H_2O_2 + Fe^{2+} \rightarrow HO^- + HO^\bullet + Fe^{3+}$$

From the reactions above, it can be concluded that each $H^\bullet$ will produce three Fe^{3+}. Each H_2O_2 (radiolytic) will produce two Fe^{3+} ions and each $HO^\bullet$ will produce one Fe^{3+}. So, the overall yield in presence of O_2 will be:

$$G(Fe^{3+}) = 3G(H^\bullet) + 2G(H_2O_2) + G(HO^\bullet)$$

When organic impurities are present in the Fricke dosimeter solution, an increase in the yield of ferric ion is observed [3.16]. The addition of chloride ions in a Fricke dosimeter reduces the effect of impurities by converting the $HO^\bullet$ radicals to the chloride atom so that a normal yield is obtained.

$$Cl^- + HO^\bullet + H^+ \rightarrow Cl^\bullet + H_2O$$
$$Cl^- + Cl^\bullet \rightarrow Cl_2^{\bullet -}$$
$$Cl_2^{\bullet -} + Fe^{2+} \rightarrow 2Cl^- + Fe^{3+}$$

Dosimetry for radiation processing: Industrial EB accelerators and large gamma irradiation facilities are generally employed for high dose irradiation and hence require different kind of dosimetric systems. A variety of solid state dosimeters, especially polymer based dosimeters in the form of thin films, are utilized for dosimetry at this type of accelerator. Of these, FWT-60 radiochromic dye film and cellulose triacetate film dosimeters are commercially available and have been reported to be particularly useful in various applications [3.17–3.19]. These are secondary dosimeters that must be calibrated against a primary dosimeter or a well characterized dosimeter. Another option is alanine dosimetry. Radiation generated radicals trapped in alanine crystals are stable and can be quantified by electron paramagnetic resonance. Complete systems consist of alanine tablets and/or strips used as small size dosimeters, dedicated electron paramagnetic resonance setups and software, and calibration sets (see Refs [3.11, 3.20–3.24]).

Dose mapping requires the placement of dosimeters throughout a representative product load. For consistency in positioning and ease of locating the dosimeters, it is helpful to define a three dimensional grid throughout the product load. The points of planar intersection provide reference locations. The use of multiple dosimeters at a given location will increase the confidence in the dose reading at that location.

In the industrial EB sterilization of medical items such as boxes of surgical gloves, the dosimeters, for example, cellulose triacetate films of 125 μm thickness, are positioned at several places on the surface and in the bottom part of the box to represent the overall surface dose distribution and depth–dose distribution in the box. The absorbed doses are measured by the increment of optical densities of the cellulose triacetate film at 280 nm. The optical density can be measured using a UV spectrophotometer. The cellulose triacetate film dosimeter is calibrated using the primary dosimeter, which is a calorimeter that includes a graphite probe placed in a thermally insulating box made of expanded polystyrene.

For a gamma irradiation plant, routine dosimeters such as ceric-cerous sulphate solution, radiochromic, PMMA and Fricke dosimeters are among the common dosimeters used by the industry.

Absorbed dose in sample: The measurement of the absorbed dose by the product is important to ensure that a dose sufficient for the intended purpose has been given. This is to avoid overexposure to radiation, which can cause damage to the products, or underexposure, which can mean that the dose absorbed by the product is not sufficient to fulfil the intended purpose.

The absorbed dose measured by the dosimeter will effectively represent the dose absorbed by the sample only when the following conditions are met: (i) the dosimeter and the sample are homogeneous; (ii) both have the same size, density and atomic composition; and (iii) both are irradiated under the same conditions. A simple and widely used method to achieve these conditions is to use equal volumes of dilute solutions of the sample and the dosimeter, and to irradiate them in turn using the same container at the same position in the radiation field. Therefore, experimental conditions must be suitably controlled for accurate measurement of the absorbed dose, D, in the sample. However, often these conditions cannot be met and in such cases a calculation must be carried out to obtain the absorbed dose in the sample. For electromagnetic radiation such as ^{60}Co γ rays, the absorbed dose in the dosimeter (D_D) and in the sample material (D_M) are related as shown in Eq. (3.4).

$$D_M = D_D \times (\mu/\rho)_D (\mu/\rho)_M \tag{3.4}$$

where $(\mu/\rho)_D$ and $(\mu/\rho)_M$ represent the mass energy absorption coefficients of the dosimeter and of the material sample, respectively.

3.4.5. Comparative aspects of radiation chemistry of solids and liquids

Solids: The nature of the changes produced in a solid depends upon the type of material being irradiated, and for this purpose, solids can be divided into metals, ionic crystals and organic compounds. All types of ionizing radiation produce ionized and excited atoms in the solids. In addition, the irradiation of solids with heavy particles (protons, deuterons, α particles) can result in the dislodging of an appreciable number of atoms from their normal lattice positions [3.4]. Gamma rays and X rays can also cause atomic displacements if their energies are sufficiently high. The irradiation of metals using ionizing radiation does not generally lead to any permanent effect as the positive holes created by the ionization are rapidly refilled by recombining with other electrons available from the common pool. However, the displacement of atoms can cause some changes in physical properties such as the electrical resistance of the material. Irradiation of ionic crystals such as alkali halides results in the development of absorption bands in the UV and visible regions. These bands are called F bands and the defects responsible for these bands are called F centres. The coloured F bands are generally easily bleached when exposed to light or heat. Besides this, covalent bonds present in the solid may also be broken, resulting in chemical changes, e.g. nitrates may decompose to yield nitrites and oxygen. Organic compounds, whether of low molecular weight, or of high molecular weight, as polymers are, can also undergo radiolysis when exposed to ionizing radiation. Monomers such

as trioxane can be polymerized in the solid state to yield polymeric materials. On the other hand, long chain polymeric materials can undergo cross-linking and chain scission reactions when exposed to ionizing radiation (see Section 4.5). In addition, trapped free radicals in the irradiated solid substrates have also been reported [3.25].

Liquids: Although the initial effect of ionizing radiation on liquids is the same with regard to ionization and excitation, the nature of the final products depends upon the properties of the liquid, such as viscosity and dielectric constant. For example, the irradiation of water mainly leads to the formation of radical species, $HO^{\bullet}$ and $H^{\bullet}$, and hydrated electrons (as well as some molecular products such as H_2 and H_2O_2), while benzene mainly gives singlet and triplet excited states and a small yield of polymeric material on irradiation [3.26, 3.27]

3.4.6. Radiation-chemical reactions in aqueous solutions

3.4.6.1. Generation of the primary species

Understanding the radiation chemistry of water is important, particularly in the context of the radiation processing of carbohydrates, since they can be irradiated in aqueous solution, suspensions or pastes, and even solid state irradiation may involve the presence of absorbed moisture. The sequence of processes occurring can be divided into three stages:

— The physical stage, consisting of energy transfer from radiation (photons and particles) to the atomic or electronic system of molecules. Its duration is of the order of 10^{-15} s.
— The physicochemical stage, consisting of processes leading to the establishment of thermal equilibrium to form chemical species in the spur. The time frame is typically 10^{-11} s.
— The chemical stage, consisting of the diffusion of the chemical species from the spur and their reaction with surrounding reactants.

The whole process can be summarized as: electron ejection → further ionization → thermalization → solvation by orientated water molecules, as described in detail below.

The passage of high energy ionizing radiation through water or dilute aqueous solutions initially gives electrons, positively charged water ions and excited water molecules [3.28]:

$$H_2O \rightarrow e^-, H_2O^*, H_2O^{\bullet +}$$

The ejected electron loses energy via further ionization and excitation events and finally becomes thermalized and solvated [3.29].

$$e^- + n\ H_2O \rightarrow e_{aq}^-$$

The positive radical ions, $H_2O^{\bullet +}$, are thought to be energetically very unstable and to decompose in 10^{-13} seconds, giving H^+ ions and $HO^\bullet$ radicals [3.28].

$$H_2O^{\bullet +} \rightarrow H^+ + HO^\bullet$$
$$H_2O^{\bullet +} + H_2O \rightarrow H_3O^+ + HO^\bullet$$

H_2O^* represents an excited water molecule which may ionize, dissociate or simply return to the ground state [3.29].

$$H_2O^* \rightarrow H^+ + HO^\bullet$$
or
$$H_2O^* \rightarrow e^- + H_2O^{\bullet +}$$

The primary species either react with one another within the spur or diffuse into the bulk of the solution [3.30].

Further H atoms are produced through the reaction of the solvated electron with protons [3.25].

$$e_{aq}^- + H^+ \rightarrow H^\bullet$$
$$(k = 2.2 \times 10^{10}\ mol^{-1} \cdot dm^3 \cdot s^{-1})$$

The molecular products H_2 and H_2O_2 are formed through the reactions [3.31]:

$$H^\bullet + H^\bullet \rightarrow H_2$$
$$(k = 7.8 \times 10^9\ mol^{-1} \cdot dm^3 \cdot s^{-1})$$
$$e_{aq}^- + e_{aq}^- \rightarrow H_2 + 2OH^-$$
$$(k = 5 \times 10^9\ mol^{-1} \cdot dm^3 \cdot s^{-1})$$
$$HO^\bullet + HO^\bullet = H_2O_2$$
$$(k = 5.5 \times 10^9\ mol^{-1} \cdot dm^3 \cdot s^{-1})$$

A considerable fraction of radicals formed in the spur are reconverted to water [3.30, 3.32]:

$$H^\bullet + HO^\bullet = H_2O$$
$$(k = 2 \times 10^{10}\ mol^{-1} \cdot dm^3 \cdot s^{-1})$$
$$H_3O^+ + OH^- \rightarrow 2H_2O$$

($k = 1.4 \times 10^{10}$ mol^{-1}·dm^3·s^{-1})

$e_{aq}^- + HO^\bullet \rightarrow OH^-$

($k = 3 \times 10^{10}$ mol^{-1}·dm^3·s^{-1})

In summary, hydrated electrons, hydrogen atoms and hydroxyl radicals are formed in the spurs very close to one another, and some of them are able to react with other species to regenerate water or the molecular products H_2 as well as H_2O_2, while the remainder escape into the bulk solution. This spur expansion is completed in about 10^{-7} s. Thus, in the nanosecond timescale, the different processes ultimately produce hydrated electrons (e_{aq}^-), $HO^\bullet$, $H^\bullet$ and the molecular products H_2 and H_2O_2. These species are also known as primary species, though this is not intended to mean that they are the first entities to be formed, as shown below.

$H_2O \rightarrow e_{aq}^-, HO^\bullet, H^\bullet, H_2O_2, H_2, H^+, OH^-\ldots$

For low linear energy transfer radiation such as γ rays from ^{60}Co and fast electrons (compared to swift heavy ions undergoing high linear energy transfer), in the pH range of 3–11, the following *G* values of the primary species (in mol/J) are generally accepted [3.33].

$G(e_{aq}^-) = G(HO^\bullet) = 0.28$ μmol J^{-1}

$G(H^\bullet) = 0.6\ G(H_2) = 0.047$ μmol J^{-1}

$G(H_2O_2) = 0.0725$ μmol J^{-1}

The hydrated electrons and hydrogen atoms are powerful reducing agents, while the hydroxyl radical is a powerful oxidizing agent. These species subsequently react with solutes present in the system at low concentrations. Their main properties are outlined in Section 3.4.6.2.

3.4.6.2. Properties of the primary species

(a) The hydrated electron

The hydrated electron may be represented as an electron surrounded by a small number of orientated water molecules and behaving in many ways like a single charge anion of about the same size as the iodide ion. It is a powerful reducing agent and its reaction is an electron transfer process represented by:

$e_{aq}^- + S^{n+} \rightarrow S^{(n-1)+}$

where n is the charge on the solute, the rate constant for this reaction range from 16 $dm^3 \cdot mol^{-1} \cdot s^{-1}$ (reaction with water) up to the diffusion controlled limit, but the activation energy is invariably small ((6−30) $kJ \cdot mol^{-1} \cdot K^{-1}$). This suggests that the magnitude of the rate constant is governed by the entropy of the activation, and the controlling factor here appears to be a suitable vacant orbital in the acceptor molecule. Thus, molecules with no vacant low lying orbitals, such as water, simple alcohol, amine or ether molecules, react slowly [3.29].

The absorption spectrum of e_{aq}^- has a maximum at approx. 715 nm. Some important features of hydrated electrons are listed in Table 3.2.

TABLE 3.2. PROPERTIES OF THE HYDRATED ELECTRON

Property	Value	Reference
G value (1/100 eV)	2.7 (at time $\leq 10^{-7}$ s)	[3.32]
Radius of charge distribution	(0.21–3) nm	[3.33]
Redox potential	2.9 V	[3.27]
Half-life	2.1×10^{-4} s (in neutral water) 7.8×10^{-4} s (in basic solution)	[3.25] [3.25]
Diffusion constant	4.96×10^{-5} cm^2 s^{-1}	[3.33]
Absorption maximium	715 nm	[3.33]
ε at 715 nm	1.85×10^4 $mol \cdot dm^{-3} \cdot s^{-1}$	[3.33]

The intense absorption band in the visible region of the spectrum makes the reactions of e_{aq}^- very easy to follow using pulse radiolysis combined with kinetic spectroscopy, i.e. an optical detection system [3.34].

(b) Hydrogen atoms

Hydrogen atoms are the minor reducing radicals in neutral and alkaline solutions, whereas more are formed in acidic solutions through the reaction:

$$e_{aq}^- + H_3O^+ \rightarrow H^\bullet + H_2O$$

$H^{\bullet}$ does not absorb in the accessible wavelength range. Nevertheless, many of its rate constants have been measured using competition kinetics [3.35].

The hydrogen atom generally reacts with organic compounds by abstracting H from saturated molecules and adding to the centres of unsaturation. In strongly basic solutions (pH > 10), the H atom may react with OH^- through the reaction:

$$H^{\bullet} + OH^- \leftrightarrow e_{aq}^- + H_2O$$

The standard electrode potential of the hydrogen atom, $E°$, is given to be −2.3 V [3.25]. Hydrogen atoms are less powerful reducing agents than are hydrated electrons [3.27].

(c) Hydroxyl radical

Hydroxyl radicals, $HO^{\bullet}$, have a standard reduction potential of +2.8 V in acidic solution and are therefore a strong oxidant. In addition to radiolysis of water, $HO^{\bullet}$ radicals can be produced by the photodissociation of H_2O.

The $HO^{\bullet}$ radical absorbs weakly in the UV region. Its absorption coefficient, $\varepsilon = 370 \times \text{mol}^{-1} \cdot \text{dm}^3 \cdot \text{cm}^{-1}$ at 260 nm, is very small. For this reason, rate constants for its reaction are obtained using competition methods or by observing the formation of the products [3.36].

Hydroxyl radicals readily oxidize inorganic ions; the reaction is usually represented as an electron transfer process:

$$HO^{\bullet} + S^n \rightarrow S^{n+1} + OH^-$$

The $HO^{\bullet}$ radical is electrophile when reacted with organic molecules and, like the hydrogen atom, abstracts H from saturated molecules and is able to add to unsaturations. However, the hydroxyl radical is less selective and more reactive than the hydrogen atom in abstraction reactions, as can be seen in Table 3.3.

To study the action of hydroxyl radicals, solutions may be saturated with nitrous oxide, when radiolytically produced e_{aq}^- are converted to $HO^{\bullet}$ radicals that represent almost 90% of the free radical pool [3.27].

$$e_{aq}^- + N_2O \rightarrow HO^{\bullet} + OH^- + N_2$$

TABLE 3.3. RATE CONSTANT FOR SELECTED REACTION OF $HO^{\bullet}$ RADICAL AND $H^{\bullet}$ ATOM

Solute	Reaction type	$\times 10^{-7}$ dm^3·mol^{-1}·s^{-1}	
		$HO^{\bullet}$	$H^{\bullet}$
$CH{=}CHCONH_2$	Addition	450	1800
C_6H_6	Addition	530	53
$C_6H_5NO_2$	Addition	340	170
C_2H_5OH	Abstraction	180	1.7
CH_3OH	Abstraction	84	0.16

The logarithmic acid dissociation constant, pK_a, of the $HO^{\bullet}$ radical has been measured as 11.9 ± 0.2 [3.31]. The significance of this reaction is that in alkaline solution, hydroxyl radicals are converted into $O^{-\bullet}$, which does not readily add to olefinic or aromatic groups, although it abstracts hydrogen atoms at a rate comparable to that of the hydroxyl radical.

$$HO^{\bullet} \leftrightarrow O^{-\bullet} + H^{+}$$

(d) The perhydroxyl radical and its anion

The perhydroxyl radical is not a significant primary radical under low linear energy transfer irradiation. It is an important secondary species in oxygenated solutions [3.37] as a result of the reaction of oxygen which is an efficient scavenger for e_{aq}^{-} and $H^{\bullet}$ atoms, according to:

$$e_{aq}^{-} + O_2 \rightarrow O_2^{-\bullet}$$
$$H^{\bullet} + O_2 \rightarrow HO_2^{\bullet}$$

The two reactions have approximately equal rate constants ($k \approx 1.9 \times 10^{10}$·mol^{-1}·dm^3·s^{-1} [3.30]).

$HO_2^{\bullet}$ is formed in acidic solutions, whereas in neutral solutions, the $O_2^{-\bullet}$ form is found as shown:

$$HO_2^{\bullet} \leftrightarrow O_2^{-\bullet} + H^{+}$$

The pK_a of $HO_2^{\bullet}$ is 4.9. Both forms can act as mild oxidants and are reductant, although $HO_2^{\bullet}$ tends to be the stronger oxidant and $O_2^{\bullet -}$ the stronger reductant (E° = 0.56 V and 0.3 V for $O_2^{\bullet -}$ and $HO_2^{\bullet}$, respectively).

The perhydroxyl radical is unreactive with most organic compounds unless the latter contain weakly bonded hydrogen, e.g:

$$HO_2^{\bullet} + RSH \rightarrow H_2O_2 + RS$$

The reaction of certain metal ions with H_2O_2 also produces $HO_2^{\bullet}$:

$$H_2O_2 + Ce^{4+} \rightarrow Ce^{3+} + HO_2^{\bullet} + H^+$$

In the absence of other reactions, perhydroxyl radicals react together forming H_2O_2.

$$HO_2^{\bullet} + HO_2^{\bullet} \rightarrow H_2O_2 + O_2 \qquad \text{(rate constant } k_{aa})$$
$$HO_2^{\bullet} + O_2^{\bullet -} + H^+ \rightarrow H_2O_2 + O_2 \qquad \text{(rate constant } k_{ab})$$
$$O_2^{\bullet -} + O_2^{\bullet -} + 2\,H^+ \rightarrow H_2O_2 + O_2 \qquad \text{(rate constant } k_{bb})$$

where $k_{aa} = 8.6 \times 10^5 \cdot mol^{-1} \cdot dm^3 \cdot s^{-1}$, $k_{ab} = 1.0 \times 10^8\ mol^{-1} \cdot dm^3 \cdot s^{-1}$, and $k_{bb} \leq 0.35\ mol^{-1} \cdot dm^3 \cdot s^{-1}$ [3.30, 3.38].

3.4.7. The radiation chemistry of simple organic compounds

When an organic molecule A–B is exposed to high energy ionizing radiation, two processes occur simultaneously, namely: (1) ionization of the molecule by expulsion of a low energy electron from the bonding orbital, resulting in the formation of ions AB^+ and e^- and (2) excitation of the molecule, which brings the A–B bond to a high energy state AB^*. These primary species undergo several secondary processes such as recombination and molecular, dissociation. At the same time, the excited state $A–B^*$ can either relax by energy emission or undergo homolysis leading to the formation of a pair of free radicals (Fig. 3.10). The exact nature of the reaction depends on the nature of the bond, the rigidity of the matrix and on irradiation conditions, such as dose rate, the temperature of irradiation and the presence of dissolved gases or other impurities.

The former homolytic process may induce chain reactions that can turn into a chemical amplification of the primary effect. Most of the chemical processes caused by ionizing radiations are interpreted in terms of free radical mechanisms [3.39].

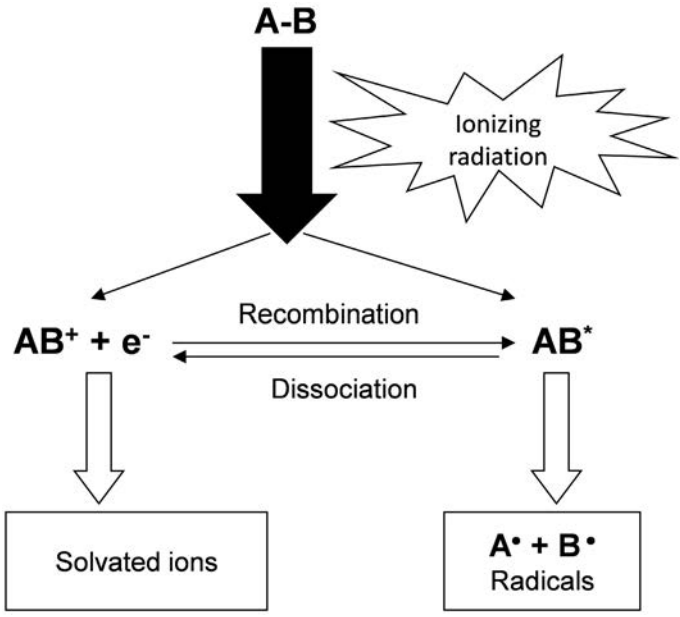

FIG. 3.10. Scheme of radiation effects on organic materials.

3.5. RADIATION EFFECTS ON POLYMERS

The use of radiation in the processing of synthetic polymers for cross-linking purposes is one of the most successful applications of radiation technology after sterilization. In this case, radiation technology is considered the most efficient technique, is cost effective compared to the conventional techniques and has high productivity, while maintaining if not exceeding quality standards. For natural polymers such as polysaccharides, radiation is used mainly to degrade the large molecules into smaller sizes, in terms of oligomers at room temperature, and is easy to control. However, with a certain arrangement and under specific conditions, radiation has been shown to cross-link polysaccharides. Therefore, such techniques have been used for producing commercial products (see Chapter 4).

3.5.1. Irradiation of polymers in the solid state

When a polymer in a solid state is subjected to ionizing radiation, the initial physical processes are the same as those occurring with simple organic molecules, i.e. ionization and excitation of the polymer molecules, which occur owing to the direct effect of radiation. Depending on the ultimate use, the range of absorbed

dose that is applied to materials covers several orders of magnitude [3.40]. However, at low doses, polymers are generally not significantly degraded, in contrast with bacteria and viruses, which can be killed. This difference makes it possible to widely apply radiation induced sterilization processes to medical supplies, which are often made of and packaged in polymers. Chain reactions, essentially polymerizations, can be achieved with medium doses, as a result of the chemical amplification by purely thermal processes of radiation induced initiation. Processes involving single steps or short kinetic chain length reactions require much higher doses. This is generally the case for the radiation cross-linking of rubbers and thermoplastics.

When polymers are submitted to high energy radiation, contrasting behaviours are observed, with a dominant effect of cross-linking or of chain scission (Fig. 3.11), depending on the nature of the repetition units. The general trends of the competition between cross-link formation (x) and chain scission (s) can be discussed for some common polymers on the basis of the values of G(s) and G(x) listed in Table 3.4.

The formation of gaseous products such as H_2, CH_4 and CO generally takes place with two dominant reactions affecting the polymer chains, namely scission and cross-linking. When irradiation is carried out in the presence of air or oxygen, oxidation is an additional reaction that may interfere with the radiation induced free radical processes. Polyethylene (PE) and poly(vinyl chloride) form networks, whereas poly(methyl methacrylate) (PMMA) degrades strongly with the evolution of low molecular weight fragments. EB lithography utilizes this degradative property to engrave nanometric lines in PMMA films for electronic applications. Copolymers including repeating units with intrinsically opposite behaviour can be synthesized with appropriate compositions to control the

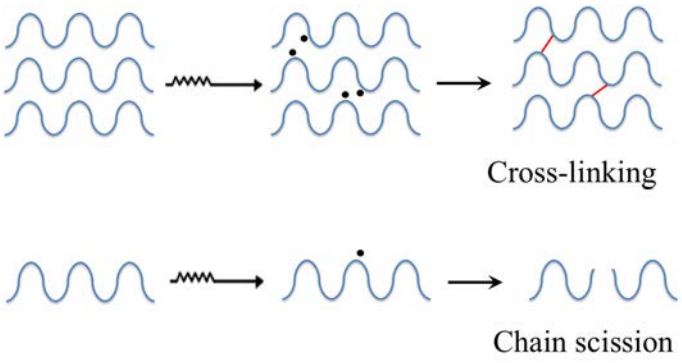

FIG. 3.11. Schematic representation of competing radiation induced polymer scission and cross-linking.

TABLE 3.4. RADIOLYTIC YIELD VALUES OF CROSS-LINKING *G*(x) AND OF SCISSION *G*(s) FOR SOME COMMON POLYMERS

Polymer[a]	Physical state	Chemical structure	*G*(x)[b]	*G*(s)[b]
Polyethylene[c]	Semi-crystalline	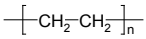	0.3	0.09
Polypropylene[c]	Semi-crystalline	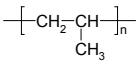	0.25	0.11
Polybutadiene	Elastomer	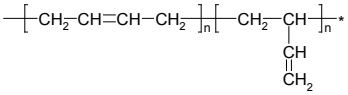	0.38	—
Poly(methyl acrylate)	Amorphous	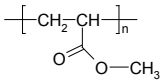	0.055	0.018
Poly(n-butyl acrylate)	Amorphous	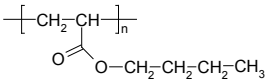	0.063	0.018
Poly(t-butyl acrylate)	Amorphous	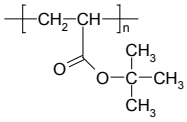	0.016	0.018
Poly(methyl methacrylate)	Glassy	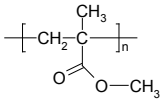	—	0.12–0.35
Poly(vinyl chloride)[d]	Essentially glassy	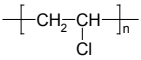	0.033	0.023
Polystyrene	Glassy	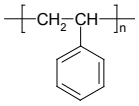	0.005	<0.002
Poly(ethylene terephtalate)	Semi-crystalline	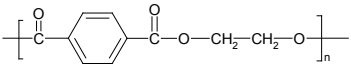	0.003–0.02	0.007–0.02

[a] Ionization at 25°C in the absence of oxygen.
[b] In µmol/J, data from Ref. [3.41].
[c] Dependent on microstructure and of crystallinity.
[d] Unplasticized.

overall behaviour [3.42]. The presence of tertiary or quaternary carbon atoms in the main chain has a determining influence on behaviour under irradiation, though the reactivity of side chains can compensate or even overcome the behaviour assigned to the main chain. Polymers including aromatic moieties as side groups (polystyrene) or in the main chain poly(ethylene terephthalate) give a strongly attenuated response to high energy radiation. It must be added — to avoid oversimplification — that morphological and ambience parameters (microstructure, crystallinity, glassy or rubbery state, degree of plasticization and presence of oxygen) may strongly affect the results.

3.5.1.1. Cross-linking

Cross-linking is the largest commercial application for which the radiation processing of plastic materials is used. Polymers with interbridged chains can withstand higher service temperatures without flowing and/or while retaining their functional properties. Generally, the materials exhibit better mechanical and chemical resistance after cross-linking. Processing is performed at high speed under the EB without requiring heating to high temperature or the use of cross-linkers necessary in the conventional chemical method.

Many types of plastic based products containing elastomers are processed by radiation cross-linking to improve their performance in insulated electric wires and cables, multilayered films for cooking pouches, shape memory tubes, pressure resistant water pipes, expandable foams, automotive parts exposed to motor heat, etc. Unsaturated additives are sometimes used to promote radiation cross-linking, in order to improve productivity or to favourably influence the inherent trend to competing cross-linking and scissioning.

Irradiation can be usefully exploited for stabilizing polymer blends, avoiding physical phase separation of the components or making it possible to block an unstable morphology of practical interest by sudden cross-linking. Various other applications take advantage of the shape memory effect that results from the radiation cross-linking of semi-crystalline thermoplastic polymers and blends. As an example, resettable fuses for electrical engineering, heat-shrinkable tubings and multilayered complexes for food packaging are produced on an industrial scale.

3.5.1.2. Degradation and post-irradiation oxidation

Other important industrial applications are based on the various chemical effects induced by radiation and resulting in scissioning, branching and partial oxidation. If those effects are well-controlled, the cumulated degradation effects can improve the processability or the compatibility of the plastic in blends

with other materials. A representative example is the treatment of fluorinated polymers that facilitates their melt processing. Radiation oxidized polypropylene is also used for elaborating fibre reinforced composite materials with enhanced performance. However, for many other applications, the very efficient reaction of generated macroradicals with dissolved and gradually diffusing oxygen forms peroxy derivatives that will induce the long term degradation of polymer properties. Chain reactions induced by the thermal or photochemical decomposition of peroxy compounds may result in the ruin of the structural and functional properties of the materials. Irradiated polymers therefore usually include antioxidants in order to minimize the detrimental effect of radio-oxidation. The risk of degradation on ageing is a limitation to the development of radiation sterilizable materials for biomedical devices. Some nanolithographic processes take advantage of the surface oxidation induced by X rays or EB for enhancing resolution.

3.5.1.3. Changes in physical properties

Irradiation of polymeric material may alter the physical properties of polymers either reversibly or irreversibly. The reversible changes generally occur at low doses while irreversible changes are typically associated with high doses. The irradiation of polymers generally increases their electric conductivity owing to the formation of mobile charge carriers (electrons, holes or ions) and is termed radiation conductivity. It generally consists of two components: (1) pulse conductivity induced by the high transient dose rates of pulse irradiation, and (2) stationary conductivity induced by a lower sustained dose rate in continuous irradiation. Once the radiation source is removed, radiation induced conductivity decays over a period that varies from a few minutes to hours, depending upon the nature of the polymer. The electric properties of a polymer can also be altered as a consequence of the chemical changes produced by irradiation. For example, cross-linked PE retains its high specific resistance at high temperatures making it useful as an insulator. On the other hand, the conductivity of poly(vinyl chloride) is permanently increased by irradiation and the increase is proportional to the degree of de-chlorination.

The mechanical properties of polymers are significantly dependent on the molecular weight of the polymer. Cross-linking and chain scission reactions can significantly alter these properties. Cross-linking reactions are generally associated with an increase in elastic modulus, while an increase in creep rate is associated with chain scission reaction.

3.5.2. Radiation grafting on polymers

Grafting is when a monomer is polymerized onto the backbone of a preformed polymer that has a different monomer unit. Either chemical reagents or high energy irradiation is used to activate the polymer chains. Branching, and even cross-linking, occurs when functional monomers grow on activated macroradicals. The growth of functional monomers on activated macroradicals leads to branching and possibly to cross-linking (Fig. 3.12).

Radiation grafting can be performed by a number of methods. In simultaneous grafting, the polymer backbone (in the form of a solid material or dissolved chains) is irradiated in the presence of a monomer, usually in a deoxygenated solution of the latter (Fig. 3.13). This is the easiest, one step approach to radiation grafting. The main drawback is the parallel formation of homopolymer. This leads to monomer losses and to the necessity of removing the homopolymer after synthesis. Homopolymer formation can be reduced by applying suitable additives, for instance Fe(II) salts, when grafting is performed in aqueous solution.

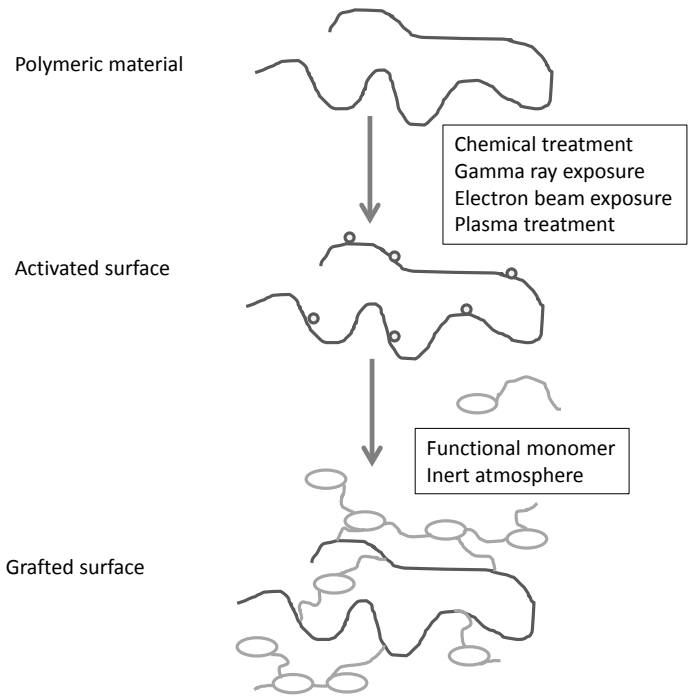

FIG. 3.12. Grafting of a monomer on preformed polymeric backbone leading to infinite branching and cross-linking.

The idea of pre-irradiation grafting is based on irradiation of the polymeric backbone alone in order to generate labile reaction centres, which can be subsequently used to trigger grafting when, after irradiation, the backbone is contacted with the monomer. In principle, at least when dealing with a semi-crystalline polymer, one may use free radicals trapped in the crystalline regions as the labile reaction centres (Fig. 3.14) during irradiation in the absence of oxygen. More often, another option is used, based on irradiation of the polymeric backbone material in the presence of oxygen (Fig. 3.15).

This results in the formation of peroxides and hydroperoxides, which are relatively stable at room temperature. When such an activated polymer is contacted with a monomer at an elevated temperature, the labile O−O bonds in peroxides and hydroperoxides break, giving rise to radicals, which in turn initiate grafting as shown in Fig. 3.15. While pre-irradiation grafting is a more complex and time consuming two step process, it reduces the risk of homopolymer formation, and the two steps can be separated in time and space.

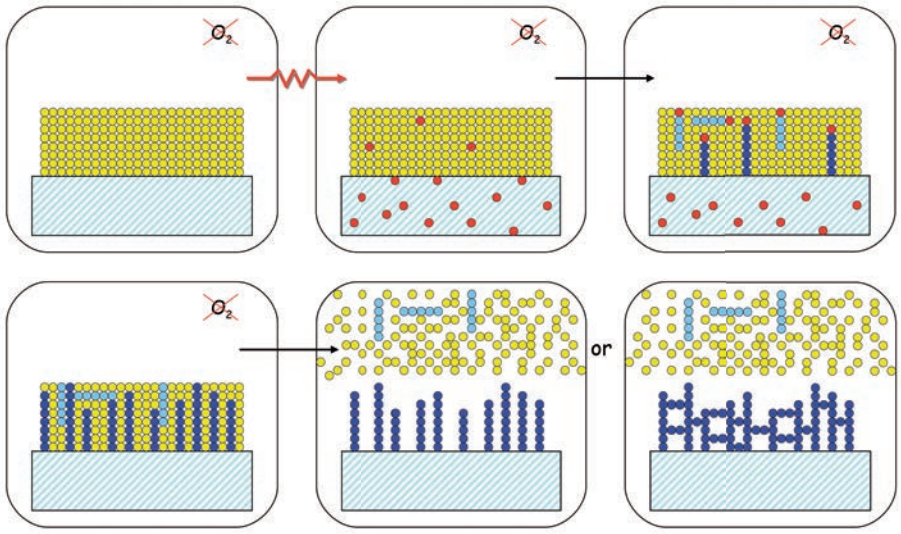

FIG. 3.13. A scheme of direct (simultaneous) radiation grafting. Red dots denote radicals, yellow dots — monomer molecules, blue dots — monomer molecules incorporated in the grafted chains, pale blue dots — monomer molecules incorporated in the homopolymer chains.

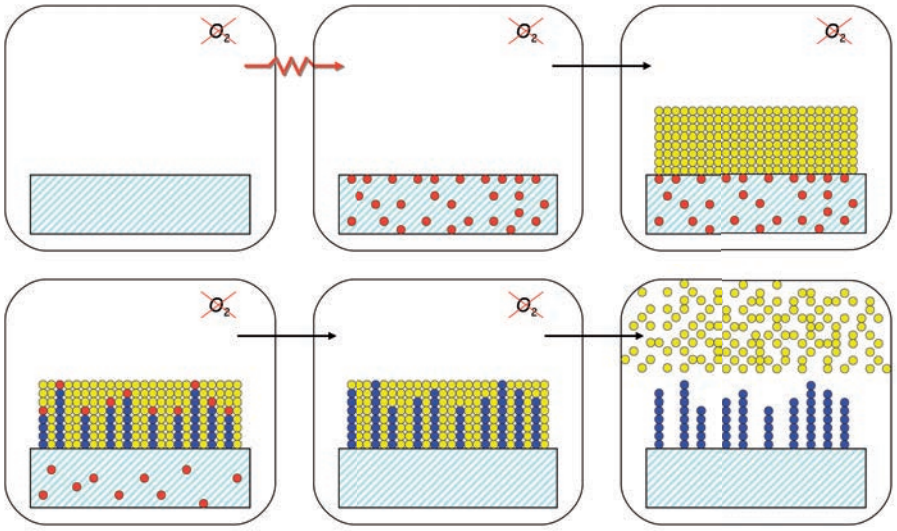

FIG. 3.14. A scheme of pre-irradiation grafting (irradiation in the absence of oxygen). Red dots denote radicals, yellow dots — monomer molecules, blue dots — monomer molecules incorporated in the grafted chains.

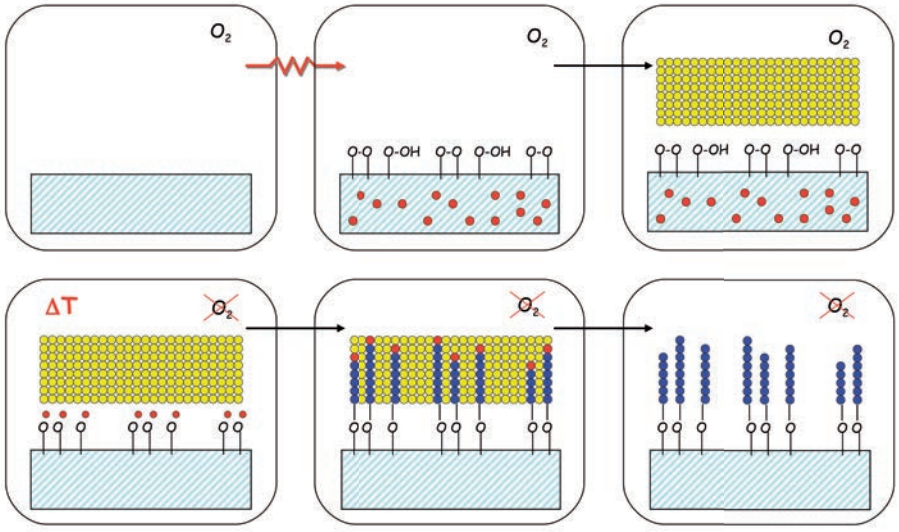

FIG. 3.15. A scheme of pre-irradiation grafting (irradiation in the presence of oxygen). Red dots denote radicals, yellow dots — monomer molecules, blue dots — monomer molecules incorporated in the grafted chains.

3.5.3. Irradiation of polymers in solution

An important aspect of the radiation treatment of polymers is irradiation in solution, where indirect effects, caused by the absorption of ionizing radiation energy by solvent molecules, dominate over direct action on macromolecules. Since in the case of polysaccharides the solvent is usually water (pure or containing low-molecular-weight additives), this subsection will focus on the irradiation of polymers in aqueous solution.

When dilute aqueous solutions of polymers are subjected to ionizing radiation, most of the energy is absorbed by water. Hydroxyl radicals, hydrogen atoms and solvated electrons are formed as the initial reactive intermediates (see Section 3.4.6.). These very active species may in turn attack the macromolecules, leading to the formation of reactive sites on the polymer chains. If the polymer does not possess any groups capable of a fast reaction with the solvated electrons, or if such a reaction is not desirable, it is common to saturate the solution with nitrous oxide that scavenges electrons and that converts them into additional hydroxyl radicals. A typical reaction of the latter species with macromolecules, unless the repeating unit contains one or more aromatic rings and/or double carbon–carbon bonds, is the abstraction of a hydrogen atom. As a result of this process, a radical is formed on the polymer chain. H atoms formed by the radiolysis of water react with polymers in a similar way to OH radicals; however, this reaction is usually less important because a much lower number of H atoms are formed (approximately 10% of the $HO^{\bullet}$ yield in the N_2O saturated solutions) and the rate constants of their attack on polymer chains are lower.

In an oxygen-free system, the fate of polymer radicals depends to some extent on the chemical structure of the polymer, but a general scheme of the possible reactions can be drawn, as shown in Fig. 3.16.

Transformations of polymer radicals (reactions 2–7 in Fig. 3.16) can be divided into reactions involving one radical (2–3) and reactions involving two radicals. The former group includes chain scission (degradation) (2) and radical transfer (H atom transfer), which may occur between two separate chains or within the same chain. Reactions involving two radicals are recombination (cross-linking, 4–5) and disproportionation (6–7). Each of them may occur either between two radicals localized on two separate chains or along the same chain. From the practical point of view, the most important processes are degradation and intermolecular cross-linking, which lead to a decrease in molecular weight or an increase in molecular weight, the formation of branched structures and, under suitable conditions, to the formation of three dimensional cross-linked structures, e.g. gels. Intramolecular cross-linking may be of importance for synthesizing nanogels and microgels.

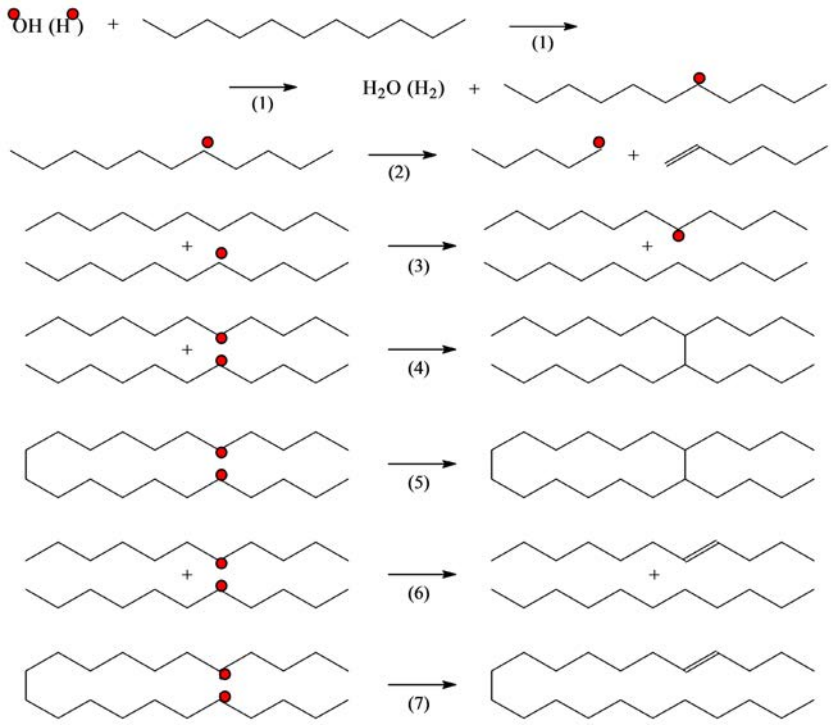

FIG. 3.16. Formation and typical reactions of carbon centred, mid-chain polymer radicals generated by the irradiation of a polymer in aqueous solution.

In polymer solutions that contain oxygen, the initially generated carbon centred macroradicals react with oxygen to form the corresponding peroxyl radicals. This is a fast, practically diffusion controlled reaction with a rate constant of the order of 10^9 $dm^3 \cdot mol^{-1} \cdot s^{-1}$ (cf. Ref. [3.43]). The chemistry of peroxyl radicals is often complex (for a review, see Ref. [3.44]). The following facts seem to be important in the current context. Neither peroxyl nor oxyl radicals can form stable bonds (cross-links) upon recombination (recombination of oxyl radicals is expected to proceed with low yields only, and the formed peroxide bond cannot be considered a stable cross-link). Peroxyl radicals may initiate chain reactions owing to their ability to abstract hydrogen atoms from:

— A neighbouring carbon atom along the chain;
— Another chain segment (as shown in Fig. 3.17);
— Another chain.

In this way, a carbon centred radical is regenerated, which, upon reaction with oxygen, re-creates a peroxyl radical, leaving behind a hydroperoxide (Fig. 3.17). Since a peroxyl radical is re-formed, the kinetic chain may go on, and in fact, it is often found that oxygen consumption and/or yield of peroxides and hydroperoxides by far exceeds the initial radical yield [3.43, 3.45].

If located in a favourable structural position, the peroxyl radical may also undergo a transformation where the $HO_2^{\bullet}/O_2^{-\bullet}$ radical is eliminated (for details, see Section 4.3) [3.30, 3.46]. In this way, the number of radicals on the polymer chain may decrease.

However, the main reaction by which peroxyl radicals at aliphatic polymer chains in solution are believed to decay is their mutual reversible recombination to form an unstable tetroxide, which decomposes mainly by forming unstable oxyl radicals [3.47, 3.48]. The latter are prone to rearrange on chain breakage, leaving behind a terminal alkyl radical. Such a radical reacts with oxygen, and, if it happens to abstract an H atom from a mid-chain position, the kinetic chain may propagate with further oxidation and/or chain breakage (Fig. 3.18) [3.49]. Such chain processes have been observed for a number of synthetic hydrophilic polymers, for instance, poly(ethylene oxide) [3.45] and poly(acrylic acid) [3.43]. In the latter case, the yield of chain scission was as high as 14×10^{-7} mol/J, i.e. much higher than the initial yield of peroxyl radicals. The hypothesis that

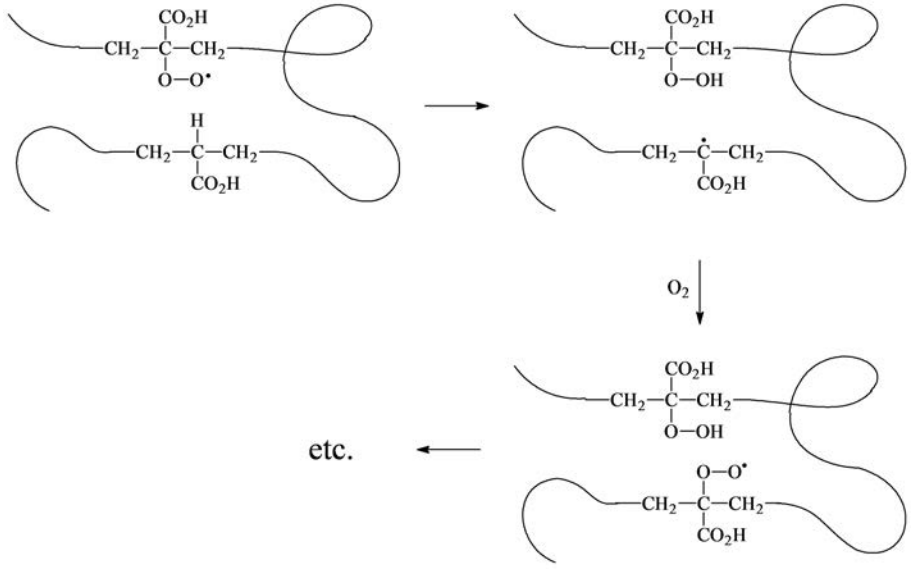

FIG. 3.17. Diagram of chain oxidation reaction in a polymer irradiated in the presence of oxygen (poly(acrylic acid) in this example).

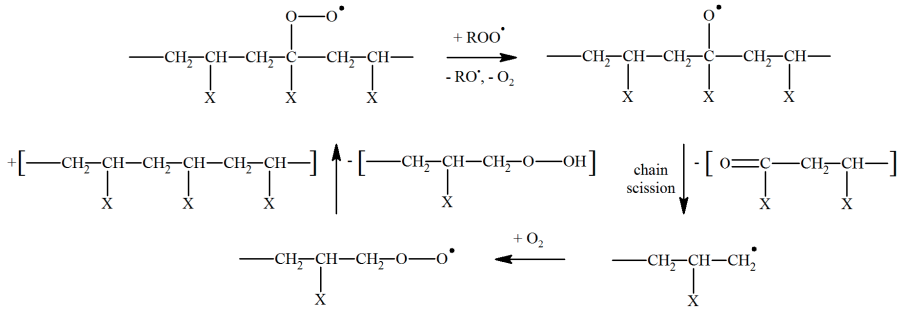

FIG. 3.18. Schematic representation of chain reaction leading to degradation (chain scission) in polymers irradiated in the presence of oxygen.

the mutual recombination of peroxyl radicals forms the transient tetroxide is supported by kinetic data, in which the decay of peroxyl radicals has often been found to be kinetically of second order with respect to the free radical concentration (e.g. Ref. [3.50]).

3.6. EVALUATION OF RADIATION INDUCED EFFECTS IN POLYMERS

The effects induced by radiation in macromolecular systems can be investigated and quantified by a number of techniques (see Chapter 6), bringing valuable information at different dimension scales (at the functional group, monomer unit and macromolecule level).

The preferred approach consists of monitoring the changes occurring during continuous or pulsed irradiation with time resolved spectroscopic, conductometric or light scattering methods. Post-irradiation measurements of chemical and structural modifications allow the assessment of most of the major transformations induced by radiation by more conventional and readily available methods.

3.6.1. Experimental methods for studying radiation induced reactions

The radiation induced transformations of the highest importance in polymer processing, i.e. degradation and intermolecular cross-linking, manifest themselves as changes in molecular weight distributions and average molecular weights. A number of methods can be used to follow and quantify these changes. The most significant ones are mentioned below.

Probably the simplest method is based on viscometry. It may be time consuming, but it is a robust method that is relatively insensitive to minor

amounts of impurities, aggregates and microgels formed in the system, and measurements do not require sophisticated, expensive equipment. Using a simple Ubbelohde viscometer in a temperature controlled bath and measuring the flow time of the solvent and several dilutions of the polymer solution obtains the value of intrinsic viscosity, which, using the Mark–Houwink equation, can be recalculated into the viscosity-average molecular weight [3.51]. A disadvantage is that viscosity measurements must be made at precisely the same conditions for which the Mark–Houwink constants are known. Moreover, the result indicates only whether degradation or cross-linking prevails, while no information is provided on the change in molecular weight distribution. In addition, the value determined as the viscosity-average molecular weight corresponds neither to the absolute number-average nor to the weight-average molecular weight, both of which are necessary for calculating the radiation-chemical yields of degradation and cross-linking.

Static light scattering allows the determination of the weight-average molecular weight, and changes in the latter, caused by irradiation of the studied polymer [3.52, 3.53]. Being an absolute method, it does not require any calibration. The intensity of light scattered by a polymer solution is measured as a function of polymer concentration and scattering angle. Readings obtained for pure solvent are subtracted from the results. The data are most often subsequently processed according to the Zimm method, yielding weight-average molecular weight. While it used to be a relatively time consuming method when performed using a goniometer-type apparatus, modern set-ups allow for simultaneous measurements at multiple angles, thus significantly shortening the measurement time. Disadvantages are a high cost of equipment, a complete or near complete lack of information about molecular weight distribution and a sensitivity to even minor amounts of large impurities (aggregates, microgels or dust). In addition, the refractive index increment (*dn/dc*) of the studied polymer should be known or needs to be determined accurately.

In a form of gel permeation chromatography (GPC), high performance liquid chromatography GPC, a polymer is fractionated on a porous column filling according to macromolecular size [3.54, 3.55]. As a result, a distribution of retention times is obtained. Re-calculation of this distribution to give the distribution of molecular weights can be accomplished in a number of ways, the choice of which may depend on the availability of standards of the studied polymer and/or on the availability of detectors. A single detector (usually a differential refractometer) can be used, and can yield precise results when standards of the studied polymers are available. At the other extreme, a combination of three detectors including a light scattering detector means that the method can be treated as absolute, and no standards are required. The equipment and columns are relatively expensive, but when all parameters are properly set, the

measurement is relatively fast. There may be problems if cross-linking dominates (leading to branched structures) while calibration is made based on linear chains — the accuracy at a high molecular weight range may be less than perfect, but this problem should not occur if three detectors are used. The big advantage is the result — a distribution of molecular weights, which is particularly useful for studying radiation induced reactions, especially in cases where degradation and cross-linking occur concomitantly. From the chromatographic trace, number- and weight-average molecular weights can be calculated and these can be applied for calculating the radiation-chemical yields of degradation and cross-linking.

Changes in molecular weights of polynucleotides (mainly DNA) and proteins can be assessed by gel electrophoresis [3.54, 3.56–3.60].

Molecular weight is not the only parameter of polymers affected by the action of ionizing radiation. Radiation induced reactions and physical processes can also alter the molecular size, chemical composition and physical structure (including crystallinity).

The size of macromolecules is related to the molecular weight, but strict correlation between these two parameters exists only for linear chains, e.g. when irradiation of linear chains causes only degradation. In other cases, especially involving inter- and/or intramolecular cross-linking, size, if this is of interest, should be determined independently. The choice of method depends on the parameter to be determined. The radius of gyration (R_g) of a macromolecule (nanogel, aggregate, etc.) can be determined by static light scattering (see above), using either a standalone apparatus or a light scattering detector coupled with GPC. The practical lower limit of R_g that can be determined by static light scattering is approximately 0.05 of the wavelength of the incident light. The hydrodynamic radius, R_h, can be measured by dynamic light scattering [3.60–3.64]. Using modern apparatus, measurements are technically easy and fast, although attention should be paid to the choice of algorithms used in the calculations.

Changes in the chemical composition of a polymer induced by irradiation can be assessed by spectroscopy (Fourier transform infrared spectroscopy (FTIR), UV-Vis, nuclear magnetic resonance (NMR)), elemental analysis or by specific tests for the presence and quantity of functional groups. At moderate doses, the extent of chemical changes when compared to the number of groups retaining their structure may be very small and difficult to follow, in particular by FTIR. The spectrum of available methods can be broadened and the precision for qualitative and quantitative detection of chemical changes can be increased by performing model studies on molecules that are low-molecular-weight analogues of the studied polymer, for instance, an analogue of a monomer unit or a few monomer units. The precise analysis of irradiation products for such models can

be performed by liquid or gas chromatography (usually after derivatization of products), coupled with mass spectrometry detection.

The crystallinity of polymer samples can usually be determined by differential scanning calorimetry [3.65–3.67]. Usually, data on the enthalpy of melting of a fully crystalline sample of the same polymer are necessary to quantify the degree of crystallinity.

Radiation induced reactions are usually very fast, especially in the liquid phase. While studying final products, e.g. by determining molecular weight after irradiation or by identifying and quantifying stable molecular products, can provide valuable information regarding the reaction mechanism, a precise description of this mechanism usually requires an insight into the structures of reactive intermediates and into the kinetics of radiation induced reactions. For solid state irradiation (and in exceptional cases, also in liquids), this can be accomplished by room temperature electron spin resonance measurements as a function of time after irradiation. Even more can be learned by either performing the irradiation at a low temperature (e.g. 77 K) and making electron spin resonance measurements while gradually raising the temperature of the irradiated sample, or by using spin traps [3.68–3.84].

Radiation induced reactions in polymer solutions can be studied by pulse radiolysis [3.85, 3.86]. A short pulse of fast electrons from an accelerator initiates the reactions, which are subsequently followed using fast detection methods. For most studies on polymer solutions, a nanosecond time resolution is sufficient; many reactions of interest take place in micro- or milliseconds. A typical method of detection is fast spectrophotometry. A beam of light passes through the cell in which the solution is pulse irradiated. Time resolved measurements of changes in absorbance after the pulse are recorded at various wavelengths. This allows the construction of absorption spectra of reactive intermediates and the following of their time evolution. A knowledge of the spectra and reaction kinetics of intermediates often allows the determination of the reaction mechanism (cf. Refs [3.82, 3.87, 3.88]). For studies on polymer solutions, two other detection systems can be applied in pulse radiolytic experiments. Polyelectrolytes, including charged polysaccharides, can be studied using conductometric detection [3.89–3.93]. Light scattering detection is used to selectively follow kinetics and yields of reactions involving changes in molecular weight (degradation, cross-linking) [3.43, 3.94–3.99].

3.6.2. Calculation of radiation-chemical yields of degradation and cross-linking

3.6.2.1. Radiation yields of degradation and of intermolecular cross-linking

When studying radiation effects in polymers in the solid state, in solution or in more complex systems, there is a need to quantify the efficiency of two main reactions, i.e. degradation (chain scission, not to be confused with depolymerization) and intermolecular cross-linking. In a single act of degradation (chain scission), a polymer chain is split into two shorter fragments. In a single act of intermolecular cross-linking, two independent polymer chains are linked together to form a larger macromolecule, the mass of which is the sum of the masses of the two parent chains.

The radiation-chemical yield of degradation, $G(\mathrm{s})$ (mol/J), is defined as:

$$G(\mathrm{s}) = \frac{n_{\mathrm{cb}}}{E} \tag{3.5}$$

where n_{cb} [mol] is the number of chain break events which took place in the polymer sample (irrespective of whether it is a dry polymer or a solution) upon absorption by the sample of energy E (J) of ionizing radiation.

Similarly, the radiation-chemical yield of intermolecular cross-linking, $G(\mathrm{x})$ (mol/J), is defined as:

$$G(\mathrm{x}) = \frac{n_{\mathrm{x}}}{E} \tag{3.6}$$

where n_{x} (mol) is the number of intermolecular cross-linking events that took place in the polymer sample (irrespective of whether it is a dry polymer or a solution) upon absorption by the sample of energy E (J) of ionizing radiation. The number of cross-linking events, n_{x}, can also be understood as the number of cross-links (cross-linking bonds) formed in the sample.

For simplicity, further in this section the term cross-linking will be solely used to refer to intermolecular cross-linking.

3.6.2.2. Solid polymers

In solid polymer samples, the general equations allowing the determination of $G(\mathrm{s})$ and $G(\mathrm{x})$ in polymers undergoing simultaneous degradation and cross-linking on the basis of changes in average molecular weight of the polymer are:

$$G(\mathrm{x}) - G(\mathrm{s}) = \frac{1}{D}\left(\frac{1}{\bar{M}_{\mathrm{n0}}} - \frac{1}{\bar{M}_{\mathrm{n}}}\right) \tag{3.7}$$

$$4G(\mathrm{x}) - G(\mathrm{s}) = \frac{2}{D}\left(\frac{1}{\bar{M}_{\mathrm{w0}}} - \frac{1}{\bar{M}_{\mathrm{w}}}\right) \tag{3.8}$$

where D (J/kg) denotes the dose of ionizing radiation absorbed by the sample, and $\bar{M}_{\mathrm{n0}}$ and $\bar{M}_{\mathrm{n}}$ (kg/mol) are number-average molecular weights before and after absorbing the dose, D, respectively, and $\bar{M}_{\mathrm{w0}}$ and $\bar{M}_{\mathrm{w}}$ (kg/mol) are the weight-average molecular weights before and after absorbing D, respectively. Equation (3.7) is valid for any initial molecular weight distribution of the polymer, while Eq. (3.8) is valid for the most probable distribution where $\bar{M}_{\mathrm{w0}} / \bar{M}_{\mathrm{n0}} = 2$.

Equations (3.7) and (3.8) can be simplified if, as is the case for most irradiated polysaccharides under typical conditions, it can be assumed that no cross-linking takes place or that its yield is negligible.

Assuming $G(\mathrm{x}) = 0$, the following is obtained:

$$G(\mathrm{s}) = \frac{1}{D}\left(\frac{1}{\bar{M}_{\mathrm{n}}} - \frac{1}{\bar{M}_{\mathrm{n0}}}\right) \tag{3.9}$$

$$G(\mathrm{s}) = \frac{2}{D}\left(\frac{1}{\bar{M}_{\mathrm{w}}} - \frac{1}{\bar{M}_{\mathrm{w0}}}\right) \tag{3.10}$$

These equations are based on the works of Charlesby [3.100, 3.101]. Since then, they have been used by many research groups in various forms and versions, and for various polymeric systems [3.102–3.106]. As questions may arise as to the correctness of the particular forms of these equations and, what is of significant importance, on their applicability to systems other than solid polymer samples, these questions are addressed below.

Equation (3.9) is derived for the case of a solid polymer sample (containing no or negligible amounts of other components). It is assumed that our solid polymer sample of a mass m (kg) consists of chains of the initial number-average molecular weight of $\bar{M}_{\mathrm{n0}}$ (kg/mol). The number of chains present in the sample before irradiation, n_0 (mol), is:

$$n_0 = \frac{m}{\bar{M}_{\mathrm{n0}}} \tag{3.11}$$

It is assumed that the sample is now irradiated, causing the chains to break into shorter fragments. It is easy to imagine that if p breaks of each chain (p is a dimensionless number) are caused, the number of resulting chains will be $p + 1$. Moving from the breaking of a single chain to a real situation where n_0 (mol) chains are broken, each of them at p sites on average, the number of resulting chains, n (mol), will be:

$$n = n_0 \times (p + 1) \tag{3.12}$$

where p (the average number of breaks of each chain) can be written as:

$$p = \frac{n_{\text{cb}}}{n_0} \tag{3.13}$$

n_{cb} (mol) being the total number of chain break events which took place in the polymer sample. Thus:

$$n = n_0 \times \left(\frac{n_{\text{cb}}}{n_0} + 1 \right) \tag{3.14}$$

The final number-average molecular weight is denoted $\bar{M}_{\text{n}}$ (kg/mol). Since n is defined as:

$$n = \frac{m}{\bar{M}_{\text{n}}} \tag{3.15}$$

the following is obtained:

$$\frac{m}{\bar{M}_{\text{n}}} = \frac{m}{\bar{M}_{\text{n0}}} \times \left(\frac{n_{\text{cb}}}{n_0} + 1 \right) \tag{3.16}$$

Equation (3.17) can be rearranged to obtain n_{cb}:

$$\frac{1}{\bar{M}_{\text{n}}} = \frac{1}{\bar{M}_{\text{n0}}} \times \left(\frac{n_{\text{cb}} \times \bar{M}_{n0}}{m} + 1 \right) \tag{3.17}$$

$$\frac{1}{\bar{M}_{\text{n}}} = \frac{n_{\text{cb}}}{m} = \frac{1}{\bar{M}_{\text{n0}}} \tag{3.18}$$

$$n_{\text{cb}} = m \left(\frac{1}{\bar{M}_{\text{n}}} - \frac{1}{\bar{M}_{\text{n0}}} \right) \tag{3.19}$$

Since the absorbed dose, D (J/kg), is defined as the energy of ionizing radiation, E (J), absorbed by the sample, which is of a mass equal to m (kg):

$$D = \frac{E}{m} \tag{3.20}$$

$$G(\text{s}) = \frac{n_{\text{cb}}}{E} = \frac{n_{\text{cb}}}{D\, m} \tag{3.21}$$

$$G(\mathrm{s}) = \frac{1}{D}\left(\frac{1}{\bar{M}_{\mathrm{n}}} - \frac{1}{\bar{M}_{\mathrm{n0}}}\right) \tag{3.22}$$

Using this form requires using $\bar{M}_{\mathrm{n0}}$ and $\bar{M}_{\mathrm{n}}$ in (kg/mol), which is numerically equivalent to kilodalton (kDa). A dose value in Gy = J/kg gives G(s) in mol/J, which is a SI compatible unit, and no numerical factors or unit recalculations are necessary.

3.6.2.3. Multicomponent systems including polymer solutions

Polymer solutions are an interesting example of systems where the polymer in question is a component in a bi- or multicomponent system. In Eq. (3.19), m (kg) denotes the mass of the polymer. The dose for a multicomponent system is defined as:

$$D = \frac{E}{m_{\mathrm{s}}} \tag{3.23}$$

where m_{s} (kg) is the total mass of the sample which absorbed the energy, E. It should be noted that if components other that the polymer are present, $m \neq m_s$. Therefore:

$$G(\mathrm{s}) = \frac{n_{\mathrm{cb}}}{E} = \frac{n_{\mathrm{cb}}}{D\, m_{\mathrm{s}}} \tag{3.24}$$

$$G(\mathrm{s}) = \frac{m}{D\, m_{\mathrm{s}}}\left(\frac{1}{\bar{M}_{\mathrm{n}}} - \frac{1}{\bar{M}_{\mathrm{n0}}}\right) \tag{3.25}$$

In a polymer solution, m_{s} (kg) is the mass of the solution. The solution volume is denoted V (dm^3) and the solution density as ρ (kg/dm^3). Since $m_{\mathrm{s}} = V \times \rho$:

$$G(\mathrm{s}) = \frac{m}{DV\rho}\left(\frac{1}{\bar{M}_{\mathrm{n}}} - \frac{1}{\bar{M}_{\mathrm{n0}}}\right) \tag{3.26}$$

The polymer concentration is denoted c (kg /dm^3), and $c = m / V$, giving:

$$G(\mathrm{s}) = \frac{c}{D\,\rho}\left(\frac{1}{\bar{M}_{\mathrm{n}}} - \frac{1}{\bar{M}_{\mathrm{n0}}}\right) \tag{3.27}$$

Equations (3.25) and (3.27), which are valid for multicomponent systems, are clearly different from Eq. (3.9), which is valid for neat, solid polymer samples,

since the polymer content (or concentration) in the multicomponent system must be taken into account. Similarly, instead of Eq. (3.9), for a multicomponent system the following is valid:

$$G(\mathrm{s}) = \frac{2c}{D\,\rho}\left(\frac{1}{\bar{M}_{\mathrm{w}}} - \frac{1}{\bar{M}_{\mathrm{w0}}}\right) \tag{3.28}$$

3.6.3. Calculation of gelation parameters

The sol-gel analysis is important for characterization as it can be used to estimate parameters such as cross-linking and degradation yields and gelation dose, which can be correlated with some physicochemical properties. The relationship between sol fraction and absorbed dose according to the Charlesby–Pinner equation [3.101, 3.107, 3.108] is shown in Eq. (3.29). This equation has been widely reported for linear polymers such as CMC [3.109].

$$s + \sqrt{s} = \frac{p_0}{q_0} + \frac{2}{q_0 \mu_{2,0} D} \tag{3.29}$$

where:

s is the sol fraction (s = 1 gel fraction);

p_0 is the degradation density, i.e. the average number of main chain scissions per monomer unit and per unit dose;

q_0 is the cross-linking density, i.e. the proportion of monomer units cross-linked per unit dose;

$\mu_{2,0}$ is the initial weight-average degree of polymerization;

and D is the absorbed dose in Gy.

The Charlesby–Rosiak equation, Eq. (3.30), is used to avoid inaccuracies resulting from unknown molecular weight distributions of polymers [3.108, 3.110]. Equation (3.30) can be used to estimate the radiation parameters of linear polymers of any initial weight distribution and is also applicable in systems with a monomer or branched polymer as the initial material [3.111].

$$s + \sqrt{s} = \frac{p_0}{q_0} + \left(2 - \frac{p_0}{q_0}\right)\frac{D_{\mathrm{v}} + D_{\mathrm{g}}}{D_{\mathrm{v}} + D} \tag{3.30}$$

where:

D is the absorbed dose in Gy;

D_g is the gelation dose — the dose required for the first insoluble gel to appear; and D_v is the virtual dose — the dose required to change the distribution of molecular weight of the polymer in such a way that the relation between weight-average and number-average molecular weight would be equal to 2.

However, a limitation of the Charlesby–Pinner equation is that it neither considers the eventuality of chain reactions nor the possible dose dependence of the reactivity of monomer units. As a consequence, most of the experimental data of radiation polymerization will not obey this equation. It has recently been shown that chain reactions, as well as polydispersity and structure, explain most of the deviation from the ideal Charlesby–Pinner behaviour that is found in irradiated polymers [3.112].

Equations (3.29) and (3.30) allow the calculation of not only the gelation dose, D_g, but also the ratio between the radiation yields of scission and cross-linking, by:

$$G(\mathrm{s})/G(\mathrm{x}) = 2p_0/q_0 \tag{3.31}$$

It should be noted that D_g, G(s) and G(x) can also be assessed by other methods (see e.g. Ref. [3.83]).

3.7. CONCLUSION

The main features of radiation processing in the domain of polymers have been briefly presented in this chapter. Efficient treatments aiming at the improvement of the properties of thermoplastics and rubber have been made available for decades and continue to be improved. The current trends show the enormous potential of radiation based processes to address environmental concerns by proposing equally performing and societally acceptable alternatives to outdated technologies based on unsuitable chemistries and unreasonable energy consumption. Both commodity and technological products will increasingly rely on radiation treatment of polymers. Use of radiation in recycling technologies and for the utilization of biomass is expected to play an increasing role in a near future. In this respect, polysaccharides occupy a central position, the various basic and applied aspects of which will be developed in the following chapters.

ACKNOWLEDGEMENTS

This work was supported in part by the National Science Centre, Poland (Grant No. 2012/07/B/ST4/01429).

REFERENCES TO CHAPTER 3

[3.1] INTERNATIONAL ATOMIC ENERGY AGENCY, Trends in Radiation Sterilization of Health Care Products, IAEA, Vienna (2008).
[3.2] ERSHOV, B.G., Radiation technologies: their possibilities, state and prospects of applications, Her. Russ. Acad. Sci. **83** (2013) 437–8.
[3.3] UNITED STATES DEPARTMENT OF ENERGY, Accelerators for America's Future, USDOE, Washington, DC (2009).
[3.4] SPINKS, J.W.T., WOODS, R.J., Introduction to Radiation Chemistry, 3rd edn, Wiley, New York (1990).
[3.5] FARHATAZIZ, RODGERS, M.A.J. (Eds), Radiation Chemistry: Principles and Applications, VCH, New York (1987).
[3.6] INTERNATIONAL COMMISSION ON RADIATION UNITS AND MEASUREMENTS, Radiation Quantities and Units, Report No. 33, ICRU, Bethesda, MD (1980).
[3.7] INTERNATIONAL COMMISSION ON RADIATION UNITS AND MEASUREMENTS, Radiation Dosimetry: Electron Beams with Energies between 1 and 50 MeV, Report No. 35, ICRU, Bethesda, MD (1984).
[3.8] ATTIX, F.H., ROESCH, W.C., TOCHILIN, T. (Eds), Radiation Dosimetry, Academic Press, New York (1966).
[3.9] KASE, K.R., BJARNGARD, B.E., ATTIX, F.H. (Eds), The Dosimetry of Ionizing Radiation, Academic Press, New York (1987).
[3.10] HOLM, N.W., BERRY, R.J., Manual on Radiation Dosimetry, Marcel Dekker, New York (1970).
[3.11] MEHTA, K., GIRZIKOWSKY, R., Alanine-ESR dosimetry for radiotherapy. IAEA experience, Appl. Radiat. Isot. **47** 11–12 (1996) 1189–1191.
[3.12] FRICKE, H., MORSE, S., The relation of chemical, colloidal and biological effects of roentgen rays of different wave lengths to the ionization which they produce in air. II. The action of roentgen rays on solutions of ferrosulphate in water, Am. J. Roentgenol. Radium Ther. **18** (1927) 426–430.
[3.13] FRICKE, H., MORSE, S., The action of X-rays on ferrous sulphate solutions, Phil. Mag. **7** (1929) 129–141.
[3.14] FRICKE, H., HART, E.J., The oxidation of Fe^{++} to Fe^{+++} by the irradiation with X-rays of solutions of ferrous sulfate in sulfuric acid, J. Chem. Phys. **3** (1935) 60–61.
[3.15] CLARK, G.L., Encyclopedia of X-rays and Gamma Rays, Chapman & Hall, London (1963).

[3.16] AL-ASSAF, S., Characterisation and Radiation Sensitivity of Biopolymer Hylan, MSc Thesis, Univ. Salford (1994).
[3.17] McLAUGHLIN, W.L., MILLER, A., FIDAN, S., PEJTERSEN, K., BATSBERG PEDERSEN, W., Radiochromic plastic films for accurate measurement of radiation absorbed dose and dose distributions, Radiat. Phys. Chem. **10** (1977) 119–127.
[3.18] INTERNATIONAL COMMISSION ON RADIATION UNITS AND MEASUREMENTS, The Dosimetry of Pulsed Radiation, Report No. 34, ICRU, Bethesda, MD (1982).
[3.19] BUXENDALE, J.H., BUSI, F. (Eds), The Study of Fast Processes and Transient Species by Electron Pulse Radiolysis, NATO Adv. Study Inst. Series, Series C: Mathematical and Physical Sciences, Riedel, Dordrecht, Netherlands (1982).
[3.20] KOJIMA, T., TACHIBANA, H., HARUYAMA, Y., TANAKA, R., OKAMOTO, J., Recent progress in JAERI alanine/ESR dosimetry system, Radiat. Phys. Chem. **42** 4–6 (1993) 813–816.
[3.21] McLAUGHLIN, W.L., DESROSIERS, M.F., Dosimetry systems for radiation processing, Radiat. Phys. Chem. **46** 4–6 (1995) 1163–1174.
[3.22] REGULLA, D., "Alanine dosimetry – A versatile dosimetric tool", Radiation Protection and Dosimetry, Biological Effects of Radiation, Vol. 25/3 (DOSSEL, O., SCHLEGEL, Eds), Springer, Berlin (2009) 477–481.
[3.23] SCHOENBACHER, H., FUERSTNER, M., VINCKE, H., High-level dosimetric methods, Radiat. Prot. Dosim. **137** 1–2 (2009) 83–93.
[3.24] INTERNATIONAL ATOMIC ENERGY AGENCY, Dosimetry for Radiation Processing, IAEA-TECDOC-1156, IAEA, Vienna (2000).
[3.25] SPINKS, J.W.T., WOODS, R.J., Introduction to Radiation Chemistry, 2nd edn, Wiley Interscience, New York (1976).
[3.26] ALLEN, A.O., The Radiation Chemistry of Water and Aqueous Solutions, Van Nostrand, Princeton, NJ (1961).
[3.27] SWALLOW, A.J., Radiation Chemistry – An Introduction, Longman, London (1973).
[3.28] O'DONNELL, J.H., SANGSTER, D.F., Principles of Radiation Chemistry, American Elsevier, New York (1970).
[3.29] BUXTON, G.V., "Basic radiation chemistry of liquid water", The Study of Fast Processes and Transient Species by Electron Pulse Radiolysis (Proc. NATO Adv. Study Inst., Capri, Italy, 1981) (BAXENDALE, H.J., BUSI, F., Eds), Springer, Dordrecht, Netherlands (1982) 241–266.
[3.30] VON SONNTAG, C., The Chemical Basis of Radiation Biology, Taylor and Francis, London (1987).
[3.31] BUXTON, G.V., GREENSTOCK, C.L., HELMAN, W.P., ROSS, A.B., Critical review of rate constants for reactions of hydrated electrons, hydrogen atoms and hydroxyl radicals ($OH^{\bullet}/O^{-\bullet}$) in aqueous solution, J. Phys. Chem. Ref. Data **17** (1988) 513–886.
[3.32] KLASSEN, N.V., "Primary products in radiation chemistry", Radiation Chemistry. Principles and Applictions (FARHATAZIZ, RODGERS, M.A.J., Eds) VCH Publishers, New York (1987) 29–64.

[3.33] BUXTON, G.V., "Radiation chemistry of the liquid state. (1) Water and homogeneous aqueous solutions", Radiation Chemistry: Principles and Applications (FARHATAZIZ, RODGERS, M.A.J., Eds.) VCH, New York (1987) 321–349.

[3.34] MATHESON, M.S., DORFMAN, L.M., Pulse Radiolysis, MIT Press, Cambridge, MA (1969).

[3.35] ANABAR, M., FARHATAZIZ, ROSS, A.B., Selected Specific Rates of Reaction of Transient from Water in Aqueous Solution II. Hydrogen Atom, United States Department of Commerce, National Bureau of Standards, Washington, DC (1975).

[3.36] DORFMAN, L.M., ADAMS, G.E., Reactivity of the Hydroxyl Radical in Aqueous Solutions, United States Department of Commerce, National Bureau of Standards, Washington, DC (1973).

[3.37] BIELSKI, B.H.J., GEBICKI, J.M., Species in irradiated oxygenated water, Adv. Radiat. Chem. 2 (1970) 177–279.

[3.38] BIELSKI, B.H.J., CABELLI, D.E., ARUDI, R.L., ROSS, A.B., Reactivity of HO_2/O^{2-} radicals in aqueous solution, J. Phys. Chem. Ref. Data **14** (1985) 1041–1100.

[3.39] LUND, A., SHIOTANI, M., Radical Ionic Systems Properties in Condensed Phases, Kluwer, Dordrecht, Netherlands (1991).

[3.40] BLY, J.H., Electron Beam Processing, International Information Associates, Yardley, PA (1988).

[3.41] COQUERET, X., "Obtaining high-performance polymeric materials by irradiation", Radiation Chemistry: From Basics to Applications in Material and Life Sciences (SPOTHEIM-MAURIZOT, M., MOSTAFAVI, M., DOUKI, T., BELLONI, J., Eds), EDP Sciences, Les Ulis, France (2008) 131–150.

[3.42] TURGIS, J.D., VERGE, C., COQUERET, X., Composition effects on the EB-induced cross-linking of some acrylate and methacrylate copolymers, Radiat. Phys. Chem. **67** (2003) 409–413.

[3.43] ULANSKI, P., BOTHE, E., HILDENBRAND, K., ROSIAK, J.M., VON SONNTAG, C., Hydroxyl-radical-induced reactions of poly(acrylic acid); a pulse radiolysis, EPR and product study. Part II. Oxygenated solution, J. Chem. Soc. Perkin Trans. 2 **1996** (1996) 23–28.

[3.44] VON SONNTAG, C., SCHUCHMANN, H.-P., The elucidation of peroxyl radical reactions in aqueous solution with the help of radiation-chemical techniques, Angew. Chem. Int. Ed. Engl. **30** (1991) 1229–1253.

[3.45] ISILDAR, M., SCHUCHMANN, M.N., SCHULTE-FROHLINDE, D., VON SONNTAG, C., Oxygen uptake in the radiolysis of aqueous solutions of nucleic acids and their constituents, Int. J. Radiat. Biol. **41** (1982) 525–533.

[3.46] VON SONNTAG, C., Free radical reactions of carbohydrates as studied by radiation techniques, Adv. Carbohydr. Chem. Biochem. **37** (1980) 7–77.

[3.47] BENNETT, J.E., BROWN, D.M., MILE, B., Studies by electron spin resonance of the reactions of alkylperoxy radicals. Part 2. Equilibrium between alkylperoxy radicals and tetroxide molecules, Trans. Faraday Soc. **66** (1970) 397–405.

[3.48] HOWARD, J.A., "Self-reactions of alkylperoxy radicals in solution (1). in: Organic Free Radicals", ACS Symposium Ser. **69** (1978) 413–432.

[3.49] ROSIAK, J.M., ULANSKI, P., Synthesis of hydrogels by irradiation of polymers in aqueous solution, Radiat. Phys. Chem. **55** (1999) 139–151.
[3.50] ULANSKI, P., BOTHE, E., ROSIAK, J.M., VON SONNTAG, C., OH-Radical-induced crosslinking and strand breakage of poly(vinyl alcohol) in aqueous solution in the absence and presence of oxygen. A pulse radiolysis and product study, Makromol. Chem. **195** (1994) 1443–1461.
[3.51] KURATA, M., TSUNASHIMA, Y., "Viscosity – molecular weight relationships and unperturbed dimensions of linear chain molecules", Polymer Handbook, 4th edn (BRANDRUP, J., IMMERGUT, E.H., GRULKE, E.A., Eds), Wiley, Hoboken, NJ (1999) 1–83.
[3.52] HUGLIN, M.B., Light Scattering from Polymer Solutions, Academic Press, London (1972).
[3.53] KRATOCHVIL, P., Classical Light Scattering from Polymer Solutions, Elsevier, Amsterdam (1987).
[3.54] VIOVY, J.L., LESEC, J., Separation of macromolecules in gels: Permeation chromatography and electrophoresis, Adv. Polym. Sci. **114** (1994) 1–41.
[3.55] SAUNDERS, G., Polymer analysis by gel permeation chromatography – A historical perspective, LC-GC Europe **17** 12 (2004) 650–655.
[3.56] ROBERTS, G.A., DRYDEN, D.T.F., "DNA electrophoresis: Historical and theoretical perspectives", DNA Electrophoresis (MAKOVETS, S., Ed.), Methods in Molecular Biology No. 1054, Humana Press, New York (2013) 1–9.
[3.57] VIOVY, J.L., Electrophoresis of DNA and other polyelectrolytes: Physical mechanisms, Rev. Mod. Phys. **72** 3 (2000) 813–872.
[3.58] ZHANG, L., DANG, F., BABA, Y., Microchip electrophoresis-based separation of DNA, J. Pharmaceut. Biomed. **30** 6 (2003) 1645–1654.
[3.59] KLEPARNIK, K., BOCEK, P., DNA diagnostics by capillary electrophoresis, Chem. Rev. **107** 11 (2007) 5279–5317.
[3.60] BURCHARD, W., Dynamic light scattering method of polymer solutions, Macromol. Symp. **101** (1996) 103–113.
[3.61] DAUTZENBERG, H., Polyelectrolyte complex formation: Role of a double hydrophilic polymer, Macromol. Chem. Phys. **201** (2000) 1765–1773.
[3.62] ABAD, L.V., et al., Dynamic light scattering studies of irradiated kappa carrageenan, Int. J. Biol. Macromol. **34** 1–2 (2004) 81–88.
[3.63] ABAD, L., et al., Comparative studies on the conformational change and aggregation behavior of irradiated carrageenans and agar by dynamic light scattering, Int. J. Biol. Macromol. **42** 1 (2008) 55–61.
[3.64] HENKE, A., et al., The structure and aggregation of hydrogen-bonded interpolymer complexes of poly(acrylic acid) with poly(N-vinylpyrrolidone) in dilute aqueous solution, Macromol. Chem. Phys. **212** 23 (2011) 2529–2540.
[3.65] FYANS, R.L., BRENNAN, W.P., EARNEST, C.M., The evolution of differential scanning calorimetry: a review, Thermochim. Acta **92** C (1985) 385–390.
[3.66] FREIRE, E., Differential scanning calorimetry, Method. Mol. Biol. **40** (1995) 191–218.

[3.67] SIMON, S.L., Temperature-modulated differential scanning calorimetry: Theory and application, Thermochim. Acta **374** 1 (2001) 55–71.
[3.68] SHIMADA, S., ESR studies on molecular motion and chemical reactions in solid polymers in relation to structure, Prog. Polym. Sci. **17** 6 (1992) 1045–1106.
[3.69] KAPTAN, Y., PEKCAN, O., GUVEN, O., Determination of diffusion coefficient of oxygen into polymers by using electron spin resonance spectroscopy II, Poly (vinyl acetate), J. Appl. Polym. Sci. **44** 9 (1992) 1595–1599.
[3.70] SZAJDZINSKA-PIETEK, E., PILLARS, T.S., SCHLICK, S., PLONKA, A., Electron spin resonance study of polymer self-assembling: Cationic spin probes in aqueous solutions of poly(ethylene-co-methacrylic acid) (EMAA) ionomers, Macromolecules **31** 14 (1998) 4586–4594.
[3.71] YAMADA, B., WESTMORELAND, D.G., KOBATAKE, S., KONOSU, O., ESR spectroscopic studies of radical polymerization, Prog. Polym. Sci. **24** 4 (1999) 565–630.
[3.72] VEKSLI, Z., ANDREIS, M., RAKVIN, B., ESR spectroscopy for the study of polymer heterogeneity, Prog. Polym. Sci. **25** 7 (2000) 949–986.
[3.73] ASSINK, R.A., et al., Analysis of hydroperoxides in solid polyethylene by MAS 13C NMR and EPR, Macromolecules **33** 11 (2000) 4023–4029.
[3.74] VON SONNTAG, J., JANOVSKA, I., NAUMOV, S., MEHNERT, R., Free radical copolymerisation of N-methylmaleimide and 2,3-dihydrofuran initiated by their radical cations. A low temperature EPR study of a binary system, Macromol. Chem. Phys. **203** 3 (2002) 580–585.
[3.75] SZAJDZINSKA-PIETEK, E., SCHLICK, S., Self-assembling of ion-containing polymers and surfactants in aqueous solutions studied by ESR and fluorescence probes, J. Mol. Liq. **117** 1–3 (2005) 153–164.
[3.76] SALIH, M.A., BUTTAFAVA, A., RAVASIO, U., MARIANI, M., FAUCITANO, A., EPR investigation on radiation-induced graft copolymerization of styrene onto polyethylene: Energy transfer effects, Radiat. Phys. Chem. **76** 8–9 (2007) 1360–1366.
[3.77] KASSER, M.J., SILVERMAN, J., AL-SHEIKHLY, M., EPR simulation of polyenyl radicals in ultrahigh molecular weight polyethylene, Macromolecules **43** 21 (2010) 8862–8867.
[3.78] EL FRAY, M., PRZYBYTNIAK, G., PIATEK-HNAT, M., KORNACKA, E.M., Physical effects of radiation processes in poly(aliphatic/aromatic-ester)s modified with e-beam radiation, Polymer **51** 5 (2010) 1133–1139.
[3.79] CHUMAKOV, M.K., et al., Electron beam induced grafting of N-isopropylacrylamide to a poly(ethylene-terephthalate) membrane for rapid cell sheet detachment, Radiat. Phys. Chem. **80** 2 (2011) 182–189.
[3.80] HINDERBERGER, D., EPR spectroscopy in polymer science, Top. Curr. Chem. **321** (2012) 67–89.
[3.81] WALO, M., PRZYBYTNIAK, G., SADLO, J., Radiation-induced radicals in aliphatic poly(ester urethane)s studied by EPR spectroscopy, J. Mol. Struct. **1036** (2013) 488–493.

[3.82] ULANSKI, P., BOTHE, E., HILDENBRAND, K., ROSIAK, J.M., VON SONNTAG, C., Hydroxyl-radical-induced reactions of poly(acrylic acid): a pulse radiolysis, EPR and product study. Part I. Deoxygenated aqueous solution, J. Chem. Soc. Perkin Trans. **2** (1996) 13–22.

[3.83] FILIPCZAK, K., et al., Poly(e-caprolactone) biomaterial sterilized by E-beam irradiation, Macromol. Biosci. **6** 4 (2006) 261–273.

[3.84] WACH, R.A., MITOMO, H., YOSHII, F., ESR investigation on gamma-irradiated methylcellulose and hydroxyethylcellulose in dry state and in aqueous solution, J. Radioanal. Nucl. Chem. **261** 1 (2004) 113–118.

[3.85] TABATA, Y., Pulse Radiolysis of Irradiated Systems, CRC Press, Boca Raton, FL (1991).

[3.86] VON SONNTAG, C., SCHUCHMANN, H.-P., Pulse radiolysis, Methods Enzymol. **233** (1994) 3–20.

[3.87] CHARLESBY, A., et al., "15. Pulse radiolysis studies of aqueous polymer-thiourea systems", Pulse Radiolysis (EBERT, M., KEENE, J.P., SWALLOW, A.J., BAXENDALE, J.H., Eds), Academic Press, London (1965) 193–201.

[3.88] BEHAR, D., RABANI, J., Pulse radiolysis of poly(styrenesulfonate) in aqueous solutions, J. Phys. Chem. **92** (1988) 5288–5292.

[3.89] JANATA, E., Pulse radiolysis conductivity measurements in aqueous solutions with nanosecond time resolution, Radiat. Phys. Chem. **19** (1982) 17–21.

[3.90] BOTHE, E., QURESHI, G.A., SCHULTE-FROHLINDE, D., Rate of OH radical induced strand break formation in single stranded DNA under anoxic conditions. An investigation in aqueous solutions using conductivity methods, Z. Naturforsch. **38c** (1983) 1030–1042.

[3.91] DEEBLE, D.J., et al., The kinetics of hydroxyl-radical-induced strand breakage of hyaluronic acid. A pulse radiolysis study using conductometry and laser-light-scattering, Z. Naturforsch. **45c** (1990) 1031–1043.

[3.92] ULANSKI, P., VON SONNTAG, C., OH-Radical-induced chain scission of chitosan in the absence and presence of dioxygen, J. Chem. Soc. Perkin Trans. **2** (2000) 2022–2028.

[3.93] ULANSKI, P., BOTHE, E., HILDENBRAND, K., VON SONNTAG, C., Free-radical-induced chain breakage and depolymerization of poly(methacrylic acid). Equilibrium polymerization in aqueous solution at room temperature, Chem. Eur. J. **6** (2000) 3922–3934.

[3.94] BECK, G., KIWI, J., LINDENAU, D., SCHNABEL, W., On the kinetics of polymer degradation in solution-I. Laser flash photolysis and pulse radiolysis studies using the light scattering detection method, Eur. Polym. J. **10** (1974) 1069–1075.

[3.95] LINDENAU, D., HAGEN, U., SCHNABEL, W., On the dynamics of DNA in aqueous solution. Pulse radiolysis studies using light scattering detection method, Radiat. Environ. Biophys. **13** (1976) 287–294.

[3.96] WASHINO, K., SCHNABEL, W., Radiation induced molecular size changes in native and denatured deoxyribonucleic acid under anoxic conditions. A pulse radiolysis study, Makromol. Chem. **183** (1982) 697–709.

[3.97] SCHNABEL, W., DENK, O., GRÖLLMANN, U., RAAP, I.A., WASHINO, K., On the reactions of macroradicals in solution. A pulse radiolysis study, Radiat. Phys. Chem. **21** (1983) 225–231.

[3.98] LUBIS, R., OLEJNICZAK, J., ROSIAK, J., KROH, J., System for measurement of changes of LSI in polymer solution after electron pulse, Radiat. Phys. Chem. **36** (1990) 249–252.

[3.99] ROSIAK, J., OLEJNICZAK, J., PEKALA, W., Fast reactions of irradiated polymers. I. Crosslinking and degradation of polyvinylpyrrolidone, Radiat. Phys. Chem. **36** (1990) 747–755.

[3.100] CHARLESBY, A., Molecular-weight changes in the degradation of long-chain polymers, Proc. Roy. Soc. Ser. A **224** (1954) 120–128.

[3.101] CHARLESBY, A., Atomic Radiation and Polymers, Pergamon Press, Oxford (1960).

[3.102] SCHNABEL, W., Polymer Degradation. Principles and Practical Applications, Hanser, Munich (1981).

[3.103] HILL, D.J.T., O'DONNELL, J.H., WINZOR, C.L., WINZOR, D.J., Evaluation of scission and crosslinking yields in "γ"-irradiated poly(acrylic acid) and poly(methacrylic acid) from weight- and Z- average molecular weight determined by sedimentation equilibrium, Polymer **31** (1990) 538-542.

[3.104] O'DONNELL, J.H., "Chemistry of Radiation Degradation of Polymers", Radiation Effects of Polymers, ACS Symposium Series No. 475 (CLOUGH, R.L., SHALABY, S.W., Eds), American Chemical Society, Washington, DC (1991) 402–413.

[3.105] ERSHOV, B.G., Radiation-chemical degradation of cellulose and other polysaccharides, Russ. Chem. Rev. **67** (1998) 353–375.

[3.106] FILIPCZAK, K., et al., Porous polymeric scaffolds for bone regeneration, E-Polymers **5** 1 (2005) Paper 11.

[3.107] ROSIAK, J.M., Gel/sol analysis of irradiated polymers, Radiat. Phys. Chem. **51** 1 (1998) 13–17.

[3.108] OLEJNICZAK, J., ROSIAK, J., CHARLESBY, A., Gel/dose curves for polymers undergoing simultaneous crosslinking and scission, Radiat. Phys. Chem. **37** 3 (1991) 499–504.

[3.109] LIU, P., ZHAI, M., LI, J., PENG, J., WU, J., Radiation preparation and swelling behavior of sodium carboxymethyl cellulose hydrogels, Radiat. Phys. Chem. **63** 3–6 (2002) 525–528.

[3.110] ROSIAK, J., OLEJNICZAK, J., CHARLESBY, A., Determination of the radiation yield of hydrogels crosslinking, Radiat. Phys. Chem. **32** 5 (1988) 691–694.

[3.111] WACH, R.A., MITOMO, H., NAGASAWA, N., YOSHII, F., Radiation crosslinking of methylcellulose and hydroxyethylcellulose in concentrated aqueous solutions, Nucl. Instr. Meth. B **211** 4 (2003) 533–544.

[3.112] JONES, R.A., WARD, I.M., TAYLOR, D.J.R., STEPTO, R.F.T., Reactions of amorphous PE radical-pairs in vacuo and in acetylene: a comparison of gel fraction data with Flory-Stockmayer and atomistic modelling analyses, Polymer **37** (1996) 3644–3657.

Chapter 4

RADIATION MODIFICATION OF POLYSACCHARIDES

S. AL-ASSAF, S.K.H. GULREZ
Hydrocolloids Research Centre, Institute of Food Science and Innovation,
University of Chester,
Chester, United Kingdom

R. CZECHOWSKA-BISKUP, R.A. WACH, J.M. ROSIAK, P. ULANSKI
Institute of Applied Radiation Chemistry, Faculty of Chemistry
Lodz University of Technology
Lodz, Poland

4.1. INTRODUCTION

There has been significant interest in the application of ionizing radiation for the modification of polysaccharides. The fact that polysaccharides are natural, biocompatible and biodegradable has resulted in their application in various fields such as healthcare, agriculture and environmental protection. This chapter, therefore, provides (a) an overview of the basic radiation chemistry of polysaccharides in dilute aqueous solution and in paste-like and solid states and (b) a review of the historical as well as contemporary literature in this field. Additionally, the mechanisms leading to these significant changes in structural and subsequently physical properties are highlighted.

Table 4.1 lists selected references that specifically discuss the effects of radiation on polysaccharides. The methodology used in these studies observed changes in molecular weight, rheology, viscometry, UV spectroscopy and FTIR. Since the mechanism and yields of the main radiation-induced reactions differ between irradiation of the substances in the solid state and in aqueous solutions (including paste-like states), the references in the table are categorized by state.

4.2. IRRADIATION OF POLYSACCHARIDES IN THE SOLID STATE

When polysaccharides are irradiated in the solid state, the formation of radicals in molecular chains is induced; macroradicals are produced by direct energy transfer to the macromolecule, and primarily radicals are generated

TABLE 4.1. LIST OF SELECTED REFERENCES SHOWING THE EFFECTS OF RADIATION ON POLYSACCHARIDES IN AQUEOUS SOLUTION AND IN THE SOLID STATE

Material	References for radiation effects	
	In aqueous solution	In solid state
CMC	[4.1–9]	[4.1, 4.10–12]
Hydroxyethyl cellulose, hydroxypropyl cellulose	[4.1, 4.13–17]	[4.1, 4.2, 4.13, 4.15, 4.18]
Chitin, chitosan & derivatives	[4.5, 4.19–37]	[4.19, 4.25, 4.30, 4.32, 4.34, 4.37–56]
Cellulose & derivatives	[4.13, 4.20, 4.57–60]	[4.13, 4.20, 4.59, 4.61–80]
Starch & derivatives	[4.5, 4.20, 4.57, 4.81–84]	[4.79, 4.82, 4.85–97]
D-glucose	[4.58, 4.98–104]	[4.105–109]
Hyaluronan & hyaluronic acid	[4.20, 4.57, 4.110–119]	[4.113, 4.118, 4.120–122]
Glucomannan, galactomannan	[4.123–125]	[4.125–131]
Alginate	[4.27, 4.57, 4.132–141]	[4.135, 4.136, 4.142–146]
Carrageenan	[4.138, 4.147–152]	[4.143, 4.150, 4.152–155]
Dextran	[4.57, 4.62, 4.156–163]	[4.62, 4.164, 4.165]
Pectin	[4.57, 4.164, 4.166–171]	[4.62, 4.142, 4.171, 4.172]
Agar	[4.57, 4.149, 4.173–175]	[4.143, 4.176–183]
GA	[4.184, 4.185]	[4.186–189]
Xanthan, β glucan	[4.190–193]	[4.194–196]

owing to the moisture present. Figure 4.1 shows the process of degradation of polysaccharides to low molecular weight products.

The scission of glycosidic bonds is predominantly responsible for the reduction in the molecular weight of macromolecules during the irradiation of polysaccharides in the solid state.

Degradation and the resulting changes in average molecular weights are often quantified as radiation yields of degradation (G(s), see Section 3.6.2), which is defined as the number of chain break events per unit of absorbed energy. Care should be taken when measuring, reporting or comparing radiation-chemical yields in solid polysaccharides, since moisture content can strongly influence the reaction pathways and yields. This is due to the contribution of water radiolysis, where the yields of radicals are significantly higher than in dry polysaccharides (see Section 4.3).

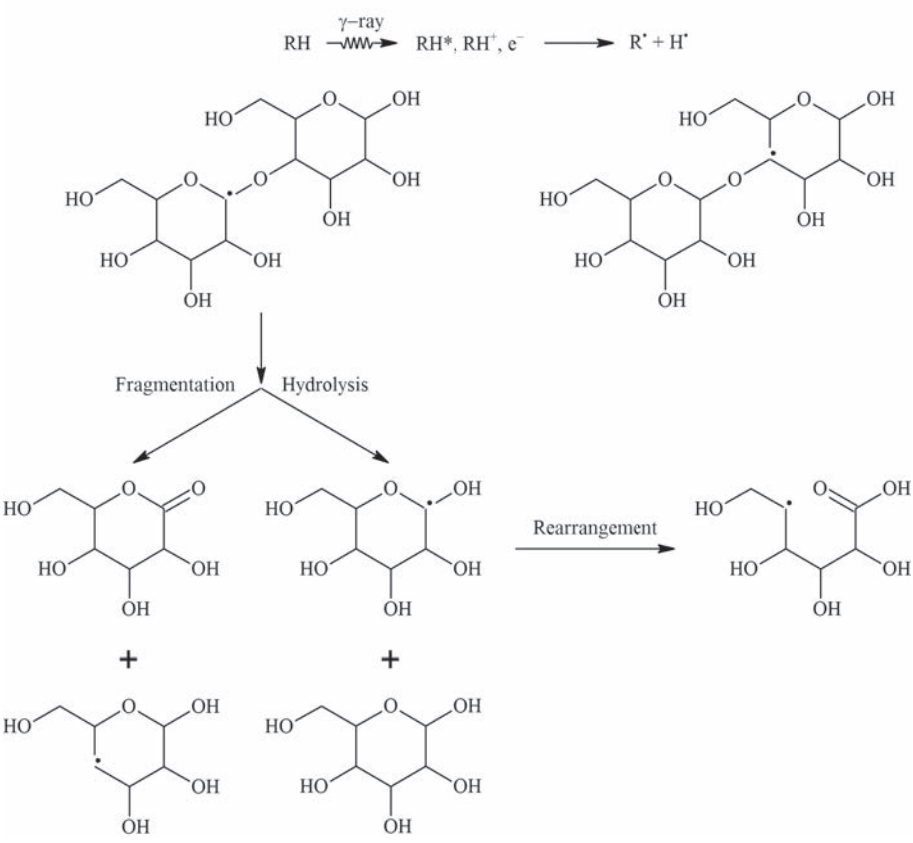

FIG. 4.1. Events in the solid state radiation of carbohydrates; the glycosidic bond cleavage and chain scission of cellobiose upon solid state irradiation.

4.3. IRRADIATION OF POLYSACCHARIDES IN AQUEOUS SOLUTION

When the dilute aqueous solution of a polysaccharide is subjected to ionizing radiation, most of the radiation energy is absorbed by water, while the absorption of ionizing radiation by the polymer itself can be neglected (see Chapter 3, Sections 3.4.6 and 3.5.3). Thus, the free radical reactions in the studied polysaccharide are induced by indirect effect, i.e. not through direct absorption of energy by the solute itself, but by absorption of radiation energy by water molecules leading to the formation of water-derived radicals [4.197], which subsequently attack polysaccharide molecules.

Understanding the mechanism and kinetics of radiation induced reactions is important for the rational design of applications and technological processes. In particular, knowledge of the radiolytic yields and rate constants of elementary reactions involved in what are often complex processes allows the prediction, by calculation and/or simulation, of the optimum conditions (concentrations of substrates and additives, dose, dose rate, temperature, etc.) to reach the desired irradiation outcome.

As stated in Sections 3.4.6.1 and 3.4.6.2, the radiolysis of water yields $HO^{\bullet}$ radicals, hydrated electrons and hydrogen atoms. Their radiation-chemical yields, expressed as G values (mol/J) are identical for ^{60}Co γ rays and high energy electrons.

The reactivity of hydrated electrons towards carbohydrates is low (typically $k < 5 \times 10^6$ $dm^3 \cdot mol^{-1} \cdot s^{-1}$) [4.110, 4.197, 4.198]. In laboratory tests, the hydrated electron can be readily converted into further $HO^{\bullet}$ by saturating the solution with N_2O ($k = 9.1 \times 10^9$ $dm^3 \cdot mol^{-1} \cdot s^{-1}$) [4.198].

Hydroxyl radicals react with low-molecular-weight carbohydrates by abstraction of carbon-bound hydrogens with a rate constant of $k > 1 \times 10^9$ $dm^3 \cdot mol^{-1} \cdot s^{-1}$, while the reactivity of H atoms is more than an order of magnitude lower [4.112, 4.198]. It has been shown that selectivity of the reaction of $HO^{\bullet}$ with carbohydrates is low [4.197, 4.199, 4.200], i.e. hydrogen atoms are abstracted from all positions with a similar probability. This leads to the formation of radicals located at various carbon atoms (Fig. 4.2).

Owing to a different reaction geometry, the rate constants of the reactions of $HO^{\bullet}$ radicals with polymers, when expressed in $dm^3 \cdot (\text{mol of repeating unit})^{-1} \cdot s^{-1}$, are lower than for low-molecular-weight analogues. The rate constants depend on the molecular weight, the conformation of the macromolecules and, to a certain extent, also on their concentration [4.201–4.205].

Only a small amount of data on the rate constants of H abstraction from polysaccharides by $HO^{\bullet}$ radicals are available. For hyaluronic acid (polyanionic) of an average molecular weight $\overline{M}_w > 10^6$ Da, $k = 7–9 \times 10^8$ $dm^3 \cdot mol^{-1} \cdot s^{-1}$ has been reported [4.110, 4.111], while for dextran (neutral) of $\overline{M}_w \approx 10^5$ Da, a value in

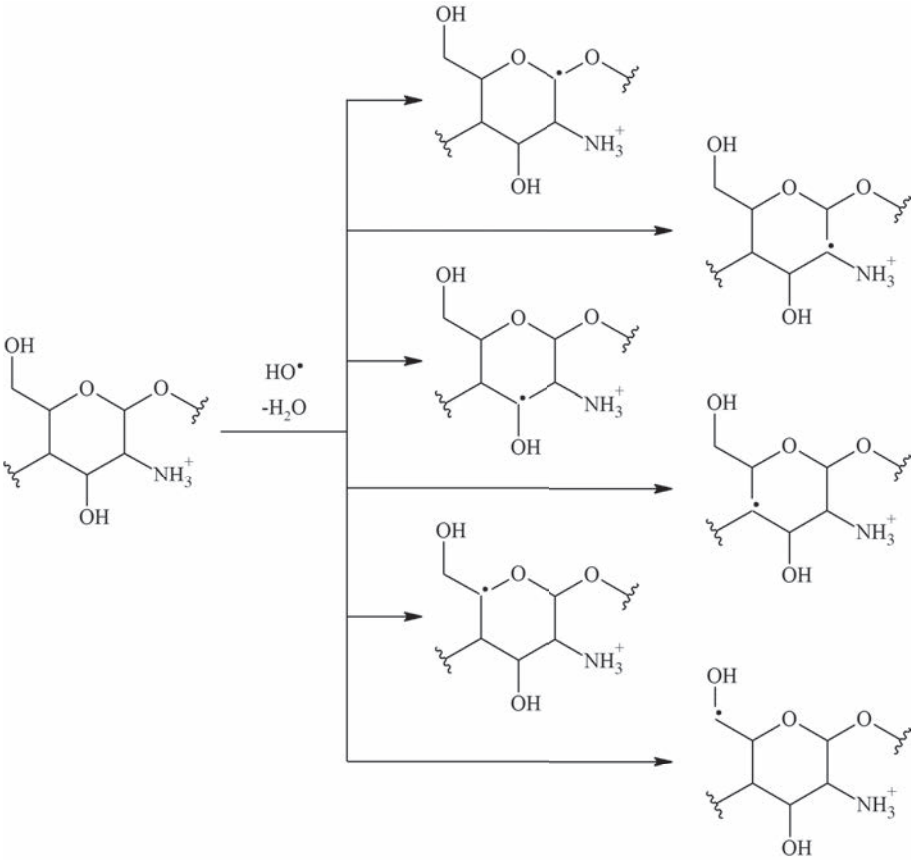

FIG. 4.2. Structures of radicals formed upon HO• attack on a polysaccharide molecule, shown in the example of chitosan.

the order of only 1×10^7 $dm^3 \cdot mol^{-1} \cdot s^{-1}$ is calculated from the data of Ref. [4.201]. The difference is attributed mostly to the different charge density, and partially to various different conformations of these polymers. Phillips and Moody [4.62] showed that neutral carbohydrates show no significant reaction with e^-_{aq}, but that the connective tissue glycosaminoglycans (such as hyaluronic acid) have a measurable activity. Hydroxyl radicals are about twice as effective as hydrogen atoms in attacking hyaluronic acid and inducing chain cleavage, while solvated electrons induce very little degradation [4.110]. Hydroxyl radicals react very rapidly with another ionic polysaccharide, CMC; the rate constant is about 1×10^9 $dm^3 \cdot mol^{-1} \cdot s^{-1}$ for the polymer bearing charges along the chain (at neutral pH), and it is independent of the DS of the CMC [4.6]. However, this value decreases

to 6×10^8 $dm^3 \cdot mol^{-1} \cdot s^{-1}$ for the neutralized form of carboxyl moieties, in which a more coiled conformation of chains is expected. For chitosan, a polycationic polysaccharide of a weight-average molecular weight of 4×10^5 Da, the rate constant of the reaction with $HO^•$ radicals is 6.4×10^8 $dm^3 \cdot mol^{-1} \cdot s^{-1}$ [4.21]. While somewhat slower than for simple sugars, these reactions are still very fast, in most cases providing complete scavenging of hydroxyl radicals by polysaccharide molecules even at low concentrations, so that the yield of the formed polysaccharide radicals is close to the initial $HO^•$ yield.

The polymers listed in Table 4.1 above degrade upon irradiation in diluted aqueous solution, irrespective of their conformation and structure, because, owing to the low polymer concentration, the chains of these polymers are not dense enough (i.e. the critical overlap concentration is not reached) for recombination of the chain derived radicals to occur. Additionally, the glycosidic bond breaks caused by radical transformations occur quite quickly [4.21, 4.111]. These radical transformations may cause other changes in the chemical structure as well as degradation [4.197, 4.206]. Figure 4.3 illustrates the reactions that occur during the aqueous radiolysis of chitosan in the absence of oxygen and shows how chain breakage is caused by hydrolysis, rearrangment and fragmentation.

Radiation degradation yields have been reported (Table 4.1) for κ, ι, and λ carrageenans in the solid state, in a paste-like state of 4% concentration and in 1% aqueous solution. The yield, G(s) was $2.3–2.7 \times 10^{-7}$ mol/J for irradiation in the solid state and $1.0–1.2 \times 10^{-7}$ mol/J for irradiation in the aqueous state, showing that carrageenan is more susceptible to degradation when in its solid state. In the paste-like state, yields were found to be 0.3×10^{-7} mol/J, probably owing to simultaneous cross-linking [4.150]. The degradation yield for κ carrageenan in aqueous solution was dependent on its conformation, with the helical conformation giving a G(s) value of 0.7×10^{-7} mol/J, compared with the value of 1.2×10^{-7} mol/J given by the coiled conformation. This difference results from the interchain stabilization offered by the helical conformation, which makes it more likely that interchain cross-linking of the free radicals will occur [4.151].

Lower G(s) values were found for galactomannans, $0.85–1.07 \times 10^{-7}$ mol/J, suggesting that they are less susceptible to degradation.

Several polysaccharides such as α D-glucose [4.58, 4.207–4.209], cellulose and its derivatives [4.1], amylose and starch [4.82, 4.209, 4.210], and chitin and chitosan [4.27, 4.211] have reportedly undergone degradation when subjected to radiation in their solid state.

In Sections 4.1 and 4.2, this chapter has only considered irradiation in oxygen-free conditions. However, in oxygenated solutions, the initially formed carbon-centred radicals such as those shown in Fig. 4.2 react with oxygen forming the corresponding peroxyl radicals (as shown in the first step of the reaction in Fig. 4.2). The latter may in turn undergo a variety of reactions, leading

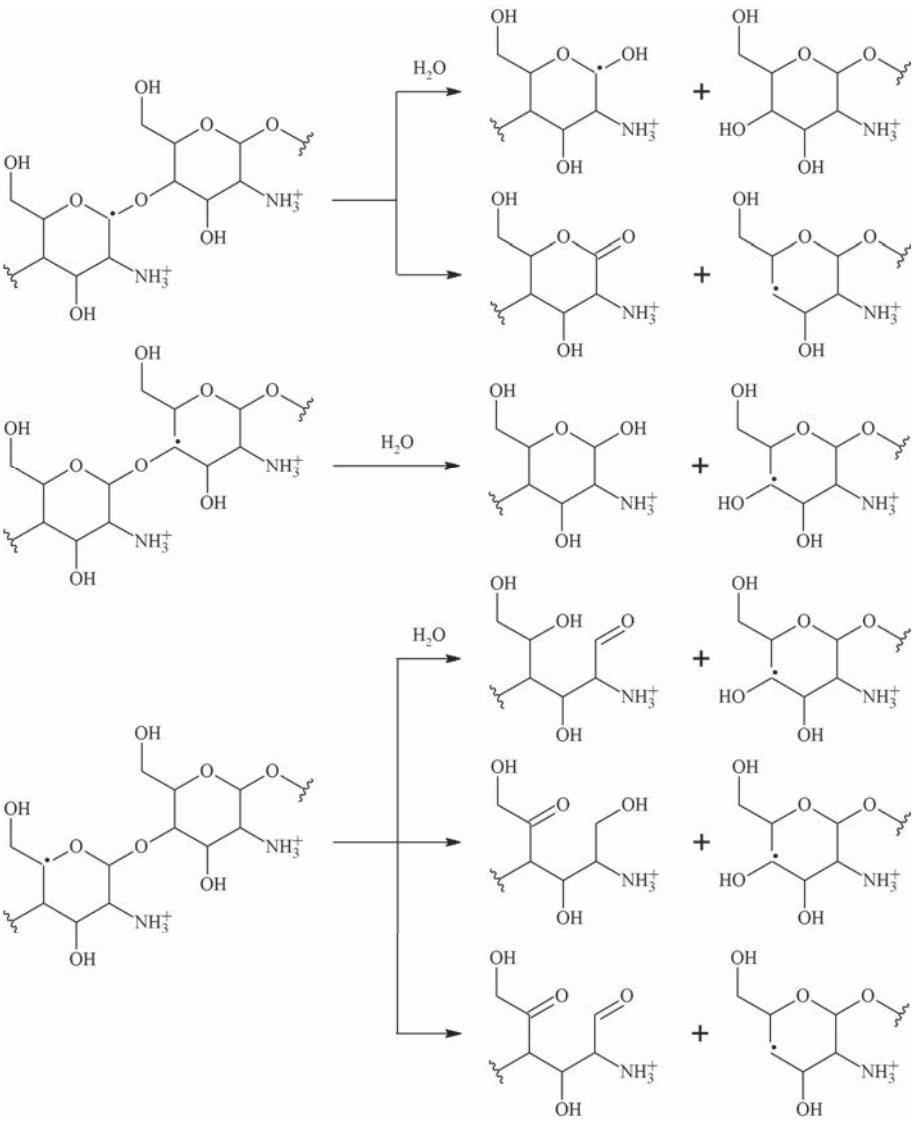

FIG. 4.3. Various hydrolysis, rearrangement and fragmentation reactions during radiolysis of chitosan in oxygen-free aqueous solution.

to chain breaks, ring opening and stable oxidation products typically containing carbonyl groups.

In contrast to many synthetic polymers that preferentially undergo cross-linking when irradiated in the absence of oxygen, and degrade when

irradiated in its presence, polysaccharides degrade when irradiated, irrespective of the presence or absence of oxygen. An interesting effect observed for a number of polysaccharides irradiated in solution is that the radiation-chemical yield of degradation, $G(s)$, tends to be lower in the presence of oxygen than in its absence. Such a protective effect, in contrast to the oxygen enhancement of degradation typical for synthetic polymers, has been observed for cellobiose [4.206, 4.212], hyaluronic acid [4.110, 4.111] and chitosan [4.21].

An example of a peroxyl radical reaction other than chain scission is shown below for chitosan. Peroxyl radicals located in an α position to a hydroxyl or amino group have a tendency to spontaneously eliminate $HO_2^{\bullet}/O_2^{-\bullet}$. A diagram of this reaction is shown in Fig. 4.4.

This effect can be utilized to quantify α hydroxyalkyl peroxyl radicals. The formation of $O_2^{\bullet-}$ can be monitored with tetranitromethane by following the formation of the nitroform anion, which absorbs strongly at 350 nm [4.213].

$$O_2^{-\bullet} + C(NO_2)_4 \rightarrow C(NO_2)_3^{-} + NO_2^{\bullet}$$

For chitosan, it has been found that the fraction of radicals eliminating $HO_2^{\bullet}/O_2^{-\bullet}$ is approx. 55%, while the expected fraction of H atoms abstracted by $HO^{\bullet}$ from the positions which can lead to α hydroxy or α amino radicals is 57%. This indicates that in fact $HO^{\bullet}$ attack on a polysaccharide is close to random, i.e. the probabilities of abstracting any one hydrogen atom are similar [4.21].

In oxygenated solutions, superoxide radicals are produced by hydrated electrons reacting with oxygen, and perhydroxyl radicals are formed by hydrogen atoms. The perhydroxyl radicals are generally unreactive with organic compounds unless they contain hydrogen that is weakly bonded [4.214, 4.215].

Superoxide radicals play an important role in joints affected by arthritis because they interact with the bio-polymers, such as hyaluronan, that lubricate the joint. Reference [4.114] reviews two potential mechanisms by which hydroxyl radicals are generated. These mechanisms involve the reaction of superoxide radicals in processes catalysed by metal ions, and their dismutation and subsequent reaction with hydrogen peroxide. These processes may influence

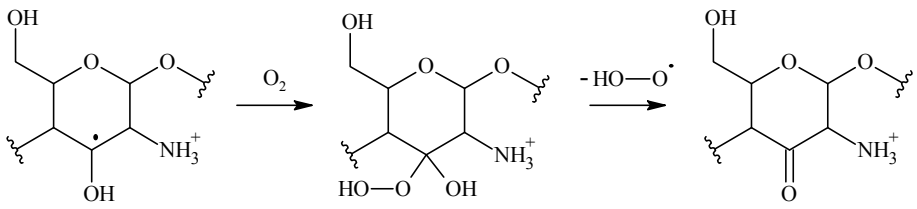

FIG. 4.4. Diagram of a peroxyl radical reaction in chitosan.

the radiolysis of polysaccharides in oxygen-containing aqueous solutions by increasing the yield of degradation in the presence of transition metal ions.

4.4. RADIATION GRAFTING ON POLYSACCHARIDES

Grafting is most often performed to combine valuable properties of two or more polymers, for instance, to link in a single material the good mechanical properties and low price of a commodity polymer with the desired special properties or functionalities at the surface. For example, the grafting of acrylic acid (AAc) onto polypropylene leads to a sturdy polymeric material with an hydrophilic, pH sensitive, ion-binding surface. The general mechanism and methods of radiation induced grafting are discussed in Section 3.5.2. Grafting on polysaccharides can be initiated by the use of high energy radiation such as gamma and EB. A few examples are described below.

Reference [4.216] reports the preparation of CMC in hydrogel form by grafting it with AAc under irradiation with EB in aqueous solution. EB irradiation initiates free radical polymerization of AAc on a backbone of CMC. The product of water radiolysis is helpful for abstracting protons from macromolecular backbones. The irradiation of CMC and the monomer produces free radicals that can combine to form a hydrogel. The authors suggested that such an AAc based hydrogel could be used for the recovery of metal ions such as copper, nickel, cobalt and lead. They also reported the use of hydrogels in skin dressings.

Reference [4.217] describes a starch based hydrogel prepared by grafting poly(vinyl alcohol) (PVA). Starch was first dissolved in water to form a gel-like solution, then added to a PVA solution, heated at 90°C for 30 mins and continuously stirred to form a homogeneous mixture. The investigation showed that there was a grafting reaction between PVA and starch molecules in addition to the cross-linking of the PVA molecules caused by irradiation. It was found that amylose of starch was an important reactive component, which also governed the properties of the starch/PVA blend hydrogel.

Reference [4.218] reports the preparation of thermo- and pH sensitive hydrogels from chitosan and *N*-isopropylacrylamide (NIPAAm) using graft copolymerization of chitosan. The grafting percentage and grafting efficiency was shown to increase in proportion with the monomer concentration and the total absorbed dose. The hydrogels that were prepared displayed good thermo- and pH sensitivity and swelling properties.

A new approach to grafting on polysaccharides has recently been proposed by Barsbay and Güven [4.219]. It is based on the combination of radiation initiation and controlled free radical polymerization techniques [4.220–4.222]. The main advantage of this method is that the graft chains are of uniform length.

This allows the preparation of surfaces with desired, tunable and well-defined properties. This approach has been used, for instance, to graft styrene and sodium 4-styrene sulphonate on cellulose [4.223, 4.224].

4.5. RADIATION CROSS-LINKING OF POLYSACCHARIDES

A generalization frequently met in the literature is that polysaccharides are classified as radiation-degrading polymers and degradation is the only direction of molecular weight change observed upon irradiation of polysaccharides. This is, in fact, true in most cases under typical conditions. While controlled radiation induced degradation of polysaccharides can be useful for many applications, it has been a longstanding desire of radiation and polymer chemists and technologists to design processes where polysaccharide chains could be cross-linked by radiation. This would allow for a full control (decrease and increase) of molecular weight by radiation techniques and, what is more important, for synthesizing polysaccharide based gels. Owing to the many beneficial properties of natural polymers, chiefly biocompatibility, biodegradability and derivation from sustainable resources, products that use them are expected to have a broad application range and in some aspects to have comparable or even better properties than gels based on synthetic polymers [4.225].

Within the last decade, a number of methods to achieve radiation induced cross-linking of polysaccharides have been invented and developed. Some of them are briefly described below. For other options, see Refs [4.54, 4.226, 4.227].

4.5.1. Cross-linking mediated by alkyne gas

References [4.184, 4.228] report a process that can modify natural polysaccharides such as CMC, GA, dextran and gelatin in the solid state using high energy radiation to first increase the molecular weight and then produce a hydrogel. The process uses ionizing radiation in the presence of an alkyne gas that serves as a meditator, and is illustrated in Fig. 4.5. It offers the possibility of modifying the structure of polysaccharides in a controlled manner, and could be applied to other similar substances.

The method has already been used with polysaccharides from a variety of origins and with a variety of structures, such as collagen, gelatin, casein and combinations of these with plant proteins. In these polymers, cross-linking occurs upon irradiation in the presence of acetylene gas, leading to the formation of macromolecules that have an increased molecular weight and improved functionalities. The increase in molecular weight may be four fold if the polysaccharide structure is highly branched at doses up to 10 kGy; doses up

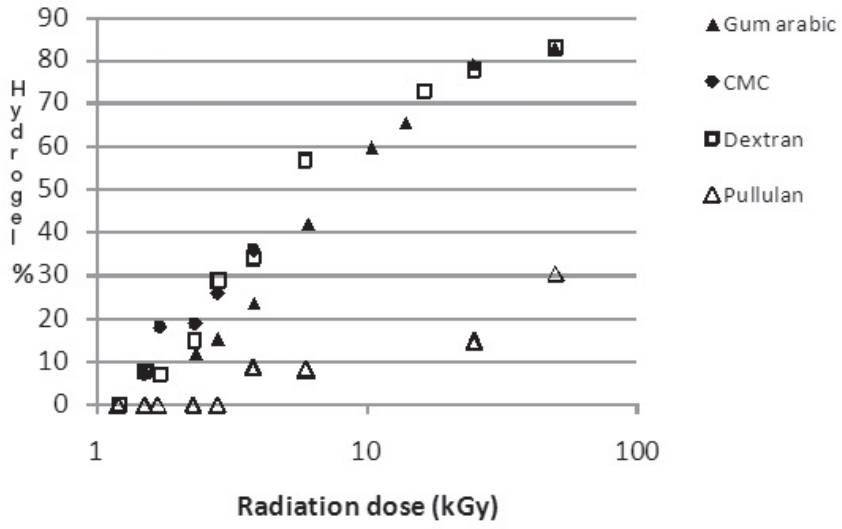

FIG. 4.5. Formation of hydrogel as a function of absorbed dose for polysaccharides irradiated in the solid state in the presence of alkyne gas. The percentage of hydrogel was calculated from the mass recovery obtained by the GPC multi angular laser light scattering method as described in Chapter 6.

to 50 kGy can produce hydrogels. If the polysaccharide structure is a straight chain, similar changes can be achieved at doses of 1–3 kGy. A dose of as much as 25 kGy may be needed to produce similar results in proteins.

A potential mechanism for cross-linking upon irradiation in the solid state is shown in Fig. 4.6. R_1H and R_2H are macromolecular chains. A free radical ($R_1^{\bullet}$) is produced by direct radiation and adds to the acetylene, producing a radical with a double bond. The addition takes places slowly. The resulting reactive radical with a double bond abstracts a hydrogen atom from a nearby polysaccharide chain to produce two radicals, one on the original acetylene adduct and another on a nearby polysaccharide chain ($R_2^{\bullet}$). The radicals recombine, creating a cross-linked stable radical with a fair degree of mobility. The stable radical either recombines with acetylene, with a radical generated by the action of the ionizing radiation or with another similar radical thereby forming a cross-linked network [4.228].

The irradiation of CMC in the solid state also shows that irradiation can be used to achieve structural changes. An initial mean of 1.55×10^5 Da is increased three fold to 4.44×10^5 Da at a dose of 1.5 kGy. Additionally, polydispersity increases from 2 to 2.8 and R_g from 36 nm to 52 nm. At the higher doses, a hydrogel is formed and can be seen in solution. The gelation of this solution, if controlled, can give stable gels and a range of consistencies from soft and pourable

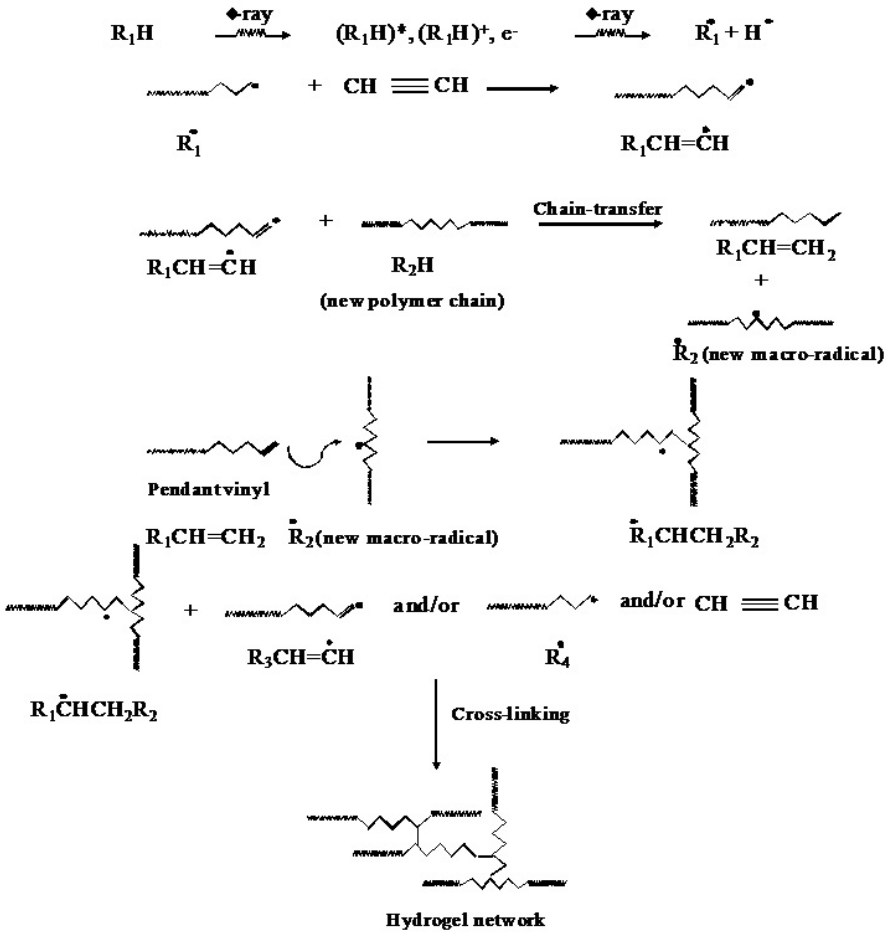

FIG. 4.6. Schematic illustration of radiation cross-linking in polymers in the solid state when irradiated in the atmosphere of acetylene.

to very firm can be achieved. A ten fold increase in G' and G'' can be achieved at a frequency of 0.1 Hz [4.184, 4.229]. The increase in molecular weight can be controlled, and hydrogel formation increases linearly with absorbed doses. As shown in Fig. 4.5, 83% hydrogel formation can be achieved at a dose of approximately 50 kGy and visco-elastic properties were shown to have increased. An increase in $\bar{M}_w$ from initial value of 2.34×10^6 Da to a maximum of 4.58×10^6 Da was observed [4.184].

The irradiation of pullulan, which is a hydrocolloid that is also slightly branched, showed that the $\bar{M}_w$ increases from 4.17×10^5 Da to 6.81×10^5 Da at a dose of 1.7 kGy and that, as shown in Fig. 4.5, 30% of the original substance was

converted to hydrogel. As expected with the increase in $\bar{M}_w$, the G' values show that the rheological properties are enhanced.

An investigation of gelatin found that its molecular weight can be increased if it is irradiated in the solid state. The increase in molecular weight and the resultant gelling properties can be varied, meaning that different products with different properties can be produced [4.184]. Identical behaviour has been induced in casein in the form of its sodium salt. The same processes can be applied to other polysaccharides such as xanthan, pectin, carrageenan, gellan, welan, GG, LBG, alginate, starch, heparin, chitin and chitosan [4.229, 4.230].

The modification of κ carrageenan by irradiation in the solid state shows that even without using gelling agents, hydrogel formation and increased visco-elasticity can be achieved [4.231]; the optimum dose range for this purpose is 5–10 kGy as the gel fraction is reduced by degradation caused by a higher dose. The irradiation of carrageenan led to the production of nearly 78% hydrogel with an improvement in viscosity nearly four fold that of control material. Visco-elasticity could be improved at moderate doses owing to the increased molecular weight and resultant formation of hydrogel. Following this modification by irradiation, the strength of κ carrageenan was shown to have increased compared with the control. The increase in strength was proportional with absorbed dose and reached its maximum at an absorbed dose of 5 kGy. The mechanical properties of the sample also improved owing to the aggregation of longer superhelical rods.

Various mixes of water soluble polymers, of both synthetic and natural origins, were investigated using the same technique and it was found that such mixes confer synergistic benefits on the functionalities of the mixes. For example, a 1:1 mixture of poly(N-vinylpyrrolidone) (PVP) and GA in the solid state was irradiated at 3.1 kGy and at 10.4 kGy, and a significant improvement in visco-elasticity (G') was achieved when the components were processed together compared with when they were processed separately. The results are shown in Fig. 4.7.

The same technique was applied to various mixed systems of water soluble polymers of synthetic and natural origin and the result showed synergistic effects on the functionalities of these mix systems. One such example is the irradiation of a mixture (1:1) of PVP and GA in the solid state, which was then prepared as a solution for rheological measurements.

4.5.2. Cross-linking in the paste-like state

As discussed earlier, in aqueous solutions of polymers, ionizing radiation interacts with the solute chiefly through indirect effect, i.e. involving transient species of water radiolysis. Water soluble polysaccharides subjected to

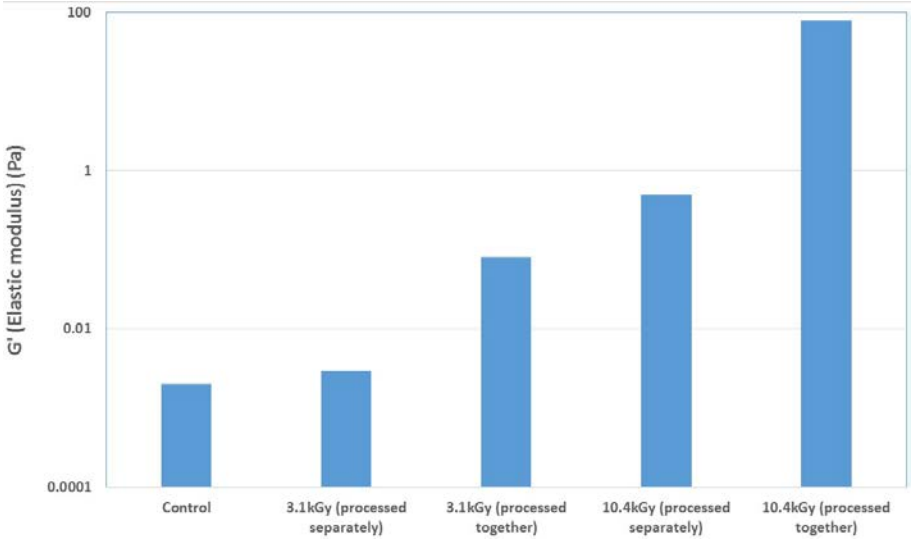

FIG. 4.7. Elastic modulus (G') at 0.1 Hz plotted as a function of oscillation frequency for 10% aqueous solution of a PVP-GA blend system modified in the solid state.

irradiation in diluted solutions undergo instant degradation, typically with a degradation yield greater than that for degradation in the solid state [4.26]. The search to cross-link polysaccharides without additives using irradiation has led to an innovative method, which relies on irradiation in the paste-like state. Several etherified cellulose derivatives with various values of DS with functional side groups irradiated in concentrated solutions were found [4.26] to undergo cross-linking simultaneously to the commonly observed degradation. In such cases water, besides generating radicals at a relatively high yield, acts as a plasticizer, allowing for a nearly unrestricted motion of polysaccharide segments and whole macromolecules. A certain mobility of chain segments is critical for the recombination of macroradicals, i.e. the cross-linking reaction, which results in an increase of the average molecular weight of the polymer. Thus, the presence of water definitely changes not only the mechanisms of energy transfer to macromolecules, but also the further reactions of macroradicals.

Hydroxypropyl cellulose, methyl cellulose (MC) and hydroxyethyl cellulose irradiated in concentrations exceeding 10–20% in water (depending on the irradiation conditions and initial molecular weight of the polymer) form hydrogels. For instance, hydroxyethyl cellulose polymers of DS 2.0 and weight-average molecular weight of 200 kDa, 310 kDa and 580 kDa irradiated by EB (vacuum-deaerated samples irradiated without access of air) form gels up to the maximum gel fraction 50–60%, for which gelation doses (D_g) were 21 kGy,

9.6 kGy and 4.6 kGy, respectively [4.14]. Similarly, for synthetic polymers cross-linked in aqueous solution, the maximum gel fraction that can be obtained for the same irradiation conditions does not depend on the initial molecular weight of the polymer, which, on the other hand, greatly affects the D_g.

A strong dependence of cross-linking and degradation yields on the concentration was observed for various polysaccharides exposed to ionizing radiation in aqueous solutions. CMC with a broad range of DS values irradiated by either gamma rays or EB easily forms hydrogels when irradiated in concentrated solutions. For instance, the yield of degradation during irradiation of aqueous solutions of CMC with a DS of 2.2 remains constant (0.5×10^{-7} mol/J) but the yield of cross-linking steadily increases (from 0.2×10^{-7} mol/J to 2.2×10^{-7} mol/J) with increasing concentration (at 10 wt% and 60 wt%, respectively; the limit is maintained homogeneity of the CMC–water mixture). Therefore, the maximum gel fraction increases, and the D_g decreases with increasing concentration (Figs 4.8 and 4.9) [4.2]. The possibility of the recombination of radicals on adjacent chains increases if the chains are in close proximity to one another (i.e. the concentration is high), especially when electrostatic repulsion of macromolecules is an obstacle, as in the case of polyions such as CMC.

DS by side groups plays an important role in directing pathways of radiation initiated reactions. In certain conditions, irradiation of CMC with a lower DS, e.g. 0.8, results in a somewhat smaller maximum gel fraction, which increases for CMC with higher DS. Also, for the same irradiation conditions, the D_g decreases with increasing DS of the CMC. This is evident because radicals created on side chains of polysaccharide derivatives participate in cross-linking reactions of the macromolecules [4.4].

The general conclusion can be drawn that high concentration and high DS of cellulose derivatives, and more generally, water soluble polysaccharides with certain functional groups, are beneficial for the radiation formation of gels, owing to the advantage of the cross-linking yield over the degradation yield. Both the high concentration and high DS of cellulose derivatives and, more generally, water soluble polysaccharides with certain functional groups favour cross-linking over degradation when they are irradiated, and are therefore appropriate for gel formation. This idea is schematically presented for the example of CMC irradiated in aqueous solution in Fig. 4.10. A relatively higher concentration is required to obtain macroscopic gel for CMC with lower DS, whereas for a high DS of 2.2, the gels are obtained at a concentration as low as 5 wt%.

The radiation processing of polysaccharides at high concentration have been further explored in other examples cross-linked by irradiation without additives, which include GA [4.185], carboxymethylated starch [4.81], CM chitin and chitosan [4.232, 4.233] and others (details given in Table 4.2).

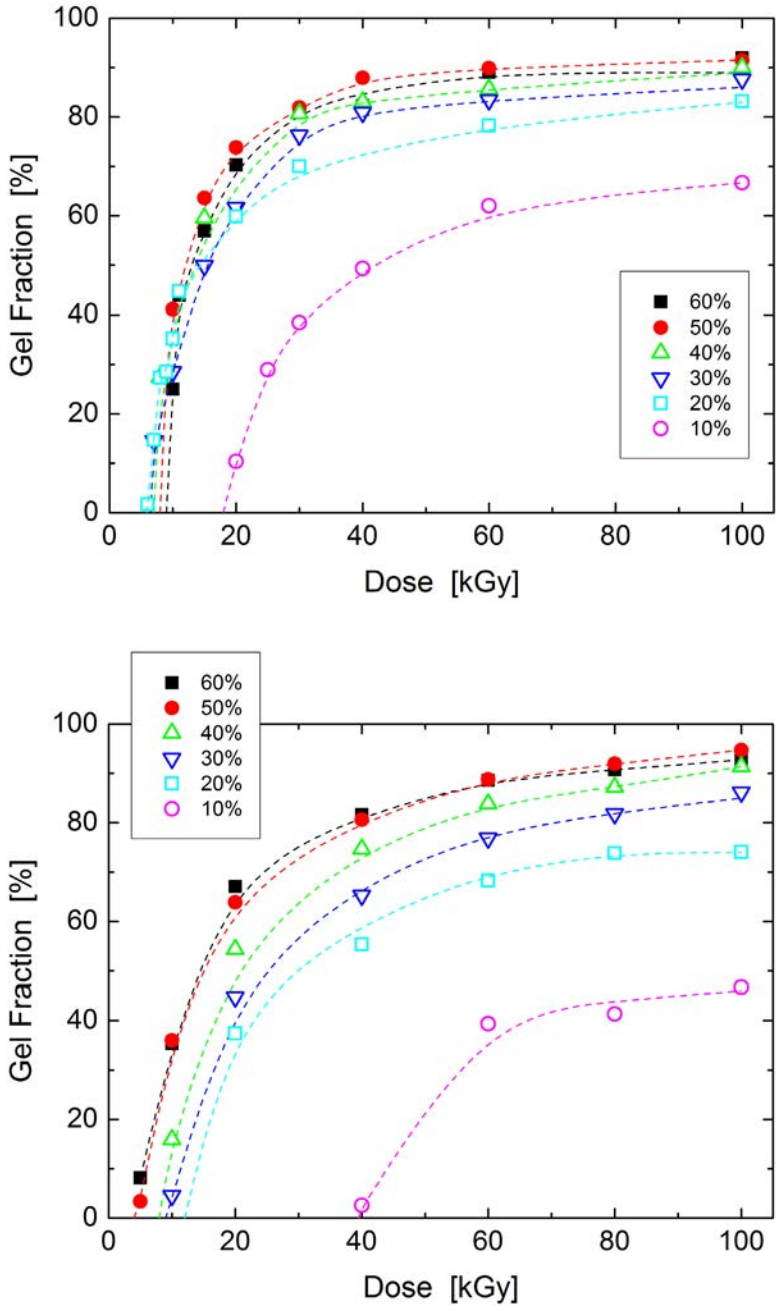

FIG. 4.8. Gel fraction as a function of dose and concentration of CMC (DS = 2.2) upon irradiation in oxygen-free solution by gamma rays (upper panel) and by EB (lower panel). CMC concentrations are indicated in the graph. Data from Ref. [4.2].

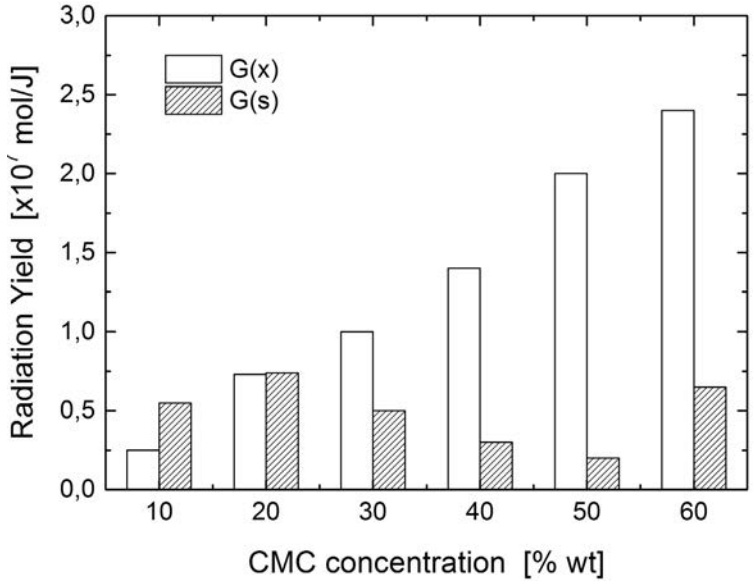

FIG. 4.9. Radiation-chemical yields of cross-linking G(x) and chain scission G(s) as a function of CMC (DS = 2.2) concentration for EB irradiation in deoxygenated aqueous solution. Data are from Ref. [4.2].

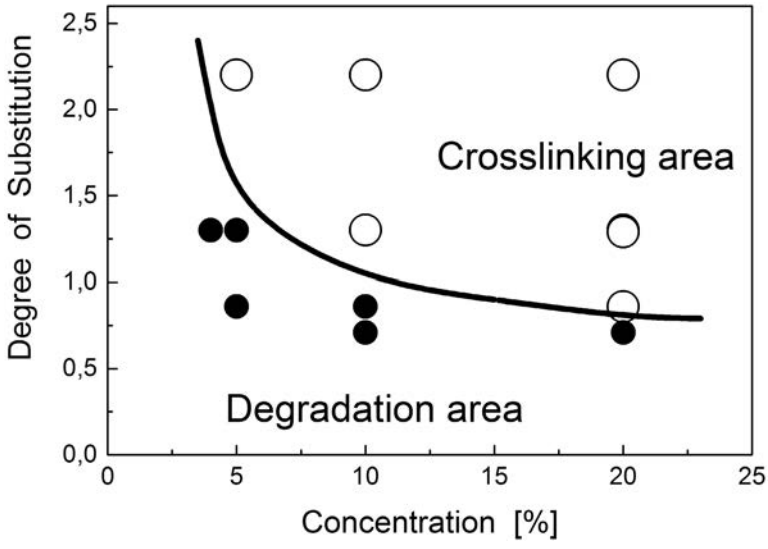

FIG. 4.10. Dependence of the dominating reaction (cross-linking vs. degradation) on concentration and DS of CMC. Data from Ref. [4.1].

TABLE 4.2. IRRADIATION OF DIFFERENT POLYMERS IN A PASTE-LIKE STATE WITH THE MAXIMUM AMOUNT OF HYDROGEL OBTAINED AND THEIR PROPOSED APPLICATIONS

Polymer	Maximum hydrogel yield	Proposed application	Reference
CMC	55% at 30 kGy	Wound care, anti-bedsore mats, superabsorbent for stock excrement	[4.1]
	50% at 80 kGy		[4.2]
	40% at 100 kGy		[4.234]
	60% at 80 kGy		[4.5]
CM chitin	70% at 100 kGy	Biomedical field	[4.233]
	70% at 80 kGy		[4.232]
CM chitosan	55% at 200 kGy	Biomedical field	[4.233]
	45% at 70 kGy		[4.232]
CM starch	70% at 10 kGy	Food and cosmetics	[4.82]
	40% at 2 kGy		[4.81]
Dihydroxypropyl chitosan	50% at 150 kGy		[4.235]
GA	50–60% at 49.8 kGy	Food, cosmetic, agricultural and hygienic materials	[4.185]
Hydroxyethyl cellulose	60% at 200 kGy		[4.14]
Hydroxypropyl cellulose	90% at 50 kGy		[4.13]
Methyl cellulose	65% at 50 kGy		[4.14]
Carageenan			[4.149]

As well as macroscopic hydrogels, nano-structures of cross-linked polysaccharide chains have also been developed [4.84]. Taking advantage of

knowledge of the concentration and dose rate factors influencing the outcome of radiation treatment, the conditions of irradiation of CM starch were chosen to promote intramolecular cross-linking. Such nanogels made of a natural polymer containing culture medium may be applied as an efficient feed or substrate for the culture of microorganisms or cells.

Dose rate is an important factor in radiation initiated reactions. For most polysaccharides (hydroxypropyl cellulose, hydroxyethyl cellulose, MC, CM chitosan), a high dose rate, i.e. irradiation with EB, is preferred. During processing with gamma rays, polysaccharides may also form cross-linked structures, but the maximum gel fraction is usually not as high as in the case of EB irradiation, the gelation dose is higher and in some cases (e.g. MC, hydroxyethyl cellulose) the gels degrade at higher absorbed doses [4.14, 4.232, 4.233]. On the other hand, CMC behaves in the same manner across a broad range of dose rates, from 1 kGy/h to 10 kGy/h to more than 10 kGy/min (Fig. 4.11). It was found that very stable radicals are responsible for these phenomena. Long lived radicals, with half-lives of tens of minutes, were detected by pulse radiolysis and laser flash photolysis methods, both with spectrometric detection [4.6, 4.236].

Another important factor, the pH of the solutions subjected to irradiation, deeply affects the susceptibility of ionic polysaccharides to cross-link. The

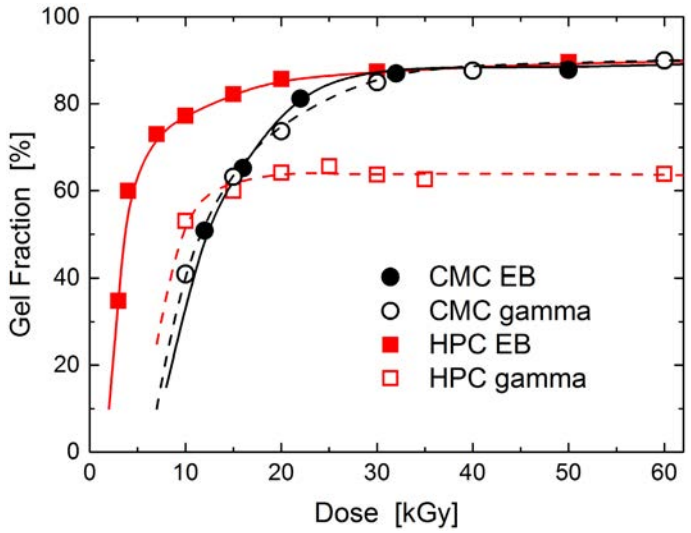

FIG. 4.11. Gel fraction as a function of dose in deoxygenated aqueous solutions of CMC ($\bar{M}_w$ = 5.2 × 10^5 Da, DS = 2.2, concentration 40%) and hydroxypropyl cellulose ($\bar{M}_w$ = 1.25 × 10^6 Da, DS = 3, concentration 20%) irradiated by gamma rays or EB. Data from Refs [4.2, 4.13].

neutralization of charges of the side groups greatly facilitates the recombination of radicals localized on distinct macromolecules. Therefore, a reduction of concentration of CMC may achieve efficient cross-linking when the ionic groups are in a neutral state. Irradiation even of dilute (e.g. 0.7%) solutions of CMC of a DS of 2.3 at a pH of 2 results in the formation of macroscopic gels. This is illustrated in Fig. 4.12, along with the equilibrium degree of swelling (mass of water embedded by 1 g dried gel, as determined after neutralization and the removal of the soluble material) of obtained CMC hydrogel [4.234, 4.237].

Gel is formed at doses as low as 1–2 kGy with a relatively high insoluble part, i.e. about 45%. In diluted solution when the polymer chains are kept at a certain distance from one another by electrostatic repulsion, radicals on the chains have very little possibility to recombine to form cross-linking bonds, despite their relatively long lifetime.

Therefore, not only concentration and DS, but also other factors, such as dose and dose rate and the pH of the solution subjected to irradiation, are important variables that, if correctly selected, facilitate the mechanism leading to the cross-linking of polysaccharides.

Similarly to networks based on synthetic polymers, polysaccharide based hydrogels formed by radiation techniques are susceptible to swelling in appropriate media. The manner of swelling is characteristic for radiation formed hydrogels; that is, the degree of swelling is the highest just after the network has been created and decreases sharply with increasing absorbed dose when

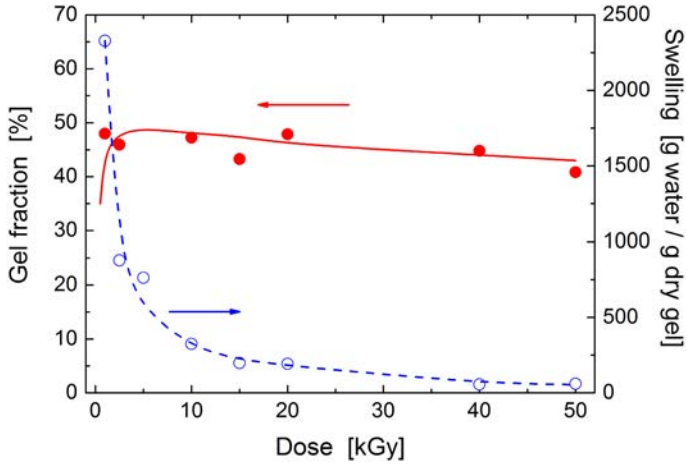

FIG. 4.12. Gel fraction and equilibrium degree of swelling as a function of dose in EB irradiated N_2O saturated solutions of CMC ($\overline{M}_w$ = 7.4 × 10^5 Da, DS 2.34, pH 2 ($HClO_4$), CMC concentration 0.7% wt/wt.) [4.235].

the number of cross-links increases, resulting in a firm gel with smaller voids within the mesh. Hydrogels of polysaccharides that undergo stimuli responsive transitions retain these characteristics. For instance, networks of temperature responsive hydroxypropyl cellulose reveal quite a broad transition at approx. 40°C, below which the gel is in a swollen state, while at a higher temperature, the gel contracts rapidly [4.13]. Poly-ion based gels are prone to swelling–shrinking behaviour depending on the pH and ionic strength of the environment. CMC gels exist in a swollen form at a pH over the pK_a value of carboxyl groups, which for polysaccharides bearing these anionic groups is usually about 4.2–4.4. Below this specific pH, the hydrogel reduces its volume several folds for CMC of a DS of 2.2 formed from 30 wt% aqueous solution by gamma rays at a dose of 100 kGy [4.4]. For this polymer, the degree of swelling reduces continuously with the increasing ionic strength of the immersing solution. Gels of polysaccharides with two distinct ionic groups of opposite charge may reveal two transitions as a function of change of medium pH in their swelling characteristics. Hydrogels of CM chitosan bearing carboxyl groups (DS 0.96) and amine groups (DDA 94%) formed in 30 wt% aqueous solution by EB irradiation at 30 kGy reveal pH responsive swelling (Fig. 4.13 [4.233]). Expansion of the network is due to ionization of one of the groups — the electrostatic repulsion of charges on the macromolecules causes maximum extension of the cross-linked chains, which is limited by the tensile contraction of the polymer network. Whereas in a solution of a pH between 3 and 6, the hydrogel tends to reduce in size owing to mutual

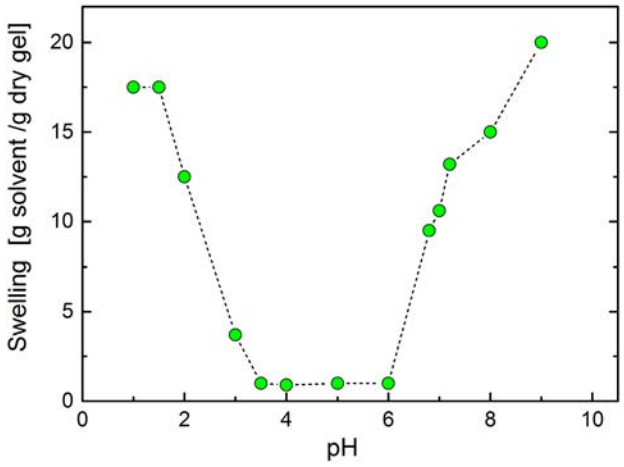

FIG. 4.13. Swelling of CM chitosan gel obtained by radiation cross-linking as a function of pH of the swelling medium. Data are from Ref. [4.233].

neutralization of the charges, the attraction of functional groups with opposite charges contracts the gel. The % hydrogel produced by irradiation of various polysaccharides together with their proposed applications are summarized in Table 4.2.

The basic mechanism of polysaccharide cross-linking in a paste-like state can be summarized as follows. Since such a system, in general, comprises a significant fraction of a polymer, radicals generated on polymer chains result either from the direct effect of radiation when radiation interacts directly with a polymer or from an indirect effect involving the products of water radiolysis, predominantly OH radicals. In such a system, the concentration of polymer should be optimum, i.e. the higher the concentration, the better, yet assuring uniform hydration of chains, without clusters devoid of water molecules, to ensure that polymeric material is well plastified with water, i.e. in order to reduce segmental mobility restictions. At the same time chains are at the closest possible distance for the polysaccharide radicals to recombine and form a cross-linked hydrogel network. The concentration needed for the modification depends on the structure, DS, distribution of substitution group and initial molecular weight. The other important factor contributing to gel formation is the DS — a higher DS is advantageous for cross-linking. Besides the fact that, in some cases, substituting groups can make macromolecules more hydrophilic, the radicals localized on side chain methylene groups may participate in recombination resulting in cross-linking bond formation. Other conditions such as temperature and especially the pH variation of the solution influence the yield of cross-linking and degradation, as they may directly control conformation of the macromolecules.

4.6. POST-IRRADIATION EFFECTS

When a polysaccharide is irradiated in solution, free radical reactions are fast and occur in principle only during irradiation. When irradiation is stopped, radicals decay almost instantly (although some exceptions to this rule may be found, see e.g. Refs [4.6, 4.238–4.241] for discussion of long lived polymer radicals in aqueous medium), and radiation effects cease just after irradiation.

However, if a partially crystalline polysaccharide is irradiated in the solid state (or in any other state where the partially crystalline structure is retained), some of the initially formed radicals may become trapped in crystalline regions and may remain there for a long time (hours, months or even longer) after irradiation [4.242]. These ‘frozen’ radicals may slowly migrate to the boundaries of crystalline regions, where they may undergo reactions governed by similar mechanisms to those occurring directly under irradiation. Besides the very slow migration, other processes (changes in crystalline structure due to external

conditions and migration of traces of water) may make these dormant radicals available for reaction. Post-irradiation effects may occur for samples irradiated and stored both in the presence and absence of oxygen.

Figure 4.14 shows changes in the number-average molecular weight of chitosan following gamma irradiation. A slow but distinct decrease of molecular weight is observed, indicating chain scission taking place for a few weeks after irradiation [4.41, 4.243].

Protecting a polysaccharide against such post-irradiation effects is difficult. Typically, one cannot melt crystallites without destroying the polysaccharide by thermal degradation. One may destroy the radicals by dissolving and recovering chitosan after irradiation, but when performing the synthesis on a large scale, this may be a costly operation.

Post-irradiation processes should be taken into consideration in applications of radiation technology for polysaccharide processing or sterilization if the crystalline phase is present during irradiation (typically when solid polysaccharides are irradiated). These processes may lead to long term changes in properties and may reduce the shelf life of products. This could be mitigated to some extent by the proper planning of radiation processing, taking post-irradiation effects into account, i.e. by degrading a polysaccharide to the upper limit of the useful range of molecular weight, and allowing the post-irradiation effects to

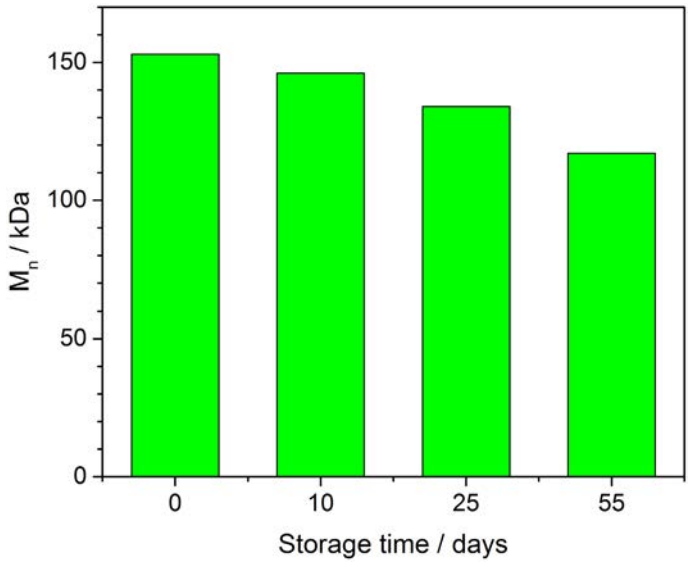

FIG. 4.14. Number-average molecular weight of chitosan as a function of time after gamma irradiation (50 kGy). Sample irradiated and stored in air (based on Ref. [4.243]).

cause a very slow degradation while the molecular weight still remains in the acceptable range for a relatively long time.

For more detailed information, the reader is directed to reviews of the radiation chemistry of carbohydrates [4.20, 4.33, 4.66, 4.197, 4.244–4.248] and references cited therein.

ACKNOWLEDGEMENTS

This work has been supported in part by the National Science Centre, Poland, as part of project 2012/07/B/ST4/01429. P. Ulanski thanks P. Sawicki (Institute of Applied Radiation Chemistry, Lodz) for assistance in preparing some of the reaction drawings.

REFERENCES TO CHAPTER 4

[4.1] FEI, B., WACH, R.A., MITOMO, H., YOSHII, F., KUME, T., Hydrogel of biodegradable cellulose derivatives. I. Radiation-induced crosslinking of CMC, J. Appl. Polym. Sci. **78** 2 (2000) 278–283.

[4.2] WACH, R.A., MITOMO, H., YOSHII, F., KUME, T., Hydrogel of biodegradable cellulose derivatives. II. Effect of some factors on radiation-induced crosslinking of CMC, J. Appl. Polym. Sci. **81** 12 (2001) 3030–3037.

[4.3] LIU, P., ZHAI, M., LI, J., PENG, J., WU, J., Radiation preparation and swelling behavior of sodium carboxymethyl cellulose hydrogels, Radiat. Phys. Chem. **63** 3–6 (2002) 525–528.

[4.4] WACH, R.A., MITOMO, H., NAGASAWA, N., YOSHII, F., Radiation crosslinking of carboxymethylcellulose of various degree of substitution at high concentration in aqueous solutions of natural pH, Radiat. Phys. Chem. **68** 5 (2003) 771–779.

[4.5] YOSHII, F., et al., Hydrogels of polysaccharide derivatives crosslinked with irradiation at paste-like condition, Nucl. Instr. Meth. B **208** 1–4 (2003) 208–320.

[4.6] WACH, R.A., et al., Rate constants of reactions of carboxymethylcellulose with hydrated electron, hydroxyl radical and the decay of CMC macroradicals. A pulse radiolysis study, Polymer **45** 24 (2004) 8165–8171.

[4.7] LIU, P., PENG, J., LI, J., WU, J., Radiation crosslinking of CMC-Na at low dose and its application as substitute for hydrogel, Radiat. Phys. Chem. **72** 5 (2005) 635–638.

[4.8] CHOI, J., et al., Controlling the radiation degradation of carboxymethylcellulose solution, Polym. Degrad. Stab. **93** 1 (2008) 310–315.

[4.9] CHOI, J., et al., Effect of electron beam irradiation on the viscosity of carboxymethylcellulose solution, Nucl. Instr. Meth. B **266** 23 (2008) 5068–5071.

[4.10] SEBERT, P., BOURNY, E., ROLLET, M., Gamma irradiation of carboxymethylcellulose: Technological and pharmaceutical aspects, Int. J. Pharm. **106** 2 (1994) 103–108.
[4.11] LEE, H.S., et al., Investigation on radiation degradation of carboxymethylcellulose by ionizing irradiation, Appl. Radiat. Isot. **67** 7–8 (2009) 1513–1515.
[4.12] YE, J., PEI, Y., Degradation of carboxymethyl cellulose (CMC) in solid state by electron beams, Nucl. Techn. **35** 7 (2012) 512–514.
[4.13] WACH, R.A., MITOMO, H., YOSHII, F., KUME, T., Hydrogel of radiation-induced cross-linked hydroxypropylcellulose, Macromol. Mater. Eng. **287** 4 (2002) 285–295.
[4.14] WACH, R.A., MITOMO, H., NAGASAWA, N., YOSHII, F., Radiation crosslinking of methylcellulose and hydroxyethylcellulose in concentrated aqueous solutions, Nucl. Instr. Meth. B **211** 4 (2003) 533–544.
[4.15] WACH, R.A., MITOMO, H., YOSHII, F., ESR investigation on gamma-irradiated methylcellulose and hydroxyethylcellulose in dry state and in aqueous solution, J. Radioanal. Nucl. Chem. **261** 1 (2004) 113–118.
[4.16] PEKEL, N., YOSHII, F., KUME, T., GÜVEN, O., Radiation crosslinking of biodegradable hydroxypropylmethylcellulose, Carbohyd. Polymer **55** 2 (2004) 139–147.
[4.17] FURUSAWA, K., et al., Structural and kinetic modification of aqueous hydroxypropylmethylcellulose (HPMC) induced by electron beam irradiation, Phys. A: Statist. Mech. Appl. **353** 1–4 (2005) 9–20.
[4.18] SEBERT, P., ANDRIANOFF, N., ROLLET, M., Effect of gamma irradiation on hydroxypropylmethylcellulose powders: Consequences on physical, rheological and pharmacotechnical properties, Int. J. Pharm. **99** 1 (1993) 37–42.
[4.19] ERSHOV, B.G., et al., Radiation destruction of chitin, Russ. J. Appl. Chem. **66** (1993) 540–545.
[4.20] ERSHOV, B.G., Radiation-chemical degradation of cellulose and other polysaccharides, Russ. Chem. Rev. **67** (1998) 353–375.
[4.21] ULANSKI, P., VON SONNTAG, C., OH-Radical-induced chain scission of chitosan in the absence and presence of dioxygen, J. Chem. Soc. Perkin Trans. 2 **2000** (2000) 2022–2028.
[4.22] JARRY, C., et al., Effects of steam sterilization on thermogelling chitosan-based gels, J. Biomed. Mat. Res. **58** 1 (2001) 127–135.
[4.23] JARRY, C., LEROUX, J.C., HAECK, J., CHAPUT, C., Irradiating or autoclaving chitosan/polyol solutions: Effect on thermogelling chitosan-β-glycerophosphate systems, Chem. Pharm. Bull. **50** 10 (2002) 1335–1340.
[4.24] CHOI, S.W., AHN, J.K., LEE, W.D., BYUN, W.M., PARK, J.H., Preparation of chitosan oligomers by irradiation, Polym. Degrad. Stabil. **78** (2002) 533–538.
[4.25] YOKSAN, R., AKASHI, M., MIYATA, M., CHIRACHANCHAI, S., Optimal gamma-ray dose and irradiation conditions for producing low-molecular-weight chitosan that retains its chemical structure, Radiat. Res. **161** 4 (2004) 471–480.
[4.26] CZECHOWSKA-BISKUP, R., ROKITA, B., ULANSKI, P., ROSIAK, J.M., Radiation-induced and sonochemical degradation of chitosan as a way to increase its fat-binding capacity, Nucl. Instr. Meth. B **236** (2005) 383–390.

[4.27] WASIKIEWICZ, J.M., YOSHII, F., NAGASAWA, N., WACH, R.A., MITOMO, H., Degradation of chitosan and sodium alginate by gamma radiation, sonochemical and ultraviolet methods, Radiat. Phys. Chem. **73** 5 (2005) 287–295.

[4.28] HUANG, L., ZHAI, M., PENG, J., LI, J., WEI, G., Radiation-induced degradation of carboxymethylated chitosan in aqueous solution, Carbohyd. Polymer **67** 3 (2007) 305–312.

[4.29] KANG, B., DAI, Y., ZHANG, H., CHEN, D., Synergetic degradation of chitosan with gamma radiation and hydrogen peroxide, Polym. Degrad. Stabil. **92** 3 (2007) 359–362.

[4.30] ZHAO, L., MITOMO, H., Radiation effects on dihydroxypropyl-chitosan, Polym. Degrad. Stabil. **93** 8 (2008) 1607–1610.

[4.31] EL-SAWY, N.M., ABD EL-REHIM, H.A., ELBARBARY, A.M., HEGAZY, E.S.A., Radiation-induced degradation of chitosan for possible use as a growth promoter in agricultural purposes, Carbohyd. Polymer **79** 3 (2010) 555–562.

[4.32] VANICHVATTANADECHA, C., et al., Effect of gamma radiation on dilute aqueous solutions and thin films of N-succinyl chitosan, Polym. Degrad. Stabil. **95** 2 (2010) 234–237.

[4.33] MAKUUCHI, K., Critical review of radiation processing of hydrogel and polysaccharide, Radiat. Phys. Chem. **79** (2010) 267–271.

[4.34] PASANPHAN, W., RIMDUSIT, P., CHOOFONG, S., PIROONPAN, T., NILSUWANKOSIT, S., Systematic fabrication of chitosan nanoparticle by gamma irradiation, Radiat. Phys. Chem. **79** 10 (2010) 1095–1102.

[4.35] DUY, N.N., PHU, D.V., ANH, N.T., HIEN, N.Q., Synergistic degradation to prepare oligochitosan by gamma-irradiation of chitosan solution in the presence of hydrogen peroxide, Radiat. Phys. Chem. **80** 7 (2011) 848–853.

[4.36] HIEN, N.Q., PHU, D.V., DUY, N.N., LAN, N.T.K., Degradation of chitosan in solution by gamma irradiation in the presence of hydrogen peroxide, Carbohyd. Polymer **87** 1 (2012) 935–938.

[4.37] TAHTAT, D., MAHLOUS, M., BENAMER, S., NACER KHODJA, A., LARBI YOUCEF, S., Effect of molecular weight on radiation chemical degradation yield of chain scission of gamma-irradiated chitosan in solid state and in aqueous solution, Radiat. Phys. Chem. **81** 6 (2012) 659–665.

[4.38] KUME, T., TAKEHISA, M., "Effect of gamma-irradiation on chitosan", Proc. 2nd Int. Conf. on Chitin and Chitosan, Sapporo, Japan, 1982 (1982) 66–70.

[4.39] PLISKO, E.A., SHCHELKUNOVA, L.I., NUD'GA, L.A., Changes in the properties of chitosan under the action of gamma-irradiation, Zh. Prikl. Khim. **50** (1977) 2040–2044 (in Russian).

[4.40] ERSHOV, B.G., ISAKOVA, O.V., ROGOZHIN, S.V., GAMZAZADE, A.I., LEONOVA, E.U., Radiation-chemical transformations of chitosan, Dokl. Akad. Nauk SSSR **295** (1987) 1152–1156 (in Russian).

[4.41] ROSIAK, J.M., ULANSKI, P., KUCHARSKA, M., DUTKIEWICZ, J., JUDKIEWICZ, L., Radiation sterilization of chitosan sealant for vascular prostheses, J. Radioanal. Nucl. Chem. **159** (1992) 87–96.

[4.42] WENWEI, Z., XIAOGUANG, Z., LI, Y., YUEFANG, Z., JIAZHEN, S., Some chemical changes in chitosan induced by gamma-ray irradiation, Polym. Degrad. Stabil. **41** 1 (1993) 83–84.
[4.43] SUKHOV, N.L., ESR spectra of gamma-irradiated chitosan and its complexes with metals, High Energy Chem. **32** 5 (1998) 290–293.
[4.44] HAI, L., DIEP, T.B., NAGASAWA, N., YOSHII, F., KUME, T., Radiation depolymerization of chitosan to prepare oligomers, Nucl. Instr. Meth. B **208** 1–4 (2003) 466–470.
[4.45] RAMNANI, S.P., CHAUDHARI, C.V., PATIL, N.D., SABHARWAL, S., Synthesis and characterization of crosslinked chitosan formed by gamma irradiation in the presence of carbontetrachloride as a sensitizer, J. Polym. Sci. Pol. Chem. **42** 15 (2004) 3897–3909.
[4.46] DESAI, K.G., HYUN, J.P., Study of gamma-irradiation effects on chitosan microparticles, Drug Deliv. **13** 1 (2006) 39–50.
[4.47] CZECHOWSKA-BISKUP, R., et al., Diet supplement based on radiation-modified chitosan and radiation-synthesized polyvinylpyrrolidone microgels. Influence on the liver weight in rats fed fat- and cholesterol-rich diet, J. Appl. Polym. Sci. **105** (2007) 169–176.
[4.48] TAHTAT, D., UZUN, C., MAHLOUS, M., GÜVEN, O., Beneficial effect of gamma irradiation on the N-deacetylation of chitin to form chitosan, Nucl. Instr. Meth. B **265** 1 (2007) 425–428.
[4.49] HUANG, L., PENG, J., ZHAI, M., LI, J., WEI, G., Radiation-induced changes in carboxymethylated chitosan, Radiat. Phys. Chem. **76** 11–12 (2007) 1679–1683.
[4.50] KIM, M.K., CHOI, Y.J., NOH, I., Control of chitosan molecular weight with cyclotron ion beam irradiation, J. Phys. Chem. Solids, **69** 5–6 (2008) 1577–1580.
[4.51] KIM, M.S., CHOI, Y.J., PARK, H.S., NOH, I., Analysis of chitosan irradiated with high-energy cyclotron ion beams, J. Phys. Chem. Solids **69** 5–6 (2008) 1569–1572.
[4.52] GRYCZKA, U., et al., The mechanism of chitosan degradation by gamma and e-beam irradiation, Radiat. Phys. Chem. **78** 7–8 (2009) 543–548.
[4.53] ZELINSKA, K., SHOSTENKO, A.G., TRUSZKOWSKI, S., Radiolysis of chitosan, High Energy Chem. **43** 6 (2009) 501–504.
[4.54] RAMAPRASAD, A.T., et al., Preparation of crosslinked chitosan by electron beam irradiation in the presence of CCl_4, J. Appl. Polym. Sci. **111** 2 (2009) 1063–1068.
[4.55] ZAINOL, I., AKIL, H.M., MASTOR, A., Effect of gamma irradiation on the physical and mechanical properties of chitosan powder, Mat. Sci. Eng. C **29** 1 (2009) 292.
[4.56] TASKIN, P., CANISAG, H., SEN, M., The effect of degree of deacetylation on the radiation induced degradation of chitosan, Radiat. Phys. Chem. **94** (2013) 236–239.
[4.57] PHILLIPS, G.O., Advances in Carbohydrates, Academic Press (1961).
[4.58] PHILLIPS, G.O., BAUGH, P., Molecular environment effects in the radiation decomposition of a-D-glucose, Nature **198** 4877 (1963) 282–283.
[4.59] NAKAMURA, Y., OGIWARA, Y., PHILLIPS, G.O., Free radical formation and degradation of cellulose by ionizing radiations, Polym. Photochem. **6** (1985) 135–159.
[4.60] TOTH, T., BORSA, J., TAKACS, E., Effect of preswelling on radiation degradation of cotton cellulose, Radiat. Phys. Chem. **67** 3–4 (2003) 513–515.

[4.61] BLOUIN, F.A., ARTHUR, J.C., Jr., The effects of gamma radiation on cotton, Textile Res. J. **28** (1958) 198–204.
[4.62] PHILLIPS, G.O., MOODY, G.J., The chemical action of gamma radiation on aqueous solutions of carbohydrates, Int. J. Appl. Radiat. Is. **6** C (1959) 78–85.
[4.63] PHILLIPS, G.O., BAUGH, P.J., MCKELLAR, J.F., VON SONNTAG, C., "Interaction of radiation with cellulose in the solid state", Cellulose Chemistry and Technology (ARTHUR, J.C., Jr., Ed.), ACS Symposium Series No. 48, American Chemical Society, Washington, DC (1977) 313–333.
[4.64] DAVID, C., DARO, A., MONNOYE, D., Utilization of waste cellulose. I. Gamma irradiation and hydrolysis with dilute sulphuric acid, Eur. Polym. J. **16** 12 (1980) 1159–1166.
[4.65] BEARDMORE, D.H., FAN, L.T., LEE, Y.H., Gamma-ray irradiation as a pretreatment for the enzymatic hydrolysis of cellulose, Biotechnol. Lett. **2** 10 (1980) 435–438.
[4.66] ERSHOV, B.G., KLIMENTOV, A.S., The radiation chemistry of cellulose, Russ. Chem. Rev. **53** (1984) 1195–1207.
[4.67] DZIEDZIELA, W.M., KOTYNSKA, D.J., Functional groups in gamma-irradiated cellulose, Radiat. Phys. Chem. **23** 6 (1984) 723–725.
[4.68] SULTANOV, K., ESR spectra of native cellulose gamma-irradiated at 300K, Vysokomol. Soedin. B **33** 5 (1991) 392.
[4.69] KUZINA, S.I., et al., Effect of gamma-rays on the properties of the cellulose nitrate detector, Eur. Polym. J. **27** 7 (1991) 703–706.
[4.70] CHIPARA, M.I., et al., ESR investigations of electron-beam irradiated cellulose nitrate, Radiat. Meas. **23** 4 (1994) 709–714.
[4.71] KUDOH, H., SASUGA, T., SEGUCHI, T., KATSUMURA, Y., High-energy-ion-irradiation effects on polymer materials: 4. The sensitivity of cellulose triacetate and poly(methyl methacrylate), Polym. J. **37** 14 (1996) 2903–2908.
[4.72] TAKACS, E., et al., Effect of gamma-irradiation on cotton-cellulose, Radiat. Phys. Chem. **55** 5–6 (1999) 663–666.
[4.73] ILLER, E., KUKIELKA, A., STUPILSKA, H., MIKOLAJCZYK, W., Electron-beam stimulation of the reactivity of cellulose pulps for production of derivatives, Radiat. Phys. Chem. **63** 3–6 (2002) 253–257.
[4.74] KOVALEV, G.V., BUGAENKO, L.T., The plasticizing effect of water on gamma-irradiated cellulose, Polym. Sci. B **44** 3–4 (2002) 108–110.
[4.75] EMMI, S.S., et al., Formation of radical cations and dose response of a-terthiophene-cellulose triacetate films irradiated by electrons and gamma rays, Radiat. Phys. Chem. **63** 1 (2002) 53–58.
[4.76] MAGGI, L., et al., Chemical and physical stability of hydroxypropylmethylcellulose matrices containing diltiazem hydrochloride after gamma irradiation, J. Pharm. Sci. **92** 1 (2003) 131–141.
[4.77] DUBEY, K.A., PUJARI, P.K., RAMNANI, S.P., KADAM, R.M., SABHARWAL, S., Microstructural studies of electron beam-irradiated cellulose pulp, Radiat. Phys. Chem. **69** 5 (2004) 395–400.
[4.78] DRISCOLL, M., et al., Electron beam irradiation of cellulose, Radiat. Phys. Chem. **78** 7–8 (2009) 539–542.

[4.79] KAMEYA, H., NAKAMURA, H., UKAI, M., SHIMOYAMA, Y., Electron spin resonance spectroscopy of gamma-irradiated glucose polymers, Appl. Magn. Reson. **40** 3 (2011) 395–404.
[4.80] SUN, J., XU, L., GE, M., ZHAI, M., Radiation degradation of microcrystalline cellulose in solid status, J. Appl. Polym. Sci. **127** 3 (2013) 1630–1636.
[4.81] NAGASAWA, N., YAGI, T., KUME, T., YOSHII, F., Radiation crosslinking of carboxymethyl starch, Carbohyd. Polym. **58** 2 (2004) 109–113.
[4.82] YOSHII, F., KUME, T., Process for Producing Cross-linked Starch Derivatives and Cross-linked Starch Derivatives Produced by the Same, United States Patent 6,617,448, Int. Cl. C08B 31/00 (20060101), Sep. 2003, filed May 2001, available on-line.
[4.83] ZHAI, M., YOSHII, F., KUME, T., Radiation modification of starch-based plastic sheets, Carbohyd. Polym. **52** 3 (2003) 311–317.
[4.84] BINH, D., PHAM THI, T.H., NGUYEN, N.D., NGUYEN, T.D., NGUYEN, N.D., A study on size effect of carboxymethyl starch nanogel crosslinked by electron beam radiation, Radiat. Phys. Chem. **81** 7 (2012) 906–912.
[4.85] MISHINA, A., NIKUNI, Z., Physical and chromatographical observations of gamma-irradiated potato starch granules, Nature **184** 4702 (1959) 1867.
[4.86] ABAGYAN, G.V., KRUTOVA, Y., PUTILOVA, I.N., BUTYAGIN, P.Y., Investigation of free radicals in gamma-irradiated starch by the method of electron paramagnetic resonance, Biophysics **12** 5 (1967) 943–946.
[4.87] RAFFI, J.J., AGNEL, J.-P.L., Influence of the physical structure of irradiated starches on their electron spin resonance spectra kinetics, J. Phys. Chem. **87** (1983) 2369–2373.
[4.88] FEDOROVA, G.A., PETROV, P.T., Degradation of carboxymethylstarch under the action of gamma-radiation, Chem. Nat. Compd. **21** 1 (1985) 9–12.
[4.89] KANG, I.J., et al., Production of modified starches by gamma irradiation, Radiat. Phys. Chem. **54** 4 (1999) 425–430.
[4.90] BERTOLINI, A.C., MESTRES, C., COLONNA, P., RAFFI, J., Free radical formation in UV- and gamma-irradiated cassava starch, Carbohyd. Polym. **44** 3 (2001) 269–271.
[4.91] SHISHONOK, M.V., et al., Structure and properties of electron-beam irradiated potato starch, High Energy Chem. **41** 6 (2007) 425–429.
[4.92] CHUNG, H.J., LIU, Q., Effect of gamma irradiation on molecular structure and physicochemical properties of corn starch, J. Food Sci. **74** 5 (2009) 353–361.
[4.93] CHUNG, H.J., LIU, Q., Molecular structure and physicochemical properties of potato and bean starches as affected by gamma-irradiation, Int. J. Biol. Macromol. **47** 2 (2010) 214–222.
[4.94] SINGH, S., SINGH, N., EZEKIEL, R., KAUR, A., Effects of gamma-irradiation on the morphological, structural, thermal and rheological properties of potato starches, Carbohyd. Polym. **83** 4 (2011) 1521–1528.
[4.95] GANI, A., BASHIR, M., WANI, S.M., MASOODI, F.A., Modification of bean starch by gamma-irradiation: Effect on functional and morphological properties, LWT - Food Sci. Technol. **49** 1 (2012) 162–169.
[4.96] NEMTANU, M.R., BRASOVEANU, M., Radio-sensitivity of some starches treated with accelerated electron beam, Starch **64** 6 (2012) 435–440.

[4.97] LEE, J.S., EE, M.L., CHUNG, K.H., OTHMAN, Z., Formation of resistant corn starches induced by gamma-irradiation, Carbohyd. Polym. **97** 2 (2013) 614–617.
[4.98] BAUGH, P.J., KERSHAW, K., PHILLIPS, G.O., Radiation chemistry of carbohydrates. Part XVII. Radical processes following gamma-irradiation of frozen concentrated solutions of sucrose and D-glucose at 77 K, J. Chem. Soc. B: Phys. Org. (1970) 1482–1489.
[4.99] KAWAKISHI, S., KITO, Y., NAMIKI, M., Deoxy sugars produced by gamma-irradiation of hexoses in oxygen-free, aqueous solution, Carbohyd. Res. **30** (1973) 220–222.
[4.100] KAWAKISHI, S., KITO, Y., NAMIKI, M., Gamma radiolysis of D-glucose in aerated, aqueous solution, Carbohydr. Res. **39** 2 (1975) 263–269.
[4.101] MATSUYAMA, T., MENHOFER, H., HEUSINGER, H., ESR spin trap investigations on aqueous glucose solutions irradiated by ultrasound and gamma-rays, Int. J. Rad. Appl. Instrum. **32** 6 (1988) 735–739.
[4.102] HEUSINGER, H., Gel-permeation chromatography of solutions of d-glucose after irradiation by ultrasound and gamma-rays, Carbohyd. Res. **209** C (1991) 109–118.
[4.103] PORTENLÄNGER, G., HEUSINGER, H., Polymer formation from aqueous solutions of alpha-D-glucose by ultrasound and gamma-rays, Ultrason. Sonochem. **1** (1994) 125–129.
[4.104] SCHILLER, J., ARNHOLD, J., SCHWINN, J., SPRINZ, H., BREDE, O., ARNOLD, K., Reactivity of cartilage and selected carbohydrates with hydroxyl radicals, Free Rad. Res. **28** (1998) 215–228.
[4.105] KAWAKISHI, S., KITO, Y., NAMIKI, M., Formation of 1-deoxy-D-threo-2,5-hexodiulose by radiation induced chain reaction in crystalline D-fructose, Agr. Biol. Chem. **39** (1975) 1897–1898.
[4.106] THLERY, C.J., AGNEL, J., FREJAVILLE, C.M., RAFFI, J.J., Electron spin resonance spin-trapping analysis of gamma-induced radicals in polycrystalline a-D-glucose, J. Phys. Chem **87** 22 (1983) 4485–4488.
[4.107] ABAGYAN, G.V., APRESYAN, A.S., Reaction routes of free radicals in gamma-irradiated alpha-D-glucose, High Energy Chem. **36** 4 (2002) 229–235.
[4.108] SHARPATYI, V.A., Radiation chemistry of polysaccharides: 1. Mechanisms of carbon monoxide and formic acid formation, High Energy Chem. **37** (2003) 369–372.
[4.109] CABALLERO, I., CASTILLO, A., NAYDENOV, V., TILQUIN, B., Radiosensitivity study of glucose and trehalose to gamma irradiation, Am. Pharma. Rev. **8** 4 (2005) 50.
[4.110] MYINT, P., DEEBLE, D.J., BEAUMONT, P.C., BLAKE, S.M., PHILLIPS, G.O., The reactivity of various free radicals with hyaluronic acid: steady-state and pulse radiolysis studies, Biochim. Biophys. Acta **925** (1987) 194–202.
[4.111] DEEBLE, D.J., et al., The kinetics of hydroxyl-radical-induced strand breakage of hyaluronic acid. A pulse radiolysis study using conductometry and laser-light-scattering, Z. Naturforsch. **45c** (1990) 1031–1043.
[4.112] DEEBLE, D.J., PHILLIPS, G.O., BOTHE, E., SCHUCHMANN, H.-P., VON SONNTAG, C., The radiation-induced degradation of hyaluronic acid, Radiat. Phys. Chem. **37** (1991) 115–118.

[4.113] REHAKOVA, M., BAKOS, D., SOLDAN, M., VIZAROVA, K., Depolymerization reactions of hyaluronic acid in solution, Int. J. Biol. Macromol. **16** (1994) 121–124.
[4.114] AL-ASSAF, S., et al., The enhanced stability of the cross-linked hylan structure to the hydroxyl (OH) radicals compared with the uncross-linked Hyaluran, Radiat. Phys. Chem. **46** (1995) 207–217.
[4.115] AL-ASSAF, S., HAWKINS, C.L., PARSONS, B.J., DAVIES, M.J., PHILLIPS, G.O., Identification of radicals from hyaluronan (hyaluronic acid) and crosslinked derivatives using electron paramagnetic resonance spectroscopy, Carbohyd. Polym. **38** 1 (1999) 17–22.
[4.116] AL-ASSAF, S., MEADOWS, J., PHILLIPS, G.O., WILLIAMS, P.A., PARSONS, B.J., The effect of hydroxyl radicals on the rheological performance of hylan and hyaluronan, Int. J. Biol. Macromol. **27** 5 (2000) 337–348.
[4.117] AL-ASSAF, S., NAVARATNAM, S., PARSONS, B.J., PHILLIPS, G.O., Chain scission of hyaluronan by carbonate and dichloride radical anions: Potential reactive oxidative species in inflammation? Free Radical Bio. Med. **40** 11 (2006) 2017–2018.
[4.118] STERN, R., KOGAN, G., JEDRZEJAS, M.J., SOLTES, L., The many ways to cleave hyaluronan, Biotechnol. Adv. **25** (2007) 537–580.
[4.119] LAL, M., Radiation induced depolymerization of hyaluronic acid (HA) in aqueous solutions at pH7.4, J. Radioanal. Nucl. Chem. **92** (1985) 105.
[4.120] ARMAND, G., BAUGH, P.J., BALAZS, E.A., PHILLIPS, G.O., Radiation protection of hyaluronic acid in the solid state, Radiat. Res. **64** 3 (1975) 573–580.
[4.121] CHOI, J., KIM, J.K., KIM, J.H., KWEON, D.K., LEE, J.W., Degradation of hyaluronic acid powder by electron beam irradiation, gamma ray irradiation, microwave irradiation and thermal treatment: A comparative study, Carbohyd. Polym. **79** 4 (2010) 1080–1085.
[4.122] SYNYTSYA, A., et al., Raman spectroscopic study on sodium hyaluronate: An effect of proton and gamma irradiation, J. Raman Spec. **42** 3 (2011) 544–550.
[4.123] RAKHIMOV, D.A., KRISTALLOVICH, E., SADYKOV, M.U., MALIKOVA, M.K., Degradation of a glucomannan and a mannan under the action of gamma-radiation, Chem. Nat. Comp. **26** 1 (1990) 90–92.
[4.124] JUMEL, K., HARDING, S.E., MITCHELL, J.R., Effect of gamma irradiation on the macromolecular integrity of guar gum, Carbohyd. Res. **282** (1996) 223–236.
[4.125] PAN, T., et al., Synergetic degradation of konjac glucomannan by gamma-ray irradiation and hydrogen peroxide, Carbohyd. Polym. **93** 2 (2013) 761–767.
[4.126] ISSARANI, R., NAGORI, B.P., Effect of gamma radiation on solution viscosity of galactomannans: Influence of galactose: mannose ratio, Indian J. Chem Techn. **12** 1 (2005) 105–107.
[4.127] SEN, M., YOLACAN, B., GUVEN, O., Radiation-induced degradation of galactomannan polysaccharides, Nucl. Instr. Meth. B **265** (2007) 429–433.
[4.128] PRAWITWONG, P., TAKIGAMI, S., PHILLIPS, G.O., Effects of gamma-irradiation on molar mass and properties of Konjac mannan, Food Hydrocoll. **21** 8 (2007) 1362–1367.

[4.129] XU, Z., SUN, Y., YANG, Y., DING, J., PANG, J., Effect of gamma-irradiation on some physiochemical properties of konjac glucomannan, Carbohyd. Polym. **70** 4 (2007) 444–450.
[4.130] LI, B., et al., Effect of gamma irradiation on the condensed state structure and mechanical properties of konjac glucomannan/chitosan blend films, Carbohyd. Polym. **83** 1 (2011) 44–51.
[4.131] JIAN, W., et al., Study on preparation and separation of Konjac oligosaccharides, Carbohyd. Polym. **92** 2 (2013) 1218–1224.
[4.132] HUMPHREYS, E.R., HOWELLS, G.R., Degradation of sodium alginate by gamma-irradiation and by oxidative-reductive depolymerization, Carbohyd. Res. **16** 1 (1971) 65–69.
[4.133] LEO, W.J., McLOUGHLIN, A.J., MALONE, D.M., Effects of sterilization treatments on some properties of alginate solutions and gels, Biotechnol. Progr. **6** 1 (1990) 51–53.
[4.134] REVINA, A.A., TSYBA, I.A., PARAMONOVA, L.I., NEKHOROSHEV, M.V., Radiation stability of alginic acid and sodium alginate, Radiatsionnaya Biol. Radioekol. **36** 3 (1996) 380–386 (in Russian).
[4.135] HIEN, N.Q., et al., Growth-promotion of plants with depolymerized alginates by irradiation, Radiat. Phys. Chem. **59** 1 (2000) 97–101.
[4.136] NAGASAWA, N., MITOMO, H., YOSHII, F., KUME, T., Radiation-induced degradation of sodium alginate, Polym. Degrad. Stabil. **69** (2000) 279–285.
[4.137] LEE, D.W., et al., Effect of gamma-irradiation on degradation of alginate, J. Agr. Food Chem. **51** 16 (2003) 4819–4823.
[4.138] SONG, E.J., et al., Effect of gamma irradiation on the physical properties of alginic acid and l-carrageenan, J. Korean Soc. Food Sci. Nut. **36** 7 (2007) 902–907.
[4.139] EL-DIN, H.M.N., EL-NAGGAR, A.W.M., Characterization of gamma irradiated concentrated aqueous solutions of chitosan/sodium alginate blends and their drug uptake-release characters, J. Appl. Polym. Sci. **122** 4 (2011) 2383–2390.
[4.140] HUQ, T., et al., Effect of gamma radiation on the physico-chemical properties of alginate-based films and beads, Radiat. Phys. Chem. **81** 8 (2012) 945–948.
[4.141] LUAN, L.Q., HA, V.T.T., UYEN, N.H.P., TRANG, L.T.T., HIEN, N.Q., Preparation of oligoalginate plant growth promoter by gamma irradiation of alginate solution containing hydrogen peroxide, J. Agric. Food Chem. **60** 7 (2012) 1737–1741.
[4.142] PURWANTO, Z.I., BROEK, L.A.M.V., SCHOLS, H.A., PILNIK, W., VORAGEN, A.G.J., Degradation of low molecular weight fragments of pectin and alginates by gamma-irradiation, Acta Aliment. **27** 1 (1998) 29–42.
[4.143] ALISTE, A.J., VIEIRA, F.F., DEL MASTRO, N.L., Radiation effects on agar, alginates and carrageenan to be used as food additives, Radiat. Phys. Chem. **57** 3–6 (2000) 305–308.
[4.144] SEN, M., RENDEVSKI, S., KAVAKLI, P.A., SEPEHRIANAZAR, A., Effect of G/M ratio on the radiation-induced degradation of sodium alginate, Radiat. Phys. Chem. **79** 3 (2010) 279–282.
[4.145] SEN, M., Effects of molecular weight and ratio of guluronic acid to mannuronic acid on the antioxidant properties of sodium alginate fractions prepared by radiation-induced degradation, Appl. Radiat. Isotopes **69** 1 (2011) 126–129.

[4.146] EL-MOHDY, H.L.A., Radiation-induced degradation of sodium alginate and its plant growth promotion effect, Arab. J. Chem. (in press).
[4.147] ABAD, L., OKABE, S., KOIZUMI, S., SHIBAYAMA, M., Small-angle neutron scattering study on irradiated kappa carrageenan, Phys. B: Cond. Mat. **381** 1–2 (2006) 103–108.
[4.148] ABAD, L.V., et al., Rate constants of reactions of kappa-carrageenan with hydrated electron and hydroxyl radical, Nucl. Inst. Meth. Phys. Res. B **265** 1 (2007) 410–413.
[4.149] ABAD, L., et al., Comparative studies on the conformational change and aggregation behavior of irradiated carrageenans and agar by dynamic light scattering, Int. J. Biol. Macromol. **42** 1 (2008) 55–61.
[4.150] ABAD, L.V., et al., Radiation degradation studies of carrageenans, Carbohyd. Polym. **78** 1 (2009) 100–106.
[4.151] ABAD, L.V., et al., Radiolysis studies of aqueous kappa-carrageenan, Nucl. Instr. Meth. B **268** 10 (2010) 1607–1612.
[4.152] ABAD, L.V., RELLEVE, L.S., RACADIO, C.D.T., ARANILLA, C.T., DE LA ROSA, A.M., Antioxidant activity potential of gamma irradiated carrageenan, Appl. Radiat. Isotopes **79** (2013) 73–79.
[4.153] ABAD, L.V., et al., Dynamic light scattering studies of irradiated kappa carrageenan, Int. J. Biol. Macromol. **34** 1–2 (2004) 81–88.
[4.154] ABAD, L.V., NASIMOVA, I.R., ARANILLA, C.T., SHIBAYAMA, M., Light scattering studies of irradiated kappa- and iota-carrageenan, Radiat. Phys. Chem. **73** 1 (2005) 29–37.
[4.155] RELLEVE, L., et al., Degradation of carrageenan by radiation, Polym. Deg. Stab. **87** 3 (2005) 403–410.
[4.156] PHILLIPS, G.O., MOODY, G.J., Radiation chemistry of carbohydrates. Part II. Irradiation of aqueous solutions of dextran with gamma radiation, J. Chem. Soc. (1958) 3534–3539.
[4.157] BAUGH, P.J., MORGAN, R.E., KERSHAW, K., PHILLIPS, G.O., Radical processes following gamma-irradiation of frozen concentrated matrices of heparin and dextran sulphate, Radiat. Res. **46** 1 (1971) 217–225.
[4.158] KOMAR, V.P., BONDARENKO, N.T., ZHBANKOV, R.G., MARKEVICH, S.V., Use of IR spectroscopy for studying the structure of gamma-irradiated dextran, J. Appl. Spec. **27** 2 (1977) 1014–1016.
[4.159] KROH, J., PLONKA, A., Electron trapping in frozen gels gamma-irradiated at 77 K, Chem. Phys. Lett. **52** 2 (1977) 371–373.
[4.160] KOVALIOV, G.V., SINITSYN, A.P., BUGAENKO, L.T., Destruction of dextran under the action of gamma radiation, Vestnik Mosk. Univ. Seriya 2 Khimiya **38** 5 (1997) 357.
[4.161] KOVALEV, G.V., SINITSYN, A.P., BUGAENKO, L.T., Degradation and crosslinking of dextran in aqueous solutions by gamma-radiolysis: The role of degree of polymerization, High Energy Chem. **33** 4 (1999) 213–217.
[4.162] KOVALEV, G.V., SINITSYN, A.P., BUGAENKO, L.T., Degradation and crosslinking of dextran in aqueous solutions by gamma-radiolysis: The effect of polymer concentration, High Energy Chem. **33** 6 (1999) 370–373.

[4.163] KOVALEV, G.V., SINITSYN, A.P., BUGAENKO, L.T., Degradation and crosslinking of dextran in aqueous solutions by gamma-radiolysis: The effect of hydrogen ions, High Energy Chem. **34** 2 (2000) 74–79.
[4.164] DZAMIC, M.D., JANKOVIC, B.R., Radiation effects in pectins, Int. J. Appl. Radiat. Isot. **17** 10 (1966) 561–566.
[4.165] BACHMAN, S., ZEGOTA, A., ZEGOTA, H., Radiation sterilization of dextran irradiated in the dry state, Probl. Tech. w Med. **4** 4 (1973) 331–337.
[4.166] WAHBA, I.J., TALLMAN, D.F., MASSEY, J., Radiation-induced gelation of dilute aqueous pectin solutions, Science **139** 3561 (1963) 1297–1298.
[4.167] ZHAO, M., MOY, J., PAULL, R.E., Effect of gamma-irradiation on ripening papaya pectin, Postharvest Bio. Tech. **8** 3 (1996) 209–222.
[4.168] YU, L., REITMEIER, C.A., LOVE, M.H., Strawberry texture and pectin content as affected by electron beam irradiation, J. Food Sci. **61** 4 (1996) 844–846.
[4.169] ZEGOTA, H., The effect of gamma-irradiation on citrus pectin in N_2O and N_2O/O_2 saturated aqueous solutions, Food Hydrocoll. **13** 1 (1999) 51–58.
[4.170] ZEGOTA, H., Some quantitative aspects of hydroxyl radical induced reactions in gamma-irradiated aqueous solutions of pectins, Food Hydrocoll. **16** 4 (2002) 353–361.
[4.171] MUNARIN, F., BOZZINI, S., VISAI, L., TANZI, M.C., PETRINI, P., Sterilization treatments on polysaccharides: Effects and side effects on pectin, Food Hydrocoll. **31** 1 (2013) 74–84.
[4.172] JO, C., KANG, H., LEE, N.Y., KWON, J.H., BYUN, M.W., Pectin- and gelatin-based film: Effect of gamma irradiation on the mechanical properties and biodegradation, Radiat. Phys. Chem. **72** 6 (2005) 745–750.
[4.173] ALTMANN, G., EISENBERG, E., BOGOKOWSKY, B., Radiation sterilization of triple sugar iron agar, Int. J. Appl. Radiat. Isot. **30** 9 (1979) 527–529.
[4.174] BOGOKOWSKY, B., EISENBERG, E., ALTMANN, G., Sterilization of MacConkey agar and CLED medium by gamma-radiation, Int. J. Appl. Radiat. Isot. **34** 10 (1983) 1441–1443.
[4.175] LARISCH, W., et al., Proton beam writing of microstructures in Agar gel for patterned cell growth, Nucl. Instrum. Meth. B **269** 20 (2011) 2444–2447.
[4.176] DOSHI, Y.A., RAO, P.S., Stable agar by gamma irradiation, Nature **216** 5118 (1967) 931–932.
[4.177] NISIZAWA, M., Studies on irradiation of agar agar in the solid state: on the changes of melting point of the agar agar hydrogel and setting point of the agar agar hydrosol produced by irradiation, Radiat. Eff. **24** 3 (1975) 177–185.
[4.178] NISIZAWA, M., Studies on irradiation of agar-agar in the solid state. On the changes of visible absorption spectra and viscosity of the agar-agar/iodine complex produced by irradiation, Radiat. Phys. Chem. **19** 2 (1982) 131–135.
[4.179] NISIZAWA, M., Studies on irradiation of agar-agar in the solid state: On the changes of colloid titration value of agar-agar hydrosol produced by irradiation, Radiat. Phys. Chem. **26** 2 (1985) 227–228.
[4.180] NISIZAWA, M., Studies on irradiation of agar-agar in the solid state: On the changes of water holding capacity of agar-agar hydrogel produced by irradiation, J. Appl. Polym. Sci. **36** 7 (1988) 1673–1676.

[4.181] NISIZAWA, M., HIRANO, T., Studies on irradiation of agar-agar in the solid state. On the changes of textural property of agar-agar hydrogel produced by irradiation, J. Polym. Sci. Part C, Polym. Let. **27** 4 (1989) 123–125.

[4.182] NISIZAWA, M., HIRANO, T., Studies on irradiation of agar-agar in the solid state. On the changes of X-ray diffraction of agar-agar film produced by irradiation, J. Appl. Polym. Sci. **39** 10 (1990) 2173–2178.

[4.183] NISIZAWA, M., Studies on irradiation of agar-agar in the solid state. On the changes of thermal property of agar-agar hydrogel produced by irradiation, J. Appl. Polym. Sci. **42** 10 (1991) 2713–2716.

[4.184] AL-ASSAF, S., PHILLIPS, G.O., WILLIAMS, P.A., Controlling the molecular structure of food hydrocolloids, Food Hydrocoll. **20** 2–3 (2006) 369–377.

[4.185] KATAYAMA, T., NAKAUMA, M., TODORIKI, S., PHILLIPS, G.O., TADA, M., Radiation-induced polymerization of gum arabic (*Acacia senegal*) in aqueous solution, Food Hydrocoll. **20** 7 (2006) 983–989.

[4.186] BLAKE, S.M., DEEBLE, D.J., PHILLIPS, G.O., PLESSY, A.D., The effect of sterlizing doses of g-irradiation on the molecular weight and emulsification properties of gum arabic, Food Polysacch. **2** (1988) 407–415.

[4.187] AL-RAWI, A.M., MUSLIH, R.M., AL-HARITHY, R.S., Estimating gamma-rays dose using computer, Radiat. Phys. Chem. **35** 4–6 (1990) 754–756.

[4.188] TSUYOSHI, K., MAKOTO, N., SETSUKO, T., MIKIRO, T., Effects of irradiation by electron beam on physical properties of food polysaccharides, Nippon Shokuhin Kagaku Kogaku Kaishi **52** 8 (2005) 373–379 (in Japanese).

[4.189] FARAG ZAIED, S., MOHAMED YOUSSEF, B., DESOUKY, O., SALAH EL DIEN, M., Decontamination of gum arabic with gamma-rays or electron beams and effects of these treatments on the material, Appl. Radiat. Isot. **65** 1 (2007) 26–31.

[4.190] PARSONS, B.J., PHILLIPS, G.O., THOMAS, B., WEDLOCK, D.J., CLARKESTURMAN, A.J., Depolymerization of xanthan by iron-catalyzed free-radical reactions, Int. J. Biol. Macromol. **7** (1985) 187–192.

[4.191] BYUN, E.H., et al., Effects of gamma irradiation on the physical and structural properties of beta-glucan, Radiat. Phys. Chem. **77** (2008) 781–786.

[4.192] KIM, J.H., et al., Effects of gamma-irradiation on immunological activities of beta-glucan, Food Sci. Biotech. **18** 5 (2009) 1305–1309.

[4.193] SUNG, N.Y., et al., Immune-enhancing activities of low molecular weight beta-glucan depolymerized by gamma irradiation, Radiat. Phys. Chem. **78** 7–8 (2009) 433–436.

[4.194] SANDULA, J., EBRINGEROVA, A., PRUZINEC, J., The effect of gamma-radiation on yeast cell wall glucans, J. Radioanal. Nucl. Chem. **144** 4 (1990) 287–295.

[4.195] VODENICAROVA, M., DRIMALOVA, G., HROMADKOVA, Z., MALOVIKOVA, A., EBRINGEROVA, A., Xyloglucan degradation using different radiation sources: A comparative study, Ultrason. Sonochem. **13** 2 (2006) 157–164.

[4.196] PATEL, T.R., et al., Global conformation analysis of irradiated xyloglucans, Carbohyd. Polym. **74** 4 (2008) 845–851.

[4.197] VON SONNTAG, C., The Chemical Basis of Radiation Biology, Taylor and Francis, London (1987).

[4.198] BUXTON, G.V., GREENSTOCK, C.L., HELMAN, W.P., ROSS, A.B., Critical review of rate constants for reactions of hydrated electrons, hydrogen atoms and hydroxyl radicals ($OH^{\bullet}/O^{-}$) in aqueous solution, J. Phys. Chem. Ref. Data **17** (1988) 513.

[4.199] GILBERT, B.C., KING, D.M., THOMAS, C.B., Radical reactions of carbohydrates. Part 2. An electron spin resonance study of the oxidation of D-glucose and related compounds with the hydroxyl radical, J. Chem. Soc. Perkin Trans. **2** (1981) 1186–1199.

[4.200] GILBERT, B.C., KING, D.M., THOMAS, C.B., The oxidation of some polysaccharides by the hydroxyl radical: An E.S.R. investigation, Carbohyd. Res. **125** (1984) 217–235.

[4.201] BEHZADI, A., BORGWARDT, U., HENGLEIN, A., SCHAMBERG, E., SCHNABEL, W., Pulsradiolytische Untersuchung der Kinetik diffusionkontrollierter Reaktionen des OH-Radikals mit Polymeren und Oligomeren in wäßriger Lösung, Ber. Bunsenges. phys. Chem. **74** (1970) 649.

[4.202] MATHESON, M.S., MAMOU, A., SILVERMAN, J., RABANI, J., Reaction of hydroxyl radicals with polyehylene oxide in aqueous solution, J. Phys. Chem. **77** (1973) 2420–2424.

[4.203] BEHZADI, A., SCHNABEL, W., Kinetic studies on the influence of conformation and chain length on the reaction of hydroxy radicals with poly(acrylic acid) in solution, Macromol. **6** (1973) 824–826.

[4.204] ULANSKI, P., ZAINUDDIN, ROSIAK, J.M., Pulse radiolysis of poly(ethylene oxide) in aqueous solution. I. Formation of macroradicals, Radiat. Phys. Chem. **46** (1995) 913–916.

[4.205] BARTOSZEK, N., ULANSKI, P., ROSIAK, J.M., Reaction of a low-molecular-weight free radical with a flexible polymer chain: Kinetic studies on the OH + poly(N -vinylpyrrolidone) model, Int. J. Chem. Kinet. **43** 9 (2011) 474–481.

[4.206] ZEGOTA, H., VON SONNTAG, C., Radiation chemistry of carbohydrates, XV. OH radical induced scission of the glycosidic bond in disaccharides, Z. Naturforsch. **32b** (1977) 1060–1067.

[4.207] PHILLIPS, G.O., BAUGH, P.J., LOFROTH, G., Energy transport in carbohydrates. Part II. Radiation decomposition of D-glucose, J. Chem. Soc. A: Inorg., Phys. Theor. (1966) 377–387.

[4.208] MOORE, J.S., PHILLIPS, G.O., Radiation studies of aryl glucosides, Carbohyd. Res. **16** (1971) 79–87.

[4.209] PHILLIPS, G.O., "Energetics and Mechanisms in Radiation Biology", Radiation Effects on Carbohydrates, Academic Press, London (1968).

[4.210] PHILLIPS, G.O., YOUNG, M., Energy transport in carbohydrates. Part III. Chemical effects of gamma-radiation on the cycloamyloses, J. Chem. Soc. A: Inorg., Phys. Theor. (1966) 383–387.

[4.211] KUANG, Q.L., ZHAO, J.C., NIU, Y.H., ZHANG, J., WANG, Z.G., Celluloses in an ionic liquid: the rheological properties of the solutions spanning the dilute and semidilute regimes, J. Phys. Chem. B **112** (2008) 10234–10240.

[4.212] SCHUCHMANN, M.N., VON SONNTAG, C., The effect of oxygen on the OH-radical-induced scission of the glycosidic linkage of cellobiose, Int. J. Radiat. Biol. **34** (1978) 397–400.

[4.213] ASMUS, K.-D., HENGLEIN, A., EBERT, M., KEENE, J.P., Pulsradiolytische Untersuchung schneller Reaktionen von hydratisierten Elektronen, freien Radikalen und Ionen mit Tetranitromethan in wässriger Lösung, Ber. Bunsenges. physik. Chem. **68** (1964) 657–663.

[4.214] BIELSKI, B.H.J., GEBICKI, J.M., Species in irradiated oxygenated water, Adv. Radiat. Chem. **2** (1970) 177–280.

[4.215] BIELSKI, B.H.J., CABELLI, D.E., ARUDI, R.L., ROSS, A.B., Reactivity of $HO_2^{\bullet}$/$O_2^{-\bullet}$ radicals in aqueous solution, J. Phys. Chem. Ref. Data **14** (1985) 1041.

[4.216] SAID, H.M., ALLA, S.G.A., EL-NAGGAR, A.W.M., Synthesis and characterization of novel gels based on carboxymethyl cellulose/acrylic acid prepared by electron beam irradiation, React. Func. Polym. **61** (2004) 397–404.

[4.217] ZHAI, M., YOSHII, F., KUME, T., HASHIM, K., Syntheses of PVA/starch grafted hydrogels by irradiation, Carbohyd. Polym. **50** 3 (2002) 295–303.

[4.218] CAI, H., ZHANG, Z.P., PING, C.S., BING, L.H., XIAO, X.Z., Synthesis and characterization of thermo- and pH- sensitive hydrogels based on chitosan-grafted N-isopropylacrylamide via gamma radiation, Radiat. Phys. Chem. **74** 1 (2005) 26–30.

[4.219] BARSBAY, M., GÜVEN, O., A short review of radiation-induced raft-mediated graft copolymerization: A powerful combination for modifying the surface properties of polymers in a controlled manner, Radiat. Phys. Chem. **78** 12 (2009) 1054–1059.

[4.220] BRAUNECKER, W.A., MATYJASZEWSKI, K., Controlled/living radical polymerization: Features, developments, and perspectives, Prog. Polym. Sci. **32** 1 (2007) 93–146.

[4.221] MOAD, G., SOLOMON, D.H., The Chemistry of Radical Polymerization, 2nd edn, Elsevier, Oxford (2006).

[4.222] QUINN, J.F., DAVIS, T.P., BARNER, L., BARNER-KOWOLLIK, C., The application of ionizing radiation in reversible addition-fragmentation chain transfer (RAFT) polymerization: Renaissance of a key synthetic and kinetic tool, Polymer **48** 22 (2007) 6467–6480.

[4.223] BARSBAY, M., et al., Verification of controlled grafting of styrene from cellulose via radiation-induced RAFT polymerization, Macromol. **40** 20 (2007) 7140–7147.

[4.224] BARSBAY, M., et al., RAFT-mediated polymerization and grafting of sodium 4-styrenesulfonate from cellulose initiated via gamma-radiation, Polymer **50** 4 (2009) 973–982.

[4.225] GULREZ, S., AL-ASSAF, S., PHILLIPS, G.O., "Hydrogels: Methods of preparation, characterisation and applications", Progress in Molecular and Environmental Bioengineering - From Analysis and Modeling to Technology Applications (CARPI, A., Ed.) InTech, Rijeka, Croatia (2011) 117–151.

[4.226] PAPARELLA, A., PARK, K., Synthesis of polysaccharide chemical gels by gamma-ray irradiation, ACS Symp. Ser. **620** (1996) 180–187.

[4.227] RAMNANI, S.P., CHAUDHARI, C.V., PATIL, N.D., SABHARWAL, S., Synthesis and characterization of crosslinked chitosan formed by gamma irradiation in the

presence of carbontetrachloride as a sensitizer, J. Polym. Sci. A: Polym. Chem. **42** 15 (2004) 3897–3909.

[4.228] AL-ASSAF, S., PHILLIPS, G.O., WILLIAMS, P.A., PLESSIS, T.A., Application of ionizing radiations to produce new polysaccharides and proteins with enhanced functionality, Nucl. Instr. Meth. B **265** (2007) 37–43.

[4.229] PHILLIPS, G.O., PLESSIS, T.A.D., AL-ASSAF, S., WILLIAMS, P.A., Biopolymers Obtained by Solid State Irradiation in an Unsaturated Gaseous Atmosphere, United States Patent 6,610,810.

[4.230] PHILLIPS, G.O., PLESSIS, T.A.D., AL-ASSAF, S., WILLIAMS, P.A., Biopolymers Obtained by Solid State Irradiation in an Unsaturated Gaseous Atmosphere, United States Patent 6,841,644, Int. Cl. C08B 37/00 (20060101), Aug. 2003, filed Mar. 2001, available on-line.

[4.231] GULREZ, S., AL-ASSAF, S., PHILLIPS, G.O., "Characterisation and radiation modifcation of carrageenan in solid state", Radiation Processing Technology Applications (KHANDAL, R.K., Ed.), Shriram Institute for Industrial Research, New Delhi (2010) 519–531.

[4.232] WASIKIEWICZ, J.M., et al., Radiation crosslinking of biodegradable carboxymethylchitin and carboxymethylchitosan, J. Appl. Polym. Sci. **102** 1 (2006) 758–767.

[4.233] ZHAO, L., MITOMO, H., NAGASAWA, N., YOSHII, F., KUME, T., Radiation synthesis and characteristic of the hydrogels based on carboxymethylated chitin derivatives, Carbohyd. Polym. **51** 2 (2003) 169–175.

[4.234] WACH, R.A., et al., Hydroxyl-radical-induced crosslinking and radiation-initiated hydrogel formation in dilute aqueous solutions of carboxymethylcellulose, Carbohyd. Polym. **112** (2014) 412–415.

[4.235] XU, G.Y., CHEN, A.M., LIU, S.Y., YUAN, S.L., WEI, X.L., Effect of $C^{12}NBr$ on the viscoelasticity of gel containing xanthan gum/Cr(III), Acta Phys.-Chim. Sin. **18** (2002) 1043–1047 (in Chinese).

[4.236] WACH, R.A., KUDOH, H., ZHAI, M., MUROYA, Y., KATSUMURA, Y., Laser flash photolysis of carboxymethylcellulose in an aqueous solution, J. Polym. Sci., Part A: Polym. Chem. **43** 3 (2005) 505–518.

[4.237] WACH, R., ROKITA, B., BARTOSZEK, N., unpublished data.

[4.238] GÖRLICH, W., SCHNABEL, W., Investigations on the influence of charge density on the mutual deactivation of polyion-macroradicals. II., Eur. Polym. J. **9** (1973) 1298–1296.

[4.239] BEHAR, D., RABANI, J., Pulse radiolysis of poly(styrenesulfonate) in aqueous solutions, J. Phys. Chem. **92** (1988) 5288–5292.

[4.240] ULANSKI, P., BOTHE, E., HILDENBRAND, K., ROSIAK, J.M., VON SONNTAG, C., Hydroxyl-radical-induced reactions of poly(acrylic acid): a pulse radiolysis, EPR and product study. Part I. Deoxygenated aqueous solution, J. Chem. Soc. Perkin Trans, **2** 1996 (1996) 13–22.

[4.241] ULANSKI, P., BOTHE, E., HILDENBRAND, K., VON SONNTAG, C., ROSIAK, J.M., The influence of repulsive electrostatic forces on the lifetimes of poly(acrylic acid) radicals in aqueous solution, Nukl. **42** (1997) 425–436.

[4.242] AUGSTEN, C., KNOLLE, W., MADER, K., Characterizing the influence of electron irradiation on scleroglucan, Carbohyd. Polym. **72** 4 (2008) 707–718.
[4.243] ULANSKI, P., ROSIAK, J.M., "Radiation-induced degradation of chitosan", Chitin World (KARNICKI, Z.S., BRZESKI, M.M., BYKOWSKI, P.J., WOJTASZ-PAJAK, A., Eds), Wirtschaftsverlag NW, Bremerhaven, Germany (1994) 575–582.
[4.244] PHILLIPS, G.O., Radiation chemistry of carbohydrates, Adv. Carbohyd. Chem. Biochem. **16** (1961) 13–58.
[4.245] MYERS, L.S., Jr., "Radiation chemistry of nucleic acids, proteins, and polysaccharides", The Radiation Chemistry of Macromolecules (DOLE, M., Ed.), Vol. 2, Academic Press, New York (1973) 323–374.
[4.246] KOCHETKOV, N.K., KUDRJASHOV, L.I., CHLENOV, M.A., Radiation Chemistry of Carbohydrates (PHILLIPS, G.O., Ed.), Pergamon Press, Oxford (1979)
[4.247] PHILLIPS, G.O., "The effect of radiation on carbohydrates", The Carbohydrates (PIGMAN, W., HORTON, D., WANDER, J.D., Eds), Academic Press, New York (1980) 1217–1297.
[4.248] VON SONNTAG, C., Free radical reactions of carbohydrates as studied by radiation techniques, Adv. Carbohyd. Chem. Biochem. **37** (1980) 7–77.

Chapter 5

EFFECTS OF POLYSACCHARIDE STRUCTURAL PARAMETERS ON RADIATION INDUCED DEGRADATION

M. SEN, P. TASKIN, O. GÜVEN

5.1. INTRODUCTION

Considerable attention has recently been directed to the modification and preparation of low-molecular-weight fractions by radiation induced degradation of oligosaccharides of κ carrageenan, sodium alginate (NaAlg) [5.1–5.4] and chitosan [5.5–5.10] for agricultural and biomedical applications.

For example, Nagasawa et al. [5.10] have investigated the effect of radiation on alginates in the solid state and in aqueous solution. It was found that NaAlg degraded after irradiation in both the solid state and aqueous solution, and the degradation in solution was considerably greater than that in the solid state. Degradation yields, G(s), of NaAlg were found in this study to be 1.9 (sc/eV) (0.197 μmol/J) and 55 (sc/eV) (5.72 μmol/J) in the solid state and in aqueous solution, respectively.

In another study performed by Wasikiewicz et al. [5.11], ultrasonic, UV and gamma degradations of NaAlg and chitosan were investigated. It was found that for both polymers the most effective degradation method, from the energetic point of view, was gamma radiation with a G(s) of 0.55×10^{-7} mol/J for 1% alginate, and 4.53×10^{-7} mol/J for 1% chitosan. However, considering the reaction time, the UV method was the most effective, with a reaction rate constant, k, of 0.52 h^{-1} for alginate and 1.6 h^{-1} for chitosan.

In Refs [5.10, 5.11], as in other studies [5.12], the effect of the structural parameters of the polysaccharide type of natural polymers was not considered. Only in the recent studies by Sen et al. [5.13–5.15] are the effects of the structural parameters of some polysaccharides on radiation induced degradation considered in detail.

5.2. EFFECT OF MANNOSE–GALACTOSE RATIO (M/G) ON THE RADIATION STABILITY OF GALACTOMANNANS

Galactomannans are polysaccharides that are found in the endosperm of the seeds of legumes. Structurally, they consist of a β(1-4)-D-mannose

backbone to which galactose units are attached with an α(1-6) linkage. Of the known galactomannans, GG, LBG and TG are the most used in applications in the food, pharmaceutical and chemical industries. GG has a mannose–galactose ratio (M/G) of approximately 2, whereas the M/G ratio is 3 for TG and 4 for LBG, respectively [5.16]. The functional and physical properties of these polysaccharides (including solubility, gelling behaviour and viscosity) are related to their molecular structure, polymerization, sugar composition and degree and distribution of branching [5.17]. Their popularity as thickening agents or stabilizers is mainly due to their high viscosity at low concentrations.

The degradation of linear polysaccharides is essential for many industrial applications. For example, guar solutions, which are used as hydraulic fracturing fluids in oil and gas recovery, need to be degraded to facilitate the outflow of oil. In addition, to understand the solution properties of guar as well as other water soluble bio-polymers, it is often necessary to degrade the native polymer to prepare samples with various molecular weights [5.18]. The degradation of polysaccharides has been widely studied. Though acid and enzymatic hydrolysis [5.19–5.21] are the most common methods of degradation, other methods such as thermal [5.18], γ irradiation [5.22], extrusion, ultrasonication [5.21, 5.23] and free radical degradation have also been reported [5.24].

The method most commonly used for the degradation of galactomannans is enzymatic hydroloysis. Only one source on the degradation of GG with γ rays in solution is available: Jumel et al. [5.25] investigated the effect of gamma irradiation in a 0−10 kGy dose range on the absolute molecular weight and viscosity properties of GG samples in solution. The molecular weight and viscosity of the GG was found to decrease on irradiation, and to decrease particularly steeply at low absorbed doses (0.1 kGy to 0.8 kGy). The decrease in both molecular weight and viscosity was much slower at high doses. Reference [5.25] also reports investigations in the change in the number of chain breaks per molecule $G(s)$. They concluded that $G(s)$ values at the lower absorbed doses were higher than that at the higher absorbed doses, i.e. more molecules were affected by the low absorbed doses [5.25].

In the recent study of Sen et al. [5.13], GG, TG and LBG samples underwent irradiation in the solid state. Changes in their molecular weights were determined by size exclusion chromatographic analysis. The authors recorded changes in viscosity in relation to temperature and absorbed dose, and $G(s)$ and the degradation rate were studied.

From the result of this study, the GPC chromatograms of LBG irradiated in the dose range of 2.5−75 kGy are shown in Fig. 5.1 as examples. Similar unimodal distributed chromatograms can also be obtained for GG and TG samples. As the absorbed dose increases, the GPC of the LBG sample shifts to

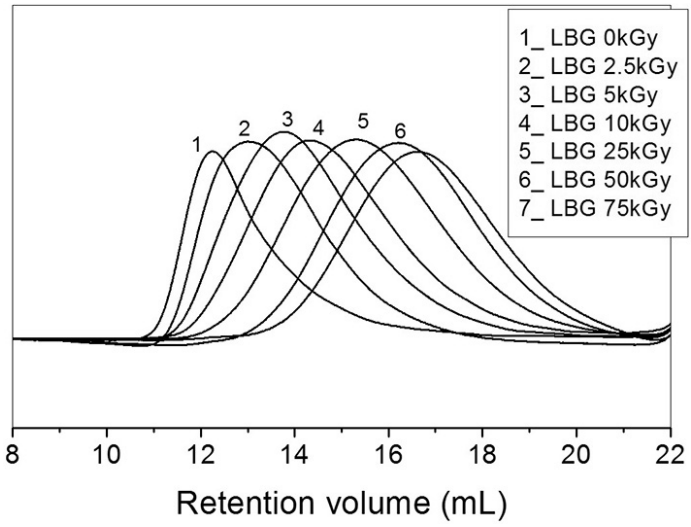

FIG. 5.1. Size exclusion chromatograms of irradiated LBG [5.13].

higher retention volumes indicating that the molecular weight of the sample is decreased by irradiation.

The change of weight ($\bar{M}_w$) and of number-average ($\bar{M}_n$) molecular weights with absorbed dose is shown in Figs 5.2(a) and 5.2(b), respectively.

For the determination of the G(s) values, $1/\bar{M}_n$was plotted against dose for all samples, which is shown in Fig. 5.3, as are the degradation rate constants. G(s) values were calculated using the intercepts. The calculated G(s) values are 0.113 ± 0.002, 0.111 ± 0.006 and 0.088 ± 0.010 μmol/J for GG, TG and LBG, respectively. It is concluded that G(s) values are dependent on the structure

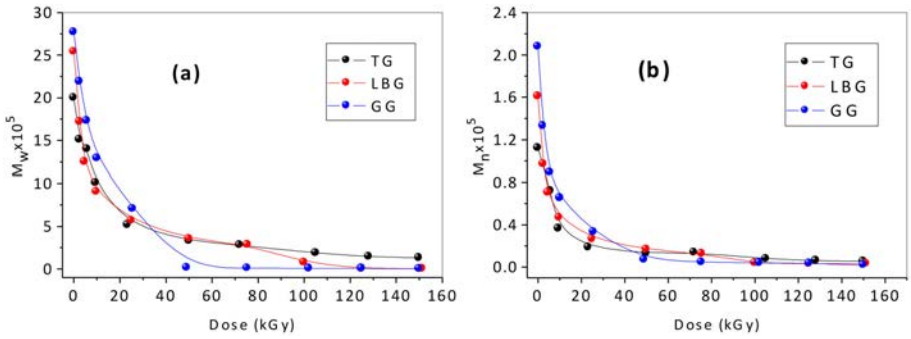

FIG. 5.2. The change in (a) weight-average molecular weight (b) number-average molecular weight of galactomannans with dose [5.13].

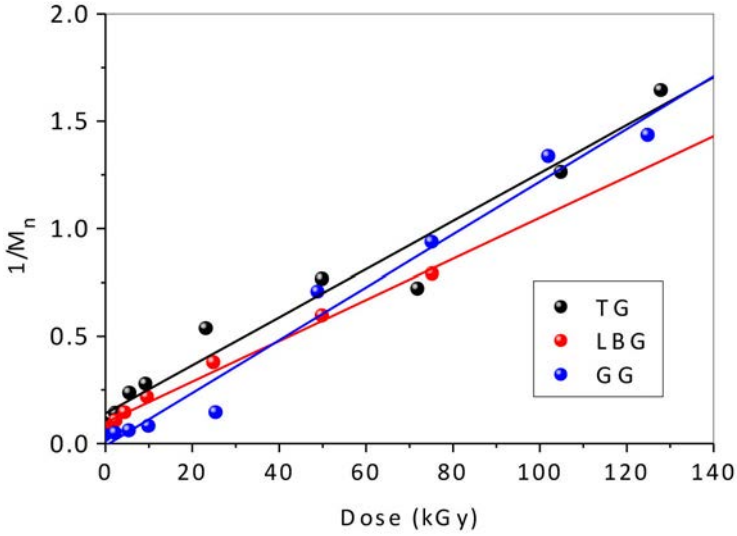

FIG. 5.3. $1/\bar{M}_n$ vs. dose plot to determine G(s) values of GG, TG and LBG [5.13].

(G/M ratio) of the sample and follow an order of GG > TG > LBG for these initial molecular weights. When the chemical structures of these gums are examined, it is found that GG has one galactomannan unit attached to the backbone per two monomeric units of the backbone, while TG has one per three monomeric units and LBG has one per four monomeric units. It can be concluded that the *G*(s) value increases with an increase in the G/M ratio and/or molecular weight of the unirradiated sample.

The equation given by Jellinek [5.26] is modified and used in the determination of degradation rate. If *N* is the average number of bond cleavages per original polymer molecule, this value can be calculated by:

$$N = \bar{M}_{n0} / \bar{M}_{nD} - 1 \tag{5.1}$$

where $\bar{M}_{n0}$ and $\bar{M}_{nD}$ are the $\bar{M}_n$ at time zero and after irradiation to a certain dose (*D*), respectively. *N* is also named the degree of scission. If the rate of chain scission is assumed to be independent of the length of the chain and of chain position, *N* can be assumed to be a linear function of absorbed dose:

$$N = \bar{M}_{n0} / \bar{M}_{nD} - 1 = k(\bar{M}_{n0} / m_0)D \tag{5.2}$$

where k is the rate constant and m_0 is the molecular weight of a monomer unit. Equation (5.2) can be rewritten as:

$$1/\bar{M}_{nD} - 1/\bar{M}_{n0} = (k/m_0)D \tag{5.3}$$

Degradation rate constants for GG, TG and LBG were determined using the information shown in Fig. 5.4. Determined degradation rate constants for GG, TG and LBG are given in Table 5.1; their values show that the degradation rate is at least partly dependent on the initial chain length found in the gum. As can be seen from Fig. 5.2, the molecular weights of the gums also follow the same order. It can be concluded that as the G/M ratio and the original molecular weight increase, the effect of irradiation on the molecular weight and rheological properties of the sample become more pronounced and the M/G ratio is one factor affecting the chain scission yield of galactomannans.

TABLE 5.1. DEGRADATION RATE CONSTANTS OF GG, TG AND LBG [5.13]

Polymer	Degradation rate constant (1/kGy)
GG	12.9 ± 0.95
LBG	7.93 ± 0.56
TG	7.44 ± 0.98

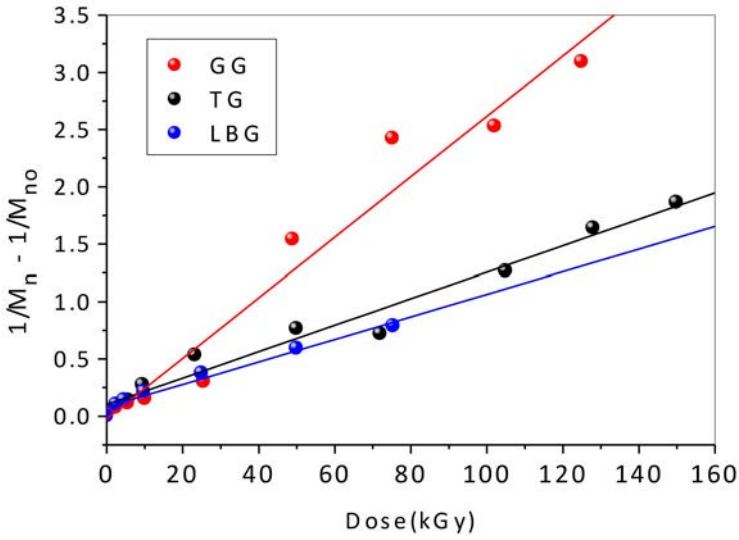

FIG. 5.4. Plot of ($1/\bar{M}_n - 1/\bar{M}_{n0}$) against dose to determine degradation rate constants of GG, TG and LBG [5.13].

5.3. EFFECT OF GULURONIC ACID/MANNURONIC ACID RATIO ON THE RADIATION INDUCED DEGRADATION OF NaAlg

Alginate is a natural polysaccharide and is found in seaweed. It is an unbranched binary copolymer of (1-4)-linked residues of β D-mannuronic acid and α L-guluronic acids. Alginic acid and its water soluble sodium salt have long been used for food, pharmaceutical and chemical applications that require highly viscous solutions. They are used as thickening agents, in medicines, as stabilizers and as plant growth stimulators [5.1, 5.27, 5.28]. Aqueous solutions of NaAlg form stable gels in the presence of multivalent cations such as Ca^{2+} and Mg^{2+}. Reference [5.29] reports that gel formation occurs because of ionic interaction between guluronic acid residues from at least two alginate chains and cations, and yields a 3-D network of alginate molecules that fit the 'egg-box model' (see Fig. 2.6). The properties of alginate gels vary according to their ratio of mannuronic to guluronic acids, the frequency and size of the guluronic acid blocks they are made up of and the molecular weight of the polymer [5.30, 5.31]. The selective binding of certain alkaline earth metal ions increases with increasing content of the α L-guluronic acid (g) residues in the chain. However, polymannuronate blocks and alternating blocks are close to being non-selective.

The radiation induced degradation of NaAlg with different G/M ratios was first investigated by Sen et al. [5.14]. The results of this study found changes in the weight ($\overline{M}_w$) and number-average ($\overline{M}_n$) molecular weights related to irradiation dose, and these are shown in Fig. 5.5.

The rapid decrease in $\overline{M}_n$ and $\overline{M}_w$ shows that degradation was the only mode of action of radiation on NaAlg. For the determination of the G(s) values, $1/\overline{M}_n$ was plotted against dose for all samples (Fig. 5.6). G(s) values were then

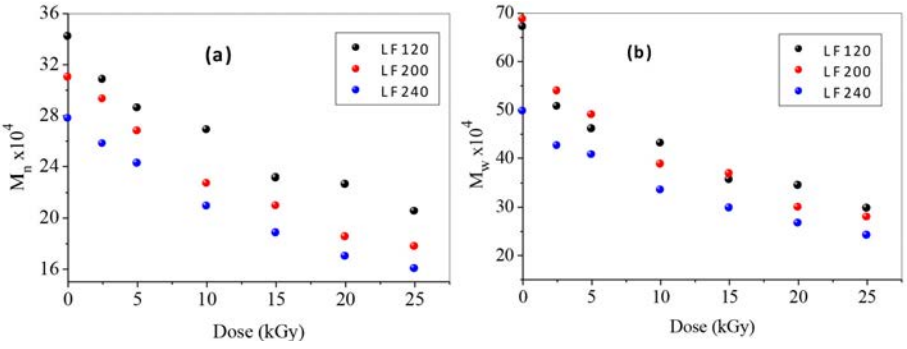

FIG. 5.5. Change in the (a) number-average molecular weight and (b) weight-average molecular weight of NaAlgs with dose [5.14].

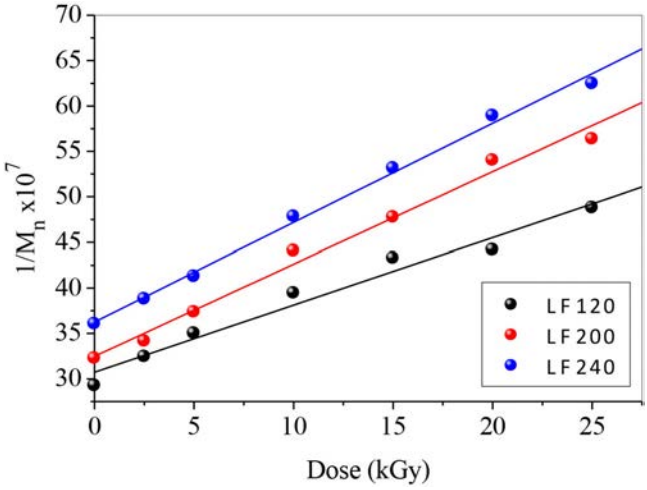

FIG. 5.6. Plot of $1/\bar{M}_{n0}$ versus dose for the determination of the G(s) values of NaAlgs [5.14].

calculated using the intercepts. The calculated *G*(s) values were 0.073 ± 0.009, 0.100 ± 0.005 and 0.1088 ± 0.003 μmol/J for LF120, LF200 and LF240 NaAlg, respectively. It was concluded that *G*(s) values were dependent on the structure (guluronic acid to mannuronic ratio) of the sample and followed the order LF240 > LF200 > LF120 or 70/30 < 50/50 < 45/55 guluronic acid to mannuronic acid ratio.

When the chemical structures of NaAlgs were examined, it was seen that their properties varied widely depending on the composition of the alginate molecule (i.e. the ratio of mannuronic to guluronic acids, the frequency and size of guluronic acid blocks and the molecular weight of the polymer), and the concentrations of alginate and cations at the time of gelation. It was concluded that the *G*(s) value increased with a decrease in the guluronic acid to mannuronic acid ratio. This increase was attributed to the decrease of radical–radical recombination reactions due to the stiff and extended nature of alginate chains. Reference [5.32] reports that the diaxial linkage in guluronic blocks causes a large, hindered rotation around the glycosidic linkage that could account for the stiff and extended nature of alginate chains.

The modified Jellinek equation [5.26] was used by Sen at al. [5.14] in the determination of the degradation rate. Degradation rate constants for NaAlgs were determined using the $(1/\bar{M}_n - 1/\bar{M}_{n0})$ versus dose curves. The determined degradation rate constants for NaAlgs are given in Table 5.2. The results reported in Ref. [5.14] show that the degradation rate was dependent on the G/M ratio for these initial molecular weights.

TABLE 5.2. DEGRADATION RATE CONSTANTS OF NaAlgs [5.14]

Polymer	G/M	k (kGy^{-1})
LF120	70/30	$4.27 \times 10^{-10} \pm 4.2 \times 10^{-11}$
LF200	50/50	$5.86 \times 10^{-10} \pm 4.0 \times 10^{-11}$
LF240	45/55	$6.30 \times 10^{-10} \pm 2.0 \times 10^{-11}$

Reference [5.14] reports that changes in viscosity upon irradiation at different polymer concentrations and with different shear rates were investigated for NaAlg samples. Figure 5.7 shows the change of viscosity with shear rate for LF120 NaAlg when unirradiated and when irradiated at 2.5 kGy and at 5.0 kGy.

Shear rate versus shear stress and shear rate versus viscosity curves become linear at an absorbed dose of approximately 2.5 kGy for LF120 NaAlg. The same behaviour was observed for the other NaAlgs. The linearity of these plots indicated that the samples showed Newtonian fluid properties. It could be concluded that LF120 NaAlg lost its pseudoplastic fluid behaviour, and that the change in flow behaviour from non-Newtonian to Newtonian took place upon irradiation even at very low doses.

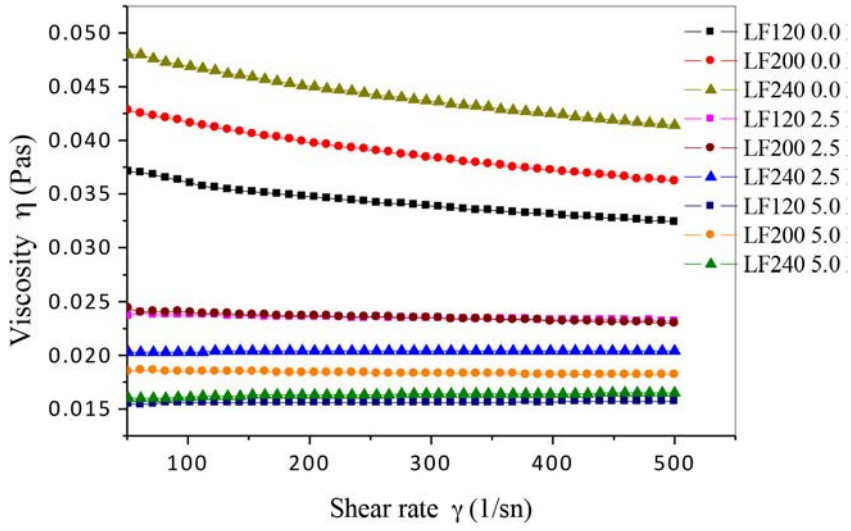

FIG. 5.7. Change in the viscosity with shear rate for LF120 NaAlg irradiated at the indicated doses [5.14].

Viscosimetric studies performed using different polymer concentrations and at different shear rates clearly indicate that the change in specific viscosity of NaAlg solutions depends on the shear rate and concentration of the solution. For the determination of the limiting viscosity number of NaAlgs for zero shear rate and concentration, the rheological data were reanalysed and the η_{sp}/c values were plotted against ($c + 0.001 \times \gamma$). The representative curves for the determination of [η] are shown in Fig. 5.8. Similar curves were obtained for the other NaAlgs. The percentage decrease in [η] upon irradiation is shown in Fig. 5.9. These results clearly indicate not only that the rheological properties of the irradiated and molecular-weight-reduced alginates were solely controlled by the ratio of guluronic acid to mannuronic acid, but also that the frequency and size of the guluronic acid blocks were important parameters. Despite the lower molecular weight and lower G/M ratio, the slower decrease in the value of [η] for LF240 on irradiation was probably because of the presence of more gg blocks in the main chain. Experimental viscosimetric data of alginate solutions indicate that the stiffness of the chain blocks increased in the order mannuronic–guluronic < mannuronic–mannuronic < guluronic–guluronic [5.32].

The authors concluded that as the guluronic acid to mannuronic acid ratio decreased, the effect of irradiation on the molecular weight and rheological properties of the sample became more pronounced and that the G/M ratio was one of the factors affecting the chain scission yield of NaAlg irradiated in the solid state. All NaAlg samples showed a pseudoplastic behaviour up to a certain dose, and Newtonian flow behaviour above that dose.

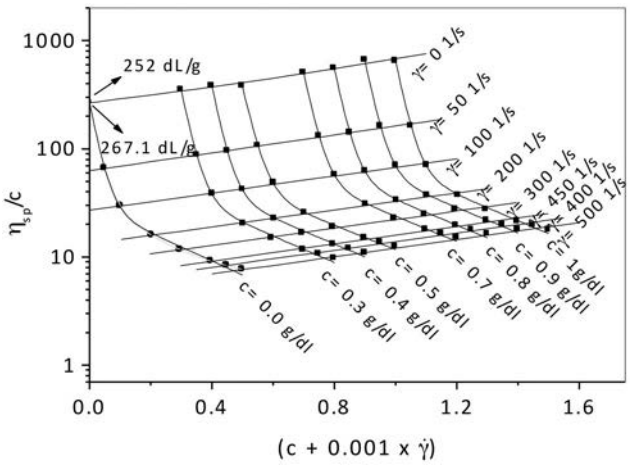

FIG. 5.8. A plot for the determination of the limiting viscosity number of LF120 NaAlg for zero shear rate and zero concentration [5.14].

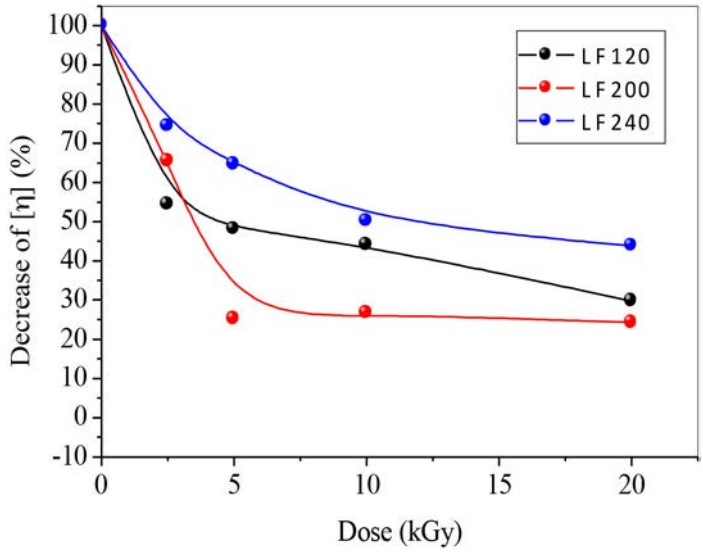

FIG. 5.9. Percentage decrease in the limiting viscosity number for LF120 NaAlg with dose [5.14].

In recent years, studies have focused on the degradation of natural polymers in accelerated conditions using additional OH radical generating systems such as hydrogen peroxide [5.33, 5.34], ammonium persulphate [5.35] and nitrous oxide [5.36], in order to reduce absorbed dose in large scale production. OH-radical-induced chain scission of chitosan in the absence and presence of dioxygen are explained in detail in Ref. [5.37].

Sen and Atile [5.15] investigated the effect of water and H_2O_2 on the radiation induced degradation of NaAlgs with different G/M ratios in 2% aqueous solutions and in H_2O_2-containing solutions by irradiating at various doses (2.5 kGy, 5 kGy, and 10 kGy) using a Gammacell 220 type ^{60}Co gamma irradiator at room temperature in air. The dose rate was 30 Gy/h. For aqueous solution irradiations, NaAlg was firstly dried in a vacuum oven and then dissolved in pure water by stirring for 24 h. For the irradiation in H_2O_2 solution, H_2O_2 was added to the polymer solution. The concentration of H_2O_2 in solution was 2%.

For the investigation of the effect of gamma rays on the molecular weight of NaAlgs, their $\bar{M}_n$ and $\bar{M}_w$ values were evaluated using GPC. Unimodal chromatograms were obtained for all NaAlg samples. As the absorbed dose increased, higher retention volumes were found using GPC, suggesting that irradiation decreased the sample's molecular weight. Figure 5.10 shows changes in the weight and in number-average molecular weights against absorbed dose.

Figure 5.10 indicates that H_2O_2 shows a synergistic effect on the degradation of NaAlg. The G/M ratio is also an important factor controlling this synergistic

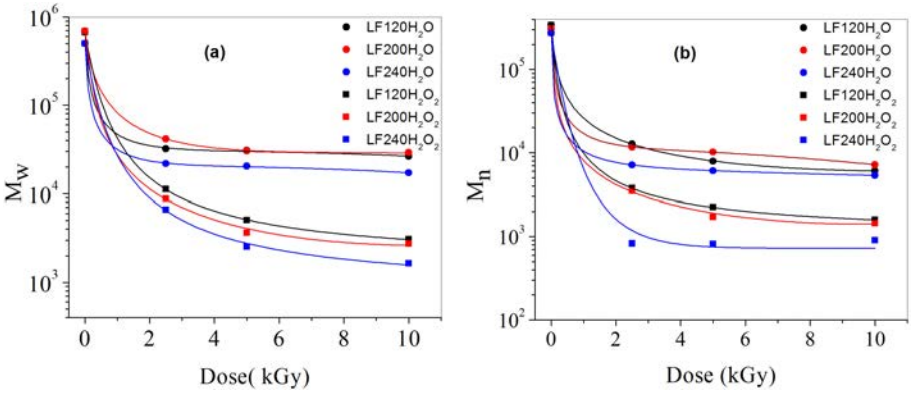

FIG. 5.10. Change in the (a) weight and (b) number-average molecular weight of NaAlgs with dose in aqueous solution with and without H_2O_2 [5.15].

effect. To obtain a better understanding of the effect of irradiation media on the accelerated degradation of NaAlg, LF240 NaAlg was irradiated both in the solid state and in aqueous solution. The changes in $\bar{M}_w$ with absorbed dose are illustrated in Fig. 5.11.

The synergistic effect of H_2O and H_2O_2 was also analysed with chain scission yield G(s) value. The G value, equal to mmol of scission events per J

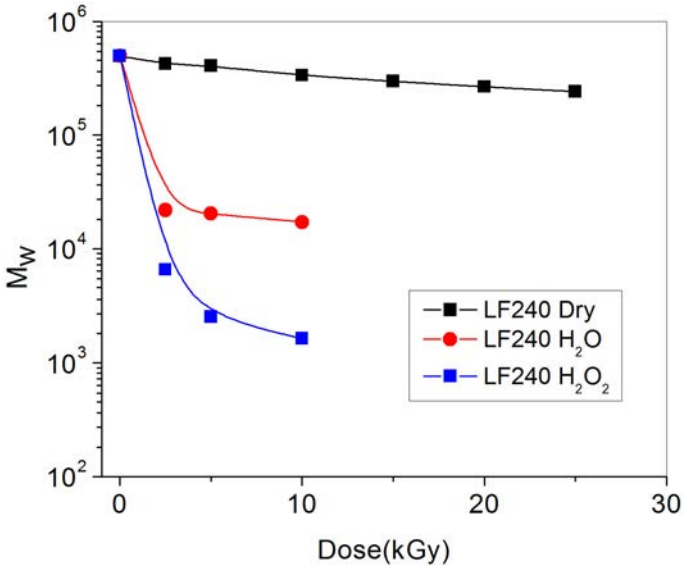

FIG. 5.11. Variation of $\bar{M}_w$ values of LF240 NaAlg with dose in dry state and in aqueous solution with and without H_2O_2 [5.15].

of energy absorbed, has been customarily used to measure radiation-chemical yield. Chain scission decreases the molecular weights of polymer molecules and cross-linking processes increase it. Therefore, measurement of the changes in molecular weight averages and distribution with dose can help to quantify these processes.

If scission is the only mode of action of radiation, Refs [5.38, 5.39] state that the radiation-chemical yield of degradation, $G(s)$ (mol/J), can be determined with the following equation:

$$G(s) = c / D_d (1/\bar{M}_{nD} - 1/\bar{M}_{n0}) \quad (5.4)$$

As has been indicated above, in order to obtain quantitative information on chain scission yields, $(1/\bar{M}_w - 1/\bar{M}_{w0})$ and $(1/\bar{M}_n - 1/\bar{M}_{n0})$ vs. dose diagrams can be constructed (Figs 5.12 (a) and (b)).

From the overall slope of the linear parts of the curves in Fig. 5.12 (0–2.5 kGy), it was found that the only mode of action of radiation is chain scission. Although it is possible to calculate a value for $G(s)$ from the overall slope of the linear parts of the curves in Fig. 5.12, the authors have preferred to calculate individual values of $G(s)$ as a function of dose using Eq. (5.4). The effects of irradiation media and dose on the $G(s)$ value for NaAlgs with different G/M ratios are given in Table 5.3. The effect of NaAlg type or the G/M ratio on the radiation induced degradation yields in aqueous solution irradiations was also examined. As can be seen from Fig. 5.13, the G/M ratio is an important factor controlling the degradation rate of NaAlg not only in dry irradition but also in aqueous solution irradiation. The conclusion is that chain scission yield ($G(s)$) values are dependent on the G/M ratio of the sample and followed the

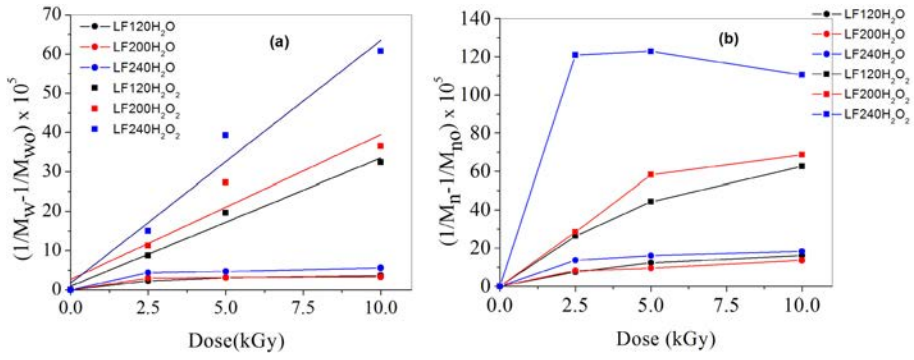

FIG. 5.12. Variation of (a) $(1/\bar{M}_w - 1/\bar{M}_{w0})$ and (b) $(1/\bar{M}_n - 1/\bar{M}_{n0})$ values of LF240 NaAlg with dose [5.15].

order LF240 > LF200 > LF120 or 70/30 < 50/50 < 45/55, with the G/M ratio similar to the dry state.

TABLE 5.3. DEGRADATION YIELD OF NaAlgs IRRADIATED WITH GAMMA RAYS IN DRY FORM (γ/DRY) AQUEOUS SOLUTION (γ/H_2O) AND HYDROGEN PEROXIDE SOLUTION (γ/H_2O_2) [5.15]

	G(s) value of NaAlg (μmol/J)								
Irradiation mode	LF120			LF200			LF240		
	2.5 kGy	5.0 kGy	10 kGy	2.5 kGy	5.0 kGy	10 kGy	2.5 kGy	5.0 kGy	10 kGy
γ/dry	0.127	0.115	0.102	0.196	0.162	0.148	0.382	0.240	0.186
γ/ H_2O	0.903	0.618	0.363	1.180	0.628	0.328	1.751	0.939	0.562
γ/H_2O_2	4.498	4.924	4.240	4.494	4.924	4.241	6.011	7.849	6.070

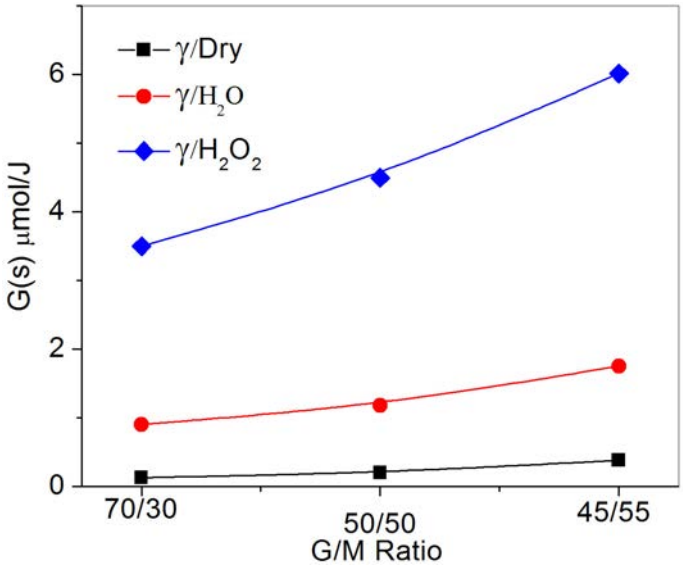

FIG. 5.13. The effect of guluronic acid/mannuronic acid ratio on the radiation induced degradation yields in aqueous solution irradiations. Absorbed dose is 2.5 kGy [5.15].

5.4. EFFECT OF THE DEGREE OF DEACETYLATION (DD) ON THE RADIATION INDUCED DEGRADATION OF CHITOSAN

Chitin, which is a structural element of the exoskeletons of crabs and shrimp and of the cell walls of fungi, is one of the most abundant biodegradable natural polymers in the world, after cellulose. Chitosan is produced commercially by the deacetylation of chitin. The degree of deacetylation (DD), which determines the content of free amino groups in polysaccharides, can be employed to differentiate between chitin and chitosan. It is very well known that the DD is one of the most important chemical characteristics of chitin and chitosan, and could influence the performance of chitosan in many of its applications [5.40].

Considerable attention has recently, especially in the last decade, been directed to the modification and preparation of low-molecular-weight fractions or oligosaccharides of chitosan by radiation induced degradation in the dry state or in aqueous solutions with various concentrations. These were intended for use mainly in plant growth promoter, plant protector and tissue engineering applications [5.35, 5.41].

In the literature, the general consensus is that the irradiation state (dry, or aqueous solution), the presence of hydroxy generating groups and the initial molecular weight of chitosan are important factors in controlling its radiation induced degradation behaviour. However, no relationship has yet been established between the DD and the radiation stability of chitosan.

In a more recent study, the effects of the DD of chitosan with a molecular weight of ~330 kDa and various DDs (78%, 80%, 88.6% and 97.4%) on their radiation stability were investigated [5.43]. The chitosan samples were irradiated with gamma rays at doses of 0–35 kGy, employing a low dose rate (3 Gy/h) in air at ambient temperature in the solid state. The DD of the unirradiated or irradiated chitosan was determined by ^{1}H-NMR spectroscopy and the degradation was monitored in detail by careful GPC and viscosimetric analyses of their respective molecular weights before and after irradiation. The Charlesby–Pinner equation was used to determine the radiation-chemical yield, G(s). It was found that the G(s) values increased with the DD value of chitosan at every absorbed dose within a dose range of 0–35 kGy. The results of this study, changes in the number-average molecular weight with absorbed dose, are shown in Fig. 5.14.

For the determination of the G(s) values, $(1/\overline{M}_n - 1/\overline{M}_{n0})$ was plotted against dose for all samples (Fig. 5.15). Then, G(s) values were calculated by using the intercepts. The calculated G(s) values were 1.36, 1.37, 1.62 and 2.07 μmol/J for 78, 80, 88.6, and 97.4% deacetylated chitosan, respectively. The change in the scission yield and % reduction of limiting viscosity number (Fig. 5.16) was attributed to the change in the coiled and extended nature of the chitosan chains that is a result of a change in the DD.

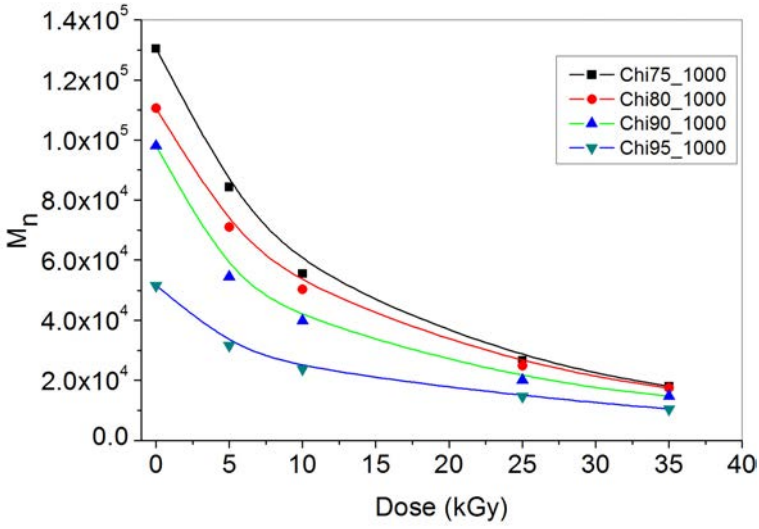

FIG. 5.14. Change in the number-average molecular weight of chitosan with dose [5.43].

It is known that the extent of the coiling character of chitosan is inversely proportional to its DD. It was concluded that the high degree of coiling in the chitosan chains could result in a more compact structure that might enhance the radical–radical combinations on the chains, which would thus lower the rate of degradation and hence reduce the *G*(s) values.

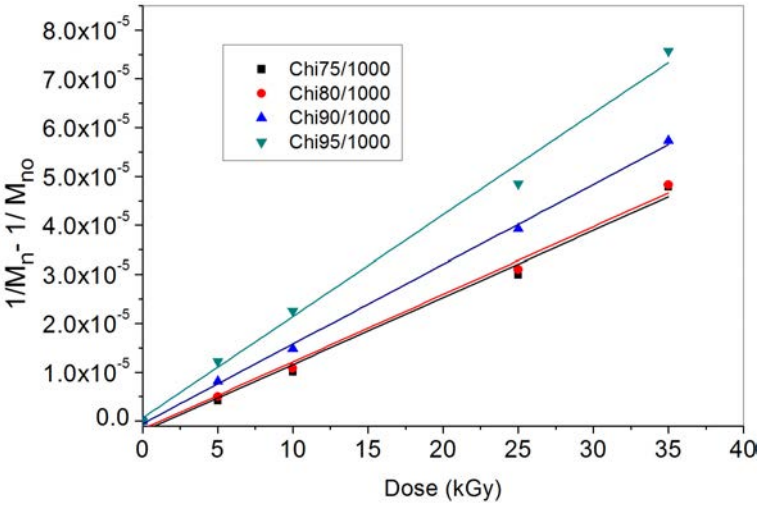

FIG. 5.15. Variation of $(1/M_n - 1/M_{n0})$ values of chitosans with dose [5.40].

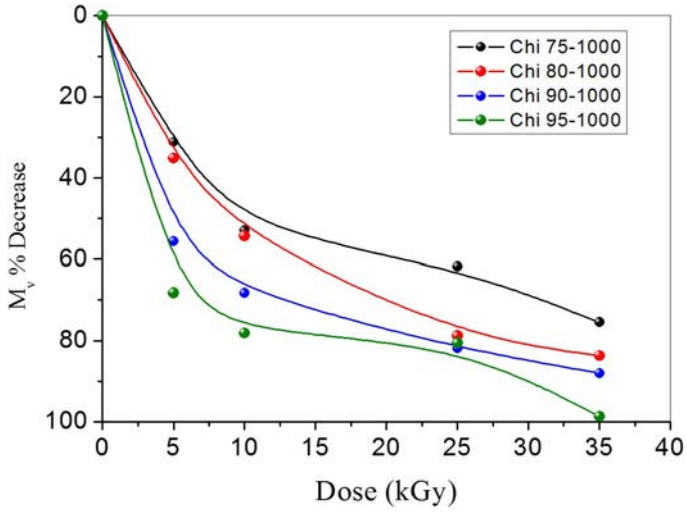

FIG. 5.16. Percentage decrease of viscosity-average molecular weight of chitosan with dose [5.40].

ACKNOWLEDGEMENTS

The authors gratefully acknowledge the support provided by the IAEA through Research Contract No. 14475/R0, the support provided by TUBITAK as part of the 106T442, 109T872 and 112T628 projects, and the support provided by the Scientific Research Projects Coordination Unit of Hacettepe University through Research Contract No. 08G702001.

REFERENCES TO CHAPTER 5

[5.1] HIEN, N.Q., et al., Growth-promotion of plants with depolymerized alginates by irradiation, Radiat. Phys. Chem. **59** (2000) 97–101.

[5.2] AFTAB, T., et al., Enhancing the growth, photosynthetic capacity and artemisinin content in *Artemisia annua* L. by irradiated sodium alginate, Radiat. Phys. Chem. **80** (2011) 833–836.

[5.3] LUAN, L.Q., NAGASAWA, N., HA, V.T.T., HIEN, N.Q., NAKANISHI, T.M., Enhancement of plant growth stimulation activity of irradiated alginate by fractionation, Radiat. Phys. Chem. **78** (2009) 796–799.

[5.4] MOLLAH, M.Z.I., KHAN, M.A., KHAN, R.A., Effect of gamma irradiated sodium alginate on redamaranth (*Amaranthus cruentus* L.) as growth promoter, Radiat. Phys. Chem. **78** (2009) 61–64.

[5.5] CZECHOWSKA-BISKUP, R., ROKITA, B., ULANSKI, P., ROSIAK, J.M., Radiation-induced and sonochemical degradation of chitosan as a way to increase its fat-binding capacity, Nucl. Instrum. Meth. Phys. Res. B **236** (2005) 383–390.

[5.6] ZAINOL, I., MDAKIL, H., MASTOR, A., Effect of γ-irradiation on the physical and mechanical properties of chitosan powder, Mater. Sci. Eng. **C29** (2009) 292–297.

[5.7] NGUYEN QUOC HIEN, "Radiation degradation of chitosan and some biological effects", Radiation Processing of Polysaccharides, IAEA-TECDOC-1422, IAEA, Vienna (2004) 67–73.

[5.8] RELLEVE, L., et al., Degradation of carrageenan by radiation, Polym. Degrad. Stabil. **87** (2005) 403–410.

[5.9] THAMA, L.X., et al., Effect of radiation-degraded chitosan on plants stressed with vanadium, Radiat. Phys. Chem. **61** (2001) 171–175.

[5.10] NAGASAWA, N., MITOMO, H., YOSHII, F., KUME, T., Radiation-induced degradation of sodium alginate, Polym. Degrad. Stabil. **69** (2000) 279–285.

[5.11] WASIKIEWICZ, J.M., YOSHII, F., NAGASAWA, N., WACH, R.A., MITOMO, H., Degradation of chitosan and sodium alginate by gamma radiation, sonochemical and ultraviolet methods, Radiat. Phys. Chem. **73** (2005) 287–295.

[5.12] KUME, T., NAGASAWA, N., YOSHII, F., Utilization of carbohydrates by radiation processing, Radiat. Phys. Chem. **63** (2002) 625–627.

[5.13] SEN, M., YOLACAN, B., GÜVEN, O., Radiation induced degradation of Galactomannan polysaccharides, Nucl. Instr. Meth. Phys. Res. B **265** (2007) 429–433.

[5.14] SEN, M., RENDEVSKI, S., AKKAS KAVAKLI, P., SEPEHRIANAZAR, A., Effect of G/M ratio on the radiation induced degradation of sodium alginate, Radiat. Phys. Chem. **79** (2010) 279–282.

[5.15] SEN, M., ATIK, H., The antioxidant properties of oligo sodium alginates prepared by radiation-induced degradation in aqueous and hydrogen peroxide solutions, Radiat. Phys. Chem. **81** (2012) 816–822.

[5.16] PICOUT, D.R., ROSS-MURPHY, S.B., JUMEL, K., HARDING, S.E., Pressure cell assisted solution characterization of polysaccharides. 2. Locust bean gum and tara gum, Biomacromol. **3** (2002) 761–767.

[5.17] PRADO, B.M., KIM, S., ÖZEN, B.F., MAUER, L.J., Differentiation of carbohydrate gums and mixtures using Fourier Transform Infrared Spectroscopy and chemometrics, J. Agric. Food Chem. **53** (2005) 2823–2829.

[5.18] CHENG, Y., BROWN, K.M., PRUD'HOMME, R.K., Preparation and characterization of molecular weight fractions of guar galactomannans using acid and enzymatic hydrolysis, Int. J. Biol. Macromol. **31** (2002) 29–35.

[5.19] COTE, G.L., Low-viscosity α-D-glucan fractions derived from sucrose which are resistant to enzymatic digestion, Carbohydr. Polym. **19** (1992) 249–252.

[5.20] CHENG, Y., BROWN, K.M., PRUD'HOMME, R.K., Enzymatic degradation of guar and substituted guar galactomannans, Biomacromol. **1** (2000) 782–788.

[5.21] TAYAL, A., KHAN, S.A., Degradation of a water-soluble polymer: Molecular weight changes and chain scission characteristics, Macromol. **33** (2000) 9488–9493.

[5.22] WILLET, J.L., MILLARD, M.M., JASBERG, B.K., Extrusion of waxy maize starch: melt rheology and molecular weight degradation of amylopectin, Polymer **38** (1997) 5983–5989.
[5.23] SZU, S.C., ZON, G., SCHNEERSON, R., ROBBINS, J.B., Ultrasonic irradiation of bacterial polysaccharides. Characterization of the depolymerized products and some applications of the process, Carbohydr. Res. **152** (1986) 7–20.
[5.24] REDDY, T.T., TAMMISHETTI, S., Free radical degradation of guar gum, Polym. Degrad. Stab. **86** (2004) 455–459.
[5.25] JUMEL, K., HARDING, S.E., MITCHELL, J.R., Effect of gamma irradiation on the macromolecular integrity of guar gum, Carbohydr. Res. **282** (1996) 223–236.
[5.26] JELLINEK, H.H.G., Degradation of Vinyl Polymers, Wiley and Sons, New York (1955).
[5.27] ØSTBERG, T., LUND, E.M., GRAFFNER, C., Calcium alginate matrices for oral unit administration. IV. Release characteristics in different media, Int. J. Pharm. **112** (1994) 241–248.
[5.28] GARCIA, A.M., GHALY, E.S., Preliminary spherical agglomerates of water soluble drug using natural polymer and cross-linked technique, J. Control. Rel. **40** (1996) 179–186.
[5.29] GRANT, G.T., MORRIS, E.R., REES, D.A., SMITH, P.J.C., THOM, D., Biological interactions between polysaccharides and divalent cations: the egg-box model, FEBS Letters **32** (1973) 195–198.
[5.30] SMIDSROD, O., Molecular basis for some physical properties of alginates in gel state, J. Chem. Soc., Faraday Trans. **57** (1974) 264–267.
[5.31] KLOCK, G., et al., Production of purified alginates suitable for use in immunoisolated transplantation, Appl. Microbiol. Biotechnol. **40** (1994) 638–643.
[5.32] SMIDSROD, O., GLOVER, R.M., WHITTINGTON, S.G., The relative extension of alginates having different chemical composition, Carbohydr. Res. **27** (1973) 107–118.
[5.33] DUY, N.N., PHU, D.V., ANH, N.T., HIEN, N.Q., Synergistic degradation to prepare oligochitosan by gamma-irradiation of chitosan solution in the presence of hydrogen peroxide, Radiat. Phys Chem. **80** (2011) 848–853.
[5.34] KANG, B., DAI, Y.D., ZHANG, H.Q., CHEN, D., Synergetic degradation of chitosan with gamma radiation and hydrogen peroxide, Polym. Degrad. Stab. **92** (2007) 359–362.
[5.35] EL-SAWY, N.M., ABD EL-REHIM, H.A., ELBARBARY, A.M., HEGAZY, E.S.A., Radiation-induced degradation of chitosan for possible use as a growth promoter in agricultural purposes, Carbohydr. Polym. **79** (2010) 555–562.
[5.36] HUANG, L., ZHAI, M., PENG, J., LI, J., WEI, G., Radiation-induced degradation of carboxy methylated chitosan in aqueous solution, Carbohydr. Polym. **67** (2007) 305–312.
[5.37] ULANSKI, P., VON SONNTAG, C., OH-Radical-induced chain scission of chitosan in the absence and presence of dioxygen, J. Chem. Soc. Perkin Trans. **2** (2000) 2022–2028.
[5.38] CHARLESBY, A., Atomic Radiation and Polymers, Pergamon Press, New York (1960).

[5.39] JANIK, I., KASPRZAK, E., AL-ZIER, A., ROSIAK, J.M., Radiation crosslinking and scission parameters for poly(vinyl methyl ether) in aqueous solution, Nucl. Instr Meth. Phys. Res. B **208** (2003) 374–379.

[5.40] PHILLIPS, G.O., WILLIAMS, P.A., Handbook of Hydrocolloids, Woodhead Publishing Series in Food Science, Technology and Nutrition No. 173, Woodhead Publishing, Cambridge (2009).

[5.41] DUY, N.N., PHU, D.V., ANH, N.T., HIEN, N.Q., Synergistic degradation to prepare oligochitosan by γ-irradiation of chitosan solution in the presence of hydrogen peroxide, Radiat. Phys. Chem. **80** (2012) 848–853

[5.42] TASKIN, P., CANISAĞ, H., SEN, M., The effect of degree of deacetylation on the radiation induced degradation of chitosan, Radiat. Phys. Chem **94** (2014) 236–239.

Chapter 6

ANALYTICAL TECHNIQUES FOR THE CHARACTERIZATION OF POLYSACCHARIDES

S. AL-ASSAF
Hydrocolloids Research Centre, Institute of Food Science and Innovation,
University of Chester,
Chester, United Kingdom

6.1. INTRODUCTION

The biological, physical and physiological functions of polysaccharides are directly related to their molecular weight, shape and size. Accurate characterization is, therefore, vital for a better understanding of their structure–property relationships. This chapter reviews some of the techniques and methodologies commonly used for the characterization of polysaccharides, with a specific focus on methods related to size and conformation in aqueous solution. Additionally, this chapter places an emphasis on how these techniques (absolute or relative) are used to determine the effect of irradiation qualitatively and quantitatively. Furthermore, it discusses specific techniques designed for the characterization of polysaccharide based hydrogels.

6.2. METHODS

6.2.1. Percentage loss on drying

The loss on drying is simply the amount of water (moisture) present in the solid sample, which gives an indication of the nature of sample (e.g. whether it is fresh or old) and whether it has been stored properly. This parameter is typically defined as not more than 10%, 12% or 15% for spray dried GA, carrageenan and xanthan, respectively. The measurement is typically carried out as follows: Around 0.5–1.0 g of test material (powder form) should be accurately weighed directly into an aluminium pan and placed in an oven (preferably a convection oven) and dried at 105°C to a constant weight. The Joint Expert Committee on Food Additives of the Food and Agriculture Organization of the United Nations and the World Health Organization defines the heating time of 2 h, 2.5 h and 5 h for the spray dried forms of pectin, xanthan and GA, respectively. The sample is then

moved to a desiccator and allowed to cool for 30 min to reach room temperature. The loss of weight can be calculated using the following equation:

$$\text{Percentage loss on drying} = (W_i - W_d)/W_i \times 100 \quad (6.1)$$

where W_i and W_d are the weight of the initial and the dry sample, respectively.

6.2.2. Solubility

Polysaccharides are water soluble owing to the presence of many hydroxyl groups. The quality of the solvent is determined according to its solubility and a solvent can be described as good when the molecules are fully hydrated. It should be noted, however, that heating is sometimes necessary to obtain a true solution. Aggregation due to the presence of hydrophobic groups or batches can lead to partial solubility. Other factors such as the presence of metal ions or ability of the polymer chains to associate via hydrogen bonding can also lead to the presence of an insoluble fraction which is often referred to as hydrogel or gel. Hydrogel can also be produced following the modification of polysaccharides (see Chapter 4). An uncomplicated approach to the determination of an insoluble gel fraction in a system involves the observation of the formation of insoluble matter on dispersal of the polysaccharide in water in a cylindrical vial. Whether shaking or stirring is needed and how long either is needed for are dependent on the molecular weight of the polymer, with high-molecular-weight materials needing a longer shaking or stirring time than low-molecular-weight polymers. Bulk viscosity can be measured by turning the vial upside down.

The basic techniques for the characterization of hydrogels derived from polysaccharides or from water soluble polymers are concerned with measuring and quantifying the absorption and swelling as described in Sections 6.2.2.1 and 6.2.2.2.

6.2.2.1. Method A

A more accurate measure of solubility than simple observation that is recommended by the Joint Expert Committee on Food Additives is essentially the determination of the insoluble fraction, i.e. the hydrogel fraction. This can be determined by weighing after vaccum filtration has been carried out. This method has been modified by changing the solvent from a mild alkaline to water [6.1, 6.2]. The weight (W_1) of a 70 mm glass fibre paper (pore size 0.7 or 1.2 μm) is determined following drying in an oven at 105°C for 1 hour and subsequent cooling in a desiccator containing silica gel. Depending on the test material, 1−2 %wt (s) dispersion can be prepared in distilled water, which is then subjected to overnight hydration at room temperature. The hydrated dispersion is then

centrifuged for 2−5 minutes at 2500 rpm prior to filtration under vacuum. Drying of the filter paper is carried out in an oven at 105°C, following which it is cooled to a constant weight (W_2). The percentage of soluble and insoluble fractions can then be calculated using the equation below:

$$\text{Per cent insoluble fraction} = (W_2 - W_1)/S \times 100 \quad (6.2)$$

Different sizes of mesh will be chosen depending on the material being investigated. In Ref. [6.3], a 20 mesh steel screen (1041 μm) was used to determine the gel fraction.

6.2.2.2. Method B

Another method specifically defines the dispersion time of the test materials in deionized water for 16 h [6.4] or 48 h at room temperature [6.5]. The gel fraction (insoluble) is then measured as follows:

$$\text{Gel fraction} = (W_d / W_i) \times 100 \quad (6.3)$$

where W_i is the initial weight of the dried sample and W_d is the weight of the dried insoluble part of the sample following extraction with water.

6.2.3. Swelling

6.2.3.1. Method A

The Japanese Industrial Standard K8150 method is used to measure the swelling of hydrogels. The dry hydrogel is immersed in deionized water on a roller mixer for 48 at room temperature. After swelling, the hydrogel is filtered by a stainless steel 30 mesh net (681 μm). The following equation is used to calculate the swelling [6.5]:

$$\text{Swelling} = (W_s - W_d) / W_d \quad (6.4)$$

where W_s is the weight of hydrogel in the swollen state and W_d is the weight of hydrogel in the dry state. Various terms such as “swelling ratio” [6.6], “equilibrium degree of swelling” [6.7] and “degree of swelling” [6.8] have been used for this type of measurement.

6.2.3.2. Method B

An alternative method of measuring the swelling of a hydrogel is to disperse it in a dry state into 25–30 mL of water in a universal vial for 48 h at room temperature. This mixture is centrifuged to separate the water bound matter from the free unabsorbed water, which is removed. Method A, as described in Section 6.2.3.2, is then used to measure the swelling.

6.2.3.3. Method C

The Japanese Industrial Standard K7224 also offers a method for measuring the swelling of a hydrogel. The gel, in a dry state, is immersed in deionized water for 16 h at room temperature. The mixture is then filtered using an 100 mesh stainless steel filter (149 μm). The following equation is used to calculate the swelling [6.9]:

$$\text{Swelling} = (C/B) \times 100 \tag{6.5}$$

where C is the weight of hydrogel obtained after drying and B is the weight of the insoluble portion after extraction with water.

6.3. LIMITING VISCOSITY NUMBER (INTRINSIC VISCOSITY)

Dilute polymer solutions exhibit a characteristic feature: their viscosity is considerably higher than that of either a pure solvent or a dilute solution of small molecules. Dilute solution viscometry is based on the measurements of the increase in viscosity of a dilute polymer in solution in a particular solvent and at a particular temperature. The magnitude of the viscosity increase is related to the dimensions of the polymer molecules in solution, which is affected by the polymer's structure, the shape of its molecules, its degree of polymerization and by polymer–solvent interactions [6.10]. Capillary viscometry is based on the time it takes for a certain volume of polymer solution to flow through a thin capillary compared to the time for the solvent to flow (see Fig. 6.1). The flow time for either is proportional to the viscosity of the liquids, and inversely proportional to the density. For dilute polymer solutions, the density term is assumed to be that of the solvent. At least four dilutions can be made in situ using the solvent. Two or three readings should be made for each dilution and the average taken. The relative viscosity for the lowest and highest concentrations should be in the region of 1.2–2.0 to ensure that all measurements are in the diluted region. Capillary viscometric measurements of dilute polymer solutions are, therefore,

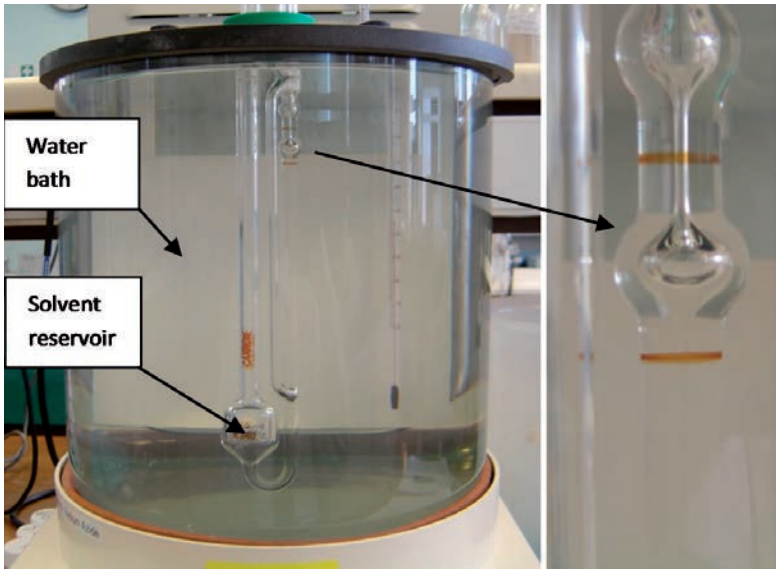

FIG. 6.1. Ubbelohde dilution viscometer housed in a water bath to maintain the desired temperature for measurements.

extremely valuable for the characterization of polymers, as attested by their widespread use. Charged polymers (polyelectrolytes) at low ionic strength exist in solution as extended coils owing to intramolecular charge repulsions. Charge repulsions can be eliminated by charge screening, when the polymer is dissolved in a solvent with a high concentration of electrolyte. Experimentally, the viscosity of a polymer solution is measured relative to that of the solvent, thus giving the relative viscosity:

$$\eta_{rel} = t_{solution} / t_{solvent} \tag{6.6}$$

where $t_{solution}$ and $t_{solvent}$ are the flow times of the polymer solution and solvent, respectively. The specific viscosity, η_{sp}, can be obtained from:

$$\eta_{sp} = (\eta_{solution} - \eta_{solvent}) / \eta_{solvent} \tag{6.7}$$

$$\eta_{sp} = (\eta_{rel} - 1) \tag{6.8}$$

The reduced viscosity and inherent viscosity may be defined as follows:

$$\eta_{red} = \eta_{sp}/c \tag{6.9}$$

$$\eta_{inh} = \ln\eta_{rel}/c \tag{6.10}$$

where c is the polymer concentration (mg/dL). If relative viscosity measurements are made under constant high ionic strength and by extrapolating the plot of the reduced or the inherent viscosity against concentration to infinite dilution, the intrinsic viscosity can be obtained in the same way as for uncharged polymers as given in Eq. (6.11).

$$[\eta] = \lim_{c\to 0} \eta_{red} = \lim_{c\to 0} \eta_{inh} \tag{6.11}$$

Experimentally, a plot of reduced viscosity as a function of concentration will give a straight line with an intercept equal to the intrinsic viscosity as given by the Huggins equation, Eq. (6.12). Alternatively, the intrinsic viscosity could be obtained by plotting the inherent viscosity as a function of the concentration as shown by Kraemer's equation, Eq. (6.13).

$$\eta_{sp}/c = [\eta] + k'[\eta]^2 c \tag{6.12}$$

$$(\ln \eta_{inherent})/c = [\eta] + k'' [\eta]^2 c \tag{6.13}$$

A typical Huggins and Kraemer plot to determine intrinsic viscosity is shown in Fig. 6.2. Generally, Huggins and Kraemer plots intersect at zero concentration as shown in Fig. 6.2, and the average value of the intercepts is used as the intrinsic viscosity. However, in the presence of aggregation, the Huggins and Kraemer plots will not intersect at zero concentration [6.11]. In such cases, the value of the intercept of the Huggins plot at zero concentration is often used as the intrinsic viscosity. Huggins and Kraemer constants can be calculated with following equations:

$$k' = d_{Huggins}/[\eta]^2 \tag{6.14}$$

$$k'' = d_{Kraemer}/[\eta]^2 \tag{6.15}$$

where d is the slope of the curve. The value for the Huggins constant is approximately 0.4 for many completely water soluble polysaccharides, and any higher values (>1) are usually taken as an indication of aggregation [6.12–6.14].

The limiting viscosity number or intrinsic viscosity $[\eta]$ is an index of the size of isolated polymer coils, and it has units of reciprocal concentration.

The molecular weight or, more accurately, the viscosity-average molecular weight ($\bar{M}_v$) can be evaluated from viscosity data if a correlation can be established between $[\eta]$ and the weight-average molecular weight. This approach

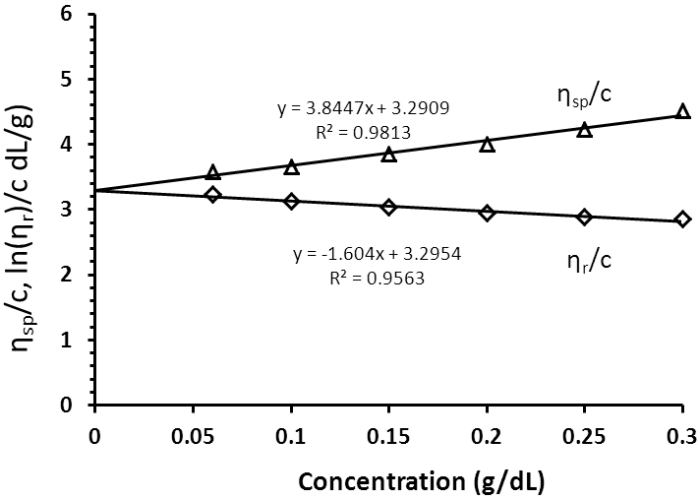

FIG. 6.2. Plot of reduced and inherent viscosities as a function of concentration for the determination of the intrinsic viscosity of sugar beet pectin in 0.1M NaCl at 25°C.

requires knowing or being able to determine the appropriate K and *a* values in the Mark–Houwink equation:

$$[\eta] = K\bar{M}_v^{\,a} \tag{6.16}$$

Mark–Houwink parameters are constants for a given polymer, which depend on the ionic strength and temperature of the solution and can be determined from a plot of log intrinsic viscosity versus log $\bar{M}_w$. $\bar{M}_w$ can be determined by an absolute technique such as light scattering, as described below. The *a* value is an effective parameter of polymer conformation and polymer–solvent interactions. If *a* is 0.6−0.8, the polymer is in random coil configuration in solution, and if the *a* value is greater than 0.8, the polymer behaves as a rigid rod. A value of zero indicates a spherical conformation.

A further variable in intrinsic viscosity measurements is the capillary viscometer itself. Ideally, all measurements should relate to the zero shear rate and a shear rate correction factor should be used specifically for high molecular weight polysaccharides that exhibit non-Newtonian behaviour even in diluted solutions (see Chapter 2). A further variable that can affect measurements is the purity of the sample and it is therefore recommended to dissolve the test material in the solvent and dialyse against the same solvent to ensure the same composition of the solvent throughout the measurements.

Both the Huggins and Kraemer equations are applicable in the diluted region. At higher concentrations ($c > 1/[\eta]$), experimental data show upward curvature when plotted according to the Huggins equation. However, some other equations have been reported for the determination of intrinsic viscosity using the extrapolation of experimental data and are below. Equation (6.17) is the linear Martin equation and Eq. (6.18) is the Schulz−Blaschke equation.

$$\ln (\eta_{sp}/c) = \ln[\eta] + k_M[\eta]c \tag{6.17}$$

$$\eta_{sp}/c = [\eta] + k_{SB}[\eta]\eta_{sp} \tag{6.18}$$

where c is the polymer concentration, and k_M and k_{SB} are the respective constants. η_{sp} is dependent on concentration and interaction forces. Plots of $\ln (\eta_{sp}/c)$ against c and η_{sp}/c against η_{sp} are straight lines with the intrinsic viscosity as the intercept. These two equations are applicable to a relatively higher range of concentrations than the Huggins and Kraemer equations.

6.4. GPC

GPC is a technique used for the separation of macromolecules by molecular size. It has been generally considered synonymous with other terms such as size exclusion chromatography, gel filtration chromatography and steric exclusion chromatography. GPC is primarily used to obtain molecular weight distribution information for polymeric materials. It provides information about the molecular weight, i.e. number, weight and Z averages ($\bar{M}_n$, $\bar{M}_w$, $\bar{M}_z$) as well as the molecular weight distribution (and polydispersity) of a polymer sample. When a sample is injected into a GPC column, the polymer molecules are separated according to their hydrodynamic volumes; therefore, polymer molecules larger than the pores of the packing material cannot enter the pores and are eluted at the interstitial volume V_i (also known as the void volume of the column). It should be noted that no fraction of the sample can be eluted before the interstitial volume has passed through the column. Small molecules, however, have access to the pores and will therefore elute at the sum of both the interstitial and pore volume, i.e. $V_i + V_p$. Molecules that have sizes between the above two extreme values will have access to only a part of the pore volume and will therefore be eluted at the elution volume V_e:

$$V_e = V_i + K_{SEC} V_p \tag{6.19}$$

where V_e is the elution volume, V_i is the interstitial volume and V_p is the pore volume. K_{SEC} is the equilibrium constant of a sample in size exclusion chromatography ($0 < K_{SEC} < 1$). Although GPC is an easy, economical and reproducible technique for the molecular weight characterization of a polymer sample, a limitation of using it alone is that it only gives correct weight-average molecular weight ($\bar{M}_w$) values for polymers for which standard polymer samples with well known molecular weights are available. In order to obtain an absolute molecular mass value for a sample, standards with known molecular masses must be used to obtain a suitable calibration curve. Also, the technique is very sensitive to flow rate variation, and to avoid any misinterpretation, internal standards should be used whenever possible.

6.5. LIGHT SCATTERING

Light scattering from dilute polymer solutions is another method for the determination of $\bar{M}_w$, radius of gyration and the second virial coefficient. When a beam of electromagnetic waves strikes atoms or molecules in a medium, the electrons are displaced and oscillate about their equilibrium positions with the same frequency as the incident exciting beam. This forces the electrons to move in one direction and the nuclei in the opposite direction, which results in an induced transient dipole in the atoms or molecules. As a consequence, the atoms or molecules will act as a secondary scattering centre by re-emitting the light in all directions. If a plane polarized light source is used, 99%+ of this re-emitted light will be in a plane perpendicular to the direction of the polarization. The intensity of the scattered light is proportional to the molar mass of the sample multiplied by the concentration of the sample and, crucially, this measurement is independent of the sample conformation.

Light scattering can be affected by intermolecular interaction (interaction between two neighbouring chains) producing a non-ideality. This non-ideality, the second virial coefficient, can be measured with light scattering using a series of different concentrations, but researchers most often prefer to work with dilute solutions to minimize these interactions since in this regime, the polymer molecules are separated by large distances. This situation is typified by chromatographic separation. In practice, molecular weights ($\bar{M}_w$) as low as that of sucrose (3.4×10^2) and as high as those of proteins of a magnitude of 10^9 can be measured.

Light of a uniform wavelength is emitted from a source, typically a laser, and passes through a cell containing the polymer solution of interest (Fig. 6.3). Multi-detectors are positioned at varying angles to simultaneously measure the intensity of light scattered $I(\theta)$.

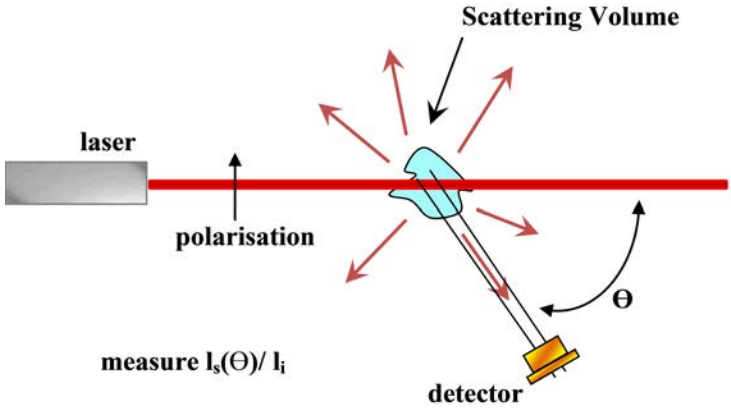

FIG. 6.3. The path of light scattered through a polymer solution. Reproduced with permission from Wyatt Technology.

The incident light, I_0 and scattered light, $I(\theta)$, in light scattering experiments are related by the Rayleigh ratio, $R(\theta)$, given by Eq. (6.20):

$$R(\theta) = \frac{I(\theta)}{I_0} \tag{6.20}$$

The light scattering intensity of a polymer solution is proportional to the product of its molecular weight (M), concentration (c) and the specific refractive index value (dn/dc), as given in Eq. (6.21):

$$I_{\text{scattered}} \propto M\, c\left(\frac{dn}{dc}\right)^2 \tag{6.21}$$

The weight-average molecular weight can be calculated using Eq. 6.22:

$$\frac{\mathrm{K}^* c}{R(\theta)} = \frac{1}{\bar{M}_{\mathrm{w}}} + 2A_2 c + \ldots \tag{6.22}$$

where:

K^* is an optical constant given by Eq. (6.23) below;
c is the solute concentration by weight of the polymer;
$R(\theta)$ is the excess scattered intensity ratio (Rayleigh ratio) of the molecular solution of concentration c at angle θ;
$\bar{M}_{\mathrm{w}}$ is the weight-average molecular weight;

and A_2 is the second virial coefficient that accounts for the solvent–solute interactions mentioned above.

$$\mathrm{K}^* = \frac{4\pi^2 n_0^2}{N_\mathrm{A}\lambda_0^4}\left(\frac{dn}{dc}\right)^2 \tag{6.23}$$

Equation (6.22) is only valid at all angles for small particles or molecules of dimensions of less than $\lambda'/20$, where $\lambda' = \lambda_0/n_0$, as small particles scatter the light isotropically. This is known as the Rayleigh–Gans–Debye limit. Here, λ_0 is the wavelength in vacuo of the incident beam and n_0 is the refractive index of the solvent. Polymer molecular dimensions are usually much larger than $\lambda'/20$. The obvious way to improve this limit would be to increase the wavelength of the incident light; however, in practice this is not done on a routine basis as problems of fluorescence and absorption tend to occur at the higher wavelengths. Larger particles or polymer molecules can still be examined as in a multiple angle detector system; the intensity of the light scattered is recorded at many angles [6.15, 6.16].

The light scattering intensity exhibits an angular dependence for particles above 10 nm in size (i.e. molecules with a major dimension larger than $\lambda°/20$ of the light's wavelength). This is usually the case in polymer solutions. Consequently, such variation depends on the size of the molecule, the wavelength of the light λ, and the observation angle θ. The Rayleigh-Gans-Debye approximation combines the light scattering principles of Eq. (6.22) and its angular dependence according to Eq. (6.24):

$$I_{\text{scattered}}(\theta) \propto R(\theta) = \mathrm{K}^* McP(\theta)\left[1 - 2A_2 McP(\theta)\right] \tag{6.24}$$

where

M is the molecular weight;
c is the polymer concentration;

and $P(\theta)$ is the form factor, corresponding to the angular variation of the scattered intensity as a function of the mean square radius, R_g, of the particle.

The larger the R_g, the larger the angular variation will be. A_2 enters the light scattering equation as a correction factor for concentration effects.

The *dn/dc* is the specific refractive index increment, which is the change in the refractive index of a polymer solution relative to the change of polymer concentration (see Eq. 6.23). The *dn/dc* value depends on (a) the type of polymer; (b) the type of solvent in which it is measured, and (c) the wavelength, and it is required to accurately determine the molecular weight by light scattering. For

greatest accuracy, the *dn/dc* used in light scattering experiments should have been obtained for the polymer solvent system at the wavelength and temperature used in the light scattering detector. The *dn/dc* can be obtained from the literature or measured directly with a differential refractive index detector using a series of polymer concentrations and measuring the change in refractive index, Δn, at the wavelength of the incident beam. A plot of Δn as a function of concentration is then constructed and by extrapolation to zero concentration, the *dn*/*dc* value is obtained.

The technique of multi angular laser light scattering (MALLS) can be used in batch mode by constructing a Zimm plot. A Zimm plot is a graphical representation of light scattering data in which the angular and concentration dependence of the scattering is displayed in a single plot. The weight-average molecular weight ($\bar{M}_w$), the radius of gyration (R_g), and the second virial coefficient (A_2) can be determined by measuring the scattered intensity as a function of angle for a series of dilute concentrations. These parameters are obtained by plotting $K^*c/R(\theta)$ against $\sin^2(\theta/2) + kc$, where k is the stretch factor, an arbitrary constant used to spread out the data and is only present to give a suitable scale to the graph obtained (changing the value has no effect on the results). A value of $k = 1/c_{max}$, where c_{max} is the maximum concentration used, has been reported [6.15]. Extrapolation of the data to zero concentration is needed to calculate the second virial coefficient. The double extrapolation to zero angle and zero concentration intercepts the $K^*c/R(\theta)$ axis at a value equal to the inverse of molecular weight (Eq. (6.25)). The second virial coefficient is obtained from the initial slope of the concentration dependence after extrapolation to zero concentration, while the root mean square radius is obtained from the initial slope of the angular dependence after extrapolation to zero angle.

$$\left(\frac{K^*c}{R(\theta=0)}\right)_{c\to 0} = \frac{1}{\bar{M}_w} \tag{6.25}$$

There are a variety of mathematical formulas that can be used to project to zero angle, with the Zimm formula being the most commonly used, but Debye and Berry methods are also possible (as are others based on models). These methods differ in the quantity used on the ordinate (Y axis) but the abscissa (X axis) is always the same, i.e. $\sin^2(\theta/2) + kc$, whereas, the ordinates are $R_\theta/(K^*c)$, $(K^*c)/R_\theta$ and $\sqrt{(K^*c)/R_\theta}$ for Debye, Zimm and Berry plots, respectively. The choice of extrapolation method can have a large impact on the obtained results in terms of accuracy. For polymer molecules with a smaller size (root mean square radius of <50 nm), the errors due to extrapolation are rather small, and are often independent of the method used. However, for large sized random coil polymers, the Berry method with a linear fit shows the highest accuracy of all three methods.

A linear fit to the lowest reliable angular data plotted according to the Berry method is the most advisable procedure when there is no prior knowledge of the polymer structure and size [6.17]. In each event, it is essential for an accurate determination to be made in order to be able to see the relationship between the line used by the relative formalisms and the real data, so as to be able to judge accurately which should be used.

One of the difficulties associated with static light scattering in the batch mode is the need to ensure that all solutions are dust free to obtain a true measure of the scattering intensity. Even a few particles of μm size will have a disproportionate effect on the result as these particles scatter so much light. Additionally, the concentration needs to be accurately determined. Furthermore, some polysaccharides have been shown to be sensitive to shear degradation following the passage through the kind of small size filters often used to obtain a dust free solution [6.18]. This mixer can be coupled with MALLS and a concentration detector as shown in the flow chart (Fig. 6.4) using the example of Calypso system. Figure 6.5 shows an example of a Berry plot for the determination of the molecular weight of hyaluronan using CG-MALLS.

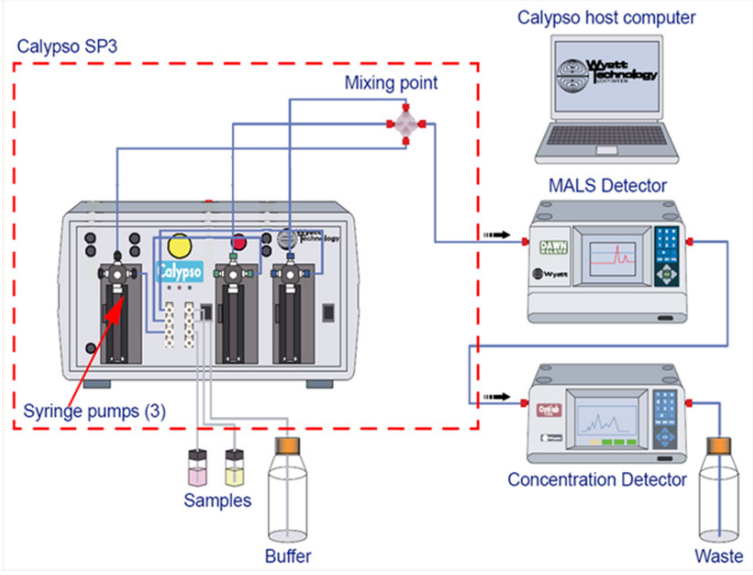

FIG. 6.4. Flow chart of concentration gradient linked to the MALLS detector (also known as a MALS detector) and concentration detector used for the generation of the Berry plot shown in Fig. 6.5. Reproduced with permission from Wyatt Technology.

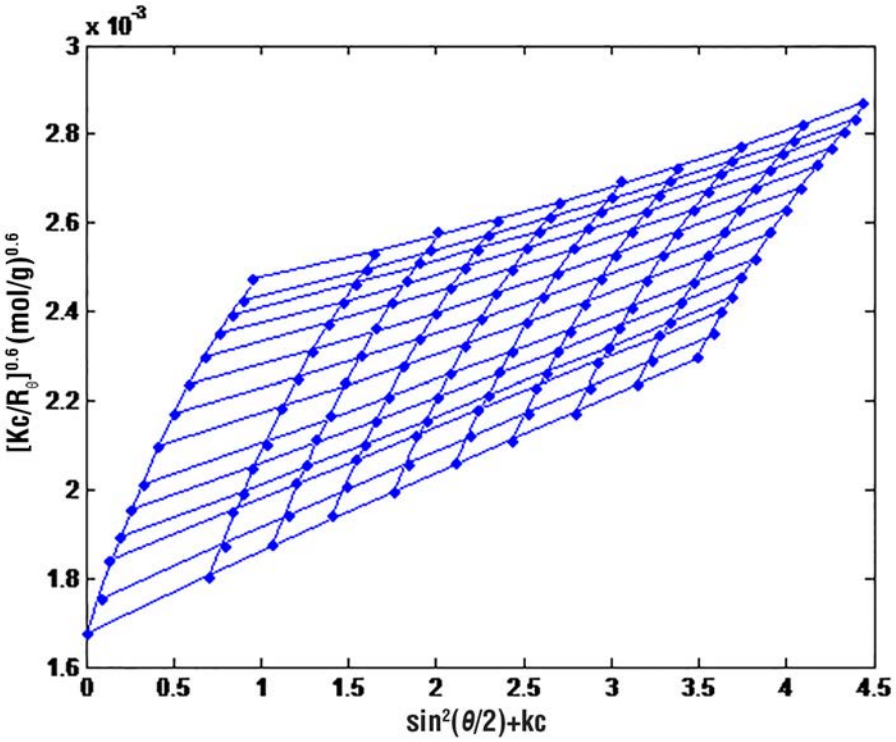

FIG. 6.5. Example of a Berry plot where $(Kc/R_\theta)^{0.5}$ is plotted against $\sin^2(\theta/2)$ + kc over a range of concentrations of hylauronan in 0.1M NaCl.

6.6. GPC-MALLS

The coupling of GPC with an on-line light scattering detector and a concentration sensitive detector (refractive index detector) results in a powerful tool for polymer characterization. Other detectors, such as viscometric or UV, can also be added to the system to provide additional information about the test material. The advantage of such a system over the conventional GPC method is that it is an absolute method and as such does not require either polymer standards or calibration curves to determine a value. Also, such a coupled system is insensitive to flow rate and other changes in chromatographic conditions. It will also give a measure of the molecular weight that is not affected by conformation changes or column interactions, an important factor when dealing with large, complex molecules, along with radius data where the size is large enough (>10–15 nm).

To obtain consistent interpretation, highly polydisperse samples need to be separated using fractionation techniques, the most common of these being GPC. GPC-MALLS techniques offer additional information such as weight-average and number-average values for both mass and size, distributions of the molecular weight and mean square radii. Additionally, they are also useful in obtaining information on branching conformations and the shapes of macromolecules in solution, a factor which is found in the log ratio of the molecular weight and R_g. A schematic presentation of a typical GPC-MALLS system is shown in Fig. 6.6.

There are many available commercial suppliers of the various detectors used in this system. All essentially measure the light scattering intensity and use the refractive index detector to determine the concentration of the fraction (often called slice) to create a plot similar to that already explained in the batch mode above. When the sample is fractionated through a GPC-MALLS-RI system, the software measures the excess Rayleigh ratio ($R(\theta)$) and sample concentration for each slice. A Debye, Zimm or Berry plot, for example, can be constructed for each slice by the extrapolation method, as shown in Fig. 6.7 below.

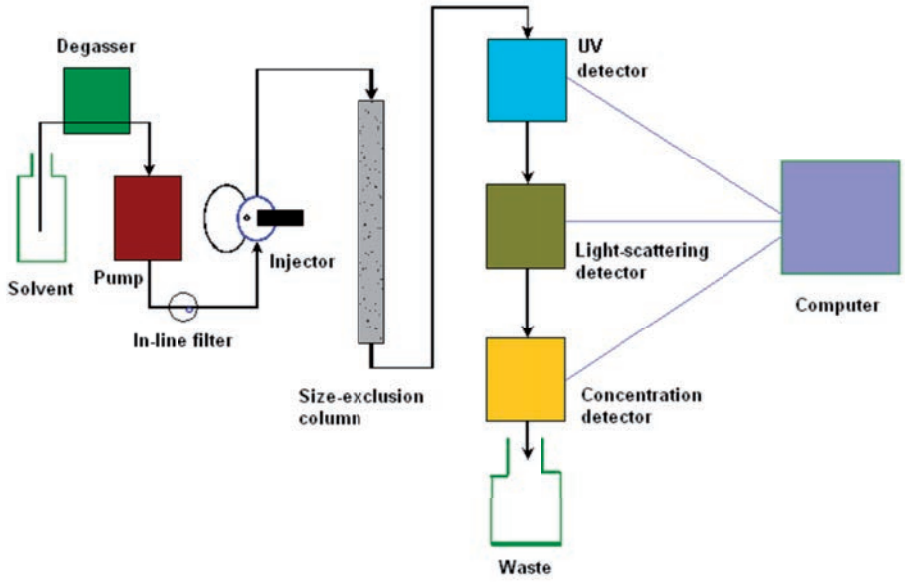

FIG. 6.6. A typical GPC-MALLS flow diagram. Solvent enters the degasser and is pumped through an in-line filter before the sample is injected and passes through the columns. The fractions are then detected by various detectors.

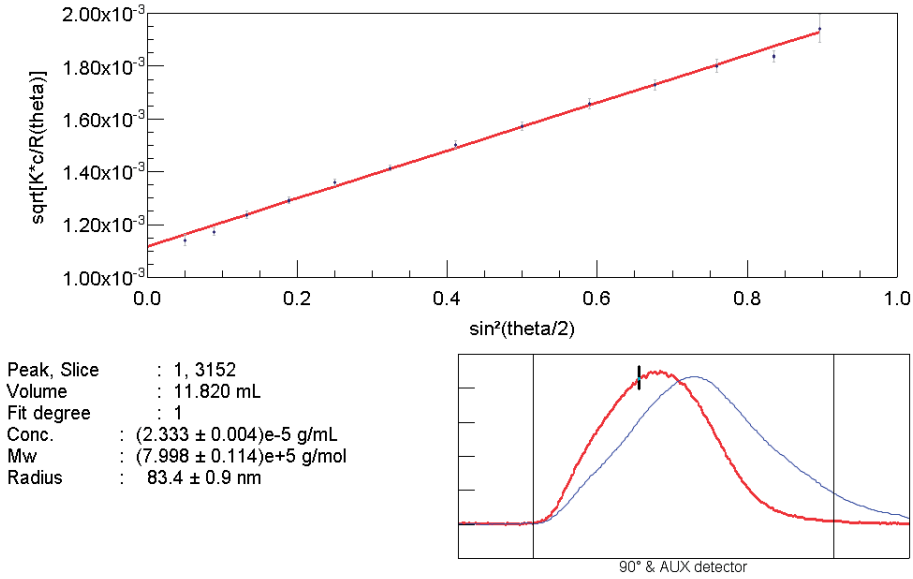

FIG. 6.7. Example of extrapolating the data obtained from multiple detectors corresponding to one slice (fraction) using Berry fitting method with a fit degree of 1.

In a Debye plot, the intercept at zero angle will give the value. Astra software, for example, can compute weight-average molecular weight ($\bar{M}_w$), number-average molecular weight ($\bar{M}_n$), molecular weight distributions, polydispersity index ($\bar{M}_w/\bar{M}_n$) and radius of gyration (R_g) by using the following equations. Equation (6.26) to obtain the weight-average molecular weight, Eq. (6.27) to obtain the number-average molecular weight and Eq. (6.28) to obtain the *z* average mean square radius:

$$\bar{M}_w = \frac{\sum(c_i M_i)}{\sum c_i} \tag{6.26}$$

$$\bar{M}_n = \frac{\sum c_i}{\sum \frac{c_i}{M_i}} \tag{6.27}$$

$$\langle r^2 \rangle_z = \frac{\sum c_i M \langle r^2 \rangle_i}{\sum (c_i M_i)} \tag{6.28}$$

where c_i and M_i are the concentration and the molecular weight for each slice, respectively. The *z* average mean square radius of gyration, defined as the average distance from the centre of gravity of a polymer coil to the chain end, is shown schematically in Fig. 6.8 and given by $\langle r_g^2 \rangle = \Sigma r_i^2 m_i / M$.

A typical elution profile of GA following fractionation by GPC is shown in Fig. 6.9. References [6.19–6.22] report an elution profile of *Acacia senegal* and the determination of the weight-average molecular weight ($\bar{M}_w$) for the whole gum and for two of its components.

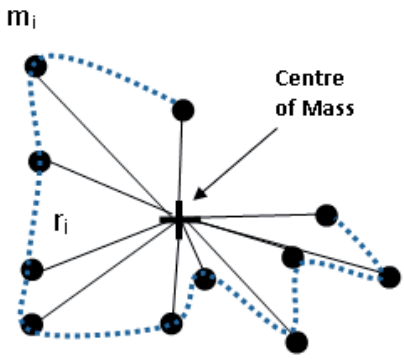

FIG. 6.8. Schematic representation of the mean square radius relating to the distribution of the mass within the molecule.

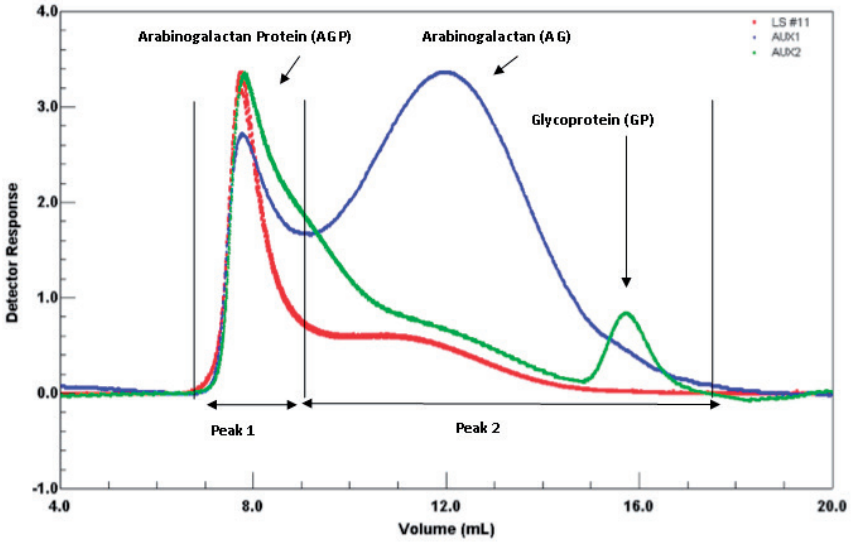

FIG. 6.9. GPC elution profile monitored by light scattering, refractive index and UV for control GA.

Molecular weight distribution can be depicted as cumulative or differential. The cumulative molecular weight distribution is defined as the weight fraction of a sample with a molar mass of less than M. For low molecular weight, the cumulative molecular weight distribution approaches zero, and for high molecular weight W(M) approaches unity. An example is shown in Fig. 6.10 for various polysaccharides using a GPC-MALLS system, which not only shows the differences in molecular weight distribution but also the effect of treatment on the same samples. The technique can be also used to show the difference in molecular weight parameters following processing or a given treatment [6.23]. Figure 6.11 shows the molecular weight distribution of hyaluronan aqueous solution following irradiation for various radiation doses [6.24].

Additionally, an accurate characterization of the material using GPC-MALLS allows the subsequent determination of the insoluble fraction (hydrogel) in a polymeric system to be quantified [6.25, 6.22]. The GPC-MALLS technique can also be used to quantify the hydrogels of several hydrocolloids such as GA, gelatin and pullulan using mass recovery [6.22, 6.26]. The mass recovery data calculated from the GPC refractive index correlate with the actual amount of hydrogel (insoluble fraction) obtained for dextran following irradiation in the solid state and in the presence of alkyne gas [6.22] (Fig. 6.12).

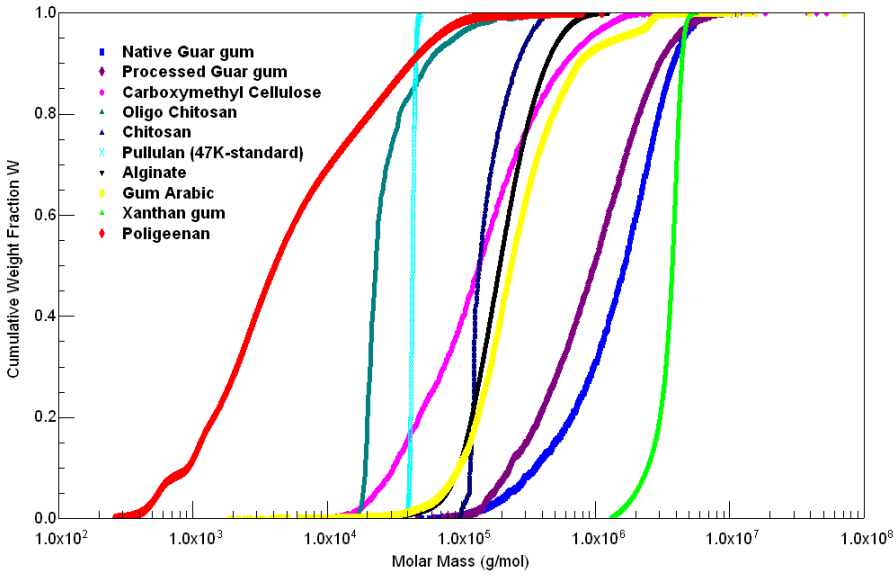

FIG. 6.10. Cumulative molecular weight plot of native GG, processed GG, CMC, oligochitosan, chitosan, pulluan, GA, xanthan gum and poligeenan obtained by GPC-MALLS.

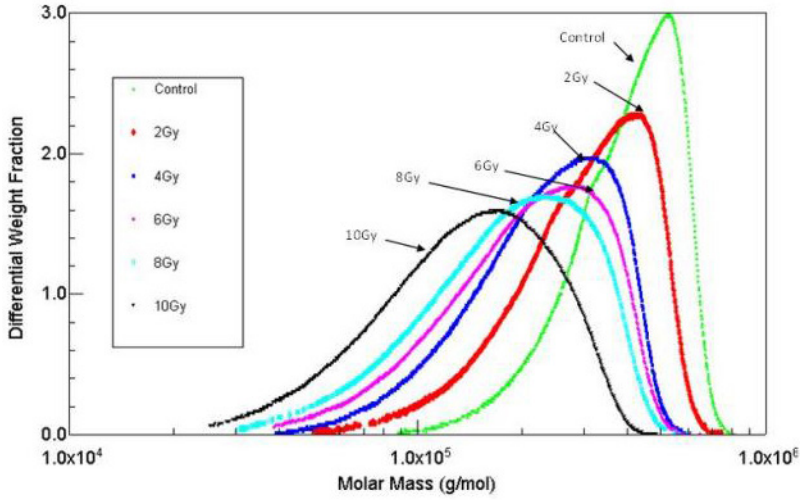

FIG. 6.11. An example of the molecular weight distribution of hyaluronan solutions following the reaction with hydroxyl radicals. Hyaluronan aqueous solution at pH7 saturated with N_2O was irradiated at various radiation doses using a gamma source at a dose rate 0.55 Gy/min and then injected into the GPC-MALLS system.

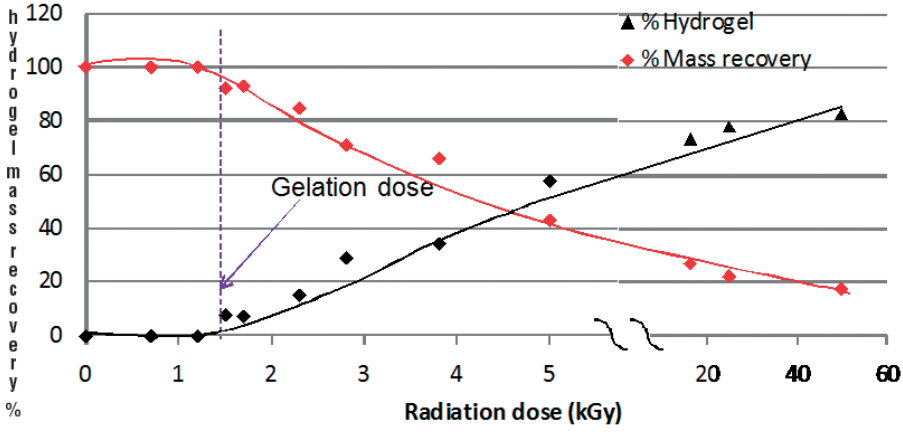

FIG. 6.12. Correlation between mass recovery data obtained from GPC-MALLS for dextran and the amount of hydrogel formed as a function of radiation dose.

6.7. DYNAMIC LIGHT SCATTERING (DLS)

Dynamic light scattering (DLS) is a well established technique for measuring particle size over the size range from a few nanometres to a few μm. Dynamic light scattering (also known as quasi-elastic light scattering and photon correlation spectroscopy) is particularly suited for the measurement of the size and size distribution of particles, emulsions and molecules dispersed or dissolved in a liquid.

Particles, emulsions and molecules in suspension undergo Brownian motion. This is the motion induced by the bombardment by solvent molecules that themselves are moving owing to their thermal energy. If the particles or molecules are illuminated with a laser, the intensity of the scattered light fluctuates at a rate that is dependent on the size of the particles. Analysis of these intensity fluctuations yields the velocity of the Brownian motion and hence the particle size can be calculated using the Stokes–Einstein relationship given below.

$$R_H = \frac{k_B T}{6\pi\eta_0 D_0} \tag{6.29}$$

Traditionally, rather than presenting the data in terms of diffusion coefficients, the data are processed to give the size of the particles (radius or diameter). The hydrodynamic diameter or Stokes radius, R_H, derived from this method gives the size of a spherical particle that would have a diffusion coefficient equal to that of the polymer molecule, and the data are commonly presented as the fraction of particles as a function of their diameter. The diameter that is measured in DLS is called the hydrodynamic diameter and can be used to understand how a particle diffuses within a fluid. The diameter obtained by this technique is that of a sphere that has the same translational diffusion coefficient as the particle being measured. Most polysaccharide molecules are not spherical. They have a hydrodynamic size that can be different from their true size and that may not be a reliable measure of molecular mass [6.27].

Reference [6.28] describes how, in the DLS technique, dynamic information of the particles is derived from an autocorrelation of the intensity trace recorded during the experiment. The following equation can be used to generate the second order autocorrelation curve from the intensity trace [6.28]:

$$g^2(\boldsymbol{q};\tau) = \frac{\langle I(t)I(t+\tau)\rangle}{\langle I(t)\rangle^2} \tag{6.30}$$

where $g^2(\boldsymbol{q};\tau)$ is the autocorrelation function at a particular wave vector, $\boldsymbol{q}$, and delay time, τ, and I is the intensity. The autocorrelation function $g^2(\boldsymbol{q};\tau)$ is the measure of correlation between the scattered intensity of the initial and final states. With time, eventually the correlation starts to exponentially decay to zero [6.29]. A typical correlation function of correlation coefficient against time for a xanthan aqueous solution is shown in Fig. 6.13.

Relevant equations are the Siegert equation, which is shown in Eq. (6.31), Eq. (6.32), which is used to derived the translational diffusion coefficient, and the Stokes-Einstein equation, which is shown in Eq. (6.33).

$$g^2(\boldsymbol{q};\tau) = 1 + \beta\left[g^1(q:\tau)\right]^2 \tag{6.31}$$

where β is a correction function dependent on the geometry and alignment of the laser beam in the light scattering set-up.

$$g^2(\boldsymbol{q};\tau) = \exp(-\Gamma\tau)... \tag{6.32}$$

$$\Gamma = \boldsymbol{q}^2 D_t \tag{6.33}$$

where Γ is the decay rate. For Eq. (6.32) it is necessary to calculate a wave vector, $\boldsymbol{q}$, for which Eq. (6.34) can be used. The wave vector $\boldsymbol{q}$ is the difference between the scattered and non-scattered beam, which relates to the refractive index of the solvent.

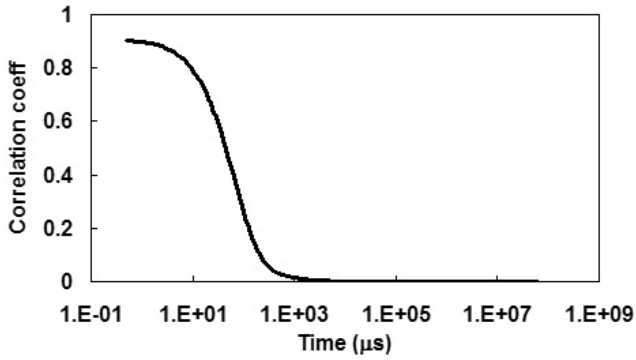

FIG. 6.13. Correlogram for xanthan showing the decay of intensity with time obtained using Zetasizer Nano ZetaSizer (Malvern Instruments, UK). Measurement conditions: 0.25 mg/mL xanthan dissolved in 0.1M $LiNO_3$, heated for 20 min in a sealed vial and subsequently filtered through 0.8 and 1.2 µm filters.

$$\boldsymbol{q} = \frac{4\pi n_0}{\lambda} \sin\left(\frac{\theta}{2}\right) \tag{6.34}$$

where:
λ is the incident laser wavelength;
n_0 is the refractive index of the sample

and θ is the angle at which the detector is located with respect to the sample cell.

Most polymers, and therefore most polysaccharides, are polydisperse systems. For such systems the autocorrelation function is calculated as shown in Eq. (6.35).

$$g^1(\boldsymbol{q};r) = \sum_{i=1}^{n} G_i(\Gamma_i)\exp(-\Gamma_i\tau) = \int G(\Gamma)\exp(-\Gamma\tau)d\Gamma \tag{6.35}$$

Some methods that have been developed to extract information from autocorrelation functions are described in Refs [6.30, 6.31] and include the CONTIN algorithm. A CONTIN fit to obtain size distribution from the first order autocorrelation function is shown in Fig. 6.14 for xanthan gum using the same data shown in Fig. 6.13.

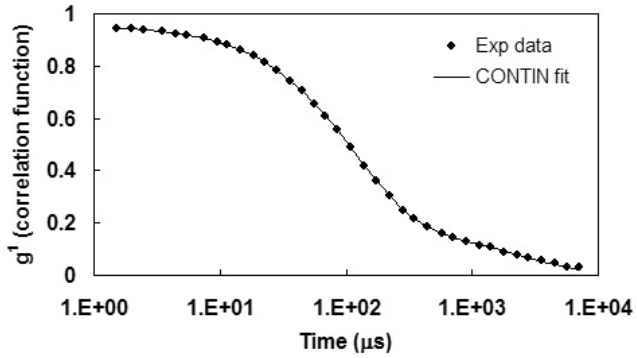

FIG. 6.14. Experimental data for the first order autocorrelation function (g^1) obtained by DLS and its corresponding fit (CONTIN) to obtain size distribution. Measurements were performed as described for Fig. 6.13.

6.8. RHEOLOGY

Rheology is the study of deformation and flow of matter and can be defined in terms of viscosity and elasticity. A good understanding of the terms stress and strain is essential for understanding this technique. The type of deformation commonly found in rheology using a rotational rheometer is simple shear. This can be illustrated with a rectangular bar of height h (Fig. 6.15). The lower surface is stationary and the upper plate is linearly displaced by an amount equal to δL. Each element is subject to the same level of deformation so the size of the element is not relevant. The angle of shear, γ, may be calculated as:

$$\tan(\gamma) = \frac{\delta L}{h} \tag{6.36}$$

With small deformations, the angle of shear (in rad) is equal to the shear strain (also denoted γ), $\tan \gamma = \gamma$. The shear stress, τ, on a material is defined as force, F, acting per initial unit area, A, which results in deformation or strain, γ.

$$\tau = \frac{F}{A} \tag{6.37}$$

It is important to measure the rheological properties of polymers under varying conditions of stress and strain in order to understand their performance in a process or under particular end use conditions. Shear strain may be generated using parallel plate, cone and plate or concentric cylinder fixtures as shown in Fig. 6.16 [6.32].

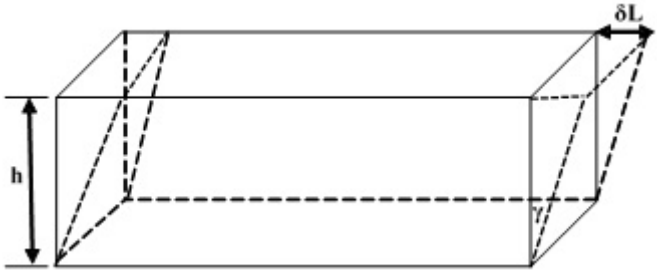

FIG. 6.15. Shear deformation of a rectangular bar. The solid lines represent the original shape.

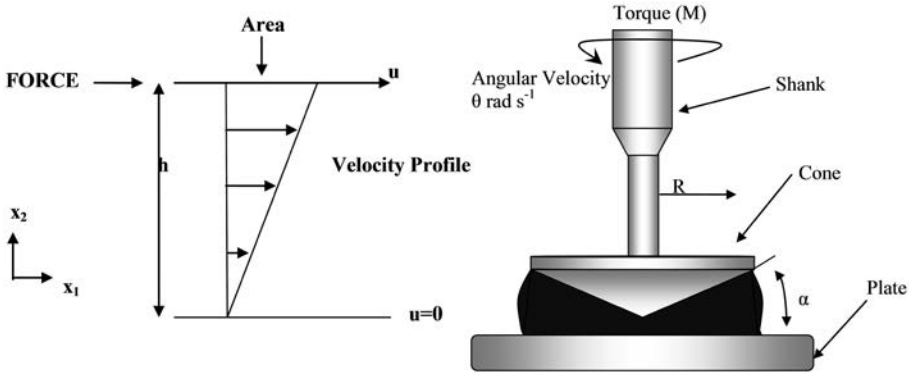

FIG. 6.16. Velocity profile between rotating cone and stationary plate.

6.8.1. Shear viscosity

The shear viscosity of a polysaccharide solution can be studied by subjecting the solution to continuous shearing at a constant rate which can be accomplished using either cone plate, cylindrical or parallel plate geometry with solution in the gap between the plates. Cone plate geometry has an advantage since it has low inertia and generates a uniform shear rate across the sample, but owing to the small gap between the plates, it is not fit for the measurement of large particle dispersion (containing hydrogels). For dispersions or solutions containing hydrogels, parallel plates with adjustable geometry gaps are more appropriate. In theory, both geometries produce similar velocity profiles. The lower plate is fixed and the upper plate moves at a constant velocity, u, which can be thought of as an incremental change in position divided by a small time period, $\delta L/\delta t$. A force per unit area on the plate is required for motion resulting in a shear stress (τ) on the upper plate that conceptually could also be considered to be a layer of fluid. The flow described above is steady simple shear and the shear rate (also called the strain rate) is defined as the rate of change of strain:

$$\gamma = \frac{d\gamma}{dt} = \frac{d}{dt}\left(\frac{\delta L}{h}\right) = \frac{\tau}{\eta} \tag{6.38}$$

The shear viscosity (η) of the fluid is defined as the ratio of applied stress, τ, to the shear rate, $\dot{\gamma}$.

$$\eta = \frac{\tau}{\dot{\gamma}} \tag{6.39}$$

When the viscosity of a fluid is independent of the shear rate it is said to be a Newtonian fluid (see Chapter 2.4); examples are low molecular weight materials such as water and glycerine. However, non-Newtonian fluids are classified in two categories: (a) shear thinning fluids whose viscosity reduces because of applied shear (most polymeric solutions fall into this category); (b) shear thickening fluids whose viscosity increases with increasing shear rate (such as sand and corn flour). Figure 6.17 shows the different flow curves of these different categories of fluids.

For a few of the polymeric solutions, viscosity remains unaltered at a very low shear rate, i.e. they show a Newtonian trend. This can be attributed to the fact that although the imposed deformation in one region leads to the breaking of entanglements in the polymeric solution, an equal number of new entanglements are formed; therefore, the overall solution viscosity remains the same. For other polymeric solutions, no Newtonian region is observed at a low shear rate, indicating the presence of yield stress (i.e. an energy barrier that must be overcome if a solution is to flow) in such solutions. It is possible to determine zero shear viscosity for the first kind of solution by extrapolating the flow curve to zero shear rates. However, at a reasonably high shear rate, entire solutions exhibit shear thinning behaviour [6.32, 6.33].

Flow behaviour of a fluid is represented by a plot of viscosity, η, versus shear rate, $\dot{\gamma}$. A typical flow curve of a polysaccharide solution (CMC, 1 wt% aqueous solution in distilled water) is shown in Fig. 6.18. Owing to the chain's characteristics, the flow curves usually show a non-Newtonian character, which is characterized by a critical shear rate over which the viscosity decreases when the shear rate increases. The first part of the curve is called the Newtonian plateau, where the viscosity is independent of $\dot{\gamma}$; in this domain the viscosity has to be measured to determine the intrinsic viscosity as discussed above.

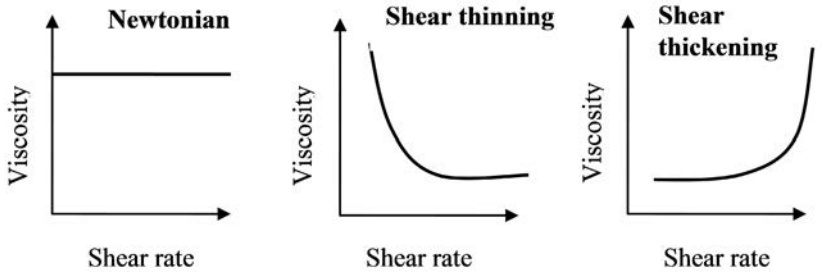

FIG. 6.17. Flow curve of Newtonian and non-Newtonian fluids of the shear thinning and shear thickening types.

The critical shear rate $\dot{\gamma}_c$ decreases when the molecular weight increases or when the polymer concentration increases [6.34, 6.35].

Using steady shear data (an example is shown in Fig. 6.18), the zero shear viscosity of samples can be determined using different fitting models. The equation for the Cross model is shown in Eq. (6.40) below [6.32, 6.36]. This model can be broken down into two components — a model known as the Sisko model (Eq. (6.41)) that includes the infinite shear plateau and the power law region (Eq. (6.42)), and the Williamson model (Eq. (6.43)) covering the zero shear plateau and power law region. Other models of a similar form to the Cross model have been developed, such as the Carreau model (Eq. (6.44)).

$$\eta = \eta_\infty + \frac{\eta_0 - \eta_\infty}{1 + \mathrm{K}_1(\dot{\gamma})^n} \tag{6.40}$$

$$\eta = \eta_\infty + \mathrm{K}_1\left[d\dot{\gamma}/dt\right]^{n-1} \tag{6.41}$$

$$\eta = \mathrm{K}_1\left[d\dot{\gamma}/dt\right]^{n-1} \tag{6.42}$$

$$\eta = \eta_0 + \mathrm{K}_1\left[d\dot{\gamma}/dt\right]^{n-1} \tag{6.43}$$

$$\frac{\eta - \eta_\infty}{\eta - \eta_0} = \frac{1}{\left[1 + (\mathrm{K}_1\dot{\gamma})^2\right]^{(n-1)^{1/2}}} \tag{6.44}$$

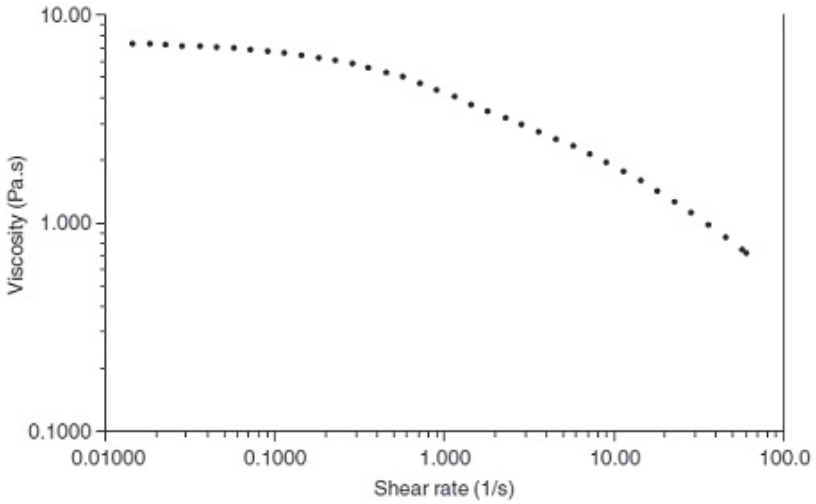

FIG. 6.18. Flow curve of CMC solution prepared at 1 wt% concentration in distilled water, measured at 25°C.

where

η_0 is viscosity at zero shear rate;
η_∞ is viscosity at infinite shear rate;
$[d\dot{\gamma} / dt]$ is change in shear rate with time;

and K_1 is the time constant.

The power law is the simplest model to describe the shear rate dependency of polymeric fluids. The Sisko model can be used at high shear rates, where the power law fails. The Williamson model can be used for low shear rate data where the power law fails to be fit. The Cross model can be applied only when there is a full range of data including the high and low shear Newtonian plateaux as well as a non-Newtonian shear thinning region [6.37, 6.38].

Figure 6.19 shows the zero shear viscosity data for a CMC sample obtained by using the best fitted model option, i.e. the Williamson model. Despite the lack of a steady state plateau in the low shear rate region, the standard error was only about 5% when extrapolating the shear viscosity to the zero axis.

Additionally, the data was also fitted to the modified Cross model suggested by Morris (Fig. 6.20). The relation between shear rate and zero shear viscosity for a random coil polysaccharide is given as follows [6.39]:

$$\eta = \frac{\eta_0}{\left[1 + (\dot{\gamma} / \dot{\gamma}_{1/2})^{0.76}\right]} \tag{6.45}$$

where $\dot{\gamma}_{1/2}$ is the shear rate required to reduce η_0 to $\eta_0/2$. In order to determine the zero shear viscosity of hydrocolloids by the Morris method, the stepped flow measurements were carried out in a range of shear rate (0.1–1000 s^{-1}). At each shear rate, $\dot{\gamma}$, the value of 0.76 was calculated and the result was multiplied by the corresponding viscosity, η, to obtain $\eta * \dot{\gamma}^{0.76}$. The graph was plotted for η (vertical axis) against $\eta * \dot{\gamma}^{0.76}$ (horizontal axis) and the best straight line was fitted. The intercept on the vertical axis gives zero shear viscosity (η_0). The result obtained by the alternative Morris method for the same sample, 5, was 12.87 Pa/s (Fig. 6.20). The two values are very close to one another, suggesting that the data are reliable.

6.8.2. Oscillation measurements

Polymer solutions exhibit neither completely liquid- nor completely solid-like behaviour and are termed viscoelastic solutions. The viscoelasticity of a polymer solution can be quantified by carrying out oscillation measurements,

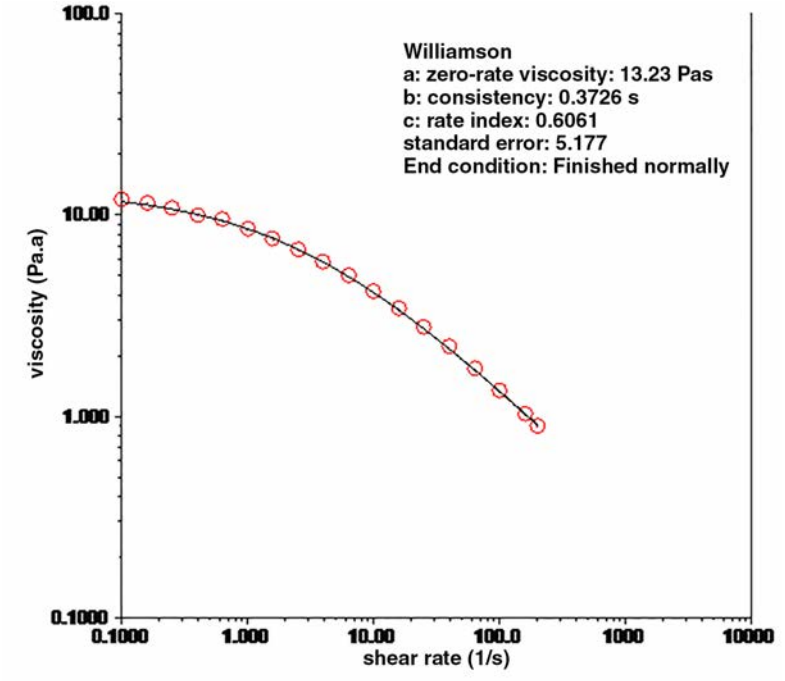

FIG. 6.19. Zero shear viscosity determined using the best fitting model option in TA software for a CMC sample (sample 5 measured at 2.5% in distilled water, at 25°C).

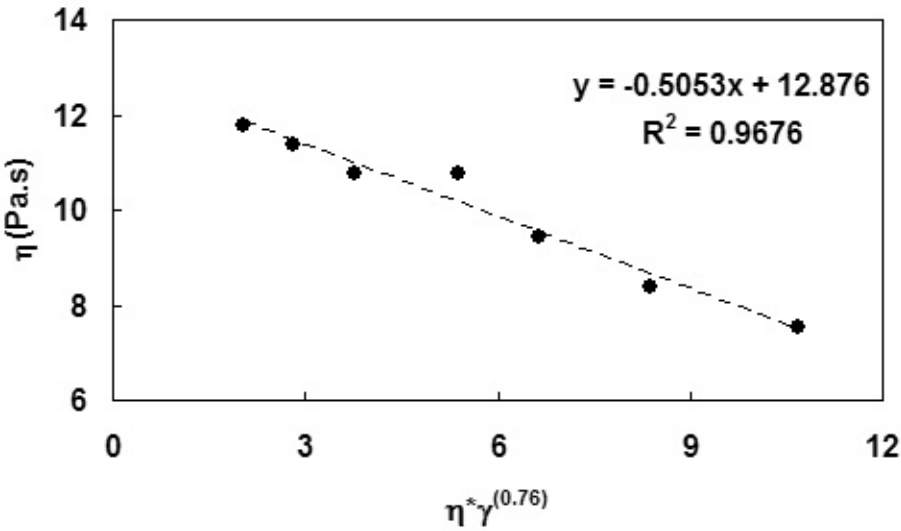

*FIG. 6.20. A plot of viscosity as a function of η * γ.l0.76 for the determination of zero shear viscosity according to the Morris method.*

the principle of which involves oscillating the polymer solution back and forth (using geometries such as parallel plate, cone and plate or cylinder) at a low frequency instead of rotating it at a high shear rate as for flow measurement. It is a non-destructive test in which the structure of the polymer is not broken, so it can show the properties of a solution under deformation before flow. The test solution is oscillated through a fixed stress or strain amplitude at an angular frequency, ω, and the resultant storage and loss modulus are derived. The data is often presented as a function of frequency, F, as this allows simulation of multiple timescales in one test. Typically, stress and/or strain-controlled, rotational rheometers are used to measure properties such as storage modulus, G', loss modulus, G'', and phase angle, tan δ, as a function of frequency, ω = 1/time, and temperature. An example of an experiment with a stress-controlled rheometer, in which a fixed stress is applied and the resulting deformation is measured, is shown in Fig. 6.21.

The ratio of input stress to the measured strain is defined as the complex modulus, G^*. It is the measure of stiffness of material, and higher the G^* value, the tougher the material will be. The phase angle, δ, is the measure of the elasticity of the material. A high phase angle indicates a viscous solution, while lower phase angles indicate a material with elastic behaviour. For a purely elastic material, the input stress and measured strain are exactly on phase, therefore the phase angle is zero. For a purely viscous material, the input stress and measured strain are a quarter of a cycle out of phase, so the phase angle is 90°. The following equations are involved in measuring the viscosity (η^*) and the viscous–elastic ratio of a polymer solution when oscillated at an angular frequency ($\omega = 2\pi \times$ frequency in Hz). At low frequency, since elastic contribution to the viscosity is negligible, complex viscosity is equal to dynamic viscosity in magnitude; i.e. $\eta^* = \eta'$. This is shown in Eq. (6.46) (storage modulus), Eq. (6.47) (loss modulus) and Eq. (6.48) (complex viscosity).

$$G' = G^* \cos\delta \tag{6.46}$$

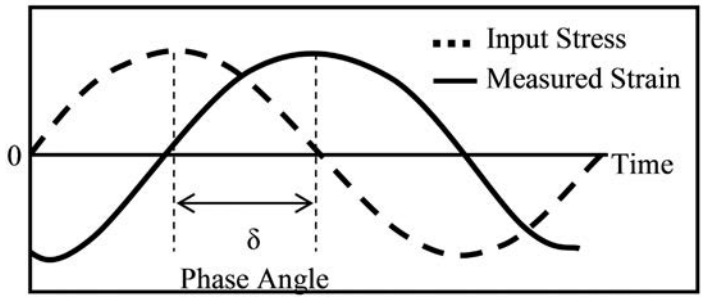

FIG. 6.21. Principle of oscillation measurement.

$$G' = G^* \sin\delta \tag{6.47}$$

$$\eta^* = \sqrt{\frac{(G')^2 + (G'')^2}{\omega}} \tag{6.48}$$

A prerequisite for oscillation measurement is making sure that within the frequency region, the input stress or strain is not high enough to break the structure of a polymeric solution. In other words, the test must be carried out within the linear viscoelastic region of the polymer solution being tested. The linear viscoelastic region of a polymeric solution is defined as a region wherein the entity of structure does not break when stress or strain is applied. Initially, a strain sweep test is conducted by varying the amplitude of a signal at a constant frequency to determine the limits of linear viscoelastic behaviour by identifying the critical value of the sweep parameter (Fig. 6.22). In the linear region, the rheological properties are independent of stress or strain [6.32, 6.40–6.42].

In oscillation measurement, a sinusoidal deformation is imposed on the solution in a large range of frequencies, and the response is a complex modulus decomposed in an in-phase response (G′ reflecting the elastic character) and an off-phase response (G″ reflecting the viscous response). An oscillation curve for a polysaccharide solution (CMC, at 1 wt% aqueous concentration in distilled water) is shown in Fig. 6.23. Generally for a polysaccharide solution G″ is larger than G′ at low frequencies until the 'cross-over' frequency (ω_0), beyond which G′ becomes larger than G″ [6.43]. The parameter ω_0 is shifted to a lower frequency when the polymer concentration or molecular weight increases.

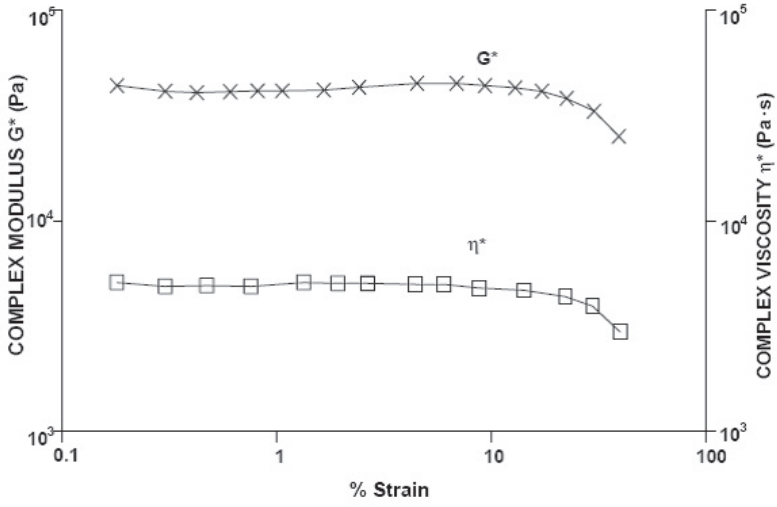

FIG. 6.22. Amplitude sweep curve for determining linear viscoelastic region.

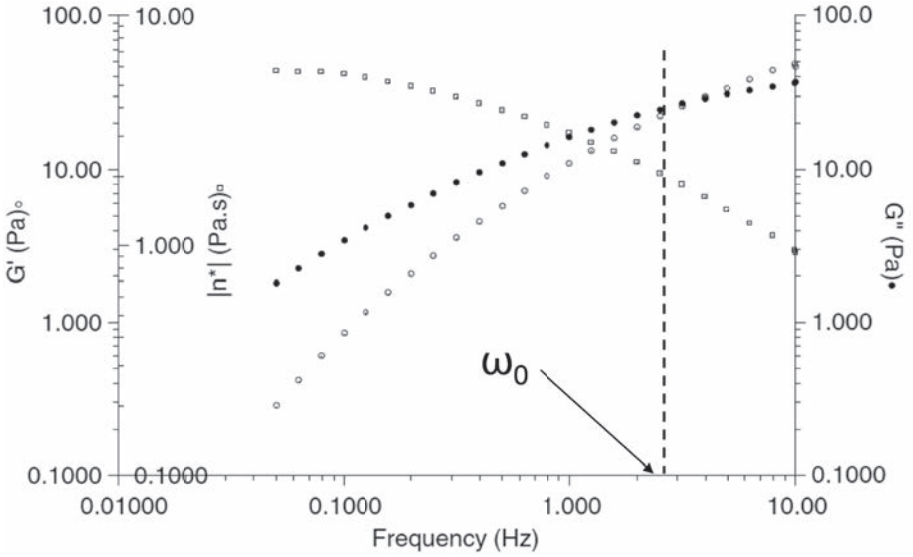

FIG. 6.23. Oscillation curve of CMC solution prepared at 1% concentration in distilled water, measured at 25°C. ω_0 is the cross-over frequency.

6.8.3. Cox–Merz relationship

The Cox–Merz relationship is used in rheology and is described in further detail in Refs [6.36, 6.44–6.46]. It states that the dynamic viscosity of a polymer is nearly equal to its steady shear viscosity at equivalent shear rate and angular frequency and is shown in Fig. 6.24.

6.9. ATOMIC FORCE MICROSCOPY

Atomic force microscopy (AFM) is a powerful technique capable of visualizing the structure of individual molecules. The images are obtained by touching the structure of the surface under investigation with a sharp tip or stylus that is mounted at the end of a flexible cantilever, allowing it to be placed gently on or very close to the sample surface with extraordinary precision (Fig. 6.25).

The force with which the tip rests on the surface under investigation should be very small in order to obtain a reliable image. When the tip is held in extremely close proximity to the sample surface, the cantilever, during the scan, bends freely up and down in response to features on the sample surface, as a result of repulsive forces. A low power laser is focused on the back of the cantilever and its deflection is detected by a photosensitive detector. Movements

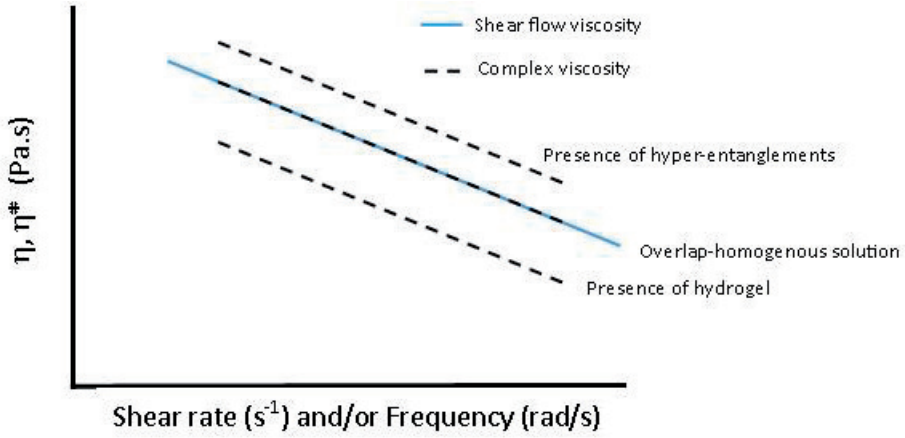

FIG. 6.24. Plot of shear flow viscosity and complex viscosity as a function of shear rate or angular frequency.

on the tip cause deflections of the laser beam which are amplified by the distance between the tip and the photo detector. An optical lever technique is the most common method for detecting and amplifying the tiny deflections experienced by the cantilever. Using this simple technology, subnanometer undulation of the tip can be detected. Methods have been described for the routine imaging

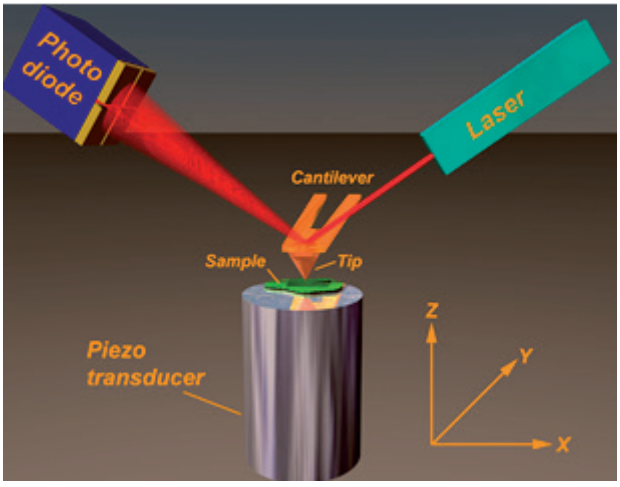

FIG. 6.25. Main features of the AFM. Image courtesy of A.P. Gunning (Institute of Food Research, Norwich, UK).

of polysaccharides by AFM using the most commonly used techniques: contact mode, non-contact mode and tapping mode [6.23, 6.47–6.50].

For example, AFM was used to investigate the effect of irradiation on modified hyaluronan (hylan) aqueous solution [6.51]. Samples were deposited on to freshly cleaved mica, air dried, and then imaged under a precipitant liquid in order to inhibit desorption or dissolution. This is a relatively mild preparative treatment and the molecules may reside within a thin film of water on the mica surface. Diluted solutions in a quantity of 10 μg mL^{-1} or 1 μg mL^{-1} were deposited onto freshly cleaved mica and allowed to dry for 10 min in air. The mica was then transferred to the liquid cell of the AFM for imaging. Examples of AFM images of hylan (modified hyaluronan) before and after irradiation in aqueous solution saturated with N_2O are shown in Fig. 6.26. The results shown in Fig. 6.26(a) show single chains and thicker bundles which have branch points to other continuous chains. Figure 6.26(b) shows long strands of molecules with little or no entanglement after the attack by •OH radicals.

This technique can also provide height measurements of individual molecules that have been used to further clarify xanthan's double helical conformation [6.23]. In addition to imaging, AFM has been successfully used to measure forces (in the nano-newton range) and record the amount of force felt by the cantilever as the probe tip is brought close to a sample surface and then pulled away. Consequently, the extent of cantilever bending provides information about the mechanics of the tip–sample interaction. Thus, information such as the mechanical modulus of the sample as well as long-range attractive or repulsive forces between the probe tip and the sample surface can be determined through such measurements. The application of AFM force measurements have been described in detail [6.52].

There have been significant advances in the field of AFM. The technique is now widely established and applied in various industrial sectors to solve

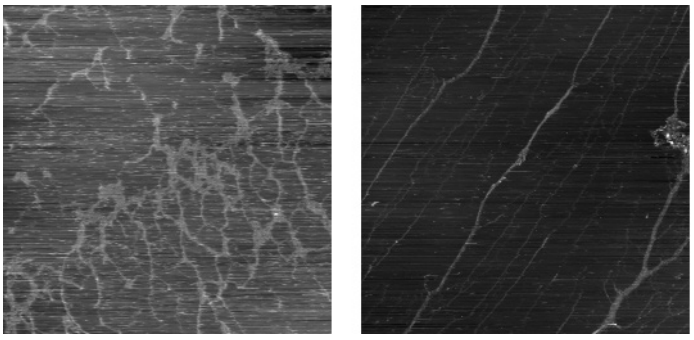

FIG. 6.26. AFM images showing the structure of cross-linked hyaluronan (Hylan) (a) before and (b) after gamma irradiation.

processing and material problems. In addition to polymeric materials, other materials being investigated include synthetic and biological membranes, metals, semiconductors, composites, glasses and thin and thick film coatings.

ACKNOWLEDGEMENTS

X. Li and S.K.H. Gulrez' results that are included in the dynamic light scattering and rheology sections are gratefully acknowledged.

REFERENCES TO CHAPTER 6

[6.1] AL-ASSAF, S., DICKSON, P.A., PHILLIPS, G.O., THOMPSON, C., TORRES, J.C., Compositions Comprising Polysaccharide Gums, Patent No. WO 2009016362 (A2), Feb. 2009, filed Jul. 2008, available on-line.

[6.2] LI, X., AL-ASSAF, S., FANG, Y., PHILLIPS, G.O., Characterisation of commercial LM-pectin in aqueous solution, Carbohyd. Polym. **92** 2 (2013) 1133–1142.

[6.3] YOSHII, F., KUME, T., Process for Producing Crosslinked Starch Derivatives and Crosslinked Starch Derivatives Produced by the Same, United States Patent No. US 6617448 B2, Sep. 2003, filed May 2001, available on-line.

[6.4] KATAYAMA, T., NAKAUMA, M., TODORIKI, S., PHILLIPS, G.O., TADA, M., Radiation-induced polymerization of gum arabic (*Acacia sengal*) in aqueous solution, Food Hydrocoll. **20** (2006) 983–989.

[6.5] NAGASAWA, N., YAGI, T., KUME, T., YOSHII, F., Radiation crosslinking of carboxymethyl starch, Carbohydr. Polym. **58** (2004) 109–114.

[6.6] LIU, P., PENG, J., LI, J., WU, J., Radiation crosslinking of CMC-Na at low dose and its application as substitute for hydrogel, Radiat. Phys. Chem. **72** 5 (2005) 635–638.

[6.7] VALLES, E., DURANDO, D., KATIME, I., MENDIZABAL, E., PUIG, J.E., Equilibrium swelling and mechanical properties of hydrogels of acrylamide and itaconic acid or its esters, Polym. Bull. **44** 1 (2000) 109–114.

[6.8] LIU, P., ZHAI, M., LI, J., PENG, J., WU, J., Radiation preparation and swelling behavior of sodium carboxymethyl cellulose hydrogels, Radiat. Phys. Chem. **63** (2002) 525–528.

[6.9] KATAYAMA, T., OGASAWARA, T., SASAKI, Y., AL-ASSAF, S., PHILLIPS, G.O., Composition Containing Hydrogel Component Derived from Gum Arabic, United States Patent No. 2008038436 (A1), 20050658003, 20050722, Feb. 2008, filed Jul. 2005, available on-line.

[6.10] AMALVY, J.I., Dilute solution viscosimetry of carboxylated acrylic lactices, Pigment & Resin Techn. **26** 6 (1997) 363–369.

[6.11] SPERLING, L.H., Introduction to Physical Polymer Science, 4th edn, John Wiley & Sons, New York, NY (2006).

[6.12] LEWANDOWSKA, K., STASZEWSKA, D.U., BOHDANECK, M., The Huggins viscosity coefficient of aqueous solution of poly(vinyl alcohol), Eur. Polym. J. **37** 1 (2001) 25–32.
[6.13] MA, X., PAWLIK, M., Intrinsic viscosities and Huggins constants of guar gum in alkali metal chloride solutions, Carbohyd. Polym. **70** 1 (2007) 15–24.
[6.14] WANG, F., SUN, Z., WANG, Y.J., Study of xanthan gum/waxy corn starch interaction in solution by viscometry, Food Hydrocoll. **15** 4–6 (2001) 575–581.
[6.15] JACKSON, C., BARTH, H.G., "Molecular weight sensitive detectors for size exclusion chromatography", Handbook of Size Exclusion Chromatography and Related Techniques, 2nd edn (WU, C.-S. (Ed.), Marcel Decker, New York, NY (2004) 99–134.
[6.16] SCHARTL, W., Light Scattering from Polymer Solutions and Nanoparticle Dispersions, Springer, Berlin (2007).
[6.17] ANDERSSON, M., WITTGREN, B., WAHLUND, K.-G., Accuracy in multiple light scattering measurements for molar mass and radius estimations. Model calculations and experiments, Anal. Chem. **75** (2003) 4279–4291.
[6.18] MILAS, M., RINAUDO, M., ROURE, I., AL-ASSAF, S., PHILLIPS, G.O., WILLIAMS, P.A., Comparative rheological behavior of hyaluronan from bacterial and animal sources with cross-linked hyaluronan (hylan) in aqueous solution, Biopolymers **59** 4 (2001) 191-204.
[6.19] AL-ASSAF, S., KATAYAMA, T., PHILLIPS, G.O., SASAKI, Y., WILLIAMS, P.A., Quality control of gum arabic, Food & Food Ingred. J. Japan **208** (2003) 771–780.
[6.20] AL-ASSAF, S., PHILLIPS, G.O., Characterisation of AGPs in Acacia gums, Food & Food Ingred. J. Japan **3** (2006) 189–197.
[6.21] AL-ASSAF, S., PHILLIPS, G.O., WILLIAMS, P.A., Studies on acacia exudate gums. Part I: the molecular weight of Acacia senegal gum exudate, Food Hydrocoll. **19** 4 (2005) 647–660.
[6.22] AL-ASSAF, S., PHILLIPS, G.O., WILLIAMS, P.A., Controlling the molecular structure of food hydrocolloids, Food Hydrocoll. **20** 2–3 (2006) 369–377.
[6.23] GULREZ, S.K.H., AL-ASSAF, S., FANG, Y., PHILLIPS, G.O., GUNNING, A.P., Revisiting the conformation of xanthan and the effect of industrially relevant treatments, Carbohydr. Polym. **90** 3 (2012) 1235–1244.
[6.24] AL-ASSAF, S., NAVARATNAM, S., PARSONS, B.J., PHILLIPS, G.O., Chain scission of hyaluronan by carbonate and dichloride radical anions: Potential reactive oxidative species in inflammation? Free Radic. Bio. Med. **40** 11 (2006) 2018–2027.
[6.25] AOKI, H., et al., Characterization and properties of Acacia senegal (L.) willd. var. Senegal with enhanced properties (Acacia (sen) SUPER GUM (TM)): Part 5. Factors affecting the emulsification of Acacia senegal and Acacia (sen) SUPER GUM (TM), Food Hydrocoll. **21** 3 (2007) 353–358.
[6.26] AL-ASSAF, S., PHILLIPS, G.O., WILLIAMS, P.A., PLESSIS, T.A.D., Application of ionizing radiations to produce new polysaccharides and proteins with enhanced functionality, Nucl. Instrum. Meth. Phys. Res. B **265** (2007) 37–44.
[6.27] ALLIANCE PROTEIN LABORATORIES, Laser Light Scattering (2016), http://www.ap-lab.com/light_scattering.htm

[6.28] HOUGH, R.-L., Rheology and Light Scattering of Telechelic Associating Polymers Based on Poly(ethylene glycol), PhD Thesis, Univ. Wales (2003).
[6.29] MALVERN, Dynamic Light Scattering (DLS), Dynamic Light Scattering DLS for Particle Size Characterization of Proteins, Polymers and Colloidal Dispersions (2016), http://www.malvern.com/en/products/technology/dynamic-light-scattering/default.aspx
[6.30] PROVENCHER, S.W., A constrained regularization method for inverting data represented by linear algebraic and integral equations, Comput. Phys. Commun. **27** (1982) 213–227.
[6.31] PROVENCHER, S.W., CONTIN: A general purpose constrained regularization program for inverting noisy linear algebraic and integral equations, Comput. Phys. Commun. **27** (1982) 229–242.
[6.32] STEFFE, J.F., Rheological Methods in Food Process Engineering, 3 edn, Freeman Press, MI (1996).
[6.33] ROLFE, P., A Basic Introduction to Rheology, Malvern Instruments, Malvern, UK (2004).
[6.34] MILAS, M., RINAUDO, M., KNIPPER, M., SCHUPPISER, J.L., Flow and viscoelastic properties of xanthan gum solutions, Macromol. **23** 9 (1990) 2506–2511.
[6.35] MILAS, M., RINAUDO, M., TINLAND, B., The viscosity dependence on concentration, molecular-weight and shear rate of xanthan solutions, Polym. Bull. **14** 2 (1985) 157–164.
[6.36] TA INSTRUMENTS, Rheology Applications Note, the Principles and Applications of the Cox-Merz Rule (2009), http://www.tainstruments.co.jp/application/pdf/Rheology_Library/Rheology_Notes/RN014.PDF
[6.37] TA INSTRUMENTS, Rheology Applications Note, Rheology Software Models (Flow) (1996), http://www.tainstruments.co.jp/application/pdf/Rheology_Library/Rheology_Notes/RN009.PDF
[6.38] TA INSTRUMENTS, Rheology Instruments (2008), http://www.tainstruments.com/support/software-downloads-support/software-sorted-by-instruments/#ffs-tabbed-13
[6.39] MORRIS, E.R., Shear-thinning of 'random coil' polysaccharides: characterisation by two parameters from a simple linear plot, Carbohydr. Polym. **13** (1990) 85–96.
[6.40] BARNES, H.A., A Handbook of Elementary Rheology, Univ. of Wales, Aberystwyth, UK (2000).
[6.41] BARROW, M.S., BROWN, S.W.J., WILLIAMS, P.R., WILLIAMS, R.L., Rheology of dilute polymer solutions and engine lubricants in high deformation rate extensional flows produced by bubble collapse, J. Fluids Eng. Trans. ASME **126** 2 (2004) 162–169.
[6.42] WILLIAMS, P.A., PHILLIPS, G.O., "Introduction to food hydrocolloids", Handbook of Hydrocolloids (PHILLIPS, G.O., WILLIAMS, P.A. (Eds), Woodhead Publishing, Cambridge (2004) 1–19.

[6.43] RINAUDO, M., "Polysaccharides", Encyclopedia of Chemical Technology, Vol. 5 (OTHEMER, K., Ed.), John Wiley & Sons (2006) 549–586.
[6.44] COX, W.P., MERZ, E.H., Correlation of dynamic and steady flow viscosities, J. Polym. Sci. **28** (1958) 619–622.
[6.45] AL-HADITHI, T.S.R., BARNES, H.A., WALTERS, K., The relationship between the linear (oscillatory) and nonlinear (steady-state) flow properties of a series of polymer and colloidal systems, Colloid & Polym. Sci. **270** 1 (1991) 40–46.
[6.46] NEMOTO, J., SAKATA, M., HOSHI, T., UENO, H., KANEKO, M., All-plastic dye-sensitized solar cell using a polysaccharide film containing excess redox electrolyte solution, J. Electroanal. Chem. **599** 1 (2007) 23–30.
[6.47] GUNNING, A.P., KIRBY, A.R., MORRIS, V.J., Imaging xanthan gum in air by ac "tapping" mode atomic force microscopy, Ultramicrosc. **63** (1996) 1–4.
[6.48] KIRBY, A.R., GUNNING, A.P., MORRIS, V.J., Imaging polysaccharides by atomic force microscopy, Biopolym. **38** 3 (1996) 355–366.
[6.49] KIRBY, A.R., GUNNING, A.P., MORRIS, V.J., Imaging xanthan gum by atomic-force microscopy, Carbohydr. Res. **267** 1 (1995) 161–166.
[6.50] KIRBY, A.R., MacDOUGALL, A.J., MORRIS, V.J., Sugar beet pectin-protein complexes, Food Biophys. **1** 1 (2006) 51–56.
[6.51] AL-ASSAF, S., PHILLIPS, G.O., GUNNING, A.P., MORRIS, V.J., Molecular interaction studies on hylan using atomic force microscope and laser light scattering, Carbohydr. Polym. **47** (2002) 341–345.
[6.52] MORRIS, V.J., KIRBY, A.R., GUNNING, A.P., Atomic Force Microscopy for Biologists, 2nd edn, Imperial College Press, London (2009).

Chapter 7

DETERMINATION OF THE DEGREE OF DEACETYLATION OF CHITOSAN USING VARIOUS TECHNIQUES

M. SEN, P. TASKIN
Department of Chemistry, Hacettepe University,
Ankara, Turkey

P. ULANSKI, R. CZECHOWSKA-BISKUP, J.M. ROSIAK
Institute of Applied Radiation Chemistry, Faculty of Chemistry,
Lodz University of Technology,
Lodz, Poland

L. RAIMOND
Glyndwr University,
North Wales, Wrexham, United Kingdom

S. AL-ASSAF
Hydrocolloids Research Centre, Institute of Food Science and Innovation,
University of Chester,
Chester, United Kingdom

7.1. INTRODUCTION

Chitosan is a product of the degradation of chitin by a specific enzyme, chitinase, or a chemical treatment using, for example, an alkaline solution. Chitin and chitosan are the major constituents of shells of arthropods such as crabs, shrimps, lobsters and insects, and they are also produced extracellularly by fungi and brown algae. The structures of chitin and chitosan (Fig. 7.1) are close to cellulose, which is a polysaccharide linear of β (1→4)–D-glucose. The difference between chitin, chitosan and cellulose is the replacement of the hydroxyl group positioned in C_2 with an acetamide ($–NHCOCH_3$) group and a primary amine ($–NH_2$) for chitin and with a primary amine ($–NH_2$) for chitosan; this gives chitosan a cationic charge.

Due to this net charge, chitosan can be solubilized only in acidic solvents. Neutral and basic solvents are inadequate. Chitosan has a wide range of applications in various fields such as biotechnology, environmental and

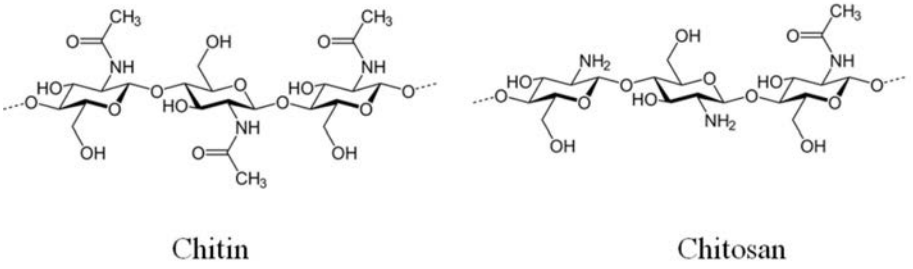

FIG. 7.1. Structure of chitin and chitosan.

biomedical engineering, cosmetics and photography. Chitosan also displays antibacterial and antifungal activities; see also Chapters 8 and 10.

There are a number of reports in the literature that deal with various aspects of chitosan solution properties and its functionality in certain applications. It should be noted that its structure, molecular weight and size as well as its DD greatly influence its functionalities. To date, there are a number of methods in use for the determination of DD as it is one of the key parameters that determine chitosan's solubility. An accurate characterization a bio-polymer is essential to understand how it can be used in a given application. Therefore, the objective of the work described in this chapter was to apply various techniques commonly used for the determination of DD and compare these methods. The final outcome of this project, as part of the Coordinated Research Project on the Development of Radiation Processed Products of Natural Polymers for Applications in Agriculture, Healthcare, Industry and Environment was to determine how various methods and treatments can affect the DD and explain the possible reasons why the values found are similar or different.

7.2. MATERIALS AND REAGENTS

Chitosan (Batch Chi 90/1000) from Heppe Medical Chitosan (Germany) with the following parameters (pH of 3–4 for 1% solution in 1% acetic acid, viscosity >10 Pa/s and a DD of 91.8%). Glacial acetic acid (CH_3COOH, assay > 99.7%), ammonium acetate (CH_3COONH_4, assay > 99%), hydrochloric acid (HCl, assay ≈ 36%), sodium chloride (NaCl) and sodium hydroxide (NaOH) were obtained from Fisher Scientific, United Kingdom. D-(+) Glucosamine HCl and N Acetyl D Glucosamine were obtained from Sigma.

7.3. RESULTS

7.3.1. FTIR

FTIR is also a widely used techniques for the determination of the DD of chitosan. Various band ratios reported in previous studies are summarized in Table 7.1 [7.1–7.13]. Contractions of the baseline in these methods are given in representative FTIR curves of chitosan in Fig. 7.2.

TABLE 7.1. SUMMARY OF FTIR METHODS WITH EVALUATED BANDS AND CALIBRATION CURVES USED IN THE DD

Method no.	Peaks evaluated	Calibration curve	Ref.
1	A1321/A1421	DD% = [2.58 − (A1320 − A3450)]/0.0104]	[7.1]
2	A1655/A3450	DD% = 100 − [(A1655 − A3450) × 155]	[7.2, 7.5]
3	A1655/A3450	DD% = 100 − [(A1655 − A3450) × 100/1.33]	[7.3, 7.7, 7.12]
4	A1655/A2870	DD% = 100 − [(A1655 − A2870) × 100/1.33]	[7.7]
5	A1320/A1420	DD% = 100 − [((A1320 − A3450) − 0.03146)/0.00226]	[7.4]
6	A1320/A3450	DD% = 100 − [((A1320 − A1420) − 0.03822)/0.003133]	[7.4]

The FTIR spectrum of the test material is shown in Fig. 7.3 with the baselines drawn according to the methods used to obtain Fig. 7.2. and the results are given in Table 7.1.

The results obtained by FTIR spectroscopy clearly show greater uncertainty when little variation in the peak height (intensity) is observed. For example, a change of 0.02 in the absorbance intensity of a peak could change the DD value by ~4%. Additionally, other factors such as the calibration curve range, the baseline correction and correction type, and the smoothing of the peaks influence the uncertainty. It was therefore concluded that the FTIR technique would not be a reliable technique for the determination of the DD value of an unknown chitosan sample if the calibration curve were not prepared in that particular laboratory and if the manipulations on the spectrum such as the baseline correction and smoothing were not well described in advance.

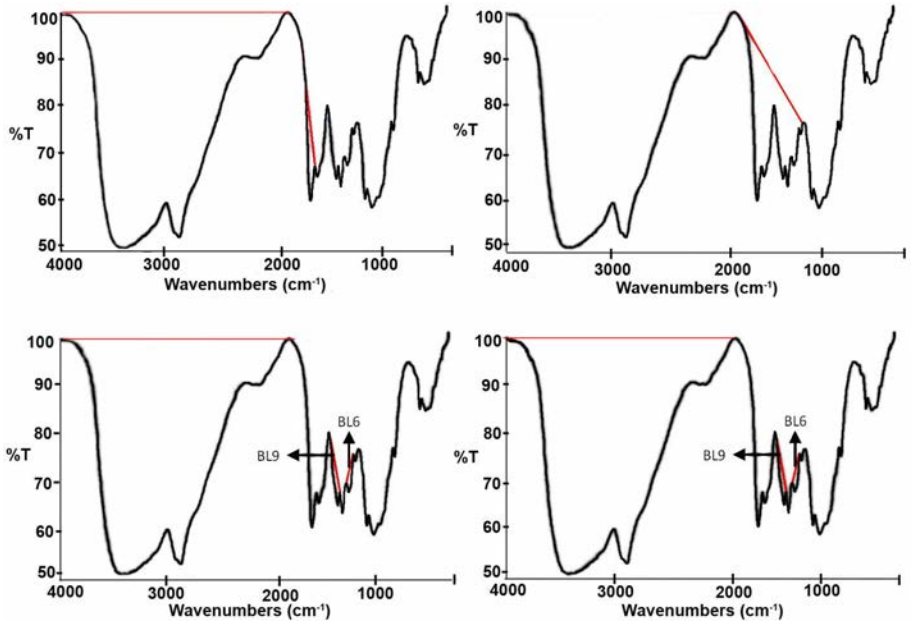

FIG. 7.2. Baseline contractions for the determination of DD in the FTIR calculations.

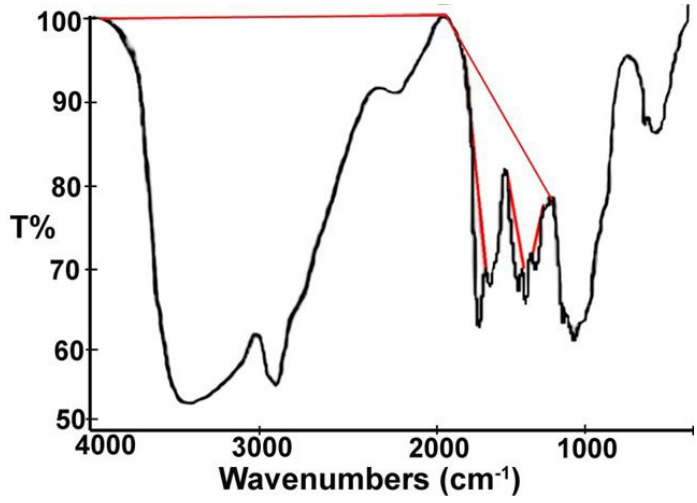

FIG. 7.3. The FTIR spectrum of Chi 90/1000 chitosan and the bands used in the calculation of the DD.

TABLE 7.2. DD VALUES OF A CHITOSAN SAMPLE DETERMINED BY FTIR

Method No.	Institute	Evaluated bands	DD value (%)
1	HU	A_{1321}/A_{1421}	95.0 ± 1.0
2	HU	A_{1655}/A_{3450}	75.8 ± 1.5
2	UL	A_{1655}/A_{3450}	78.0 ± 2.0
3	HU	A_{1655}/A_{3450}	64.8 ± 4.0
3	UL	A_{1655}/A_{3450}	85.6 ± 2.0
4	UL	A_{1655}/A_{2870}	44.9 ± 9.2
5	HU	A_{1655}/A_{3450}	89.8 ± 1.2
6	HU	A_{1320}/A_{3450}	82.8 ± 1.8
6	UL	A_{1320}/A_{3450}	89.5 ± 5.8

Note: HU = Hacettepe University, Laboratories for Radiation & Polymer Science; UL = Institute of Applied Radiation Chemistry of the Lodz University of Technology

7.3.2. Determination of DD by NMR

Many researchers have found that for the determination of DD of chitosan the H-NMR technique is simple, rapid and more precise than other known techniques such as FTIR or titration [7.14–7.16]. The structures of acetylated (glucosamine) and deacetylated (N acetyl glucosamine) units of chitosan are presented in Fig. 7.4.

Figure 7.5 presents the 400 MHz ^{1}H-NMR spectrum of chitosan (DD ~75%) at 70°C. The assignment of chitosan peaks has already been reported in the literature [7.13–7.16] and is summarized in Table 7.3. The peak at 2.0–2.1 ppm represents three protons of N acetyl glucosamine (GlcNAc) and the peak at 4.1–4.2 ppm represents an H-2 proton of glucosamine (GlcN) residues. The non-anomeric protons which are connected to the ring-skeleton in a glycosyl residue have similar electron densities and thus have similar chemical shifts. In the spectrum of the molecule, the signals of the non-anomeric protons partially overlap

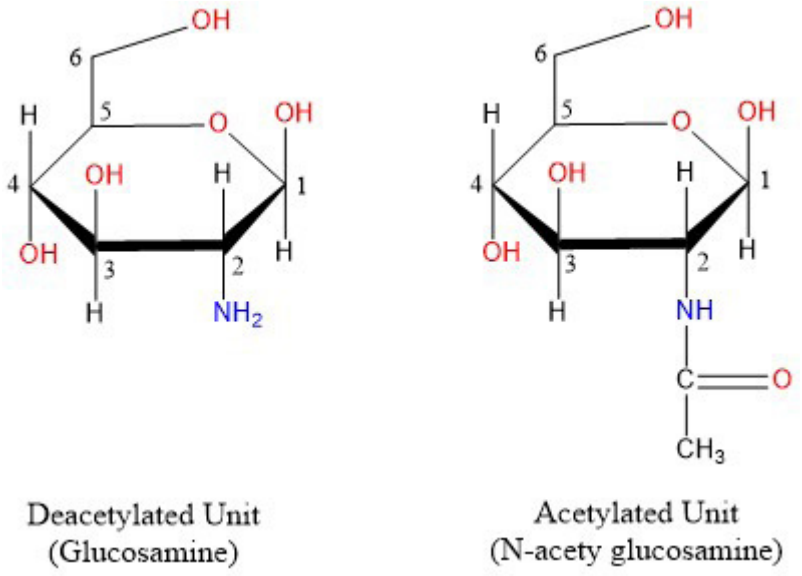

FIG. 7.4. Acetylated and deacetylated repeating units of chitosan.

and produce a broad envelope of signals in the middle of the spectrum [7.14]. All the signals are observed between 4.5 and 4 ppm. Anomeric protons (H1) are observed at higher chemical shifts. The protons of H-1 [GlcN (H-1D) and GlcNAc (H-1A)] resonate at 4.6 and 4.8 ppm, respectively. Among various bands of 1H NMR spectra, the methyl protons, 2.0–2.1 ppm, possess the highest resolution. The protons of H-1 [H1(Glc-NAc) 4.8 and H1(GlcN) 4.6 ppm] have the lowest resolution. The resolution of the H-3, H-4, H-5 and H-6 protons is also low. The signals of the latter protons overlap with the chemical shift for water value for a solvent (D_2O/CD_3COOD) at 4.05 ppm.

The typical NMR spectra of chitosan (shown in Fig. 7.5 and described above) clearly shows the protons of H-1(D), H-1(A), H-2/6, H-2(D) and H-Ac. The slight shift in the position of the protons compared with Table 7.3 is due to the working temperature.

Method 1: The DD is calculated using integrals of the peak of proton H1 of the deacetylated monomer (H1-D) and of the peak of the three protons of the acetyl group (H-Ac) [7.14, 7.17].

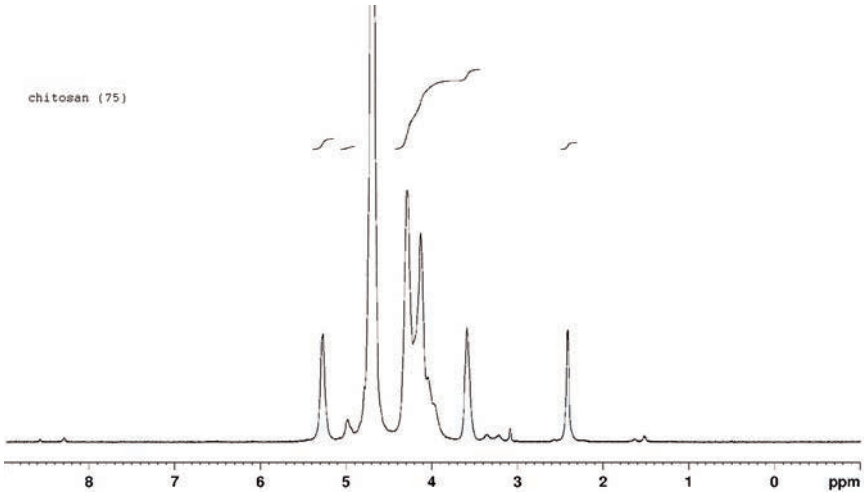

FIG. 7.5. ^{1}H-NMR spectrum of chitosan (DD is 75).

TABLE 7.3. CHEMICAL SHIFTS FOR PROTONS IN CD_3COOD/D_2O OR DCL/D_2O SOLUTION AT 65ºC

Type of proton	Position (δ, ppm)
H_1 (H_1 of GluNAc or H-1(A))	4.62–4.85
H_1 (H_1 of $GluNH_2$ or (H-1(D))	4.85–4.97
H_2 (H_2 of $GluNH_2$ or H-2(D))	4.18–4.24
H_2 (H_2 of GluNAc or H-2(A))	4.38–4.65
H_3 (H_3 of $GluNH_2$ or H-3(D))	4.52–4.87
H_3 (H_3 of GluNAc or H-3(A))	4.52–4.65
H_3, H_4, H_5, H_6, H_6'	4.74–4.34
HN–$COCH_3$ or H-Ac	1.95–2.09

$$DD(\%) = \left(\frac{H1D}{H1D + HAc/3} \right) 100 \quad (7.1)$$

Method 2: The DD is calculated with the method proposed by Hirai et al. [7.11] using the signal from protons H-2, H-3, H-4, H-5, H-6, H-6′ (H2-6) of both monomers and the peak of acetyl group (H-Ac).

$$DD(\%) = \left(1 - \left(\frac{\frac{HAc}{3}}{\frac{H26}{6}} \right) \right) 100 \quad (7.2)$$

Method 4: A DD lower than 90% can also be calculated by using the peaks of protons H1 of both the deacetylated and the acetylated monomer (H1-D, H1-A). However, this equation is not suitable for high DD values because H1-A cannot be observed in the spectrum.

$$DD(\%) = \left(\frac{H1D}{H1D + H1A} \right) 100 \quad (7.3)$$

The ^{1}H-NMR spectrum of test material is shown in Fig. 7.6. As a result of the evaluation of the ^{1}H-NMR spectra, the calculated DD values of the chitosan samples are given in Table 7.4.

TABLE 7.4. THE DD VALUES OF THE CHITOSAN SAMPLE DETERMINED BY ^{1}H-NMR

Institute	Method 1	Method 2	Method 3
HU	91.5 ± 0.5	91.9 ± 0.6	89.3 ± 0.8
UL	91.3 ± 0.7	89.4 ± 0.3	84.9 ± 1.3

Note: HU = Hacettepe University, Laboratories for Radiation & Polymer Science; UL = Institute of Applied Radiation Chemistry of the Lodz University of Technology

As can be seen from the table, the DD values calculated by Method 1 are very close to those calculated by Method 2. However, the DD values obtained by Method 3 are slightly different from those obtained by Methods 1 and 2. This difference was attributed to the low intensity of the H1A peak in the spectra. Table 7.4 also indicates that the values experimentally calculated for chitosan

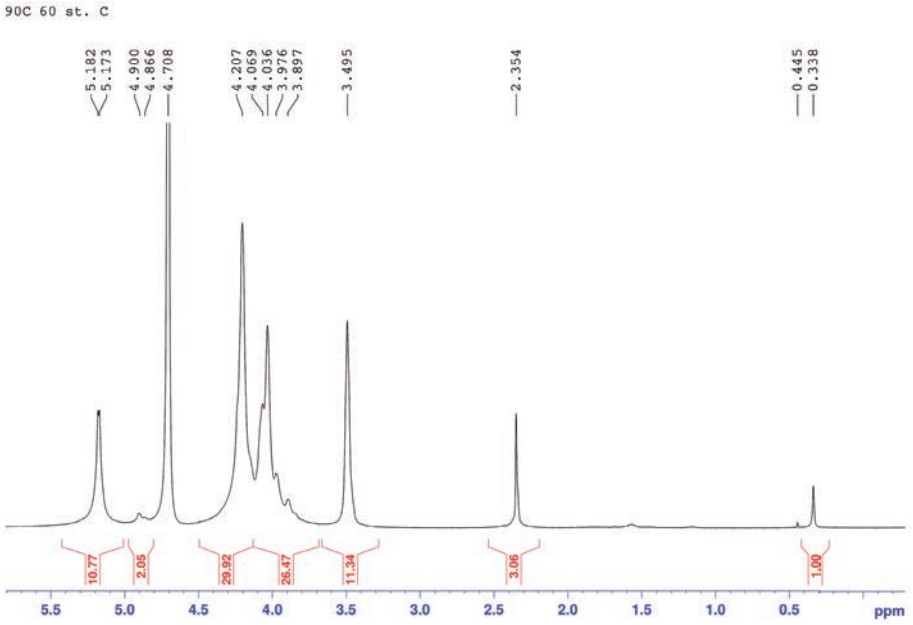

FIG. 7.6. The [1]H-NMR spectra of chitosan 90/1000.

90/1000 at Hacettepe University and at the Lodz University of Technology are very close to the value reported by the supplier (i.e. 91.8%). In conclusion, therefore, NMR seems to be the most reliable technique, particularly when used according to Methods 1 and 2.

7.3.3. Determination of DD values by titration

Various titration procedures are reported in previous studies for the determination of the DD value of chitosan. These procedures and related equations are summarized below [7.18–7.24].

7.3.3.1. Titration procedure I

In titration procedure I, dried chitosan (0.2 g) was dissolved in 20 cm^3 0.1M hydrochloric acid and 25 cm^3 deionized water [7.18]. After 30 min continuous stirring, the next portion of deionized water (25 cm^3) was added and stirring continued for 30 min. When the chitosan was completely dissolved, the solution was titrated with a 0.1M sodium hydroxide solution using an automatic burette (0.01 cm^3 accuracy). A typical titration curve is shown in Fig. 7.7.

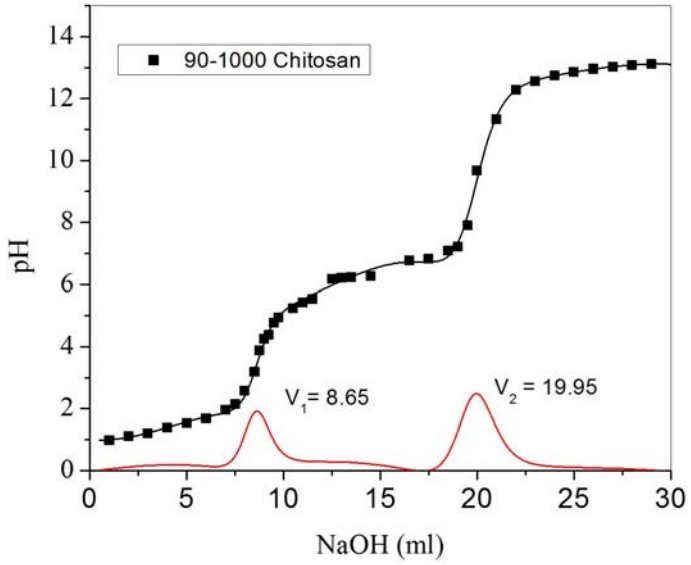

FIG. 7.7. A typical titration curve of a chitosan sample.

A curve with two inflexion points is obtained from the titration of the chitosan solution. The difference of the volumes of these two points (V_1 and V_2) corresponds to the acid consumed by the amine groups and allows the calculation of the DD values. Determination of the first derivative helps in the precise reading of V_1 and V_2. The DD of chitosan was calculated using Eq. (7.4).

$$DD(\%) = 100 - \left[2.03 \left(\frac{(V_2 - V_1)}{m + 0.0042(V_2 - V_1)} \right) \right] \tag{7.4}$$

where:

m is the weight of the sample;

V_1 and V_2 are the volumes of 0.1M sodium hydroxide solution corresponding to the deflection points (Fig. 7.7);

2.03 is a coefficient resulting from the molecular weight of the chitin monomer unit;

and 0.0042 is a coefficient resulting from the difference between the molecular weights of chitin and chitosan monomer units.

7.3.3.2. Titration procedure II

In titration procedure II, the method described by Jiang et al. [7.22] and Tan et al. [7.23] was applied, with a few modifications. Chitosan (0.20–0.25 g) was dissolved in 20 mL of 0.10M HCl and diluted with 10 mL of distilled water. The pH of the solution was adjusted to ≈2 with 0.01M NaOH and taken as the start point. Under continuous stirring, 0.250 mL of 0.1M NaOH was added, allowed to equilibirate and the pH recorded. This sequence was repeated until the pH reached a value of 4. A value of *f(x)* of the corresponding volume of NaOH added was calculated using the following equation:

$$f(x) = \left(\frac{V_o + V}{N_B} \right) \times \left(\left[H^+ \right] - \left[OH^- \right] \right) \tag{7.5}$$

where:
V_o is the volume of chitosan solution (mL);
V is the volume of NaOH added (mL);
N_B is the concentration of NaOH (M);
$[H^+]$ is the concentration of hydronium ions (M);

and $[OH^-]$ is the concentration of hydroxyl ions (M).

The linear titration curve was obtained by plotting *f(x)* against the corresponding volume of NaOH. The volume of NaOH at the end point of the titration, V_o, was estimated by extrapolating the linear titration curve to the *x* axis. The DD of the chitosan sample was calculated using the following formula.

$$DD(\%) = \frac{\varnothing}{\left[\frac{W - 161 \times \varnothing}{204} + \varnothing \right]} \times 100 \tag{7.6}$$

where:

$$\varnothing \ \frac{N_A \cdot V_A - N_B \cdot V_e}{1000}; \tag{7.7}$$

N_A is the concentration of HCl (M);
V_A is the volume of HCl (mL);
N_B is the concentration of NaOH (M);
V_e is the volume of NaOH at the end point (mL);

and W is the sample mass.

The results obtained following the determination of the DD value of chitosan 90/1000 are given in Table 7.5, with other parameters used in the equation.

TABLE 7.5. TITRATION DATA OF CHITOSAN 90/1000

V_{NaOH} (mL)	pH	[H+] (M)	pOH	[OH-] (M)	*f(x)*
0.00	2.00	1.00E-02	12.00	1.00E-12	3.23
0.25	2.04	9.12E-03	11.96	1.10E-12	2.95
0.50	2.08	8.32E-03	11.92	1.20E-12	2.69
0.75	2.14	7.24E-03	11.86	1.38E-12	2.34
1.00	2.20	6.31E-03	11.80	1.58E-12	2.04
1.25	2.27	5.37E-03	11.73	1.86E-12	1.74
1.50	2.36	4.37E-03	11.64	2.29E-12	1.41
1.75	2.48	3.31E-03	11.52	3.02E-12	1.07
2.00	2.63	2.34E-03	11.37	4.27E-12	0.76
2.25	2.86	1.38E-03	11.14	7.24E-12	0.45
2.35	3.00	1.00E-03	11.00	1.00E-11	0.32

By plotting the *f(x)* vs V_{NaOH} values given in Table 7.5, Fig. 7.8 was obtained. Then the extrapolation of the line x-intercept V_e value was calculated from Fig. 7.8:

$$V_e = \frac{-3.2783}{-1.2538} = 2.6147 \tag{7.8}$$

This value is used to calculate the value of ∅ using Eq. (7.6):

$$\varnothing = \frac{0.078 \times 20 - 0.117 \times 2.6147}{1000} = 1.254 \times 10^{-2} \tag{7.9}$$

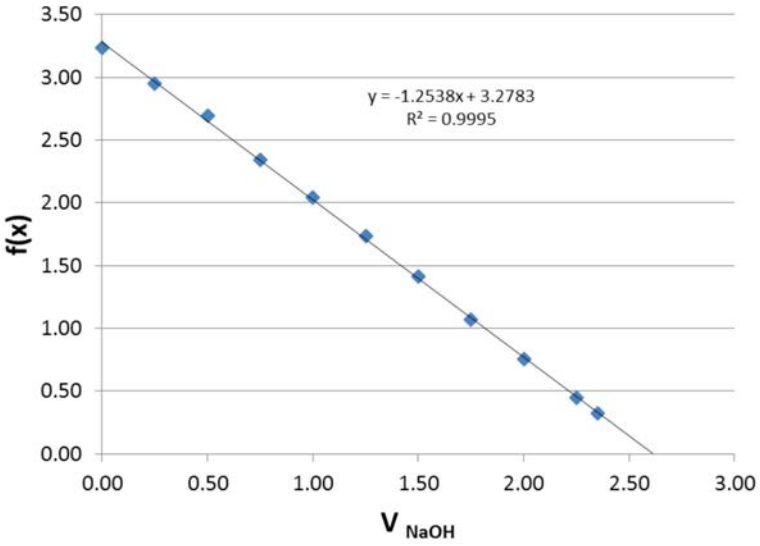

FIG. 7.8. Linear relationship between f(x) and volume of NaOH.

And finally, the DD was calculated from Eq. (7.10) as 88.8%:

$$DD(\%) = \frac{1.254\times10^{-2}}{\left[\frac{(0.2341-161\times1.254\times10^{-2})}{204}+1.254\times10^{-2}\right]}\times100 = 88.8\% \quad (7.10)$$

7.3.3.3. Titration procedure III

This procedure is a modified form of titration procedure II [7.23]. Chitosan (0.20–0.25 g) was dissolved in 20 cm^3 of 0.1 mol/dm^3 HCl and diluted with 10 cm^3 of deionized water. Under continuous stirring, 0.50 cm^3 of 0.1 mol/dm^3 sodium hydroxide was added, allowed to equilibrate and the pH of the solution was measured and recorded. This sequence was repeated until the pH reached a value of 4. The same calculation as in titration procedure II was used.

7.3.3.4. Titration procedure IV

In this procedure, 0.125 g of chitosan was dissolved in 25 cm^3 aqueous solution of 0.1 mol/dm^3 hydrochloric acid and stirred for 30 min for complete dissolution. The solution was titrated with 0.1 mol/dm^3 NaOH. The degree of deacetylation was calculated as follows [7.24]:

$$NH_2\% = \left[\frac{(C_1V_1 - C_2V_2)\ 0.016}{G(100 - W)}\right]100 \tag{7.11}$$

where:

C_1 is the concentration of HCl (mol/dm^3);
C_2 is concentration of NaOH (mol/dm^3);
V_1 is the volume of HCl (cm^3);
V_2 is the volume of NaOH (cm^3);
0.016 is the molecular weight of NH_2 in 1 cm^3 0.1 mol/dm^3 HCl (g);
G is the sample weight (g);

and W is the water percentage of the sample; DD (%) = NH_2 % / 9.94% × 100% where 9.94% is the theoretical NH_2 percentage obtained.

Figure 7.7 shows an example titration curve for chitosan solution using titration procedure IV. The first maximum corresponds to the neutralization of HCl and the second to the amount of NaOH needed for the neutralization of the protonated amine groups. Because chitosan had previously been dried to a constant weight, expression (100 − W) was skipped.

The procedures used, the experimentally calculated DD values of chitosan 90/1000 determined by titration are summarized in Table 7.6; the centre at which the work was performed is also indicated. Results indicate that the experimentally calculated values of the chitosan 90/1000 at the three different centres are very close to each other.

TABLE 7.6. THE DD VALUES OF THE CHITOSAN SAMPLE DETERMINED BY TITRATION

Institute	Titration procedure	DD value
UL	I	87.7 ± 1.4
GU	II	88.8 ± 1.2
HU	III	88.9 ± 0.5
UL	IV	85.6 ± 0.4

Note: HU — Hacettepe University; UL — Lodz University of Technology; GU — Glyndwr University.

7.3.4. Determination of DD by the UV method

For the determination of the DD of chitosan samples, the method proposed by Wu and Zivanovic [7.25] was used. The diagram of the three step procedure for the determination of the degree of acetylation values for chitin and chitosan is given in Fig. 7.9. The standard solutions of GlcNAc and GlcN were prepared in 0.85% phosphoric acid at concentrations of 0, 10, 20, 30, 40 and 50 μg/mL. The calibration curve was obtained by plotting the first derivative UV values at 200 nm (H200) as a function of GlcNAc and GlcN concentration. The UV spectra of GlcNAc and GlcN are shown in Fig. 7.10. The first derivative curves of GlcNAc and GlcN are presented in Fig. 7.11. By plotting the first derivative UV values at those wavelengths against the concentrations of GlcNAc to perform linear regression analysis, the best linear regression was obtained at 200 nm. Thus, the first derivative value at 200 nm was chosen for the DD measurements in this study and represented by the symbol of H200. A plot of H200 values against the concentrations of N acetyl D glucosamine in the range of 0–50 μg/mL resulted in a good linear regression with the R^2 value of 0.994 (Fig. 7.12).

The value of the DD was calculated as:

$$DD(\%) = 100 - \left[\frac{\frac{m_1}{203.21}}{\frac{m_1}{203.21} + \frac{m_2}{161.17}} \right] \times 100 \tag{7.12}$$

where:

m_1 is the mass of GlcNAc in the 1 mL chitin or chitosan solution (Step 2; Fig. 7.9), calculated from the calibration curve by the corresponding H200;

m_2 is the mass of glucosamine in the 1 mL chitin/chitosan solution (Step 2; Fig. 7.9), and is given by Eq. (7.13).

$$m_2 = M - m_1 \tag{7.13}$$

where M is given by Eq. (7.14):

$$M = (M_1 \times M_3) / (M_1 + M_2) \tag{7.14}$$

where

m_1 is the mass of the solid chitin/chitosan sample taken for analysis (100 ± 10 mg);

m_2 is the mass of 20 mL of 85% phosphoric acid (Step 1; Fig. 7.9);

and M_3 is the mass of the 1 mL chitin/chitosan solution in the concentrated phosphoric acid (Step 2; Fig. 7.9).

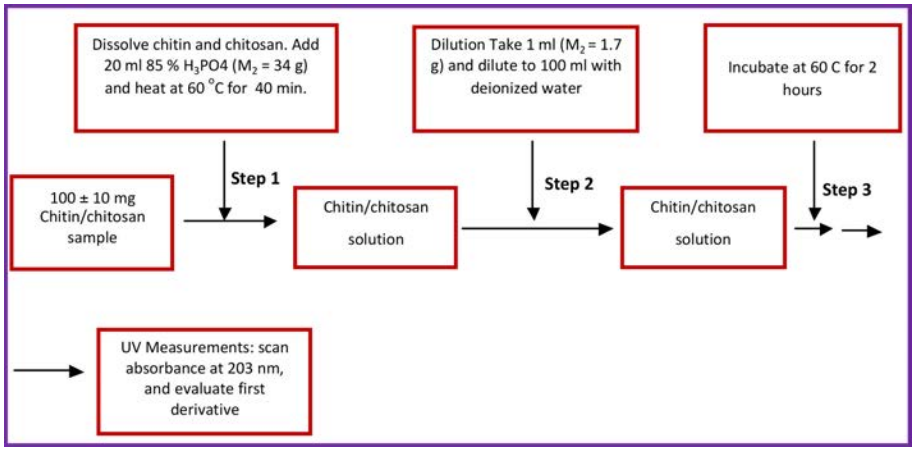

FIG. 7.9. Diagram of the three step procedure for the determination of the DD values for chitosan.

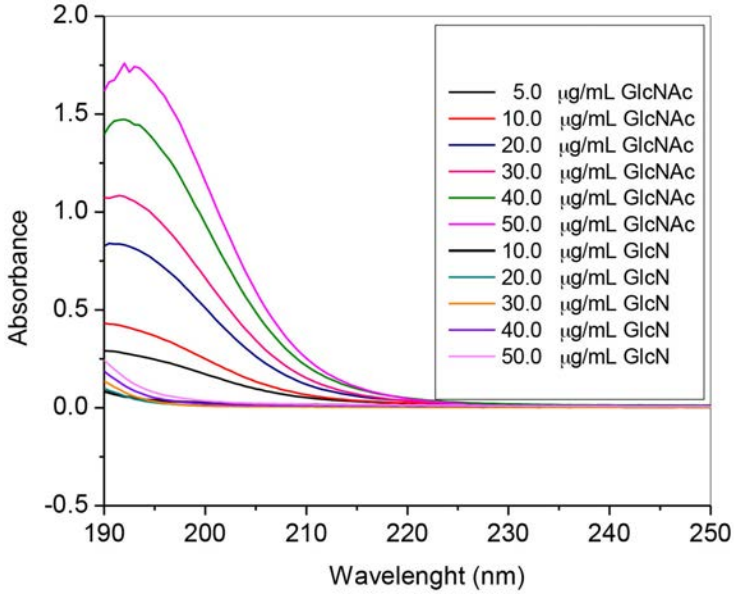

FIG. 7.10. UV spectra of GlcNAc and GlcN standards at concentrations from 0 to 50 µg/mL.

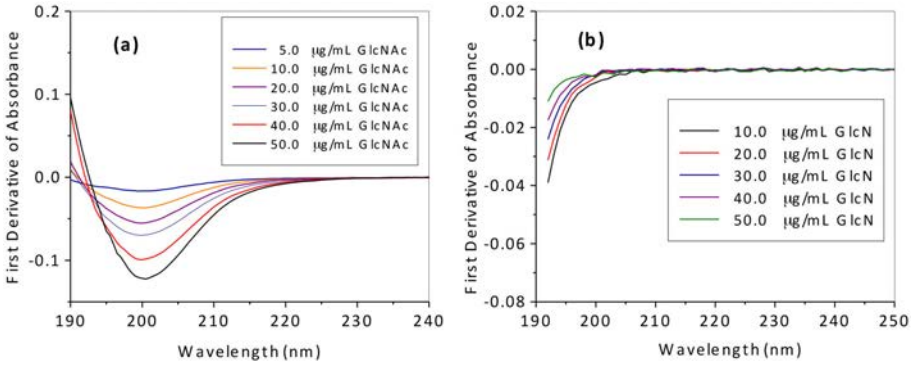

FIG. 7.11. (a) First derivative UV spectra of GlcNAc. (b) First derivative UV spectra of GlcN.

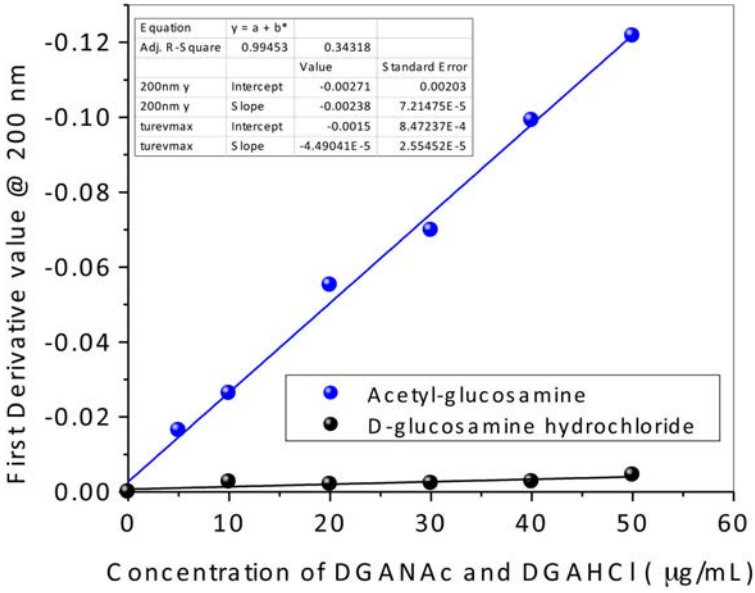

FIG. 7.12. UV calibration curves for GlcNAc, and GlcN from the first derivative peak maximum at 200 nm.

The UV spectra of the chitosan 90/1000 sample and their first derivative curves are shown in Fig. 7.13. The DD values determined are summarized in Table 7.7. As can be seen from the table, the DD values determined for the chitosan samples are very close to those found by the ^{1}H-NMR technique.

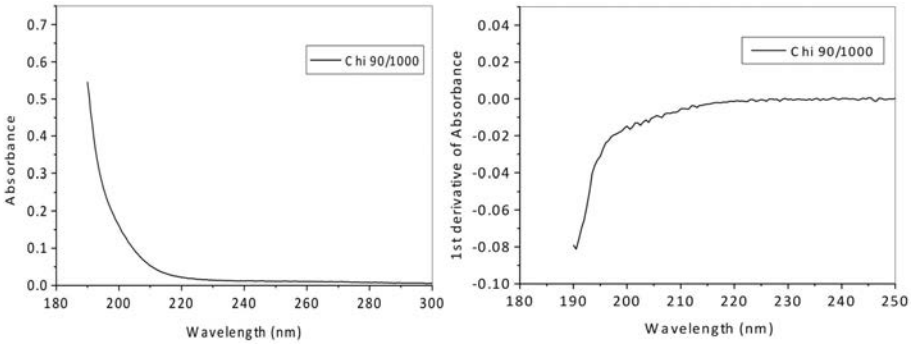

FIG. 7.13. (a) UV spectra; (b) first derivative of UV spectra of the chitosan 90/1000 samples.

TABLE 7.7. THE DD VALUES OF THE CHITOSAN SAMPLE DETERMINED BY TITRATION

Institute	DD value chitosan 90/1000
HU	91.2 ± 0.5
UL	89.4 ± 0.1

Note: HU — Hacettepe University; UL — Lodz University of Technology.

7.4. SUMMARY AND CONCLUSION

Four different techniques were used for the determination of the DD values of the chitosan 90/1000 samples in this study. The DD values determined experimentally by each method are summarized in Table 7.8.

TABLE 7.8. THE DD VALUES OF THE CHITOSAN SAMPLE DETERMINED BY DIFFERENT METHODS

	Method				
Institute	FTIR	Potentiometric titration	UV	NMR	HMC value
HU	64.8–95.0	98.9 ± 0.5	91.2 ± 0.5	91.5 ± 0.5	91.8
UL	44.9–89.5	87.7 ± 1.4	89.4 ± 0.1	91.3 ± 0.7	91.8
GU	—	88.8 ± 1.2	—	—	91.8

Note: HU — Hacettepe University; UL — Lodz University of Technology; GU — Glyndwr University.

On the basis of all these experiments (the results shown here are for one standard chitosan sample, but in fact the same experiments were performed for many samples of different DD), it is concluded that a laboratory intending to use FTIR for determination of the DD of chitosan should first establish its own calibration curve based on the 1655 cm^{-1} and 3450 cm^{-1} peaks using well characterized standard samples, and then use this curve or equation for measurements on real samples, keeping conditions constant and applying a baseline correction as recommended by Tahtat el al. [7.1]. The main advantages of FTIR techniques are the low price of the chemicals used, the easy sample preparation and measurement, and the moderately priced and generally available equipment (FTIR spectrometer). The main disadvantages of FTIR techniques are their moderate to poor reproducibility, the difficulties involved in the setting the baselines (operator dependent results) and their sensitivity to humidity, impurities (particularly protein residues) and instrument settings.

^{1}H-NMR is currently the best and most accurate method for the determination of the DD of chitosan. While this technique itself cannot be treated as ideal or absolute, it is justified to consider it the reference method. The main advantages of this technique are the more precise methods for the determination of the DD of chitosan, making it suitable as the reference method, the relatively easy sample preparation (except for the solubilization problem) and its highly reproducible results with small standard errors. Its disadvantages are the very expensive chemicals and apparatus involved, the needs for highly qualified staff for maintenance and operation, the great length of time needed for sample preparation, and the limited solubility and long dissolution time of some chitosan samples at the required high concentrations.

Potentiometric titration, when based on selected procedures and standard analytical solutions of well known concentrations, is the most reliable and robust of the non-NMR methods. The main advantages of this technique are that it yields reasonable DD values (but still 3–5% lower than ^{1}H-NMR), it is a simple experimental procedure, using easily accessible chemicals and equipment that has a low cost. Its disadvantages are the time consuming measurements needed and the requirement for standard solutions of precisely known concentrations.

UV-Vis, when carefully performed, seems to produce good results, but the procedure is quite time consuming and the presence of contaminants may influence the spectra and hence the final result.

ACKNOWLEDGEMENTS

J.M. Rosiak would like to thank S. Jankowski (Faculty of Chemistry, Lodz University of Technology) and his staff for performing the NMR measurements on chitosan samples. M. Sen gratefully acknowledges the support provided by the Scientific Research Projects Coordination Unit of Hacettepe University through Research Contract No. 013D04601002. Heppe Medical Chitosan (Germany) contributed reagents for some of the work described in this chapter.

REFERENCES TO CHAPTER 7

[7.1] TAHTAT, D., UZUN, C., MAHLOUS, M., GÜVEN, O., Beneficial effect of gamma irradiation on the N-deacetylation of chitin to form chitosan, Nucl. Instrum. Meth. Phys. Res B **265** (2007) 425–428.

[7.2] GUINESI, L.S., CAVALHEIRO, E.T.G., The use of DSC curves to determine the acetylation degree of chitin/chitosan samples, Thermochim. Acta **444** (2006) 128–133.

[7.3] ZAINOL, I., AKIL, H.M., MASTOR, A., Effect of γ-irradiation on the physical and mechanical properties of chitosan powder, Mat. Sci. Eng. C **29** (2009) 292–297.

[7.4] BRUGNETTO, J., LIZARDI, J., GOYCOOLEA, F.M., ARGÜELLES-MONAL, W., DESBRIÉRES, J., An infrared investigation in relation with chitin and chitosan characterization, Polymer **42** (2001) 3569–3580.

[7.5] BAXTER, A., DILLON, M., TAYLOR, K.D., ROBERTS, G.A.F., Improved method for IR determination of the degree of N-acetylation of chitosan, Int. J. Bio. Macromol. **14** (1992) 166–169.

[7.6] DUARTE, M.L., FERREIRA, M.C., MARVAO, M.R., ROCHA, J., An optimized method to determine the degree of acetylation of chitin and chitosan by FTIR spectroscopy, Int. J. Bio. Macromol. **31** (2002) 1–8.

[7.7] DOMARD, A., RINAUDO, M., Preparation and characterization of fully deacetylated chitosan, Int. J. Bio. Macromol. **5** (1983) 49–52.

[7.8] MIYA, M., IWAMOTO, R., YOSHIKAWA, S., MIMA, S., I.R. spectroscopic determination of CONH content in highly deacetylated chitosan, Int. J. Bio. Macromol. **2** (1980) 323–324.

[7.9] SHIGEMASA, Y., MATSUURA, H., SASHIWA, H., SAIMATO, H., Evaluation of different absorbance ratios from infrared spectroscopy for analyzing the degree of deacetylation in chitin, Int. J. Bio. Macromol. **18** (1996) 237–242.

[7.10] SANNAN, T., KURITA, K., OGURA, K., IWAKURA, Y., Studies on chitin: (7) IR spectroscopic determination of degree of deacetylation, Polymer **19** (1978) 458–459.

[7.11] SABINS, S., BLOCK, L. H., Improved infrared spectroscopic method for the analysis of degree of N-deacetylation of chitosan, Polym. Bull. **39** (1997) 67–69.

[7.12] KASAAI, M.R., A review of several reported procedures to determine the degree of N-acetylation for chitin and chitosan using infrared spectroscopy, Carbohyd. Polym. **71** (2008) 497–508.

[7.13] SHIGEMASA, Y., MATSUURA, H., SASHIWA, H., SAIMATO, H., An Improved IR Spectroscopic Determination of Degree of Deacetylation of Chitin , Advances in Chitin Science, Vol. 1 (DOMARD, A., et al. (Eds)), André, Lyon (1996) pp. 204.

[7.14] KASAAI, M.R., Determination of the degree of N-acetylation for chitin and chitosan by various NMR spectroscopy techniques: A review, Carbohydr. Polym. **79** (2010) 801–810.

[7.15] HIRAI, A., ODANI, H., NAKAJIMA, A., Determination of degree of deacetylation of chitosan by 1H NMR spectroscopy, Polym. Bull. **26** (1991) 87–94.

[7.16] VÄRUM, K.M., ANTHONSEN, M.W., GRASDALEN, H., SMİDSRØD, O., Determination of the degree of N-acetylation and the distribution of N-acetyl groups in partially N-deacetylated chitins (chitosans) by high-field NMR spectroscopy, Carbohyd. Res. **211** (1991) 17–23.

[7.17] LAVERTU, M., A validated, 1H NMR method for the determination of the degree of deacetylation of chitosan, J. Pharm. Biomed. Anal. **32** (2003) 1149–1158.

[7.18] MUZZARELLI, R.A.A., Chitin, Pergamon Press, Oxford (1977).

[7.19] WOJTASZ-PAJAK, A., KOLODZIEJSKA, I., DEBOGORSKA, A., MALESA-CIECWIERZ, M., Enzymatic, physical and chemical modification of krill chitin, Bull. Sea Fish. Inst. **143** (1998) 29–40.

[7.20] TOLIMATE, A., et al., On the influence of deacetylation process on the physicochemical characteristics of chitosan from squid chitin, Polymer **41** (2000) 2463–2469.

[7.21] CZECHOWSKA-BISKUP, R., et al., "Examination of plant fat- and cholesterol binding by chitosan of various molecular weights – preliminary data", Progress on Chemistry and Application of Chitin and Its Derivatives, Vol. 10 (STRUSZCZYK, H., Ed.), Polskie Towarzystwo Chitynowe, Lodz (2004) 121–130.

[7.22] JIANG, X., CHEN, L., ZHONG, W., A new linear potentiometric titration method for the determination of deacetylation degree of chitosan, Carbohydr. Polym. **54** (2003) 457–463.

[7.23] TAN, S.C., KHOR, E., TAN, T.K., WONG, S.M., The degree of deacetylation of chitosan: Advocating the first derivative UV spectrophotometry method of determination, Talanta **45** (1998) 713–719.

[7.24] JIA, Z., SHEN, D., Effect of reaction temperature and reaction time on the preparation of low-molecular-weight chitosan using phosphoric acid, Carbohydr. Polym. **49** (2002) 394–400.

[7.25] WU, T., ZIVANOVIC, S., Determination of the degree of acetylation (DA) of chitin and chitosan by an improved first derivative UV method, Carbohydr. Polym. **73** (2008) 248–253.

Chapter 8

RADIATION PROCESSING OF ALGINATE, CHITOSAN AND CARRAGEENAN AND THEIR APPLICATIONS AS PLANT GROWTH PROMOTERS

K. ZAMAN
Malaysian Nuclear Agency,
Bangi, Malaysia

N. QUOC HIEN, D. VAN PHU, L. QUANG LUAN
Vietnam Atomic Energy Research Institute,
Research and Development Center for Radiation Technology,
Ho Chi Minh City, Viet Nam

M.N. CLOZZAL, M.D. DIVO, E.B. GIARDINA, F. VILELLA
Departamento de Producción Vegetal,
Universidad de Buenos Aires,
Buenos Aires, Argentina

E.E. SMOLKO, L. CERCHIETTI
Centro Atómico Ezeiza,
Comisión Nacional de Energía Atómica,
Buenos Aires, Argentina

8.1. INTRODUCTION

This chapter will specifically discuss the extraction, radiation processing and application of alginate, chitosan and carrageenan as plant growth promoters. Furthermore, the biological activities of oligosaccharides derived from the above mentioned polysaccharides will also be addressed.

8.2. RADIATION PROCESSING

8.2.1. Radiation degradation of alginate

Alginate is a natural polysaccharide composed of two building blocks of monomer units, namely D-mannuronic and L-guluronic acid, attached by random

1,4-glycoside linkages [8.1, 8.2]. Alginates are extracted from brown seaweeds, in which 18−40% of the total plant expressed as alginic acid. The brown seaweed Sargassum is shown in Fig. 8.1.

The annual production of alginate is about 30 000 t [8.2]. For most applications, for example, for use in food and drink, pharmaceutical products, cosmetics, bioengineering and agriculture, alginates are sold for US $5–20/kg [8.2].

Alginate is a linear copolymer with homopolymeric blocks of (1-4)-linked β D-mannuronate (M) and its C-5 epimer α L-guluronate (G) residues, respectively, covalently linked together in different sequences or blocks (Fig. 8.2).

FIG. 8.1. Sunlight dried brown seaweed (Sargassum) used for alginate extraction in Viet Nam.

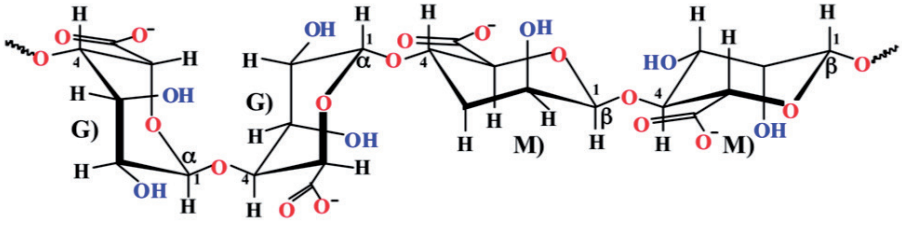

FIG. 8.2. The molecular structure of alginate.

Oligoalginate was reported to have several novel properties, such as plant growth promotion [8.3–8.5], plant elicitation [8.6] and effects on bifidobacterial growth [8.7]. Nagasawa et al. studied in detail the radiation degradation of NaAlg in powder form and in solution by irradiation with gamma rays from a ^{60}Co source [8.8], as shown in Fig. 8.3.

A detailed methodology for calculating chain scission yield is presented in Chapter 3. Radiation degradation yield G(s) can be used to evaluate the susceptibility of a polymer to degradation upon irradiation as a bulk material. G(s) is calculated based on Eqs (8.1) and (8.2) [8.9, 8.10]:

$$G(\mathrm{s})(scissions/100\ \mathrm{eV}) = N_A(1/\bar{M}_n - 1/\bar{M}_{n0})/6.24\times10^{16}D \quad (8.1)$$

$$G(\mathrm{s})(scissions/100\ \mathrm{eV}) = 2\times N_A(1/\bar{M}_w - 1/\bar{M}_{w0})/6.24\times10^{16}D \quad (8.2)$$

where

$\bar{M}_{n0}$ and $\bar{M}_n$ are the number-average molecular weight;
$\bar{M}_{w0}$ and $\bar{M}_w$ are the weight-average molecular weight of the polymer before and after irradiation;
D is the absorbed dose (kGy);

and N_A is Avogadro's number.

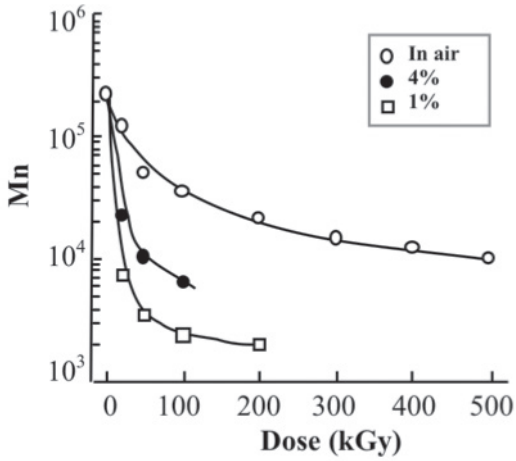

FIG. 8.3. Changes in the number-average molecular weight (M_n) of alginate irradiated in form powder and in aqueous solutions 1% and 4% with various doses in air.

Alternatively, $G(s)$ (scissions/100 eV) can be converted to $G(s)$ (μmol/J) by multiplying by 0.10364 [8.11]. Thus, as presented in Fig. 8.4, Nagasawa et al. calculated the $G(s)$ to be 1.9, 55 and 18 scissions/100 eV, that is, equal to 0.197 μmol/J, 5.700 μmol/J and 1.866 μmol/J for alginate in powder form, 1% and 4% aqueous solution, respectively [8.8]. Generally, if one uses Eq. (8.1) or Eq. (8.2) for the calculation, $G(s)$ will increase with decreasing polymer concentration in the solution. Accordingly, the higher the concentration of the polymer in the solution, the lower the $G(s)$ value is.

In addition, taking into account the concentration, C, of polymer in solution, then $G(s)$ is calculated with Eqs (8.3) and (8.4) [8.11]:

$$G(\mathrm{s})(\mu\mathrm{mol/J}) = CN_{\mathrm{A}}(1/\bar{M}_{\mathrm{n}} - \bar{M}_{\mathrm{n0}})/6.24\times10^{19}D \tag{8.3}$$

$$G(\mathrm{s})(\mu\mathrm{mol/J}) = 2\times CN_{\mathrm{A}}(1/\bar{M}_{\mathrm{w}} - \bar{M}_{\mathrm{w0}})/6.24\times10^{19}D \tag{8.4}$$

where C is the concentration of the polymer in solution (g/dm^3).

If Eq. (8.3) or Eq. (8.4) is used for calculation, the $G(s)$ will decrease with the polymer concentration in the solution. Accordingly, the lower the concentration of the polymer in solution, the lower the $G(s)$. In the particular case of the $G(s)$ values reported by Nagasawa et al. [8.8], if Eq. (8.3) is used then the $G(s)$ values will be 0.057 μmol/J and 0.076 μmol/J for 1% and 4% alginate solution, respectively.

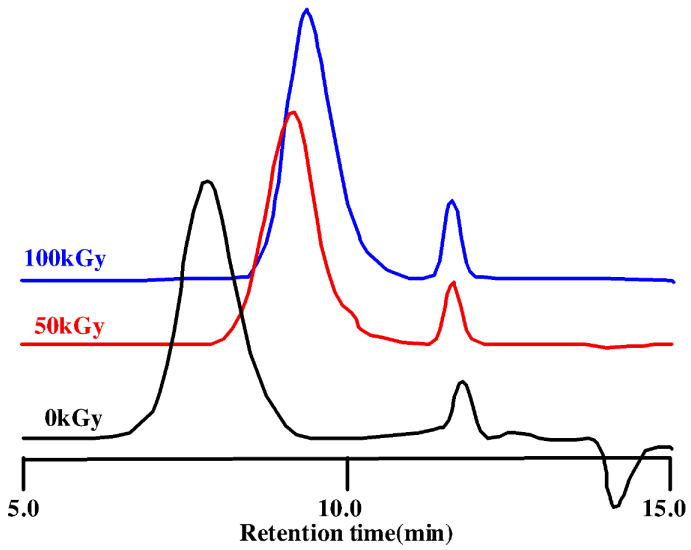

FIG. 8.4. GPC elution curves of alginate irradiated at 0, 50 and 100 kGy in aqueous solution.

Furthermore, low energy electron beams can be used for the degradation of polysaccharides and particularly for alginate in aqueous solution. Table 8.1 shows the molecular weight ($\bar{M}_w$) and $\bar{M}_w$ distribution index ($\bar{M}_w/\bar{M}_n$) of alginate subjected to gamma ^{60}Co radiation and a low energy electron beam [8.12].

TABLE 8.1. MOLECULAR WEIGHT OF ALGINATE IRRADIATED BY GAMMA CO-60 RADIATION AND A LOW ENERGY ELECTRON BEAM

	Alginate powder	Alginate solution 5%	
	0 kGy	Gamma Co-60 (10 kGy/h) 40 kGy	Low energy electron beam (250 keV, 10 mA 35 min)
$\bar{M}_w$	136 700	8 900	12 700
$\bar{M}_n$	50 700	7 400	7 800
$\bar{M}_w/\bar{M}_n$	2.70	1.20	1.62

In general, when polysaccharides are irradiated, oligosaccharides are produced as a result of chain scission, as seen from the shifting of the GPC peaks to longer retention times (Fig. 8.4). These oligosaccharides usually also have a narrower molecular weight distribution (Table 8.1).

8.2.2. Radiation degradation of chitosan

Chitosan is a linear aminopolysaccharide (polyglucosamine) derived from chitin, a naturally abundant mucopolysaccharide poly β (1→4)-linked N acetyl D-glucosamine, by alkali deacetylation. Its molecular structure is shown in Fig 8.5.

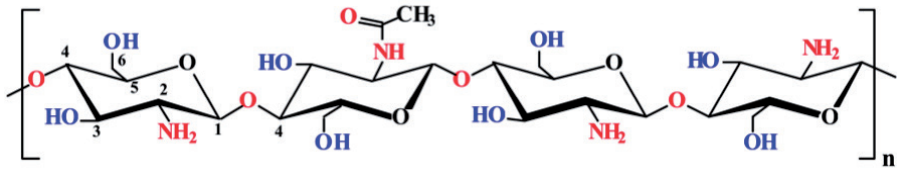

FIG. 8.5. The molecular structure of chitosan with a DD of ~70% (NH_2 70%, NH-$COCH_3$ 30%).

Chitosan has a wide range of applications, for example in wastewater treatment, in medicine and cosmetics, in food, including functional food, and in agriculture [8.13–8.16]. The production of chitin and chitosan is currently based on crab and shrimp shells discarded as food industry waste and Fig. 8.6 shows various sources of chitin and chitosan. The global annual estimate of shellfish processing discards is more than one million metric tonnes [8.13] and the disposal of shellfish wastes has been a challenge for most shellfish processing countries. Therefore, production of value added products such as chitin, chitosan, oligomers and their derivatives for utilization in different fields is of utmost interest.

The production of low molecular weight oligochitosan by irradiation (γ ray, EB) is being carried out in many radiation processing research centres because of the beneficial properties and potential applications of the end products in different fields. Chitosan of a weight-average molecular weight from 10 000 to about 100 000 is considered low $\bar{M}_w$ chitosan, while the $\bar{M}_w$ of oligochitosan is generally less than 10 000. Chitosan prepared from chitin by the deacetylation process generally has a high $\bar{M}_w$, which in many cases limits its applications. The low $\bar{M}_w$ chitosan and its oligomer have some special biological properties which are different from those of the ordinary high $\bar{M}_w$ chitosan, such as an antioxidant property [8.17–8.18], antimicrobial property [8.19–8.22], antitumor activity [8.23] and immunity stimulation in animals [8.24, 8.25] and plants [8.26–8.28]. Recent reviews on the topic have been published by Kim and Rajapakse [8.29] and Xia et al. [8.30]. A variety of techniques including chemical

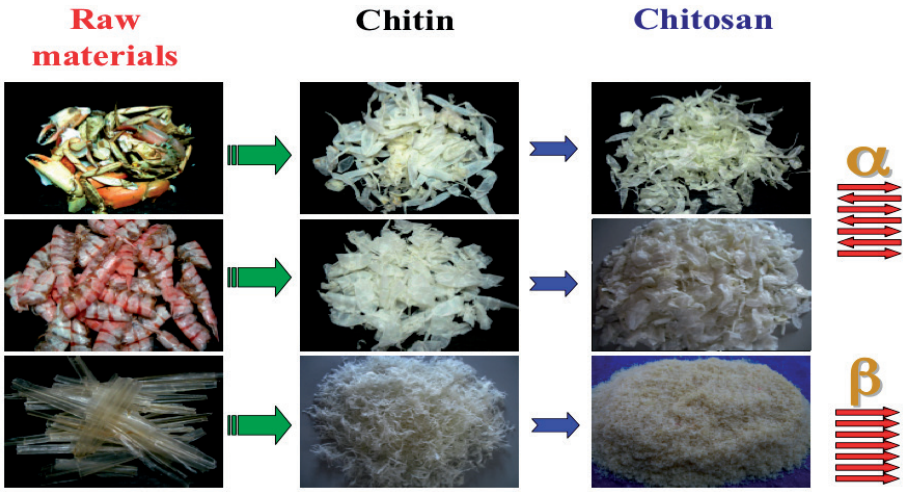

FIG. 8.6. The major sources for chitin and chitosan production from shrimp, crab shells and squid pens.

and enzymatic hydrolysis and radiation degradation processes can be used to prepare low $\bar{M}_w$ chitosan and its oligomer, as described by Makuuchi [8.31]. However, radiation (γ ray, EB) is a useful environmentally friendly processing technology for the degradation of polymers [8.32]. Figure 8.7 shows the effect of gamma irradiation on the degradation of the molecular weight of dry chitosan in the form of powder or flakes.

Accordingly, low $\bar{M}_w$ chitosan can be conveniently prepared by the irradiation of high $\bar{M}_w$ chitosan in powder or flake form [8.26, 8.33–8.35]. Ulanski and Rosiak [8.33] reported G(s) values of 0.9, 1.1 and 1.3 scissions/100 eV for chitosan powder irradiated in a vacuum, in air and in oxygen, respectively. However, Czechowska-Biskup et al. [8.36] reported the highest G(s) value for chitosan irradiated in air (G(s) = 0.6 μmol/J equal to 5.79 scissions/100 eV). The reason for the difference in G(s) may be due to many factors that need further study.

Oligochitosan has been produced in most cases by the irradiation of chitosan in solution [8.26, 8.36, 8.37]. G(s) values were found to be 0.058 μmol/J, 0.08 μmol/J and 0.10 μmol/J for 1%, 3% and 5% chitosan solutions, respectively, based on the molecular weight presented in Fig. 8.8 and calculated using Eq. (8.4). Wasikiewicz et al. reported a rather higher G(s) (0.353 μmol/J) for 1% chitosan solution [8.38]. The reason for this may be the difference in the DD of chitosan used for these studies.

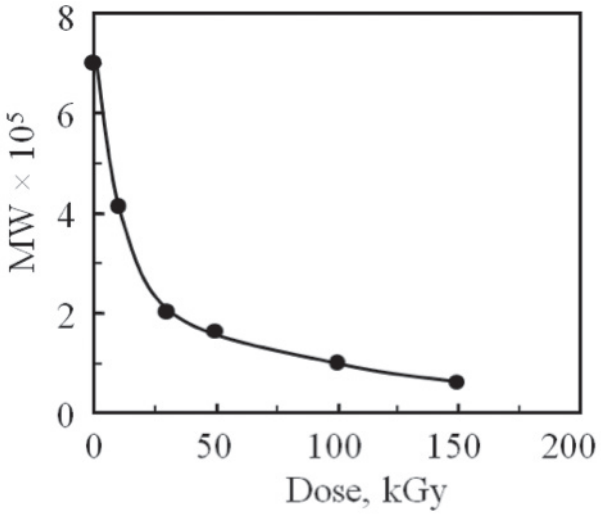

FIG. 8.7. Molecular weight of chitosan irradiated by ^{60}Co gamma ray in powder and flake form in air as a function of absorbed dose.

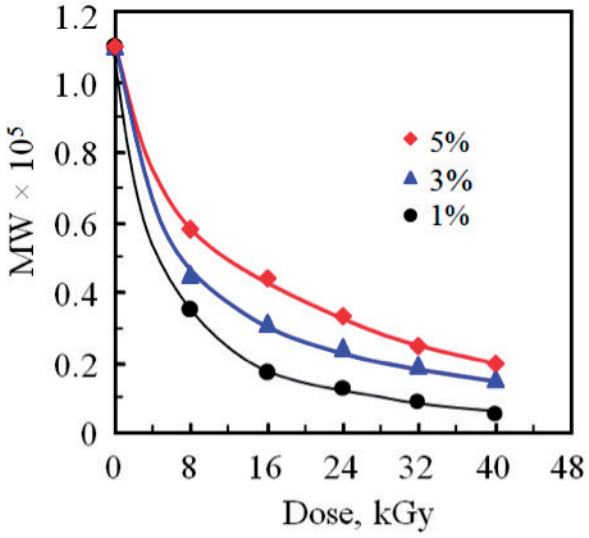

FIG. 8.8. Molecular weight of chitosan in solutions of 1%, 3% and 5% irradiated with ^{60}Co gamma rays as a function of absorbed dose.

It is usually more expensive to produce oligochitosan using enzymatic hydrolysis than using oxidative degradation [8.31]. In addition, this chemical process has some drawbacks, such as low production yields and higher pollution risks to the environment [8.29]. Unfortunately, there are some disadvantages associated with oxidative degradation, such as the chemical structure changes caused by the formation of carboxyl groups, deamination, breakage of the glucoside ring [8.39] and high irradiation doses.

Thus, in order to degrade chitosan effectively, synergistic degradation by combination of hydrogen peroxide (H_2O_2) with γ ray [8.40–8.42], UV light [8.43] and microwave irradiation [8.44] has been studied. According to the results reported by Kang et al. [8.40] and El-Sawy et al. [8.41], chitosan in a suspension or paste form mixed containing a rather high H_2O_2 concentration (10–30%) was degraded by γ irradiation to prepare oligochitosan in a high dose range from 20 kGy to more than 100 kGy. Furthermore, according to the the synergic effect of γ ray and H_2O_2 for the degradation of β chitosan in solution reported by Hien et al. [8.42], oligochitosan with a $\bar{M}_w$ of less than 10 000 can be produced in a low dose range of up to 16 kGy with the addition of a small amount of 1% H_2O_2 to a 5% beta chitosan solution; this method reduces the cost of production to an acceptable level (see Fig. 8.9).

However, according to the experiences of large scale oligochitosan production plants, where chitosan solution is irradiated (200 L/batch

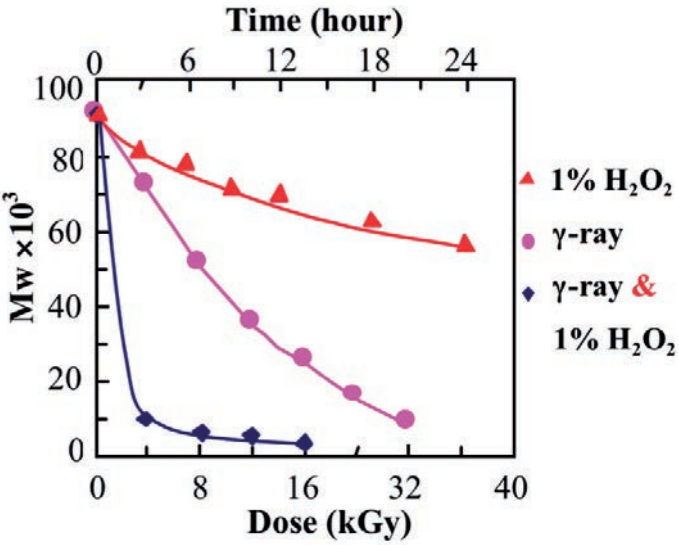

FIG. 8.9. Changes in weight-average molecular weight of β chitosan treated with H_2O_2, γ ray and H_2O_2/γ ray versus treatment time and dose (dose rate: 1.33 kGy/h).

in Viet Nam, 500 L/batch in Indonesia and 2000 L/cycle in Malaysia), it was recognized that highly viscous chitosan solution (>3%) is not suitable for processing. Therefore, a study on preparing oligochitosan with various $\bar{M}_w$ below 10 000 by γ irradiation of 3% chitosan solution containing H_2O_2 at various concentrations (0.25–1%) has been proposed [8.45]. The influence of varying dose on the change in molecular weight and in the radiation degradation yield of chitosan was investigated. The synergistic degradation effect induced by γ rays and H_2O_2 was also calculated based on the percentage of the reduction ($\bar{M}_w \times 100/\bar{M}_{w0}$) of chitosan molecular weight [8.42].

8.2.3. Radiation degradation of carrageenan

Carrageenan is a collective term for polysaccharides prepared by alkaline extraction (and modification) from red seaweed (*Rhodophyceae*), mostly of the genera *Chondrus*, *Eucheuma*, *Gigartina* and *Iridaea*. Different seaweeds produce different types of carrageenan. Carrageenan consists of alternating 3-linked β D-galactopyranose and 4-linked a D-galactopyranose units.

All carrageenan are high molecular weight polysaccharides including repeating galactose units and 3,6 anhydrogalactose, both sulphated and non-sulphated. The units are joined by alternating α 1-3 and β 1-4 glycosidic linkages as shown in Fig. 8.10.

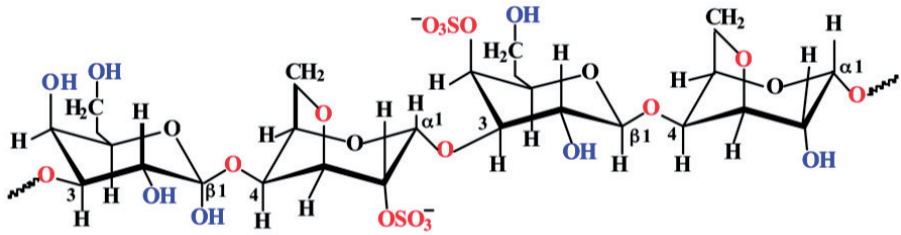

FIG. 8.10. The molecular structure of carrageenan.

There are three main commercial classes of carrageenan:

— Kappa (κ): strong and rigid gels. Gels with potassium ions that contain 1 sulphate ($-OSO_3$) group per repeating unit.
— Iota (ι): soft gels. Gels with calcium ions that contain 2 $-OSO_3$ groups per repeating unit.
— Lambda (λ): does not gel, contains 3 $-OSO_3$ groups per repeating unit.

Carrageenans are large and highly flexible molecules that curl, forming helical structures. This gives them the ability to form a variety of different gels at room temperature. They are widely used in sectors such as the food industry as thickening and stabilizing agents.

Relleve et al. [8.46] showed that carrageenan degraded easily upon irradiation without adding any chemical additives at ambient temperature. The weight-average $\bar{M}_w$ of κ carrageenan at various absorbed doses in solid form and at 1% and 4% concentration is shown in Fig. 8.11. The $\bar{M}_w$ of carrageenan decreases continuously with increasing dose. The dose needed to degrade carrageenan in the gel state is very much less than for solid carrageenan. This is due to the indirect effect of radiation brought about by the water molecules. As shown in Fig. 8.11, the dose required to obtain κ carrageenan with a molecular weight of 2.5×10^4 is about 500 kGy in the solid state, 100 kGy at 4% and 10 kGy at 1% gel. Thus, carrageenan of different molecular weights can be readily obtained by gamma ray irradiation of the carrageenan powder or gel at various absorbed doses.

Since the three types of carrageenan have varying amounts of sulphate content, the obtained carrageenan oligomers have varying degrees of sulphation. It was also shown that radiation has caused the loss of sulphate groups in κ, ι and λ carrageenan, as shown in Fig. 8.12. The study also showed that desulphation almost remained constant above 10 kGy. About 90%, 83% and 71% of the sulphate remained in the irradiated κ, ι and λ carrageenan, respectively.

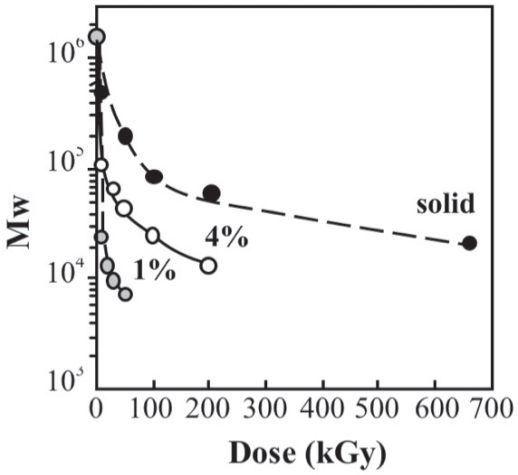

FIG. 8.11. Weight-average molecular weight of κ carrageenan irradiated at various doses in the solid and 1% and 4% gel states.

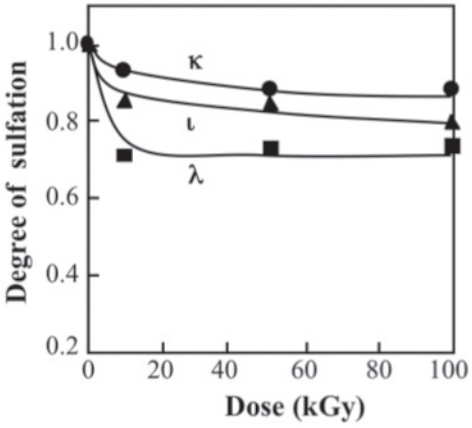

FIG. 8.12. Degree of sulphation of carrageenan at various absorbed doses.

From the extensive study by Relleve et al. [8.46], it can be concluded that the radiation degradation of carrageenan will cause the degradation of the molecular weight of the carrageenan as well as the loss of part of the sulphate groups that are important factors influencing the applications of radiation processed carrageenan in agriculture.

8.3. PILOT SCALE PRODUCTION OF OLIGOCHITOSAN BY GAMMA IRRADIATION

In the region of Asia and the Pacific, several pilot scale facilities for the gamma irradiation of liquid such as natural rubber latex and aqueous solutions of chitosan have been established in several countries: in India, Indonesia (Fig. 8.13), Malaysia (Fig. 8.14) and Viet Nam. All the pilot scale plants are batch type irradiation plants except the plant in Malaysia, which is designed for the continuous irradiation of the natural rubber latex and later designed for the production of radiation processed oligochitosan for use as a plant growth promoter and plant elicitor as shown in Fig. 8.14.

In the pilot scale production of oligochitosan in Malaysia, a two step gamma irradiation process was employed [8.47]. Currently, the liquid gamma irradiator is set to deliver an absorbed dose of 12 kGy, and for this reason, the chitosan powder has to be partially degraded using another gamma irradiation plant that delivers 50 kGy. The viscosities of chitosan powder, 2% or 3% chitosan powder in 2% lactic acid, before and after irradiation, are shown in Table 8.2. The viscosity of 3% chitosan in 2% lactic acid after irradiation at 50 kGy is slightly higher than the viscosity of natural rubber latex and this formulation was selected for this study. In view of the low activity of the ^{60}Co of the plant, i.e.

FIG. 8.13. Irradiation tank used for gamma irradiation of chitosan aqueous solution for the production of oligochitosan, 1000 m^3 per batch, in Indonesia.

FIG. 8.14. Mixing and storage tanks (top left), pumping system (top right), irradiation room (bottom left) at the gamma irradiation pilot plant facility for continuous production of oligochitosan (bottom right), 2000 m^3 per cycle, in Malaysia.

94.0 kCi (3.478 TBq), with a dose rate of 0.86 kGy/hr, the cycle time for 1500 m^3 of oligochitosan at 12 kGy is 14.0 h. However, the cycle time can be shorter if the ^{60}Co is higher in strength. The gamma plant in Malaysia is a dry source type and was designed for a 1.0 MCi (37 000 TBq) ^{60}Co source. The irradiated chitosan solution, which is in the form of oligochitosan, is continuously pumped into the storage tank. The oligochitosan was in an acidic condition and was neutralized using a sodium hydroxide solution before being applied to the field as shown in Table 8.3. Whenever necessary, a preservative can also be added to the oligochitosan solution to enable a long period of storage. A total volume of 2300 m^3 of oligochitosan with a concentration of ~20 000 ppm per cycle can be prepared.

TABLE 8.2. VISCOSITY COMPARISON OF DIFFERENT CHITOSAN CONCENTRATIONS BEFORE AND AFTER IRRADIATION AT 50 kGY

Formulation	Dose (kGy)	Viscosity (mPa·s)
2CL2	0	234.98
	50	15.16
3CL2	0	315.26
	50	35.50
Latex	0	20.00

TABLE 8.3. pH OF THE IRRADIATED CHITOSAN

Formulation	pH at 50 kGy	pH at 12 kGy	Final pH (adjusted with NaOH)
3CL2	4.40	4.58	5.03

In Table 8.4, the viscosity-average molecular weight of irradiated chitosan dropped significantly [8.47]. However, the drop in molecular weight is reduced to 9% when the absorbed dose further increases to 75 kGy. Further increases in absorbed dose did not compensate for the decrease in the molecular weight of the chitosan. Therefore, an absorbed dose of 50 kGy was chosen to degrade the chitosan for further processing in the liquid formed using a liquid gamma irradiator.

After the degradation of chitosan powder at 50 kGy, the chitosan was further degraded to produce small molecules of oligochitosan with a molecular weight of 10 000 or below. In this process, the irradiation was carried out on the degraded chitosan in solution form, 3% chitosan in 2% lactic acid (3CL2) in the presence of 0.1–0.3% hydrogen peroxide. Hydrogen peroxide is used to impact synergetic effects that facilitate the reduction of the molecular weight of degraded chitosan powder in aqueous solution when exposed to 12 kGy gamma radiation. Table 8.4 shows the molecular weights of degraded chitosan and oligochitosan produced after the irradiation of chiotsan powder and 3CL2 aqueous solution made from chitosan powder at different doses.

TABLE 8.4. MOLECULAR WEIGHT OF CHITOSAN AND OLIGOCHITOSAN: PRE-IRRADIATION OF CHITOSAN POWDER AND SUBSEQUENT IRRADIATION OF OLIGOCHITOSAN

Chitosan powder pre-irradiation	$\bar{M}_w$	$\bar{M}_w$ after irradiation at 12 kGy (3CL2 + 0.3% H_2O_2)
0 kGy	218 269	—
25 kGy	81 574	12 684
50 kGy	36 564	10 453
75 kGy	33 358	10 000
100 kGy	32 219	6 657

There was a slight reduction in the molecular weight of the oligochitosan (3CL2) above 12 kGy. The $\bar{M}_w$ of oligochitosan from degraded chitosan of 50 kGy and 75 kGy are not much different at around 10 000, as shown in Fig. 8.15 [8.47]. The pre-irradiation process of chitosan powder that produces low-molecular-weight chitosan was carried out at 50 kGy, and was followed by the irradiation of the lactic acid solution of low-molecular-weight chitosan at 12 kGy to produce oligochitosan.

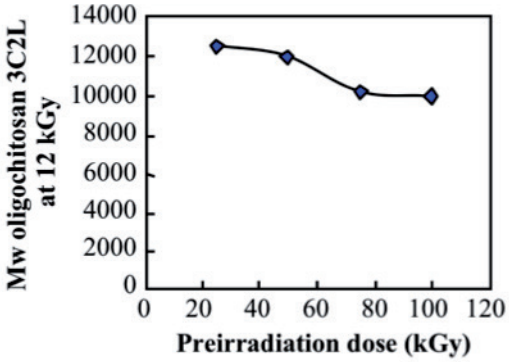

FIG. 8.15. $\bar{M}_w$ of oligochitosan after 12 kGy absorbed dose.

A brief protocol for the preparation of oligochitosan to be used as a plant elicitor and growth promoter for agriculture applications is as follows:

— Take chitosan with a DD of 70–80% and an $\bar{M}_w$ of approx. 2.0×10^5. If the molecular weight of the dry chitosan is rather high, it can be reduced using gamma irradiation.
— Dissolve chitosan in lactic acid (1.5–2%) with a concentration of 30 g/L.
— Keep standing overnight and then filter through a stainless steel net (100 mesh).
— Add H_2O_2 to the chitosan solution to a final concentration of 0.3–0.5%.
— Irradiate the chitosan/H_2O_2 solution at an average dose of 10.0–12.0 kGy.
— Neutralize the irradiated chitosan solution by adding NaOH 2M to pH5.0–6.0.
— Add preservative (0.2% sodium benzoate, alcohol or other).
— Package final product as a biotic elicitor for plants.
— Characteristics of the biotic elicitor and plant growth promoter oligochitosan:
    • Oligochitosan concentration: 20–30 g/L (20 000–30 000 ppm);
    • Molecular weight ($\bar{M}_w$): $5.0–10.0 \times 10^3$;
    • pH ~5.0–6.0;
    • Appearance: yellowish liquid;
    • Maximum storage period: 2 years.

8.4. BIOLOGICAL EFFECT OF OLIGOSACCHARIDES ON PLANT TISSUE CULTURE

Degraded alginate was found to have several novel properties that can be useful in agriculture. It was reported that degraded alginate had successfully acted as a plant growth promoter [8.3, 8.6, 8.48, 8.49] and had enhanced the activity of some enzymes such as alcohol dehydrogenase, lactate dehydrogenase and chitinase [8.6, 8.50, 8.51]. Degraded chitosan has also been reported to have various biological activities in plants [8.16, 8.52–8.60]. It has been shown that various plant cells can respond to fragments of chitin and chitosan and initiate defence reactions leading to an accumulation of antibiotic phytoalexins to prevent infection of fungal diseases, stimulate plant growth and induction of the root system and strengthen plant stems [8.49, 8.59, 8.61].

Degraded alginate is usually produced using an alginate degrading enzyme such as alginate lyase [8.3, 8.6, 8.49, 8.60, 8.62, 8.63] and degraded chitosan that has been used for study has so far been obtained by enzymatic [8.64–8.68] or chemical degradation methods [8.39, 8.68–8.70] Irradiation has been found

to be a useful method for the degradation of polysaccharides and it is expected to be applied as a simple and useful tool for the degradation of alginate and chitosan [8.4, 8.71]. In addition, the biological activities of irradiated alginate for plants have not been investigated in detail. Recently, it has been found that the irradiated product of alginate, chitosan and carrageenan have interesting effects on plants [8.5, 8.46, 8.72–8.75], therefore, this section presents the biological activity of radiation degraded alginate, chitosan and carrageenan on the growth and development of plants in tissue culture.

Some plants used for tissue culture are chrysanthemum (*Chrysanthemum morifolium*), lisianthus (*Eustoma grandiflorum*), limonium (*Limonium latifolium*) and potato plants. Some bioactivity tests are described below.

8.4.1. Shoot proliferation activity test

To investigate the effect of absorbed dose (for the degradation of alginate) on the growth of shoot clusters, 20 shoots of chrysanthemum, limonium and lisianthus were cultured in a vessel containing Murashige and Skood's medium [8.76] with 3% sucrose, 0.8% agar, 0.3 mg/L 6-benzylaminopurin, 0.1mg/L 1-napthylacetic acid and 50mg/L alginate or chitosan of various $\bar{M}_w$. To investigate the effect of concentration on plant growth promotion, alginate ($\bar{M}_w$ ~14 kDa) or chitosan ($\bar{M}_w$ ~16 kDa) was supplemented into the culture medium at a concentration of 5–200 mg/L. The cultures were incubated for 25 days.

8.4.2. Plantlet propagation test

For plantlet culture, 20 plant shoots of chrysanthemum, limonium and lisianthus were cultured in a vessel containing half-strength Murashige and Skood's medium, 3% sucrose, 0.8% agar and 100 mg/L alginate or 50 mg/L chitosan that was irradiated at various doses; this was used as is for chrysanthemum and supplemented with 1 mg/L indole 3-butyric acid for lisianthus and limonium. To investigate a suitable concentration for the intended use, irradiated alginate and chitosan were supplemented at 5–200 mg/L. The media was adjusted to pH5.8 before autoclaving at 121°C for 15 min. All the cultures were incubated in a Biotron at 25 ±1°C with a photoperiod of 12 h per day. Cultures were incubated for 15 days for chrysanthemum and 20 days for limonium and lisianthus.

8.4.3. Transfer to soil

A hundred plantlets of chrysanthemum, limonium and lisianthus were removed and washed gently with tap water. The plantlets were then transferred to pots containing a mixture of soil and fertilizer and cultivated for 30 days in a greenhouse.

8.4.4. Data collection and statistical analysis

For the alginate test, the controls were carried out under the same conditions but without the supplementation of alginate. In the case of chitosan, the control was supplied with the same content of acetic acid used for dissolving the chitosan sample. All the cultures were incubated in a Biotron with a photoperiod of 12 h per day.

To evaluate the shoot proliferation rate, the number of shoots was determined by counting those that were higher than 0.5 cm. For the plantlet propagation test, the shoot height and root length were measured with a millimetre ruler. All the experiments were run as three blocks with three replicates for each treatment. The data were statistically analysed by variance analysis (ANOVA) with $LSD_{0.05}$ (the least significant difference at 5% probability level) and mean ± SE. The degree of growth promotion was calculated by the following expression: [Growth promotion degree, %] = [100 × (Evaluation of the treated bed)]/[Evaluation of the untreated bed].

8.4.5. Biological activity of irradiated alginate

8.4.5.1. Treatment with irradiated alginate leads to enhancement of shoot proliferation

Oligosaccharides have been reported to have biological effects on the growth of plants, particularly on the morphogenetic process, root and shoot elongation, antibiotic induction and enzyme activity [8.59]. The weight-average molecular weight ($\bar{M}_w$) of polysaccharides is proposed to determine its biological activity [8.63, 8.77]. This study investigates the most appropriate $\bar{M}_w$ of alginate for use for growth promotion activity in plants in tissue culture.

Alginates of various $\bar{M}_w$ are used to grow the shoot cluster, and the effect is quantified by observing the shoot proliferation rate. Table 8.5 shows that the supplementation of the growing media with irradiated alginate of $\bar{M}_w \sim$ 5.7–20.5 kDa increased the number of shoots. The $\bar{M}_w$ of alginate that offered the most efficient growth promotion of the shoot clusters of the tested plants was found to be about 14.2 kDa.

The effect of the concentration of enzymatically degraded alginate on various plants was studied and the optimum concentration was found at 300 mg/L [8.3, 8.49]. The data in Table 8.6 indicate that supplementation with irradiated alginate at a concentration of 50–70 mg/L exhibited a significant effect on the enhancement of the shoot proliferation rate for all the tested plants.

TABLE 8.5. EFFECT OF DOSE ABSORBED BY ALGINATE ON SHOOT PROLIFERATION RATE OF PLANTS

Absorbed dose (kGy)	$\bar{M}_w \times 10^3$	Number of shoots		
		Chrysanthemum	Lisianthus	Limonium
Control[a]	—	2.87	4.37	2.62
0	904.9	2.77	4.60	2.82
10	97.2	2.95	4.85	2.68
30	34.9	2.90	4.58	4.01
50	20.5	4.34	4.30	4.20
75	14.2	4.41	4.67	4.65
100	10.9	4.21	4.87	4.37
150	7.9	4.14	4.88	4.31
200	5.7	4.42	4.87	4.42

[a] Control without supplement of irradiated alginate.

TABLE 8.6. EFFECT OF IRRADIATED ALGINATE (14.2 kDa) CONCENTRATION ON SHOOT PROLIFERATION RATE OF PLANTS

Irradiated alginate concentration (mg/L)	Number of shoots		
	Chrysanthemum	Lisianthus	Limonium
0	2.63	4.83	4.58
5	2.77	4.92	4.58
10	2.95	4.48	5.07
30	4.32	4.66	5.20
50	4.10	4.95	5.40
70	4.70	4.33	5.47
100	4.25	4.32	5.28
150	4.58	4.33	5.20
200	4.42	4.29	5.11

8.4.5.2. Growth promotion activity of irradiated alginate in plantlet propagation

Tomoda et al. [8.49] revealed that degraded alginate had high positive effects on the root length of barley seedlings (2.4 mm/h) and on the tuber mass of Japanese radishes (324% increase in mass). For plantlet propagation, the induction of the root is an important stage in the formation of a plantlet from a shoot. The irradiated alginate promotes the growth of chrysanthemum plantlets, which are shown in Fig. 8.16 [8.5]. Treatment with alginate of a $\bar{M}_w$ of 10.9–14.2 kDa increases plants' shoot height (by 9.0–20.5%), root length (by 11.6–12.1%) and fresh biomass (by 19.0–32.6%). The treatment of plants with alginate of a $\bar{M}_w$ higher than 14.2 kDa or lower than 5.6 kDa gives no significant difference. The growth promotion effects of irradiated alginate on lisianthus and limonium are shown in Fig. 8.17 and Fig. 8.18 [8.5]. A remarkable increase in shoot height, root length and fresh biomass are observed in beds supplemented with alginate with $\bar{M}_w$ from 5.7–20.5 kDa for lisianthus and from 7.9–20.5 kDa for limonium. Alginate of a $\bar{M}_w$ higher than 20.5 kDa shows no significant effect on the development process for both plants, suggesting that these products are not suitable as plant growth promoters. Based on these results, it can be concluded that the alginate of a $\bar{M}_w$ of ~14.2 kDa shows the highest growth promotion effect in tissue culture for all tested plant varieties. Therefore, an irradiated alginate product of a $\bar{M}_w$ of ~14.2kDa was selected to investigate the optimal concentration of alginate.

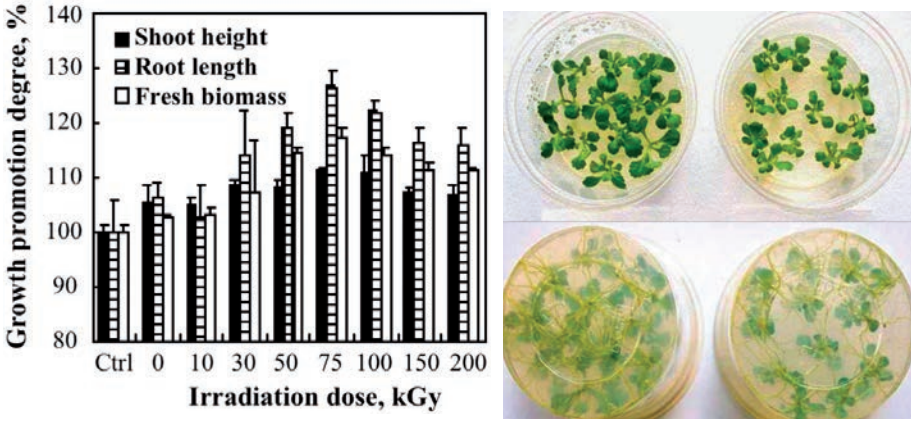

FIG. 8.16. Effect of irradiated alginate $\bar{M}_w$ on the growth of chrysanthemum.

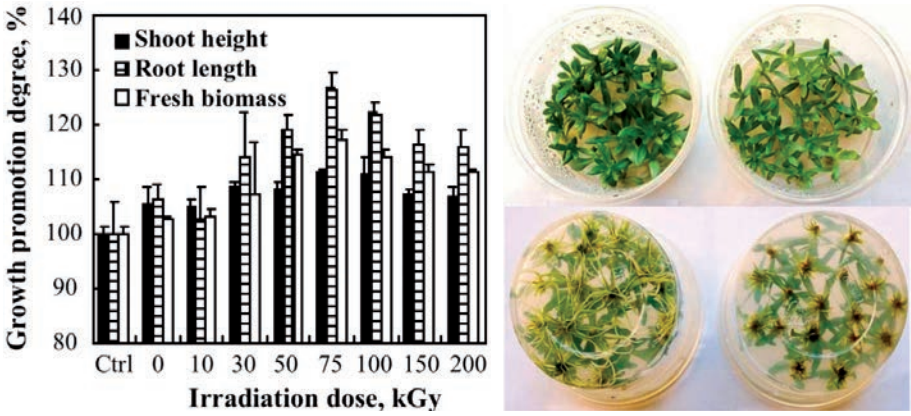

FIG. 8.17. Effect of irradiated alginate $\bar{M}_w$ on the growth of lisianthus.

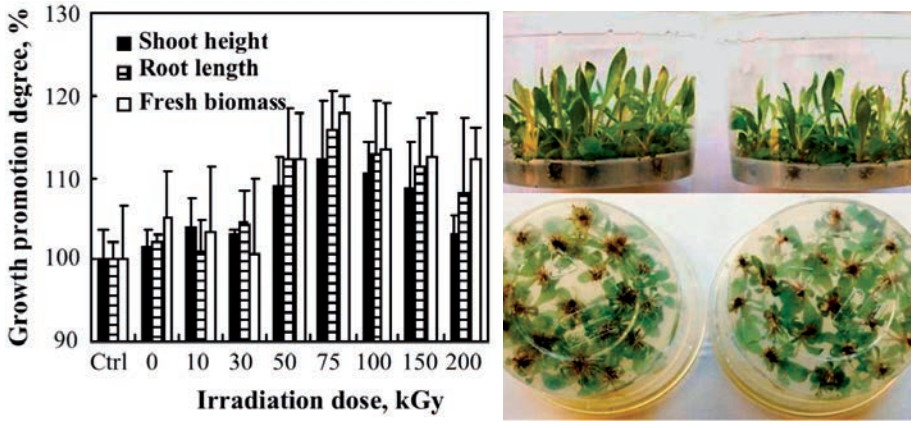

FIG. 8.18. Effect of irradiated alginate $\bar{M}_w$ on the growth of limonium.

Using irradiated alginate with an $\bar{M}_w \sim 14.2$ kDa, the optimum concentration for plant growth was investigated and the results are shown in Fig. 8.19. It can be observed that the supplementation of the growing medium with 50–200 mg/L irradiated alginate of an $\bar{M}_w \sim 14.2$kDa shows a significant effect on the induction and development of roots, enhances the shoot height and fresh biomass of chrysanthemum. Treatment with 50–200 mg/L irradiated alginate increases the root length, shoot height and fresh biomass of this plant by 16.9–39.4%, 14.1–24.2% and 9.7–19.4%, respectively, compared with the untreated control. In case of lisianthus, the increase in root length (8.9–14.6%), shoot height (6.2–14.4%) and fresh biomass (8.1–9.9%) were observed with 50–200 mg/L

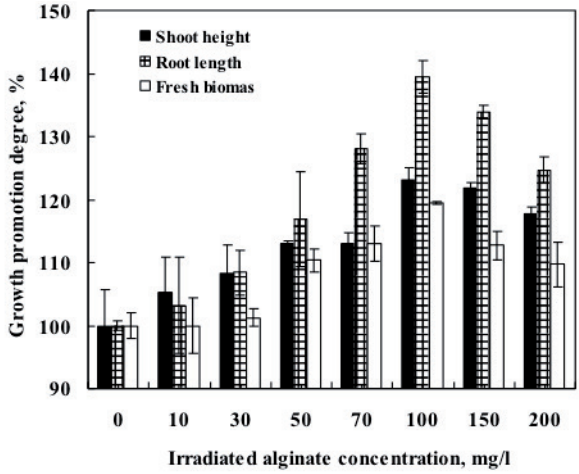

FIG. 8.19. Effect of irradiated alginate concentration on the growth of chrysanthemum.

irradiated alginate (Fig. 8.20). For limonium, the results in Fig. 8.21 show that the same concentrations of irradiated alginate enhanced root length (9.7–12.9%), shoot height (9.3–16.6%) and fresh biomass (11.7–16.6%). The most effective concentration of irradiated alginate for plantlet culture of chrysanthemum, limonium and lisianthus was found to be 100 mg/L.

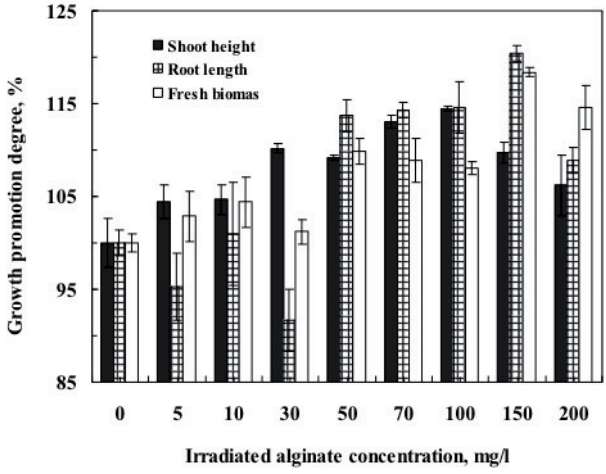

FIG. 8.20. Effect of irradiated alginate concentration on the growth of lisianthus.

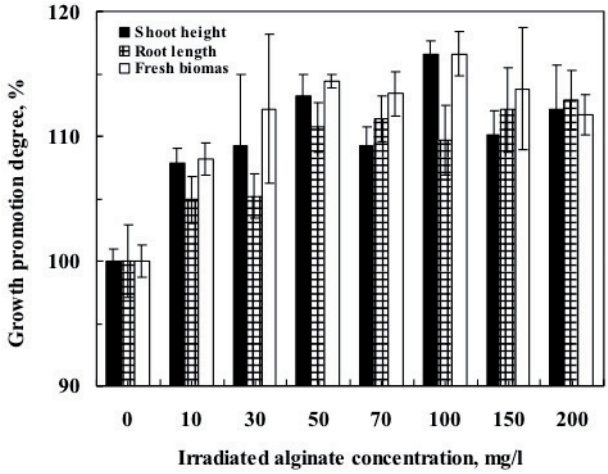

FIG. 8.21. Effect of irradiated alginate concentration on the growth of limonium.

8.4.6. Biological activity of irradiated chitosan

8.4.6.1. Enhancement of shoot proliferation by irradiated chitosan

Chitosan solution of 10% was selected for the preparation of irradiated chitosan. The effect of the $\bar{M}_w$ of irradiated chitosan on the growth of shoot clusters was investigated. The results in Table 8.7 indicate that the supplementation of irradiated chitosan of $\bar{M}_w$ ~ 16.4–27.8 kDa significantly increased the shoot proliferation rate of chrysanthemum (by 14.5%), limonium (by 17.9%) and lisianthus (by 69.0%) compared to the untreated control. Chitosan with a $\bar{M}_w$ ~ 16.4 is found to be the optimum product for promoting the growth of all the tested plants. Table 8.8 records the effect of irradiated chitosan concentration on the proliferation rates of chrysanthemum, limonium and lisianthus. When irradiated chitosan is added to culture media, the growth of the shoot cluster is promoted.

The optimum concentration of chitosan degraded by enzymatic and chemical methods has been investigated on plants by several authors and has been reported to be 100 mg/L for wheat and 500 mg/L for tomato plants [8.56]. In the present study, as indicated in Table 8.9, the growth effect of appropriate concentrations of irradiated chitosan was different for the plants studied. In particular, chrysanthemums treated with solutions containing 70–150 mg/L irradiated chitosan were found to have increased their shoot proliferation rates by 5.7–6.6%. For lisianthus, supplementing with irradiated chitosan of

TABLE 8.7. EFFECT OF IRRADIATED CHITOSAN ON SHOOT PROLIFERATION RATE OF PLANTS

Absorbed dose (kGy)	$\bar{M}_w \times 10^3$	Number of shoots		
		Chrysanthemum	Lisianthus	Limonium
Control[a]	—	2.71	22.2	2.90
0	194.66	2.83	2.25	4.13
10	129.50	2.80	2.32	4.93
30	66.07	2.92	2.43	4.47
50	39.20	2.79	2.57	4.53
75	27.79	4.04	2.53	4.53
100	16.40	4.10	2.61	4.90
150	11.34	2.72	2.38	4.75
200	9.90	2.30	2.35	4.09

[a] Control treated with the same content of acetic acid but without chitosan.

TABLE 8.8. EFFECT OF DOSE ABSORBED BY CHITOSAN ON SHOOT PROLIFERATION RATE OF PLANTS

Absorbed dose (kGy)	Number of shoots		
	Chrysanthemum	Limonium	Lisianthus
Control	2.71	2.22	2.22
0	2.83	2.25	2.25
10	2.80	2.32	2.32
30	2.92	2.43	2.43
50	2.79	2.57	2.57
75	4.04	2.53	2.53
100	4.10	2.61	2.61
150	2.72	2.38	2.38
200	2.30	2.35	2.35

concentrations of 50–100 mg/L promotes a shoot proliferation rate of 19.8–22.4%. Treatment with 30–100 mg/L irradiated chitosan increased the shoot proliferation rate of limonium by 16.8–35.7%. It can be said that, as with irradiated alginate, irradiated chitosan can also have a positive effect on the shoot proliferation of plants.

TABLE 8.9. EFFECT OF IRRADIATED CHITOSAN CONCENTRATION ON THE SHOOT PROLIFERATION RATE OF PLANTS

Concentration (mg/L)	Number of shoots		
	Chrysanthemum	Limonium	Lisianthus
0	4.18	4.17	4.95
5	4.13	4.32	4.75
10	4.25	4.53	4.67
30	4.24	4.85	4.63
50	4.34	5.45	4.73
70	4.39	4.82	4.82
100	4.36	5.15	4.83
150	4.37	4.50	4.07

8.4.6.2. Growth promotion activity of irradiated chitosan on plantlet propagation

Irradiated chitosan was also tested for its effect on the growth of chrysanthemum, lisianthus and limonium plantlets. As shown in Fig. 8.22, treatment with irradiated chitosan of a $\bar{M}_w$ of ~39.2–11.3 kDa led to a remarkable increase in the shoot height (14.6–22.3%) and fresh biomass (5.0–7.1%) of chrysanthemums compared with those of the untreated control, while a significant effect on root length (growth of 21.6–23%) is only observed upon treatment with irradiated chitosan of $\bar{M}_w$ ~ 17.8–16.4 kDa. The supplementation with irradiated chitosan also increases the growth of lisianthus plantlets. In particular, treatment with irradiated chitosan of a $\bar{M}_w$ ~ 17.8–16.4 kDa increases shoot height by 10.4–17.5%, while the increase in root length (18.6–44.6%) and fresh biomass (36.0–55.2%) is observed upon treatment with irradiated

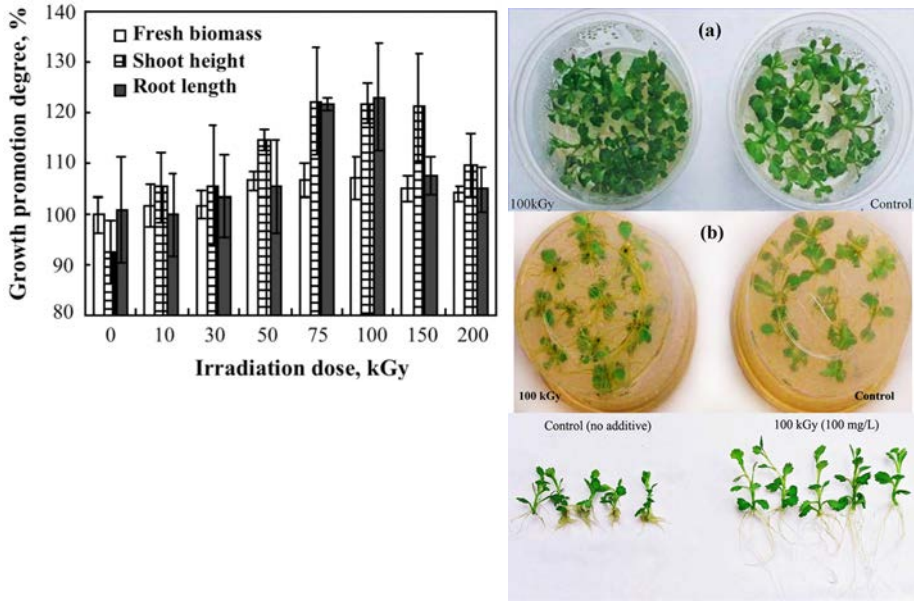

FIG. 8.22 . Effect of irradiated chitosan $\bar{M}_w$ on the growth of chrysanthemum.

chitosan of a $\bar{M}_w$ ~ 39.2–11.3 kDa and 17.8–16.4 kDa, respectively. Similarly, the treatments of irradiated chitosan with $\bar{M}_w$ ~ 39.2–11.3 kDa show a significant effect in limonium on the root length (increase of 76.9–167.9%), shoot height (increase of 9.0–11.4%) and fresh biomass (increase of 37.2–48.3%) compared with those of untreated control. The highest effect for the root growth of this plant is obtained with irradiated chitosan of $\bar{M}_w$ ~ 11.3 kDa, while the greatest increase in fresh biomass is observed upon treatment with the irradiated chitosan product of $\bar{M}_w$ ~ 16.4 kDa.

Thus, irradiated chitosan products with $\bar{M}_w$ ~ 39.2–11.3 kDa have a positive effect on the growth of shoot clusters and plantlets of all the tested plants. The combination of all the results obtained from the three tested plants indicates that the irradiated chitosan of a $\bar{M}_w$ ~ 16.4 kDa is the optimal product for growth promotion.

8.4.7. Biological activity of irradiated carrageenan

The molecular weights of the irradiated carrageenan obtained at 10, 20, 30 and 50 kGy are determined by GPC to be 24 kDa, 13 kDa, 10 kDa and 7 kDa, respectively [8.46]. As shown in Fig. 8.23, unirradiated carrageenan evidently inhibited the growth of potato plants in tissue culture while carrageenan irradiated at 30 kGy ($\bar{M}_w$ ~ 10 kDa) showed the highest inhibition effect. Compared

with control, the fresh biomass and shoot height increased by 35% and 15%, respectively. However, the effect of irradiated carrageenan on root length was insignificant.

In summary, the irradiation of of alginate, chitosan and carrageenan can confer plant growth promotion properties on them. The products of irradiated natural polysaccharides show positive effects on plant growth promotion in tissue culture.

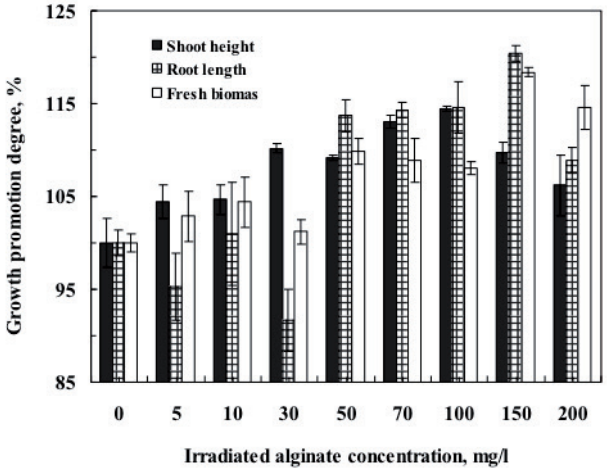

FIG. 8.23. Effect of irradiated carrageenan on the growth of potato plants.

8.5. FIELD TRIALS OF OLIGOCHITOSAN AS A PLANT ELICITOR AND GROWTH PROMOTER

A field trial is an experiment conducted on a large area or a large quantity of plants under conditions that are thought to be representative for a particular type of commercial operation. This type of trial is important when transforming a traditionally small scale, production based sector into a large scale agribusiness that contributes to economic growth and sustainability.

In Malaysia, a field trial was conducted on 24 ha of rice fields. It was the largest field trial conducted on the application of oligochitosan as a plant growth promoter and plant elicitor on rice plantations in the region. Basically, the field trial was designed using 8 field plots of 1.0 ha size per plot, in triplicate, with a total area of 24 ha [8.78]. The plots were used as described below.

Plots T1 and T2 (3 replicates in each plot) were the control plots and were soaked in commercial local growth promoter for 24 h and tossed for another 24 h before sowing to the fields. These rice plots were given pesticide treatment according to the normal local practices.

Plots T3, T4 and T5 (3 replicates in each plot) were soaked in water for 24 h and tossed for another 24 h before sowing to the fields. These rice plots were sprayed with oligochitosan at concentrations of 20 ppm, 40 ppm and 100 ppm, respectively, 42 days and 72 days after planting.

Plots T6, T7 and T8 (3 replicates in each plot) were soaked in water for 24 h and then soaked in 20 ppm oligochitosan for 30 min. They were then tossed for another 24 h prior to sowing to the fields. These rice plots were sprayed with oligochitosan at concentrations of 20 ppm, 40 ppm and 100 ppm, respectively, 42 days and 72 days after planting.

A smaller field trial, of slightly less than 1.0 ha, of the application of oligochitosan as a plant growth promoter on rice plantations was also conducted in another rice field in a different area 150 km away from the first field trial. The second rice field is well known for its fertility for rice growing. In this field trial, only 3 plots were designated: control, 40 ppm and 100 ppm oligochitosan, with triplicates in each plot. In each 1 ha plot, 5 quadrants of 1 m^2 in size were identified for the collection of data on physical growth, fungal diseases, yield and rice seed characterization.

8.5.1. Field trial of the use of oligiochitosan on rice seedlings for transplanting

Rice seedling trials have been conducted at both rice plantation areas described above. The following compares the growth rates of rice seedlings treated with oligochitosan with those treated with a commercial product 15 days before being transferred to the paddy field.

The effects of oligochitosan on the growth of rice seedlings were significant, as shown in Figs 8.24 to 8.26, and can be summarized as follows:

— The growth of rice seedlings increased by 22.8–24.3% on burned rice husk substrate and by 14.0% on commercial soil when sprayed with oligochitosan compared with when they were sprayed with commercial nutrients. This indicates that the type of soil or substrate also significantly affected the growth rate of the rice seedlings. However, relatively, the growth of rice seedlings sprayed with oligochitosan in any soil or substrate is much faster than when they are sprayed with commercial nutrients, although oligochitosan has no nutrients that can provide additional essential elements to the seedling. Figure 8.25 clearly shows that the height of the

rice seedlings at 8 days after treatment with oligochitosan was much greater than that of the seedlings treated with commercial nutrients. Similarly, the root growth of the rice seedlings treated with oligochitosan was significantly increased compared with rice seedlings treated with commercial nutrients, as shown in Fig. 8.27.

— The usual time taken for rice seedlings to become mature plants can be shortened from 15 days to 10–12 days. The growth of roots was faster and was well spread on the substrates and the seedlings were ready to be transferred to the field 10–12 days after planting rather than at the usual 15 days.

From the above rice seedling trials, it can be concluded that oligochitosan enhances the growth of rice seedlings without adding nutrients and can consequently reduce the time taken for rice seedlings to become mature plants and thereby reduce costs.

Figure 8.28 shows the rice seedlings at the site waiting to be transferred to the fields on the 15th day. Figure 8.29 shows the method of transplanting the rice seedlings to the fields using a transplanter.

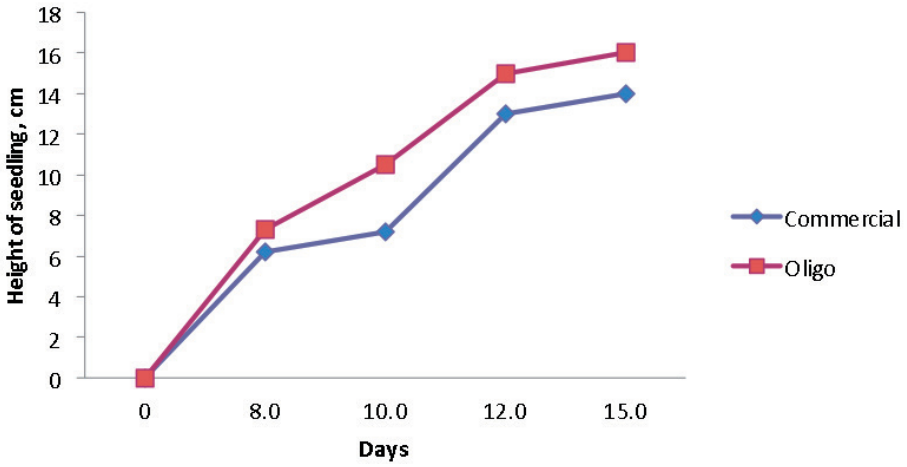

FIG. 8.24. Growth rate of rice seedlings in the wet season (October–February).

FIG. 8.25. Height of rice seedlings at 8 days.

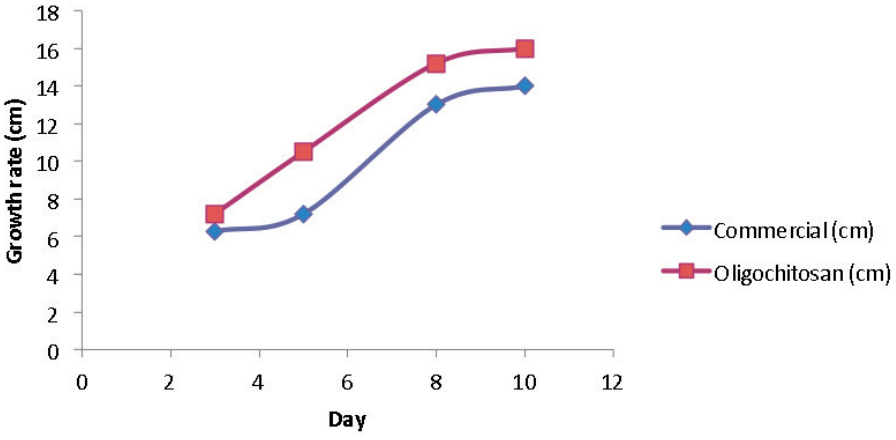

FIG. 8.26. Growth rate of rice seedlings during the dry season (March–July).

FIG. 8.27. Root growth at 8 days.

FIG. 8.28. Rice seedlings.

FIG. 8.29. Transplanting rice seedlings.

8.5.2. Field trials of the use of oligiochitosan during rice planting

Rice seeds were harvested 112 days after planting. The total yield of rice seeds per experimental plot at the Federal Land Consolidation and Rehabilitation Authority at Seberang Perak and in the Agriculture Department of the Ministry of Agriculture at Tanjung Karang are given in Table 8.10 and Table 8.11 respectively. The field trials at FELCRA were designed as described below.

TABLE 8.10. RICE YIELDS 2008–2010 FOR FIELD TRIALS CONDUCTED AT FELCRA (M) BERHAD, SEBERANG PERAK

	Rice yield when sprayed with 40 ppm oligochitosan			
	Large area, 24 ha		Small area, 1 ha	
	Season 2/2008	Season 1/2009	Season 1/2010	Season 2/2010
% increase over control T1	7.3	5.5	9.14	20
% increase over control T2	4.5	4.6	4.1	14.6

The T1 and T2 plots were not treated with oligochitosans but one was sprayed with fungicides and one was not; both were used as controls. Plots T3–T8 were not sprayed with fungicides but were only sprayed with oligochitosan at different concentrations.

FELCRA's Seberang Perak rice crop plantation area is a low yield rice area, with a yield per ha of not more than 5.9 in 2008−2010. Unfortunately, the rice yields decreased between 2008 and 2010. The average increase in rice yield when oligochitosan is used is about 4.5% to 7.0% higher than the control plots T1 and T2; the large field trial area was 24 ha in size. However, when the field trial was conducted in a smaller plot area of about 1 ha, the increase in rice yield is quite significant at 9.0–20.0% [8.78]. The vast differences in the increase in yield were due to the management of the field trial plots against pests such as rats, golden snails, birds and weedy rice and against unfavourable weather. For a 24 ha field trail, more workers would be required to manage the plots in the same way.

Nevertheless, most of the rice plots sprayed with oligochitosan had higher yields than the plots sprayed with fungicides (T2). This demonstrates the effectiveness of oligochitosan as a plant elicitor inducing the rice crops to protect themselves against fungi.

TABLE 8.11. RICE YIELDS IN 2011 IN TANJUNG KARANG, SELANGOR

Plot	Treatment	Area (ha)	2nd trial, Jul.–Dec. 2011 (wet season)			1st trial, Jan.–Jun. 2011 (dry season)		
			Weight (t)	Weight/ha (t)	Increase (%)	Weight (t)	Weight/ha (t)	Increase (%)
T1	Control, no fungicides, no oligochitosan	0.0437	0.420	9.6110	—	0.240	5.4920	—
T2	40 ppm oligochitosan	0.0437	0.433	9.9161	4.17	0.276	6.3310	15.28
T3	100 ppm oligochitosan	0.0437	0.430	9.8398	2.38	0.276	6.3310	15.28
Average				9.7890			6.0513	

The average rice yield at Tanjung Karang during the dry season was about 6.0 t/ha, and during the wet season it was 9.0 t/ha. Tanjung Karang is one of Malaysia's high yield rice areas. During the dry season, the rice plots that were sprayed with oligochitosan produced a 15% increase in yield compared with control [8.78]. However, during the high season, when the yield of rice is at the optimum 9.0 t/ha, the application of oligochitosan does not produce a significant effect [8.78].

From the results of the above field trials, it can be concluded that:

— Oligochitosan enhances the yield of rice crops.
— An oligochitosan concentration of 40 ppm is sufficient to enhance the yield of rice crops.
— The effectiveness of oligochitosan as a plant growth promoter can be clearly seen during the wet season (off season).
— Oligochitosan seems capable of acting as a plant elicitor against fungus, hence the use of chemical fungicides may become unnecessary.

In Viet Nam, field tests were carried out to investigate the effect of oligochitosan on sugarcane and rice growth. A randomized block design in triplicate was used for the study. Oligochitosan of $\bar{M}_w$ 6000–10 000 with a DD of 70–90% was sprayed three times on crop plants [8.56]. In the case of sugarcane, the optimum concentration of oligochitosan was found to be 30 ppm. This concentration achieved a disease index reduction for *Ustilago scitamines* and *Colletotrichum falcatum* of 50–80% and a productivity increase of 11–13 % (which amounts to 6–8 t/ha) [8.56]. Figure 8.30 shows the field trial in rice, while the effect of oligochitosan on disease index and productivity is summarized in Table 8.12 [8.56].

It has been shown that an oligochitosan concentration of 15 ppm reduced the disease index of *Pyricularia grisea* on the leaves to 63% and increased productivity by 26%.

Additionally, Dzung and Thang have carried out investigations in peanut [8.61], soybean [8.79] and coffee (Dzung et al. [8.80]) plants. They used a 20–50 ppm oligochitosan solution for the foliar spraying of peanut leaves, and obtained a productivity increase of 20–40% (Table 8.13).

The productivity of soybean plants increased by about 30% when the seeds were soaked in a 0.4% oligochitosan solution, which also decreased the rate of rust disease [8.79].

In a field test of the effect of oligochitosan on the growth of coffee plants, it was shown that when sprayed with a 60 ppm oligochitosan solution, the growth of branches increased by about 20%, and an increase in the height of the plants, their stem diameter and number of leaves was observed [8.80].

FIG. 8.30. Field test of the elicidation and growth promotion effects of oligochitosan, produced by gamma irradiation, on rice in Viet Nam.

TABLE 8.12. THE EFFECT OF OLIGOCHITOSAN ON DISEASE INDEX AND PRODUCTIVITY IN RICE

Conc. of oligochitosan ppm	Leaf DI		Panicle DI		Productivity	
	Index (%)	Compared with control (%)	Ratio (%)	Compared with control (%)	Tonne/ha	Increase (%)
15	14.4	62.88	10.0	34.1	6.8	25.93
30	15.3	66.81	12.0	40.9	6.0	11.11
60	16.0	69.87	15.3	52.2	6.3	16.67
Control (H_2O)	22.9	100	29.3	100	5.4	—

TABLE 8.13. EFFECT OF OLIGOCHITOSAN ON THE PRODUCTIVITY OF PEANUTS

	Oligochitosan (ppm)				
	0 (control)	20	30	40	50
Productivity (kg)	4.05	4.64	4.74	4.29	4.81
Compared with control (%)	100	119.3	122.6	140.7	124.8

In addition, El-Sawy et al. studied the effect of radiation-degraded chitosan on the growth of broad bean plants [8.41]. They concluded that degraded chitosan has a positive effect not only on plant growth but also on the productivity of broad bean plants.

In conclusion, oligochitosan is very effective at inducing a defence response to disease infection in plants. In addition, the treatment with oligochitosan not only reduced the disease index but also increased productivity. Thus, oligochitosan has a potential application in agriculture as a biotic elicitor and a growth promoter for plants.

8.6. APPLICATION IN HYDROPONICS CULTURE

The plants tested were rice, soybean, barley and lettuce. Irradiated alginate was used in a growth promotion test. The results shown in Fig. 8.31 indicate that a suitable concentration of degraded alginate for the growth promotion of rice was found to be about 50 ppm [8.4, 8.20]. Alginate irradiated in powder form also exhibited an effect for plant growth promotion (Fig. 8.32).

The results given in Table 8.14 show that irradiated alginate product enhances the growth and development of plants, increases the activity of phytoalexin enzymes and increases the crop yield.

Irradiated alginate of various $\bar{M}_w$ has also been tested for the production of 'clean' vegetables (i.e. produced without artificial chemicals) using hydroponics systems. It was shown that all irradiated alginate products affect the stimulation of growth and development of Chinese mustard (Fig. 8.33) and lettuce plants (Fig. 8.34) compared to the control (not treated with irradiated alginate) and the unirradiated sample ($\bar{M}_w \sim 930$ kDa). The optimal $\bar{M}_w$ of irradiated alginate for growth promotion activity in Chinese mustard and lettuce was also found to be 14.2 kDa.

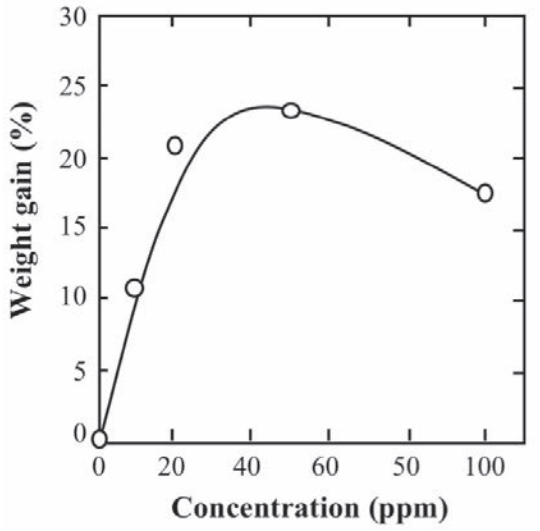

FIG. 8.31. Effect of the concentration of irradiated alginate ($\bar{M}_w$ ~ 7000) on the growth of rice plants.

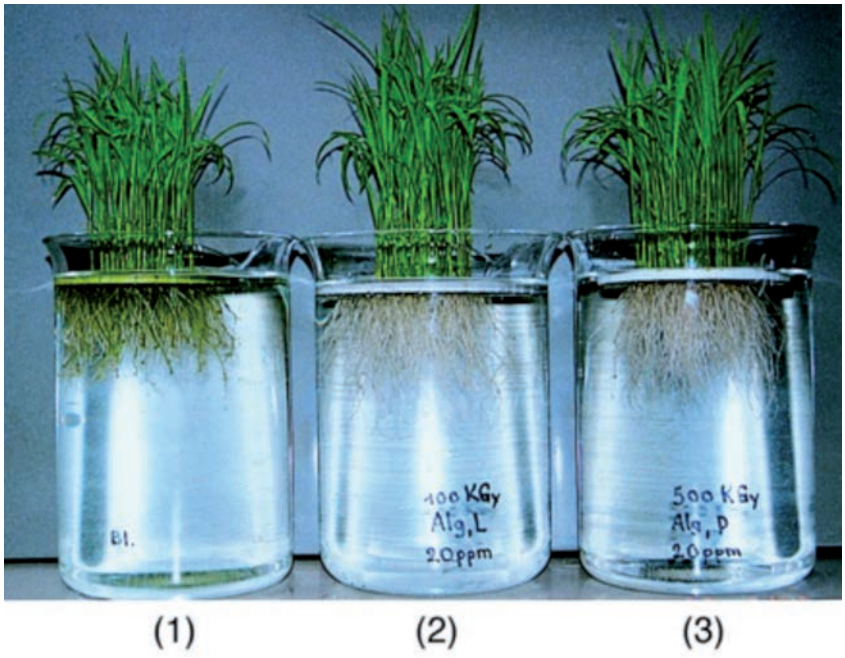

FIG. 8.32. Growth of rice plants: (1) not treated with alginate, (2) treated with 20 ppm alginate irradiated at 100 kGy in 4% solution and (3) treated with 20 ppm alginate irradiated at 500 kGy in powder form.

TABLE 8.14. ENHANCEMENT OF THE CROP YIELD OF SOYBEAN PLANTS CULTURED IN HYDROPONICS WITH IRRADIATED ALGINATE

Samples	Weight of dried seed, g/plant
Control	4.47 ± 0.13 (100%)
Irradiated alginate	4.73 ± 0.08 (107.5%)

In Viet Nam, irradiated alginate has been applied by Saigon Thuy Canh for clean vegetable production using hydroponics technology on a large scale (see Fig. 8.35) because of the high yield and increased quality indicated by parameters such as a high dried matter content and a low nitrate content.

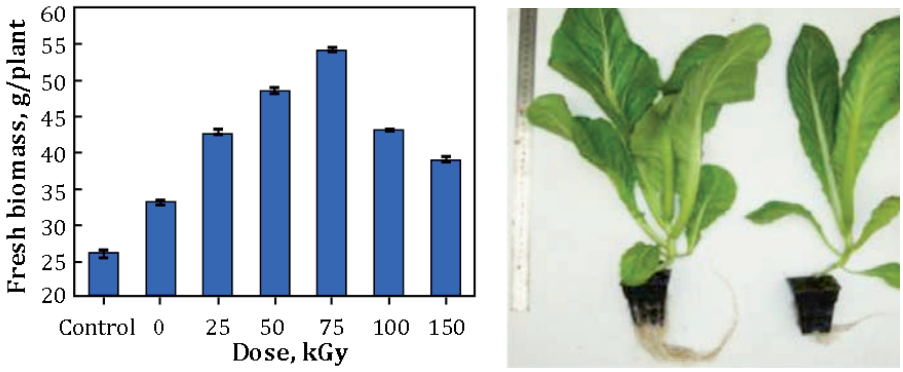

FIG. 8.33. Effect of $\bar{M}_w$ of alginate on the growth of Chinese mustard in hydroponics culture.

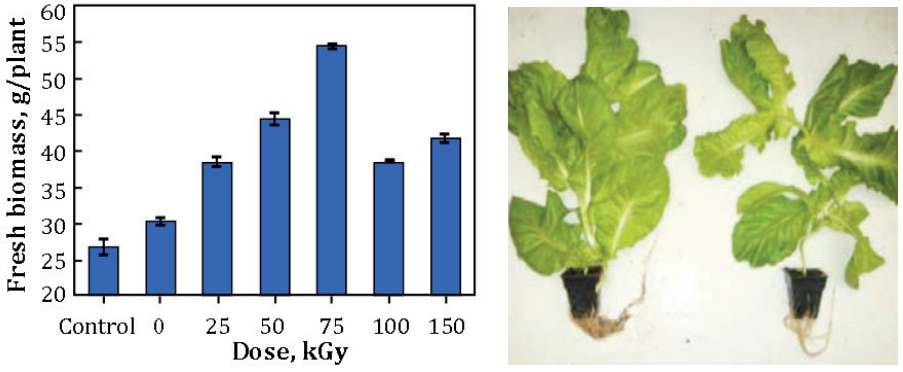

FIG. 8.34. Effect of M_w of alginate on the growth of lettuce in hydroponics.

FIG. 8.35. Large scale application of irradiated alginate for production of vegetables without using artificial chemicals.

8.7. APPLICATION BY LEAF FOLIAR SPRAYING ON PLANTS

The treatment of seedlings of horticulture plants such as carrots, cabbage, tea, spinach, tomato and lettuce plants with foliar spraying of various irradiated polysaccharides has been shown to have positive effects. Leaf foliar spraying of carrot plants with oligoalginate produced by the radiation degradation method increases their productivity by about 50% compared with that of the control, and the optimum concentration is 40–80 ppm [8.81]. In addition, the quality of carrots was improved, giving a higher total sugar content and lower nitrate content (see Table 8.15). The maximum level of nitrate content in green vegetables is 500 mg/kg fresh (equal to 500 ppm).

Leaf foliar spraying of oligoalginate on tea plants was shown to increase productivity by about 20% compared with that of control at the optimum concentration of 50–100 ppm [8.81]. In addition, the content of soluble substances and the tanin of the tea product was higher (Tables 8.16 and 8.17), indicating that the quality of tea treated with oligoalginate is higher (Figs 8.36 and 8.37).

TABLE 8.15. EFFECT OF FOLIAR SPRAYING WITH OLIGOALGINATE ON CARROT PRODUCTIVITY AND QUALITY

Oligoalginate concentration (ppm)	Leaf biomass (t/ha)	Productivity		Nitrate content		Sugar content	
		Compared with control (%)		mg/kg fresh	Compared with control (%)	g/kg fresh	Compared with control (%)
Control	21.1	35.8	100.0	615	100.0	6.29	100.0
20	27.3	46.9	130.9	491	79.9	7.26	115.5
40	26.5	50.7	141.5	458	74.5	8.25	131.4
60	29.6	57.3	159.5	448	72.9	8.64	137.4
80	28.4	52.8	147.5	446	72.6	9.02	144.3
100	25.3	47.2	131.7	451	74.4	10.37	165.0
120	26.0	47.0	131.2	453	74.7	10.02	159.4
$LSD_{0.05}$	—	4.3					

TABLE 8.16. EFFECT OF OLIGOALGINATE ON PRODUCTIVITY OF TEA PLANTS

Oligoalginate concentration (ppm)	0 (control)	25	50	100	200
Productivity (ton/ha[a])	5.35	5.91	6.32	6.39	5.75
Compared with control (%)	100	110.5	118.1	119.4	107.3

[a] Least significant difference 0.05 = 0.25.

FIG. 8.36. Field application of oligoalginate (T&D 4DD) to tea plants.

FIG. 8.37. Oligoalginate commercial product produced by γ irradiation method in Viet Nam.

TABLE 8.17. EFFECT OF OLIGOALGINATE ON TEA PRODUCT CONTENT OF SOLUBLE SUBSTANCES AND TANIN

Oligoalginate	Soluble substances (g/100 g)	Compared with control (%)	Tanin content (g/100 g)	For control (%)
Control, 0 ppm	38.9 ± 2.0	100	12.3 ± 0.9	100
50 ppm	46.2 ± 2.3	118.7	15.9 ± 1.4	128

It was also reported by Mollah et al. [8.82] that foliar spraying of irradiated alginate on red amaranth plants increased their average weight gain (Fig. 8.38).

Some of the work that was carried out at the University of Buenos Aires under a N–S orientated greenhouse improved for seedling production (Fig. 8.39) is described below. The growth and development of seedlings of horticultural species that were foliar sprayed with various irradiated polysaccharides were compared with those grown in untreated control plots. Plants were obtained in plugs and grown in soilless culture in order to control the presence of all essential nutrients, using a perlite and sphagnum peat (50% volume/volume) substrate (Fig. 8.40) and a nutrient solution (Hoagland). The spray solutions were applied twice a week, and prepared from the solid form just before application. At the

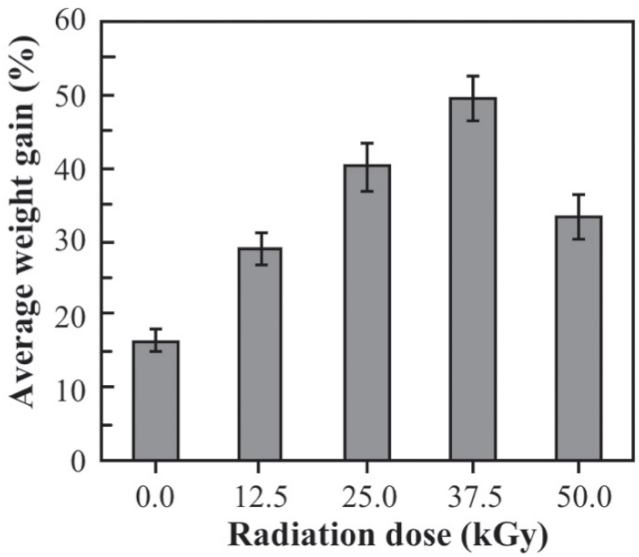

FIG. 8.38. Effect of irradiated alginate treatment (150 ppm) on weight gain of red amaranth (Amarathus cruentus L.).

FIG. 8.39. Greenhouse for production of seedlings in plugs and pots.

FIG. 8.40. Soilless culture components: compost, vermiculite, perlite and sphagnum peat.

end of the experiments, the seedlings and plants were harvested, the dry weights (drying was carried out in a ventilated oven at 60ºC for a week) of their leaves (including petioles), stems and roots were registered and their shoot–root ratio calculated. The data were analysed using the statistical software InfoStat and Duncan test.

Four groups of alginate samples irradiated with 0, 500, 750 and 1000 kGy and a control (water) were applied to spinach (S*pinacia oleracea* L.), cabbage (*Brassica oleracea* L.) and tomato (*Solanum lycopersicum* L.) (Figs 8.41–8.43). Polysaccharide solutions for foliar spraying were prepared in 20 and 100 ppm concentrations. The aerial biomass, shoot–root ratio, chlorophyll (measured using a soil plant analysis development (SPAD)-502 meter), Polyphenol (measured using the Folin–Ciocalteu method) and Anthocyanin (measured using the differential pH method) were measured [8.83].

Radiation-processed alginate, carrageenan and chitosan were used as plant growth promoters in cabbage, tomato and lettuce (*Lactuca sativa* L.) (Fig. 8.44). The alginate, carrageenan and chitosan were dry gamma irradiated with 0, 50, 100 and 300 kGy doses. The average $\bar{M}_w$ of alginate and carrageenan versus

absorbed doses are shown in Figs 8.45 and 8.46. They were foliar sprayed as aqueous solutions in 100 ppm concentration. To analyse a possible vegetal growing compensation effect under nutrient stress conditions, different nitrogen availability was provided (N200: complete solution, 200 ppm N; N50: deficient, 50 ppm N). The chlorophyll leaf content was estimated using a SPAD-502 meter [8.84].

FIG. 8.41. Spinach plants at an early stage of the growing period.

FIG. 8.42. Cabbage plants at an early stage of the growing period.

FIG. 8.43. Tomato plants at an early stage of the growing period.

FIG. 8.44. Lettuce plants at the final stage of the growing period.

The alginate, carrageenan and chitosan were irradiated in air in the solid state (in powder form) with gamma rays of ^{60}Co at the semi-industrial irradiation plant of the National Atomic Energy Commission's Ezeiza Atomic Centre and at the private industrial irradiation plant IONICS, in Don Torcuato, Buenos Aires Province. The irradiation took place in air at room temperature at a dose rate of 10 kGy/h.

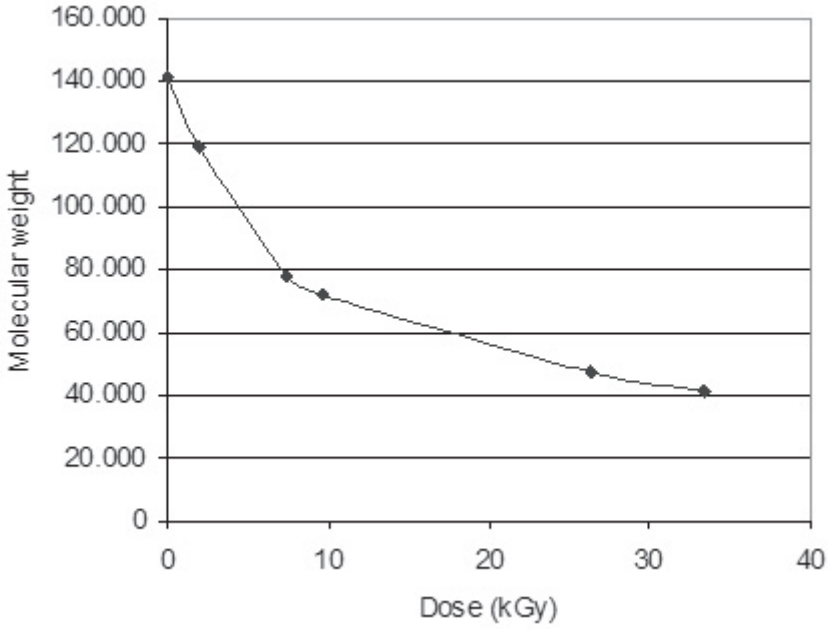

FIG. 8.45. Average viscosity molecular weight of alginate in Da vs. absorbed dose in kGy.

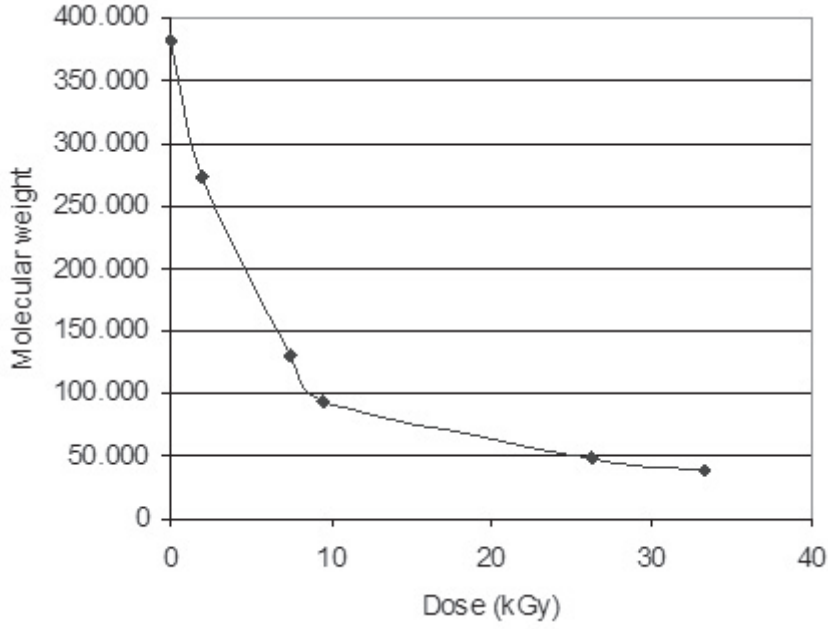

FIG. 8.46. Average viscosity molecular weight of carrageenan in Da vs. absorbed dose in kGy.

In this study, the allometric measures or proportions that are usually used in the analysis of plant growth were employed, for example, to estimate leaf area and leaf chlorophyll content, by non-destructive methods.

8.7.1. Leaf area estimation

The most common measurements for the determination of plant growth are the length and width of leaves to estimate leaf area; the length or diameter of the fruits to estimate growth; and the exchange of CO_2 and water vapour from leaves or fruits measured with cameras. In general, it is assumed that such measurements do not alter the normal development of plants (even if thigmomorphogenesis is sometimes cited as affecting the morphology and physiology of plants, it is impossible to make an exact quantitative prediction because different mechanical disturbances are not comparable, and there may also be interaction with environmental factors).

A non-destructive model has been adjusted to estimate leaf area for each species. Leaf areas of a representative number of leaves from all experiments and at different crop stages were measured with an area meter (LI-COR Model 3100 Area Meter), and correlated to their respective length and width. In this way, growth analysis can be done avoiding periodic harvests (destructive measurement). In tomatoes, 315 leaves were measured, obtaining a high correlation model between length and leaf area (Fig. 8.47).

8.7.2. Leaf chlorophyll content

The determination of chlorophyll by acetone extraction is a method used to estimate a crop's nutritional status as regards nitrogen, magnesium and iron content, and has the drawback of requiring specialized equipment and a lengthy analysis time. The amount of chlorophyll determined by this traditional method has a high correlation with the units registered by a chlorophyll meter. Based on the principle that part of the radiation reaching the foliage is absorbed by chlorophyll, and the rest of the light detected by the device is converted into an electrical signal, this methodology is widely used in crops with the aim of instantaneously determining nitrogen needs. Non-destructive techniques to estimate chlorophyll content have been adjusted for all the horticultural species in the study. The objective was to correlate extractable chlorophyll with the values obtained by means of a SPAD-502 meter (a Soil Plant Analysis Development chlorophyll meter manufactured by Minolta), avoiding destructive measurements.

Leaves of different colours, from pale yellow (chlorotic) to intense green, were selected from several plants. These were cut in 1 cm^2 fragments and readings were immediately taken with the chlorophyll analyser. The concentration of

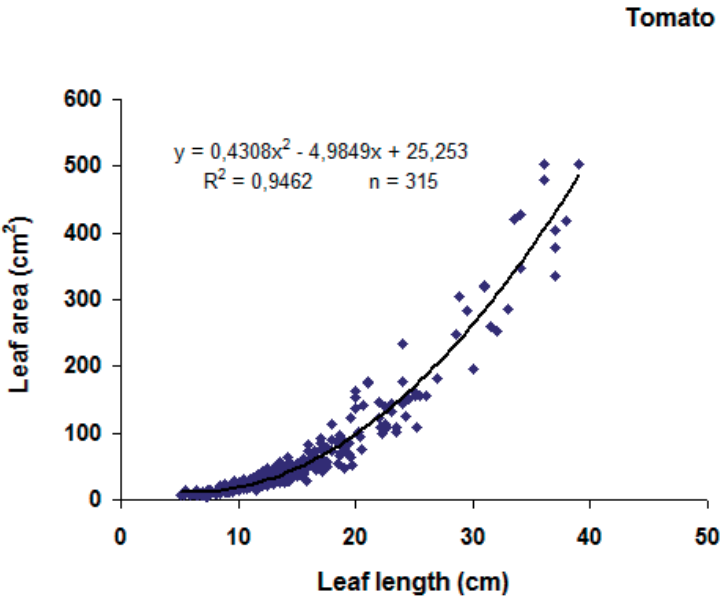

FIG. 8.47. Calibration curve of tomato leaf area vs. leaf length.

extractable chlorophyll was determined by N, N dimethylformamide (Inskeep and Bloom method) and measured with a spectrophotometer (Life Science UV/VIS Spectrophotometer DU530, Beckman).

The leaf chlorophyll content was correlated with the SPAD meter reading and converted to absolute values using the calibration curves shown in Figs 8.48–8.50.

In the high dose experiment, different biomass accumulations and partitioning was found in spinach, cabbage and tomato, Tables 8.18–8.20 respectively, depending on the radiation level received by the alginate and its spray concentration.

For aerial biomass, shoot–root ratio and chlorophyll content, treatments are considered effective when the statistical values are higher than the control values, as these parameters indicate a better growth performance and therefore a yield increase. When polyphenol and anthocyanin values are lower than controls, treatments are considered positive.

In spinach, the aerial biomass and shoot–root ratio increased with the application of alginate in any dose or concentration, whereas the chlorophyll content was higher when the lower concentration of 20 ppm was used. Polyphenol decreased with the spray applications compared with the control, but no effect in anthocyanin content was caused. In cabbage, both aerial biomass and chlorophyll

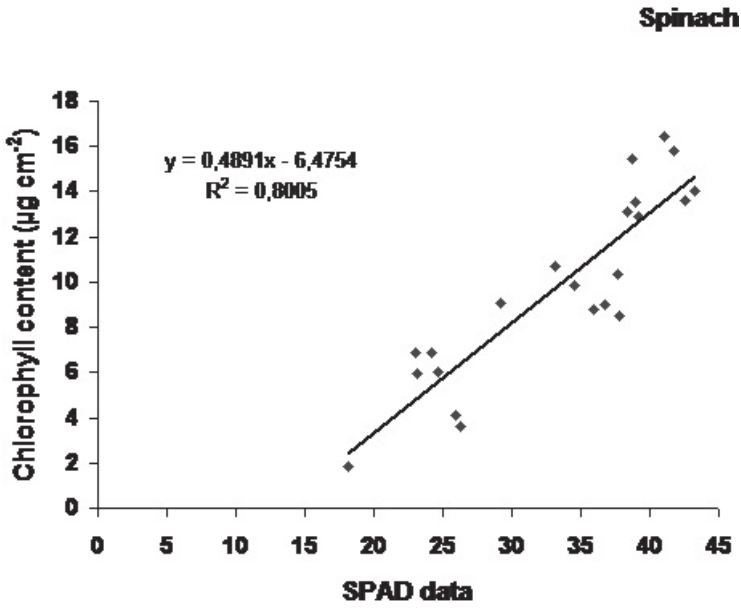

FIG. 8.48. Calibration curve of extractable chlorophyll content of spinach vs. SPAD meter readings.

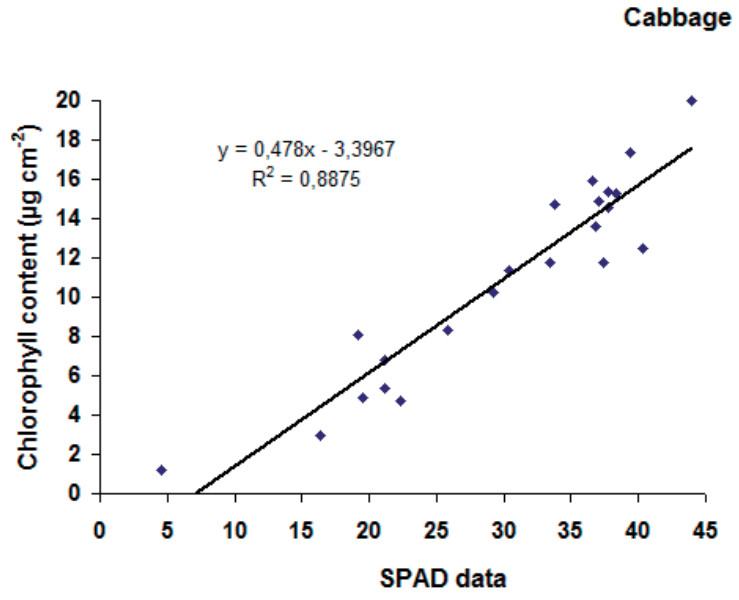

FIG. 8.49. Calibration curve of extractable chlorophyll content of cabbage vs. SPAD meter readings.

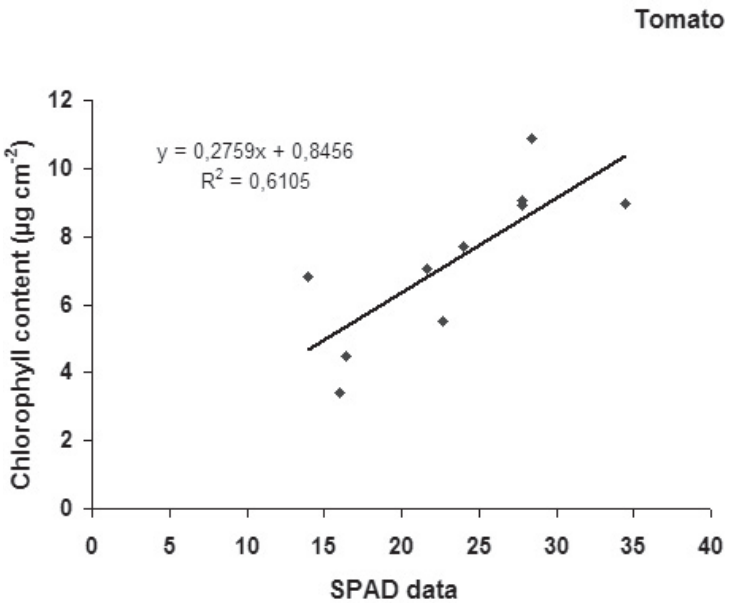

FIG. 8.50. Calibration curve of extractable chlorophyll content of tomato vs. SPAD meter readings.

content increased with the lower concentrations, but shoot–root ratio only increased with the 100 ppm concentration, independent of the radiation doses.

The polyphenol and anthocyanin contents were not modified. Tomato presented higher aerial biomass only with 20 ppm concentrations, but a lower shoot–root ratio, which means a proportionally greater radicular biomass than the other treatments. No differences in chlorophyll, polyphenol or anthocyanin contents, compared with the control, were shown.

In the low dose experiments, different chlorophyll contents were found in the three species depending on the polysaccharide, radiation level and nitrogen availability (Table 8.21).

High dose experiments with 120 determinations gave a whole efficiency of the treatments of 80%, 70% and 35% for spinach, cabbage and tomato, respectively. Analysing the use of alginate solutions of 20 ppm or 100 ppm concentration, a more effective result for the former dilution was found: 66.6% for the average, but 95%, 75% and 35% for spinach, tomato and cabbage, respectively. The dose of radiation led to an increase in effectiveness of 64.3%, 60%, 70% and 50% for 0 kGy, 500 kGy, 750 kGy and 1000 kGy, respectively.

In a low dose experiment, the application of polysaccharides had different effects on the chlorophyll contents depending on the crop and N availability (Table 8.22). When nitrogen was provided in 200 ppm concentration, tomato and

TABLE 8.18. AERIAL BIOMASS, SHOOT–ROOT RATIO AND CHLOROPHYLL, POLYPHENOL AND ANTHOCYANIN CONTENTS IN SPINACH

	Aerial biomass (mg)		Shoot–root ratio		Chlorophyll content (μg/cm^2)		Polyphenol (mg/100 g fresh weight)		Anthocyanin[a] (mg/100 mg fresh weight)	
Control	36		2.60		10.67		0.34		0.30	
kGy	20 ppm	100 ppm	20 ppm	100 ppm	20 ppm	100 ppm	20 ppm	100 ppm	20 ppm	100 ppm
0	127	86	4.93	4.32	11.20	10.32	0.20	0.17	0.20	0.43
500	136	88	5.02	4.28	11.49	10.51	0.16	0.11	0.23	2.53
750	120	80	5.11	4.70	11.45	10.79	0.14	0.12	0.13	1.23
1000	124	90	1.68	4.97	10.68	9.66	0.16	0.20	0.00	2.77

[a] Anthocyanin (mg/100 mg) × 10^{-2} fresh weight.

TABLE 8.19. AERIAL BIOMASS, SHOOT–ROOT RATIO AND CHLOROPHYLL, POLYPHENOL AND ANTHOCYANIN CONTENTS IN CABBAGE

	Aerial biomass (mg)		Shoot–root ratio		Chlorophyll content (μg/cm^2)		Polyphenol (mg/100g fresh weight)		Anthocyanin[a] (mg/100 mg fresh weight)	
Control	448		2.34		16.37		0.20		0.40	
kGy	20 ppm	100 ppm	20 ppm	100 ppm	20 ppm	100 ppm	20 ppm	100 ppm	20 ppm	100 ppm
0	536	447	2.80	4.89	17.74	16.67	0.21	0.26	0.00	0.03
500	512	456	4.42	6.12	17.48	16.99	0.21	0.18	0.07	0.63
750	534	452	2.35	4.34	17.87	16.49	0.22	0.17	0.27	0.73
1000	562	434	2.63	4.21	17.86	16.53	0.22	0.27	0.57	1.93

[a] Anthocyanin (mg/100 mg) × 10^{-2} fresh weight.

TABLE 8.20. AERIAL BIOMASS, SHOOT–ROOT RATIO AND CHLOROPHYLL, POLYPHENOL AND ANTHOCYANIN CONTENTS IN TOMATO

	Aerial biomass (mg)		Shoot–root ratio		Chlorophyll content (μg/cm^2)		Polyphenol (mg/100g fresh weight)		Anthocyanin[a] (mg/100 mg fresh weight)	
Control	290		4.83		8.81		0.34		0.17	
kGy	20 ppm	100 ppm	20 ppm	100 ppm	20 ppm	100 ppm	20 ppm	100 ppm	20 ppm	100 ppm
0	397	341	2.28	4.51	8.71	8.74	0.34	0.39	0.27	0.13
500	412	278	2.45	4.80	8.79	8.71	0.39	0.39	0.17	0.33
750	392	378	2.30	4.55	8.69	8.89	0.34	0.30	0.00	0.43
1000	388	368	2.09	4.19	8.63	8.63	0.37	0.46	0.23	0.10

[a] Anthocyanin (mg/100 mg) × 10^{-2} fresh weight.

TABLE 8.21. CHLOROPHYLL CONTENT IN LETTUCE, CABBAGE AND TOMATO

		Chlorophyll content (μg cm^{-2})					
	Dose (kGy)	Lettuce		Cabbage		Tomato	
Nitrogen availability		N200	N50	N200	N50	N200	N50
Control		4.90	4.67	17.35	15.34	8.42	7.50
Alginate	0	4.67	4.42	19.15	15.56	9.34	7.84
	50	4.80	4.69	18.75	14.76	9.01	7.49
	100	5.05	4.73	19.46	15.64	9.40	7.64
	300	4.80	4.48	19.51	17.21	9.03	7.42

TABLE 8.21. CHLOROPHYLL CONTENT IN LETTUCE, CABBAGE AND TOMATO (cont).

		Chlorophyll content (μg cm^{-2})					
	Dose (kGy)	Lettuce		Cabbage		Tomato	
Carrageenan	0	4.40	4.80	18.79	17.04	9.44	7.16
	50	4.94	4.54	19.87	15.79	9.18	7.39
	100	4.94	4.58	18.98	14.81	9.37	7.22
	300	5.26	4.42	18.93	15.19	9.13	7.51
Chitosan	0	5.05	4.64	19.77	15.16	8.98	7.58
	50	5.50	4.79	18.43	14.73	9.38	7.45
	100	5.80	4.73	19.06	15.28	9.32	7.63
	300	5.57	4.88	19.32	15.63	9.11	7.59

TABLE 8.22. CHLOROPHYLL AVERAGE INCREASE

	Chlorophyll increase (%)		
Nitrogen availability	Cabbage	Tomato	Lettuce
mg/L			
200	10.48	9.50	4.46
50	1.50	−0.13	−0.81

cabbage increased their chlorophyll content by 10% in all treatments compared with control. Lettuce increased its chlorophyll content by a similar percentage but only upon application of chitosan.

In general, the 100 kGy dose showed the best results, with 77.7% effectiveness. Tomato, lettuce and cabbage had an improvement in chlorophyll content of 83%, 66.6% and 54.1%, respectively. Chitosan, alginate and

carrageenan were more effective in producing increments in chlorophyll, with increases of 84.3%, 66.6% and 58.3%, respectively.

Under N deficiency (50 ppm N), all the species and treatments presented lower chlorophyll contents than with 200 ppm N. However, with alginate and chitosan applications, independent of the dose, higher values were obtained in tomato. The same response was observed for lettuce in chitosan treatments.

In conclusion, irradiated alginates applied as a foliar spray did not improve chlorophyll content in lettuce, cabbage or tomato when less nitrogen was available. However, under N200 treatments, alginate application increased the chlorophyll content in cabbage and tomato, independent of the radiation dose.

Carrageenan applications showed the same response, and also the same values as those registered under alginate treatments. On the other hand, chitosan presented the best performance for the three species, with a similar chlorophyll content under nitrogen low availability, and a higher content when this element was available.

Aerial biomass as leaf content was 377% higher in spinach treated with alginate irradiated with 500 kGy dose and a solution containing 20 ppm N. Leaves increased the aerial biomass by 125% in cabbage and 142% in tomato when treated with alginate irradiated with 500 kGy.

Generally, the decrease of anthocyanin and polyphenol was in the order of 212% and 130% respectively.

REFERENCES TO CHAPTER 8

[8.1] CLARE, K., “Alginate”, Industrial Gums — Polysaccharides and Their Derivatives, (WHISTLER, R.L., BEMLLER, J.N., Eds), Academic Press, New York (1993) 105–144.

[8.2] ERTESVAG, H., VALLA, S., Biosynthesis and applications of alginates, Polym. Deg. Stab. **59** (1998) 85–91.

[8.3] YONEMOTO, Y., et al., Promotion of germination and shoot elongation of some plants by alginate oligomers prepared with bacteria alginate lyase, J. Ferment. Bioeng. **75** (1993) 68–70.

[8.4] HIEN, N.Q., et al., Growth-promotion of plants with depolymerized alginates by irradiation, Rad. Phys. Chem. **59** (2000) 97–101.

[8.5] LUAN, L.Q., et al., Biological effect of radiation-degraded alginate on flower plants in tissue culture, Biotechnol. Appl. Biochem. **38** (2003) 283–288.

[8.6] AKIMOTO, C., AOYAGI, H., TANAKA, H., Endogenous elicitor-like effects of alginate on physiological activities of plant cells, Appl. Microbiol. Biotechnol. **52** (1999) 429–436.

[8.7] AKIYAMA, H., et al., Effect of depolymerized alginates on the growth of bifidobacteria, Biosci. Biotech. Biochem. **56** 2 (1992) 355–356.
[8.8] NAGASAWA, N., MITOMO, H., YOSHII, F., KUME, T., Radiation-induced degradation of sodium alginate, Polym. Deg. Stab. **69** (2000) 279–285.
[8.9] CHARLESBY, A., Atomic Radiation and Polymers, Pergramon Press (1960).
[8.10] WOOD, R.T., PIKAEVI, A.K., "Radiation processing", Applied Radiation Chemistry, Wiley, New York (1994).
[8.11] JANIK, I., KASPRZAK, E., AL-ZIER, A., ROSIAK, J.M., Radiation crosslinking and scission for poly(vinyl methyl ether) in aqueous solution, Nucl. Instr. Meth. Phys. Res. B **208** (2003) 374–379.
[8.12] YOSHII, F., "Radiation degradation of marine polysaccharides by low energy electron beam", Proceedings of the FNCA 2002 Workshop on Application of Electron Accelerator (Proc. Workshop Takasaki, Japan, 2002), JAERI, Tokyo (2003) 42–47.
[8.13] KNORR, D., Recovery and utilization of chitin and chitosan in food processing waste management, Food Technol. J. **45** (1991) 114–122.
[8.14] HIRANO, S., Chitin biotechnology applications, Biotechnol. Annu. Rev. **2** (1992) 237–258.
[8.15] SHAHIDI, F., ARACHCHI, J.K.V., JEON, Y.T., Food applications of chitin and chitosan, Trends Food Sci. Technol. **10** (1999) 37–51.
[8.16] KUMAR, M.N.V.R., A review of chitin and chitosan applications, React. Funct. Polym. **46** (2000) 1–27.
[8.17] TOMIDA, H., et al., Antioxidant properties of some different molecular weight chitosans, Carbohydr. Res. **344** (2009) 1690–1696.
[8.18] FENG, T., DU, Y., LI, J., HU, Y., KENNEDY, F.J., Enhancement of antioxidant activity of chitosan by irradiation, Carbohydr. Polym. **73** (2008) 126–132.
[8.19] LIU, N., et al., Effect of MW and concentration of chitosan on antibacterial activity of Escherichia coli, Carbohydr. Polym. **64** (2006) 60–65.
[8.20] ZHENG, L.Y., ZHU, J.F., Study on antimicrobial activity of chitosan with different molecular weights, Carbohydr. Polym. **54** (2003) 527–530.
[8.21] JEON, Y., PARK, P., KIM, S., Antimicrobial effect of chitooligosaccharides produced by bioreactor, Carbohydr. Polym. **44** (2001) 71–76.
[8.22] MATSUHASHI, S., KUME, T., Enhancement of antimicrobial activity of chitosan by irradiation, J. Sci. Food Agric. **73** (1997) 237–241.
[8.23] QIN, C.Q., DU, Y.M., XIAO, L., LI, Z., GAO, X.H., Enzymic preparation of water-soluble chitosan and their antitumor activity, Int. J. Biol. Macromol. **31** (2002) 111–117.
[8.24] LUO, L., et al., Immune response, stress resistance and bacterial challenge in juvenile rainbow trouts Oncorhynchus mykiss fed diets containing chitosan-oligosaccharides, Curr. Zool. **56** (2009) 416–422.
[8.25] HUANG, R.L., et al., Dietary oligochitosan supplementation enhances immune status of broiler, J. Sci. Food Agric. **87** 1 (2007) 153–159.
[8.26] HIEN, N.Q., "Radiation degradation of chitosan and some biological effects", Radiation Processing of Polysaccharides, IAEA-TECDOC-1422, IAEA, Vienna, (2004) 67–73.

[8.27] RODRIGUEZ, A.T., et al., Induction of defense response of *Oryza sativa* L. against *Pyricularia grisea* (Cooke) Sacc. by treating seeds with chitosan and hydrolyzed chitosan, Pest. Biochem. Physiol. **89** (2007) 206–215.

[8.28] YIN, H., ZHAO, X., DU, Y., Oligochitosan: A plant diseases vaccine—A review, Carbohydr. Polym. **82** (2010) 1–8.

[8.29] KIM, S.K., RAJAPAKSE, N., Enzymatic production and biological activities of chitosan oligosaccharides (COS): A review, Carbohydr. Polym. **62** (2005) 357–368.

[8.30] XIA, W., LIU, P., ZHANG, J., CHEN, J., Biological activities of chitosan and chitooligosaccharides, Food Hydrocoll. **25** (2011) 170–179.

[8.31] MAKUUCHI, K., Critical review of radiation processing of hydrogel and polysaccharide, Radiat. Phys. Chem. **79** (2010) 267–271.

[8.32] HAJI-SAEID, M., SAFRANY, A., SAMPA, M.H.O., RAMAMOORTHY, N., Radiation processing of natural polymers: The IAEA contribution, Radiat. Phys. Chem. **79** (2010) 255–260.

[8.33] ULANSKI, P., ROSIAK, J.M., Preliminary study on radiation-induced changes in chitosan, Radiat. Phys. Chem. **39** (1992) 53–57.

[8.34] CHMIELEWSKI, A.G., et al., Chemical-radiation degradation of natural oligoamino-polysaccharides for agricultural application, Radiat. Phys. Chem. **76** (2007) 1840–1842.

[8.35] ZAINOL, I., AKIL, H.M., MASTOR, A., Effect of γ-irradiation on the physical and mechanical properties of chitosan powder, Mater. Sci. Eng. C **29** (2009) 292–297.

[8.36] CZECHOWSKA-BISKUP, R., ROKITA, B., ULANSKI, P., ROSIAK, J.M., Radiation-induce and sonochemical degradation of chitosan as a way to increase its fat-binding capacity, Nucl. Instr. Meth. Phys. Res. B **236** (2005) 383–390.

[8.37] CHOI, S.W., AHN, J.K., LEE, W.D., BYUN, W.M., PARK, J.H., Preparation of chitosan oligomers by irradiation, Polym. Degrad. Stab. **78** (2002) 533–538.

[8.38] WASIKIEWICZ, M.J., YOSHII, F., NAGASAWA, N., WACH, A.R., MITOMO, H., Degradation of chitosan and sodium alginate by gamma radiation, sonochemical and ultraviolet methods, Radiat. Phys. Chem. **73** (2005) 287–295.

[8.39] QIN, C.Q., DU, Y.M., XIAO, L., Effect of hydrogen peroxide treatment on the molecular weight and structure of chitosan, Polym. Degrad. Stab. **76** (2002) 211–218.

[8.40] KANG, B., DAI, D.Y., ZHANG, Q.H., CHEN, D., Synergic degradation of chitosan with gamma radiation and hydrogen peroxide, Polym. Degrad. Stab. **92** (2007) 359–362.

[8.41] EL-SAWY, N.M., ABD EL-REHIM, H.A., ELBARBARY, A.M., HEGAZY, E.A., Radiation-induced degradation of chitosan for possible use as a growth promoter in agricultural purposes, Carbohydr. Polym. **79** (2010) 555–562.

[8.42] HIEN, N.Q., PHU, D.V., DUY, N.N., ANH, T.N., LAN, N.T.K., Degradation of chitosan in solution by gamma irradiation in the presence of hydrogen peroxide, Carbohydr. Polym. **87** (2012) 935–938.

[8.43] WANG, S.M., HUANG, Q.Z., WANG, Q.S., Study on the synergetic degradation of chitosan with ultraviolet light and hydrogen peroxide, Carbohydr. Res. **340** (2005) 1143–1147.

[8.44] SHAO, J., YANG, Y., ZHONG, Q., Study on preparation of oligoglucosamine by oxidative degradation under microwave irradiation, Polym. Degrad. Stab. **82** (2003) 395–398.

[8.45] DUY, N.N., PHU, D.V., ANH, T.N., HIEN, N.Q., Synergistic degradation to prepare ologochitosan by gamma-irradiation of chitosan solution in the presence of hydrogen peroxide, Radiat. Phys. Chem. **80** (2011) 848–854.

[8.46] RELLEVE, L., et al., Degradation of carrageenan by radiation, Polym. Degrad. Stab. **87** (2005) 403–410.

[8.47] MOHD DAHLAN, K., et al., A Pilot Scale Production and Field Trial Study of Radiation Processed Chitosan as Plant Growth Promoter for Rice Crops (2009), http://www-naweb.iaea.org/napc/iachem/meetings/RCMs/RC-1091-2_report_complete.pdf

[8.48] THERKELSEN, G.H., "Carragenan", Industrial Gums — Polysaccharides and Their Derivatives (WHISTLER, R.L., BEMLLER, J.N., Eds), Academic Press, New York (1993) 145–180.

[8.49] TOMODA, Y., UEMURA, K., ASACHI, T., Promotion of barley root elongation hypoxic condition by Alginate Lyase Lysate (A.L.L.), Biosci. Biotech. Biochem. **58** (1994) 202–204.

[8.50] RYAN, C.A., FARMER, E.E., Oligosaccharide signaling in plants: A current assessment, Ann. Rev. Plant Physiol. Mol. Biol. **42** (1991) 651–674.

[8.51] INUI, H., YAMAGUCHI, Y., HIRANO, S., Elicitor actions of N-acetylchitooligosaccharides and Laminarioligosaccharides for chitinase and L-phenylalanine ammonia-lyase induction in rice suspension culture, Biosci. Biotech. Biochem. **61** (1997) 975–978.

[8.52] TAY, L.P., KHOH, L.K., LOH, C.S., KHOR, E., Alginate-chitosan coacervation in production of artificial seed, Biotechnol. Bioeng. **42** (1993) 449–454.

[8.53] BITTELLI, M., FLURY, M., CAMPBEL, G.S., NICHOLS, E.J., Reduction of transpiration through foliar application of chitosan, Agr. Forest Meteorol. **107** (2001) 167–175.

[8.54] KENDRA, A.F., HADWIGER, L.A., Characterization of smallest chitosan oligomer that is maximally antifungal to *Fusarium solani* and elicits pisatin formation in *Pisum sativum*, Exp. Mycol. **8** (1984) 276–281.

[8.55] INUI, H., KOSAKI, H., UNO, Y., TABATA, K. HIRANO, S., Introduction of chitinase in rice callus treated with chitin derivatives, Agr. Biol. Chem. **55** (1991) 3107–3109.

[8.56] HIEN, Q.H., Study of Chemical Treatment Combined with Radiation to Prepare Biotic Elicitor for Utilization in Agriculture (2009), http://www-naweb.iaea.org/napc/iachem/meetings/RCMs/RC-1091-2_report_complete.pdf

[8.57] YAMADA, A., SHIBUYA, N., KODAMA, O., AKATSUKA, T., Induction of phytoalexin formation in suspension rice cells by N-acetylchitooligosaccharides, Biosci. Biotech. Bioch. **57** (1993) 405–409.

[8.58] DOARES, S.H., SYROVETS, T., WEILER, E.W., RYAN, C.A., "Oligogacturonides and chitosan activate plant defensive genes through the octadecanoid pathway", Proc. Nat. Acad. Sci. USA **92** (1995) 4095–4098.

[8.59] VANDER, P., VÅRUM, K.M., DOMARD, A., GUEDDARI, N.E.E., MOERSCHBACHER, B.M., Comparison of the ability of partially N-acetyled

chitosans and chitooligosaccharides to elicit resistance reaction in wheat leaves, Plant Physiol. **118** (1998) 1353–1359.

[8.60] IWAMOTO, Y., et al., Purification and characterization of bifunctional alginate lyase from Alteromonas sp. Strain No. 272 and its action on saturate oligomeric substrates, Biosci. Biotech. Biochem. **65** (2001) 133–142.

[8.61] DZUNG, N.A., THANG, N.T., Effect of chitooligosaccharides on the growth and development of peanut (*Arachis hypogea* L.), Proc. Sixth Asia-Pacific on Chitin, Chitosan Symposium (KHOR, E., HUTMACHER, D., YONG, L.L., Eds), Singapore (2004).

[8.62] AOYAGI, H., et al., Promotion effect of alginate on chitinase production by *Wasabia japonica*, Biotechnol. Tech. **10** (1996) 649–654.

[8.63] NATSUME, M., KAMO, Y., HIRAYAMA, M., ADACHI, T., Isolation and characterization of alginate-derived oligosaccharides with root growth-promoting activities, Carbohydr. Res. **258** (1994) 187–197.

[8.64] AIBA, S.I., Preparation of N-acetylchitooligosaccharides from lysozymic hydrolysates of partially N-acetylated chitosans, Carbohydr. Res. **261** (1994) 297–306.

[8.65] QIN, C., DU, Y., ZENG, F., LIU, Y., ZHOU, B., Effect of hemicellulase on the molecular weight and structure of chitosan, Poly. Degrad. Stab. **80** (2003) 435–441.

[8.66] CHENG, C.Y., LI, Y.K., An aspergillus chitosanase with potential for large-scale preparation of chitosan oligosaccharides, Biotechnol. Appl. Biochem. **32** (2000) 197–204.

[8.67] ZHANG, H., NEAU, S.H., In vitro degradation of chitosan by a commercial enzyme preparation: Effect of molecular weight and degree of deacetylation, Biomater. **22** (2001) 1653–1658.

[8.68] JIA, Z., SHEN, D., Effect of reaction temperature and reaction time on preparation of low-molecular weight chitosan using phosphoric acid, Carbohydr. Polym. **49** (2002) 393–396.

[8.69] TOMMERAAS, K., VÅRUM, K.M., CHRISTENSEN, B.E., SMIDSROD, O., Preparation and characterization of oligosaccharides produce by nitrous acid depolymerisation of chitosans, Carbohydr. Res. **333** (2001) 137–144.

[8.70] HSU, S.C., DON, T.M., CHIU, W.Y., Free radical degradation of chitosan with potassium persulfate, Polymer Degrad. Stab. **75** (2002) 73–84.

[8.71] KUME, T., NAGASAWA, N., YOSHII, F., Utilization of carbohydrates by radiation processing, Radiat. Phys. Chem. **63** (2002) 625–627.

[8.72] LUAN, L.Q., NAGASAWA, N., HA, V.T.T., KUME, T., YOSHII, F., NAKANISHI, T.M., Biological effect of irradiated chitosan plant on plant in vitro, Biotechnol. Appl. Biochem. **41** (2005) 49–57.

[8.73] LUAN, L.Q., NAGASAWA, N., TAMADA, M., NAKANISHI, T.M., Enhancement of plant growth activity of irradiated chitosan by fractionation, Radioisot. **55** 1 (2006) 21–27.

[8.74] LUAN, L.Q., NAGASAWA, N., HA, V.T.T., NAKANISHI, T.M., A Study of degradation mechanism of alginate by gamma-radiation, Radioisot. **58** 1 (2009) 1–11.

[8.75] LUAN, L.Q., NAGASAWA, N., HA, V.T.T., HIEN, N.Q., NAKANISHI, T.M., Enhancement of plant growth stimulation activity of irradiated alginate by fractionation, Radiat. Phys. Chem. **78** (2009) 796–799.

[8.76] MURASHIGE, T., SKOOG, F., A revised medium for rapid growth and bioassay with tobacco tissue cultures, Plant Physiol. **15** (1962) 473–497.

[8.77] IWASAKI, K., MATSUBARA, Y., Purification of alginate oligosaccharides with root growth-promotion activity toward lettuce, Biosci. Biotech. Bioch. **64** (2000) 1067–1070.

[8.78] MOHD DAHLAN, K., et al., "A pilot scale production and field trial study of radiation processed chitosan as plant growth promoter for agricultural applications", IAEA Technical Report of the 3rd and Final Meeting of the IAEA/CRP Project on Development of Radiation Processed Products of Natural Polymers for Application in Agriculture, Healthcare, Industry and Environment, Working Material, IAEA, Vienna (2011).

[8.79] DZUNG, N.A., THANG, N.T., "Effects of chitooligosaccharides prepared by enzyme degradation on the growth of soy bean", Proc. 5th Asia Pacific Chitin and Chitosan Symposium (SUCHIVA, K., CHANDRKRACHANG, S., METHACANON, P., PETER, M.G., Eds), National Metals and Materials Center, Bangkok (2003).

[8.80] DZUNG, N.A., KHANH, V.T.P., DZUNG, T.T., Research on impact of chitosan oligomer on biophysical characteristics, growth, development and drought resistance of coffee, Carbohydr. Polym. **84** 2 (2011) 751–755.

[8.81] HIEN, N.Q., et al., "Radiation degradation of alginate and some results of biological effect of degraded alginate on plants", Proceedings of the Takasaki Workshop on Bilateral Cooperations (Proc. Workshop, Takasaki, 1999) JEARI, Tokyo (2000) 94–100.

[8.82] MOLLAH, M.Z.I., KHAN, M.A., KHAN, R.A., Effect of gamma irradiated alginate on red amaranth (*Amaranthus cruentus* L) as growth promoter, Radiat. Phys. Chem. **78** (2009) 61–64.

[8.83] DIVO DE SESAR, M.D., Integración de Estudios Fisiológicos, Histológicos y Bioquímicos del Proceso de Enraizamiento, Rustificación y Crecimiento Posterior de Especies de Importancia Agronómica Suplementadas con Citoquininas, PhD Thesis, Buenos Aires Univ. (2005).

[8.84] CLOZZA, M.N., Crecimiento y Desarrollo en Tomate Platense (*Lycopersicon esculentum* Mill.): Análisis del Efecto de la Nutrición Mineral, PhD Thesis, Valencia Univ. (2010).

Chapter 9

ANTIMICROBIAL AND ANTIOXIDANT PROPERTIES OF OLIGOSACCHARIDES

M. SEN
Department of Chemistry, Hacettepe University,
Ankara, Turkey

N. QUOC HIEN, D. VAN PHU, L. QUANG LUAN
Vietnam Atomic Energy Institute,
Hanoi, Viet Nam

K. ZAMAN
Malaysian Nuclear Agency,
Bangi, Malaysia

L.V. ABAD, L.S. RELLEVE, C.T. ARANILLA, C.D.T. RACADIO
A.M. DE LA ROSA
Philippine Nuclear Research Institute,
Quezon City, Philippines

D. TAHTAT, M. MAHLOUS, S. BENAMER, A. NACER KHODJA
Department of Irradiation Technology,
Nuclear Research Center of Algiers,
Algiers, Algeria

9.1. INTRODUCTION

In recent years, the potential antimicrobial activity of oligosaccharides (such as chitosan, alginate and carrageenan) and their derivatives has received considerable attention. Numerous studies were conducted showing that oligosaccharides could be effective against different groups of microorganisms, such as bacteria, yeast and fungi. Some of the results reported are summarized in this chapter.

9.2. THE ANTIMICROBIAL ACTIVITY OF CHITOSAN

Chitosan or its derivatives have been proven more effective against gram-positive bacteria than gram-negative bacteria [9.01]. The effect may be attributed to their cell wall composition: the cell wall of a gram-positive bacterium (e.g. *Bacillus subtilis)* is composed of the peptide polyglycogen, which forms a network with many pores, allowing chitosan to enter the cell easily and disturb its metabolism. However, the cell wall of a gram-negative bacterium (e.g. *Escherichia coli*) is made up of a thin membrane of peptidoglycan and an outer membrane of lipopolysaccharides and phospholipids, which constitute a barrier against chitosan. For gram-positive bacteria (except for *Lactobacillus sp*.), chitosan with 470 kDa was the most effective antimicrobial substance , whereas for gram-negative bacteria, chitosan with 1106 kDa was the most effective.

In one study [9.2], a chitosan derivative, N carboxybutyl chitosan, was tested against 298 different pathogenic microorganisms displaying bactericidal and bacteriostatic activities. Marked morphological alterations in treated microorganisms were found [9.2]. Low-molecular-weight chitosan did not display systematically higher antimicrobial activity, but this was found for a specific molecular weight range.

These results were confirmed by antibacterial tests conducted in solid and liquid media against *Escherichia coli* with chitosan of a molecular weight of $\overline{M}_{w1}$ = 88.3 kDa and $\overline{M}_{w2}$ = 17.4 kDa, respectively. The inhibition diameters in the solid medium were 35 mm and 28.25 mm for $\overline{M}_{w1}$ and $\overline{M}_{w2}$, respectively. More significant results were obtained in the liquid medium, where the counts were 28×10^2 cfu/mL and 294×10^2 cfu/mL for $\overline{M}_{w1}$ and $\overline{M}_{w2}$, respectively. The initial bioburden was 615×10^6 cfu/mL. These two tests confirmed that the chitosan of a molecular weight of 88.3 kDa is more effective in bacterial growth inhibition than that of a molecular weight of 17.4 kDa [9.1].

Qin et al. [9.3] studied the antibacterial activity of chitosan in a molecular weight range of 1.4 to 400 kDa, and found that the highest antimicrobial effect was obtained for $\overline{M}_w$ 78 kDa and 48 kDa. Liu et al. [9.4] reported that antimicrobial activity is more pronounced for low $\overline{M}_w$ in the range of 55 to 155 kDa. Lam and Diep [9.5] studied the antifungal activity of chitosan of an $\overline{M}_w$ varying from 72.5 to 139 kDa and found that the highest activity corresponded to a $\overline{M}_w$ of 122 kDa.

Li et al. [9.6] reported that the molecular weight of chitosan and the species of bacteria made a big difference to the antibacterial activity. Chitosan with a molecular weight of 50 kDa exhibited higher antibacterial activity against *Pseudomonas aeruginosa* and *Escherichia coli* than against *Proteus mirabilis*. In the presence of 3 kDa chitosan oligomers, higher inhibition was observed against *Pseudomonas aeruginosa* and *Proteus mirabilis* than against

Escherichia coli. However, high molecular weight chitosan of 1000 kDa inhibited *Proteus mirabilis* more effectively than it did the other two bacterial species. This study [9.6] demonstrated the excellent antibacterial activity of chitosan against three species of gram-negative bacteria, although to a different extent. This difference can be attributed to the different molecular weight of chitosan and the characteristics of the bacterial species. Chitosan's antibacterial activity is related to the surface characteristics of the cell wall and increases in proportion with increasing hydrophilicity or a negative charge of the cell surface. Chitosan increases the permeability of the outer membrane and disrupts bacterial cells membranes. Interactions between $-NH_3$ in chitosan and −C=O or −P=O groups in *Escherichia coli* were analysed by FTIR.

Several studies have found a higher antibacterial activity of chitosan compared with chitosan oligomers. Sekiguchi et al. [9.7] investigated the antibacterial activities of chitosan oligomers of a molecular weight from 2.35 to 21.6 kDa against various bacteria [9.7]. The growth of *Bacillus cereus* on agar plates was suppressed by 0.2%−0.3% chitosan oligomer with a $\bar{M}_w$ of 11 kDa. Uchida et al. [9.8] reported that chitosan oligomer II, which is a mixture of triose and tetraose, failed to display antibacterial activity against *Escherichia coli* at a concentration of 0.5 g/100 mL, while chitosan oligomer I, which is a mixture of tetraose and heptose, possessed antibacterial activity [9.8].

Chitosan's antimicrobial action is influenced by intrinsic and extrinsic factors, for example, by the type of chitosan, its degree of polymerization, the host nutrient constituency, the substrate chemical and/or nutrient composition and the substrate water activity [9.9]. The inactivation and growth inhibition of mould and yeasts seems to depend on the concentration of the chitosan and the pH and temperature of the media [9.10].

A higher temperature and a lower pH of food increased the bactericidal effect of chitosan prepared from shrimp against *Escherichia coli*. This effect might be explained by the changed permeability of the membrane, induced by crosslink formation between polycations of chitosan and anions on the bacterial surface [9.11].

The DD of chitosan plays also a very important role in antibacterial activity. When the antimicrobial activity of chitosans with different DD was investigated against three gram-negative bacteria and five gram-positive bacteria, it was found that the 75% deacetylated chitosan showed more effective antimicrobial activity compared with that of 90% and 50% deacetylated chitosan [9.12].

An increase in the positive charge of chitosan resulted in stronger binding to the bacterial cell walls [9.13]. The relationship between antimicrobial activity, number of charges and $\bar{M}_w$ has been studied. It was shown that degraded chitosan was more effective than plain chitosan, which was attributed to the interaction of the −COOH group with the NH_2 group [9.14].

The concentration of chitosan also plays a very important role in antibacterial activity. It was observed that the antibacterial activity of chitosan increased in proportion with the concentration of chitosan, the minimum inhibitory concentration being 0.005 g/L for both *Escherichia coli* and for *Bacillus subtilis*, for the initial bioburden of DO = 0.08 at λ = 625 nm [9.15].

It was reported that when PVA blend was prepared with chitosan (471 kDa), the diameter of inhibition zone for *Escherichia coli* and *Bacillus subtilis* did not change when the concentration of chitosan (0.05%−1%) in the blend was increased. This may suggest that the release of chitosan is governed by its molecular weight, independently of its concentration. Indeed, when chitosan of a molecular weight of 101 kDa replaced chitosan of a molecular weight of 471 kDa in the blend, with an increase of chitosan concentration from 0.25% to 1%, the diameter of inhibition zones also increased. The amount of released chitosan increased with the increase of its concentration in the blend, owing to its low molecular weight [9.1]. Several mechanisms have been suggested as the cause of the inhibition of bacteria cells by chitosan. The first proposed mechanism is that the interaction with anionic groups on the cell surface, because of its polycationic nature, causes the formation of an impermeable layer around the cell, which prevents the transport of essential solutes. It has been demonstrated by electron microscopy that the site of action is the outer membrane of gram-negative bacteria. The permeabilizing effect has been observed at slightly acidic conditions in which chitosan is protonated [9.16]. The second proposed mechanism involves the inhibition of the RNA and protein synthesis by permeation into the cell nucleus [9.17].

Other mechanisms have also been proposed. Chitosan may inhibit bacterial growth by acting as a chelating agent rendering metals, essential nutrients or trace elements unavailable for the organism to grow at its normal rate. Chitosan is able to interact with flocculate proteins, but this action is highly pH dependent [9.18]. The antimicrobial action of chitosan against filamentous fungi could be explained by a more direct disturbance of membrane function [9.19]. However, it is not clear whether the antimicrobial activity of chitosan is caused by growth inhibition or cell death.

9.3. ANTIMICROBIAL ACTIVITY OF LOW-MOLECULAR-WEIGHT CHITOSAN FOR USE ON PLANTS

It has been reported that foliar spraying with chitosan can control infection caused by fungal, bacterial and viral pathogens on plants [9.20]. In addition to the direct effect of antimicrobial activity, chitosan induces a series of defence reactions correlating with the activation of the immune system. It has also been

recognized in many studies that the antimicrobial activity of chitosan depends on its molecular weight ($\overline{M}_w$), DD, pH of medium, concentration and of course, the strains of the microbes [9.21–9.30]. The radiation degradation of chitosan can cause enhancement of antifungal and antimicrobial activity [9.25, 9.26, 9.29]. Table 9.1 shows the inhibition effect of chitosan and irradiated chitosan on the growth of various fungi [9.25]. The same results were also obtained by Matsuhashi and Kume [9.24] and Liu et al. [9.26]. Their studies showed that low-molecular-weight chitosan ($\overline{M}_w \sim 100\ 000$) has good antibacterial activity.

TABLE 9.1. INHIBITION EFFECT OF CHITOSAN AND IRRADIATED CHITOSAN ON GROWTH OF VARIOUS FUNGI

Fungi	Minimum inhibiting concentration (μg/mL) of chitosan for suppression of fungi		
	Non-irradiated	Irradiated[a]	Enhancement ratio (%)
Phytophthora cactorum	300	250	16.7
Fusarium oxysporum	1150	800	30.4
Aspergillus awamori	400	250	37.5
Exobasidium vexans	1000	550	45.0
Septoria chrysanthemum	700	350	50.0
Gibberella fujikuroi	400	250	37.5
Septobasidium theae	1450	1000	31.0
Colletotrichum sp.	1500	1050	30.0

[a] Chitosan irradiated at 75 kGy in powder form.

Ben-Shalom et al. [9.29] investigated whether grey mould caused by *Botrytis cinerea* could be controlled in cucumber plants by foliar spraying with 0.1% chitosan before and after inoculation. The results revealed that spraying on leaves 1 h after inoculation induced less control of the disease (48%) than spraying before inoculation (35%). By foliar spraying of irradiated chitosan, the blast disease index was reduced remarkably (see Fig. 9.1).

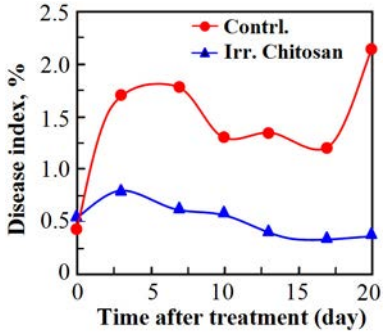

FIG. 9.1. Effect of foliar spraying of irradiated chitosan for suppression of disease on rice.

There are few published references related to the effect of chitosan on yield, but some studies reported that pre-harvest application of chitosan solutions increased yield at harvest [9.30–9.33]. An increase of tomato yield was correlated with the concentration of chitosan applied to soil inoculated with *Fusarium oxysporum* before transplanting seedlings [9.31]. The yield of rice and soybeans increased remarkably (20–40%) upon foliar spraying with chitosan solution [9.32–9.34].

Based on the results of antimicrobial activity, it can be concluded that chitosan has potential as a natural agent for controlling plant diseases. A commercial fungicide product made from irradiated chitosan (Gold Rice) in Viet Nam is shown in Fig. 9.2.

FIG. 9.2. Commercial fungicide product made from irradiated chitosan (Gold Rice) in Viet Nam.

9.4. EFFECTS OF OLIGOCHITOSAN ON RICE

One of the most important defences of plant tissues against disease infection is their ability to produce phytoalexin which is an antibiotic synthesized in response to pathogens or elicitors. At an effective concentration, phytoalexins can slow phytopathogen growth and development. Phytoalexins in rice leaves, momilactones, were first reported by Cartwright et al. [9.35]. The study of Agrawal et al. also indicated that after 72 h of treatment with chitosan, momilactone-A in rice leaves increased to values higher than 10 000 ng/50 mg fresh weight (FW) (Fig. 9.3) [9.36].

Rodiguez et al. [9.37] investigated whether the treatment of rice seed, *Oryza sativa* L., with chitosan and hydrolysed chitosan induced a defensive response against *Pyricularia grisea*, the fungus that causes rice blast [9.37]. They found that plants grown from seeds treated with chitosan and hydrolysed chitosan (oligochitosan) were more resistant to blast disease compared with non-treated plants (positive control). A similar study in China was reported in Ref. [9.38] and is summarized in Table 9.2.

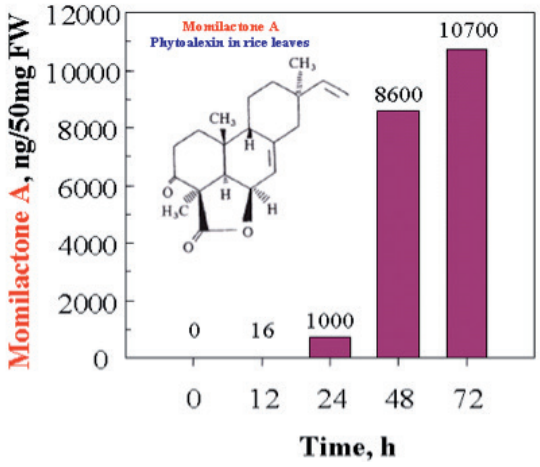

FIG. 9.3. Phytoalexin momilactone A content in rice leaves treated with chitosan.

TABLE 9.2. THE EFFECT OF OLIGOCHITOSAN ON PLANT DISEASE CONTROL [9.38]

Plants	Plant diseases	Control rates (%)
Tobacco	Tobacco mosaic virus, potato virus	76.49–87.5
Panax notoginseng	Viral disease	>90
Tulip	*Peronospora*	84.24–88.6
Piper nigrum L.	Mosaic virus	74.54–81.3
Tomato	Solani, infestans, viral disease, bacterial wilt	84.47–88.24
Cucumber	*Peronospora*	78.96–82.65
Pepper	Viral diseases, blight, anthracnose, pepper phytophthora blight	78.58–90
Aubergine	Viral diseases	94.18–100
Chinese cabbage	Erwinia carotovora subsp.	78.62–85
Asparagus lettuce	*Peronospora*	45.80–62.3
Wax gourd	Blight	84.81–95
Cauliflower	Blackrot	64.60–64.2
Green cucumber	Blight	45.50–57.6
Cowpea	Viral diseases	31.13–58.8
Papaya	Mosaic virus	70.00–96
Watermelon	Blackrot, *Didymella bryoniae*, blight, viral diseases	81.71–85.40
Muskmelon	Powdery mildew	71.34–86.26
Banana	Banana bunchy top virus	84.70–94.6
Apple	Mosaic virus, *Venturia inaequalis*	76.68–94.85
Soybean	Viral diseases	75.10–100
Cotton plant	Cotton yellow wilt	85.50–87.2
Maize	*Sphacelotheca Reiliana*, corn northern leaf blight, corn southern leaf blight	24.90–45.35
Rice	Rice blast	71.41–92.0
Peanut	Viral diseases	24.90–26.5

9.5. SURVIVAL RATIO OF PLANTLETS TREATED WITH IRRADIATED ALGINATE

Studies have concluded that, in plant cells, oligosaccharides can be considered signalling chemicals inducing phytoalexins that protect plants from fungal infection [9.39–9.41]. Furthermore, degraded alginate has exhibited not only a remarkable growth promotion effect but also a protection effect for plants [9.42]. In the study described in Ref. [9.42], the survival ratio of all chrysanthemum, lisianthus and limonium plantlets treated with irradiated alginate was investigated after 30 days' acclimatization in greenhouse conditions. The results in Table 9.3 show that there is no significant effect on the survival ratio of the treated and untreated plantlets.

However, it can be seen from Fig. 9.4 that the treated plantlets show better growth compared with the untreated control. These results suggest that the plantlets treated with irradiated alginate show a better response to environmental influence during acclimatization in a greenhouse. Degraded alginate was reported to increase the activity of phytoalexin enzymes such as chitinase [9.43].

TABLE 9.3. THE SURVIVAL RATIO OF PLANTLETS TREATED WITH IRRADIATED ALGINATE AFTER 30 DAYS' ACCLIMATIZATION IN A GREENHOUSE

Absorbed dose (kGy)	$\bar{M}_w \times 10^3$	Plant survival (%)		
		Chrysanthemum	Lisianthus	Limonium
Control	n.a.	84.3	81.4	87.1
0	904.9	79.9	75.1	84.0
10	97.2	84.6	76.8	92.1
30	34.9	75.5	77.1	92.6
50	20.5	87.0	84.8	92.5
75	14.2	98.7	86.0	91.9
100	10.9	89.9	86.3	91.9
150	7.9	81.8	85.2	92.5
200	5.7	78.6	80.2	91.6

FIG. 9.4. Growth of transferred flower plantlets treated with irradiated alginate after 30 days' acclimatization in a greenhouse; (a) chrysanthemum, (b) lisianthus and (c) limonium.

9.6. THE ANTIOXIDANT PROPERTIES OF OLIGO NaAlgs

In recent years there has also been considerable interest in the identification of antioxidant properties of different type of oligosaccharides [9.44–9.46]. These include κ carrageenan [9.47], NaAlg [9.48], chitosan [9.49–9.50], carboxymethylchitosans [9.51], fucoidan and laminarin [9.52], guar and LBG [9.48].

In Refs [9.53–9.55] there is general agreement that there is a strong relationship between the molecular weight of polysaccharides and their antioxidant properties. Reference [9.56] is the only example in the literature suggesting a relationship between the molecular weight and the structural properties of a polysaccharide and its antioxidant properties. This study [9.56] investigated a NaAlg fraction with a molecular weight of 12–35 kDa with various G to M ratios. The NaAlg samples were irradiated in the solid state with gamma rays in air at ambient temperature at low dose rates. Molecular weight changes were monitored by GPC and the variation in their antioxidant properties was characterized by scavenging activity for 1,1-diphenyl-2-picrylhydrazyl free radicals (DPPH). The effect of absorbed dose this scavenging efficacy of NaAlg is shown in Fig. 9.5. Additionally, the number-average molecular weight of the NaAlg fractions was plotted against their DPPH scavenging activity (Fig. 9.6).

The evaluation of the relationship between the structural and antioxidant properties of NaAlgs showed that its antioxidant activity was independent

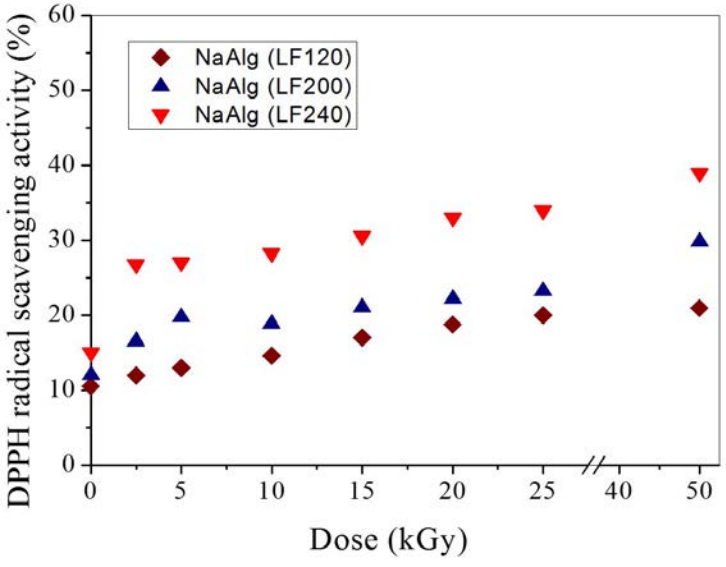

FIG. 9.5. Effect of absorbed dose on the DPPH scavenging activity of NaAlgs.

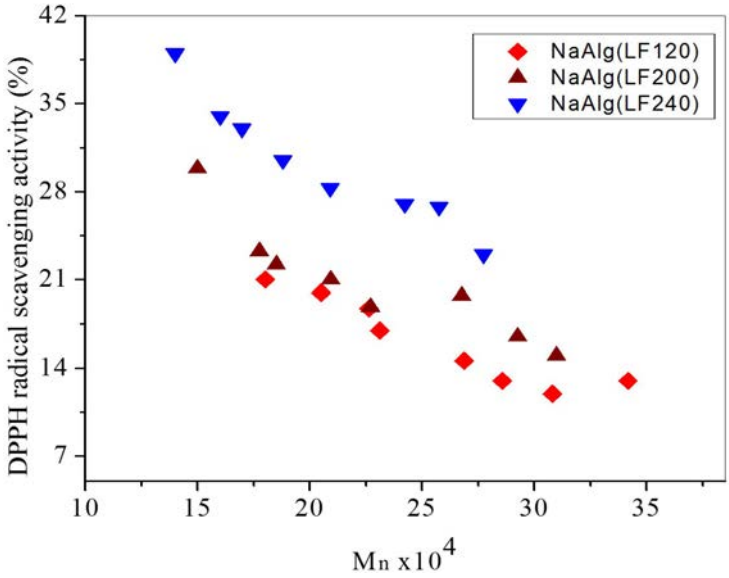

FIG. 9.6. Effect of the molecular weight and G/M of NaAlg on its DPPH scavenging activity.

of its molecular weight whereas the G/M appeared to be an important factor determining the DPPH scavenging activity of NaAlg of 12–35 kDa molecular weight.

Reference [9.57] investigated the radiation induced degradation of NaAlg with different guluronic to mannuronic acid ratios. The scavenging efficacy of the unirradiated and the dry state irradiated LF240 NaAlg was compared with LF240 NaAlg irradiated in aqueous solution in the presence of H_2O_2. As seen in Fig. 9.7, the antioxidant behaviour of NaAlg could be easily controlled by changing the irradiation medium, and 100% of the radicals (0.1 mM/mL) could be removed using only 10 mg of NaAlg. The IC_{50} values of the oligosaccharides prepared in solution by 2.5 kGy irradiation were higher than 10 mg/mL, and this value reduced to 3 mg/mL for the fractions prepared in the presence of H_2O_2.

In order to investigate the effects of the G/M of NaAlgs on their antioxidant properties, the number-average molecular weight of the fractions was plotted against their DPPH radical scavenging activity (Fig. 9.8). Figure 9.8 clearly shows that for the fractions with molecular weights below 12 kDa, the G/M was not a significant factor in controlling the antioxidant behaviour of NaAlgs. The main factor in controlling the antioxidant behaviour of the oligo NaAlgs was their molecular weight. The promotion of the antioxidant behaviour of chitosan with the decrease in molecular weight was attributed to two factors: (i) an increase in chain flexibility or a decrease in the compact structure, with radiation

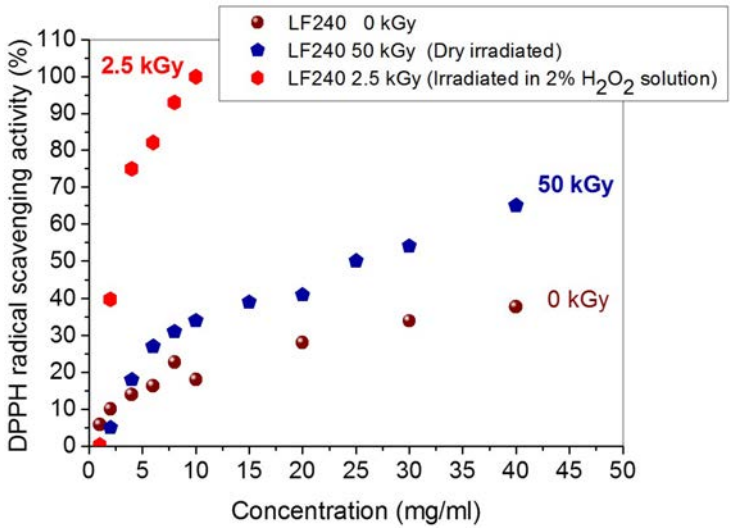

FIG. 9.7. Comparison of the scavenging efficacies of LF240 NaAlgs in the unirradiated state; after irradiation in the dry state, and after irradiation in solution in the presence of H_2O_2.

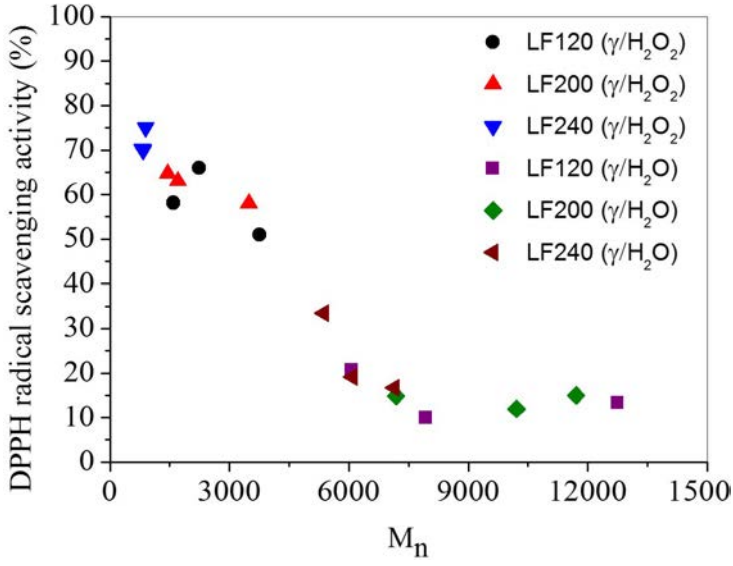

FIG. 9.8. Effects of molecular weight and G/M on the DPPH scavenging activity of NaAlgs.

inducing the degradation; (ii) the formation of more hydroxyl groups as a result of the cleavage of the glycosidic linkages in the skeletal structure [9.58] and formation of more carboxylic acid groups in the terminal mannuronic acid due to the reduction with H_2O_2 [9.59]. It is well known that these groups are the main groups controlling the antioxidant behaviour of polysaccharides.

It was concluded that the radical scavenging efficacy of NaAlgs is dependent on the structure (G/M) of the sample between the molecular weight range of 12–35 kDa, and followed the order LF240>LF200>LF120 or 70/30<50/50<45/55; the decrease in the radical scavenging efficacy with the type of NaAlg was previously attributed to the decrease in the G content [9.56].

On the other hand, as observed in this present study, below a molecular weight of approximately 12 kDa, the only parameter controlling the radical scavenging efficacy was the molecular weight, not the G/M. The independence of the radical scavenging efficacy of NaAlg below 12 kDa from the initial G/M was probably due to the change in the chain conformation or the G content, which was a result of stiffness and of the extent of degradation in aqueous solutions.

9.7. ANTIOXIDANT ACTIVITY POTENTIAL OF GAMMA IRRADIATED CARRAGEENAN

Algal polysaccharides have been demonstrated to play an important role as free radical scavengers in vitro and to provide antioxidants for the prevention of oxidative damage in living organisms [9.60]. The activity of algal polysaccharides is dependent on their structure, indicated by values such as the DS, molecular weight, sulphation position, type of sugar and glycosidic branching [9.61]. Reference [9.62] states that phosphorylated and sulphated glucans show a higher antioxidant property than glucans and other neutral polysaccharides, suggesting that polyelectrolytes such as glucan sulphate (e.g. carrageenan) might display increased scavenging activity [9.62].

Very few studies on the antioxidant properties of oligosaccharides derived from algal polysaccharides are available. Moreover, the relationships between the molecular weight of oligosaccharides and their biological activity are hardly known. It has been demonstrated that the antioxidant activities of oligosaccharides such as chitosan and κ carrageenan improve with lower molecular weights [9.63–9.65]. These low-molecular-weight polysaccharides are produced by the degradation of the parent carrageenans by chemical or enzymatic hydrolysis. Recently, degradation by radiation processing has gained much attention due to its technological effectiveness in producing low-molecular-weight fragments.

Low-molecular-weight fragments from gamma irradiated seaweed polysaccharides show enhanced antioxidant properties [9.52]. In a recent study [9.66],

κ, ι, and λ carrageenan polysaccharides were subjected to degradation by gamma irradiation and the relationship between the low-molecular-weight oligosaccahrides of different structural types, and their antioxidant activities were evaluated. The antioxidant properties of oligo κ, ι and λ carrageenans were determined by evaluating their hydroxyl radical scavenging activity, reducing power and DPPH radical scavenging capacity [9.66].

The hydroxyl radical scavenging assay is based on the degradation of deoxyribose by hydroxyl radicals generated by Fenton's reaction. The degraded products, when heated with thiobarbituric acid at an acidic pH, form a pink chromogen, the abundance of which can be measured at 532 nm. If another molecule that can react with hydroxyl radicals is added to the mixture, it will compete with deoxyribose for $HO^{\bullet}$ and thereby decrease the rate of deoxyribose degradation.

Figure 9.9 shows the scavenging effect of irradiated κ carrageenan on hydroxyl radicals. It shows that the potential of aqueous κ carrageenan to scavenge hydroxyl radicals increased with increasing concentration and radiation dose. However, at lower doses (5–10 kGy), the scavenging effects of aqueous κ carrageenan were not significantly different from one another. Likewise, solid κ carrageenan irradiated at 100 kGy showed OH radical scavenging effects comparable with those of aqueous κ carrageenan irradiated at these doses. Irradiated carrageenan at all doses exhibited a lower OH radical scavenging effect

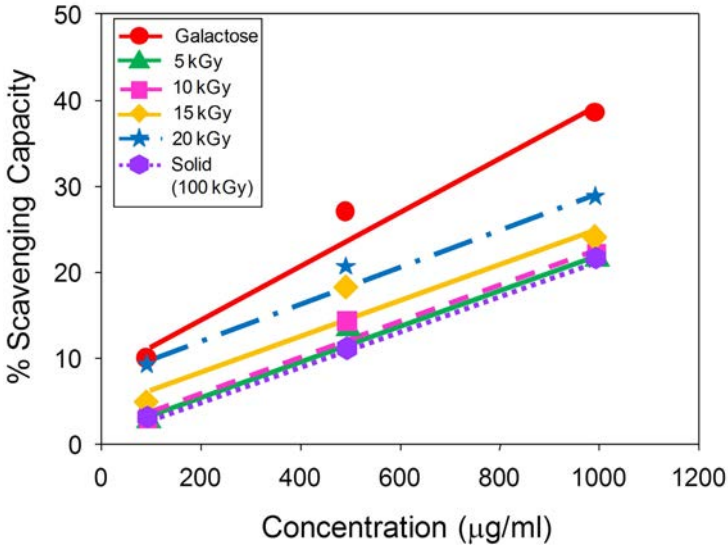

FIG. 9.9. Hydroxyl radical scavenging effect of irradiated κ carrageenan at different doses with increasing concentration.

than the reducing sugar galactose. This might be explained by the irradiation induced degradation of κ carrageenan [9.67]. Higher degradation is expected in an aqueous medium owing to the indirect effect of water radiolysis, and therefore a lower scavenging effect is observed in solid κ carrageenan irradiated at 100 kGy. Table 9.4 confirms this trend of increases in reducing sugar with increasing dose in κ carrageenan, with irradiated solid κ carrageenan having the lowest amount of reducing sugar. On the basis of these results, the source of the OH radical scavenging activity of irradiated κ carrageenan could come from its reducing end.

This result may also be caused by intramolecular and intermolecular hydrogen bonds of low-molecular-weight κ carrageenan, which become weaker than those of the high-molecular-weight ones. The weakening of the intramolecular hydrogen bonds can make the free hydroxyl in the polymer chain susceptible to attack by hydroxyl radicals [9.68].

The reducing power assay method is based on the principle that substances that have reduction potential react with potassium ferricyanide (Fe^{3+}) to form potassium ferrocyanide (Fe^{2+}), which then reacts with ferric chloride to form a ferric ferrous complex that has an absorption maximum at 700 nm [9.69]. It has been reported by some researchers that antioxidant effect is concomitant with the development of reducing power [9.70]. Reducing properties are generally associated with the presence of reductones. These break the free radical chain by hydrogen atom donation. Additionally, they also react with certain precursors of peroxide, thus preventing its formation [9.71]. In this assay, the yellow colour of

TABLE 9.4. REDUCING SUGAR CONTENT OF IRRADIATED CARRAGEENANS AT DIFFERENT DOSES

Dose (kGy)	% Reducing sugar			
	1% aqueous κ	1% aqueous ι	1% aqueous λ	Solid κ
5	4.9	4.1	2.5	—
10	6.1	4.2	4.3	—
15	6.7	6.3	5.0	—
20	8.3	6.9	6.7	—
100	—	—	—	2.1

the test solution changes to various shades of green and blue, depending upon the reducing power of each sample.

Figure 9.10 shows the reducing power of κ carrageenan at different doses with respect to a known antioxidant — ascorbic acid. The reductive potential of the κ carrageenan increased proportionally to oligomeric concentration and dose. It was found to reach a maximum at 50 kGy within the dose range investigated. The reducing capacity of κ carrageenan was low compared with ascorbic acid.

The efficacy of κ carrageenan irradiated at 50 kGy was 40 times lower than ascorbic acid. This corresponds to a concentration of 1 000 μg/mL and 2 000 μg/mL κ carrageenan for every 25 and 50 μg/mL of ascorbic acid, respectively.

Figure 9.11 shows the reducing power of oligosaccharides from irradiated κ, ι and λ carrageenan with increasing concentration. Aqueous κ carrageenan, as could be expected, had a higher reducing power than solid κ carrageenan irradiated at 100 kGy. The reducing power of the different carrageenan oligosaccharides increased as follows: κ>ι>λ. This order has a similar trend to that of the amount of reducing sugar produced from the different carrageenans. κ carrageenan, followed by ι carrageenan, generally had higher reducing sugar (Table 9.4) than

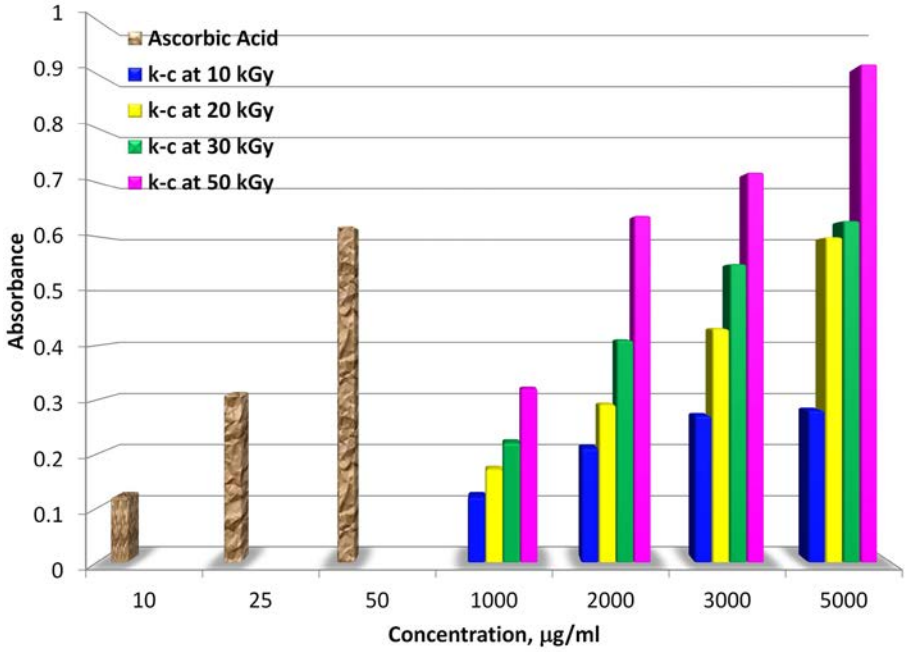

FIG. 9.10. Reducing power of κ carrageenan (κC) at different doses with increasing concentration.

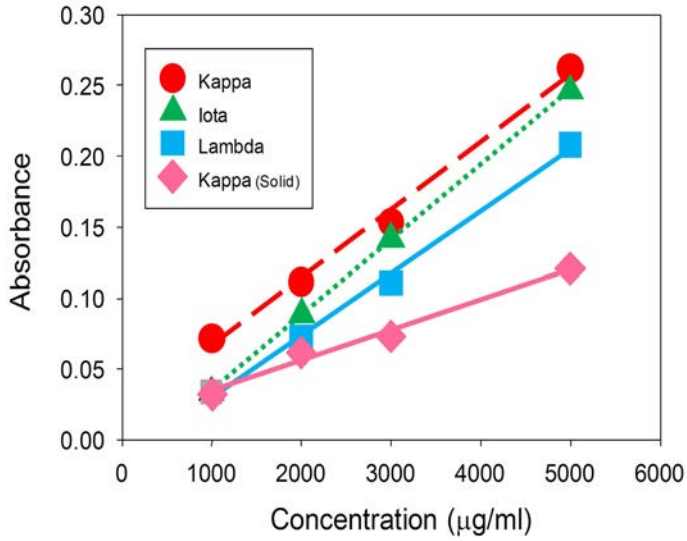

FIG. 9.11. Reducing power of irradiated κ, ι and λ carrageenan (5 kGy) with increasing concentration.

λ carrageenan. At increasing concentrations, however, the reducing power of κ carrageenan tended to approach the values of ι carrageenan. This would imply that the reducing sugar is not the only causal factor in increasing the reducing power of carrageenans. It is likely that the amount of sulphates may also play a role in the reducing power of carrageenan; κ carrageenan has only one sulphate compared with ι and λ carrageenan, which have two and three, respectively.

Figure 9.12 shows the reducing power of κ, ι and λ carrageenan irradiated at different doses. At lower doses (<10 kGy), κ carrageenan had higher reducing capacities that the other two carrageenans. However, beyond a dose of 10 kGy, its reductive potential tended to be lower than ι and λ. This again is in accordance with the values of reducing sugar, although the amount of reducing sugar in κ carrageenan leveled off at 10 kGy. In addition, cleavage of the sulphate group is expected with dose [9.72]. Thus, decrease in reducing power ability is more pronounced at higher doses.

These results indicate the dependence of the reducing power of the carrageenans with their reducing sugar. The reducing capacity is generally associated with the presence of reducing sugars and might be due to hydrogen-donating ability [9.73]. A similar study conducted on irradiated chitosan also shows increasing reductive capacity with increasing dose [9.74]. In addition, these results also suggest that degree of sulphation may influence the reducing power of carrageenans.

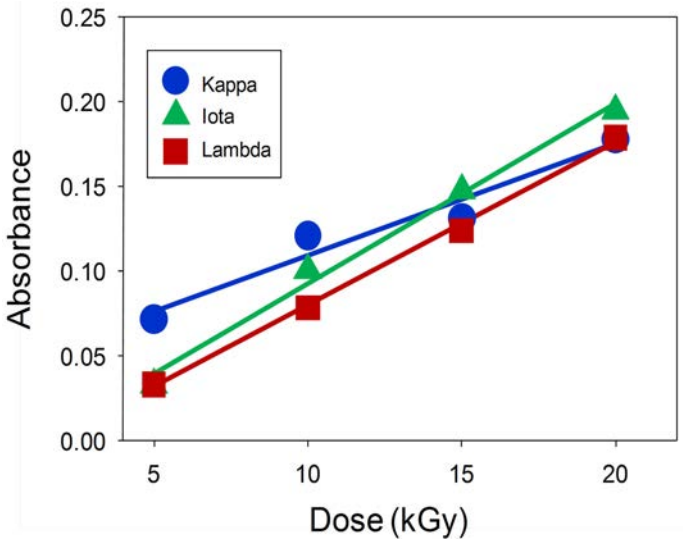

FIG. 9.12. Reducing power of irradiated κ, ι and λ carrageenan (500 μg) as a function of dose.

The DPPH radical is a stable radical that can readily undergo reduction by an antioxidant, AH, which can be demonstrated by the following reaction:

$$DPPH + AH \rightarrow DPPH - H + A$$

It has been reported that the radical scavenging activity of seaweeds is mostly related to their phenolic or polyphenolic contents. Aside from phenolic groups, the presence of other functional groups in the whole molecule, such as double bonds, and their conjugation to –OH groups and ketonic groups (as in the case of ascorbic acid) also play an important role in their antioxidant properties. If two active hydroxyl groups are present in the polymer chains, this may affect the scavenging ability of carrageenan via the typical H-abstraction reaction with free radicals [9.75]. Low-molecular-weight polysaccharides have also an influence on antioxidant activity [9.74], which can be attributed to their reducing sugar content. The DPPH radical scavenging capacity of irradiated κ carrageenan is shown in Fig. 9.13. The curves indicated an increasing trend with increasing concentration as well as with increasing dose. At higher doses of 15 and 20 kGy, its radical scavenging effect reached saturation at concentrations of 1500 and 1000 μg/mL, respectively.

Figure 9.14 shows the DPPH radical scavenging capacity of the different types of carrageenans as a function of dose. Similar to the results on the reducing power and OH radical scavenging capacity of irradiated aqueous carrageenan, it

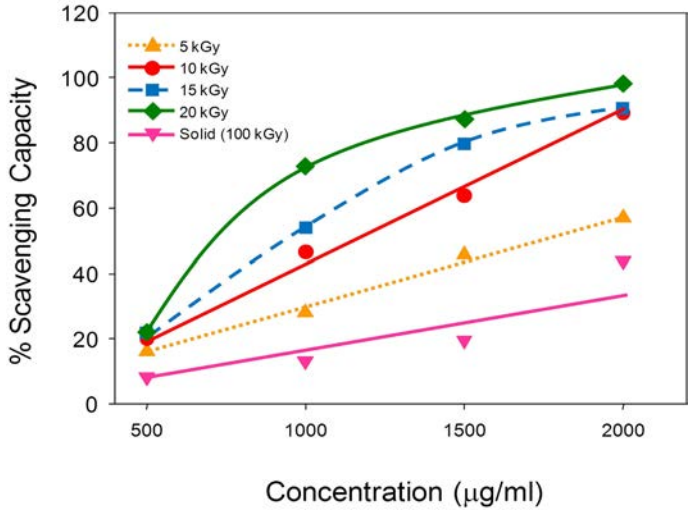

FIG. 9.13. DPPH radical scavenging capacity of aqueous κ carrageenan at different doses with increasing concentration.

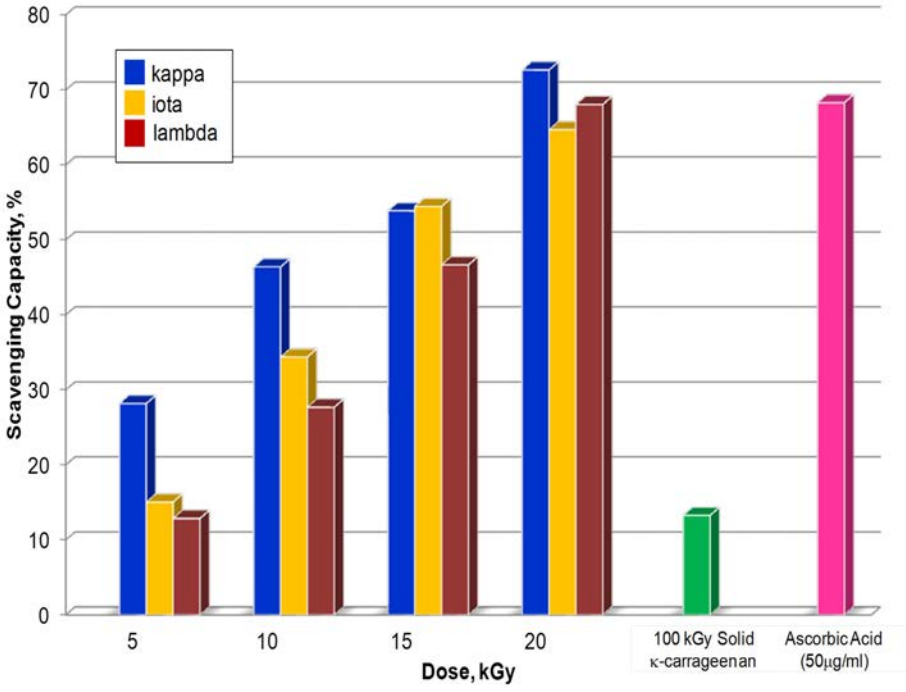

FIG. 9.14. DPPH radical scavenging capacity of carrageenans (500 μg) at different doses.

had higher radical scavenging capacity than that of solid carrageenan irradiated at 100 kGy. This again is mainly due to the amount of reducing sugar generated by irradiation. Carrageenan solutions irradiated at 20 kGy had a DPPH radical scavenging capacity approximately ten times lower than that of ascorbic acid. Its scavenging capacity increased in the order of λ<ι<κ at doses of 5–10 kGy, which is comparable to the results of the reducing power capacity. Reference [9.76] reports that sulphated polysaccharides from red and brown algae display scavenging action, with and λ carrageenan being more effective than κ and ι carrageenans [9.76]. However, current results find that the scavenging capacity of carrageenans increases in the following order: λ<κ/ι<κ/β<κ<iks[1] [9.77]. This indicates that sulphation degree is not the only parameter responsible for this property.

Unlike the results on the reducing power of κ carrageenan showing that beyond a dose of 10 kGy, its reductive potential tended to be lower than ι and λ, the increase in DPPH radical scavenging capacity proportional to concentration was not affected by dose. Thus, it can be assumed that the degree of sulphation, as explained earlier, does not affect DPPH radical scavenging capacity in carrageenans. A related study [9.72] also indicates that the scavenging capacities of different carrageenans strongly depends on their concentration, and structure of a sample, e.g. the degree of sulphation, is not considered an important factor for this action. Aside from the formation of reducing ends, irradiation can promote the formation of double bonds and ketonic groups in κ carrageenan that could possibly explain its consistency in increasing DPPH radical scavenging activity with dose.

To summarize, carrageenan oligomers obtained by gamma irradiation exhibited antioxidant properties as determined by hydroxyl radical scavenging activity, reducing power and DPPH radical scavenging capacity assay. The type of carrageenan has also an influence on its antioxidant activity, which follows the order λ<ι<κ. The degree of sulphation and the cleavage of sulphate groups with irradiation have also an influence on the reducing power of the carrageenan oligomers. These results may be useful in looking for an effective, non-toxic bioactive substance that could play an important role as a free radical scavenger for preventive medicine applications.

[1] This is a new type of carrageenan, iks carrageenan, which is not discussed elsewhere in this publication.

REFERENCES TO CHAPTER 9

[9.1] TAHTAT, D., et al., Influence of some factors affecting antibacterial activity of PVA/chitosan based hydrogels synthesized by gamma irradiation, J. Mat. Sci.: Mat. Med. **22** (2011) 2505–2512.

[9.2] MUZZARELLI, R., et al., Antimicrobial properties of N-carboxylbutyl chitosan, Antimicrob. Agents Chemother. **34** (1990) 2019–2023.

[9.3] QIN, C., et al., Water-solubility of chitosan and its antimicrobial activity, Polym. Degrad. Stab. **63** (2006) 367–374.

[9.4] LIU, N., et al., Effect of MW and concentration of chitosan on antimicrobial activity of *Escherchia coli*, Carbohydr. Polym. **64** (2006) 60–65.

[9.5] LAM, N.D., DIEP, T.B., A preliminary study on radiation treatment of chitosan for enhancement of antifungal activity tested fruit-spoiling strains, Nucl. Sci. Technol. **2** (2003) 54–60.

[9.6] LI, X.F., FENG, X.Q., YANG, S.A., A mechanism of antibacterial activity of chitosan against Gram-negative bacteria, Food Sci. **31** (2010) 148–151.

[9.7] SEKIGUCHI, S., et al., "Molecular weight dependency of antimicrobial activity by chitosan oligomers", Food Hydrocolloids: Structures, Properties, and Functions (NISHINARI, K., DOI, E., Eds), Springer, New York, (1993) 71–75.

[9.8] UCHIDA, Y., IZUME M., OHTAKARA, A., "Preparation of chitosan oligomers with purified chitosanase and its application", Chitin and Chitosan (BRAEK, G.S., ANTHONSEN, T., SANDFORD, P., Eds), Elsevier, London (1989) 373–382.

[9.9] CUERO, R.G., Antimicrobial action of exogenous chitosan, EXS **87** (1999) 315–333.

[9.10] ROUT, S.K. Physicochemical, Functional, and Spectroscopic Analysis of Crawfish Chitin and Chitosan as Affected by Process Modification, MS Thesis, Seoul Nat. Univ. (2001).

[9.11] TSAI, G.J., SU, W.H., Antibacterial activity of shrimp chitosan against *Escherichia coli*, J. Food Protect. **62** (1999) 239–243.

[9.12] PARK, P.J., JE, J.Y., BYUN, H.G., MOON, S.H., KIM, S.K., Antimicrobial activity of hetero-chitosans and their oligosaccharides with different molecular weights, J. Micro. Biotech. **14** (2004) 317–323.

[9.13] GERASIMENKO, D.V., AVDIENKO, I.D., BANNIKOVA, G.E., ZUEVA, O.Y., VARLAMOV, V.P., Antibacterial effects of water-soluble low molecular-weight chitosans on different microorganisms, Appl. Biochem. Microbiol. **40** (2004) 254–261.

[9.14] KIM, K.W., THOMAS, R.L., LEE, C., PARK, H.J., Antimicrobial activity of native chitosan, degraded chitosan, and O-carboxymethylated chitosan, J. Food Protect. **66** (2003) 1495–1498.

[9.15] LATRECHE, N., BENAMEUR, M., Etude de l'effet du poids moléculaire du chitosane, incorporé dans un hydrogel à base de PVA radio-synthétisé, sur l'activité antibactérienne, Mémoire de fin d'études en vue de l'obtention du diplômed'ingénieur d'état en Biologie, Univ. Sci. Technol. Houari Boumediene, Bab Ezzouar, Algiers (2009).

[9.16] HELANDER, I.M., NURMIAHO-LASSILA, E.L., AHVENAINEN, R., RHOADES, J., ROLLER, S., Chitosan disrupts the barrier properties of the outer membrane of Gram-negative bacteria, Int. J. Food Microbiol. **71** (2001) 235–244.

[9.17] LIU, X., YUN, L., DONG, Z., ZHI, L., KANG, D., Antibacterial action of chitosan and carboxymethylated chitosan, J. Appl. Polym. Sci. **79** (2001) 1324–1334.

[9.18] ROLLER, S., COVILL, N., The antifungal properties of chitosan in laboratory media and apple juice, Int. J. Food Microbiol. **47** (1999) 67–77.

[9.19] FANG, S.W., LI, C.F., SHIH, D.Y.C., Antifungal activity of chitosan and its preservative effect on low-sugar candied kumquat, J. Food Protec. **57** (1994) 136–140.

[9.20] POSPIESZNY, H., CHIRKOV, S., ATABEKOV, J., Induction of antiviral resistance in plant by chitosan, Plant Sci. **79** (1991) 63–68.

[9.21] LIU, N., et al., Effect of MW and concentration of chitosan on antibacterial activity of *Escherichia coli*, Carbohydr. Polym. **64** (2006) 60–65.

[9.22] ZHENG, L.Y., ZHU, J.F., Study on antimicrobial activity of chitosan with different molecular weights, Carbohydr. Polym. **54** (2003) 527–530.

[9.23] JEON, Y., PARK, P., KIM, S., Antimicrobial effect of chitooligosaccharides produced by bioreactor, Carbohydr. Polym. **44** (2001) 71–76.

[9.24] MATSUHASHI, S., KUME, T., Enhancement of antimicrobial activity of chitosan by irradiation, J. Sci. Food Agric. **73** (1997) 237–241.

[9.25] HIEN, N.Q., "Radiation degradation of chitosan and some biological effects", Radiation Processing of Polysaccharides, IAEA-TECDOC-1422, IAEA, Vienna, (2004) 67–73.

[9.26] LIU, X.F., GUAN, Y.L., YANG, D.Z., LI, Z., YAO, K.D., Antibacterial action of chitosan and carboxymethylated chitosan, J. Appl. Polym. Sci. **79**, (2001) 1324–1335.

[9.27] BHASKARA REDDY, M.V., BELKACEMI, K., CORCUFF, R., CASTAIGNE, F., ARUL, J., Effect of pre-harvest chitosan sprays on post-harvest infection by *Botrytis cinerea* and quality of strawberry fruit, Postharvest Biol. Techn. **20** (2000) 39–51.

[9.28] XU, J., ZHAO, X., HAN, X., DU, Y., Antimicrobial activity of oligochitosan against *Phytophthora capsici* and other plant pathogenic fungi in vitro, Pesticide Biochem. Phys. **87** (2007) 220–228.

[9.29] BEN-SHALOM, N., ARDI, R., PINTO, R., AKI, C., FALLIK, E., Controlling grey mound caused by *Botrytis cinerea* in cucumber plants by means of chitosan, Crop Protect. **22** (2003) 285–290.

[9.30] LAFONTENE, P.J., BEHAMOU, N., Chitosan treatment: an emerging strategy for enhancing resistance of greenhouse tomato plants to infection by *Fusarium oxysporum f. sp. Radicis-lycopersici*, Biocontrol Sci. Tech. **6** (1996) 111–124.

[9.31] CHANDRKRACHANG, S., "The application of chitin and chitosan in agriculture in Thailand", Advances in Chitin Science, Vol. 5 (SUCHIVA, K., CHANDRKRACHANG, S., METHACANON, P., PETER, M.G., Eds), National Metal and Materials Technology Center, Bangkok (2002) 458–462.

[9.32] DZUNG, N.A., THANG, N.T., "Effect of oligoglucosamine prepared by enzyme degradation on the growth of soybean", Advances in Chitin Science, Vol. 5 (SUCHIVA, K., CHANDRKRACHANG, S., METHACANON, P., PETER, M.G., Eds), National Metal and Materials Technology Center, Bangkok (2002) 463–467.

[9.33] ANGELOVA, Z., GEORGIEV, S., ROOS, W., Elicitation of plants, Biotechnol. Eq. **20** 2 (2006) 72–82.
[9.34] KEEN, N.T., Specific elicitors of plant phytoalexin production: Determinants of race specificity in pathogens, Sci. **187** (1975) 74–75.
[9.35] CARTWRIGHT, D., LANGCAKE, P., PRYCE, R.J., LEWORTHY, D.P., RIDE, J.P., Chemical activation of host mechanisms as a basis for crop protection, Nat. **27** (1977) 511–513.
[9.36] AGRAWAL, G.K., et al., Chitosan activates defense/stress response(s) in the leaves of *Oryza sativa* seedlings, Plant Physiol. Biochem. **40** (2002) 1061–1069.
[9.37] RODRIGUEZ, A.T., et al., Induction of defense response of *Oryza sativa* L. against *Pyricularia grisea* (Cooke) Sacc. by treating seeds with chitosan and hydrolyzed chitosan, Pest. Biochem. Physiol. **89** (2007) 206–215.
[9.38] YING, H., ZHAO, X., DU, Y., Oligochitosan: A plant diseases vaccine - A review, Carbohydr. Polym. **82** (2010) 1–8.
[9.39] KENDRA, A.F., HADWIGER, L.A., Characterization of smallest chitosan oligomer that maximally antifungal to *Fusarium solani* and elicits pisatin formation in *Pisum sativum*, Exper. Mycol. **8** (1984) 276–281.
[9.40] INUI, H., KOSAKI, H., UNO, Y., TABATA, K. HIRANO, S., Introduction of chitinase in rice callus treated with chitin derivatives, Agri. Bio. Chem. **55** (1991) 3107–3109.
[9.41] VASYOKOVA, N.I., et al., Modulation of plant resistance to diseases by water-soluble chitosan, Appl. Biochem. Microbiol. **37** (2001) 104–107.
[9.42] AOYAGI, H., et al., Promotion effect of alginate on chitinase production by *Wasabia japonica*, Biotech. Techn. **10** (1996) 649–654.
[9.43] YAMADA, A., SHIBUYA, N., KODAMA, O., AKATSUKA, T., Induction of Phytoalexin formation in suspension rice cells by N-acetylchitooligo saccharides, Biosci. Biotech. Bioch. **57** (1993) 405–409.
[9.44] SUN, L., WANG, C., SHI, Q., MA, C., Preparation of different molecular weight Polysaccharides from *Porphyridium cruentum* and their antioxidant activities, Int. J. Biol. Macromol. **45** (2009) 42–47.
[9.45] XING, R., et al., Relevance of molecular weight of chitosan and its derivatives and their antioxidant activities in vitro, Bioorgan. Med. Chem. **13** (2005) 1573–1577.
[9.46] XING, R., et al., Antioxidant activity of differently region selective chitosan sulfates in vitro, Bioorgan. Med. Chem. **13** (2005) 1387–1392.
[9.47] YUAN, H., et al., Preparation and in vitro antioxidant activity of κ-carrageenan oligosaccharides and their over sulfated, acetylated, and phosphorylated derivatives, Carbohydr. Res. **340** (2005) 685–692.
[9.48] TROMMER, H., NEUBERT, R.H.H., The examination of polysaccharides as potential antioxidative compounds for topical administration using a lipid model system, Int. J. Pharm. **298** (2005) 153–163.
[9.49] XIE, W., XU, P., LIU, Q., Antioxidant activity of water-soluble chitosan derivatives, Bio. Med. Chem. Lett. **11** (2001) 1699–1701.
[9.50] YEN, M.T., YANG, J.H., MAUC, J.L., Antioxidant properties of chitosan from crab shells, Carbohydr. Polym. **74** (2008) 840–844.

[9.51] SUN, T., ZHOU, D., MAO, F., ZHU, Y., Preparation of low-molecular weight Carboxymethyl chitosan and their superoxide anion scavenging activity, Eur. Polym. J. **43** (2007) 652–656.

[9.52] CHOI, J., et al., Application of gamma irradiation for the enhanced physiological properties of polysaccharides from seaweeds, Appl. Radiat. Isotopes **67** (2009) 1277–1281.

[9.53] SMIDSROD, O., GLOVER, R.M., WHITTINGTON, S.G., The relative extension of alginates having different chemical composition, Carbohydr. Res. **27** (1973) 107.

[9.54] KLOCK, G., et al., Production of purified alginates suitable for use in immune isolated transplantation, Appl. Microbiol. Biotech. **40** (1994) 638–643.

[9.55] SEN, M., RENDEVSKI, S., AKKAS KAVAKLI, P., SEPEHRIANAZAR, A., Effect of G/M ratio on the radiation-induced degradation of sodium alginate, Radiat. Phys. Chem. **79** (2009) 279–282.

[9.56] SEN, M., Effects of molecular weight and ratio of guluronic acid to mannuronic acid on the antioxidant properties of sodium alginate fractions prepared by radiation induced degradation, Appl. Radiat. Isotopes **69** (2011) 126–129.

[9.57] SEN, M., ATIK H., The antioxidant properties of oligo sodium alginates prepared by radiation-induced degradation in aqueous and hydrogen peroxide solutions, Radiat. Phys. Chem. **81** (2012) 816–822.

[9.58] NAGASAWA, N., MITOMO, H., YOSHII, F., KUME, T., Radiation-induced degradation of sodium alginate, Polym. Degrad. Stab. **69** (2000) 279–285.

[9.59] YANG, Z., LI, J.P., GUAN, H.S., Preparation and characterization of oligomannuronates from alginate degraded by hydrogen peroxide, Carbohydr. Polym. **58** (2004) 115–121.

[9.60] KUMAR, K.S., GANESAN, K., SUBBA RAO, P., Antioxidant potential of solvent extracts of *Kappaphycus alvarezii* (Doty) Dotyan edible seaweed, Food Chem. **107** (2008) 289–295.

[9.61] YUAN, H., et al., Preparation and in vitro antioxidant activity of κ-carrageenan oligosaccharides and their oversulfated, acetylated, and phosphorylated derivatives, Carbohydr. Res. **340** (2005) 685–692.

[9.62] TSIPALI, E., et al., Glucans exhibit weak antioxidant activity, but stimulate macrophage free radical activity, Free Rad. Biol. Med. **30** (2001) 393–402.

[9.63] XING, R., et al., Relevance of molecular weight of chitosan and its derivatives and their antioxidant activities in vitro, Bioorg. Med. Chem. **13** (2005) 1573–1577.

[9.64] KIM, K., TOMAS, R., Antioxidative activity of chitosans with varying molecular weights, Food Chem. **101** (2007) 308–313.

[9.65] KAUR, R., THUKRAL, A., ARORA, S., Attenuation of free radicals by an aqueous extract of peels of safedmusli tubers *Chlorophytum borivilianum* Santet Fernand, J. Chin. Clin. Med. **5** (2010) 7–11.

[9.66] ABAD, L.V., et al., NMR analysis of fractionated irradiated κ-carrageenan oligomers as plant growth promoter, Radiat. Phys. Chem. **80** (2011) 977–982.

[9.67] ZHONG, Z., et al., The preparation and antioxidant activity of the sulfanilamide derivatives of chitosan and chitosan sulfates, Bioorgan. Med. Chem. **15** (2007) 3775–3782.

[9.68] SUN, T., TAO, H., XIE, J., ZHANG, S., XU, X., Degradation and antioxidant activity of κ-carrageenans, J. Appl. Polym. Sci. **117** (2010) 194–199.
[9.69] JOSHI, V., VERMA, T., SHETTY, P., Antioxidant potential of *Bauhinia purpurea* Linn. leaves, Int. J. Pharm. Res. **1** (2009) 51–55.
[9.70] DUH, P.D., Antioxidant activity of Burdock (*Arctium lappa* Linné): Its scavenging effect on free-radical and active oxygen, J. Am. Oil Chem. Soc. **75** (1998) 455–461.
[9.71] JAYAPRAKASHA, G., SINGH, R., SAKARIAH, K., Antioxidant activity of grape seed (*Vitis vinifera*) extracts on peroxidation models in vitro, Food Chem.**73** (2001) 285–290.
[9.72] ABAD, L.V., et al., Radiation degradation studies of carrageenans, Carbohydr. Polym. **78** (2009) 100–106.
[9.73] SHIMADA, K., FUJIKAWA, K., YAHARA, K., NAKAMURA, T., Antioxidative properties of xanthan on the autoxidation of soybean oil in cyclodextrin emulsion, J. Agric. Food. Chem. **40** (1992) 945–948.
[9.74] FENG, T., DU, Y., LI, J., HU, Y., KENNEDY, J.F., Enhancement of antioxidant activity of chitosan by irradiation, Carbohydr. Polym. **73** (2008) 126–132.
[9.75] SIRIWARDHANA, N., LEE, K., KIM, S., HA, J., JEON, Y., Antioxidant activity of *Hizikia fusiformis* on reactive oxygen species scavenging and lipid peroxidation inhibition, Food Sci. Technol. Int. **9** (2003) 339–346.
[9.76] ROCHA DE SOUZA, M.C., et al., Antioxidant activities of sulfated polysaccharides from brown and red seaweeds, J. Appl. Phycol. **19** (2007) 153–160.
[9.77] SOKOLOVA, E.V., et al., In vitro antioxidant properties of red algal polysaccharides, Biomed. Preven. Nutr. **1** (2011) 161–167.

Chapter 10

RADIATION PROCESSING OF NATURAL POLYMERS FOR MEDICAL AND HEALTHCARE APPLICATIONS

L.V. ABAD
Philippine Nuclear Research Institute,
Quezon City, Philippines

10.1. INTRODUCTION

Hydrogels are cross-linked networks composed of polymer chains with hydrophilic structures, and are sometimes found as gels with water as the dispersion medium. Some examples are soft contact lenses, wound dressings, drug delivery systems, implants, biosensors and crystals of superabsorbent polymers. These have found wide application, especially in the biomedical field and in other healthcare areas. Moreover, their functions have recently been extended to the agricultural, industrial and environmental fields. Hydrophilic polymeric networks can absorb water in amounts from 10% of their dry weight up to thousands of times their dry weight; examples are found in super water absorbents for farming and hydrogels used in healthcare products. The networks attain an equilibrium swelling state that depends on the polymer–water interaction parameter and cross-link density. The network chains (cross-links) are usually formed by covalent or ionic bonds, although physical cross-links, such as entanglements, hydrogen bonds, hydrophobic and van der Waals interactions, can also provide three dimensional networks but with different characteristics (Fig. 10.1).

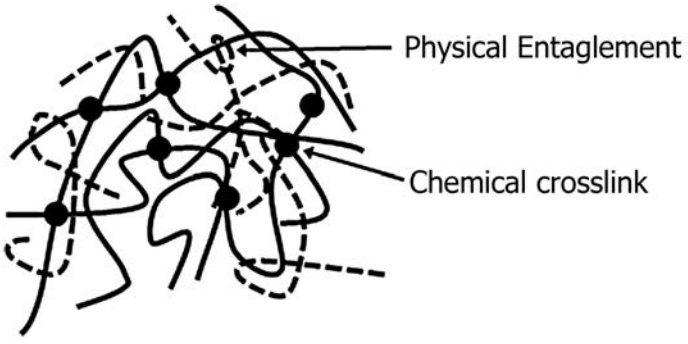

FIG. 10.1. Network structure in hydrogels.

They are called permanent or chemical gels when they are composed of covalently cross-linked networks. On the other hand, if they are composed of physically cross-linked networks, they are called reversible or physical gels, as their network interactions are reversible, and can easily be disrupted by changes in physical conditions or the application of stress. Hydrogels can be made up of synthetic polymers, natural polymers or a combination of both. Hydrogels can be synthesized by polymerization and cross-linking of a monomer or monomer mixtures (in bulk or in solutions), or by cross-linking of polymers. Details about these various methods are given below.

In the design of hydrogels for biomedical applications, certain considerations have to be taken into account. Medical devices that would come into contact with blood, tissues and body fluids or implants that would replace certain tissues have to fulfill specific requirements such as non-toxicity, functionality, sterilizability and biocompatibility (i.e. not provoking a toxic, injurious or immunological response in living tissue) [10.1].

The first known chemically synthesized hydrogel for biomedical applications is poly(vinyl alcohol) (PVA), which is used in surgery under the trade name Ivalon. It was cross-linked with formaldehyde that can withstand autoclaving temperatures. Tissue reaction to the implanted Ivalon was reported to be very mild, but after prolonged periods, shrinkage and calcification has been observed. However, Ivalon's application in plastic surgery and as bone and post nucleation implants was widely reported as successful [10.2]. In the 1950s, a hydrophilic polymer, based on hydroxyethyl methacrylate (HEMA), and cross-linked with diesters of methacrylic acid and mono, di and triethylene glycols was synthesized [10.3]. This poly-HEMA was primarily used as the main component of contact lenses. Between then and now, it has been used for various medical purposes in combination with other hydrophilic and hydrophobic polymers.

The interest in the application of radiation to obtain hydrogels for biomedical purposes began in the late 1960s. Research was mainly focused on using hydrogel matrices to immobilize biologically active species and on using hydrogels as drug delivery systems and enzyme traps. The modification of material surfaces was also investigated, with the aim of improving hydrogel's biocompatibility and ability to bond antigens and antibodies [10.4, 10.5]. Recently, hydrogels prepared by radiation processing have gained more attention because of the 'cleanliness' of the process; materials can be cross-linked without the addition of additives (e.g. sensitizers and catalysts), meaning that no chemical residues are left in the products. This improves the biocompatibility of the hydrogel. Other advantages of the radiation processing of hydrogels include: (a) the possibility of initiating the reaction at any temperature; (b) the wide variety of monomers and polymers to choose from, including those that cannot be polymerized by classical chemical

initiation; (c) the possibility of controlling the degree of cross-linking; (d) the possibility of simultaneous synthesis and sterilization; and (e) the possibility of the simultaneous immobilization of bioactive materials without any loss in their activity [10.6]. The properties of hydrogels (such as pore size, swelling–shrinking kinetics and water content) can be controlled by the synthesis conditions. Absorbed dose, dose rate, type of monomer(s) and concentration (ratio), and irradiation temperature all affect the properties of the gel, which permits the appropriate selection of a tailor-made preparation of a product for a specific application.

Most commercially available hydrogels are made up of synthetic polymers. In recent years, natural polymers have been looked at with renewed interest because of their unique characteristics such as inherent biocompatibility, biodegradability and easy availability. The first successfully commercialized radiation processed hydrogel for burn dressings was made up of a water soluble polymer, PVP, and PE glycol and a natural polymer, agar. It was commercialized under the trade name HDR or AQUA-GEL and marketed mainly in Central Europe [10.7, 10.8]. Since then, efforts have been made by the IAEA to promote the use of radiation technology for the modification of natural polymers for use as hydrogels for biomedical applications. Various IAEA CRPs and regional cooperative agreements (RCAs) have been implemented specifically for this purpose [10.9].

10.2. THE RADIATION CHEMISTRY OF HYDROGELS

The radiation chemistry of aqueous polymeric solutions has already been described in Chapters 3 and 4. When a polymer solution is subjected to ionizing radiation, reactive intermediates are produced in the form of macroradicals. This can result from the direct action of radiation on polymeric chains or from the indirect effect, i.e. the reaction of the intermediates generated in water with macromolecules. Among all the water radiolysis products, hydroxyl radicals have been shown to be the main species responsible for reactivity transfer from water to the polymer chains. The values of the rate constants of the reaction of OH radicals with water soluble polymers (polyethylene oxide, PVAL, PVP and poly(vinyl methyl ether)) are higher than 10^8 $dm^3 \cdot mol^{-1} \cdot s^{-1}$ as determined by pulse radiolysis [10.10–10.13]. Hydroxyl radicals abstract hydrogen atoms from macromolecules forming macroradicals. The macroradicals generated from the polymers recombine to form intermolecular cross-links. The yield of intermolecular cross-links, $G(x)$, defined as the number of cross-links formed in the system upon absorption of 1 J of ionizing radiation energy, expected for this reaction (without considering other side reactions, e.g. intramolecular

cross-linking) would be $G(x) = 1.6 \times 10^{-7}$ mol/J for deoxygenated (i.e. saturated with Ar or N_2) solutions and approx. 3.0×10^{-7} mol/J for solutions saturated with nitrous oxide [10.14]. The concentration of the polymer and the dose rate influences the competition reactions between inter- and intramolecular cross-linking. The higher the polymer concentration, the more likely it becomes that two recombining radicals can be found on different chains. On the other hand, high dose rates combined with a low polymer concentration may result in the generation of a large number of radicals on each chain. This reduces the probability and yield of intermolecular recombination. Figure 10.2 illustrates both intermolecular (a) and intramolecular (b) cross-linking. Chain scissions may also occur simultaneously with intermolecular cross-linking, especially in oxygenated solutions. In oxygen-containing polymer solutions, the macroradicals react with oxygen to form peroxyl or oxyl radicals. These peroxyl or oxyl radicals do not form stable cross-links upon recombination [10.14]. One of the main reaction pathways leads to chain scission. When radical terminating reactions are slow, peroxyl radicals can undergo a chain reaction of hydrogen atom abstraction followed by a reaction of the alkyl radical formed with oxygen. In this way, the degradation products, terminal peroxyl radicals, can rearrange into mid-chain peroxyl radicals that can initiate further chain scissions [10.15]. Such chain processes have been observed in PAAc [10.16]. Degradation products from the chain scission reaction of poly(ethylene oxide) in the presence of oxygen have also been observed [10.17, 10.18]. Thus, in the synthesis of hydrogels, gel formation can generally be efficiently formed in oxygen-free systems. These simultaneous cross-linking and scission reactions are well discussed theoretically using mathematical expressions to calculate gel (cross-link) and sol (scission) fractions [10.19, 10.20].

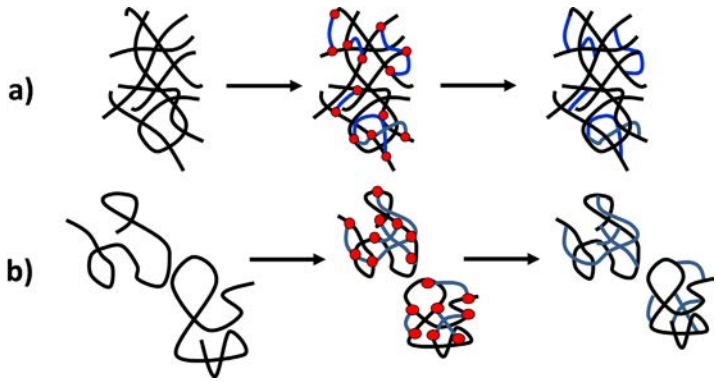

FIG. 10.2. Schematic representation of (a) intermolecular and (b) intramolecular cross-linking in polymers. The dots on the macromolecules are free radical sites.

Gamma or EB irradiation of water soluble polymers blended with natural polymers results in the simultaneous cross-linking of the water soluble polymers and the degradation of the natural polymer. A combination of these processes may form a hydrogel with a network structure of a semi-interpenetrating polymer network whereby the natural polymer is physically entangled within the cross-linked water soluble polymers. Aside from this network, there is a possibility that portions of the degraded natural polymer can be grafted onto the PVP. A study on PVP κ carrageenan shows the presence of a grafted network in which κ carrageenans are grafted onto a PVP backbone. Thermal gravimetric analysis indicates a new degradation peak found between the peaks of κ carragenan and the cross-linked PVP [10.21].

10.3. RADIATION CROSS-LINKING OF NATURAL POLYMER DERIVATIVES

Natural polymers are known to degrade upon exposure to ionizing radiation. Thus, natural polymers alone could not form hydrogels by the radiation method. They have to be blended with water soluble polymers to form a semi-interpenetrating polymer network. Synthetic polymers without natural polymers can be useful as hydrogels but the addition of natural polymers can improve their physicomechanical properties remarkably. This function will be discussed in Section 10.6. Recently, studies have shown that derivatives of natural polymers, such as carboxy methyl (CM) cellulose [10.22, 10.23], CM starch [10.24], CM chitin/chitosan [10.25] and CM carrageenan [10.26] can be cross-linked. The initial process involves the derivatization reaction of the desired polysaccharide with monochloroacetic acid in the presence of sodium hydroxide [10.27–10.29]. The carboxymethylation process may be performed in repetitive cycles to increase its DS. The titration method and NMR spectroscopy can determine the DS of the derivative [10.30–10.34]. The CM polysaccharides are then irradiated in a paste-like state (20–50% concentration) to form a hydrogel. The process is illustrated in Fig. 10.3. The cross-linking of the CM derivatives depends on the initial polymer concentration and the DS. Figure 10.4 shows that a higher DS is favourable to cross-linking. For the same dose, a higher gel fraction is achieved at a higher DS [10.35].

10.4. CHARACTERIZATION OF HYDROGELS

The most important properties of hydrogels related to their functions are gel fraction, degree of swelling and tensile strength (TS) or gel strength. These

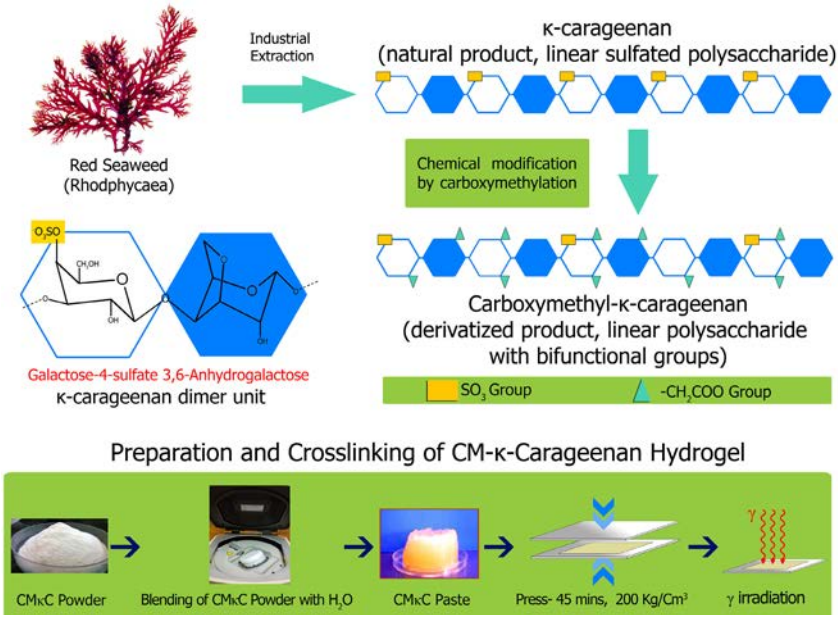

FIG. 10.3. Synthesis of cross-linked CM carrageenan hydrogel.

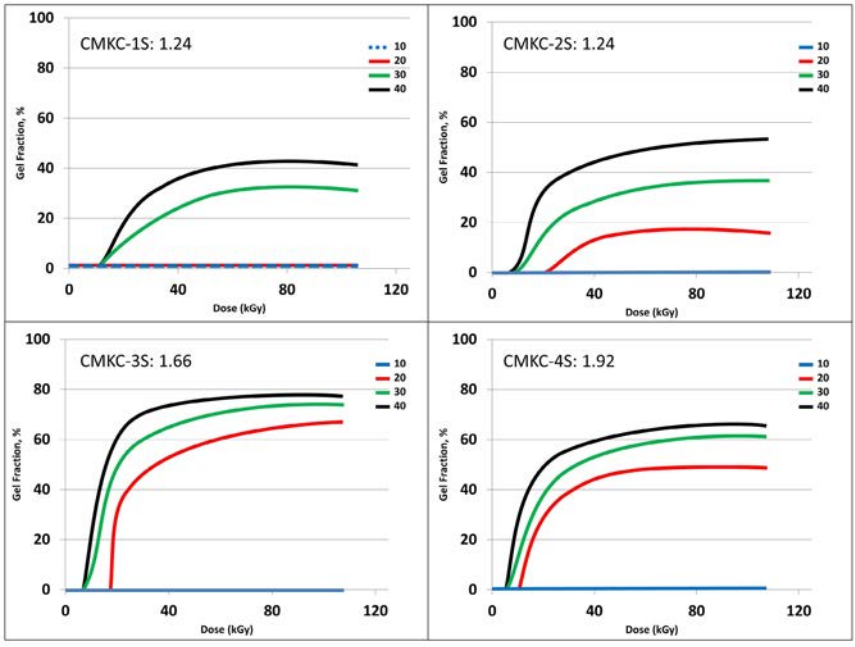

FIG. 10.4. Gel fraction of CM-κ-carrageenan at varying DS and concentrations.

properties are interrelated and depend on the degree of cross-linking as well as the cross-linking density of the polymer. A hydrogel that has a low degree of cross-linking will naturally have lower non-soluble fractions (gel fractions). The three dimensional network forms a loose network structure which allows more free water to diffuse into the network and therefore increases the degree of swelling. Hydrophilic functional groups such as –OH, –COOH, $–CONH_2$ and $–SO_3H$ present in the hydrogel are capable of absorbing water and increase the degree of swelling. More cross-links would mean more stable chemical bonds and consequently they give a higher TS or gel strength. When the cross-link density becomes so high, the network becomes so tight that the hydrogel loses its flexibility and becomes brittle. Both the degree and density of cross-linking depend on the absorbed radiation dose. Typical curves showing the relationship of gel fraction, degree of swelling and TS or gel strength as a function of irradiation dose are shown in Fig. 10.5.

Another factor affecting the cross-linking of hydrogels is the presence of inhibitors such as glycols and even natural polymers themselves since they compete with the available free radicals. Thus, the parameter related to the concentration of polymers can be tailored in such a way that the final product

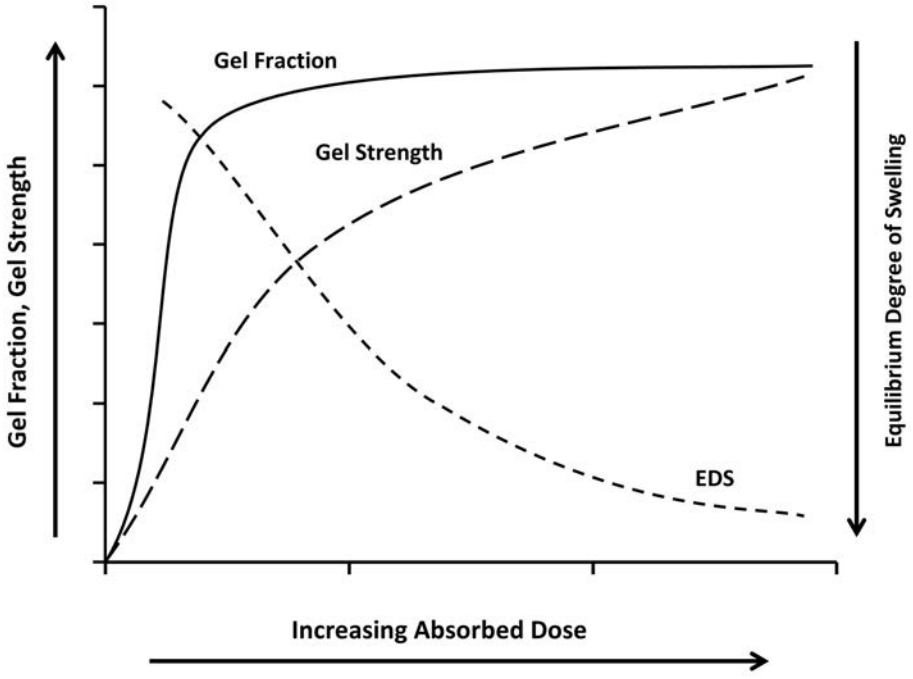

FIG. 10.5. Relationship of gel fraction, equilibrium degree of swelling and gel strength with dose.

would have the appropriate properties needed for a specific purpose. It should be noted, as mentioned earlier, that the presence of air (oxygen) can also inhibit the formation of cross-links in hydrogels. Some practical procedures for the measurement of gel fraction and degree of swelling (as discussed in Chapter 6) are suggested below.

10.4.1. Calculation of the gel fraction

The dried sample of hydrogel is immersed in distilled water (changing the water several times) for 48 h at room temperature. Alternatively, the dried hydrogel is placed in a wire mesh (small enough so that disintegrated hydrogels will not pass through) and placed in bottled containers with sufficient water. The hydrogels are then autoclaved for 30 min. The autoclaved hydrogels are washed with distilled water and dried. The gel fraction is calculated as follows:

$$\text{Gel fraction} = \frac{W_d}{W_i} \tag{10.1}$$

where W_d is the dried weight of the insoluble fraction after extraction with water and W_i is the initial weight of dried hydrogel.

10.4.2. Calculation of the degree of swelling

The dried sample of hydrogel is immersed in distilled water and allowed to swell. The hydrogels are weighed several times until no changes in weight are observed. For practical purposes, weighing can be done every 8 to 12 h. The equilibrium degree of swelling, EDS, is calculated as follows:

$$\text{EDS} = \frac{W_s}{W_i} \tag{10.2}$$

where W_s is the weight of hydrogel in its swollen state and W_i is the initial weight of the dried hydrogel. Alternatively, percentage swelling can also be used for the computation.

$$\text{Percent swelling} = \frac{W_s - W_i}{W_i} \times 100 \tag{10.3}$$

10.5. STIMULI RESPONSIVE HYDROGELS

Some hydrogels undergo changes in swelling behaviour in response to stimuli such as a change in pH, ionic strength or temperature or electric currents. Gels exhibiting a phase transition in response to changes in external conditions

are known as stimuli-responsive or 'smart' gels. Stimuli responsive hydrogels undergo abrupt volume changes in response to changes in these environmental parameters, as shown in Fig. 10.6.

The key element of pH sensitive hydrogels is the presence of polymers containing ionizable weak acidic (e.g. −COOH/−COO−) or basic moieties (e.g. $-R_2N/-R_2NH^+$) attached to a hydrophobic backbone. External pH changes cause pH sensitive hydrogels to undergo conformational chain transitions from extended to coil states or vice versa. Upon ionization, the coiled chains extend dramatically, responding to the electrostatic repulsions of the generated charges (anions or cations). Typical examples are CM cellulose, CM chitin and CM chitosan containing the negatively charge carboxy methyl group and $–NH_2$ groups. These undergo conformational transition from an extended to a coil state upon a change in pH [10.36, 10.37]. Many synthetic hydrogels have been found to display this kind of pH sensitivity. Lipid/polypeptide coated polyamide gel shows swelling behaviour in response to changing pH [10.38]. Poly(N-isopropylacrylamideco-methacrylic acid) gel membrane shows a pH response in a very narrow range, pH4.9–5.2 [10.39]. Polyaspartic gels show abrupt changes in swelling behaviour at pH7.3 [10.40]. Recent works on natural polymer blended or grafted synthetic polymer hydrogels (κ carrageenan, starch, chitosan, alginate, cellulose) also show pH sensitivity [10.41–10.45].

Thermosensitive hydrogels, on the other hand, make the chains swell or collapse at a lower critical solution temperature (LCST) owing to adjustments of the hydrophobic and hydrophilic interactions between the polymer chains and the aqueous medium. A critical solution temperature is the temperature at which a polymer solution separates from one phase to two. Therefore, the volume of temperature sensitive polymers changes as abruptly when the temperature of the medium reaches the LCST. A typical example of a thermosensitive hydrogel is

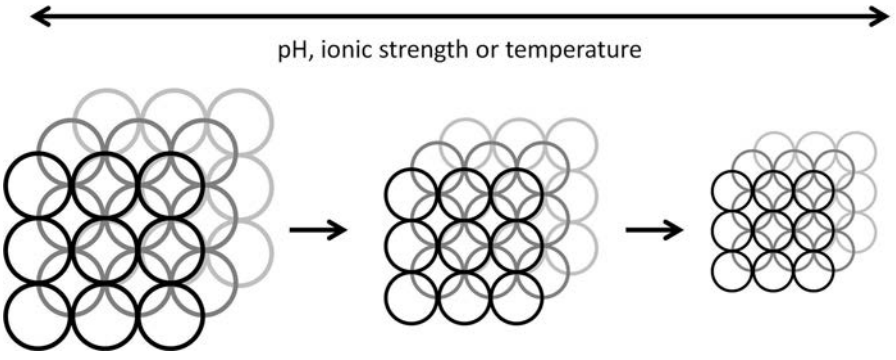

FIG. 10.6. Swelling behaviour of stimuli responsive hydrogels.

poly-N-isopropyl acrylamide (PNIPAAm) gel. The LCST of PNIPAAm has been determined to be 32°C [10.46]. PNIPAAm is hydrophilic and exists in individual chains with a coil conformation; while above the LCST, it undergoes a sharp coil-to-globule transition to form inter- and intra-chain associations, resulting in hydrophobic aggregation and depositing from the aqueous solution [10.47–10.50]. These conformational changes primarily result from dehydration at the isopropyl side groups. The LCST can be changed by modifying the functional groupings in the polymer chain, e.g. modifying PNIPAAm with a carboxyl end group that changes the LCST to 20°C [10.51]. Many hydrogels derived from synthetic copolymers of PNIPAAm have been studied for their thermosensitive attributes [10.52–10.56]. Natural polymers (cellulose, methyl cellulose, dextran, GG, CM chitosan, pullulan and chitosan) have been used as copolymers or grafted onto PNIPAAm for use as a thermosensitive gel [10.57–10.63].

The unique characteristics of stimuli responsive hydrogels are of great interest in drug delivery (the controlled release of drugs is shown in Fig. 10.7), cell encapsulation and tissue engineering [10.64]. From a biomedical point of view, the most important systems are those that are sensitive to the temperature and/or pH of the surroundings. The human body exhibits variations of pH along the gastrointestinal tract, and in some specific areas, such as certain tissues (and tumoural areas) and subcellular compartments. Quite a number of studies have been performed utilizing hydrogels for these purposes. Many of these hydrogels have been synthesized using the ‘classical’ chemical method. As mentioned in the

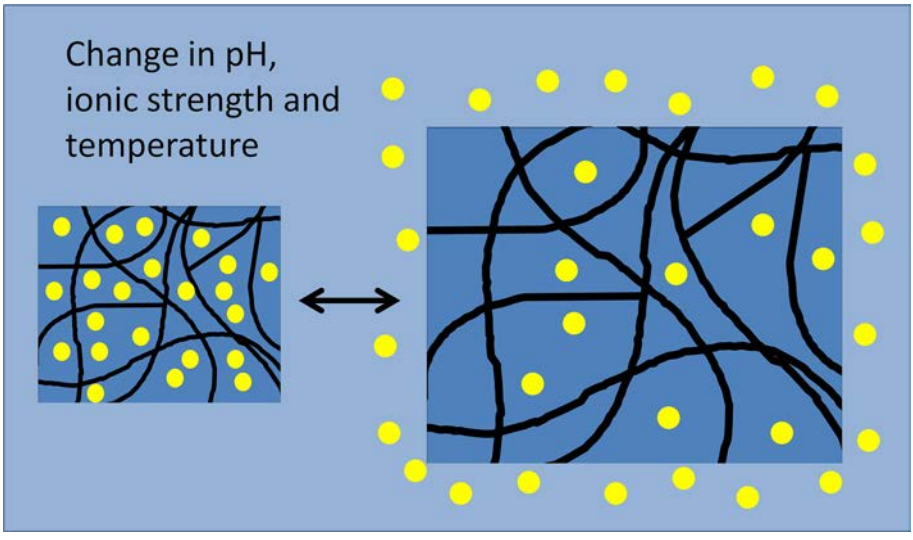

FIG. 10.7. Schematic diagram of hydrogels for controlled release of drugs.

early part of this chapter, ionizing radiation has been recognized as a very suitable alternative to this process as this does not contain the monomers, initiators, cross-linking agents and additives present in the conventional method. Several studies have already been carried out on the use of radiation for the synthesis of hydrogels for drug delivery systems:

— N vinyl pyrrolidone was studied as a therapeutic system for local release of prostaglandins for the induction of labour [10.65].
— A polymeric rod containing a mixture of poly(ethylene oxide), poly(ethylene glycol) (PEG) and the drug medroxyprogesterone was studied for the local release of anticancer agent for the treatment of endometrial carcinoma [10.66].
— Injectable PEG–morphine mixtures were studied for the prolongation of the effects of anaesthesia for patients after operation [10.67].
— Injectible PNIPAAm/anticancer (5–FU) mixtures were studied for the local chemotherapy of tumour tissue [10.67].
— pH sensitive hydrogels from β cyclodextrin grafted PEG and AAc was studied for the release of a model drug (5-Fluorouracil) [10.68].
— Psyllium N vinylpyrrolidone based hydrogels were studied for the release of an anticancer model drug (5-fluorouracil) [10.69].
— Poly[(dimethylaminoethyl methacrylate)-co-(diallyl dimethyl ammonium chloride)] hydrogels were studied as a carrier for notoginsenoside delivery [10.70].
— Polydimethylsiloxane was studied as a matrix for the release of progesterone [10.71].
— pH sensitive interpolymer polyelectrolyte complex from AAc and dimethyl aminoethyl methacrylate was studied as a colon-specific drug delivery system [10.72].
— Thermally reversible gels based on acryloyl L proline methyl ester were studied for the release of acetaminophen, an analgesic and antipyretic drug [10.73].

One of the interesting studies on stimuli responsive hydrogels produced by radiation processing has been performed by Nho et al. [10.74]. They synthesized a pH sensitive hydrogel based on PVA grafted with AAc / methacrylic acid for the oral delivery of insulin. Oral delivery of peptides and proteins to the gastrointestinal tract is one of the most challenging issues. There are many hurdles, including protein inactivation by digestive enzymes in the gastrointestinal tract, mainly in the stomach, and the poor epithelial permeability of these drugs. However, certain hydrogels may overcome some of these problems by appropriate molecular design or formulation approaches.

In Ref. [10.74], pH responsive hydrogel was used as an oral delivery carrier for insulin in order to protect the insulin from the acidic environment of the stomach. The insulin release profile of these pH responsive hydrogels both in vitro and in vivo has been investigated. The in vitro release profile of insulin obtained in both simulated gastric fluid and simulated intestinal fluid indicate that these hydrogels could be applied successfully for oral drug delivery to the gastrointestinal tract. The oral administration of insulin loaded hydrogels to rats was found to decrease their blood glucose levels for at least 4 h owing to the absorption of insulin in the gastrointestinal tract (Fig. 10.8).

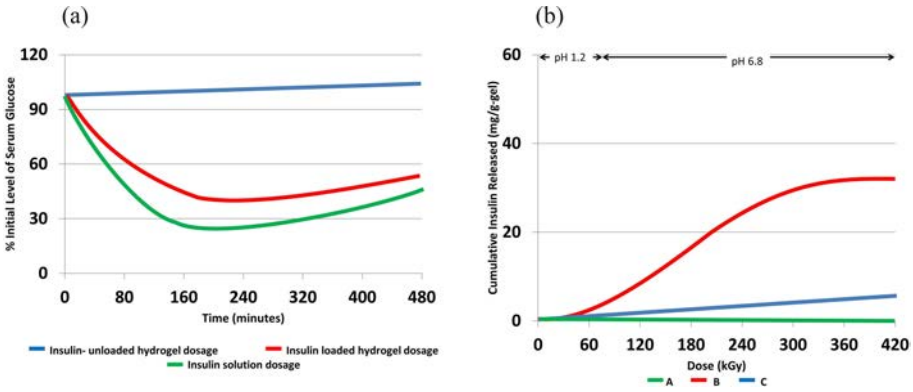

FIG. 10.8. Insulin release profile of insulin-loaded PVA-g-AAc hydrogel: (a) in vivo experiments in rats and (b) in vitro experiments at different pH.

10.6. PRODUCTS DEVELOPED FROM RADIATION PROCESSED POLYMERS FOR MEDICAL AND HEALTHCARE APPLICATIONS

A great effort has been made to use established products from radiation processed natural polymeric materials for biomedical and healthcare purposes. The IAEA, through its CRPs and RCAs, has played a significant role in fostering developments in this area. However, only very few such materials have ever reached the full commercial scale.

10.6.1. Wound care coverings

Hydrogel dressings produced using radiation technology form a small part of the global market in hydrocolloid and hydrogel products. Brands of hydrocolloids and hydrogels for wound dressing such as ConvaTec's Duo-Derm, Coloplast, Comfeel, Hollister's Restore, Smith & Nephew United's IntraSite and Replicare, none of which used radiation technology at the time of writing, dominate the

international market. Since the development of the first dressing from radiation processed PVP-agar in Poland, a number of similar wound dressings have been developed and commercialized in the local market. The formulation varies only in the type of water soluble polymer (PVP, PVA or poly(ethylene oxide)) and natural polymer (agar, carrageenan, chitosan or a combination of these natural polymers) that is used. The polymer effectively absorbs body fluids and prevents their loss, acts as an efficient barrier against bacteria, adheres well to the wound but adheres more strongly to healthy skin, exhibits high elasticity but also some mechanical strength, shows good transparency and enables oxygen to penetrate through the volume of the dressing to the wound surface [10.2]. The main advantage of the product is that sterilization and cross-linking are both carried out in a single step process by irradiation.

10.6.1.1. PVP-agar carrageenan hydrogel wound dressing

PVP hydrogel produced by irradiation in aqueous solution has been successfully applied to local wound repair in many pathologies (such as burns, ulcerations and postoperative wounds), thereby confirming its excellent biomedical properties [10.75]. It is prepared by dissolving and mixing at elevated temperature and cast into moulds, which can also be used as final packages; the moulds are irradiated at the optimum absorbed dose [10.8]. The addition of natural polymers such as carrageenan, and increasing the amount of PVP, can substantially improve the mechanical properties of the hydrogel, as shown in Fig. 10.9 [10.76]. Such improvements are essential especially when applied to wounds, as they allow the absorption of exudates without breaking, as well as comfortable handling by physicians.

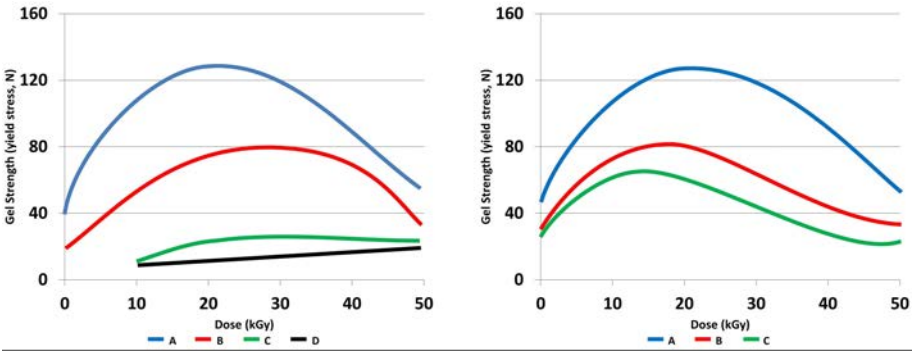

FIG. 10.9. The effect on the gel strength of the hydrogel of varying concentrations of (a) κ carrageenan — A (5%), B (3%), C (1%) and D (0%), and (b) PVP — A (15%), B (10%), C (5%).

The type of natural polymer added to PVP and other water soluble polymers can influence the physicomechanical properties of the hydrogel. Differences in functional groupings, e.g. of sulphate in carrageenan, can substantially increase the swelling behaviour of the hydrogel. The network structure becomes more hydrophilic, which can attract more water molecules inside the structure. This is illustrated in Fig. 10.10 where the degree of swelling of PVA-κ-carrageenan is higher than PVA-agar [10.77]. Aside from the degree of swelling, PVP-carrageenan forms a tougher hydrogel than PVP-agar, giving PVP-carrageenan higher mechanical properties. By nature, κ carrageenan forms a hard gel while agar is a soft gel. This property of κ carrageenan would be advantageous in the preparation step since the PVP-carrageenan gels can be easily taken out from their moulds after forming without destroying their shape. This cannot be easily done with PVP-agar. On the other hand, PVP-agar is a very flexible hydrogel while PVP-carrageenan has a tendency to become brittle. A combination of both natural polymers may form hydrogels with enhanced physicomechanical properties.

Similar to PVP-agar hydrogel, the swelling behaviour and gel fraction of PVP-κ-carrageenan are influenced by quantities of the natural polymer present in the hydrogel, as shown in Fig. 10.11 [10.78]. For the practical application of PVP-carrageenan as a wound dressing, it would require only a small amount of κ carrageenan (1–2%). At a lower concentration, κ carrageenan would not form a physical gel, while a concentration higher than 2% would be detrimental to

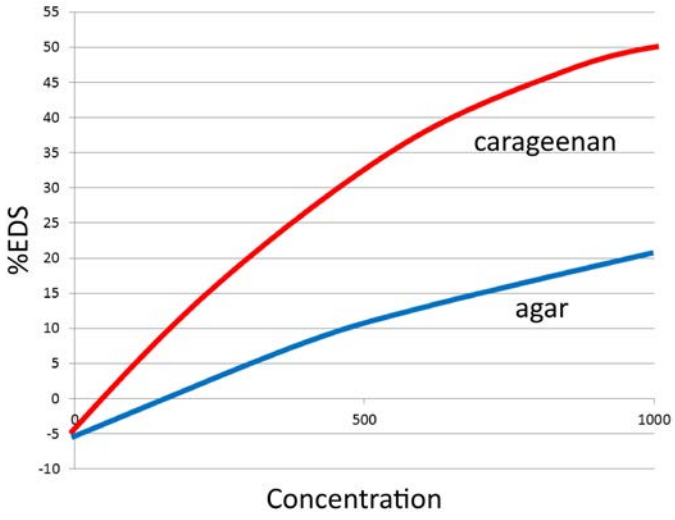

FIG. 10.10. Equilibrium degree of swelling of hydrogel (27 kGy) containing PVA (8%) at varying concentrations of agar and carrageenan.

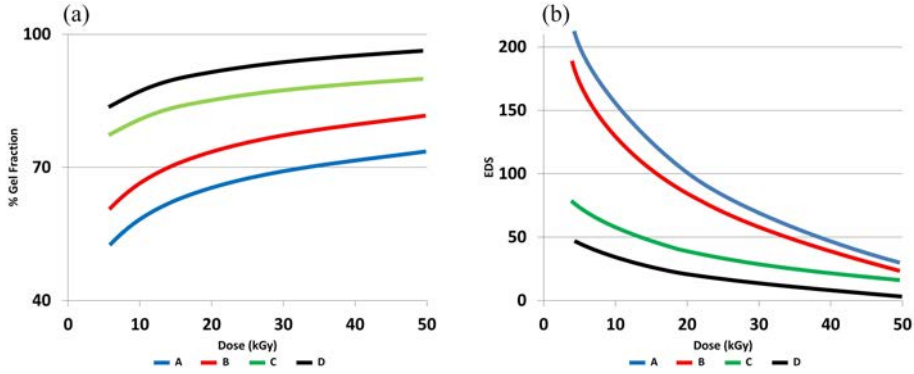

FIG. 10.11. The effect of varying concentrations of κ carrageenan — A (5%), B (3%), C (1%) and D (0%) on (a) the gel fraction and (b) the EDS of PVP-κ-carrageenan hydrogel.

the physicomechanical properties of the resulting hydrogel. Less cross-linking is expected as the quantity of the natural polymer is increased.

In the Philippines, a PVP-carrageenan hydrogel has been developed and patented [10.79]. It has been tested for use as a burn dressing. Figure 10.12 shows that the healing period of wounds dressed with the PVP-carrageenan hydrogel is similar to a wound treated with a commercial hydrocolloid. The market price of the commercial hydrocolloid would be expected to be three times higher than the PVP-carrageenan hydrogel. A similar product in the Republic of Korea also contains a PVP-carrageenan formulation. The degree of evaporation, a common problem for most hydrogels, has been minimized with the use of a polyurethane membrane. Aside from burns, this hydrogel dressing is also quite effective for decubitus ulcers [10.79]. In developing countries, where prices of imported hydrocolloid dressings are excessively high, decubitus ulcers are generally treated by daily washing with saline solution and covered with gauze. The use of PVP-carrageenan hydrogel could be a good alternative as a dressing for this type of wound. The hydrogel can cover the wound for the duration of three days,

FIG. 10.12. Healing of wound using PVP-carrageenan hydrogel and a commercial hydrocolloid [10.80].

which minimizes the disturbance of the growth of new epithelial cells caused by the daily removal of gauze and the accompanying washing. In effect, this hydrogel can be more economical than gauze as labour expenses due to daily nursing care are minimized.

10.6.1.2. Other formulations of hydrogels for wound dressing

Different formulations of radiation processed natural polymer hydrogels for wound dressings have been developed by Member States under the IAEA RCA RAS Projects 8096, 8098 and 8106. Various improvements in the synthesis of these hydrogels have also been made. In the Republic of Korea, the incorporation of aloe vera, a plant extract known to be effective in healing wounds, has been studied [10.81]. PVA/PVP/aloe vera hydrogels have a better healing effect than either the absence of a dressing or commercial polyurethane membranes. The wounds were found to heal 15 days after the PVA/PVP/aloe vera hydrogels are applied, while wounds with no dressing healed after 21 days [10.80]. A PVA/Thai silk fibroin hydrogel has also been developed in Thailand. The texture of the PVA/Thai silk fibroin hydrogel films is softer than that of pure PVA. Animal testing shows that wounds covered with PVA/silk fibroin heal faster than those covered with a commercial dressing [10.80].

Indian researchers have incorporated iodine into a hydrogel to form a blue-black complex with PVA hydrogel. Iodine is slowly released to the wound, which facilitates its healing [10.82]. In some cases of wounds with dents, e.g. bed sores, hydrogel flms are not useful since they cannot penetrate the dent in the wound. An injectable hydrogel may be useful. Malaysian researchers are developing such a kind of hydrogel from oligochitosan (Fig. 10.13).

The advantages of hydrogels from radiation processed natural polymers for topical wound coverings are unmistakable. Potential expansions of the functions of these hydrogels, for example, by incorporating them into transdermal patches for the slow release of drugs, need to be further explored.

10.6.2. Face mask

Sago starch is isolated from the trunks of the sago palm (*Metroxylon spp.*), which is otherwise known as rumbia and is found abundantly in south-east Asia. It contains high levels of polyphenolic substances with antioxidative, anti-ageing and antibacterial properties. Nuclear Malaysia has developed, by radiation processing, a sago hydrogel made up of a sago starch-PVA polymer blend to be used as a facemask [10.84]. The production process involves blending appropriate concentrations of PVA and sago starch in water, coating the mixture in a flexible cloth material as a backing, cutting, packaging and performing

FIG. 10.13. Injectable chitosan gel [10.83].

e-beam irradiation for simultaneous cross-linking and sterilization of the polymer blend. The resulting facemask provides the skin with antioxidant protection, as well as boosting its moisture level. It has bio-cleansing abilities, removes dead skin cells and has been clinically shown to treat acne.

10.6.3. Hydrogel mat

Bed sores, also known as decubitus ulcers, pressure sores and pressure ulcers, are commonly developed in patients who are bedridden and who are not properly repositioned. These are ulcerations or sores on the skin, typically over bony prominences, resulting from prolonged pressure. Bed-sores are a localized area of tissue injury that develops when soft tissue is compressed between a bony prominence and an external surface for a prolonged period of time. The external surface may be a mattress, a chair or wheelchair, or even other parts of the body. A bed sore develops when blood supply to the skin is cut off owing to prolonged pressure for more than two to three hours. As the skin dies, the bed sore first starts as a red, painful area, which eventually turns purple. If the skin is left untreated, it can break open and become infected. One concrete way to prevent the formation of bed sores is by providing soft padding in wheelchairs and beds to reduce pressure.

An innovative way of preventing bed sores has been developed in Japan [10.85]. It makes use of a CMC hydrogel mat prepared by radiation induced

cross-linking (20% CMC in water). Figure 10.14 shows the CMC mat being used in a bed. Clinical studies reveal that no bed sore was observed in 64 out of 68 subjects after their surgical operations when CMC hydrogel mats were used. This result implies that the CMC hydrogel mats can disperse body pressure and sustain the circulation of blood. These CMC hydrogel mats are commercially available in Japan with the product name 'Non-bedsore'. CMC gels are biodegradable and the waste coming from these gels can easily be converted into fertilizer by degradation with bacteria in soil.

FIG. 10.14. CMC hydrogel mat [10.83].

10.6.4. Thai silk soap

Thai silk is a well known product of Thailand and has various unique properties that make it suitable for a variety of applications in addition to uses in clothing. For example, Thai silk protein can be used as a wound dressing (Section 10.6.1) and as a skin moisturizer. Thai silk powder can easily be degraded by gamma radiation to make it miscible with water. The degraded powder can then be easily incorporated into various products such as Thai silk soap [10.86].

10.7. OTHER POTENTIAL USES OF RADIATION PROCESSED NATURAL POLYMERS

10.7.1. Bioimplant for the endoscopic treatment of vesicoureteral reflux (PVP-chitosan hydrogel)

Vesicoureteral reflux (VUR) refers to the retrograde flow of urine from the bladder into the upper urinary tract. It predisposes an individual to renal infection

or pyelonephritis by facilitating the transport of bacteria from the bladder to the upper urinary tract [10.87]. It is the most common urologic anomaly in children, has been reported in 30–50% of those who present with urinary tract infections and is a risk factor for progressive renal damage. Open surgical re-implantation or uretero neocystostomy has a high success rate of up to 98% in correcting VUR. It is an major invasive clinical procedure reserved only for persistent urinary tract infections and high grade reflux. The endoscopic treatment of VUR has gained favour in recent years as a therapeutic alternative to long term antibiotic prophylaxis and open surgery. This makes use of different tissue to augment implants injected in the peri-ureteral area. The most effective and stable subureteral implant material is a dextranomer-hyaluronic acid copolymer. The gel is injected into the bladder wall where the ureter enters the bladder, forming a bulge at the opening. The bulge reduces the size of the opening, to prevent urine from flowing backwards into the ureter. The opening is still flexible so urine can flow into the bladder, as it should. The gel is gradually replaced by the body's own tissue, so the bulge remains.

In the Philippines, an injectable gel of radiation cross-linked PVP-chitosan has been developed as a possible alternative to a dextranomer implant [10.88]. The viscosity of the material has been tested by passing the gel implant through a gauge 26 needle. Preliminary animal testing has been conducted by injecting rats subcutaneously with chitosan-PVP and using a commercial dextranomer implant as the control. The results of the test revealed comparable results for both materials. Monthly examination of the implanted sites showed no local inflammatory reactions in either group. The volume of the subcutaneous nodule indicates that after six months, the decrease in volume of subcutaneous nodules for PVP-chitosan does not differ significantly from the commercial dextranomer implant (Fig. 10.15). Histological examination of both groups showed no signs of granulation tissue formation, foreign body reaction or scar formation. The migration potential was evaluated by histological studies in the liver, kidneys and lungs for both groups, which did not show any inflammation, irritation, foreign body responses, tissue necrosis or scarring. These results reveal the potential of PVP-chitosan hydrogel as a VUR.

10.7.2. Hydrogels for treatment of atopic dermatitis (PVA-natural herb extract)

Atopic dermatitis is a common chronic pruritic inflammatory skin condition. It causes dry skin, intense itching and a raised, red rash. In severe cases, the rash forms clear, fluid-filled blisters. Atopic dermatitis is most common in babies and children. The cause of atopic dermatitis is not clear. People with atopic dermatitis seem to have very sensitive immune systems that are more likely to

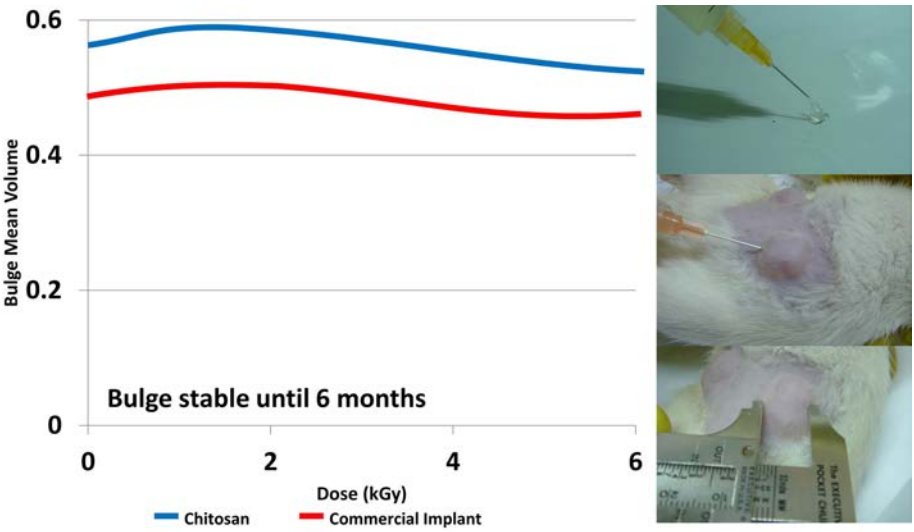

FIG. 10.15. PVP-chitosan injectable gel as a bioimplant for VUR tested subcutaneously on rats [10.89].

react to irritants and allergens. Most people who have atopic dermatitis have a personal or family history of allergies, such as hay fever (allergic rhinitis) and asthma. Its origin can be caused by both genetic (hereditary) and environmental factors. Atopic dermatitis is treated with moisturizing creams and lotions. Immunosuppressive drugs (creams and ointments) such as glucocorticoids are effective for atopic dermatitis, however, the prolonged use of these drugs may cause adverse effects owing to their non-specific immune modulation [10.90]. Recently, herbal medicines have been used to treat atopic dermatitis in some countries [10.91].

A novel therapeutic hydrogel for atopic dermatitis has been developed in the Republic of Korea. It is prepared from a radiation processed PVA hydrogel with herb extracts (*Houttuynia cordata* Thunb. and *Ulmus davidiana var. japonica* (Japanese elm) (Ato-gel)) [10.92]. *Houttuynia cordata* Thunb. has been used for the treatment of herpes simplex. The Japanese elm is a deciduous broad-leaved tree widely distributed in Asia, and its stem and root barks have been used as a traditional medicine for the treatment of oedema, mastitis, cancer, inflammation and rheumatoid arthritis. The hydrogel also contains propylene glycol as a moisturizer, which improves skin adherence. An atopic dermatitis study using BALB/c mice indicated that the application of hydrogel containing herbal extracts can minimize scratching tendency in mice to a greater extent than if the extracts are injected directly into the affected area (Fig. 10.16). Atopic

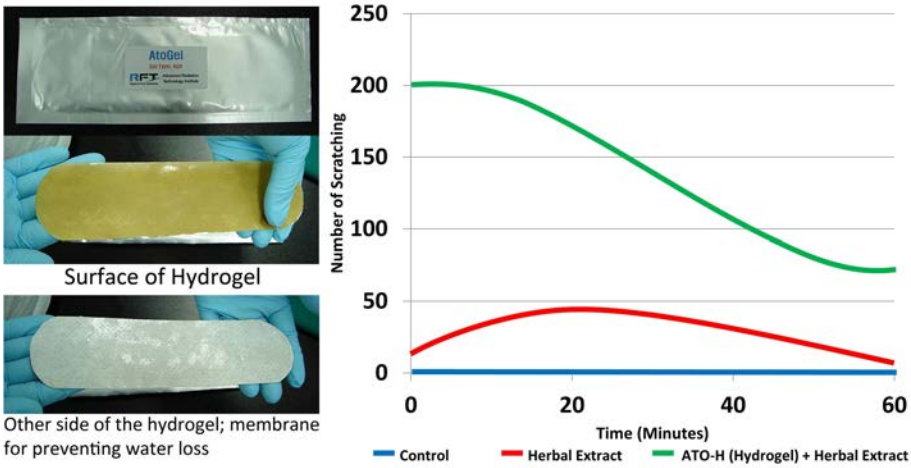

FIG. 10.16. Atopic dermatitis treatment with Ato-gel in BALB/c mice [10.93].

dermatitis patients commonly exhibit hyperproduction of immunoglobulin E. Immunoglobulin E synthesis is primarily regulated by cytokines such as IFN-γ and IL-4.

The animal study further showed that an increase in both IFN-γ and IL-4 is observed after treatment with dinitrochlorobenzene. After two weeks of application of the Ato-gel, a decrease in the levels of IFN-γ and IL-4 was observed in the mice treated with dinitrochlorobenzene mice. The effect is even higher than the effect of the commercial control gel (Fig. 10.17). The results of clinical trials suggest atopic dermatitis may heal with no recurrence. These studies reveal the efficacy of the hydrogel with herbal extracts for the treatment of AD and the synergetic effect of the combination of moisture and medicine.

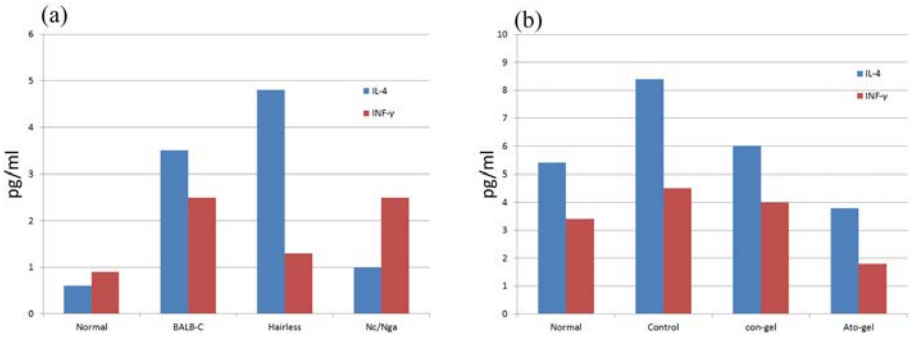

FIG. 10.17. Cytokine change (a) after treatment with dinitrochlorobenzene and (b) 2 weeks after Ato-gel treatment in BALB/c nude mouse [10.92].

10.7.3. CM cellulose hydrogels and solutions for the prevention of postsurgical adhesion

Adhesions are fibrous bands that form between tissues and organs, often as a result of injury during surgery. Adhesion formation is a natural consequence of surgery that occurs when the body tries to repair itself following the trauma of incision, cauterization or suturing, or as a result of handling or drying out of tissue owing to exposure. At the site of such damage, internal tissues that normally remain separate often become joined together, causing fibrous scar tissue to form. This process generally occurs within the first few days following surgery and can lead to further serious complications, including difficult re-operations, small bowel obstruction, female infertility and chronic debilitating pain. Adhesion can be prevented with the use of synthetic barrier membranes that stick to the internal tissues and separate the organs to prevent them from attaching to one another as they heal. The most commonly used barriers are oxidized regenerated cellulose or films of chemically modified sodium hyaluronate and CMC. Membranes from oxidized regenerated cellulose and polytetrafluroethylene have demonstrated some limited inhibition of adhesion formation in humans [10.94].

In the Republic of Korea, radiation processed CMC/PEG hydrogels and CMC/PEG hydrogel solution (2%) have been tested for the prevention of intra-abdominal adhesion in rats [10.94]. The control animals developed dense adhesions between their caecal and abdominal walls. Animals treated with the CMC/PEG hydrogel or the 2 wt% solution of the CMC/PEG hydrogel had a significantly lower average adhesion score than the controls (Fig. 10.18). At day 14, almost no residual CMC hydrogels were visible in the treated animals. These hydrogels were found to significantly reduce postsurgical adhesions in a

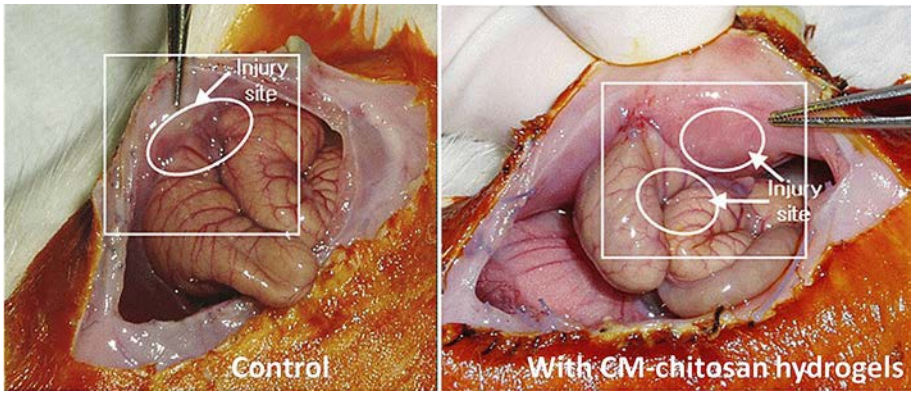

FIG. 10.18. Effect of prevention of intra-abdominal adhesion by CM chitosan hydrogels [10.95].

rat caecal abrasion model. The results are quite promising, with both materials decreasing significantly the degree of adhesion.

10.7.4. Microbial cellulose membrane for guided bone regeneration

Bone grafts and guided bone regeneration (GBR) are needed when a part of the body has a missing bone. A missing portion of bone is frequently called a bony defect. Examples of jaw bone defects are: defects surrounding roots of teeth (periodontal defects); defects which occur following tooth extraction; generalized decrease in quantity of jaw bone from trauma or long term tooth loss; defects surrounding dental implants; and defects resulting from cyst or tumour surgery. It is known that bone heals more slowly than gum tissues. Without GBR techniques, the faster healing gum would prevent the bone from maximizing its full healing potential following surgical procedures, as shown in Fig. 10.19. The concept of treatment is simple. A biocompatible membrane is placed between the gum and bone which acts as a barrier. This barrier prevents downgrowth of the gum into the underlying bone as it heals. Oftentimes, a bone graft is placed into the underlying bony irregularities, under the membrane, to help the body grow new bone. Membranes around teeth are typically designed to dissolve away, or resorb, after several weeks of healing have passed. The materials that are used as a barrier membrane for GBR procedures should meet several prerequisites. As the membrane is supposed to be implanted in the body, it must be biocompatible,

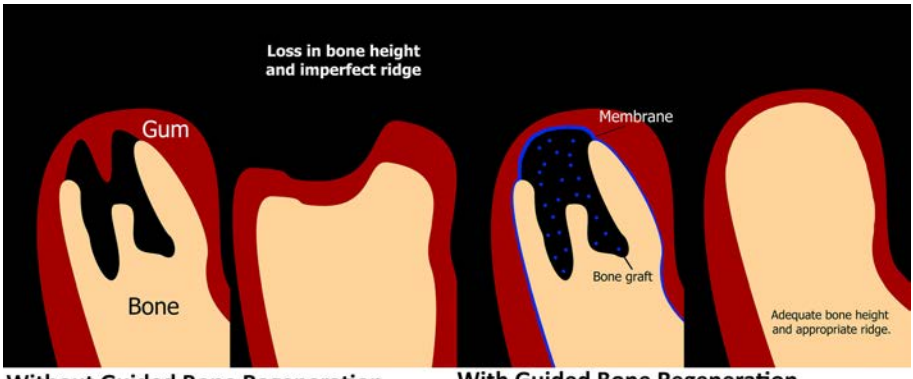

FIG. 10.19. The effect of GBR membrane for restorative dental work.

non-immunogenic and non-toxic. As avoiding the removal of the membrane after healing would be advantageous, it would be better if it were composed of biodegradable materials. The degradation time should be long enough to achieve bone regeneration before membrane disintegration. There are various commercially available products, ranging from non-resorbable materials, such as expanded polytetrafluorethylene, to bioabsorbable membranes composed of poly(lactic) acid (PLA), poly(glycolic acid), polyurethane, and so on [10.96].

An initial study on irradiated microbial cellulose membrane for possible use in GBR has been conducted in Indonesia [10.97]. Microbial cellulose is a natural polymer derived from the fermentation of *Acetobacter xylinum* in a specific growth medium. An edible gel commonly known as nata de coco is a type of MC produced by *Acetobacter xylinum* using coconut water as the micronutrient medium. It is easily produced in a variety of shapes and as a membrane, gel or film. The gamma irradiation of microbial cellulose produces two effects, sterilization and degradation. The TS results of irradiated microbial cellulose reveal a decreasing trend with time (within weeks), a property needed for an ideal GBR membrane. The pore size of irradiated microbial cellulose is far below the size of pores of soft tissue (2–15 μm), which makes it possible to use this membrane as a physical barrier for tissue invasion. Because of these properties, microbial cellulose may be used as scaffolds in GBR.

10.7.5. PVA/PVP/chitosan polymer-hydroxyapatite composite as bone substitute

Bone grafts are bone that is transplanted from one area of the skeleton to another to promote healing, strengthen bones or improve function. Bone or bone-like materials used in bone grafts may be transplanted directly from one area of an individual's skeleton to another (autografts) or from a donor (allografts) or from an artificial source. In many cases, they are used to fill in an empty space that may have been created in or between the bones by disease, injury or deformity. While the use of allograft bone has become quite common, it has some limitations due to the chance of disease transmission, and lessened effectiveness since the bone growth cells and proteins are removed during the cleansing and disinfecting process. Owing to this drawback, researchers are looking for materials that can substitute the bone. Some of these bone graft alternatives include: demineralized bone matrix containing collagen, proteins and growth factors that are extracted from the allograft bone, ceramics, coral, graft composites (combination of demineralized bone matrix and ceramics), bone morphogenetic proteins and alloplastic grafts made from hydroxylapatite (a naturally occurring mineral that is also the main mineral component of bone). Hydroxylapatite is a synthetic bone graft, which is now, like other synthetics, commonly used owing

to its osteoconduction (a three dimensional scaffold or matrix facilitating bone repair), hardness and acceptability by bone. However, the lack of mechanical properties (brittleness) and osteoinduction (acceleration of new bone formation by chemical means) limits its clinical use. Often, a combination of ceramic and polymer materials is exploited to augment bone integration of the graft material and the native host tissue e.g. poly-ε-caprolactone (PCL)-grafted hydroxyapatite nanocrystals [10.98].

To improve the mechanical and osteoinduction properties of hydroxylapatite, Indonesian researchers are developing a synthetic bone graft composite made up of irradiated PVA-PVP–chitosan polymer and hydroxylapatite [10.99]. The presence of chitosan may improve osteoinduction, whereas the elasticity of the PVA-PVP polymer may improve its mechanical properties. The resulting composite is an injectable type of synthetic bone substitute with a gel fraction of around 0.35, which can flow through a syringe. The hydroxyapatite has a particle size of 50–300 nm and is distributed homogenously in suspension. This may be applied in orthopaedic and periodontal surgeries, especially for non-invasive techniques.

10.7.6. Radiation processed natural polymers for stimuli responsive hydrogels

A small number of studies on radiation processed stimuli responsive natural polymer hydrogels have been carried out. Most of them are synthesized as grafted natural polymers. A new pH and temperature responsive hydrogel based on the chitosan grafted with PAAc, PVA, PHPMA and gelatin was developed for oral drug delivery using oxttetracycline as a model drug [10.100]. NIPAAm alginate was synthesized and showed temperature sensitivity in the release of the model drug IMC (1-[p-chlorobenzoyl]5-methanoyl-2-methylindole-3-acetic acid) [10.100]. Non-irritant bioadhesive drug release systems based on starch– AAc graft copolymers prepared by the irradiation of starch and AAc has been studied for the release of model drug theophylline (TPL) [10.101]. Hydrogels from grafted natural polymers are prepared by first dissolving the natural polymer in an appropriate solvent or by forming a film. The synthetic monomers/polymers are then added into the solution or film and irradiated at a certain dose. Drug release (antibiotic drug amoxicillin) assays from new chitosan/pHEMA membranes has also been studied [10.102]. The synthesis of AAc/chitosan hydrogels by the polymerization of AAc in the presence of chitosan has been reported to release 5-fluorouracil (5-FU, a model antimetabolic drug) using simulated gastric fluid and simulated intestinal fluid at a constant temperature of 25°C [10.103]. Figure 10.20 shows the swelling behaviour at different pH levels and the in vitro 5-FU release profiles of this hydrogel.

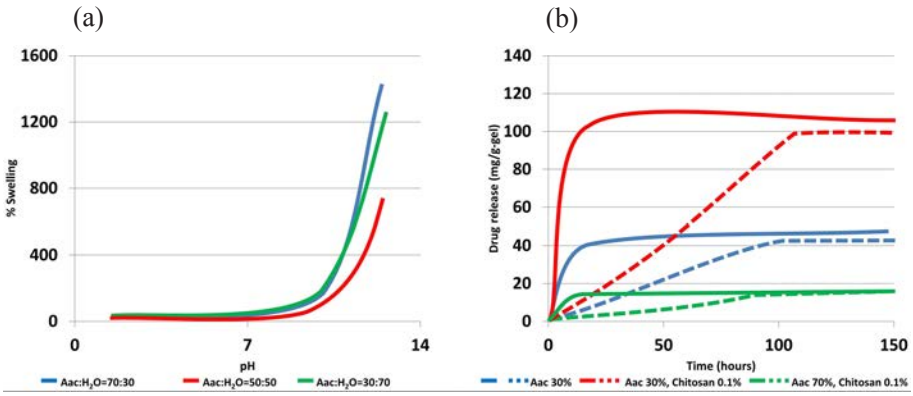

FIG. 10.20. (a) Swelling behaviour of AAc/chitosan hydrogel as a function of pH (0.1 wt % chitosan, temperature = 25°C; radiation dose = 30 kGy); (b) In vitro 5-FU release profiles of AAc/chitosan hydrogels in simulated gastric fluid (broken lines) and simulated intestinal fluid (solid lines) (radiation dose = 30 kGy).

10.8. CONCLUSION

Many of the possible medical and healthcare applications of radiation processed natural polymers mentioned in this chapter are still in the developmental stage. It may still take a long way to have these products reach the market with all the difficulties posed by passing from one stage to another, from in vitro testing to animal testing to clinical trials and obtaining the final approval from the appropriate authorities. However, intense efforts have been made to overcome these difficulties. The search for new and novel applications of these materials continues. It is hoped that these radiation processed natural polymers and products will soon be commercially and competitively available as alternatives to established products.

REFERENCES TO CHAPTER 10

[10.1] WILLIAMS, D.F., "Biofunctionality and biocompatibility", Materials Science and Technology, Medical and Dental Materials, Vol. 14, VCH Publishers, New York (1992).

[10.2] ROSIAK, J.M., ULANSKI, I.P., PAJEWSKI, L.A., YOSHII, F., MAKUUCHI, K., Radiation formation of hydrogels for biomedical purposes. Some remarks and comments, Radiat. Phys. Chem. **46** (1995) 161–168.

[10.3] WICHTERLE, O., LIM, D., Hydrophilic gels for biological use, Nat. **185** (1960) 117–118.

[10.4] KAETSU, I., Immobilization of biofunctional substances, Radiat. Phys. Chem. **18** 1–2 (1981) 343–356.
[10.5] HOFFMAN, A.S., A review of the use radiation plus chemical and biochemical processing treatments to prepare novel biomaterials, Radiat. Phys. Chem. **18** 1–2 (1981) 323–342.
[10.6] INTERNATIONAL ATOMIC ENERGY AGENCY, Radiation Synthesis and Modification of Polymers for Biomedical Applications, IAEA-TECDOC-1324, IAEA, Vienna (2002).
[10.7] ROSIAK, J.M., "Hydrogel dressings", Radiation Effects on Polymers, American Chemical Society, Washington, D.C., (1991) 271–299.
[10.8] ROSIAK, J., RUCINSKA-RYBUS, A., PEKALA, W., Method of Manufacturing Hydrogel Dressings, US Patent No. 4,871,490, Polish Patent No. 151,581, Hungarian Patent No. 204,866, UK Patent No. 2,200,643, German Patent No. 3,744,289, Oct. 1989, filed Dec. 1987.
[10.9] HAJI-SAEID, M., SAMPA, M.H., RAMAMOORTHY, N., GÜVEN, O., CHMIELEWSKI, A.G., The role of IAEA in coordinating research and transferring technology in radiation chemistry and processing of polymers, Nucl. Instrum. Meth. B **265** 1 (2007) 51–57.
[10.10] ULANSKI, P., ZAINUDDIN, Z., ROSIAK, J.M., Pulse radiolysis of poly(ethylene oxide) in aqueous solution. I. Formation of macroradicals, Radiat. Phys. Chem. **46** 4–6 (1995) 917–920.
[10.11] ULANSKI, P., BOTHE, E., ROSIAK, J.M., VON SONNTAG, C., OH-radical-induced crosslinking and strand breakage of poly(vinyl alcohol) in aqueous solution in the absence and presence of oxygen. A pulse radiolysis and product study, Macromol. Chem. Phys. **195** 4 (1994) 1443–1461.
[10.12] ROSIAK, J.M., YOSHII, F., Hydrogels and their medical applications, Nucl. Instrum. Meth. B **151** 1–4 (1999) 56–64.
[10.13] JANIK, I., ULANSKI, P., ROSIAK, J.M., Pulse radiolysis of poly(vinyl methyl ether) in aqueous solution, Formation and structure of primary radicals, Nucl. Instrum. Meth. B **151** 1(1999) 318–323.
[10.14] ROSIAK, J.M., YOSHII, F., Hydrogels and their medical applications, Nucl. Instrum. Meth. B **151** 1–4 (1999) 56–64.
[10.15] ROSIAK, J., et al., "Radiation formation of hydrogels for biomedical application", Radiation Synthesis and Modification of Polymers for Biomedical Applications, IAEA-TECDOC-1324, IAEA, Vienna (2002).
[10.16] ROSIAK, J.M., OLEJNICZAK, J., Medical applications of radiation formed hydrogels, Radiat. Phys. Chem. **42** 4–6 (1993) 903–906.
[10.17] ULANSKI, P., BOTHE, E., HILDENBRAND, K., ROSIAK, J.M., VON SONNTAG, C., Hydroxyl-radical-induced reactions of poly (acrylic acid); a pulse radiolysis, EPR and product study. Part II. Oxygenated aqueous solutions, J. Chem. Soc. Perkin Trans. II **1** (1996) 23–28.
[10.18] ISILDAR, M., SCHUCHMANN, M.N., SCHULTE-FROHLINDE, D., VON SONNTAG, C., Oxygen uptake in the radiolysis of aqueous solutions of nucleic acids and their constituents, Int. J. Radiat. Biol. **41** 5 (1982) 525–533.

[10.19] ROSIAK, J.M., Gel/sol analysis of irradiated polymers, Radiat. Phys. Chem. **51** 1 (1998) 13–17.
[10.20] OLEJNICZAK, J., ROSIAK, J., CHARLESBY, A., Gel/dose curves for polymers undergoing simultaneous cross-linking and scission, J. Radiat. Phys. Chem. **38** 1 (1991) 113–118.
[10.21] ABAD, L., RELLEVE, L., ARANILLA, C., DELA ROSA, A., Properties of radiation synthesized PVP-kappa carrageenan hydrogel blends, Radiat. Phys. Chem. **68** 5 (2003) 901–908.
[10.22] LIU, P., ZHAI, M., LI, J., PENG, J., WU, J., Radiation preparation and swelling behavior of sodium carboxymethyl cellulose hydrogels, Radiat. Phys. Chem. **63** 3–6 (2002) 525–528.
[10.23] FEI, B., WACH, R.A., MITOMO, H., YOSHII, F., KUME, T., Hydrogel of biodegradable cellulose derivatives I. Radiation-induced crosslinking of CMC, J. Appl. Polym. Sci. **78** 2 (2000) 278–283.
[10.24] NAGASAWA, N., YAGI, T., KUME, T., YOSHII, F., Radiation crosslinking of carboxymethyl starch, Carbohydr. Polym. **58** 2 (2004) 109–113.
[10.25] ZHAO, L., MITOMO, H., NAGASAWA, N., YOSHII, F., KUME, T., Radiation synthesis and characteristic of the hydrogels based on carboxymethylated chitin derivatives, Carbohydr. Polym. **51** 2 (2003) 169–175.
[10.26] ARANILLA, C., NAGASAWA, N., BAYQUEN, A., DELA ROSA, A., Synthesis and characterization of carboxymethyl derivatives of kappa-carrageenan, Carbohydr. Polym. **87** 2 (2012) 1810–1816.
[10.27] PETZOLD, K., SCHWIKAL, K., HEINZE, T., Carboxymethyl xylan—synthesis and detailed structure characterization, Carbohydr. Polym. **64** 2 (2006) 292–298.
[10.28] VARSHNEY, V.K., et al., Carboxymethylation of α-cellulose isolated from Lantana camara with respect to degree of substitution and rheological behaviour, Carbohydr. Polym. **63** 1 (2006) 40–45.
[10.29] JUN-LI Ren, RUN-CANG Sun, FENG Peng, Carboxymethylation of hemicelluloses isolated from sugarcane bagasse, Polym. Degrad. Stab. **93** 4 (2008) 786–793.
[10.30] DE ABREU, F., FILHO, S., Characteristics and properties of carboxymethylchitosan, Carbohydr. Polym. **75** 2 (2009) 214–221.
[10.31] HEINZE, T., ERLER, U., NEHLS, I., KLEMM, D., Determination of the substituent pattern of heterogeneously and homogeneously synthesized carboxymethyl cellulose by using high-performance liquid chromatography, Angew. Makromol. Chem. **215** 1 (1994) 93–106.
[10.32] HEINZE, T., PFEIFFER, K., LIEBERT, T., HEINZE, U., Effective approaches for estimating the functionalization pattern of carboxymethyl starch of different origin, Starch/Stärke **51** 1 (1999) 11–16.
[10.33] BAAR, A., KULICKE, W.-M., SZABLIKOWSKI, K., KIESEWETTER, R., Nuclear magnetic resonance spectroscopic characterization of carboxymethylcellulose, Macromol. Chem. Phys. **195** 5 (1994) 1483–1492.
[10.34] BACH TUYET, L.T., IIYAMA, K., NAKANO, J., Preparation of carboxymethyl cellulose from refiner mechanical pulp. IV. Analyses of carboxymethylated polysaccharides by the use of proton-NMR, Mokuzai Gakkaishi **31** 1 (1985) 14–19.

[10.35] ARANILLA, C., Synthesis and Radiation Crosslinking of Carboxymethyl-k-Carrageenan for Development of Hydrogels for Various Potential Applications, MS Thesis, Univ. Santo Tomas, Philippines (2008).
[10.36] ZHAI, M., et al., Laser photolysis of carboxymethylated chitin derivatives in aqueous solution. Part 2. Reaction of OH• and SO4•- radicals with carboxymethylated chitin derivatives, Biomacromol. **5** 2 (2004) 458–462.
[10.37] WACH, R., et al., Rate constants of reactions of carboxymethylcellulose with hydrated electron, hydroxyl radical and the decay of CMC macroradicals. A pulse radiolysis study, Polymer **45** 24 (2004) 8165–8171.
[10.38] KONO, K., KIMURA, S., IMANISHI, Y., pH-responsive permeability of polyamide capsule membrane coated with lipid molecules and amphiphilic polypeptides, J. Membr. Sci. **58** 1 (1991) 1–9.
[10.39] MITSUMATA, T., SUEMITSU, Y., FUJII, K., FUJII, T., TANIGUCHI, T., KOYAMA, K., pH-response of chitosan, κ-carrageenan, carboxymethyl cellulose sodium salt complex hydrogels, Polymer **44** 23 (2003) 7103–7111.
[10.40] GYENES, T., TORMA, V., GYARMATI, B., ZRINYI, M., Synthesis and swelling properties of novel pH-sensitive poly(aspartic acid) gels, Acta Biomat. **4** 3 (2008) 733–744.
[10.41] CHEN, J., LIU, M., CHEN, S., Synthesis and characterization of thermo- and pH-sensitive kappa-carrageenan-g-poly(methacrylic acid)/poly(N,N-diethylacrylamide) semi-IPN hydrogel, Mater. Chem. Phys. **115** 1 (2009) 339.
[10.42] SABOKTAKIN, M., MAHARRAMOV, A., RAMAZANOV, M., pH-sensitive starch hydrogels via free radical graft copolymerization, synthesis and properties, Carbohydr. Polym. **77** 3 (2009) 634–638.
[10.43] SHANG, J., SHAO, Z., CHEN, X., Chitosan-based electroactive hydrogel, Polymer **49** 25 (2008) 5520–5525.
[10.44] JU, H., KIM, S., LEE, Y., pH/temperature-responsive behaviors of semi-IPN and comb-type graft hydrogels composed of alginate and poly(N-isopropylacrylamide), Polymer **42** 16 (2001) 6851–6857.
[10.45] KARLSSON, J.O., GATENHOLM, P., Cellulose fibre-supported pH-sensitive hydrogels. Polymer **40** 1 (1999) 379–387.
[10.46] LYON, L.A., DEBORD, J.D., DEBORD, S.B., JONES, C.D., McGRATH, J.G., SERPE, M.J., Microgel colloidal crystals. J. Phys. Chem. B **108** 50 (2004) 19099.
[10.47] WU, C., ZHOU, S.Q., Laser light scattering study of the phase transition of poly(N-isopropylacrylamide) in water. 1. Single chain, Macromolecules **28** 24 (1995) 8381–8387.
[10.48] WINNIK, F.M., Phase transition of aqueous poly(N-isopropylacrylamide) solutions: a study by non-radiative energy transfer, Polymer **31** 11 (1990) 2125–2134.
[10.49] CHEE, C.K., RIMMER, S., SOUTAR, I., SWANSON, L., Time-resolved fluorescence anisotropy studies of the temperature-induced intramolecular conformational transition of poly(N-isopropylacrylamide) in dilute aqueous solution, Polymer **38** 2 (1997) 483–486.

[10.50] ANNAKA, M., et al., Fluorescence study on the swelling behavior of comb-type grafted poly(N-isopropylacrylamide) hydrogels, Macromolecules **35** (2002) 8173–8179.
[10.51] KANAZAWA, H., et al., Temperature-responsive chromatography using poly(N-isopropylacrylamide)-modified silica, Anal. Chem. **68** 1 (1996) 100–105.
[10.52] WEI, H., YANG, Z., ZHENG, L., SHEN, Y., Thermosensitive hydrogels synthesized by fast Diels–Alder reaction in water, Polymer **50** 13 (2009) 2836–2840.
[10.53] WANG, Z., et al., In situ formation of thermosensitive P(NIPAAm-co-GMA)/PEI hydrogels, React. Funct. Polym. **69** 1 (2009) 14–19.
[10.54] LIU, Y.Y., SHAO, Y.H., LU, J., Preparation, properties and controlled release behaviors of pH-induced thermosensitive amphiphilic gels, Biomater. **27** 21 (2006) 4016–4024.
[10.55] YIN, X., HOFFMAN, A.S., STAYTON, P.S., Poly(N-isopropylacrylamide-copropylacrylic acid) copolymers that respond sharply to temperature and pH, Biomacromol. **7** 5 (2006) 1381–1385.
[10.56] ZHANG, J., BHAT, R., JANDT, K., Temperature-sensitive PVA/PNIPAAm semi-IPN hydrogels with enhanced responsive properties, Acta Biomater. **5** 1 (2009) 488–497.
[10.57] ZHANG, J., XU, X., WU, D., ZHANG, X., ZHUO, R., Synthesis of thermosensitive P(NIPAAm-co-HEMA)/cellulose hydrogels via "click" chemistry, Carbohydr. Polym. **77** 3 (2009) 583–589.
[10.58] LIU, W., et al., A rapid temperature-responsive sol–gel reversible poly(N-isopropylacrylamide)-g-methylcellulose copolymer hydrogel, Biomater. **25** (2004) 3005–3012.
[10.59] CHEN, L., DONG, J., DING, Y.M., HAN, W.J., Swelling and mechanical properties of a temperature-sensitive dextran hydrogel and its bioseparation applications, J. Appl. Polym. Sci. **206** 19 (2005) 2435–2441.
[10.60] LI, X., WU, W., LIU, W., Synthesis and properties of thermo-responsive guar gum/poly(N-isopropylacrylamide) interpenetrating polymer network hydrogels, Carbohydr. Polym. **71** 3 (2008) 394–402.
[10.61] CHEN, J., et al., Preparation and characterization of a novel IPN hydrogel memberane of poly(N-isopropylacrylamide)/carboxymethyl chitosan (PNIPAAm/CMCS), Radiat. Phys. Chem. **76** 8–9 (2007) 1425–1429.
[10.62] MASCI, G., BONTEMPO, D., CRESCENZI, V., Synthesis and characterization of thermoresponsive N-isopropylacrylamide/methacrylated pullulan hydrogels, Polymer **43** 20 (2002) 5587–5593.
[10.63] MU, Q., FANG, Y., Preparation of thermosensitive chitosan with poly(N-isopropylacrylamide) side at hydroxyl group via O-maleoyl-N-phthaloyl-chitosan (MPCS), Carbohydr. Polym. **72** 2 (2008) 308–314.
[10.64] OKANO, T., Biorelated Polymers and Gels, Academic Press, New York (1962).
[10.65] ROSIAK, J.M., OLEJNICZAK, J., Medical applications of radiation formed hydrogels, Radiat. Phys. Chem. **42** 4–6 (1993) 903–906.
[10.66] ROSIAK, J.M., KOWALSKI, A., DEC, W., Drug delivery system for the treatment of endometrial carcinoma, Radiat. Phys. Chem. **52** 1–6 (1998) 307–311.

[10.67] KAETSU, I., "The use of radiation processing to prepare biomaterials for applications in medicine", Radiation Synthesis and Modification of Polymers for Biomedical Applications, IAEA-TECDOC-1324, IAEA, Vienna (2002).

[10.68] CHEN, J., RONG, L., LIN, H., XIAO, R., WU, H., Radiation synthesis of pH-sensitive hydrogels from β-cyclodextrin-grafted PEG and acrylic acid for drug delivery, Mater. Chem. Phys. **116** 1 (2009) 148–152.

[10.69] SINGH, B., KUMAR, S., Synthesis and characterization of psyllium-NVP based drug delivery system through radiation crosslinking polymerization, Nucl. Instrum. Meth. B **266** 15 (2008) 3341–3500.

[10.70] ZHANG, Y., et al., Radiation synthesis of poly[(dimethylaminoethyl methacrylate)-co-(diallyl dimethyl ammonium chloride)] hydrogels and its application as a carrier for notoginsenoside delivery, Eur. Polym. J. **42** 11 (2006) 2959–2967.

[10.71] MASHAK, A., TAGHIZADEH, S., In vitro progesterone release from γ-irradiated cross-linked polydimethylsiloxane, Radiat. Phys. Chem. **75** 2 (2006) 229–235.

[10.72] ALI SAID, A., Radiation synthesis of interpolymer polyelectrolyte complex and its application as a carrier for colon-specific drug delivery system, Biomater. **26** 15 (2005) 2733–2739.

[10.73] MARTELLINI, F., et al., Thermally reversible gels based on acryloyl-l-proline methyl ester as drug delivery systems, Radiat. Phys. Chem. **55** 2 (1999) 185–192.

[10.74] NHO, Y., PARK, S., KIM, H., HWANG, T., Oral delivery of insulin using pH-sensitive hydrogels based on polyvinyl alcohol grafted with acrylic acid/methacrylic acid by radiation, Nucl. Instrum. Meth. B **236** 1–4 (2005) 283–288.

[10.75] SILVER, F., DOILLON, C., Biocompatibility: Interactions of Biological and Implantable Materials, Vol. 1, VCH Publishers, New York (1989).

[10.76] MAOLIN, Z., HONGFEI, H., YOSHII, F., MAKUUCHI, K., Effect of kappa-carrageenan on the properties of poly(*N*-vinyl pyrrolidone) / kappa-carrageenan blend hydrogel synthesized by *γ*-radiation technology, Radiat. Phys. Chem. **57** 3–6 (2000) 459–464.

[10.77] VARSHNEY, L., Role of natural polysaccharides in radiation formation of PVA–hydrogel wound dressing, Nucl. Instrum. Meth. B **255** 2 (2007) 343–349.

[10.78] ABAD, L., RELLEVE, L., ARANILLA, C., BISNAR, C., DELA ROSA, A., "Philippine country report", paper presented at the IAEA RCA RAS 8106 Project Planning Mtg on Radiation Processing Applications for Health and the Environment, Bangkok, 2007.

[10.79] ABAD, L., DELA ROSA, A., Polyvinylpyrrolidone-Carrageenan Hydrogel, Philippine Patent No. 1-2000-02471, Mar. 17, 2003, filed Sep. 7, 2000; copies available at the Philippine Patent Office.

[10.80] KEWSUWAN, P., PONGPAT, S., PRASATSRISUPAB, J., "Thailand country report", paper presented at the IAEA/RCA Project Final Technical Review Mtg for RAS/8/106 on Radiation Processing Applications for Health and the Environment, Daejeon, Republic of Korea, 2009.

[10.81] PARK, K., NHO, Y., Preparation and characterization by radiation of hydrogels of PVA and PVP containing Aloe Vera, J. Appl. Polym. Sci. **91** 3 (2004) 1612–1618.

[10.82] BHARDWAJ, Y., "Indian country report", paper presented at the IAEA/RCA Project Final Technical Review Mtg for RAS/8/106 on Radiation Processing Applications for Health and the Environment, Daejeon, Republic of Korea, 2009.
[10.83] TAMADA, M., "Applications of naturally occurring polymers modified by radiation crosslinking in Japan", report presented at the IAEA RCA (RAS8/096) Mt on Modification of Natural Polymers through Radiation Processing, Quezon City, 2004.
[10.84] DAHLAN, K., HASHIM, K., MING, T., "Malaysian country report", paper presented at the IAEA/RCA Project Final Technical Review Meeting for RAS/8/106 on Radiation Processing Applications for Health and the Environment, Daejeon, Republic of Korea, 2009.
[10.85] TAMADA, M., SEKO, N., YOSHII, F., Application of radiation-graft material for metal adsorbent and crosslinked natural polymer for healthcare product, Radiat. Phys. Chem. **71** (2004) 221–225.
[10.86] HEMVICHIAN, K., "Thailand country report", paper presented at the Mid-Term Review Mtg of RAS/8/109 on Supporting Radiation Processing of Polymeric Materials for Agricultural Applications and Environmental Remediation, Kuala Lumpur, 2010.
[10.87] ELDER, J., et al., Antibiotics and surgery for vesicoureteric reflux: a meta-analysis of randomised controlled trials, J. Urol. **157** 5 (1997) 1846–1851.
[10.88] BISNAR, C., et al., Experimental study on a new bioimplant for endoscopic treatment of vesicoureteral reflux: Chitosan – polyvinyl pyrolidone (PVP) copolymer implanted subcutaneously in rat abdomen in comparison with dextranomer / hyaluronic acid copolymer (Deflux), Philipp. J. Urol. **17** (2007) 53–63.
[10.89] ABAD, L., RELLEVE, L., ARANILLA, C., DELA ROSA, A., "Philippine country report", paper presented at the IAEA/RCA Mid-term Progress Meeting of RAS/8/106 on Radiation Processing Applications for Health and the Environment, Manila, 2008.
[10.90] FURUKAWA, H., et al., Enhanced TARC production by dust-mite allergens and its modulation by immunosuppressive drugs in PBMCs from patients with atopic dermatitis, J. Dermatol. Sci. **35** 1 (2004) 35–42.
[10.91] QI, X., et al., Effects of *Bambusae caulis* in Liquamen on the development of atopic dermatitis-like skin lesions in hairless mice, J. Ethnopharmacol. **123** 2 (2009) 195–200.
[10.92] LIM, Y., et al., Preparation of hydrogels for atopic dermatitis containing natural herbal extracts by gamma-ray irradiation, Radiat. Phys. Chem. **78** 7–8 (2009) 441–444.
[10.93] SHIN, J., LIM, Y., NHO, Y., "Preparation of hydrogels for atopic dermatitis containing natural herbal extracts by gamma-ray irradiation and studies on their biological activities", Republic of Korea country report, paper presented at the IAEA/RCA Project Final Technical Review Mtg for RAS/8/106 on Radiation Processing Applications for Health and the Environment, Daejeon, Republic of Korea, 2009.
[10.94] NHO, Y., LEE, J., Reduction of postsurgical adhesion formation with hydrogels synthesized by radiation, Nucl. Instrum. Meth. B **236** 1–4 (2005) 277–282.
[10.95] NHO, Y., "Progress of Biomaterials Processing by Radiation in [the Republic of] Korea, Country Report", paper presented at the IAEA/RCA Mid-term Progress Mtg of

RAS/8/106 on Radiation Processing Applications for Health and the Environment, Manila, 2008.

[10.96] PARK, J., et al., Guided bone regeneration by poly(lactic-co-glycolic acid) grafted hyaluronic acid bi-layer films for periodontal barrier applications, Acta Biomater. **5** 9 (2009) 3394–3403.

[10.97] DARWIS, D., "Indonesian country report", paper presented at the IAEA/RCA Project Final Technical Review Mtg for RAS/8/106 on Radiation Processing Applications for Health and the Environment, Daejeon, Republic of Korea, 2009.

[10.98] NGIAM, M., et al., Fabrication of nano-hydroxyapatite/collagen/osteonectin composites for bone graft applications, Biomed. Mater. **4** 2 (2009) 4–9.

[10.99] SOKKER, H., ABDEL GHAFFAR, A., GAD, Y., ALY, A., Synthesis and characterization of hydrogels based on grafted chitosan for the controlled drug release, Carbohydr. Polym. **75** 2 (2009) 222–229.

[10.100] LEE, Y., et al., Preparation of alginate/poly(N-isopropylacrylamide) hydrogels using gamma-ray irradiation grafting, Macromol. Res. **12** 3 (2004) 269–275.

[10.101] GERESH, S., et al., Synthesis, characterization and evaluation of IPN hydrogels for antibiotic release, J. Control. Release **94** 2–3 (2004) 391–398.

[10.102] CASIMIRO, M., GIL, M., LEAL, J., Drug release assays from new chitosan/pHEMA membranes obtained by gamma irradiation, Nucl. Instrum. Meth. B **265** 1 (2007) 406–409.

[10.103] SHIM, J., NHO, Y., Preparation of poly(acrylic acid)–chitosan hydrogels by gamma irradiation and in vitro drug release, J. Appl. Polym. Sci. **90** 13 (2003) 3660–3667.

Chapter 11

RECENT DEVELOPMENTS IN SYNTHETIC AND NATURAL POLYMER BASED HYDROGELS

D. TAHTAT, S. BENAMER, A. NACER KHODJA
Department of Irradiation Technology,
Nuclear Research Center of Algiers,
Algiers, Algeria

11.1. INTRODUCTION

Polymer hydrogels are a group of materials that are gaining wide application in many fields, such as pharmacy, medicine and agriculture. During the last four decades, many works dedicated to hydrogel synthesis, characterization, formulation and application have been published.

Hydrogels are defined as three dimensional networks of hydrophilic polymers that can absorb large quantities of water and hold it while maintaining their structure [11.1, 11.2]. In the swollen state, the mass fraction of water in a hydrogel is generally much higher than the mass fraction of the polymer. The ability to swell and the extent of swelling of hydrogels are mainly governed by two factors, namely the hydrophilicity of polymer chains and the density of the cross-linking.

The three dimensional structure of the hydrogel is formed and maintained by junctions that are formed during the gelation process. Gelation is the result of the process in which the chains are connected with each other to form a three dimensional network. This may be formed by covalent bonds, hydrogen bonds, electrostatic interactions, hydrophobic interactions or physical entanglements. Depending on the nature of the cross-links that form the structure of hydrogels, these materials can offer moderate to high physical, chemical and mechanical stability in their swollen state [11.3]. The preparation and characterization of hydrogels was described in more detail in Chapter 10.

There are numerous applications of natural and synthetic hydrogels, in particular in the medical and pharmaceutical sectors. Some of the recent developments in natural and synthetic polymer based hydrogels are summarized below.

11.2. AGRICULTURE APPLICATIONS

The beneficial use of radiation cross-linked hydrogels in agriculture was studied in Egypt [11.4]. A predetermined amount of PAAm/NaAlg hydrogels was added to sandy soil and the water retention improvement within the soil and the growth of broad bean plant was monitored. An increased growth rate of the broad bean planted in PAAm/NaAlg treated soil was observed as compared with plants grown both in soil treated with only PAAm hydrogels and in untreated soil. The authors of Ref. [11.4] reasoned that the PAAm/NaAlg hydrogel, besides increasing water retention, also provides the plant with oligoalginate from the degradation of the hydrogel, thus providing the plant with a growth promoter.

11.3. MEDICAL APPLICATIONS

The development of a synthetic wound dressing that can be used for the treatment of burns, blisters, fissures and herpes labialis is currently a subject of great commercial interest [11.5]. An ideal wound dressing material should have several properties [11.6]. The first commercial synthetic hydrogel wound dressing produced by radiation processing is Aqua-gel [11.7]. It is claimed that this hydrogel is transparent, has over 90% water content, can be used to control drug dosage, offers good handling and owing to radiation processing is fully sterile. An example of a PVA hydrogel is shown in Fig. 11.1.

FIG. 11.1. Hydrogel prepared by radiation processing.

Hydrogels, which are cross-linked hydrophilic polymers, represent an important class of biomaterials in biotechnology and medicine because many hydrogels exhibit excellent biocompatibility, causing minimal inflammatory responses, thrombosis, and tissue damage [11.8]. Various formulations have been developed. A wound dressing needs to be biocompatible and protect the wound from bacterial infection while providing the moisture necessary for healing [11.9–11.11].

It was reported by Benamer et al. [11.12] that microbiological analyses show that no bacteria pass through hydrogels based on PVP during day-by-day observation over 14 days. In Figs 11.2(a) and 11.2(b) the development of bacteria on the upper surface of the gel is shown, but no bacteria colonies were found on the opposite side or deeper in the gel.

The diffusion of the culture medium into the hydrogel is shown by the change in its colouration and by the discolouration of the culture medium that had been in contact with the hydrogel (Fig. 11.2(c)). From these observations it has been concluded that nutrients from the culture medium have diffused through the hydrogel, reached the upper side and have been used by the bacteria for their development. In the absence of culture medium under the gel

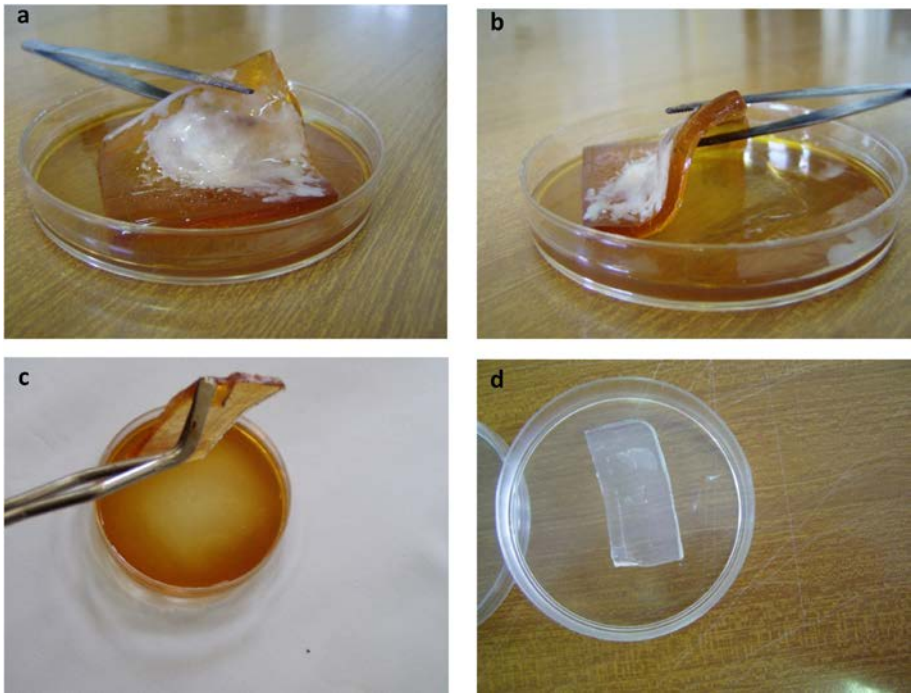

FIG. 11.2. Bacterial development on the surface of the hydrogel after 14 days' incubation.

sample, no bacterial development was observed on the upper surface of the gel (Fig. 11.2(d)). PVP hydrogel seems to be a good barrier against bacteria. So if used as a wound dressing, it assures a good protection to the wound from bacterial infection [11.12].

Hydrogels have been considered to be advantageous as a wound dressing material [11.13]. During the last decade, promising materials for wound dressing have been produced using PVP [11.12, 11.14], poly (vinyl alcohol) [11.10, 11.15], poly (ethylene oxide) [11.16] and polysaccharides such as chitosan, alginate, collagen and cellulose [11.17, 11.18].

A hydrogel produced for wound dressings should have the following properties [11.6, 11.19]:

— Forms an efficient barrier against bacteria, and also for preventing the excessive loss of body fluids;
— Allows the diffusion of oxygen to the wound;
— Soft and elastic, but mechanically strong enough;
— Good adhesion to the wound and to healthy skin, but without a tendency for excessive sticking, enabling a painless removal or exchange of the dressing without disturbing the healing process;
— Transparent, so that the healing process can be monitored without the necessity of removing the dressing;
— Enables an easy treatment of the wound with drugs;
— Absorbs exudates and bacterial toxins;
— Non-antigenic and does not provoke allergic reactions;
— Soothes pain and provides an optimal wound healing environment of constant humidity;
— Sterile, easy to use and not expensive.

Hydrogels have been used as barriers in order to improve healing response following tissue injury, and to deliver bioactive agents such as chitosan that encourage the natural reparation process. The comparative study of a hydrogel based on poly (vinyl alcohol) containing 0.25% of chitosan synthesized by gamma irradiation and evaluated as a wound dressing material in a rat burn model found that the wounds treated with PVA/chitosan hydrogel healed on the 9th day, while those treated with paraffin gauze dressing and cotton gauze (conventional treatment) healed on the 16th day. A histological analysis found that the production of new granulation tissue and epithelialization progressed better in wounds treated with hydrogel PVA/chitosan than in wounds covered with gauze. The determined values of a primary skin irritation test and mucosal membranes irritation test of the PVA/chitosan hydrogel were, respectively 0.5

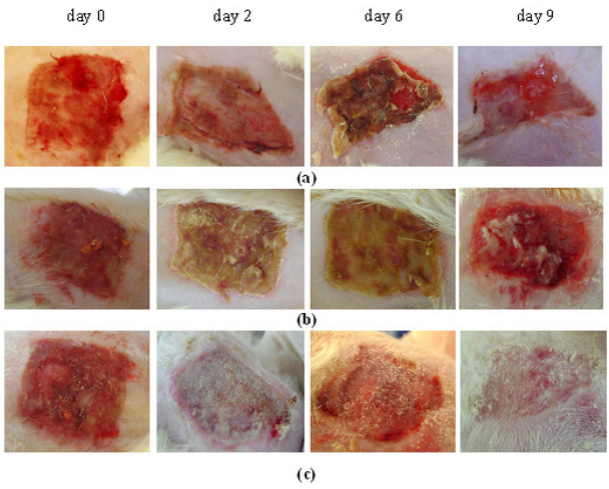

FIG. 11.3. Photographs of the macroscopic appearance of wound repair: (a) in an uncovered wound; (b) in a wound covered with paraffin gauze dressing; and (c) a wound covered with PVA/chitosan at day 0, day 2, day 6 and day 9, respectively.

and 0; these values indicate that PVA/chitosan hydrogel can be considered non-irritating to the skin [11.11].

The macroscopic appearance of the treated and untreated wounds is shown in Fig. 11.3. Two days after the burn, a hard brown scab formed, induced by inflammatory reaction. The scab was excised because it may have constituted a barrier to the chitosan contained in the hydrogel. Two days after the removal of the scab, in the group treated with PVA/chitosan, fibrin had formed (Fig. 11.3(a)); fibrin is an exudate fibrino-leukocytic. The presence of exudates on the wounds is critical as it could delay wound healing and granulation [11.20, 11.21] and therefore the fibrin was removed.

In the group that was treated with paraffin gauze and left untreated, the scab that had been removed two days earlier reformed (Figs 11.3(b) and 11.3(c)), but this did not occur in the group treated with PVA/chitosan (Fig. 11.3(a)) because hydrogel absorbs excess exudates caused by the inflammatory reaction and prevents the reconstruction of a scab, although fibrin was formed. Between day 2 and day 6, there was homogeneous formation of fibrin in the wound treated by PVA/chitosan hydrogel, whereas in the wound treated by paraffin gauze dressing and in the untreated wound (natural healing), fragments of scab (spontaneous detersion of the scab), fibrin and a coagulated area were observed. Between day 6 and day 9, in the untreated group, a light coat of scab persisted in the wound (Fig. 11.3(a)). The group that was treated with paraffin gauze dressing began to show healing and furrows at the level of closure of the wound (Fig. 11.3(b)).

In the group treated with hydrogel PVA/chitosan, full good quality healing was observed [11.11].

After removing the scab, the hydrogel PVA/chitosan is not disruptive to any of the major phases of wound healing — the inflammatory, proliferative and maturation phases — because it can be peeled off easily from the wound when the dressing needs changing, unlike paraffin gauze dressing, which adheres very closely to the wound during dressing changes, causing additional damage to the wound and disturbing healing processes [11.11].

Hydrogel is about 95% water. It has been reported that epidermal cells migrate more easily over a wet wound area than under a scab in dry wounds [11.22]. Paraffin gauze dressings and a lack of dressings produce a dry environment. Epidermal cells can migrate at a speed of about 0.5 mm/day over a moist wound surface, which is twice as fast as under a scab in dry wounds [11.23]. Chitosan molecules induce migration and enhance the functions of inflammatory cells, such as polymorphonuclear leukocytes, macrophages and fibroblasts, which are activated to produce multiple cytokines [11.24–11.26].

Figure 11.4 shows photographs of healing wound quality. Homogenous formation of the skin with a very good healing quality can be observed on day 12 (Fig. 11.4(c)), whereas on the 16th a furrow at the level of closure of the wound can be seen in groups untreated and treated with paraffin gauze, and a scar was caused (Figs 11.4(a), 11.4(b)) [11.11].

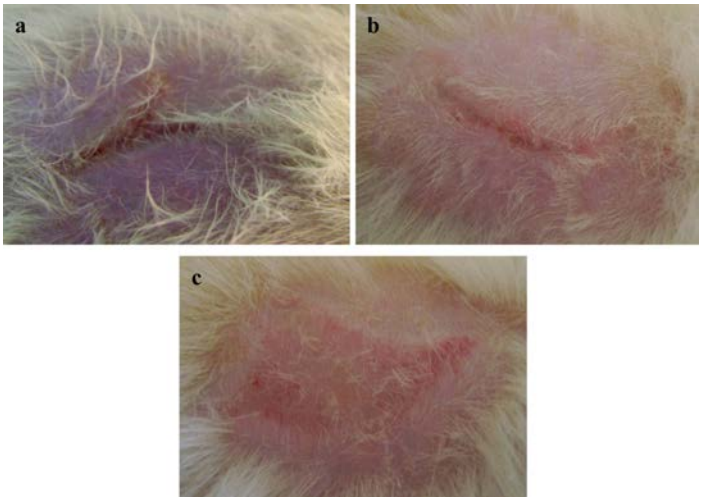

FIG. 11.4. Photographs showing the typical cicatrization wound: (a) control (untreated) on the 16th day, (b) paraffin gauze dressing on the 16th day and (c) PVA/chitosan on the 12th day.

Because of its high water absorption capacity and biocompatibility, hydrogel has been also used in drug delivery systems [11.27–11.29], sanitary pads and transdermal systems [11.30, 11.31], dental materials [11.32, 11.33], implants [11.34], injectable polymeric systems [11.35] ophthalmic applications [11.36], hybrid-type organs and stimuli-sensitive systems [11.37], in the purification of wastewater [11.38], as localized drug depots [11.39, 11.40] and for macromolecular drugs [11.41].

Researchers have engineered the physical and chemical properties of hydrogels at the molecular level to optimize their properties, such as permeability (sustained-release applications), enviro-responsive nature (pulsatile release applications), surface functionality (PEG coatings for stealth release), biodegradability (bioresorbable applications), surface biorecognition sites (targeted release and bioadhesion applications) and for controlled drug delivery applications (Fig. 11.5) [11.42].

Environmentally responsive hydrogels have been applied in a wide variety of controlled drug delivery applications. The intelligent response of these systems allows for a release that is controlled by the conditions of the environment [11.42]. Temperature responsive hydrogels have been widely used to create drug delivery systems that exhibit a pulsatile release in response to temperature changes [11.43]. In addition, pH responsive hydrogels have been applied in numerous controlled release applications. For example, pH responsive hydrogels composed of alginate/chitosan gel beads have been applied for the oral delivery of insulin [11.27].

In clinical therapy, insulin is mainly administered via the subcutaneous route, which can be the cause of pain and possible infections and therefore reduced patient compliance; oral delivery of insulin could address these issues. However, several problems are encountered in the development of oral systems for insulin delivery to the blood stream, among which are the degradation of insulin by proteolytic enzymes and the acidic environment in the stomach, and the low penetration of insulin into the blood stream [11.44]. Several methods have been proposed to improve the oral bioavailability and gastrointestinal uptake of a poorly absorbable drug such as insulin. Among these are encapsulation using a hydrogel composed of synthetic or natural polymers, which represents a promising concept. Natural polymers (polysaccharides) are attractive because they are biodegradable, biocompatible, non-toxic and safe. Alginate and chitosan cross-linked by glutaraldehyde have been successfully used [11.27].

Spherical and oval gel beads have been obtained from a NaAlg/chitosan solution at 2%, after the alginate was cross-linked with $CaCl_2$ (Fig. 11.6(a)). The beads were white and opaque after the first step and became light brown because of the cross-linking of chitosan with glutaraldehyde (Fig. 11.6(b)) [11.27].

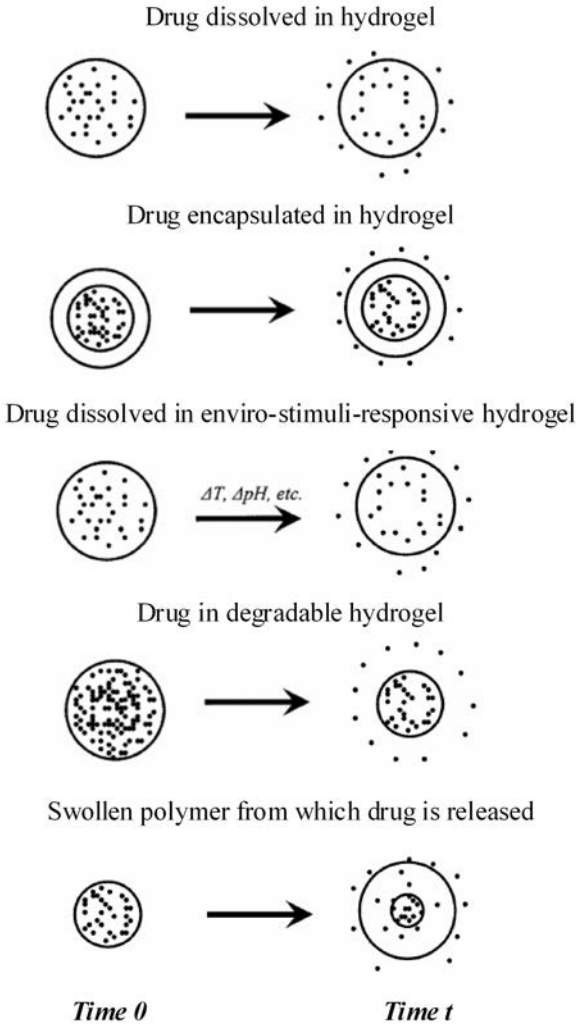

FIG. 11.5. Various delivery and release mechanisms of hydrogels [11.42].

The insulin release behaviour of alginate/chitosan gel beads was studied in simulated gastric fluid and simulated intestinal fluid, and the obtained results are represented in Fig. 11.7. The cumulative release of insulin seems to be proportional to the swelling rate of the beads [11.27]. The cumulative quantity of insulin released in the simulated intestinal fluid was enough to meet glycaemic goals. The alginate/chitosan blend gel beads could be used with a wide range of insulin dosages and at different times of release. Therefore, the investigated alginate/chitosan beads can be considered potential oral insulin carriers [11.27].

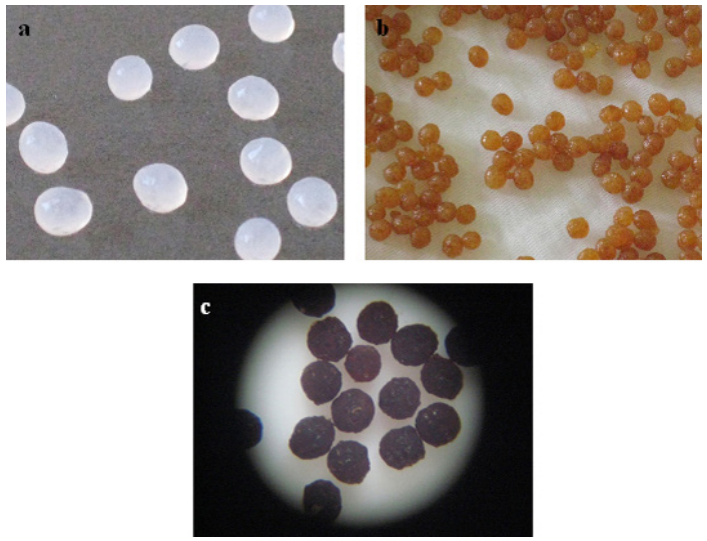

FIG. 11.6. Photographs of the typical gel beads at different steps of their preparation: (a) wet alginate/chitosan gel beads crosslinked with $CaCl_2$, (b) wet alginate/chitosan gel beads cross-linked with glutaraldehyde and (c) dry alginate/chitosan gel beads.

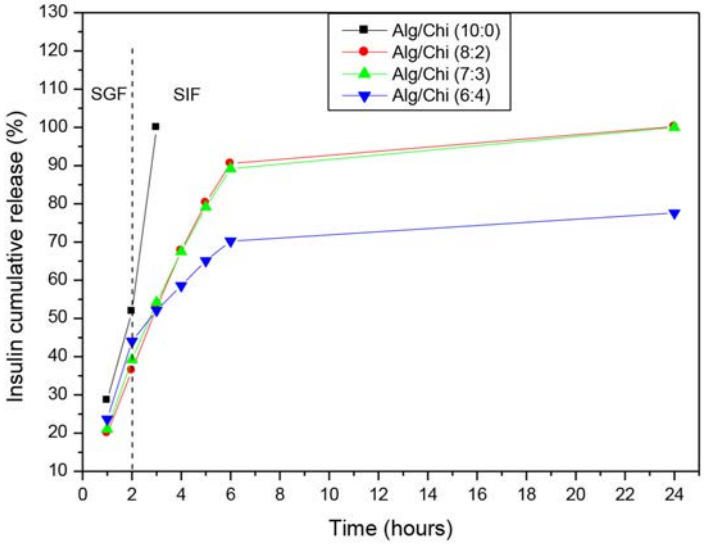

FIG. 11.7. Insulin cumulative release by alginate/chitosan beads over time.

11.4. ENVIRONMENTAL APPLICATIONS

Environmental degradation caused by human activities is a serious problem; enhanced industrial activities are responsible for a large number and amount of pollutants being emitted to the environment. Among these, toxic metal species mobilized from industrial activities and fossil fuel consumption impacts the atmospheric environment as well as water and soil, leading to their degradation [11.45].

Many environmental applications of hydrogels have been investigated. One example is the modification of raw chitosan gel beads by cross-linking with glutaraldehyde to increase their resistance to chemical and biological degradation and introducing, by a radiation grafting reaction, carboxyl groups to increase their sorption capacity. The efficiency of modified and unmodified chitosan gel beads to adsorb cadmium and lead ions, which are considered highly toxic, was investigated [11.46]. Radiation induced grafting of AAc onto chitosan gel beads was performed in solution with gamma rays from a cobalt-60 source. The removal of Pb and Cd ions with grafted chitosan gel beads from aqueous solutions was investigated. The sorption behaviour of the sorbents was examined through pH, kinetics and equilibrium measurements. Grafted chitosan beads presented a higher sorption capacity for metal ions than did unmodified chitosan gel beads [11.46]. The effect of the grafting degree on the sorbent's

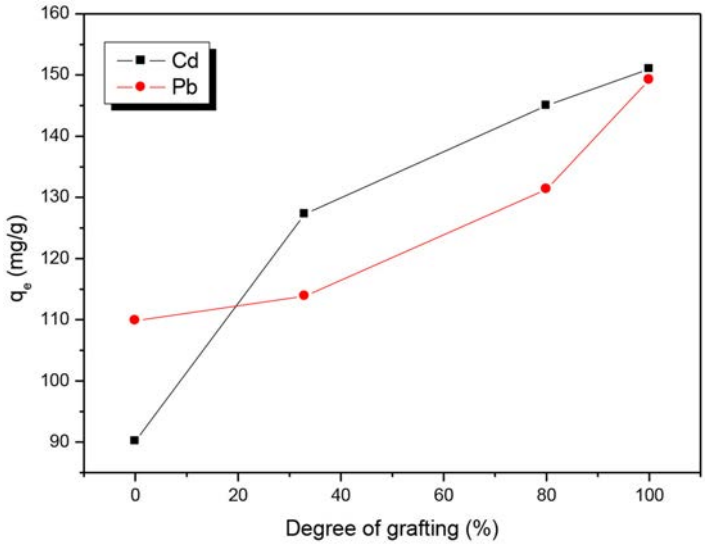

FIG. 11.8. Effect of grafting degree on adsorption capacity of Cd and Pb (initial concentration 200 mg/L, ambient temperature).

capacity to adsorb metal ions, at the same initial concentration (200 mg/L), is shown in Fig. 11.8. The general trend is that, with the increase of grafting rate, the adsorption capacity of the sorbent increases. The difference in the adsorption behaviour against the two metal ions is observed below a 33% grafting rate, where ion uptake is more pronounced for the cadmium than for the lead. Beyond 33% grafting, the adsorption capacity of both metals increased significantly. It is understandable that the increment in the adsorption capacity may be attributed to the increase of carboxylic groups that appear to play an important role in the ability to adsorb metal ions [11.46].

The effect of pH on metal ion removal by chitosan gel and chitosan-AAc gel beads is shown in Fig. 11.9. It was observed that the adsorption capacity of metal ions by chitosan gel and chitosan-AAc gel beads was almost constant over a wide pH range, though the adsorption was lower at pH3 for chitosan gel beads and almost zero for chitosan-AAc gel beads. The amino groups of chitosan gel beads are protonated in acidic pH values, which renders the sorbent positively charged. Owing to the positive charge of metal, strong coulombic repulsions are developed between them. At a higher pH of the solution, the amino groups of the sorbent are deprotonated, the repulsive forces weaken and the metal uptake increases. Chitosan becomes strongly anionic after grafting with AAc. On increasing the pH of the solution, deprotonation of the chitosan-AAc gel bead derivative is realized, and strong attractive forces between the positively charged metal and the negatively charged chitosan gel beads result in high metal ion uptake [11.46].

Hydrogel from cross-linked polyacrylamide (PAAm)/GG graft copolymers for the sorption of hexavalent chromium ions has been applied as a sorbent

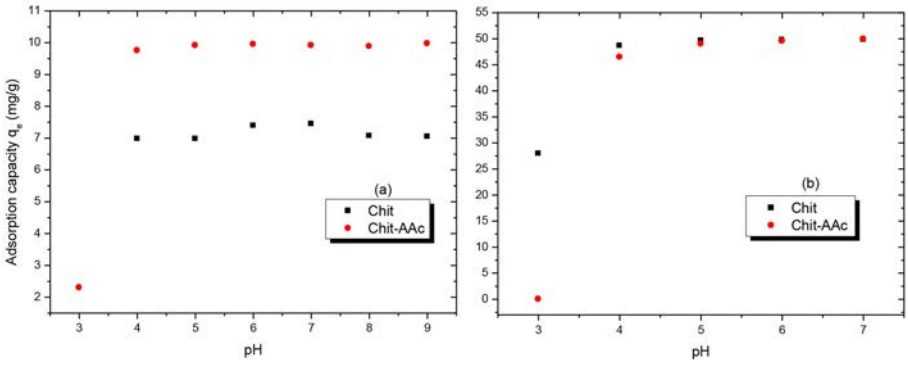

FIG. 11.9. Effect of pH on the sorption of Cd (a) and Pb (b) onto chitosan gel bead and chitosan-AAc gel bead. Initial concentrations of 10 and 50 mg/L for Cd and Pb, respectively, ambient temperature, stirred at 150 rpm.

material prepared by the polymerization grafting of acrylamide (AAm) onto GG, using a potassium bromate/thiourea dioxide redox system for initiating the polymerization reaction. The PAAm/GG graft copolymer prepared in this way was further cross-linked with glutaraldehyde to obtain a sorbent material in the form of hydrogel. It was found from the study that the sorption of Cr (VI) by the hydrogel is pH dependent and that maximum sorption was obtained at pH4. The sorption data obeyed Langmuir and Freundlich sorption isotherms. The Langmuir sorption capacity (Q_{max}) was found to be 588.24 mg/g [11.47].

REFERENCES TO CHAPTER 11

[11.1] ROSIAK, J.M., ULANSKI, P., Synthesis of hydrogels by irradiation of polymers in aqueous solution, Radiat. Phys. Chem. **55** (1999) 139–151.

[11.2] HENNINK, W.E., VAN NOSTRUM, C.F., Novel crosslinking methods to design hydrogels, Adv. Drug Deliv. Rev. **54** 1 (2002) 13–36.

[11.3] PEPPAS, N.A., Hydrogels in Medicine and Pharmacy, Vol. I, Fundamentals, CRC Press, Boca Raton, FL (2000).

[11.4] ABD EL-REHIM, H.A., Characterization and possible agricultural application of polyacrylamide/sodium alginate crosslinked hydrogels prepared by ionizing radiation, J. Appl. Polym. Sci. **101** (2006) 3572–3580.

[11.5] DARWIS, D., Role of radiation processing in production of hydrogels for medical applications, Atom Indones. **35** (2009) 85–104.

[11.6] CORKHILL, P.H., HAMILTON, C.J., TIGHE, B.J., Synthetic hydrogels. VI. Hydrogel composites as wound dressings and implant materials, Biomaterials **6** (1989) 3–10.

[11.7] ROSIAK, J.M., Hydrogel Dressings, American Chemical Society, Washington, DC (2001) 271–295.

[11.8] GRAHAM, N.B., Hydrogels: their future, Part I, Med. Device Technol. **9** (1998) 18–22.

[11.9] PURNA, S.K., BABU, M., Collagen based dressings: a review, Burns **26** (2000) 54–62.

[11.10] TAHTAT, D., et al., Influence of some factors affecting antibacterial activity of PVA/Chitosan based hydrogels synthesized by gamma irradiation, J. Mater. Sci.: Mater. Med. **22** (2011) 2505–2512.

[11.11] NACER KHODJA, A., et al., Evaluation of healing activity of PVA/chitosan hydrogels on deep second degree burn: pharmacological and toxicological tests, Burns **39** (2013) 98–104.

[11.12] BENAMER, S., MAHLOUS, M., BOUKRIF, A., MANSOURI, B., YOUCEF, S.L., Synthesis and characterisation of hydrogels based on poly(vinyl pyrrolidone), Nucl. Instrum. Methods Phys. Res. B. **248** (2006) 284–290.

[11.13] CHANDY, T., SHARMA, C.P., Chitosan as a biomaterial, Biomater. Artif. Cells Artif. Org. **18** (1990) 1–24.

[11.14] ROSIAK, J.M., ULANSKI, P., PAJEWSKI, L.A., YOSHI, F., MAKUUCHI, K., Radiation formation of hydrogels for biomedical purposes. Some remarks and comments, Radiat. Phys. Chem. **46** (1995)161–168.

[11.15] VARSHNEY, L., Role of natural polysaccharides in radiation formation of PVA-hydrogel wound dressing, Nucl. Instrum. Methods Phys. Res. B. **255** (2007) 343–349.

[11.16] TRANQUILAN-ARANILLA, C., YOSHII, F., DELA ROSA, A.M., MAKUUCHI, K., Kappa-carrageenan–polyethylene oxide hydrogel blends prepared by gamma irradiation, Radiat. Phys. Chem. **55** (1999) 127–131.

[11.17] LIU, L., BERG, R.A., Adhesion barriers of carboxymethylcellulose and PEO composite gels, J. Biomed. Mater. Res. **63** (2002) 326–332.

[11.18] KNILLA, C.J., et al., Alginate fibres modified with unhydrolysed and hydrolysed chitosans for wound dressings, Carbohydr. Polym. **55** (2004) 65–76.

[11.19] ROSIAK, J.M., et al., Radiation Formation of Hydrogels for Biomedical Applications (2002),
http://mitr.p.lodz.pl/biomat/old_site/raport/0_radiation_hydrogels.html

[11.20] SERRAA, L., DOMENECH, J., PEPPAS, N.A., Drug transport mechanisms and release kinetics from molecularly designed poly (acrylic acid-g-ethylene glycol) hydrogels, Biomater. **27** (2006) 5440–5451.

[11.21] TANVEER, A.K., KOK, K.P., A preliminary investigation of chitosan film as dressing for punch biopsy wounds in rats, J. Pharm. Pharm. Sci. **6** (2003) 20–26.

[11.22] WINTER, G.D., SCALES, J.T., Effect of air drying and dressings on the surface of a wound, Nature **197** 4 (1963) 91–2.

[11.23] WINTER, G.D., "Epidermal regeneration studied in the domestic pig", Epidermal Wound Healing (MAIBACH, H.I., ROVEE, D.T., Eds), Year Book Medical Publishers, Chicago, IL (1972) 71–112.

[11.24] UENO, H., MORI, T., FUJINAGA, T., Topical formulations and wound healing applications of chitosan, Adv. Drug Deliv. Rev. **52** (2001) 105–115.

[11.25] USAMI, Y., et al., Chitin and chitosan induce migration of bovine polymorpho-nuclear cells, J. Vet. Med. Sci. **56** 4 (1994) 761–762.

[11.26] USAMI, Y., et al., Migration of canine neutrophils to chitin and chitosan, J. Vet. Med. Sci. **56** 6 (1994) 1215–1216.

[11.27] TAHTAT, D., et al., Oral delivery of insulin from alginate/chitosan crosslinked by glutaraldehyde, Int. J. Biol. Macromol. **58** (2013) 160–168.

[11.28] OH, J.K., LEE, D.I., PARK, J.M., Biopolymer-based microgels/nanogels for drug delivery applications, Progress Polym. Sci. **34** (2009) 1261–1282.

[11.29] XU, Y., ZHAN, C., FAN, L., WANG, L., ZHENG, H., Preparation of dual crosslinked alginate–chitosan blend gel beads and in vitro controlled release in oral site-specific drug delivery system, Int. J. Pharm. **336** (2007) 329–337.

[11.30] CHEN, C.C., FANG, C.L., AL-SUWAYEH, S.A., LEU, Y.L., FANG, J., Transdermal delivery of selegiline from alginate-Pluronic composite thermogels, Int. J. Pharm. **415** 1–2 (2011) 119–128.

[11.31] KRAVCHENKO, I.A., GOLOVENKO, N.Y., LARIONOV, V.B., ALEKSANDROVA, A.I., OVCHARENKO, N.V., Effect of lauric acid on transdermal penetration of phenazepam in vivo, Bull. Exp. Biol. Med. **136** 6 (2003) 579–581.

[11.32] AL-ASSAF, S., DICKSON, P., PHILLIPS, G.O., THOMPSON, C., TORRES, J.C., Compositions Comprising Polysaccharide Gums, WO2009/016362, Feb. 2009, filed Jul. 2008, available on-line.

[11.33] DYBEK, K., KUBIS, A., ROSIAK, J.M., Studies on dressings for dental surgery use, Part 4, Effect of gamma-radiation and formaldehyde on properties of gelatinous dental dressings, Pharm. **47** (1992) 273–274.

[11.34] STASICA, P., CIACH, M., RADEK, M., ROSIAK, J.M., Approach to construct hydrogel intervertebral disc implants-experimental and numerical investigations, Eng. Biomater. **3** 9 (2000) 9–14.

[11.35] LUM, L., ELISSEEFF, J., "Injectable hydrogels for cartilage tissue engineering", Topics in Tissue Engineering (ASHAMMAKHI, N., FERRETTI, P., Eds), University of Oulu (2003).

[11.36] ALIYAR, H.A., HAMILTON, P.D., RAVI, N., Refilling of ocular lens capsule with copolymeric hydrogel containing reversible disulfide, Biomacromolecules **6** (2005) 204–211.

[11.37] KOZICKI, M., et al., Encapsulation of living cells towards artificial hybrid organs, Eng. Biomater. **7–8** (1999) 11–15.

[11.38] KARAKOYUN, N., et al., Hydrogel-biochar composites for effective organic contaminant removal from aqueous media, Desalination **280** 1–3 319–325.

[11.39] AN, Y.J., HUBBELL, J.A., Intraarterial protein delivery via intimally-adherent bilayer hydrogels, J. Control. Release **64** (2000) 205–215.

[11.40] LU, S.X., RAMIREZ, W.F., ANSETH, K.S., Photopolymerized, multilaminated matrix devices with optimized nonuniform initial concentration profiles to control drug release, J. Pharm. Sci. **89** (2000) 45–51.

[11.41] SLAUGHTER, B.V., KHURSHID, S.S., FISHER, O.Z., KHADEMHOSSEINI, A., PEPPAS, N.A., Hydrogels in regenerative medicine, Adv. Mater. **21** (2009) 3307–3329.

[11.42] PEPPAS, N.A., ZACH HILT, J., KHADEMHOSSEINI, A., LANGER, R., Hydrogels in biology and medicine: from molecular principles to bionanotechnology, Adv. Mater. **18** (2006) 1345–1360.

[11.43] SERSHEN, S., WEST, J., Implantable, polymeric systems for modulated drug delivery, Adv. Drug Deliv. Rev. **55** (2003) 439.

[11.44] LEE, V.H.L., YAMAMOTO, A., Penetration and enzymatic barriers to peptide and protein absorption, Adv. Drug Deliv. Rev. **4** (1990) 171–207.

[11.45] INTERNATIONAL ATOMIC ENERGY AGENCY, Radiation Processing: Environmental Applications, IAEA, Vienna (2007).

[11.46] BENAMER, S., et al., Radiation synthesis of chitosan beads grafted with acrylic acid for metal ions sorption, Radiat. Phys. Chem. **80** (2011) 1391–1397.

[11.47] ABDEL-HALIM, E.S., AL-DEYAB, S.S., Hydrogel from crosslinked polyacrylamide/guar gum graft copolymer for sorption of hexavalent chromium ion, Carbohydr. Polym. **86** (2011) 1306–1312.

Chapter 12

RADIATION SYNTHESIS AND CHARACTERIZATION OF NATURAL POLYMER BASED SUPERABSORBENTS

M. SEN, H. HAYRABOLULU
Hacettepe University, Department of Chemistry,
Ankara, Turkey

12.1. INTRODUCTION

Superabsorbent polymers (SAPs) are moderately cross-linked, 3-D, hydrophilic network polymers (hydrogels) that can absorb and conserve considerable amounts of aqueous fluids even under heat or pressure. Because of their unique properties, which are superior to conventional absorbents, SAPs have applications in many fields, for items such as hygienic products, disposable diapers, horticulture products, gel actuators, drug delivery systems, water-blocking tapes, coal dewatering polymers and water managing materials for the renewal of arid and desert environments [12.1]. In recent years, naturally available resources, such as polysaccharides, have drawn considerable attention for the preparation of SAPs. However, since the mechanical properties of polysaccharide based natural polymers are low, researchers have mostly focused on their improvement using natural/synthetic polymer/monomer mixtures to obtain novel SAPs [12.2].

12.2. SYNTHESIS AND CHARACTERIZATION OF THE SWELLING PROPERTIES OF AAc SODIUM SALT / LBG HYDROGELS

Sen and Hayrabolulu [12.3] synthesized a novel superabsorbent polymer with high mechanical strength by radiation induced polymerization and cross-linking of AAc sodium salt (AAcNa) in the presence of the natural polymer LBG, and characterized the substance's network structures. Liquid retention capacities and absorbency under load analyses were performed in water. For the characterization of the network structure of the semi-interpenetrating-polymer-network hydrogels, the average molecular weight between cross-links ($\bar{M}_c$) was evaluated through uniaxial compression and oscillatory rheological measurements; the advantages and disadvantages of these two techniques were compared.

The network structure was characterized by studying the swelling properties of the substances in water. The effect of degree of neutralization (DN) and pressure on the swelling behaviour of the hydrogels was examined by the swelling experiments carried out under the pressure of 2.1 kPa.

Each swelling experiment was performed until a constant value of swelling was reached for the sample in question. From the result of this study, the swelling kinetics of the AAcNa/LBG hydrogels in water under 0.0 kPa and 2.1 kPa at 25°C are presented in Figs 12.1 and 12.2. As can be seen from these figures, the AAcNa/LBG hydrogels reached equilibrium swelling in 10–20 minutes. On the other hand, the equilibrium swelling degree was lower under pressure than in pure water for each DN value (Fig. 12.3). This decrease was attributed to the increase in osmotic pressure on the gel system.

According to the experimental results, the swelling behaviour of the AAcNa/LBG hydrogels was the most affected by the DN. The swelling degree of the gels was increased from 245 to 587 with an increase in degree of DN from 50 to 90 in the absence of force. This was attributed to the increase in the number of the carboxylate groups in the gel with DN and the change in the Donnan equilibrium. The water absorbency of the completely neutralized gel (AAcNa/LBG-DN100) was lower than that of the AAcNa/LBG-DN90 gel. This decrease was probably due to the buffer action and the screen effect caused by the counterions inside the gel [12.4].

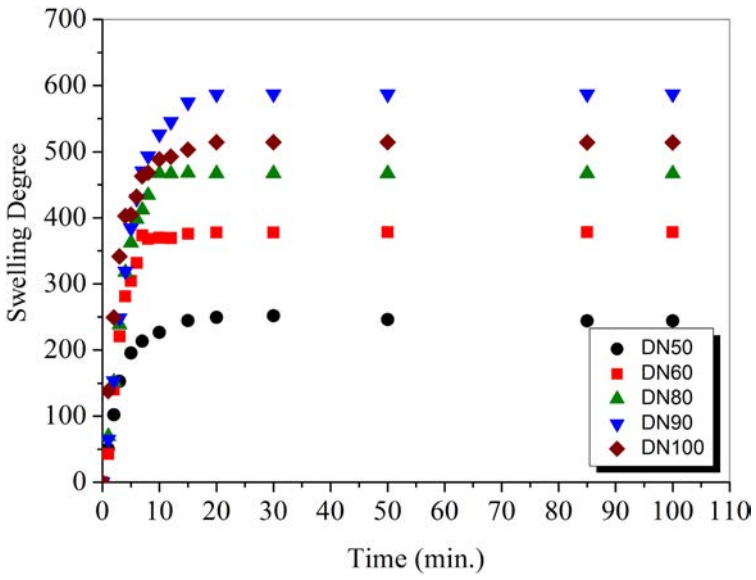

FIG. 12.1. Swelling kinetics of the AAcNa/LBG double network hydrogels under zero pressure. The DN of AAc is indicated by the legend [12.3].

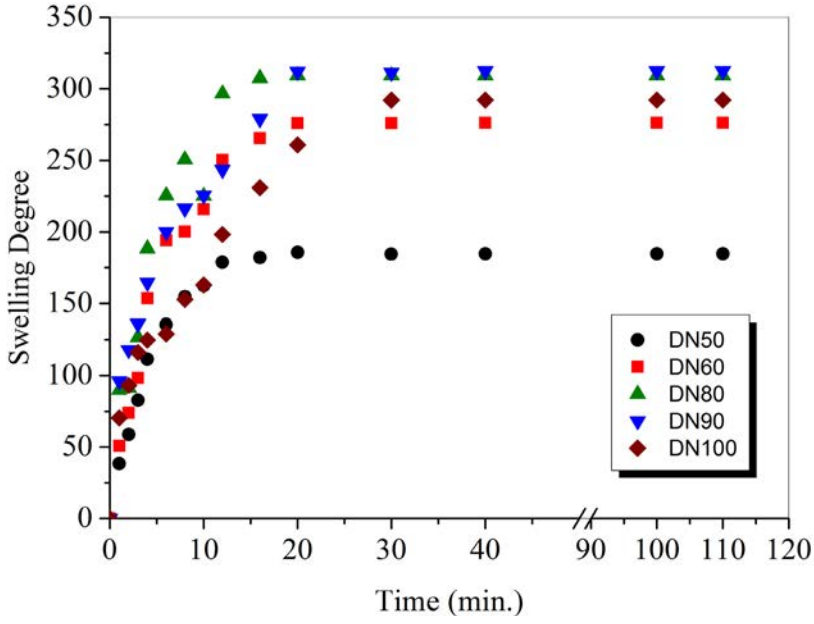

FIG. 12.2. Swelling kinetics of the AAcNa/LBG double network hydrogels under a pressure of 2.1 kPa. The DN of AAc is indicated by the legend [12.3].

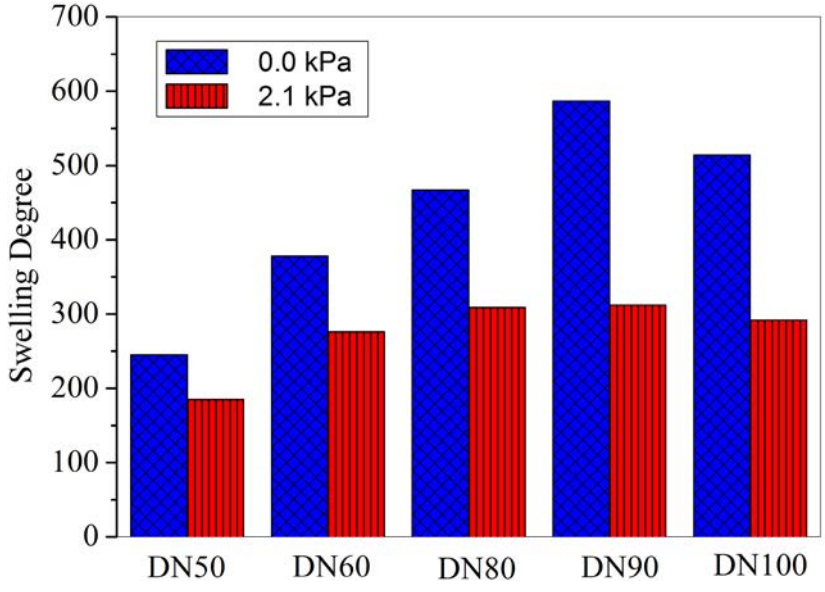

FIG. 12.3. Effects of pressure and DN on the equilibrium swelling of the AAcNa/LBG double network hydrogels [12.3].

12.2.1. Characterization of the network structure of AAcNa/LBG hydrogels

In order to determine the molecular weight between cross-links of the hydrogels prepared by means of the shear modules value, two different evaluation techniques were used in this study. The first technique was the uniaxial compression analysis performed on the swollen gels and followed with the use of a universal testing instrument. Figure 12.4 shows typical stress–strain curves for AAcNa/LBG. Shear modulus values of the hydrogels (G_m) were calculated using the elastic deformation theory and Eq. (12.1) [12.5–12.7].

$$f = G_m(\lambda - \lambda^{-2}) \tag{12.1}$$

where λ is the deformation ratio and is equal to L/L_0, and L_0 and L are the length of the undeformed and deformed hydrogels during compression, respectively. When the equation is applied to the initial stages of deformation, plots of f vs. $(\lambda - \lambda^{-2})$ yield straight lines (inset Fig. 12.4). The G_m value was calculated from the slope of the lines and is listed in Table 12.1. Using the G_m values and other relevant experimental parameters, the molecular weight between cross-links $(\bar{M}_c)_m$ values were calculated using Eq. (12.2) and collected in Table 12.1.

$$G_m = G_R = A\frac{\rho}{\bar{M}_c}RT(v_{2r})^{2/3}(v_{2m})^{1/3} \tag{12.2}$$

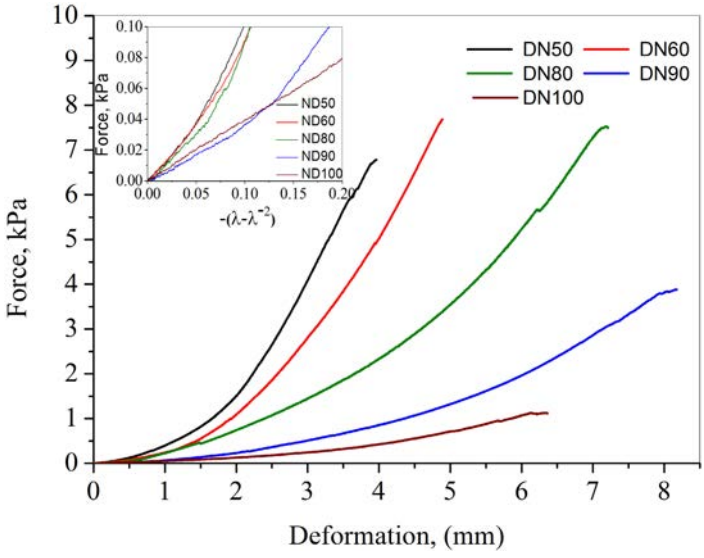

FIG. 12.4. Curves of strain vs. stress and $-(\lambda-\lambda^{-2})$ vs. stress for the AAcNa/LBG hydrogels [12.3].

TABLE 12.1. STRUCTURAL PROPERTIES OF THE AAcNa/LBG HYDROGELS

Gel Name	AAcNa/ LBG-DN50	AAcNa/ LBG-DN60	AAcNa/ LBG-DN80	AAcNa/ LBG-DN90	AAcNa/ LBG-DN100
$(v_{2m})^{1/3}$	0.1479	0.1440	0.1241	0.1104	0.0932
$(v_{2r})^{2/3}$	0.2482	0.2349	0.2334	0.2010	0.1401
ρ (kg/m^3)	1072	1100	1118	1263	1494
G_m (Pa)	2305	2120	990	850	390
G_R (Pa)	2665	2290	1020	715	180
$(\bar{M}_c)_m$ (g/mol)	42.320	44.570	81.050	81.500	124.580
$(\bar{M}_c)_R$ (g/mol)	36.570	40.280	78.820	97.120	265.580
$(v_e)_R$ (mol/cm^3)	2.533×10^{-5}	2.525×10^{-5}	1.379×10^{-5}	1.550×10^{-5}	1.199×10^{-5}
(ξ_R) (nm)	92	96	152	172	252

where

ρ is the polymer density;

$(\bar{M}_c)$ is the average molecular weight of the network chains;

v_{2m} is the polymer volume fraction of the cross-linked polymer in equilibrium with the swollen gel;

and v_{2r} is the polymer volume fraction in the relaxed state, i.e. after cross-linking but before swelling.

The prefactor A equals 1 for an affine network and $1 - 2/\Phi$ for a phantom network [12.5].

The polymer volume fractions ν_{2x} (ν_{2r} and ν_{2m}) are determined by Eq. (12.3):

$$Q = 1/\nu_{2x} = (1 + \rho/\rho_w(w^{-1} - 1)) \tag{12.3}$$

where ρ and ρ_w were the densities of the swollen gel and water and w was the weight fraction of the polymer in the relaxed and swollen gel for the determination of ν_{2r} and ν_{2m}, respectively.

As can be seen from Table 12.1, the DN of AAc strongly affected both the distance between two entanglement points and the molecular weight between cross-links of the AAcNa/LBG hydrogels. The results clearly indicate that DN was one of the important parameters affecting radiation induced polymerization and the cross-linking of AAcNa/LBG mixtures. As explained previously, the decrease in cross-link reactions is probably due to the increase in the macroradical stability with the increase in the ionization degree of AAc.

The second technique used in this study for the determination of the shear modules of the hydrogels was rheology [12.8]. The oscillatory frequency sweep test was performed in the linear viscoelastic region. Stress sweep was performed to determine the linear viscoelastic region at a frequency of 1 Hz. The results (Fig. 12.5) showed that the network structure strongly influenced the type of the deformation (elastic vs. viscose) above a critical shear rate. The shear stress was constant between 0.01–0.5% to ensure the linearity, and all frequency sweep tests were carried out at $\gamma = 0.01\%$.

The storage or elastic moduli, G_R, of the double networks, exhibited a low frequency dependence and the slopes of G_R vs. frequency curves were almost zero in a frequency range of 0.01–1 Hz (Fig. 12.6). Figure 12.6 shows that for the cross-linked hydrogels, the magnitude of G_R decreased with increasing DN up to 90% and then to 100%, similarly to the case of equilibrium swelling.

An ideal oscillatory curve has a plateau in the intermediate frequency region, which corresponds to the rubber-elasticity region. In this region, the relaxation ability of the segments is smaller than the stress velocity, thus preventing the large molecules from freely passing one another [12.8]. In the linear viscoelastic range, the network parameters, i.e. the molar mass between the two entanglement points, $(\bar{M}_c)_R$, the cross-link density (υ_e), and the mesh size (ξ) were calculated using Eqs (12.1), (12.4) and (12.5). For a homogenous network of Gaussian chains, the elastic modules of the gels swollen to equilibrium G_R were related to the network cross-link density through Eq. (12.1). The space between the chains, or mesh size, is usually characterized by the correlation length, or the distance between two adjacent cross-links [12.9–12.11].

$$\nu_e = \frac{\rho}{\bar{M}_c} \tag{12.4}$$

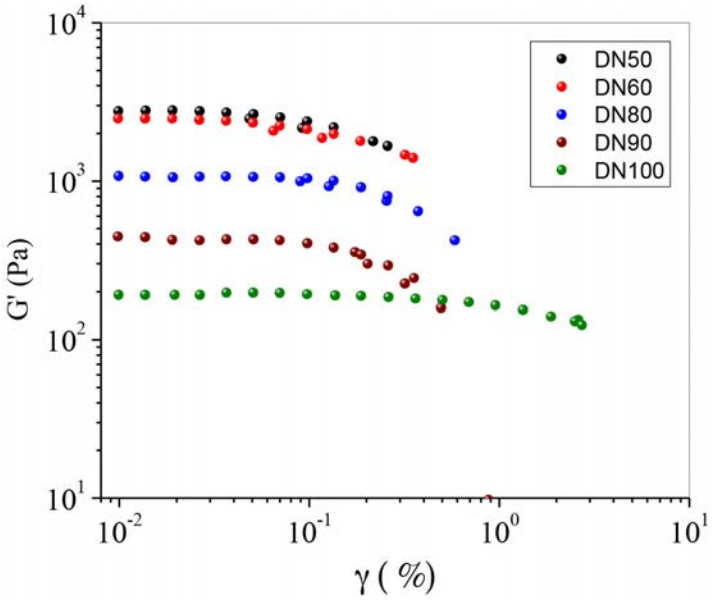

FIG. 12.5. Variation shear moduli of the AAcNa/LBG hydrogels as a function of the strain at ω = 1 Hz for various DNs [12.3].

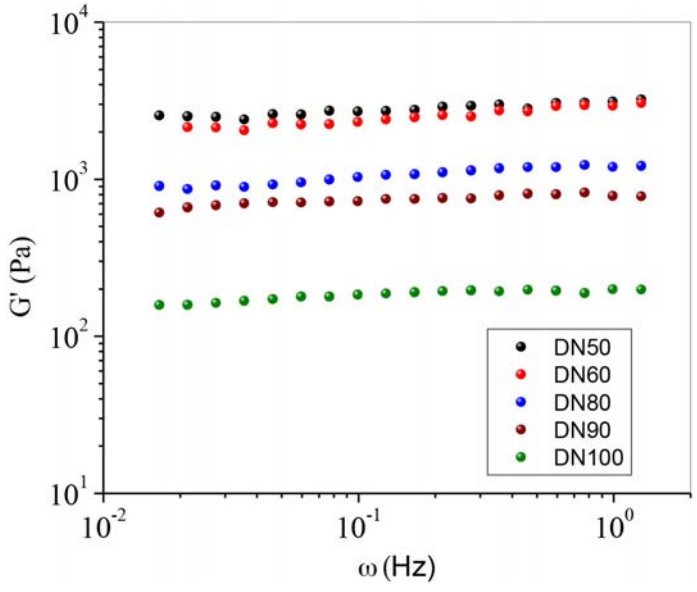

FIG. 12.6. Variation shear moduli of the AAcNa/LBG hydrogels as a function of frequency at γ = 0.01% for various DNs [12.3].

$$\xi = v_{2m}^{-1/3}\left[C_n\left(\frac{2\bar{M}_c}{M_r}\right)\right]^{1/2} l \tag{12.5}$$

where ξ is the Flory characteristic ratio or rigidity factor of the hydrogel (in this case, 6.7) [12.12], l is the carbon–carbon length (154 pm) and M_r is the molecular weight of the monomeric unit.

The elastic module values determined are listed in Table 12.1. Using the values and other relevant experimental parameters, $(\bar{M}_c)_R$ and v_e were calculated and are given in Table 12.1. The results clearly show that changes in the DN of AAc will influence the distance between adjacent cross-links in the AAc/LBG hydrogel network. Except for the completely neutralized gel system, the values obtained from rheological measurements closely followed the values calculated from the mechanical properties of the same hydrogel. The large difference in the values in the neutral gel system was attributed to their softness and the practical difficulties in the preparation of the perfectly smooth cylindrical gel pieces required for mechanical analyses. Because of the difficulty in detecting very small force values for rough surfaces, the determination of the actual onset point of the compression and the viscoelastic deformation range of the gel system was not straightforward. On the other hand, the rheological analyses were independent of the size and shape of the gel, and thus for such soft gels, the rheological measurements can provide more accurate values. Owing to the ease of adjustments of the gap distance between the plates, the initial preload value on the gels could be controlled by the user prior to the experiment. In this way, the viscoelastic deformation range can be accurately determined by a strain sweep test.

As a result of all these analyses, it could be concluded that the uniaxial compression technique could be used for the characterization of the network structure of a hydrogel along with the rheological analyses. However, a very precise control of the gel size was also needed. Since a very small deformation force could be applied in the linear viscoelastic deformation range on the gel system irrespective of its shape, rheology was an easier and more reliable technique for the characterization of the network structural parameters of the gel systems.

12.2.2. Swelling properties of AAcNa/LBG hydrogels in urine solutions

Knowledge of the swelling behaviour of superabsorbent polymers (SAPs) in salt or urine solutions is very important for the identification of their potential for use in hygiene products. The swelling kinetics of the AAcNa/LBG hydrogels in urine solutions at different temperatures and under different loads are shown

in Fig. 12.7. As can be seen from the figures, AAcNa/LBG hydrogels reach equilibrium swelling in ten minutes at all pressures. On the other hand, the equilibrium swelling degree is lower in pseudo urine solutions than in pure water. This decrease was attributed to the Donnan effect.

For the comparison of the swelling capacity of SAP prepared in this study (see Fig. 12.8) with that of commercial products already in use in hygiene products such as incontinence pads or baby's nappies (see Fig. 12.9), swelling analyses were performed, and the maximum swelling capacity of AAcNa based SAP obtained from these products was determined [12.14].

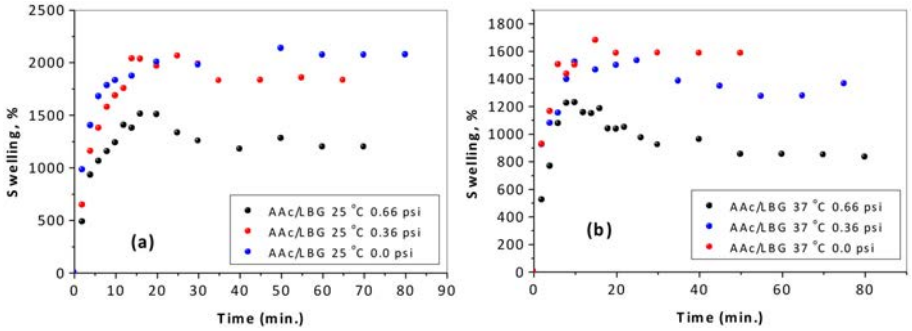

FIG. 12.7. Variation of the swelling kinetics of the AAcNa/LBG hydrogels with load in pseudo urine solutions at temperatures of: (a) 25°C and (b) 37°C [12.13].

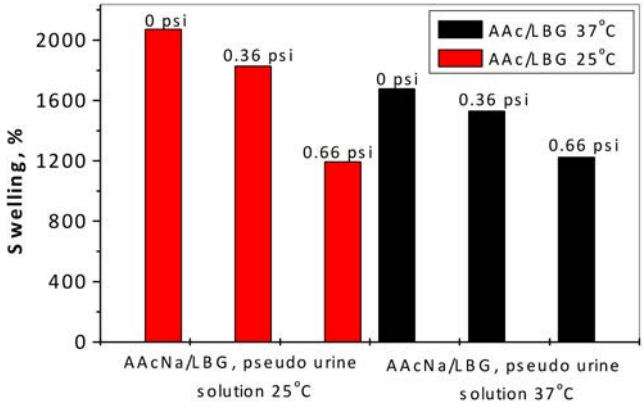

FIG. 12.8. Absorbency under load values of the AAcNa/LBG SAPs in water and pseudo urine solution at different temperatures. The loads applied on the gels are given above the respective bars [12.13].

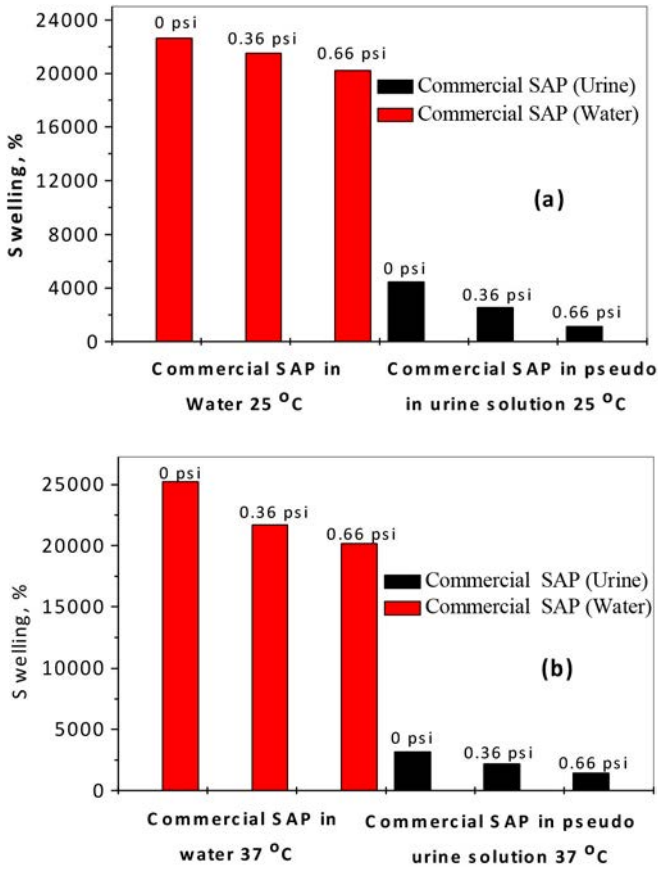

FIG. 12.9. Absorbency under load values of the commercial SAPs in water and pseudo urine solution, at temperatures of (a) 25°C (b) 37°C. The loads applied on the gels are given above the respective bars [12.13].

The maximum swelling or water retention capacities of the commercial SAPs in water and pseudo urine solution are shown in Fig. 12.9. As in the AAcNa/LBG SAP systems, the swelling degree of the commercial gels also decreased, but it decreased more abruptly with the ionic strength of the swelling medium. This decrease was attributed to the high ionic nature of the SAP system.

The absorbency under load values for AAc/Na/LBG SAP and the commercial SAP in urine solution are compared in Fig. 12.10. Figure 12.10 clearly indicates that the hydrogels prepared in this study (the LBG natural polymer interpenetrated with a synthetic monomer) are comparable, especially at high pressures.

12.3. SYNTHESIS AND CHARACTERIZATION OF CARBOXYLATED LBG HYDROGELS

In a recent study [12.15], carboxylated LBG hydrogels were prepared by irradiation in a paste-like condition, as well as by irradiation in solid state in the presence of acetylene. Sol-gel analysis was carried out in order to determine the polymer to gel conversion ratios. It was found that the swelling capacity of the hydrogels prepared in the presence of acetylene increased with dose from 19 000% to 34 000%, and the gelation percentage increased rapidly up to 5.0 kGy, and then slowed down at higher doses. While a lower gelation was observed, the cross-link density of the CLBG hydrogels prepared in the paste-like conditions was high. For the characterization of the network structure of the hydrogels, the average molecular weight between cross-links ($\bar{M}_c$) was evaluated by means of rheological analyses.

12.3.1. Preparation and characterization of CLBG

LBG was first carboxylated using a technique known as TEMPO, which is performed as follows: 0.5 g of LBG was suspended in 250 mL of deionized water overnight and then stirred at 60°C for two hours. The solution was then cooled to room temperature, and catalytic amounts of (2,2,6,6−tetramethylpiperidin−1−yl)oxyl and NaBr were added. The oxidation reaction was initiated by the drop wise addition of a NaOCl solution (the active Cl value was 11%) at 4°C. In order to obtain various oxidation ratios, 4.5 mL, 7.0 mL, 14.5 mL, 18.0 mL or 35 mL of the NaOCl solution was added to the mixture. The NaOCl/primary alcohol mol ratio was 1.2, 1.9, 4.6, 4.8 and 9.3, respectively. For the selective oxidation of polysaccharides, the pH should be around 10.2 [12.16]. The pH in this study was kept at 9−10 during the reaction by adding 0.5M of aqueous NaOH solution. When the pH decrease was very slow, the reaction was quenched by adding MeOH. Finally, the CLBG was precipitated by use of acetone.

In order to change the carboxylation degree, the NaOCl/primary alcohol mol ratio was controlled during the oxidation reaction. The effect of NaOCl/primary alcohol mol ratio on the structural changes was firstly monitored by FTIR. In Fig. 12.11(a), the spectra of the virgin LBG, and of the samples synthesized using a 4.5 mL, 7.0 mL, 14.5 mL, 18.0 mL or 28 mL of the NaOCl solution in the carboxylation reaction, respectively, are shown. For the pure LBG (Fig. 12.11), the band at 3430 cm^{-1} represents the O–H stretching vibration. The band at 2924 cm^{-1} is due to the C–H stretching of the $–CH_2$ groups. The bands due to ring stretching of galactose and mannose appear at 1641 cm^{-1} and 1657 cm^{-1}. In addition, the bands in the region of 1350–1450 cm^{-1} are due to

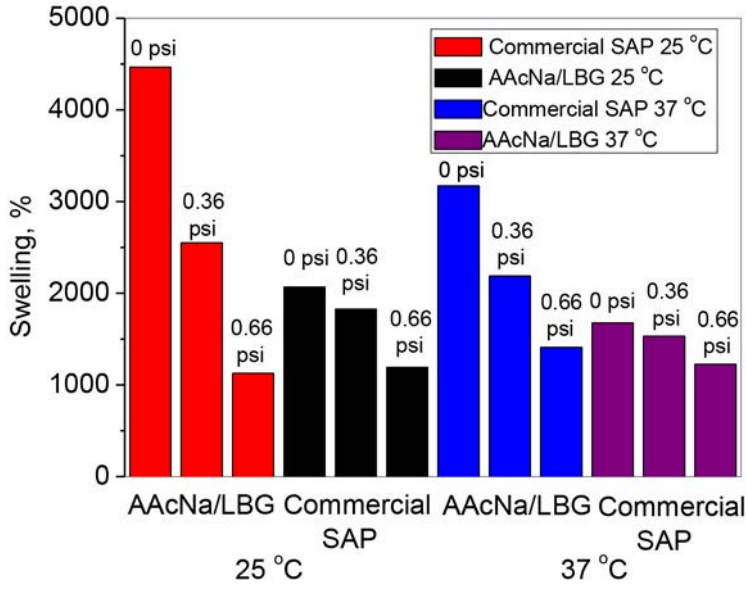

FIG. 12.10. Absorbency under load values of AAcNa/LBG and a commercial SAP in pseudo urine solution at 25°C and 37°C [12.17].

the symmetrical deformations of the CH_2 and COH groups. The bands due to the primary alcoholic $–CH_2OH$ stretching mode and CH_2 twisting vibrations appear at 1078 cm^{-1} and 1021 cm^{-1}, respectively. The weaker bands around 770 cm^{-1} are due to the ring stretching and ring deformation of the α D-(1-4) and α D-(1-6) linkages. The peak at 1729 cm^{-1} in the b–f spectra is the stretching bond of the C=O groups in the carboxylic acids. As can be seen in Fig. 12.11, the peak intensity of the C=O groups continuously increased with the amount of NaOCl. The carboxylation of the LBG was also evidenced by ^{13}C NMR analyses [12.17].

The effect of the carboxylation or the amount of NaOCl added in the reaction mixture on the molecular weight of the LBG was investigated by GPC. The chromatograph was combined with refractive index and MALLS detectors. The variations in the weight and number-average molecular weights of the CLBG as a function of the NaOCl/primary alcohol mol ratios are given in Table 12.2. As can be seen, the molecular weight of the CLBG increased with the amount of NaOCl. This increase was attributed to side esterification reactions and partial cross-linking of the LBG structure. Owing to the solubility problem of the CLBG-18 in water, the CLBG-4, CLBG-7 and CLBG-13 systems were used in the gelation experiments.

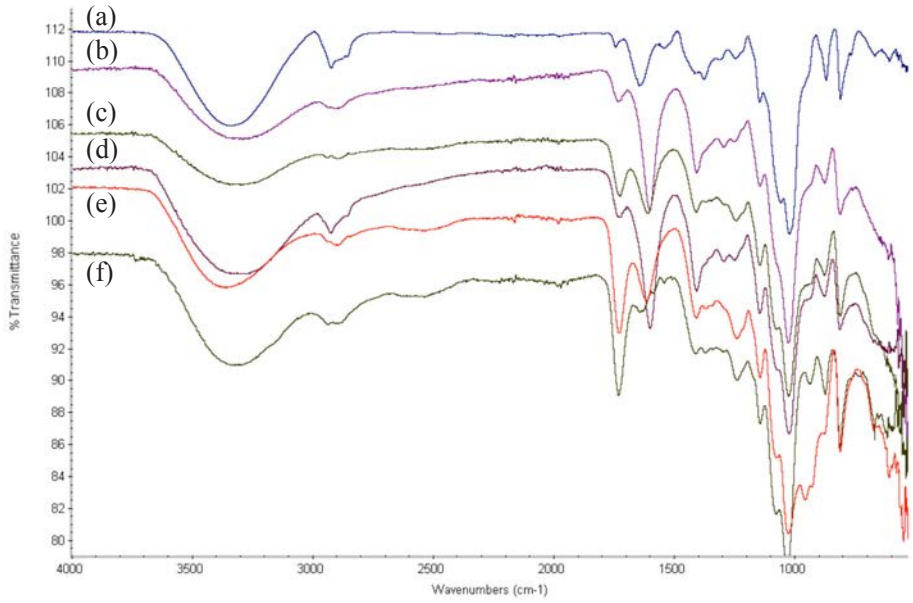

FIG. 12.11. FTIR spectrum of virgin LBG (a) and CLBGs prepared by using (b) 4.5 mL, (c) 7 mL, (d) 13.5 mL, (e) 18 mL and (f) 28 mL NaOCl in the carboxylation experiments [12.15].

TABLE 12.2. NUMBER AND WEIGHT-AVERAGE MOLECULAR WEIGHTS OF CLBG POLYMERS

Sample name	Amount of NaOCl (mL)	$\bar{M}_w$	$\bar{M}_n$	Polydispersity index
LBG	0.0	510 430	390 200	1.31
LBG-4	4.5	614 000	291 000	2.10
LBG-7	7.0	780 000	456 000	1.71
LBG-13	14.5	1 200 000	630 000	1.90
LBG-18	18.0	1 570 000	870 000	1.80
LBG-28	28.0	385 000	228 000	1.69

12.3.2. Preparation of CLBG gels in paste-like states

For the preparation of CLBG hydrogels in the paste-like state, solutions of 20% (weight/volume) LBG and CLBG were placed in tightly closed tubes and irradiated at a dose of 5.0 kGy in a Gammacell 220 type ^{60}Co gamma irradiator at room temperature, in air. Sol-gel analysis and swelling experiments were performed using the sintered gooch crucible apparatus shown in Fig. 12.12. [12.15].

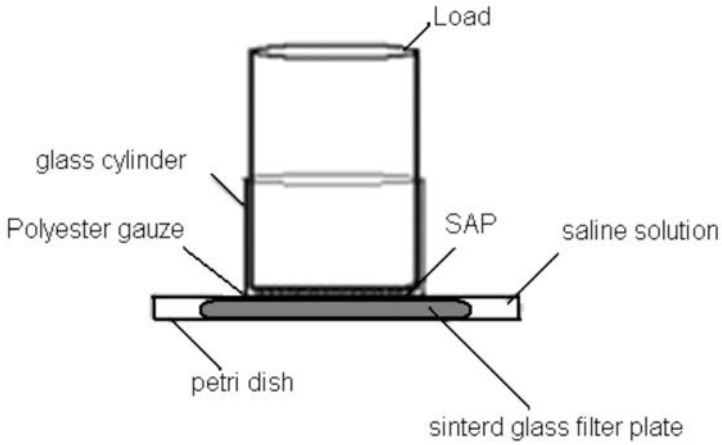

FIG. 12.12. Sintered gooch crucible apparatus used for the determination of the gelation and swelling ratios of the gels [12.15].

The gelation and swelling percentages of the prepared gels were calculated, and the results are given in Table 12.3. A gelation of 71.6% was observed for non-carboxylated LBG and the swelling percentage of this gel was only 1225%. As can be seen in Table 12.3, the swelling degree (4700%) of the CLBG of 26% was approximately four times higher than that of the LBG. On the other hand, a reduction was observed in the gelation ratio of the system.

When the carboxylation degree of the LBG was increased from 26% to 40% and 70%, neither a regular increase nor a decrease was observed in the gelation and swelling percentages of the CLBG samples. This behaviour was attributed to the partial and local cross-links formed during the carboxylation reactions that led to the inhomogeneous diffusion of water inside the gels.

12.3.3. Preparation of CLBG gels in the presence of acetylene

In order to prepare the CLBG gels in the presence of acetylene gas, 0.5 g ground dry carboxylated polymer samples were placed in glass tubes with

TABLE 12.3. EFFECT OF NaClO/PRIMER ALCOHOL MOL RATIO ON THE CARBOXYLATION DEGREE AND GELATION AND SWELLING DEGREE OF CLBG GELS PREPARED IN PASTE-LIKE STATES

NaClO/primer mol ratio	CD	Gelation % at 5 kGy dose	Swelling (%)
0.0	0.0	71.6	1225
1.2	26	25.5	4700
1.9	40	45.1	1090
4.6	70	35.8	2020

rubber lids. The glass tubes were filled with nitrogen gas and then with acetylene gas for 5 minutes. The samples were then irradiated in the gamma source up to 10 kGy.

Additionally, powdered CLBG was also irradiated in the presence of acetylene up to 10 kGy at a dose rate of 30 Gy/h. The effects of the dose and degree of carboxylation on the gelation and percentage swelling of gels are presented in Table 12.4.

TABLE 12.4. GELATION AND SWELLING % OF CLBG GELS PREPARED IN THE PRESENCE OF ACETYLENE GAS IN THE FUNCTION OF THE NaOCl/PRIMARY ALCOHOL MOL RATIO AND THE ABSORBED DOSE (DOSE RATE; 30 Gy/HOUR) [12.14]

NaClO/primary alcohol mol ratio	2 kGy		5 kGy		10 kGy	
	Gelation (%)	Swelling (%)	Gelation (%)	Swelling (%)	Gelation (%)	Swelling (%)
0.0	85.0	490	88.3	443	70	700
1.2	61.3	19020	99.5	17730	46	33945
1.9	58.0	2600	64.5	2415	35	1244
4.6	50.0	975	48.6	935	45	4270

As can be seen in Table 12.4, higher gelation ratios were observed for the gels prepared in the presence of acetylene gas in comparison to the ones prepared in paste-like conditions. The results showed that the increase in carboxylation degree had a reverse effect on gelation, as the gelation and swelling percentages decreased with the carboxylation ratio. The results also demonstrated that the cross-linking reactions occurred via different mechanisms depending on the extent of the carboxylation of the LBG when irradiations were performed in the presence of acetylene gas. When the absorbed dose was increased from 5 kGy to 10 kGy, for all carboxylation degrees, the degrees of gelation were found to decrease. As is well known, polysaccharides in dry form or in solution degrade upon irradiation [12.18–12.23]. The decrease in gelation and increase in swelling at relatively high absorbed doses (at 10 kGy, for instance) showed that the chain scission yield was more dominant than the cross-linking reactions.

Dose rate is an important parameter that controlls the degradation and cross-linking of natural polymers. For the investigation of the effect of dose rate on the gelation and swelling of the CLBG gels in the presence of acetylene gas, a CLBG sample with a carboxylation degree of 26% was also irradiated with gamma rays at a dose rate of 300 Gy/h at 2 or 5 kGy. The gelation and swelling values were calculated and are shown in Table 12.5.

TABLE 12.5. GELATION AND SWELLING % OF CLBG GELS PREPARED IN THE PRESENCE OF ACETYLENE GAS

NaClO/primary alcohol mol ratio/ Carboxylation degree	2 kGy		5 kGy	
	Gelation (%)	Swelling (%)	Gelation (%)	Swelling (%)
1.2/26	81	2250	89.5	2115

When the gelation and swelling ratio of the gels prepared at different dose rates were compared, it was found that dose rate was also an important parameter for the CLBG gels prepared in the presence of acetylene gas. For both dose rates, the gelation values increased as the absorbed dose increased. When the dose rate increased from 30 Gy/h to 300 Gy/h, the swelling percentages of the gels decreased from 19 000% to 2000%. These results indicated that the dose rate had a positive effect on gelation with a significant detractive effect on the swelling values.

As a result of the irradiation studies performed in the presence of acetylene, it was concluded that an absorbed dose of 5 kGy and a carboxylation degree of 26% were the optimal conditions for the preparation of the super adsorbent polymer of CLBG.

ACKNOWLEDGEMENTS

The authors gratefully acknowledge the support provided by the International Atomic Energy Agency through Research Contract No. 14475/R0 and the support provided by TUBITAK through Project No. 109T872.

REFERENCES TO CHAPTER 12

[12.1] BUCHHOLZ, F.L., PEPPAS, N.A., Superabsorbent Polymers: Science and Technology, ACS Symposium Series No. 573, American Chemical Society, Washington, DC (1994).

[12.2] GULREZ, S., AL-ASSAF, S., PHILLIPS, G.O., "Hydrogels: Methods of preparation, characterization and Applications", Progress in Molecular and Environmental Bioengineering, from Analysis and Modeling to Technology Applications, InTech, Rijeka, Croatia (2011).

[12.3] SEN, M., HAYRABOLULU, H., Radiation synthesis and characterization of network structure of natural/synthetic double-network superabsorbent polymers, Radiat. Phys. Chem. **81** (2012) 1378–1382.

[12.4] KONAK, C., BANSIL, R., Swelling equilibria of ionized poly(methacrylic acid) gels in the absence of salt, Polym. **30** (1989) 677–690.

[12.5] MARK, J.E., ERMAN, B., (Eds), Rubberlike Elasticity: A Molecular Primer, Wiley, New York (1998).

[12.6] MAHMUDI, N., SEN, M., RENDEVSKI, S., GÜVEN, O., Radiation synthesis of low swelling acrylamide based hydrogels and determination of average molecular weight between crosslinks, Nucl. Instrum. Meth. Phys. Res. B **265** (2007) 375–378.

[12.7] UZUN, C., HASSNISABER, M., SEN, M., GÜVEN, O., Enhancement and control of crosslinking of dimethyl aminoethyl methacrylate irradiated at low dose rate in the presence of ethylene glycol dimethacrylate, Nucl. Instrum. Meth. Phys. Res. B **208** (2003) 242–246.

[12.8] GLUCK-HIRSCHI, J.B., KOKINIA, J.L., Determination of the molecular weight between crosslinks of waxy maize starches using the theory of rubber elasticity, J. Rheol. **41** (1997) 129–139.

[12.9] TRELOAR, L.R.G., The Physics of Rubber Elasticity, 3rd edn, Clarendon Press, Oxford (2005).

[12.10] OKAY, O., DURMAZ, S., Charge density dependence of elastic modulus of strong polyelectrolyte hydrogels, Polym. **43** (2002) 1215–1221.

[12.11] PEPPAS, N.A., MIKOS, A.G., “Preparation methods and structure of hydrogels”, Hydrogels in Medicine and Pharmacy (PEPPAS, N.A., Ed.), CRC Press, Boca Raton, FL (1986) 27–54.
[12.12] PEPPAS, N.A., WRIGHT, S.L., Solute diffusion in poly(vinyl alcohol)/poly(acrylic acid) interpenetrating networks, Macromolecules **29** (1996) 8798–8804.
[12.13] HAYRABOLULU, H., Radiation Synthesis of Acrylic Acid Sodium Salt / Locust Bean Gum Semi-Interpenetrating Polymer Networks and Investigation of their Super Absorbent Behaviour, MS Thesis, Hacettepe Univ., Ankara (2011).
[12.14] SEN, M., HAYRABOLULU, H., Radiation Synthesis of Superabsorbent Polymers Based on Natural Polymers (2009), http://www-naweb.iaea.org/napc/iachem/meetings/RCMs/RC-1091-2_report_complete.pdf
[12.15] HAYRABOLULU, H., SEN, M., ÇELİK, G., AKKAS KAVAKI, P., Synthesis of carboxylated locust bean gum hydrogels by ionizing radiation, Radiat. Phys. Chem. **94** (2014) 240–244.
[12.16] PONEDEL’KINA, I.Y., KHAIBRAKHMANOVA, E.A., ODINOKOV, V.N., Nitroxide catalized selective oxidation of alcohols and polysaccharides, Russ. Chem. Rev. **79** (2010) 63–75.
[12.17] SEN, M., KAVAKLI, P.A., HAYRABOLULU, H., CELIK, G., Preparation and characterization of carboxylated locust bean gum, unpublished data.
[12.18] BLAKE, S.M., DEEBLE, D.J., PHILLIP, G.O., DU PLESSIS, A., The effect of sterilizing doses of γ-irradiation on the molecular weight and emulsification properties of gum arabic, Food Hydrocolloid. **2** (1988) 407–415.
[12.19] HAI, L., DIEP, T.B., NAGASAWA, N., YOSHII, F., KUME, T., Radiation depolymerization of chitosan to prepare oligomers, Nucl. Instrum. Meth. B **208** (2003) 466–470.
[12.20] DUY, N.N., PHU, D.V., ANH, N.T., HIEN, N.Q., Synergetic degradation to prepare oligochitosan by γ-irradiation of chitosan solution in the presence of hydrogen peroxide, Radiat. Phys. Chem. **80** (2011) 848–853.
[12.21] NAGASAWA, N., MITOMO, H., YOSHII, F., KUME, T., Radiation-induced degradation of sodium alginate, Polym. Degrad. Stabil. **69** (2000) 279–285.
[12.22] PHILLIPS, G.O., in: The Chemistry, Biology, and Medical Applications of Hyaluronan and its Derivatives (LAURENT, T.C., Ed.), Portland Press, London, Miami (1998).
[12.23] SEN, M., RENDEVSKI, S., KAVAKLI, S., AKKAS, P., SEPEHRIANAZAR, A., Effect of G/M ratio on the radiation-induced degradation of sodium alginate, Radiat. Phys. Chem. **79** (2010) 279–282.

Chapter 13

IRRADIATION OF SUGARCANE BAGASSE FOR ETHANOL PRODUCTION

C.L. DUARTE
Energetic and Nuclear Research Institute,
Radiation Technology Centre,
São Paulo, Brazil

13.1. INTRODUCTION

In recent years, there has been an increasing trend towards more efficient utilization of agro-industrial residues such as sugarcane bagasse as raw materials for industrial applications. However, the remaining bagasse continues to be a menace to the environment and a suitable utilization of this residue is an important objective to be pursued. Several processes and products that utilize sugarcane bagasse as a raw material have been reported. These include electricity generation, pulp and paper production, and products based on fermentation. Biofuels only provided around 3% of total transport fuel at the time of writing, and the development of new technologies is necessary to change this parameter over the coming decades. To change from 3% to 27% by 2050, it will be necessary to develop and commercialize new advanced fuel technologies [13.1].

The installation of power generating capacity at sugar mills is increasing all around the world. For example, Brazil recently saw this capacity grow by 500 MW in a three year period, and a significant part of the energy used on Mauritius and Réunion, France, originates from this kind of power generation. Both the federal and regional Governments of India are pushing for this kind of energy generation to be increased [13.1].

Brazil has a long tradition of using renewable energy. A review of primary energy supplies in 2010 showed that 47% was renewable, with a hydropower contribution of 14% and biomass making up 30%. This large proportion is both an advantage and a disadvantage, as Brazil is in part dependent on uncontrollable factors such as rainfall for its energy supply. The energy shortage of 2001 led to the Brazilian Government's decision to diversify its energy supply sources, favouring the inclusion of a reasonable share of thermal power plants and creating a market share for other renewable sources of energy such as wind power and biomass [13.1, 13.2].

One third of the energy that sugarcane contains is present as ethanol. The remainder is contained in fibre in the stalks and in the leaves. The sugarcane processing plants use around 93% of the bagasse — the material that remains after the juice has been extracted from the sugarcane — as fuel, and 85% of the leaves are burned before the harvest to reduce harvesting costs. The remaining leaves are left to rot on the ground. This means that for 100% of the leaves, the carbon they contain makes its way back to the atmosphere as CO_2 [13.1, 13.2].

The production rate of ethanol from sugarcane is about 6400 L/ha, and the utilization of sugarcane bagasse will make it possible to produce an additional 5600 L/ha. In addition, as a large source of lignocellulose biomass, sugarcane bagasse is a cheap and annually renewable resource suitable for producing natural cellulose fibres, and the exploitation of this by-product will also benefit the environment. The chemical modification of cellulose for the production of cellulose derivatives is one method for the production of value added products. Hemicelluloses are the second most abundant bio-polymer in sugarcane bagasse after cellulose. The preparation and the property characterization of new polymers from hemicelluloses are an important part of any research programme for the replacement of polymers prepared from petrochemicals [13.1].

Lignocellulose is the most abundant renewable biomass, and the biological conversion of different lignocellulosic feedstock, such as forest and agricultural residues, or of crops dedicated to biomass production, offers numerous benefits but its development is still hampered by economic and technical obstacles. The application of ionizing radiation can potentially enhance the processes of lignocellulosic to biofuel conversion.

13.2. FIRST GENERATION ETHANOL BIOFUEL

Conventional technologies for the production of first generation biofuels include well established processes on a commercial scale, including sugar and starch based ethanol, oil crop based biodiesel and pure vegetable oil, as well as biogas derived through anaerobic digestion.

This generation of bioethanol utilizes as its main feedstock sugarcane and corn. While these two crops have helped to stimulate the demand for bioethanol and to provide added value to the farming communities, their widespread use introduces some limitations. The use of corn is not sustainable owing to its high energy requirements during growth and the elevated cost of agricultural lands.

13.3. SECOND GENERATION ETHANOL BIOFUEL

Second generation ethanol biofuels are produced by biomass conversion to produce biofuel from lignocellulose feedstock, animal fat and plant oils, and algae as well as by converting sugar into diesel using biological or chemical catalysts. The main benefits of the production of ethanol from biomass are the protection and recovery of the environment, and the reduction of greenhouse gas emissions compared with the emissions that would have been produced by oil derivatives, and the increase in ethanol production per cultivated hectare. The production of second generation ethanol faces a number of technical constraints subject to the structural and chemical complexity of the lignocellulose feedstock and, more specifically, the conversion of cellulose and hemicellulose to fermentable sugars [13.2].

Lignocellulose biomass is a heterogeneous complex of carbohydrate polymers such as cellulose, hemicelluloses and lignin, a complex polymer of phenylpropanoid units, as well as other minor components depending on the source. The cellulose and hemicelluloses, which typically make up 65–80% of the dry mass, are polysaccharides that can be hydrolysed to sugars and eventually fermented to ethanol or converted to biodiesel. Table 13.1 gives the composition of several lignocellulose raw materials. Sugarcane bagasse contains almost 70% carbohydrates [13.2–13.6].

Cellulose shows a highly crystalline structure with rigid linear chains essentially free from side branching. Cellulose is a linear polymer of cellobiose repeating units, and the degree of polymerization is normally 10 to 100 times greater than that found in hemicelluloses. The hydroxyl groups attached to the chains provide strong intermolecular bonding. Lignin is a complex, variable, hydrophobic, cross-linked, three dimensional aromatic polymer of p-hydrophenylpropanoid units connected by C−C and C−O−C links. Lignin and hemicellulose molecules are joined through ester linkages formed by the carboxyl groups in the lignin [13.4].

Sugarcane bagasse generally contains up to 40% glucose polymer cellulose, a large part of which is in a crystalline structure; about 30% hemicellulose, as an amorphous polymer usually composed of xylose, arabinose, galactose and mannose; and 20% lignin, which cannot be easily separated into readily utilizable components owing to their recalcitrant nature towards hydrolysis. The remaining components are mineral, wax, protein and other compounds [13.5, 13.6].

TABLE 13.1. COMPOSITION OF VARIOUS LIGNOCELLULOSE RAW MATERIALS [13.2–13.6]

	Corn stover	Wheat straw	Rice straw	Sugarcane bagasse	Cotton gin trash	News print	Urban residues
				Carbohydrates (%)			
Glucose	39.0	36.6	41.0	38.1	20.0	64.4	40.0
Mannose	0.3	0.8	1.8	n.a.	4.1	16.6	8.0
Galactose	0.8	4.4	0.4	1.1	0.1	—	—
Xylose	14.8	19.2	14.8	24.3	4.6	4.6	14.0
Arabinose	4.2	4.4	4.5	4.5	4.3	0.5	4.0
				Non-carbohydrates (%)			
Lignin	15.1	14.5	9.9	18.4	17.6	21.0	20.0
Ash	4.3	9.6	4.4	4.8	14.8	0.4	1.0
Protein	4.0	4.0	—	4.0	4.0	—	—

—: not determined

13.4. STEPS TO PRODUCE BIOETHANOL FROM BIOMASS

The process of converting biomass to ethanol biofuel consists of three steps, namely pretreatment, hydrolysis and fermentation. The pretreatment is related to the delignification step, which is the liberation of cellulose and hemicelluloses from lignin. The hydrolysis process causes the depolymerization of the carbohydrate polymer, and the fermentation of the mixed hexose and pentose sugars produces ethanol.

13.4.1. Pretreatment

Pretreatment is the first step in cellulose conversion processes for bioethanol production from biomass [13.3, 13.7]. The main challenge of this step is to modify the structure and morphology of the biomass to render cellulose more accessible to the enzymes that convert the carbohydrate polymers into fermentable sugars. An effective pretreatment step must (a) reduce the size of

the particle, (b) preserve pentose units (hemicelluloses), (c) limit the formation of degradation products that adversely affect the growth of the fermentative microorganisms or inhibit enzymes, and finally, (d) minimize the energy costs.

Hydrothermal treatment consists in submitting the lignocellulosic material to a high temperature, which varies in a range of 150–220°C, and low pressure of between 827–1655 kPa in the presence of water or acid. The major reactions in hydrothermal and acid pretreatment under these conditions involve acid catalyzed hydrolysis of the lignin and hemicelluloses into low-molecular-weight, water soluble products. At higher temperatures (170–230°C) and pressures (1655–3310 kPa), the major products are carboxylic acids, mainly acetic and formic acid, formed by oxidation and fragmentation of the cellulose and hemicelluloses [13.3, 13.8–13.11].

The major drawback is the formation of by-products such as carboxylic acids, furfural and hydroxymethylfurfural formed by the dehydration reaction of xylose. This is why it is very important to keep a compromise between the temperature and time of the hydrolysis in order to obtain a maximum of glucose and cellobiose liberation while minimizing the formation of by-products [13.12–13.14].

The steam explosion process is a process in which vapour that is subject to high pressure and temperature is then subjected to a violent decompression of the system, completely disarranging the raw fibres of the lignocellulosic material. This opening in staple fibres makes a bigger area of contact with enzymes possible and increases the conversion of the cellulose to free sugars. Steam explosion is recognized as one of the most cost effective pretreatment processes for hardwoods and agricultural residues. The disadvantages of steam explosion include the destruction of a portion of the xylan fraction and the incomplete disruption of the lignin–carbohydrate matrix. The process causes hemicellulose degradation and lignin transformation due to high temperature, thus increasing the potential of cellulose hydrolysis [13.15–13.17].

13.4.2. Hydrolysis

The hydrolysis reaction breaks the cellulose down into simple sugars suitable for fermentation. The hydrolysis processes that are commonly used are chemical (acid) and enzymatic reactions. These reactions are very harsh and frequently produce toxic degradation products that interfere with the fermentation process.

The primary enzymes used in the hydrolysis of lignocellulosic materials are celullases (generally complexes of three enzymes) that break the cellulose into cello-oligomers and cellobiose (two glucose molecules). Generally, the enzymatic load is supplemented with β glucosidase, which is responsible for

the conversion of cellobiose into glucose. The enzyme dose is based on the calculation of total solids in the dry mass. This dose can vary significantly, owing to the composition of the lignocellulosic material and the nature of chemical and physical pretreatment. The cellulases and β glucosidase are inhibited by cellobiose and glucose. Sometimes surfactants can be added to reduce the adsorption of enzymes by lignin [13.5, 13.15, 13.16].

13.4.3. Fermentation

Alcoholic fermentation is a process that converts the sugar in sugarcane biomass, mainly sucrose, glucose and fructose, to ethanol. Ethanol is produced primarily from sugarcane juice, utilizing the yeast *Saccharomyces cerevisiae* for fermentation. In this process, one molecule of glucose produces two molecules of ethanol:

$$C_6H_{12}O_6 \rightarrow 2\ CH_3\text{-}CH_2\text{-}OH + 2\ CO_2 + 98.2\ kJ$$

At the end of the fermentation process, the average alcohol content typically ranges from 7% to 10%.

Glucose, galactose and mannose are six-carbon sugars (hexoses), and are readily fermented to ethanol by many naturally occurring organisms, but xylose and arabinose, which have five carbons (pentoses), are fermented by few native strains and usually at a low yield. When cellulose hydrolysis is carried out in presence of fermenting microorganisms, the process is called simultaneous saccharification and fermentation. The hydrolysis temperature, the reaction time and the acid concentration influence the generation of fermentation inhibitors [13.7, 13.13].

13.5. A REVIEW OF THE USE OF IONIZING RADIATION IN BIOETHANOL PRODUCTION

Several studies have shown that the irradiation of cotton cellulose degenerates the mechanical parameters by chain scission reaction within the cellulose molecules. It has also been reported that high energy radiation causes a decrease in the degree of polymerization and an increase in the carbonyl content of cotton cellulose. Other studies have shown that, as a pretreatment method, irradiation has similar results in terms of increasing digestibility to NaOH treatment, which is one of the most commonly used methods to upgrade foliage digestibility. When cotton cellulose is subjected to high energy radiation, free radicals are produced and react with them. This reduces the extent of

polymerization while leading to a higher carbonyl content caused by chain scission reactions in the cellulose and hemicellulose [13.12, 13.17–13.20].

Radiation processing is a powerful technology for accelerating this hydrolysis reaction because, compared with most other natural polymers, cellulose shows an unusual susceptibility to degradation by irradiation. The use of ionizing radiation increases the reactivity of cellulose towards certain reagents and decreases the violence of the process. The effects of high energy radiation on purified cellulose materials such as cotton and wood pulp have been studied, but comparatively little work has been carried out on natural biomass. Pure cellulose is readily depolymerized by radiation, but in biomass, the cellulose is intimately bound to lignin [13.3, 13.12, 13.18–13.23].

The main challenge of EB treatment is obtaining the desirable effects while applying doses no higher than those which is necessary to cause some breaks in the polysaccharide chains. The control of absorbed dose in sugarcane bagasse irradiation is very important, so that the degradation of the glucose, xylose galactose and arabinose just after liberation can be avoided, because when the sugar is irradiated alone it is more susceptible to degradation than when it is part of a mixture, as shown by experimental results [13.24], shown in Fig. 13.1, where two kinds of standard sugars were prepared by dilution in distilled water and irradiated by a gamma source in sealed vials to obtain different absorbed doses. One of them was a standard with a mixture of glucose, xylose, galactose and arabinose with concentrations of 511.3 mg/L, 520.2 mg/L, 498.1 mg/L and 483.1 mg/L, respectively. The other was a standard with 500.0 mg/L of each sugar, irradiated separately. When the mixture of different sugars were irradiated as a unique sample, the degradation results reached a much lower percentage (see Fig. 13.1).

13.5.1. The effects of radiation on the structure and composition of sugarcane bagasse

Understanding the chemical and physical mechanisms that play a role during pretreatment and improving the comprehension of the relationship between the chemical composition and physicochemical structure of lignocelluloses as it relates to the enzymatic digestibility of cellulose and hemicelluloses is fundamental for the generation of effective pretreatment models.

The structural and compositional modification of sugarcane bagasse (50% humidity) with absorbed doses from 5–150 kGy show that almost all the cellulose and hemicelluloses are converted to oligosaccharides at 70 kGy. The main by-product identified is acetic acid, which originates from the de-acetylating of hemicelluloses. There is some break in the structure of lignin, but not enough to degrade it. On the other hand, cellulose of a high

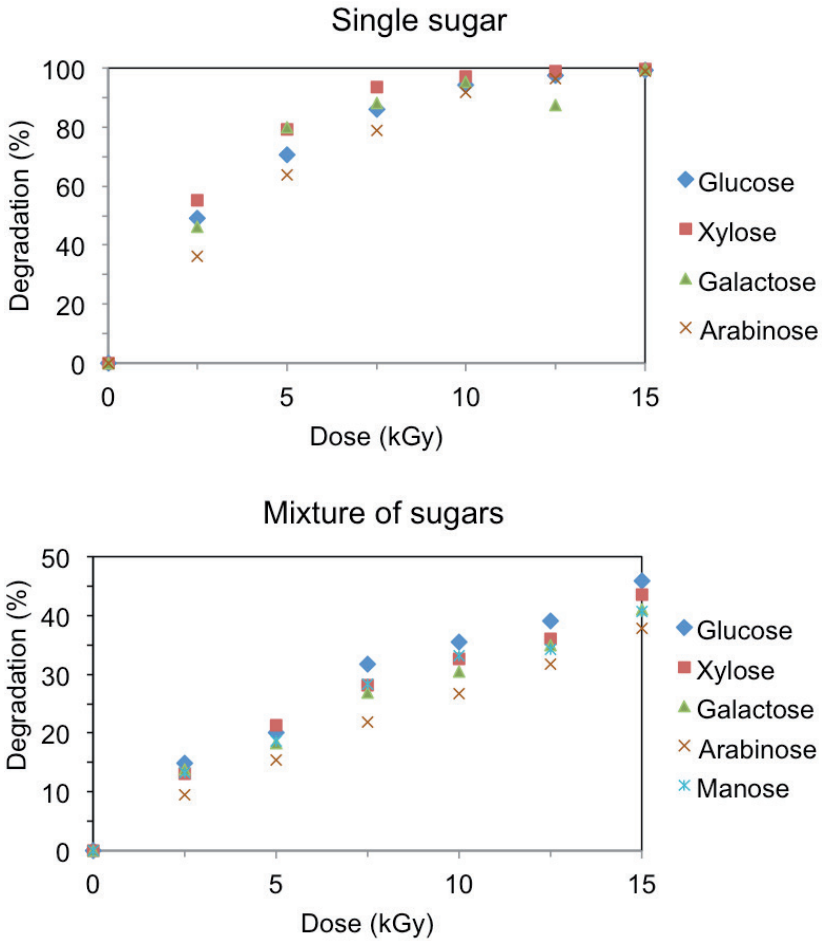

FIG. 13.1. Degradation of the sugars after gamma irradiation in (top) a sample with single sugar and (bottom) a mixed sample [13.24].

molecular weight presents a total reduction at an absorbed dose of 50 kGy. It is important to point out that the changes observed in cellulose suggest that there are some effects on the lignin structure, since the cellulose is protected by lignin and hemicelluloses. The main sugars identified are glucose and arabinose, and the water soluble cello-oligosaccharides formed by the partial degradation of cellulose and hemicelluloses is also detected. These compounds show a maximum concentration at 50 kGy and a total degradation at 100 kGy of absorbed dose. However, they are not hydrolysed to a significant extent during radiation pretreatment, because no significative increase in glucose or xylose is

found. Acid hydrolysis of the soluble extract shows a total degradation of the oligomers and an increase in xylose and glucose, as shown in Fig. 13.2. This confirms that the partial degradation of cellulose and hemicelluloses leads to the formation of cello-oligosaccharides of glucanases and xylanases [13.24].

Radiation acts initially on the branches of hemicelluloses, liberating arabinose, and then acts on the xylose polymers. The main by-product is acetic acid originating from the deacetilation of hemicelluloses. The removal of acetyl groups enhances the accessibility of the enzyme to the cellulose and increases enzymatic hydrolysis [13.24]. This sequence of interaction probably occurs because of the location of xylose in the backbone of arabinoxylan, while arabinose is located in the branches of the macromolecules where the glycosidic bonds are easier to hydrolyse, as shown in Fig. 13.3 [13.25].

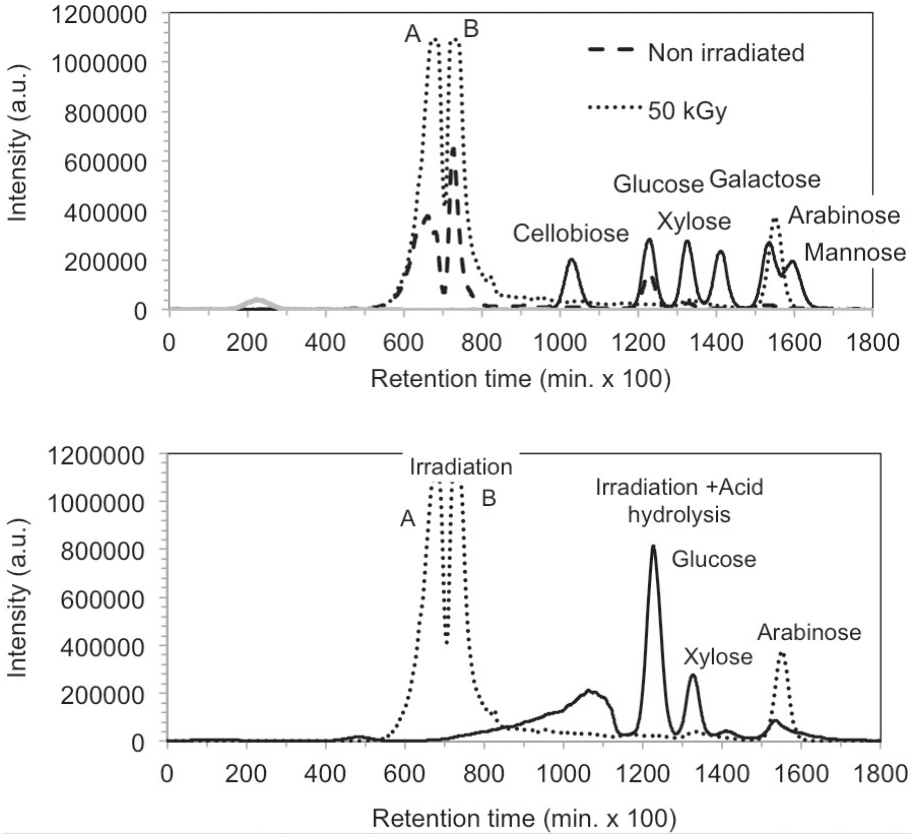

FIG. 13.2. Oligomer decomposition and xylose and glucose increase found in irradiated sugarcane bagasse (SCB) (top) after irradiation and (bottom) after acid hydrolysis [13.24].

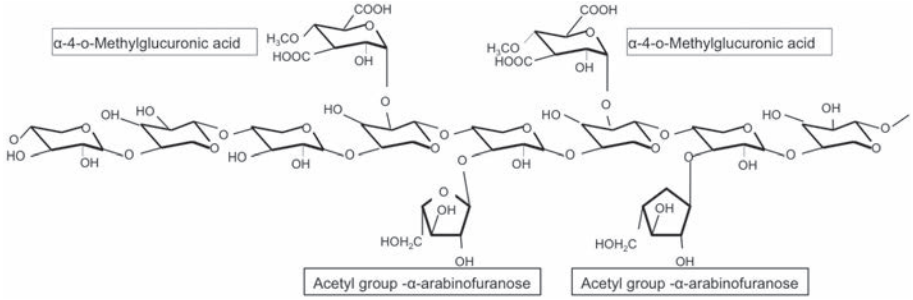

FIG. 13.3. Structure of hemicellulose of sugarcane bagasse [13.4, 13.25].

The composition of the biomass is strongly dependent on the crop, its varieties and the season. The compositional analysis is related to the proportion of cellulose, hemicelluloses, lignin, ash and soluble parts in the biomass. The National Renewable Energy Laboratory (NREL) [13.26] has developed standard procedures for the determination of the composition of different types of biomass that analyse the monosaccharide using GPC, after performing acid hydrolysis in an autoclave (121°C, 60 min).

Figure 13.4 shows a compositional analysis of untreated and EB irradiated sugarcane bagasse. Radiation processing promotes an increase in the soluble portion that is related to hemicellulose and cellulose cleavage, as shown in Fig. 13.2 [13.27].

EB irradiation was responsible for conversion of 0.5% of cellulose to glucose at a dose of 20 kGy in sugarcane bagasse with 50% moisture content. On the other hand, when the bagasse was dried for 12 h, 24 h, 36 h and 48 h, the conversion decreased, as shown in Table 13.2.

These results highlight the importance of moisture content in the formation of $OH^{\bullet}$ radicals, in addition to the radiation effect. The conversion of hemicelluloses to xylose and arabinose reaches 2% at 70 kGy, with the major part remaining as oligosaccharides. Hemicellulose conversion is calculated taking into account the mass of xylose and arabinose, and the mass of the by-products such as furfural and acetic acid, applying the respective conversion factors of the hemicelluloses (0.88 × xylose mass, 0.88 × arabinose mass, 0.72 × acetic acid mass and 1.37 × furfural mass). Furfural is the main compound formed by the oxidation of arabinose and xylose, and its degradation produces formic acid [13.3, 13.14, 13.24, 13.27].

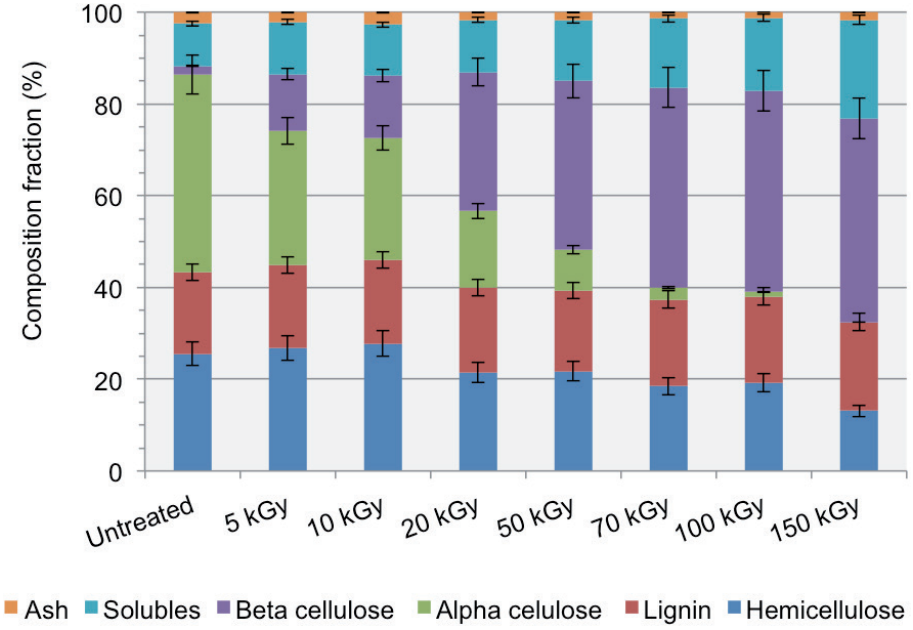

FIG. 13.4. Composition of sugarcane bagasse after EB irradiation [13.24].

TABLE 13.2 CONVERSION OF CELLULOSE TO GLUCOSE IN IRRADIATED SUGARCANE BAGASSE WITH DIFFERENT MOISTURE CONTENT [13.17]

Sugarcane bagasse samples	Absorbed dose (kGy)	Moisture content (%)	Solubility (%)	Conversion (%)
Untreated	30	49.6	9.1	0.58
Dried for 12 h	30	24.3	4.2	0.13
Dried for 24 h	30	9.5	2.3	0.12
Dried for 36 h	30	8.6	2.0	0.11
Dried for 48 h	30	5.0	1.5	0.10

13.5.2. Enzymatic conversion of irradiated sugarcane bagasse

Studies on enzymatic hydrolysis of sugarcane bagasse treated with EB irradiation were carried out using 100 g total mass in a reactor with 8% solid load (dry base) and commercial *Trichoderma reesei* cellulose preparation (Celluclast 1.5 L) supplied by Novozymes (Bagsvaerd, Denmark), with 5 FPU/g of cellulose and beta-glycosidase 0.5% (p/p), 0.08 mL surfactant EDTA and 11 mL of sodium citrate (pH4.5). The incubation was performed at 50ºC, under stirring at 175 rpm for 48 h. Conversion yields on the basis of glucose formation are calculated according to Eq. (13.1).

$$\text{Yield} = \frac{\text{Glucose final concentration} - \text{Glucose initial concentration}}{CF\left(M_{\text{bagasse}} / V\right)\left(M_{\text{glucose}} / M_{\text{cellulose}}\right)} \qquad (13.1)$$

where

CF is the fraction of cellulose in bagasse (0.420);
M_{bagasse} is the mass of bagasse;
V is the volume of the reaction;
M_{glucose} is the molar mass of glucose (180 g/mol);

and $M_{\text{cellulose}}$ is the $\bar{M}_{\text{w}}$ of cellulose (162 g/mol).

The observed yields for the enzymatic conversion of bagasse cellulose into glucose are shown in Fig. 13.5.

When irradiated at 20 kGy, the yield increases from 6% to 10% within the first 24 h of incubation, and to 20% after 48 h [13.17]. The conversion yield of cellulose to glucose did not increase for doses higher than 150 kGy. One reason for these results is the degradation of glucose by radiation, and the formation of inhibiting products.

13.6. COMBINATION OF IRRADIATION AND CONVENTIONAL PRETREATMENT TECHNOLOGIES

The combination of pretreatment technologies is intended to decrease the violence of the process and to avoid excessive sugar degradation. Another important point is the limiting of the formation of by-products with inhibiting properties during the saccharification of lignocelluloses, such as aliphatic acids (e.g. acetic, formic and levulinic acid), furan derivatives (e.g. furfural

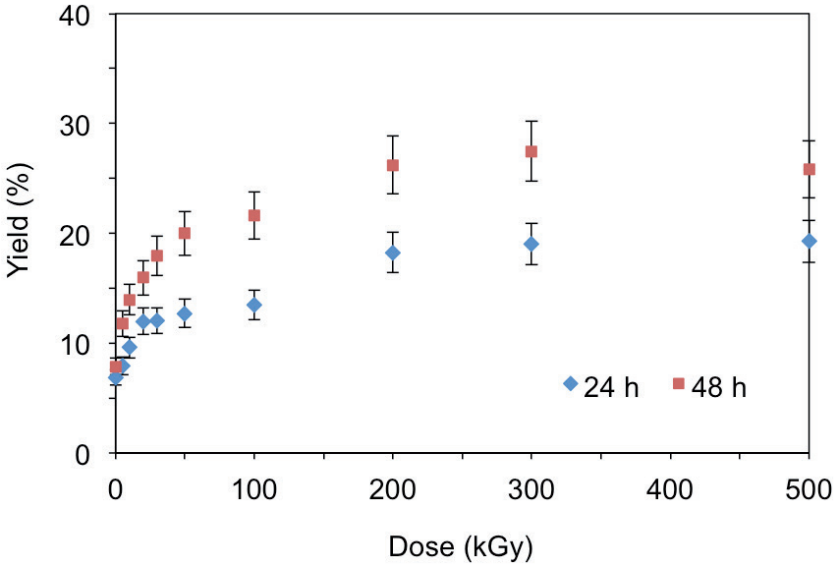

FIG. 13.5. Enzymatic conversion yield (%) of cellulose to glucose after EB irradiation of two different samples (S1 and S2) and enzymatic hydrolysis for 24 h and 48 h [13.17].

and 5-hydroxyl-methyl-furfural) and phenol compounds. These compounds might seriously inhibit enzyme activity and hence decrease the yield of glucose formation.

13.6.1. Radiation combined with hydrothermal treatment of sugarcane bagasse

The hydrothermal hydrolysis of sugarcane bagasse at 180°C after irradiation at 50 kGy leads to a total reduction in oligosaccharides, mainly because of the liberation of xylose. However, the presence of formic acid and furfural after 40 min of thermal treatment suggests that xylose and glucose decompose immediately following their liberation from hemicelluloses and cellulose. If diluted acid is used, the same amount of xylose can be liberated as before, but in this case, the time of thermal treatment is reduced from 40 min to 10 min and the absorbed dose is reduced from 50 to 10 kGy. Figure 13.6 shows the increase in solubility that is proportional to the radiation dose and hydrolysis time. Considering only irradiation, there is an increase of 16% in solubility when applying 150 kGy. Taking into account only thermal hydrolysis for 10 min, an increase of 22.7% can be observed, and with the addition of dilute acid, the solubility rate increases to 42.2%. Considering the solubility of samples that are

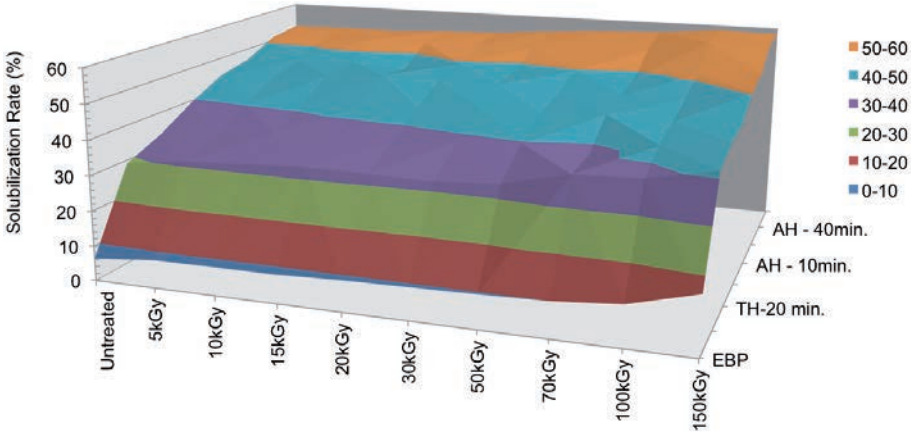

FIG. 13.6. Solubility after hydrothermal and dilute acid treatment of sugarcane bagasse irradiated at different absorbed doses [13.17].

non-irradiated and irradiated at 150 kGy, acid hydrolysis presented an increase of 1%, 3% and 6% for 10 min, 20 min and 30 min, respectively, while thermal hydrolysis showed 13%, 11% and 3% for 10, 20 and 40 min, respectively [13.27].

The conversion of hemicelluloses reached 42% after thermal treatment by 40 min for sugarcane bagasse irradiated at 50 kGy. After the addition of diluted sulphuric acid (0.1% v/v), almost all of the hemicellulose is converted to xylose and by-products, mainly furfural. Boussarsar et al. [13.28] obtained a 55% conversion of hemicellulose to xylose after 4 h at 170°C, but for 2 h the yield decreased to 48.8%. Rodrigues et al. [13.14] obtained 74.4% conversion of hemicelluloses at 130°C for 20 min and 100 mg acid/g of dry bagasse.

The enzymatic hydrolysis of cellulose in sugarcane bagasse samples submitted to EB irradiation and thermal treatment is shown in Fig. 13.7. The enzymatic conversion yield reached almost 72% in samples irradiated at 50 kGy and subjected to 60 min of thermal treatment. When dilute sulphuric acid was added, an increase in cellulose conversion was observed, however, the time was reduced. The higher value (74%) was reached after 40 min thermal treatment and 24 h enzymatic hydrolysis. Reference [13.16] describes the obtaining of 69.2% cellulose conversion when treating sugarcane bagasse at 195°C for 10 min, and 72 h of enzymatic hydrolysis, and 89.2% after delignification of these samples with NaOH 1.0% at 100°C for 1 h.

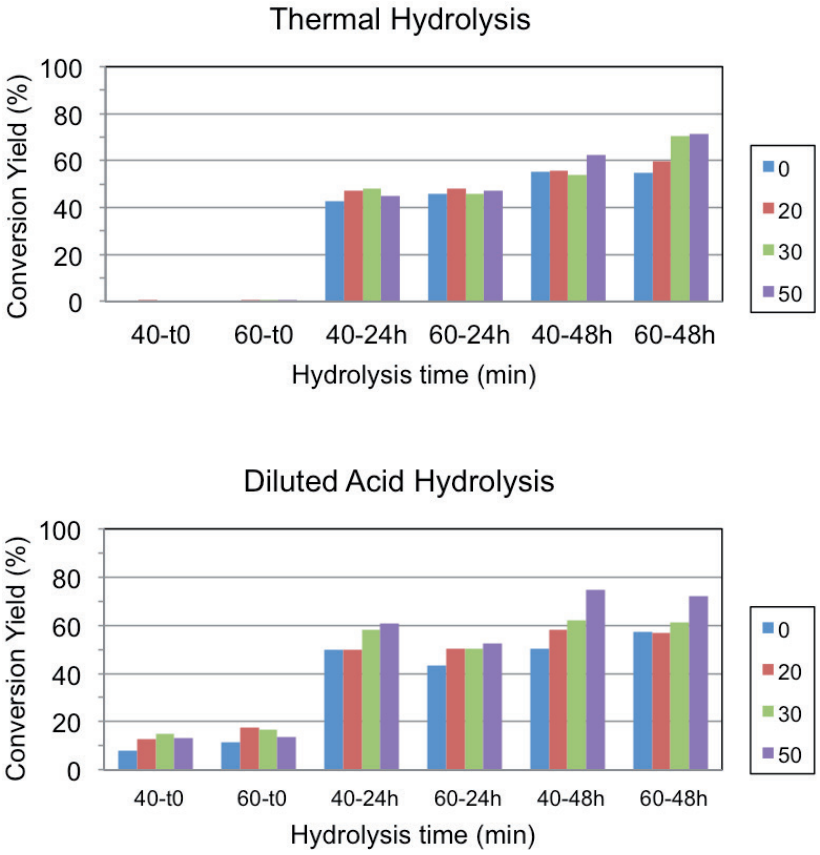

FIG. 13.7. Enzymatic conversion yield (%) of cellulose to glucose after 24 h and 48 h of enzymatic hydrolysis of irradiated sugarcane bagasse followed by thermal and acid treatment for 40 and 60 min [13.17].

13.6.2. Radiation combined with steam explosion treatment of sugarcane bagasse

Studies on the combination of steam explosion with EB irradiation were carried out using sugarcane bagasse samples steam exploded using a sealed reactor, pressurized at 15.7 kg/cm^2, heated to 200°C and kept in this condition for 10 min. After this time, the valve on the bottom of the reactor was opened, making the materials undergo an explosive decompression. These steam exploded samples were irradiated at different absorbed doses. In Fig. 13.8, the compositional analysis of these samples irradiated with an absorbed dose from 5–200 kGy are presented, including natural sugarcane bagasse and samples that

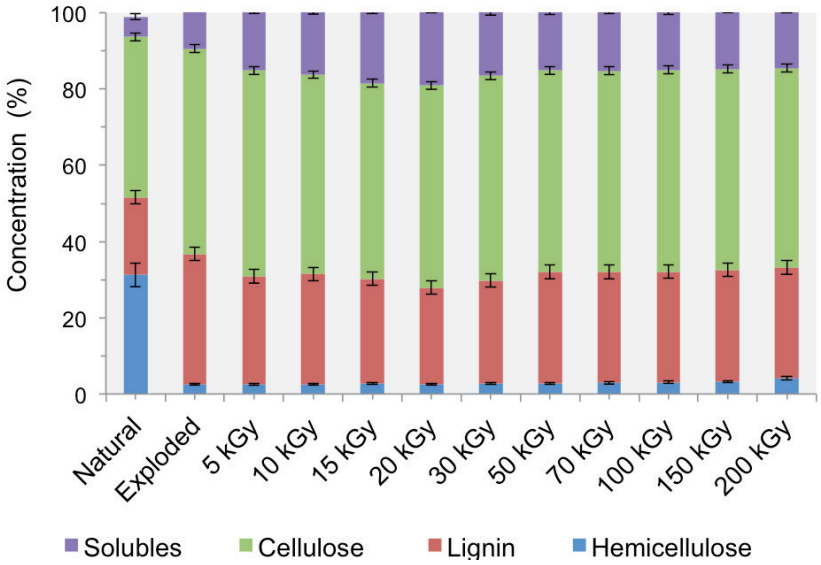

FIG. 13.8. Compositional analysis of sugarcane bagasse after steam explosion and EB irradiation at various doses [13.17].

were steam exploded without irradiation. The steam explosion showed a total removal of hemicelluloses, but lignin did not change, and after EB irradiation there was an increase in the soluble fraction.

The steam exploded sugarcane bagasse samples contained very high concentrations of furfural, which originated from the decomposition of hemicelluloses. Radiation processing can contribute to its removal, as shown in Fig. 13.9. The furfural concentration underwent a gradual reduction with the increase in absorbed dose, reaching about 60% at 200 kGy.

The FTIR spectra obtained from attenuated transmission reflectance of raw sugarcane bagasse that had been steam exploded and irradiated after steam explosion are presented in Fig. 13.10.

The band at 3350 cm^{-1} corresponds to the hydrogen bonds and its reduction indicates the disruption of hydrogen bonds of cellulose. The band at 2900 cm^{-1} corresponds to the methyl/methylene group in cellulose. The aromatic skeleton of lignin absorbs at 1660, 1630 and 1480 cm^{-1}. The bands at 1033 cm^{-1} and 900 cm^{-1} are related to crystalline and amorphous cellulose, respectively. After irradiation, the exploded bagasse does not show any modification in these structures. The main modifications after steam explosion are observed in the band at 1730 nm referring to the acid group in the structure of hemicelluloses and in the band at 1254 cm^{-1} that refers to the acetyl group. These peaks disappeared owing to the removal of hemicelluloses [13.15, 13.25, 13.29, 13.30].

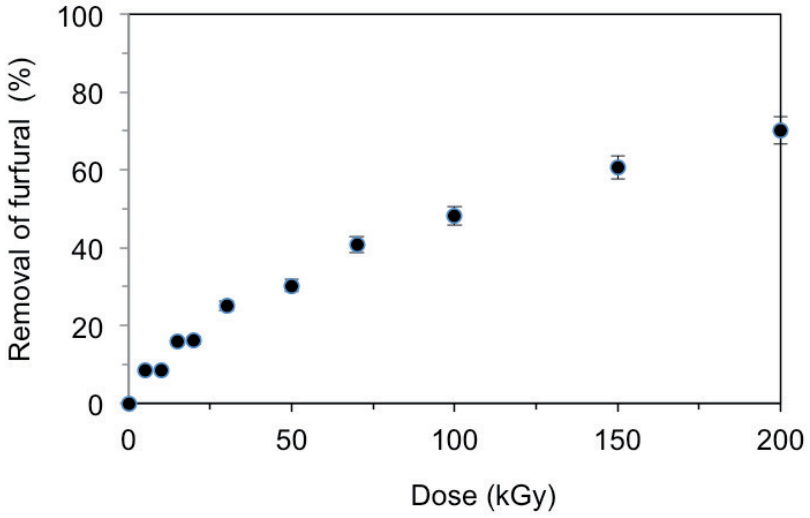

FIG. 13.9. Furfural removal after EB processing of steam exploded sugarcane bagasse [13.17].

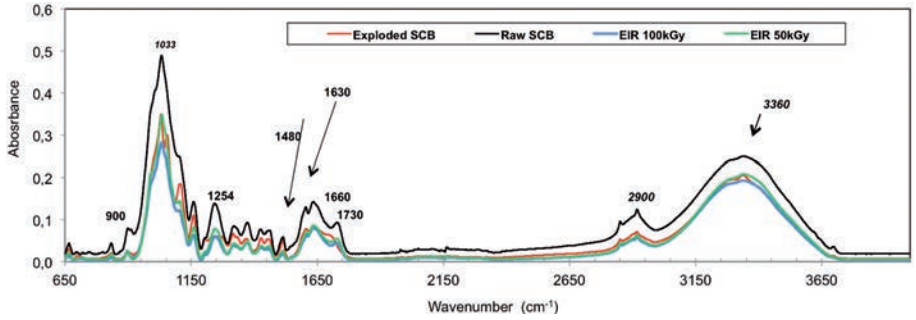

FIG. 13.10. FTIR spectra of raw sugarcane bagasse, after steam explosion, and EB processing at 50 kGy and 100 kGy [13.17].

The results of the enzymatic hydrolysis of sugarcane bagasse submitted to steam explosion and EB irradiation is shown in Fig. 13.11. An expected increase in the yield of enzymatic hydrolysis in these samples as a result of furfural degradation by irradiation has not occurred. However, the radiation showed no effect on the enzymatic hydrolysis of cellulose for absorbed doses lower than 30 kGy. At higher doses, the yield decreased. This evolution could result from glucose degradation upon irradiation, because in the steam exploded bagasse, the cellulose is not protected by the hemicelluloses.

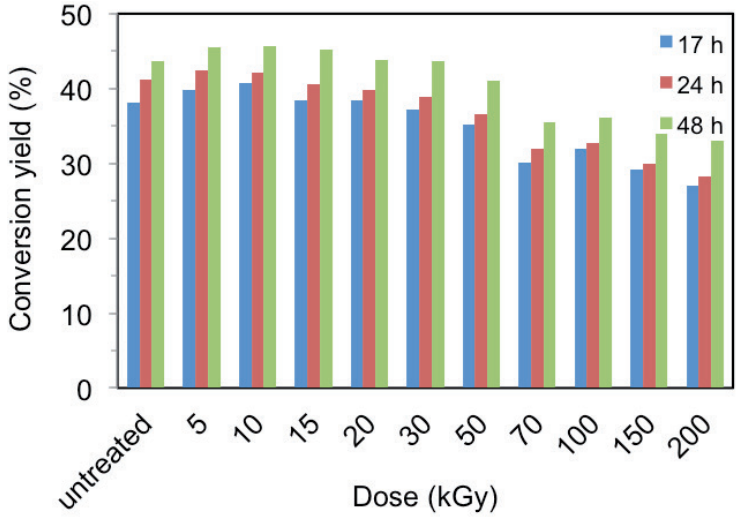

FIG. 13.11. Conversion yield of cellulose to glucose after enzymatic hydrolysis of 24 h and 48 h of steam exploded sugarcane bagasse at different absorbed doses [13.17].

13.7. FINAL CONSIDERATIONS

Concerning the present interest around the world in the development and production of second generation bioenergy, there are some areas that still need research and improvement. Examples are the development of economically feasible physical and chemical pretreatments of biomass for the hydrolysis of lignocelluloses, the development of acid catalysed and biocatalysed saccharification, the development of high performance cellulases and hydrolases, the removal of fermentation inhibitors and the development of microorganism strains. EB irradiation could be used as a competitive pretreatment method to increase the conversion yield and the production of ethanol biofuel.

The structural and chemical modifications produced by ionizing radiation in sugarcane bagasse are very important aspects of the development of second generation energy production. Improvements that will arise from the combination of pretreatment technologies will enhance the efficiency and reduce the cost of future bioethanol production.

ACKNOWLEDGEMENTS

The authors gratefully acknowledge the Research Foundation of São Paulo State, FAPESP, (BIOEN Project 08/056066-1) and the IAEA (Research Contract 4709) for their financial support.

REFERENCES TO CHAPTER 13

[13.1] HASSUANI, S.J., Biomass Power Generation: Sugar Cane Bagasse and Trash, (2005), http://www.sucre-ethique.org/IMG/pdf/CTC_energy_-_biomass_1_.pdf

[13.2] INTERNATIONAL ENERGY AGENCY, Technology Roadmap: Biofuels for Transport (2011), http://www.iea.org/publications/freepublications/publication/technology-roadmap-biofuels-for-transport.html

[13.3] BRENNER, W., RUGG, B., ARNON, J., Radiation pretreatments for optimizing the sugar yield in the acid hydrolysis of waste cellulose, Radiat. Phys. Chem. **14** (1979) 299–308.

[13.4] GLASSER, W.G., KELLY, S.S., Encyclopedia of Polymer Science and Engineering, John Wiley & Sons, New York (1987) p. 796.

[13.5] SANCHEZ, O.J., CARDONA, C.A., Trends in biotechnological production of fuel ethanol from different feedstocks, Bioresour. Technol. **99** (2008) 5270–5295.

[13.6] SUN, J.X., SUN, X.F., ZHAO, H., SUN, R.C., Isolation and characterization of cellulose from sugarcane bagasse, Polym. Degrad. Stab. **84** (2004) 331–339.

[13.7] MOSIER, N., et al., Features of promising technologies for pretreatment of lignocelluloses biomass, Biores. Technol. **96** (2005) 673–686.

[13.8] McGINNIS, G.D., PRINCE, S.E., BIERMANN, C.J., LOWRIMORE, T., Wet oxidation of model carbohydrate compounds, Carbohydr. Res. **128** (1984) 51–60.

[13.9] SILVA, V.F.N., ARRUDA, P.V., FELIPE, M.G.A., GONÇALVES, A.R., ROCHA, G.J.M., Fermentation of cellulosic hydrolysates obtained by enzymatic saccharification of sugarcane bagasse pretreated by hydrothermal processing, J. Ind. Microbiol Biotechnol. **38** 7(2010) 809–817.

[13.10] VAN WALSUM, G.P., ALLEN, S.C., SPENCER, M.J., LASER, M.S., ANTAL, M.J., LYND, L.R., Conversion of lignocellulosics pretreatment with liquid hot water to ethanol, Appl. Biochem. Biotechnol. **57** 58 (1996) 157–170.

[13.11] YU, Y., LOU, X., WU, H., Some recent advances in hydrolysis of biomass in hot-compressed water and its comparisons with other hydrolysis methods, Energy Fuels **22** (2008) 46–60.

[13.12] McLAREN, K.G., Degradation of cellulose in irradiated wood and purified celluloses, Intern. J. Appl. Rad. Isot. **29** (1978) 631–635.

[13.13] PALMQVIST, E., HAHN-HAGERDAL, B., Fermentation of lignocellulosic hydrolysates. II: inhibitors and mechanisms of inhibition, Bioresour. Technol. **74** (2000) 25–33.

[13.14] RODRIGUES, R.C.I.B., ROCHA, G.J.M., RODRIGUES, D., JR., FILHO, H.J.I., FELIPE, M.G.A., PESSOA, A.P., JR., Scale-up diluted sulfuric acid hydrolysis for producing sugarcane bagasse hemicellulose hydrolysate, Bioresour. Technol. **101** (2010) 1247–1253.

[13.15] KADAM, K.L., RYDHOLM, E.C., McMILLAN, J.D., Development and validation of a kinetic model for enzymatic saccharification of lignocellulosic biomass, Biotechnol. Progr. **20** (2004) 698–705.

[13.16] SANTOS, V.T.O., ESTEVES, P.J., MILAGRES, A.M.F., CARVALHO, W., Characterization of commercial cellulases and their use in the saccharification of a sugarcane bagasse sample pretreated with dilute sulfuric acid, J. Ind. Microbiol. Biotechnol. **38** 8 (2010) 1089–1098.

[13.17] DUARTE, C.L., RIBEIRO, M.A., OIKAWA, H., MORI, M.N., NAPOLITANO, C.M., GALVÃO, C.A., Study of thermal treatment combined with radiation on the decomposition of polysaccharides in sugarcane bagasse, Radiat. Phys. Chem. **84** (2013) 191–195.

[13.18] HAN, Y.W., CATALANO, E.A., CIEGLER, A., Chemical and physical properties of sugarcane bagasse irradiated with γ rays, J. Agric. Food Chem. **311** (1983) 34–38.

[13.19] KHAN, F., AHMAD, S.R., KRONFLI, E., γ Radiation induced changes in the physical and chemical properties of lignocelluloses, Biomacrom. **7** (2006) 2303–2309.

[13.20] SMITH, G.S., KIESLING, H.E., GALYEAN, M.L., BADER, J.R., Irradiation enhancements of biomass conversion, Radiat. Phys. Chem. **25** 1–3 (1985) 27–33.

[13.21] FOLDVÁRY, C.M, TAKÁCS, E., WOJNÁROVITS, L., Effect of high-energy radiation and alkali treatment on the properties of cellulose, Radiat. Phys. Chem. **67** (2003) 505–508.

[13.22] TAKÁCS, E., WOJNÁROVITS, L., BORSA, J., FOLDVÁRY, C., HARGITTAI, P., ZOLD, O., Effect of γ irradiation on cotton-cellulose, Radiat. Phys. Chem. **55** (1999) 663–666.

[13.23] TAKÁCS, E., WOJNÁROVITS, L., FOLDVÁRY, C., BORSA, J., SAJÓ, I., Effect of combined gamma-irradiation and alkali treatment on cotton-cellulose, Radiat. Phys. Chem. **57** (2000) 399–403.

[13.24] RIBEIRO, M.A., OIKAWA, H., MORI, M.N., DUARTE, C.L., Degradation mechanism of polysaccharides on irradiated sugarcane bagasse, Radiat. Phys. Chem. **84** (2012) 115–118.

[13.25] KUMAR, R., MAGO, G., BALAN, V., WYMAN, C., Physical and chemical characterizations of corn stover and poplar solids resulting from leading pretreatment technologies, Biores. Technol. **100** (2009) 3948–3962.

[13.26] NATIONAL RENEWABLE LABORATORY, Analytical Procedures for Standard Biomass Analysis (2010),
http://www.nrel.gov/biomass/analyticalprocedures.html

[13.27] DUARTE, C.L., RIBEIRO, M.A., OIKAWA, H., MORI, M.N., NAPOLITANO, C.M., GALVÃO, C.A., Electron beam combined with hydrothermal treatment for enhancing the enzymatic convertibility of sugarcane bagasse, Radiat. Phys. Chem. **81** (2012) 1008–1011.

[13.28] BOUSSARSAR, H., ROGÉ, B., MATHLOUTHI, M., Optimization of sugarcane bagasse conversion by hydrothermal treatment for the recovery of xylose, Bioresour. Technol. **100** (2009) 6537–6542.

[13.29] CHUNDAWAT, S.P.S., VENKATESH, B., DALE, B.E., Effect of particle size based separation of milled corn stover on AFEX pretreatment and enzymatic digestibility, Biotechnol. Bioeng. **96** 2 (2007) 219–231.

[13.30] STEWART, D., WILSON, H.M., HENDRA, P.J., MORRISON, M., Fourier-Transform Infrared and Raman Spectroscopic study of biochemical and chemical treatment of oak wood (*Quercus rubra*) and barley (*Hordeum vulgare*) straw, J. Agric. Food Chem. **43** (1995) 2219–2225.

Chapter 14

RADIATION PROCESSED POLYSACCHARIDES FOR ENVIRONMENTAL APPLICATIONS

T. KUME
Dalat University,
Dalat, Viet Nam

14.1. INTRODUCTION

Nuclear technology has contributed to creating a cleaner environment in many ways through, for example, the cleaning of water by reducing contaminants, contributing to cleaner agriculture via the sterile insect technique, food irradiation and mutation breeding, and recycling resources from wastes. The modification of natural polymers by radiation is another example of reducing environmental pollution by using an environmental friendly technology to prepare products from naturally occurring polymers such as cellulose, starch, chitin, chitosan, alginate and carrageenan.

Cellulose is the most abundant natural polymer on this planet, but a large quantity of cellulosic agricultural wastes or by-products such as sugarcane bagasse and rice straw are produced throughout the world. It has been estimated that 2 billion t of cereal straw, 500 million t of leguminous crop residues, 200 million t of sugarcane bagasse and 300 million m^3 of forest residues are generated. These agricultural wastes generated during the harvesting, handling and processing of cellulose containing plants are discarded or burned, causing serious environmental pollution problems world wide.

Chitin is the second most abundant naturally occurring polysaccharide and is found in the exoskeleton of marine organisms such as shrimps and crabs, and in cuttlebone recovered from the waste of fisheries. The utilization of chitin and its derivative chitosan is far less widespread than that of cellulose but the development of commercial applications for chitin and chitosan has expanded rapidly in recent years.

By using irradiated natural polymers, the use of chemicals, pesticides and fumigants such as ethylene oxide and methyl bromide, which are environmental biohazards, can be effectively decreased. This chapter discusses the radiation treatment of natural polymers for environmental applications such as the recovery

of wastes from industrial plants, decontamination of pathogenic microorganisms in various wastes and sewage sludge and improvement of quality of natural polymers by radiation degradation and cross-linking.

14.2. RADIATION TREATMENT OF CELLULOSIC MATERIALS

The burning and incineration of cellulosic wastes emits considerable amounts of smoke and pollutants and thereby affects surrounding areas. A number of experiments have shown that the radiation treatment of cellulosic materials induces a partial breakdown of the molecular structure that increases digestion by ruminant animals, fermentation and enzymatic degradation.

14.2.1. Recycling of cellulosic waste

A large quantity of cellulosic agricultural wastes and by-products are generated worldwide and a great deal of these becomes waste. The upgrading of these wastes by radiation technology into useful end products is a potential solution to environmental pollution. One of these applications is to convert these wastes into animal feed. Forest biomass contains 40–60% cellulose, 10–25% hemicellulose and 13–18% lignin, while agricultural waste contains 30–45% cellulose, 16–29% hemicellulose and 3–13% lignin.

For animal feed, it is strongly suggested to bring the lignin content down to less than 10% for better digestibility. A radiation fermentation process using oil palm cellulosic wastes has been shown to reduce lignin to the desired levels [14.1]. The palm oil industry is expanding in Asia and cellulosic wastes such as empty fruit bunch (EFB) and palm press fibre are increasing. Incineration of these wastes emits considerable amounts of smoke and pollutants (Fig. 14.1).

Oil palm cellulosic wastes can be converted to a material that can be used for feeding animals or growing mushrooms by radiation and fermentation treatment. The process is as follows: microorganisms in the fermentation media of EFB are removed by radiation, useful fungi are inoculated, and subsequently proteins and edible mushrooms are produced (Fig. 14.2). Among many fungi used for the digestion of EFB, *Coprinus cinereus* and *Pleurotus sajor-caju* were the most suitable microorganisms for the fermentation of EFB. The protein content increased to 13% and the crude fibre content decreased to 20%. A high yield of edible mushrooms was obtained during fermentation using *P. sajor-caju* (Fig. 14.3). EFB is a good substrate for mushroom and animal feed production, and radiation and fermentation treatment is effective for utilizing cellulosic wastes as well as reducing pollution problems. Similar results are obtained using rice straw and sugarcane bagasse.

FIG. 14.1. Environmentally polluting smoke from a factory processing oil palm [14.1].

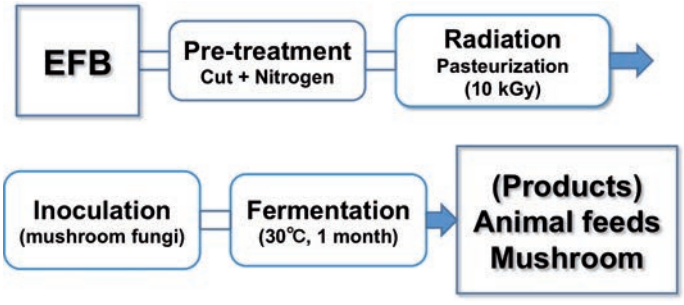

FIG. 14.2. Processing EFB into animal feed using radiation and fermentation [14.1].

14.2.2. Degradation of cellulose wood pulp for the production of viscose rayon

Viscose from cellulose wood pulp is used to produce clothing, fabric, filament, automobile tyres, packaging film and so on. It is currently manufactured mainly by a process that involves dissolving the cellulose pulp in toxic chemicals

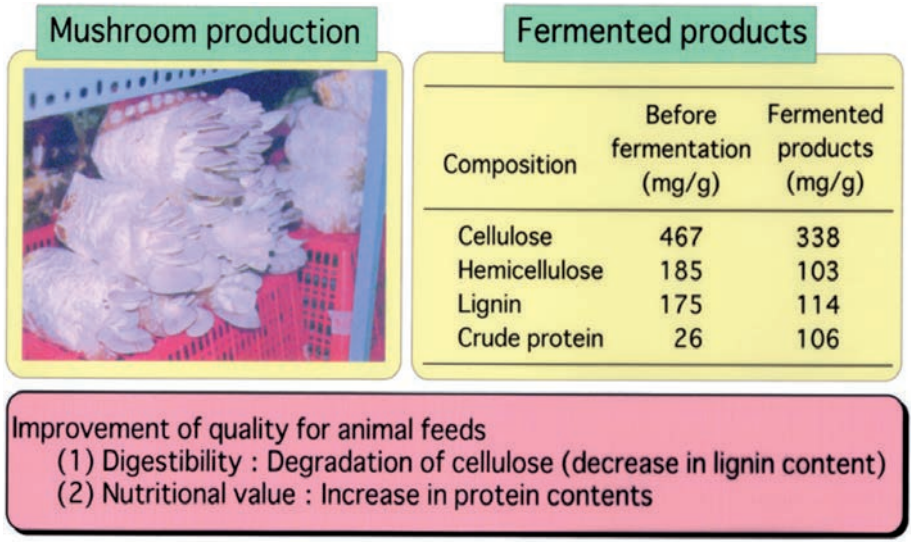

FIG. 14.3. Products from cellulosic waste obtained by radiation and fermentation treatment [14.1]. EFB was irradiated at 10 kGy and fermented at 30°C for 1 month.

such as carbon disulphide (CS_2) and also uses high concentrations of alkali and acids. In many plants, the CS_2 and hydrogen sulphide (H_2S) formed on spinning are vented to the atmosphere. These chemicals, and the zinc used in the spin bath, are toxic and cause environmental problems.

In the viscose process, cellulose is first treated with high concentrations of alkali (18–20%) to produce alkali cellulose. The alkali cellulose is incubated, or aged, in air for hours at 40°C or higher. During this ageing step, oxygen reacts with the alkali cellulose causing cleavage of the cellulose chains, which is necessary for producing viscose with the right viscosity for spinning. High concentrations (28%–36% based on cellulose) of CS_2 are then added to make a xanthate. These xanthate groups are sufficient to disrupt the forces holding the crystalline structure, thereby promoting solubilization in alkali. When the xanthate is dissolved in alkali, the resulting solution is called viscose. The viscose is spun in a bath containing high concentrations of sulphuric acid, sodium sulphate and zinc sulphate. During the spinning process, solid cellulose and CS_2 are regenerated, and H_2S is produced as a side product.

Radiation can easily react with the crystalline regions in cellulose to cause cleavage of the cellulose chains. Therefore, radiation technology can be effectively used to control the degree of polymerization of cellulose pulp as well as to enhance its reactivity towards solvents. EB processing of cellulose pulp to produce viscose can reduce CS_2 and NaOH usage [14.2]. If less CS_2 is used

(reductions of 25–40%), less CS_2 and H_2S are produced during the spinning process and smaller amounts of these chemicals are released into the atmosphere. In practice, these advantages can be utilized for reducing the concentrations of hazardous chemicals, thereby lowering the pollution emitted. The need for fewer ventilators owing to reduced emissions of toxic gases also results in significant energy savings.

14.3. THE PRODUCTION OF BIODEGRADABLE PLASTICS FROM STARCH

Synthetic polymers produced from petroleum are a major source of environmental pollution. Natural polysaccharides such as starch are totally biodegradable and are the most promising materials for the production of biodegradable plastics. Replacing these synthetic materials with biodegradable ones can contribute substantially to reducing pollution and increasing environmental friendliness.

14.3.1. Bio-foams and bio-films from sago starch

Sago starch, which is produced from the pith of the sago palm, a plant that is abundant in Malaysia, is a useful indigenous resource for biodegradable raw materials and/or composites. Sago starch on its own cannot be expanded to produce foam. However, blending sago starch with other water soluble polymers enables the blends to be expanded. EB irradiation is used to induce cross-linking in the sago blends that prevents the foam from collapsing once it has cooled down [14.3]. In comparison with the raw materials used to create other foam materials, sago starch is much cheaper than synthetic polymers of PE or polystyrene (Table 14.1). Some sago blends such as sago−PVP formulations foam very well but produce hard foams. On the other hand, sago−PVA blends produce softer and more resilient foams. Irradiation at high dose levels leads to the formation of rigid foams. As much as 80% of sago starch can be added into blends for eventual foam production (Fig. 14.4). A biodegradability test showed that more than 90% of weight was lost after 3 months burial.

Sago film is 100% biodegradable, and is designed to replace non-biodegradable film made from synthetic polymers such as PE or polypropylene. The film can be produced at various thicknesses depending on the intended application. Blends of sago film have been prepared in soft and hard formulations depending on their final applications. Sago film has good mechanical strength and good water permeability [14.3].

TABLE 14.1. DENSITY OF SAGO FOAM IN COMPARISON WITH OTHER COMMERCIAL FOAM PRODUCTS [14.3]

Foam materials	Sago	Wheat	Corn	Polyethylene	Polystyrene
Density (kg/m^3)	0.2	0.7	0.9	0.06	0.05
Cost of raw materials (RM[a]/kg)	0.80	1.70	2.30	>5.00	>5.00

[a] RM: Malaysian Ringgit; US $1 was equivalent to RM 4.13 at the time of writing.

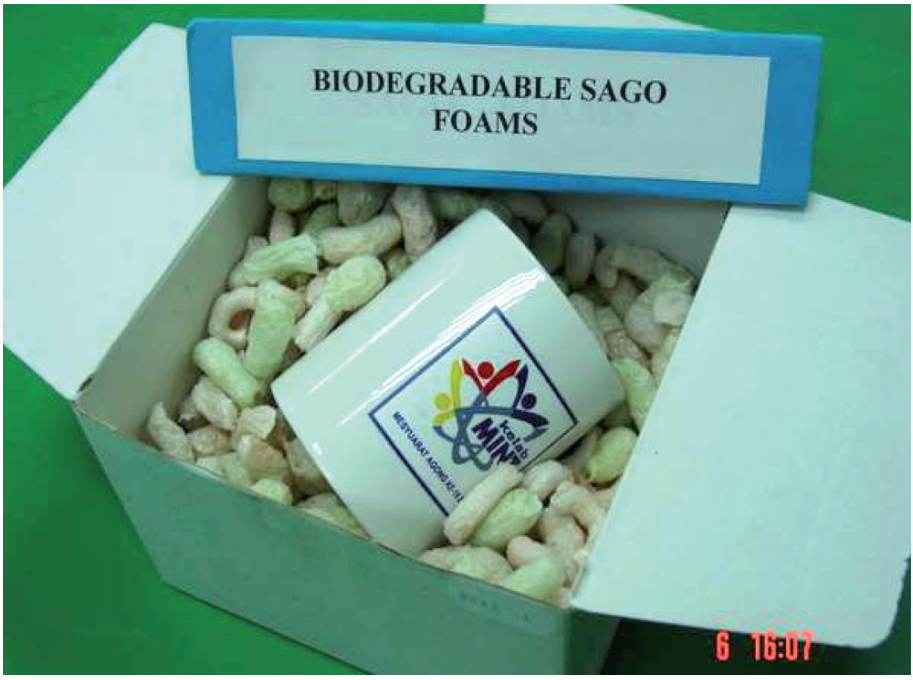

FIG. 14.4. Sago based biodegradable foam produced by radiation cross-linking of sago starch and PVA blends (photograph courtesy of Nuclear Malaysia).

14.3.2. Radiation cross-linking of PLA

PLA is a bioplastic that can be produced by the fermentation of glucose and saccharose. Enzymes (amylase, for example) act on starches such as cassava, potato, corn or sugarcane extract and produce L-lactic acid. Chemical conversion to lactide and subsequent polymerization yield PLA, which is biodegradable

and is considered a carbon neutral resource. Plants absorb carbon dioxide in air and photosynthesize starch. Although PLA synthesized from starch releases the carbon dioxide by digestion of microorganisms, it is not considered to increase the carbon dioxide concentration in the atmosphere (Fig. 14.5).

PLA has good properties as a plastic material with high strength, transparency, biodegradability and biocompatibility. However, it has low heat resistance, which leads to deformation above the glass temperature, 60°C. Cross-linking of PLA by radiation is an effective way to overcome this disadvantage and expand the utilization of PLA. Among many polyfunctional monomers tested as inducers of cross-linking of this degradable type of polymer during irradiation, it was found that triallylisocyanurate (TAIC) was the most effective [14.4]. A TAIC concentration of 3% in PLA gives a gel fraction of 80% (Fig. 14.6). The heat stability of PLA is improved by cross-linking under EB irradiation in the presence of TAIC (Fig. 14.7) and the product does not melt even at temperatures higher than 200°C. Furthermore, softness and flexibility for thin film and sheets of cross-linked PLA can be improved by soaking in plasticizer.

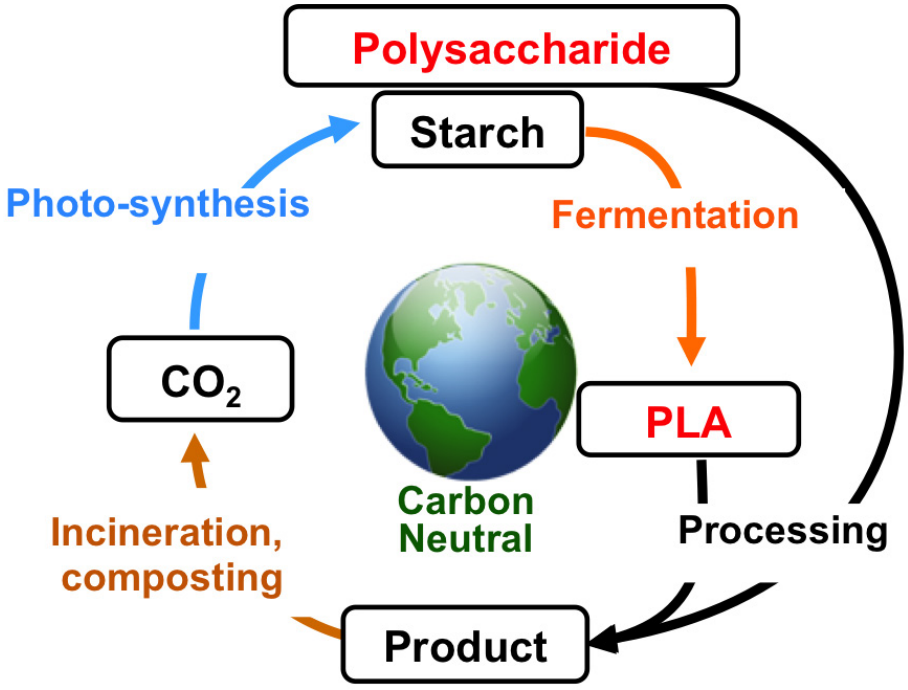

FIG. 14.5. Renewable material of PLA (figure courtesy of Japan Atomic Energy Agency).

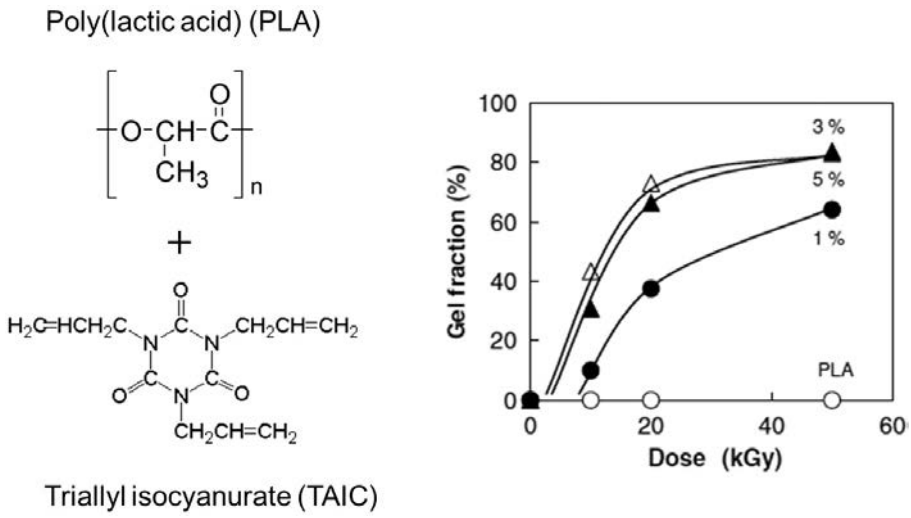

FIG. 14.6. Insoluble fraction of PLA after irradiation in the presence of TAIC as a cross-linker at a concentration ranging from 0–5 %wt [14.4].

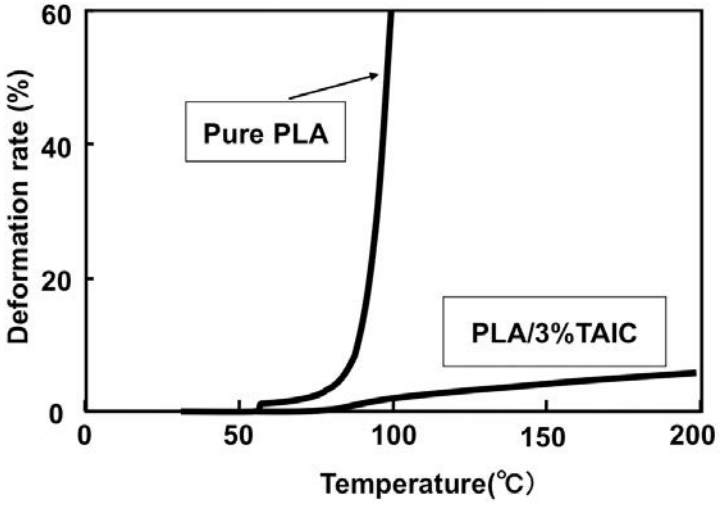

FIG. 14.7. Heat stability of unirradiated pure PLA and 50 kGy irradiated PLA with 3% TAIC [14.4].

14.4. RECOVERY AND UTILIZATION OF WASTE PROTEIN

Proteins are an important source of food and feed, but at the same time, protein by-products resulting from food processing are often discarded and can

cause environmental pollution. Radiation technology can be applied for the recovery and reuse of these proteins from waste.

The recovery of protein from wastewater from the food industry could be improved with a combination treatment of radiation and chitosan. The pathogenic microorganisms in blood wastewater from slaughterhouses were eliminated by radiation and the recovered materials could be used for animal feed [14.5]. The suspended solids in wastewater were coagulated by the addition of chitosan. The coagulation was accelerated by pre-irradiation treatment, and the acceleration reached its maximum at around 30 kGy (Fig. 14.8). Radiation causes the denaturation and aggregation of proteins via the rupture of hydrogen bonds with subsequent unfolding of molecules (Fig. 14.9). As the result, the soluble proteins become insoluble, which promotes their coagulation in wastewaters.

Combined radiation and chitosan treatment was also effective at recovering organic substances from potato starch wastewater [14.6]. Furthermore, the reduction of browning in potato starch wastewater due to the oxidation of polyphenols was also initiated by radiation treatment (Fig. 14.10). Results also showed that the irradiation at the sterilization dose was effective to recover the proteins from wastewater for animal feeds without pathogenic microorganisms.

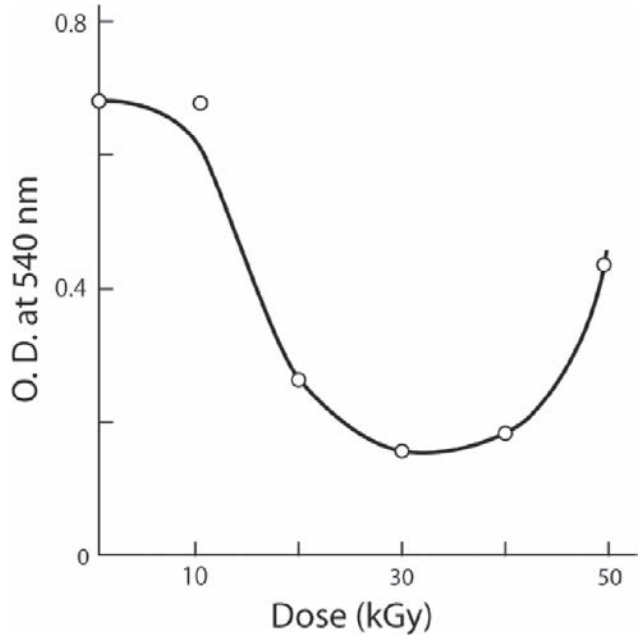

FIG. 14.8. Dose dependence of the coagulation efficiency of irradiated blood wastewater measured from the optical density (absorbance) of the supernatant after the addition of 0.01 % of chitosan [14.5].

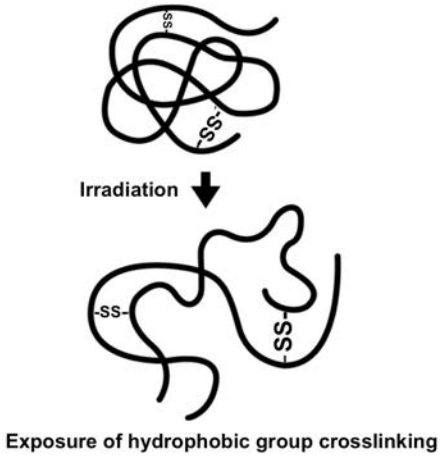

FIG. 14.9. Schematic diagram of the denaturation and structural changes in proteins upon irradiation.

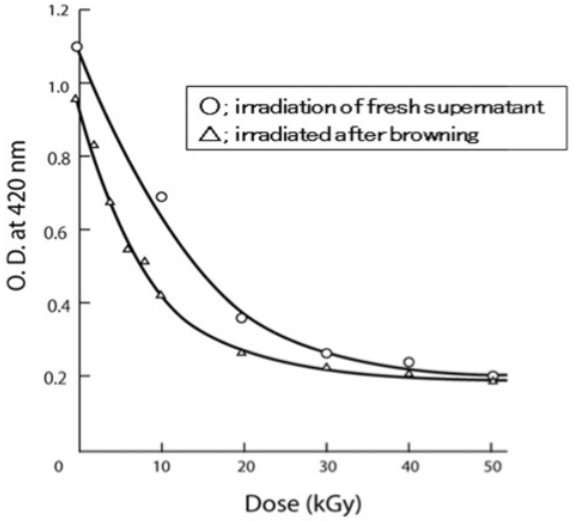

FIG. 14.10. Reduction of discolouration of potato starch wastewater by radiation [14.6].

14.5. UTILIZATION OF RADIATION DEGRADED POLYSACCHARIDES FOR ENVIRONMENTAL PURPOSES

Polysaccharides such as starch, cellulose, chitosan, carrageenan, and NaAlg undergo cleavage of the glycosidic link, producing lower fractions such as oligosaccharides. Particularly chitosan (poly β D-glucosamine) prepared

from chitin by deacetylation has unique properties as a coagulant and chelating agent. These polysaccharides can be rendered more efficient by radiation induced degradation.

14.5.1. Application as a coagulant for wastewater treatment

Polysaccharides can be irradiated in either dry or solution form at ambient temperature without any additive. Table 14.2 [14.7] shows the changes in the properties of chitosan irradiated in the dry state [14.8]. The solubility of chitosan in acetic acid (0.005%) increased with the increase in dose but the changes were small even at high doses. Surface charge was also stable and only 13% of charge decreased at 1000 kGy. The effectiveness as a coagulant for protein suspension decreased with the increase in dose and at 1000 kGy was 60% of the effectiveness as a coagulant of unirradiated chitosan. On the other hand, the viscosity of the irradiated chitosan decreased significantly at low dose (Fig. 14.11). These results show that viscosity is more radiosensitive than other properties when chitosan is irradiated in the dry state. Suspensions of heat denatured protein at pH10 were clarified with irradiated chitosan (Fig. 14.12). Chitosan irradiated at high doses in the dry state undergoes coagulation of the suspended solids even in alkaline solutions, while unirradiated chitosan is ineffective. However, the amount of chitosan required to clarify the alkaline suspension was about 10 times higher than that required for a neutral suspension. Solubility increased with increase in dose (17% for 100 kGy and 40% for 500 kGy in Fig. 14.13), contributing to the effectiveness of coagulation in alkaline suspension.

TABLE 14.2. CHANGE IN THE PROPERTIES OF CHITOSAN IRRADIATED IN THE DRY STATE [14.7]

Dose (kGy)	Solubility (%)	Relative charge (%)	Relative coagulation ability (%)
Unirradiated	2.3	100	100
1	2.3	100	97
10	2.4	101	97
100	4.0	97	87
500	16.5	92	78
1000	27.6	87	60

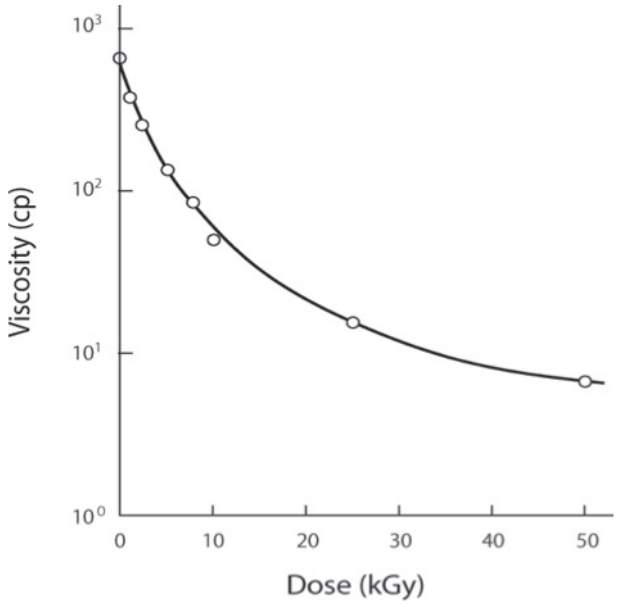

FIG. 14.11. Changes in viscosity as a function of dose for a chitosan sample irradiated in the dry state [14.8].

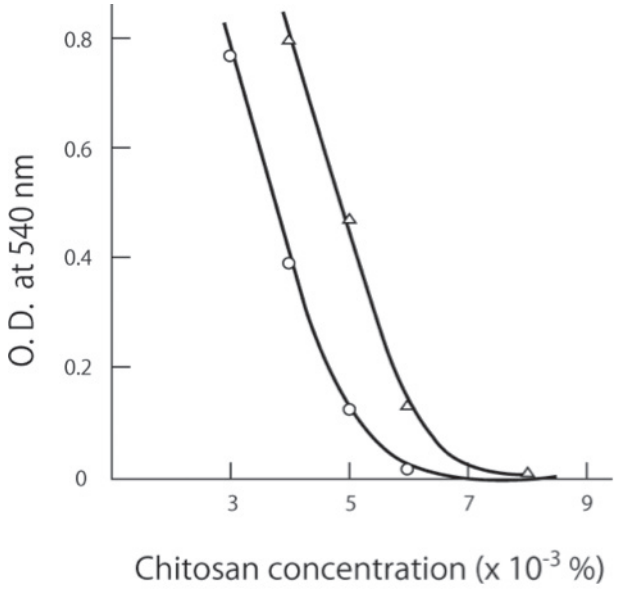

FIG. 14.12. Coagulation properties of irradiated chitosan solution at pH10: chitosan irradiated at 100 kGy (○) and 500 kGy (Δ) doses in the dry state [14.8].

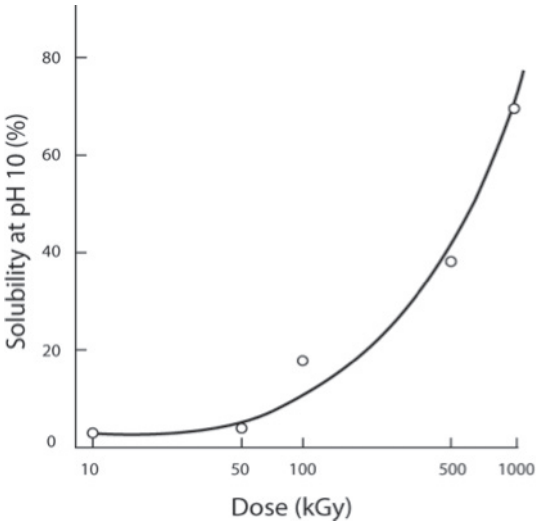

FIG. 14.13. Change in the solubility of chitosan at pH10 after irradiation in the dry state [14.8].

14.5.2. Suppression of environmental stress on plants

The potential for contamination of the environment by vanadium (V) is increasing with industrialization, since V compounds are present in fossil fuel deposits and mineral ores. When absorbed by plants, heavy metals such as V can induce stress within them. Tham et al. [14.9] investigated the effect of V on wheat, barley, soybean and rice. They concluded that although wheat and barley are more sensitive to V than rice and soybean, all seedlings were damaged at 2.5 μg/mL V, and their growth was severely reduced. The authors reported that this damage could be reduced by the application of radiation degraded chitosan. The recovery of growth and reduction of V levels in seedlings are obtained by treatments with 10–200 μg/mL chitosan irradiated at 70–200 kGy of γ rays in 1% solution (Fig. 14.14, Table 14.3) [14.9]. The reduction of V content in plants was attributed to the ability of chitosan to chelate metals in solution (Table 14.4). The transportation of V from root to shoot was visualized by bioimaging, and it became clear that this transport was suppressed by irradiated chitosan. From these results, it could be concluded that chitosan of a certain molecular weight, obtained by controlled radiation degradation, can effectively supress heavy metal stress in plants.

Lignocellulosic materials are also degraded by radiation, and extracts from oil palm fibre, sugarcane bagasse and sawdust of *fagus* are increased at 500–1000 kGy [14.8]. Figure 14.15 shows the effect of fermentation and radiation on the extraction of lignocellulose from sawdust of *fagus* in hot water. These

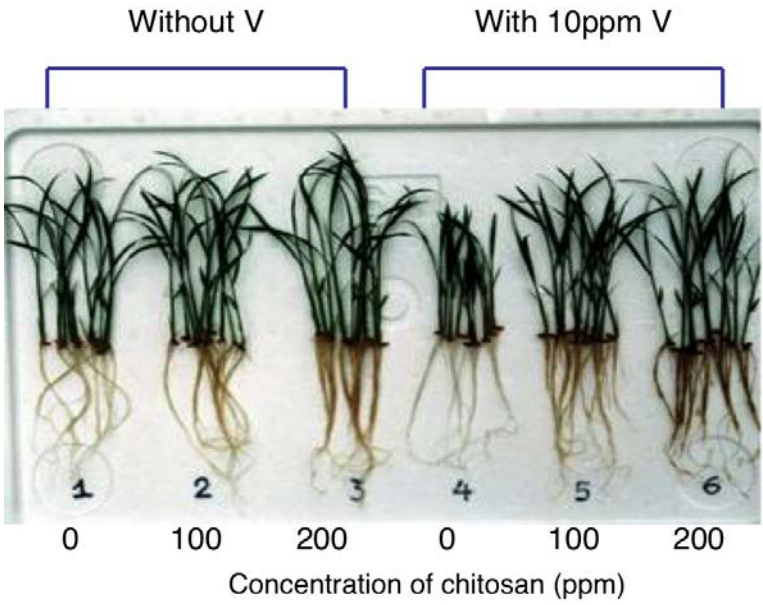

FIG. 14.14. Suppression of V damage to rice by irradiated chitosan (image courtesy of JAEA). Seedlings of plants grow for 9 days under V stress with chitosan.

TABLE 14.3. SUPPRESSION OF V DAMAGE ON RICE BY IRRADIATED CHITOSAN [14.9]

V + chitosan treatment		Dry weight of seedlings (mg/10 plants)			
		Wheat		Rice	
V (ppm)	Chitosan (ppm)	Biomass	%	Biomass	%
0	0	385 ± 42	100	190 ± 17	100
0	100	544 ± 47	141	2061 ± 6	108
0	200	540 ± 39	140	236 ± 30	124
10	0	229 ± 37	59	143 ± 12	75
10	100	350 ± 35	91	214 ± 18	113
10	200	392 ± 39	102	210 ± 18	111

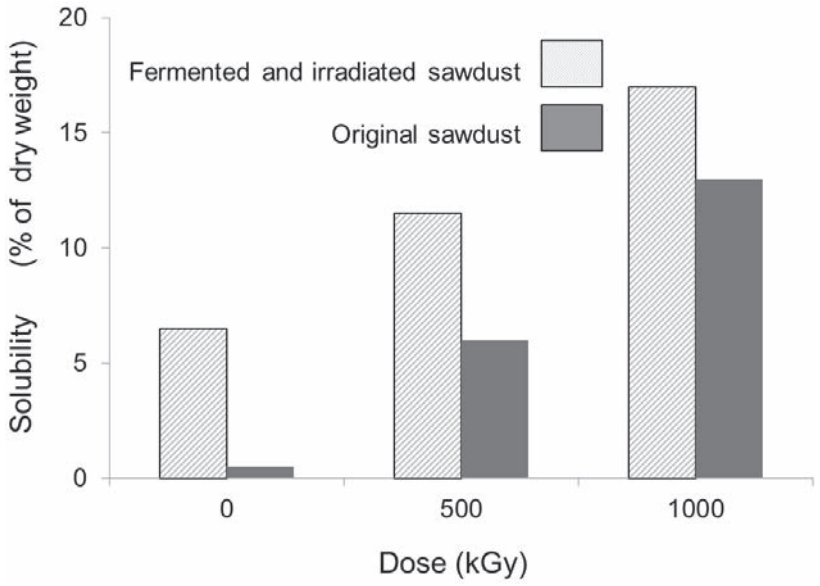

FIG. 14.15. Effect of fermentation and irradiation on the solubility of sawdust in hot water (figure courtesy of JAEA).

extracts in hot water show show a strong activity to suppress heavy metal and salt stress on plants. Salt stress at 5 mg/mL strongly inhibited the growth of rice seedlings causing a lower biomass production (62.6%) but the growth of plants suffering salt stress was clearly improved by the application of lignocellulosic extracts, especially 90 kGy irradiated extracts (Fig. 14.16). Polysaccharides irradiated at suitable doses could be used as heavy metal and salt eliminators in crop production.

TABLE 14.4. V CONTENT IN SEEDLINGS TREATED WITH IRRADIATED CHITOSAN [14.9]

V + chitosan treatment		V content in seedling (g/g dry weight)			
V (g/mL)	Chitosan (g/mL)	Wheat		Rice	
		Shoot	Root	Shoot	Root
0	0	<1	10	—	—
10	0	560	3820	530	1730
10	200	140	2100	74	1360

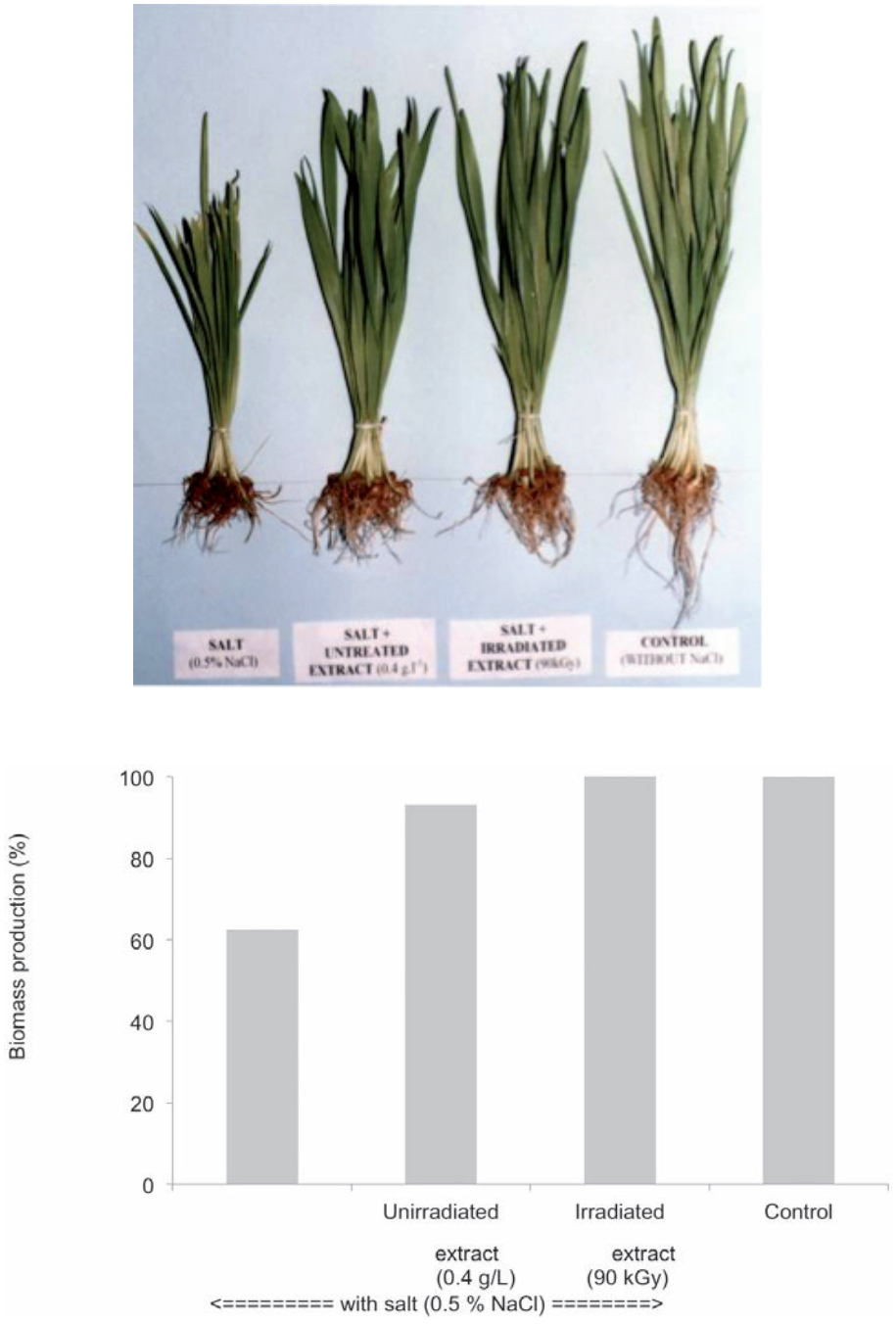

FIG. 14.16. Suppression of salt stress on rice growth by irradiated extract (image courtesy of JAEA). Salt stress: 0.5% NaCl, extract: 0.04%, dose: 90 kGy.

14.6. UTILIZATION OF RADIATION CROSS-LINKED HYDROGEL FOR ENVIRONMENTAL PURPOSES

Cellulose and its derivative CMC are well known to be radiation degradable in the solid phase and in dilute solution (below 10%). On the other hand, it was recently found that CMC can be cross-linked by irradiation in a paste-like condition of high concentration (Fig. 14.17) [14.10]; see also Chapter 4.5.2. CMC hydrogel is commercially used as a biodegradable coolant for the transportation of refrigerated fish and vegetables (Fig. 14.18).

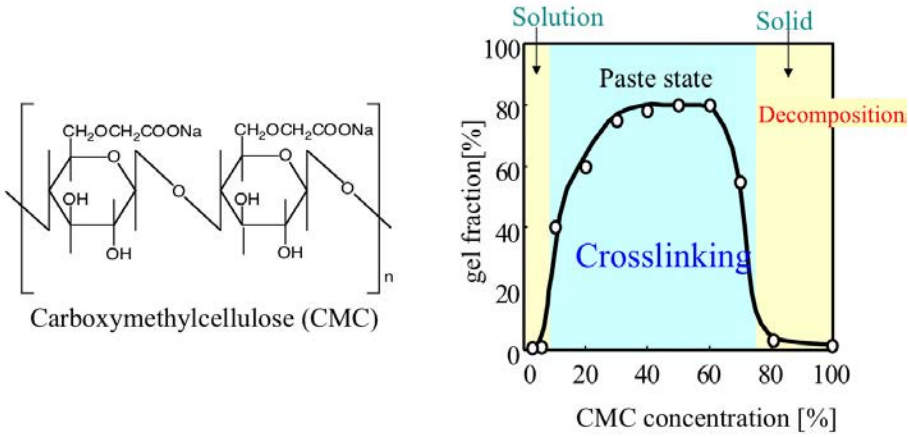

FIG. 14.17. Radiation cross-linking of CMC [14.11].

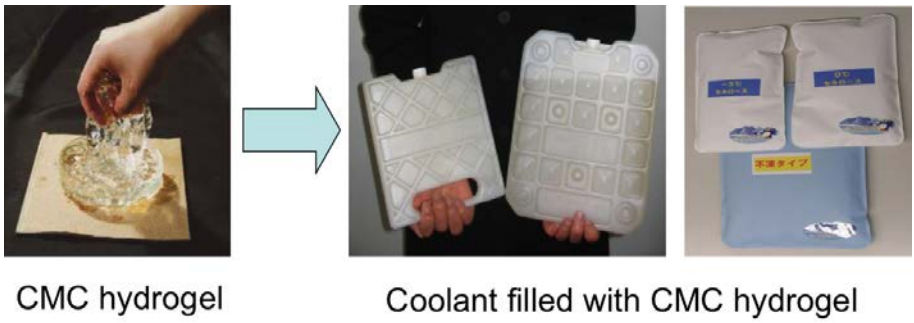

FIG. 14.18. Coolant using radiation cross-linked CMC (photograph courtesy of JAEA).

14.6.1. Treatment of industrial and agricultural wastes with CMC dry gel

Since excrement and urine from domestic animals, such as cattle and pigs, causes the pollution of river and underground water, the conversion of excrement and urine into organic fertilizer by fermentation is strongly recommended. However, excrement and urine from cattle contain 85–90% water, so a smooth fermentation process is challenging. The addition of 0.2% CMC dry gel to the fermentation process can reduce the water content to 65–70%, which is suitable for fermentation. The method developed using CMC hydrogel can enhance fermentation and reduce odour diffusion in the environment (Fig. 14.19).

The Japanese liquor shochu (alcohol content 25%) is produced by the fermentation of rice, wheat and sweet potato. Residues are formed during this process, which contain 90% water, and these are discarded in the deep sea. This sea pollution can be avoided by the utilization of shochu residue for animal feeds. In plants for the processing of animal feeds from shochu residue, the volume of corncob needed to absorb the water can be decreased from 650 kg to 200 kg/t of shochu residue by addition of 0.2% (2 kg) CMC dry gel. It is confirmed that water absorption by CMC dry gel is effective at converting shochu residue into animal feed [14.12].

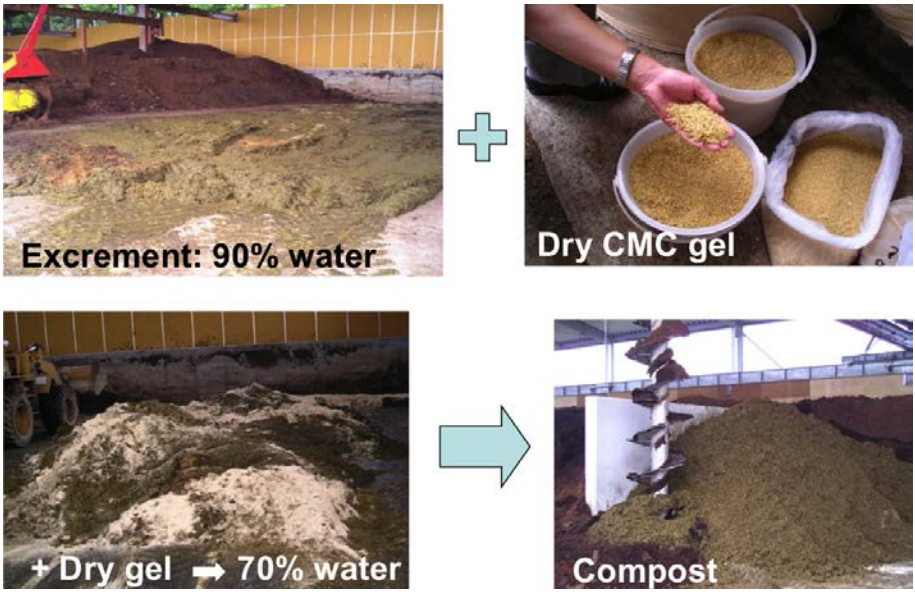

FIG. 14.19. Composting process of livestock excrement using CMC dry gel (images courtesy of JAEA). The moisture content of excrement (90%) can be decreased to 70%, a level more suitable for composting, by adding dry CMC gel.

14.6.2. Adsorption of heavy metals by CM chitosan gel

Resins derived from petroleum products are commonly used for the adsorption of heavy metals. For the security of petroleum resources and the decrease of environmental burdens, naturally occurring polymers can form the raw materials for metal ion adsorbents. Among many natural polymers, chitin/chitosan is considered to be the most interesting raw material because of its amine group. Amine groups can recover several kinds of metal ions such as copper (Cu), mercury (Hg), uranium (U), lead (Pb), chromium (Cr), molybdenum (Mo) and V, as well as the noble metals platinum (Pt) and palladium (Pd).

The cross-linking of chitin and chitosan increases the chemical stability of the adsorbent in acid media and, in particular, decreases solubility in most mineral and organic acids. Such modified chitin and chitosan has been used for metal ion recovery in acid media. Radiation is considered an environmentally friendly method for cross-linking CM chitin and CM chitosan without any cross-linking agent (Fig. 14.20). Using CM chitin and CM chitosan hydrogels cross-linked by radiation, adsorptions of various metal ions have been tested (Fig. 14.21) [14.12]. CM chitosan hydrogel adsorbed Pd, Sc, Au, Cd, V and Pt in the order of high adsorption at 240 min. The adsorption of Sc increased and attained the highest adsorption percentage in all-metal ions after 480 min. In the case of CM chitosan, Au and Pt, which are expensive noble metals because of their rare occurrence in nature, were preferentially adsorbed. The selectivity of CM chitin and CM chitosan hydrogels to noble metals can be applied not only to reduce heavy metal pollution but also to recover and recycle these important rare metals.

Radiation cross-linked CM chitosan also has a potential for use in applications relating to the separation and concentration of humic acid [14.13]. Humic substances are the most common natural polymers on the earth and it

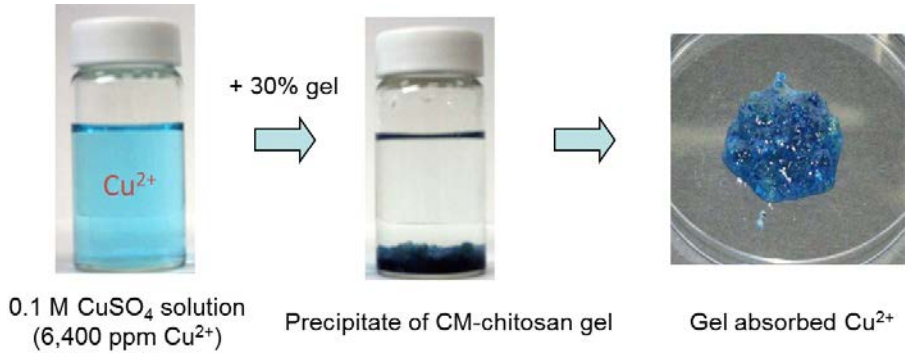

FIG. 14.20. Absorption of Cu^{2+} by CM chitosan gel (images courtesy of JAEA).

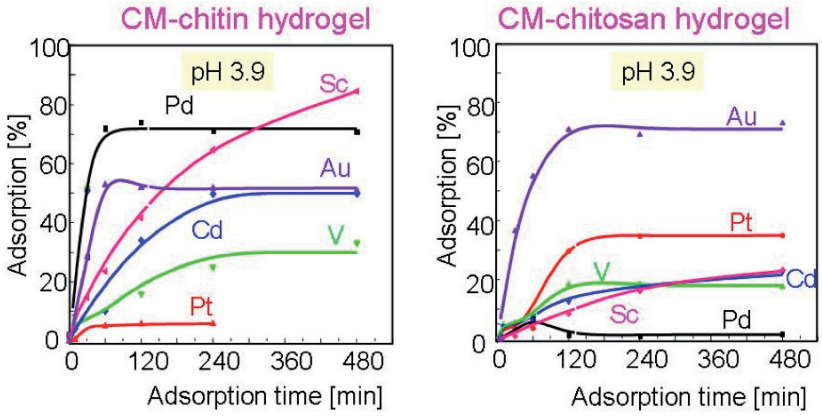

FIG. 14.21. Adsorption of various metal ions onto CM chitin and CM chitosan hydrogels [14.12].

is desirable to minimize the presence of humic substances in drinkable and industrial waters. Cross-linked CM chitosan is effective at removing humic acid under acidic pH conditions (pH < 6). The amino groups of cross-linked CM chitosan in a protonated state, which can form a surface complex with humic acid, were found to play the major role in the adsorption process.

14.7. EMERGING APPLICATIONS AND CONCLUSION

Radiation technology has contributed to improving public welfare and cleaning the environment. The main effects of radiation on natural polymers used for environmental treatment are the degradation of components, enhancement of coagulation and killing of pathogenic microorganisms. These radiation effects on natural polymers have directly contributed to the conservation of the environment in applications such as the cleaning of wastewater and utilization of discarded natural polymers. Radiation pasteurization is effectively used to utilize sewage sludge for fertilizer and for recycling of cellulosic wastes to animal feeds. Radiation treatment of proteins causes the aggregation and coagulation in solution improving the recovery from wastewater with aid of chitosan.

Bioethanol is considered a promising form of sustainable energy because of the limitation of the petroleum supply and increasing worldwide concerns about carbon dioxide emissions. An alternative source of bioethanol to corn that costs less to produce and avoids the use of food and animal feed, lignocellulose is also an abundant and suitable raw material. The rate and extent of saccharification is increased by radiation treatment, but a high dose of up to 1000 kGy is required for the degradation of lignocellulose. When radiation is combined with alkali

treatment, a reduction of cellulose crystallinity and a decrease of lignin and hemicellulose could greatly improve the hydrolysis of cellulose to fermentable reducing sugars (more details are given in Chapter 13). Further investigation is necessary, but a combination treatment with radiation and with another chemical treatment such as alkali is expected to emerge as an effective pretreatment of lignocellulose for bioethanol production.

The modification of natural polymers using radiation is an emerging technique to reduce environmental pollution. The products of degradation or cross-linking of polysaccharides by radiation can avoid damage to the environment indirectly by reducing the use of synthetic chemicals and removing toxic metals. Radiation degraded polysaccharides induce antimicrobial activity, coagulation activity, plant growth promoter and elicitor activities resulting in fewer synthetic chemicals and fertilizers being used, the cleaning of wastewater and the suppression of heavy metal and salt stress in plants. Radiation cross-linked hydrogel is also useful as a heavy metal adsorbent to remove such metals from water.

Natural polymers, which can be regenerated by the metabolism of microorganisms and plants, are materials with the potential to reduce the production of carbon dioxide, and thereby global warming. PLA synthesized from starch is one of these promising bio-polymers and radiation cross-linking enhances properties such as heat stability and softness. It is strongly suggested, wherever feasible, to replace polymers produced from fossil fuel with bio-polymers, in order to protect the environment.

REFERENCES TO CHAPTER 14

[14.1] KUME, T., et al., Study on Upgrading of Oil Palm Wastes to Animal Feeds by Radiation and Fermentation Processing, Report No. JAERI-Research 98-013, Japan Atomic Energy Research Institute, Tokai-mura, Japan (1998).

[14.2] STEPANIK, T.M., RAJAGOPAL, S., EWING, D., WHITEHOUSE, R., Electron-processing technology: A promising application for the viscose industry, Radiat. Phys. Chem. **52** (1998) 505–509.

[14.3] ZAMAN, K., HASHIM, K., GHAZALI, Z., MAHMOOD, M.A., SHARIF, J., "Radiation processing of natural polymer", Proc. of the FNCA 2006 Workshop on Application of Electron Accelerator – EB Treatment of Wastewater –, (Proc. Workshop, Daejeon, Korea, 2005), JAEA-Conf. No. 2006-006, Japan Atomic Energy Research Institute, Tokai-mura, Japan (2006) 14–22.

[14.4] NAGASAWA, N., et al., Application of poly(lactic acid) modified by radiation crosslinking, Nucl. Instr. Meth. B **236** (2005) 611–616.

[14.5] KUME, T., TAKEHISA, M., Effects of irradiation on the coagulation and disinfection of blood wastewater, Nippon Shokuhin Kogyo Gakkaishi **29** (1982) 730–732.

[14.6] KUME, T., TAKEHISA, M., Effect of irradiation for recovery of organic wastes from potato starch wastewater with chitosan, Radiat. Phys. Chem. **23** (1984) 579–582.
[14.7] LAM, N.D., NAGASAWA, N., KUME, T., Effect of radiation and fungal treatment on lignocelluloses and their biological activity, Radiat. Phys. Chem. **59** (2000) 393–398.
[14.8] KUME, T., Takehisa, M., "Effect of gamma-irradiation on chitosan", in Proc. 2nd Int. Conf. Chitin/Chitosan, Sapporo, Japan, Japan Chitin Society, Sapporo (1982) 66–70.
[14.9] THAM, L.X., et al., Effect of radiation-degraded chitosan on plants stressed with vanadium, Radiat. Phys. Chem. **61** (2001) 171–175.
[14.10] YOSHII, F., et al., Hydrogels of polysaccharide derivatives crosslinked with irradiation at paste-like condition, Nucl. Instr. Meth. B **208** (2003) 320–324.
[14.11] TAMADA, M., "Metal ion adsorption by carboxymethyl chitin and chitosan hydrogels", Proc. of the FNCA 2007 Workshop on Application of Electron Accelerator, (Proc. Workshop, Hochiminh, 2007), Japan Atomic Energy Research Institute, Tokai-mura, Japan (2008) 125–132.
[14.12] YOSHII, F., "Effective utilization of agro-waste by application of CMC dry-gel", Proc. of the FNCA 2007 Workshop on Application of Electron Accelerator (Proc. Workshop, Hochiminh, 2007), Japan Atomic Energy Research Institute, Tokai-mura, Japan (2008) 83–86.
[14.13] ZHAO, L., WASIKIEWICZ, J.M., MITOMO, H., YOSHII, F., NAGASAWA, N., Preparation and adsorption behavior for metal ions and humic acid of chitosan derivatives crosslinked by irradiation, Nucl. Sci. Tech. **18** (2007) 42–49.

Chapter 15

RADIATION PROCESSING OF STARCH BASED PLASTIC BLENDS

D. KHANDAL
Institut de Chimie Moléculaire de Reims,
University of Reims Champagne-Ardenne,
Reims, France

P. MIKUS, P. DOLE
Fractionation of Agroresources and Environment Lab,
University of Reims Champagne-Ardenne,
Reims, France

S. BAUMBERGER
Institut Jean-Pierre Bourgin,
Institut National de la Recherche Agronomique,
Versailles, France

X. COQUERET
Institut de Chimie Moléculaire de Reims,
University of Reims Champagne-Ardenne,
Reims, France

15.1. INTRODUCTION

15.1.1. Bio-based plastics

There is an increasing interest in renewable and environmentally friendly polymers from biomass for substituting synthetic polymers in various sectors and for various applications, as well as in finding new applications. Basic and applied research aims particularly to develop bio-sourced polymers for materials (for example, materials for packaging, soil mulching and for manufacturing automobile interiors), specialty products (for example, adhesives, absorbents, humectants and surfactants) and high value added products (for example, cosmetics and pharmaceutical applications) [15.1]. Despite the promising growth and inherent potential of bio-based plastics, they still account for only 1% of the total polymer market. The total technical substitution potential of the bio-based

market is considered to be almost 270 Mt, but market projections are always only a few Mt, simply because the major barriers hindering potential growth are the high production costs and technical challenges involved in scaling up the process from the laboratory to an industrial production scale [15.2].

There has been a steep growth in the market of bio-based plastics of almost 38% per year since 2003. According to the projected growth of bio-plastics, starch plastics would form the greatest proportion of bio-based plastics by the year 2020 (1.3 Mt), followed by PLA (0.8 Mt), bio-based PE (0.6 Mt), and poly(hydroxyalkanoates) (PHA) (0.4 Mt). The importance of starch can be understood from the fact that it is a renewable agricultural resource and is economical, easy to process into a thermoplastic material and biodegradable. The interest in bio-based plastics has grown over the years mainly for environmental and economic reasons rather than because of their physical or mechanical properties [15.3].

Starch polymers have played an important role for many decades in non-plastic applications. Owing to their low cost and excellent biodegradability, the use of starch as a raw material for bio-plastic production has been considered for several years and is still by far the most important of the bio-based plastics [15.4]. Research on starch based plastics began with the value addition of synthetic polymers; initially, blending bio-polymers to synthetic polymers was carried out to obtain a certain degree of biodegradability. Starch based plastics have consisted of a polyolefin including 5–20 wt% starch powder as a filling material. The starch content in blends varies from 30–80 wt% depending on the end application, with the loss of mechanical properties becoming critical at starch contents above approximately 40 wt%. Since then, the majority of polymers associated with starch have been biodegradable oil based polymers (for example, polycaprolactone (PCL), poly(butylene-succinate), poly(butylene-succinate-co-terephtalate), poly(butylene-succinate-lactate) and poly(hydroxyalkanoate-butyrate) (PHAB). Therefore, most starch blends are partially bio-based and essentially biodegradable; one example is Mater-Bi, which is prepared from starch and the copolyester Ecoflex. However, some of the polyesters with which starch is blended can potentially be made from bio-based instead of petrochemical feedstock. PLA is attracting a growing interest since it is fully bio-based. Also, the succinic acid and butane-1,4-diol present in other polyesters can now be produced industrially from biomass and can be used as a monomer for poly(butylene-succinate), poly(butylene-succinate-lactate-adipate), poly(butylene-succinate-lactate) and poly(butylene-succinate-co-terephtalate).

Starch can be used for various other applications if structural modifications conferring new functionalities are made, for example, by chemical grafting of hydrophobic moieties onto hydrophilic polysaccharides in order to improve

drug retention for drug delivery, or by complexation of metal ions for imparting electrical or magnetic properties to the final biodegradable product.

15.1.2. Starch: Structure and properties

Starch is a bio-polymer composed of anhydroglucose units that form either a linear chain, i.e. amylose, or branched chains, i.e. amylopectin (Fig. 15.1). Depending on the botanical origin of the starch, the proportions of these two main components vary.

Generally, in non-bioengineered starch, the percentage of amylose in native starch is between 25% and 40%, whereas amylopectin constitutes the major part, accounting for 60–75% of the starch granule [15.5]. Amylose-free starch also exists and is called waxy starch, which has an amylopectin content as high as 90%. The molecular weight of amylose is anywhere between 100 000 g/mol to 10^6 g/mol, with a degree of polymerization of 100 to 10 000 anhydroglucose units; amylopectin is almost 100 times larger with a molecular mass between 10^7 and 10^9 g/mol. Amylopectin is the largest known bio-polymer with a very extensively branched structure where almost 95% of the glucosidic bonds are α−1,4, and 5% of the other glucosidic bonds are α−1,6 and are involved in branching [15.6].

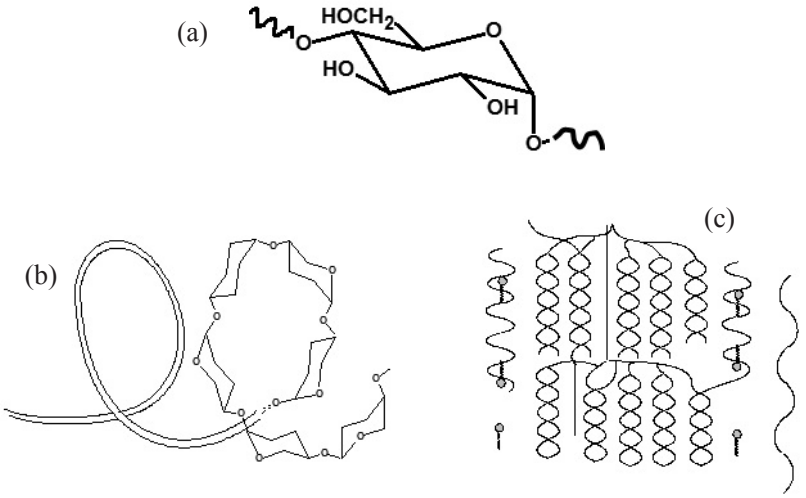

FIG. 15.1. Structure of anhydroglucose units (a), amylose (b) and amylopectin (c).

Because of the amorphous character of amylose and the crystalline character of amylopectin within the pristine granule, starch is a semi-crystalline material, with a degree of crystallinity varying between 0.17 and 0.42 [15.7]. After granule destructuring under high temperature and shearing, amylose chains are more likely than amylopectin chains to crystallize over time. Thus, amylose initially imparts an amorphous character to starch granules but after starch has been converted into an amorphous polymeric material, it is the amylopectin that retains an amorphous character for longer.

The arrangement of amylose and amylopectin chains in various definite patterns results in concentric circles of amorphous and crystalline regions [15.8]. Amylopectin linear branches are arranged in the form of double helices, whereas amylose chains adopt a single helix conformation. Depending on the arrangement of these double helices in the amylopectin chains, starch crystallinity is categorized as A type, B type or C type. The A type crystalline pattern is observed in cereal starches, such as wheat starch, while the B type is seen in tuber starches, such as potato starch. A crystalline pattern between the A and B types is called the C type, which is found in peas, beans and high amylose rice starch [15.9]. In general, amylopectin chains in all the three types of starches have different molar ratios of short and long branch chains, which is 8–12 for A type starches, 3–7 for B type starches, and 7–9 for C type starches [15.10].

For its main application as a thermoplastic material, native starch needs to be destructurized and plasticized [15.11]. The transformation of crystalline starch granules into an amorphous thermoplastic is achieved by combining mechanical energy and heat while blending the powder with water and appropriately selected additives.

For most packaging applications, thermoplastic starch needs to be blended with hydrophobic polymers that can improve the water resistance of the final material by reducing its hydrophilic character. Starch is then often extruded with hydrophobic additives or polymers; however, the final blend is physically unstable and results in the phase separation of the constituents. To overcome or retard retrogradation, starch also needs structural modifications. Therefore, conventional processing methods are essential for the preparation of thermoplastic starch but are not enough to result in a performant thermoplastic material.

The covalent grafting of synthetic thermoplastics onto starch is an attractive option for improving blend stability. This type of modification can be achieved by a variety of chemical methods. An early attempt consisted of introducing some polar functions onto a commodity plastic in order to enhance compatibility and create covalent linkages between starch and the synthetic thermoplastic. The use of EB on blends of thermoplastic starch with poly(ethylene-co-vinyl alcohol) has been previously carried out and thermoplastic starch was found to undergo degradation while poly(ethylene-co-vinyl alcohol) remained unaffected

[15.12, 15.13]. In another application orientated study, sago starch was blended with poly(vinyl alcohol), cross-linked by radiation processing and converted into foam particles by microwave heating [15.14].

New routes based on radiation processing for the controlled modification of the properties of starch based materials are being considered. Various approaches are being considered:

— The radiation grafting of a reactive plasticizer onto starch and its influence on the physical stability of plasticized starch materials;
— The blending and grafting of various types of lignin with the aim of modifying bulk water sorption and surface hydrophilicity;
— The study of the protective effects of aromatic additives including some lignin monomers with respect to irradiation of destructurized starch or model maltodextrins.

15.2. PHYSICAL STABILIZATION BY RADIATION GRAFTING OF ALLYLUREA AS A REACTIVE PLASTICIZER

Starch materials are generally amorphized by mechanical mixing at temperatures slightly higher than 100°C with low molecular weight additives such as water and glycerol that act as destructuring agents and plasticizers. A major problem with thermoplastic starch is the physical instability of the bulk material, caused by migration or phase separation of the plasticizer, as well as by retrogradation of the starch component [15.15–15.17]. A novel approach to this problem has recently been explored, by treating, with accelerated electrons, blends of native potato starch and N−allylurea (CH_2=CH−CH_2−NH−(C=O−NH_2) (AU), which result from intimate mixing at 130°C [15.18]. AU was selected as a simple unsaturated homologue of urea and was expected to have similar destructuring and plasticizing properties to starch, and poor aptitude for long chain polymerization in the amorphous blend. The typical procedure for preparing the starch based films is presented in Fig. 15.2. Starch and AU are blended in an internal mixer at 130°C for 15 min with a screw rotation speed of 50 rpm.

The blends were chopped into small cubes and quenched at −17°C immediately after processing in order to avoid physical evolution. To prepare starch films, the starting material was ground into coarse powder and transformed by compression moulding with a hydraulic press at 130°C at a pressure of 10 MPa maintained for 5 min. The loss of water during this step is negligible and the water uptake, measured after reconditioning the pressed sample at 58% relative humidity, was insignificant. After pressing, the films were stored at −17°C until the moment of analysis. Characterization of the materials and EB processing

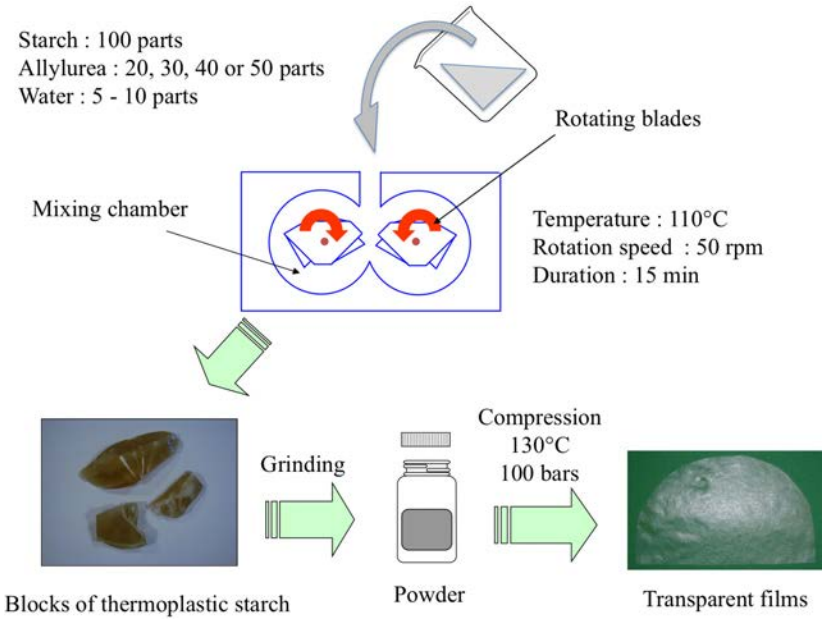

FIG. 15.2. Typical procedure for the preparation of destructurized starch blends and for the preparation of films.

of films were performed with samples reconditioned from the frozen stock just before use.

Immediately after pressing the coarse thermoplastic starch powder conditioned at 58% RH, the films were transparent and appeared visually homogeneous. This indicates that the granular structure was destroyed during processing. After 1 h of ageing, the films obtained from Starch AU30, 40 and 50 became opaque with AU molecules blooming at the sample surface (Fig. 15.3).

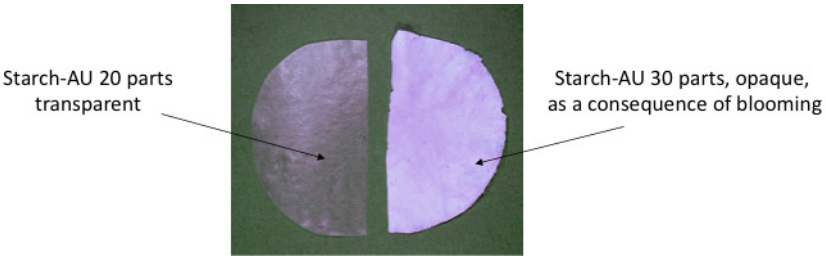

FIG. 15.3. Photographs showing AU blooming in samples of destructurized starch blends including excess amounts of AU (above 25 wt parts for 100 parts of dry starch).

The phenomenon was not observed for the lowest amount of AU, indicating that the compatibility limit was between 24 and 35 parts per 100 parts of dry starch in the given storage conditions (Fig. 15.3 and Table 15.1).

TABLE 15.1. APPEARANCE OF THERMOPLASTIC STARCH FILMS AFTER PRESSING AND AGEING

AU content (wt-parts)[a]	Optical aspect		Brittleness index[b]	
	Initial	After 1 h	Initial	After 350 h
24.5	Transparent	Transparent	0[c]	0[c]
35.3	Transparent	Opaque	0[c]	0[c]
47.1	Transparent	Opaque	0[c]	1
58.8	Transparent	Opaque	0[c]	9

[a] expressed in g/100 g of dry starch.
[b] curvature radius (mm) for folding without apparent damage.
[c] folding backwards with an angle of 180° without apparent damage.

The quantification of blend plasticization was assessed by a flexibility test. The critical curvature radius before observing breaking was used as a brittleness index for rating the thermoplastic starch materials.

The preliminary investigation showed that AU propenyl group conversion obtained by EB irradiation was associated with macroscopic physical and mechanical stabilization. The blooming phenomenon was significantly delayed.

Physical ageing of the unstable blends was monitored for various initial AU contents. EB processing of fresh films with AU contents above the solubility limit was shown to prevent phase separation, essentially as a consequence of radiation grafting onto starch of the unsaturated additive, as supported by FTIR spectroscopy (Fig. 15.4) and by solution ^{1}H-NMR. Both methods unambiguously showed the consumption of allylic unsaturations.

The presence of nitrogen in the processed blends washed with methanol supported the covalent binding of polymerized AU segments onto the base starch material. However, AU homopolymerization cannot be excluded. The sketch shown in Fig. 15.5, though somewhat simplified, gives an acceptable view of the chemical transformations induced by radiation.

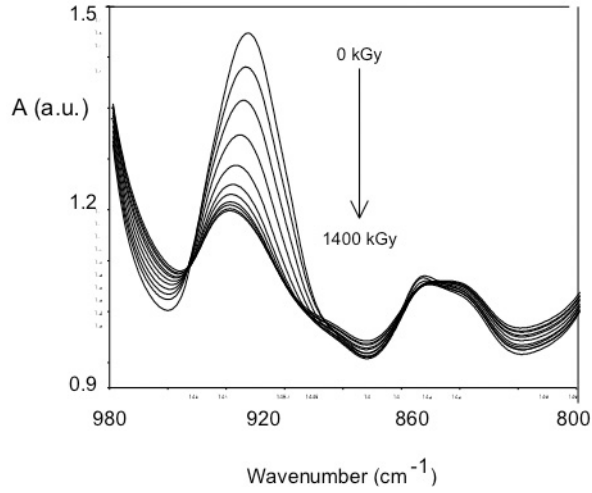

FIG. 15.4. FTIR monitoring of AU conversion upon EB irradiation of destructurized starch blends (50 wt parts for 100 parts of dry starch).

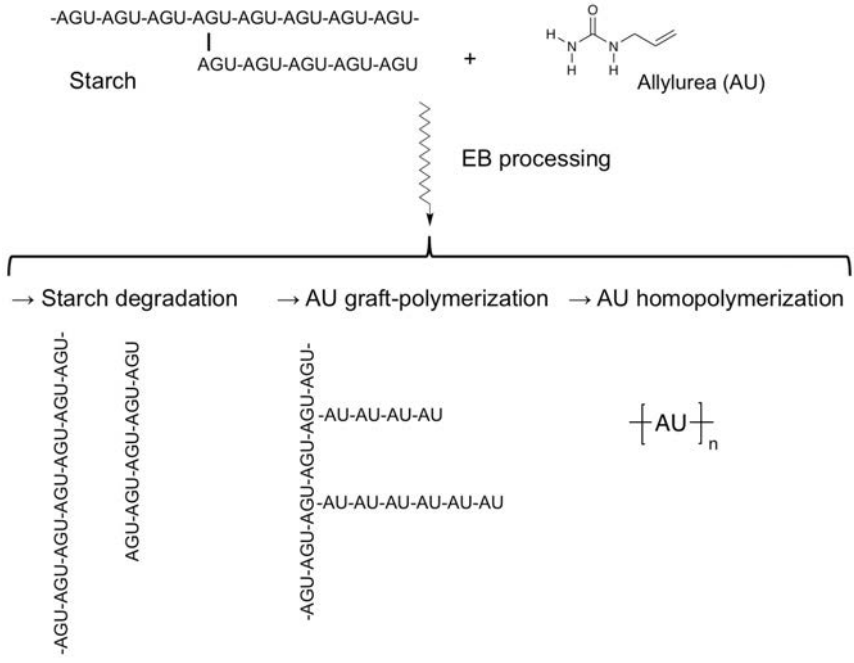

FIG. 15.5. Simplified representation of the reactions induced by EB treatment in AU blends.

X ray diffractometry was performed at the different stages of the process to check: (a) the effective amorphization of starch upon mixing; (b) the recrystallization of the incompatible AU fraction from untreated blends in the tetragonal form; and (c) the retardation or suppression of this phenomenon after EB processsing (50–800 kGy). The physical stability of the blends treated with a sufficient radiation dose was confirmed by dynamic thermomechanical analysis of samples submitted to various hygrometric conditioning, as supported by experiments conducted at stages 1, 2 and 3 of the ageing cycle described in Figs 15.6 and 15.7 [15.19, 15.20]. The recorded thermomechanical spectra of samples reconditioned at 57% relative humidity did not show any significant reference, confirming the physical stability of the radiation processed blends, presumably with low propensity to retrogradation or phase separation.

It was therefore demonstrated that AU, a radiosensitive additive, can be efficiently grafted onto starch by radiation processing of fresh samples. Radiation doses as high as 1400 kGy are required to approach complete allyl group conversion. Interestingly, not only is the migration aptitude of grafted AU molecules restricted by permanent immobilization at doses as high as 100 kGy, but grafting also seems to increase the compatibility of the free AU with the modified polysaccharide. Effective compatibilization can be induced with a

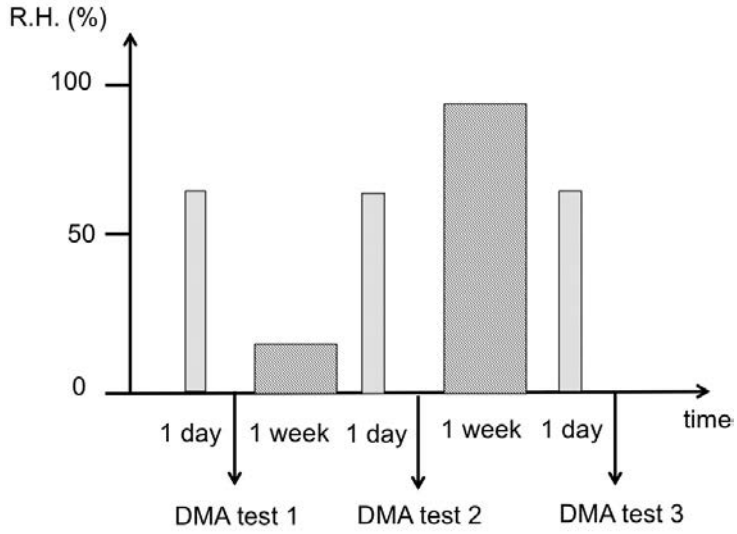

FIG. 15.6. Ageing cycle applied to the starch-AU (50 wt parts per 100 parts of dry starch) samples after 200 kGy EB irradiation to assess the stabilization of the thermomechanical behaviour.

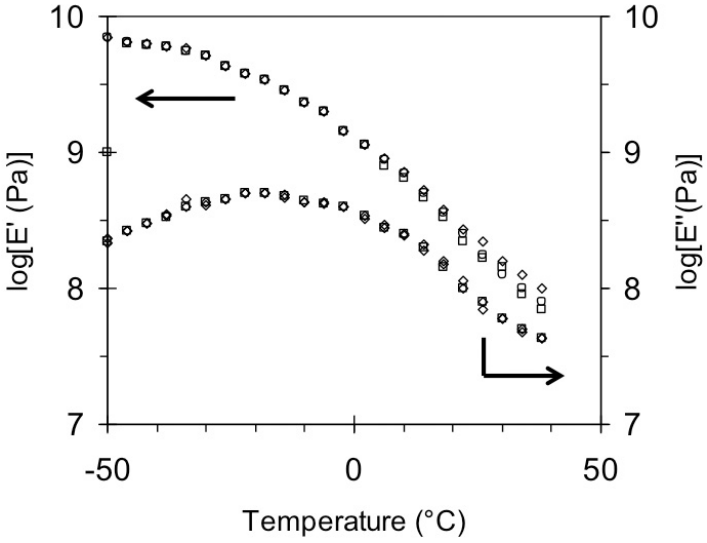

FIG. 15.7. Effects of ageing in various hygrometric conditions on the thermomechanical spectrum of reconditioned starch film plasticized with AU (50 pph) and treated with a 200 kGy dose at the stage 1 (□), 2 (○) or 3 (◇) corresponding to Fig. 15.6.

moderate radiation dose. Blended starch films containing 50 pph of AU do not show any sign of phase separation after a 200 kGy treatment. Ageing experiments in wet and dry ambiences have shown that the thermomechanical properties of the films are stable.

15.3. RADIATION PROCESSING OF STARCH–LIGNIN BLENDS

15.3.1. Potentialities of starch–lignin blends

Built on phenyl propane units linked by various carbon–carbon and ether bonds (Fig. 15.8) [15.21], lignins impart strength and waterproofing to specialized vegetal tissues [15.20]. Delignification processes employed by the pulp and paper industry yield abundant and renewable by-products referred to as industrial lignins. These lignins have been used as fillers in natural thermoplastics such as cellulose derivatives, proteins and polyesters [15.22].

Lignin and their derivatives are therefore good candidates for limiting the water sensitivity of starch based materials. In practice, they mix efficiently and form segregated domains when blended with polysaccharides [15.23]. To overcome this poor compatibility, free radical coupling reactions similar to

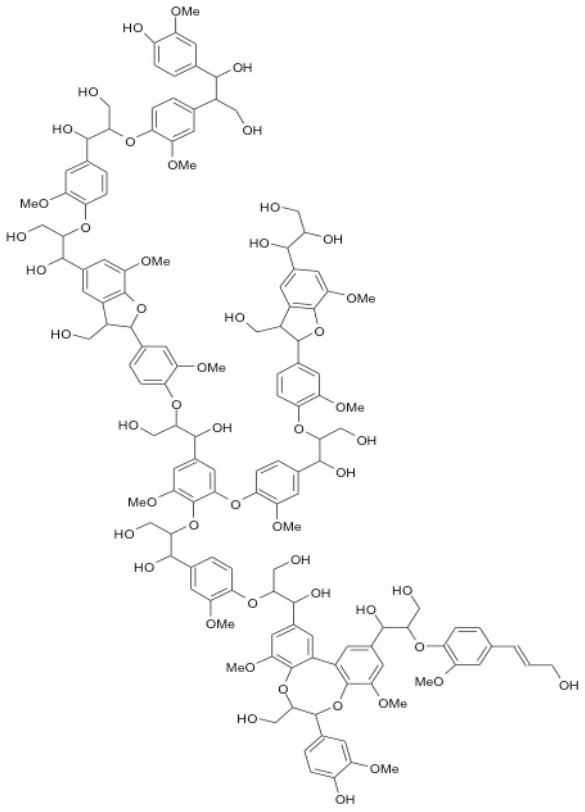

FIG. 15.8. Diagram of the structure of lignin [15.21].

those occurring in the lignification process of plants can be induced by high energy irradiation of starch–lignin blends.

It is known that lignin compounds are subject to reactions initiated by radicals upon irradiatation in an isolated state and within a polysaccharide template [15.24–15.26]. To describe this approximately, it could be expected that high energy irradiation will generate free radical species on starch and lignin molecules, thereby inducing grafting and/or cross-linking of hydrophobic lignin fragments onto starch, with some improvement in the water resistance of the thermoplastic starch materials.

The following section includes results illustrating: (a) the effective reduction of water sorption by blending starch glycerol mixtures with wheat or bagasse lignin; (b) the modification of surface properties after the treatment

of such blends by EB irradiation; (c) the biodegradability of irradiated and unirradiated starch–lignin blends.

15.3.2. Surface properties and water sorption

Thermoplastic starch based films were prepared by extrusion in the presence of glycerol as a plasticizer (30/70 glycerol/starch wt ratio), either without any lignins or with 20% or 30% industrial lignin content (lignosulphonates, wheat straw or bagasse alkali lignins). The lignin-free thermoplastic starch film that was recovered had an initial contact angle with water of $\theta_0 = 35°$. This angle rapidly decreased within a few seconds of water deposition and the water droplet was totally absorbed by the film in less than ten seconds. This behaviour reflected the hydrophilicity and wettability of the starch surface and could also be connected with the high proportion of glycerol, a very hygroscopic plasticizer.

Lignin incorporation does not increase θ_0 in the unirradiated film, but a substantial reduction of the sorption rate was observed. The equilibrium water sorption at 75% relative humidity was also found to be lower for films containing alkali lignin. Both the hydrophobic characteristics of lignin and the lower glycerol content in starch–lignin films could be responsible for this surface and bulk hydrophobization phenomenon.

After EB irradiation at a dose of 400 kGy, the presence of lignin was shown to induce an effect on the contact angle of a water droplet at the film surface. Whereas the sample that was free of any lignin additive was subject to a slight decrease of θ, a significant increase was observed with the wheat and the bagasse lignins. This effect, enhanced by larger amounts of lignin, increased the θ value from less than 30° to almost 60° for a content of 30 wt parts in bagasse lignins (Fig. 15.9).

Reduction of surface hydrophilicity prevented water from spreading or being absorbed for more than 10 min, irrespective of the lignin level (20% or 30%). Surprisingly, irradiation does not affect the water sorption of the bulk material at 75% RH for any formulation (Table 15.2).

The above supports the idea that the irradiation generates a hydrophobic surface barrier and that the overall decrease of moisture content in starch–lignin blends results essentially from a lower glycerol content compared with the lignin-free reference sample [15.27]. It has recently been shown that optimization of the material processing and irradiation conditions could lead to a contact angle as high as 110° for 80/20 starch/lignin blends, thus providing truly hydrophobic materials [15.28].

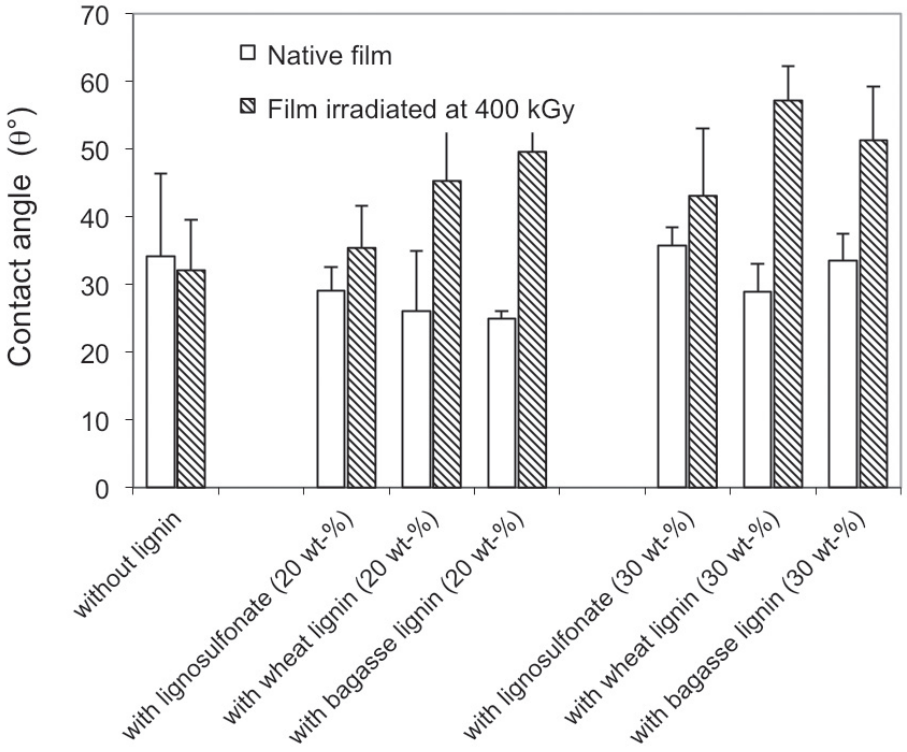

FIG. 15.9. Effects of the presence of lignin and EB irradiation on the contact angle of a water droplet on starch based films.

TABLE 15.2. EFFECTS OF THE PRESENCE OF LIGNINS AND EB IRRADIATION ON WATER SORPTION IN STARCH BASED FILMS

Blend	Water sorption (%) at 73% RH, T = 25°C	
	Unirradiated	Irradiated
Starch glycerol (no lignin)	21	21
Starch glycerol–bagasse lignins (30 phr)	17	16
Starch glycerol–wheat lignins (30 phr)	16	14
Starch glycerol–lignosulphonates (20–30 phr)	21–23	19–23

15.3.3. Physical effects of grafting on starch retrogradation

Thermoplastic starch samples including glycerol and cinnamyl alcohol (CA) as plasticizers were prepared with various compositions. The resulting thermoplastic starches were white materials that can be pressed into 2 mm thick plates for obtaining samples to be submitted to physical characterization and mechanical testing. One of the expected effects of the covalent grafting onto amorphized starch was the prevention of starch retrogradation.

The X ray diffractograms in Fig. 15.10 clearly show the beneficial effect of a 400 kGy irradiation on the stability of the amorphous state of the CA–starch blend. After ageing for one year at room temperature, the unirradiated sample exhibits some sharp and intense peaks characteristic of a retrograded material, whereas the sample irradiated at a dose of 400 kGy essentially presents an amorphous structure.

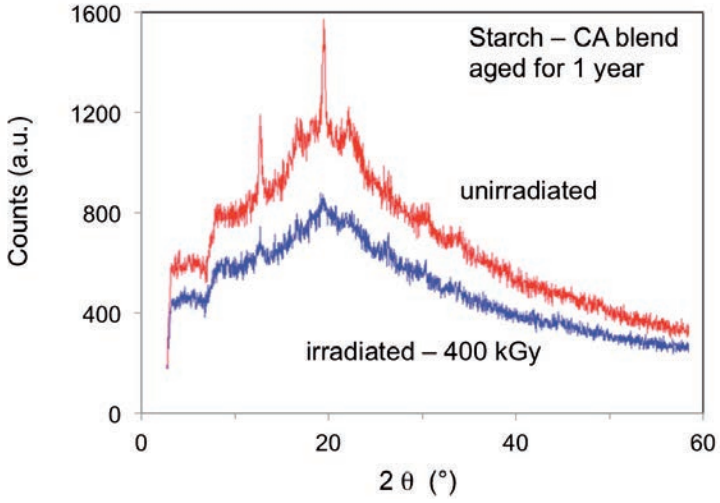

FIG. 15.10. X ray diffractograms of unirradiated and EB irradiated amorphized CA–starch blends.

15.3.4. Biodegradability of starch–lignin blends

Lignin incorporation combined with irradiation not only improves the surface properties of starch but also preserves its biodegradability, in contrast with systems involving synthetic polyolefins [15.29]. The kinetics of CO_2 release from film samples during incubation in soils showed that the materials undergo biodegradation, whatever the lignin content and absorbed dose (Fig. 15.11) [15.30]. The proportion of total carbon mineralized during 100 day

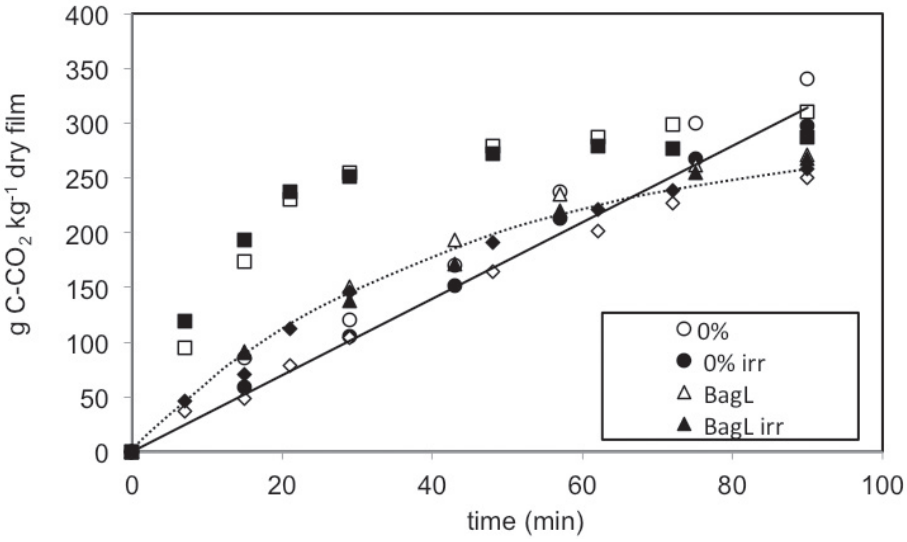

FIG. 15.11. Influence of lignin incorporation and irradiation on the biodegradation of starch based films incubated in a controlled soil.

incubation was not modified by the presence of lignins. However, it affected the biodegradation kinetics, which were linear (4% C−CO_2 kg/day) during the incubation period for the control thermoplastic starch film. Lignosulphonates increase the mineralization rate in the early weeks of incubation; this is likely due to their solubility in water.

15.4. STUDY OF MODEL BLENDS OF MALTODEXTRINES

In order to obtain an insight into the mechanism of the condensation reactions likely to occur within thermoplastic starch–lignin films under EB irradiation, the reactivity of model blends submitted to similar treatments was examined using a variety of analytical methods. Aromatic alcohols, phenols and acids with one or several functional groups present in lignins were studied and their coupling efficiency with maltodextrins when subjected to EB irradiation was evaluated. Para-methoxy benzyl (BA) and CA alcohols are simple and interesting models exhibiting the main structural features of lignin compounds. These models exhibit an aromatic ring with a benzylic or an allylic hydroxy group. Other models, including various cinnamic acids, are shown in Fig. 15.12.

This section covers results illustrating: (a) the effective reduction of water sorption by blending starch glycerol mixtures with wheat or bagasse lignin;

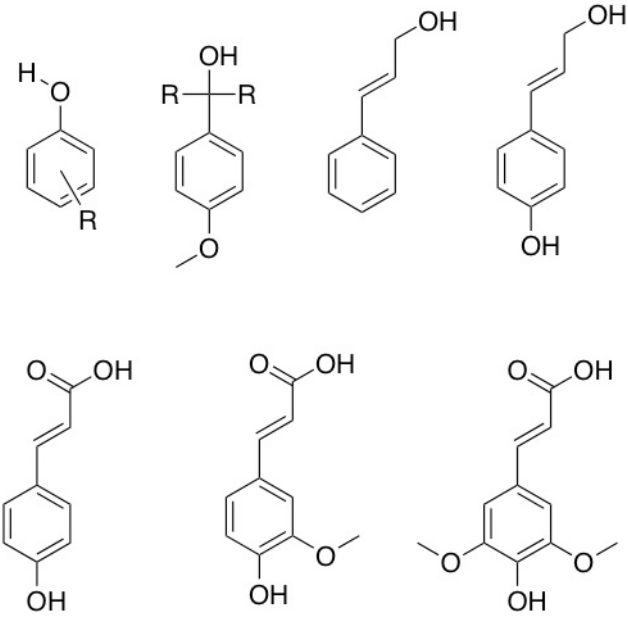

FIG. 15.12. Aromatic model compounds and lignin-like monomers used as additives in starch or maltodextrine blends.

(b) the modification of surface properties after the treatment of such blends by EB irradiation; (c) the quantification of additive conversion after irradiation of blends including model compounds, (d) the evidence of covalent coupling between maltodextrines and p−MeO−benzyl or CA based on MALDI−TOF mass spectrometry analyses.

Preliminary X ray diffraction data will be presented to support the limitation, if not the absence, of any retrogradation in starch additive blends aged for 1 year after EB irradiation.

BA and CA were blended with a maltodextrine of averaged degree of polymerization value 7 (Glucidex G19) and maltotriose (MT) as a methanolic aqueous syrup. A typical composition expressed in weight parts is: MT (70), H_2O (30), CA (10), MeOH (2). The blends were placed in sealed glass vials and were treated with an EB dose ranging from 50 to 400 kGy under conditions similar to the treatment applied to thermoplastic starch–lignin films.

MALDI−TOF mass spectrometry is a very informative method for analysing scissions and couplings altering the molecular structure of compounds subjected to various chemical treatments. The changes occurring in the maltodextrine-BA blend upon EB irradiation can be examined by comparing the MALDI−TOF spectra.

The selected expansion shown in Fig. 15.13 represents the changes observed after irradiation with a 100 kGy dose. Under these conditions, only one new peak is observed between two consecutive peaks of the Na^+ cationized oligosaccharide distribution.

The new lines correspond formally to the coupling of a single methoxybenzyl residue with loss of one molecule of water. Increasing the absorbed dose was shown to induce the appearance in the MALDI−TOF spectra of new peaks that were assigned to multiple occurrences of the same type of reaction. Adducts with m/z values of each cationized oligomer that had increased by 1 to 3 times 120 Da were clearly observable.

Determining precisely the location of the grafting reaction onto the polysaccharide will require additional study on product separation as well as spectroscopic analyses. Further studies are under way to assess the reactivity of unsubstituted and substituted benzyl alcohol exhibiting chemical functions resembling those appearing in lignins. A hypothetical mechanism following EB irradiation of BA-maltodextrine blends rationalizes observed behaviour on the basis of reported elementary free radical reactions [15.31]. The mechanism is as follows:

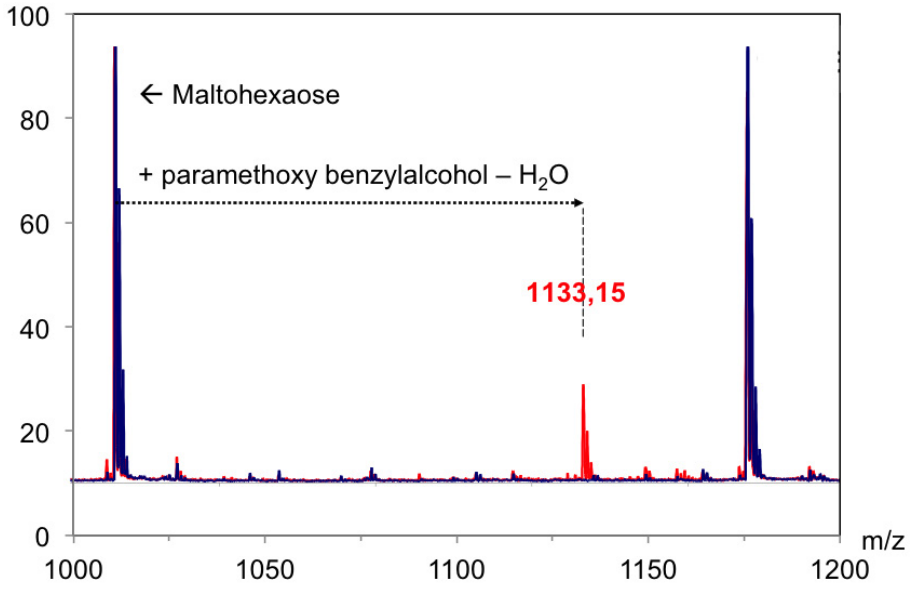

FIG. 15.13. Selected expansion of the MALDI−TOF mass spectra of maltodextrine (Glucidex G19) BA blend before and after irradiation with a 100 kGy EB dose.

— Radiolysis of the constituents:
UAG-UAG-UAG → [UAG-UAG-UAG-(H)]• + H•
H_2O → H• + HO•
Ar-CH2-OH → Ar-CH2• + HO•
— Secondary activation of polysaccharide by transfer:
UAG-UAG-UAG + R• → [UAG-UAG-UAG-(H)]• + RH
— Coupling by combination of radical species:
[UAG-UAG-UAG-(H)]• + RHAr-CH2• →
[UAG-UAG-UAG-(H) + (CH_2-AR)]

The situation is more complex with the second model of lignin used for these experiments. Because of the multifunctional structure of CA, several reactions are possible. MT, a well-defined glucose oligomer, has therefore been used instead of the maltodextrine blend Glucidex G19, in order to facilitate mass spectrometry spectra analysis (Fig. 15.14). In the unirradiated blend, the main peak corresponds to the MT(Na^+) cation appearing at m/z = 526.90 Da, and some other peaks marked with a star in the figure are attributed to the matrix or to impurities in the original MT sample.

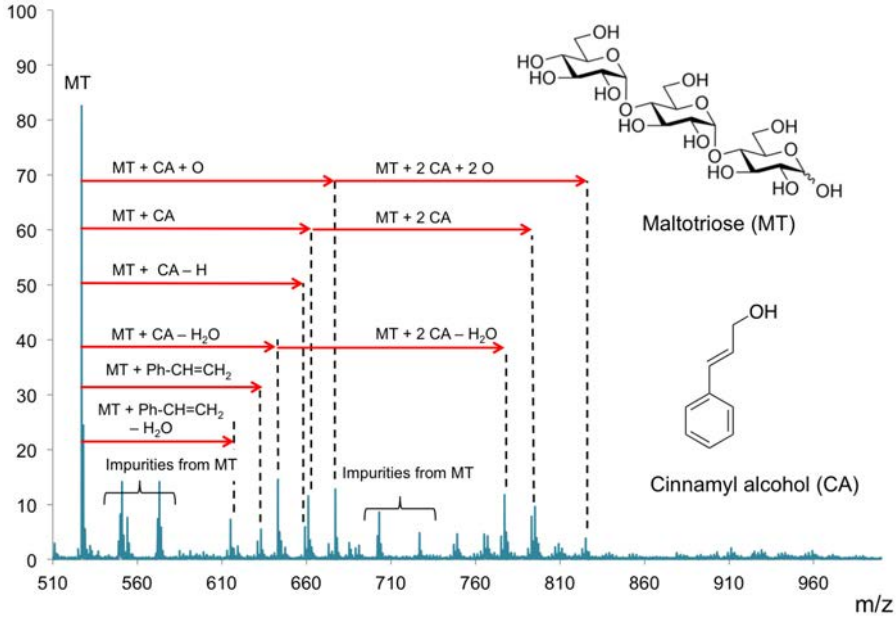

FIG. 15.14. MALDI–TOF mass spectra of MT–CA blend before and after irradiation with a 200 kGy EB dose.

In the EB-treated sample, additional peaks are detected at m/z values 642.99, 660.99, 676.98, 777.02 and 795.04. These are observed above the baseline with intensities of the unreacted MT(Na^+) line of 5–20%. The mass increase relative to the parent MT can be rounded to 116 Da, 134 Da, 150 Da, 250 Da and 268 Da. Taking into account the molecular structure of CA and its expected reactivity, a set of five plausible structures can be proposed for the adducts. The position of the couplings on the MT and on the cinnamyl moieties cannot be deduced from the spectroscopic data available at present. However, the general behaviour of free radicals generated under similar conditions can be reasonably applied to the system under consideration. Hydrogen abstraction from the anomeric C^1 atom in the anhydroglucose units is likely to occur, either by direct radiolysis or by reaction with some free radicals propagating a chain mechanism. The coupling of these free radicals MT(−H)$^\bullet$ with cinnamyl radicals Ph−CH=CH−$CH_2^\bullet$ would yield adducts with a mass increase of 116 Da relative to MT. The addition of MT(−H)$^\bullet$ radicals to the cinnamyl unsaturation would result in reactive adducts that are unlikely to propagate any polymerization, because of the substitution of the CA ethylenic group. Further transfer by hydrogen abstraction would lead to adducts with a mass increase of 134 Da.

Obviously, the repetition of this addition process, or its combination with the coupling of the cinnamyl free radical already described, can explain the formation of adducts with a mass increase of 268 (= 2 × 134) Da and of 250 (= 116 + 134) Da, respectively. Finally, the adduct with a mass increase of 150 Da might be formed by a similar addition process involving CA and an alkoxy free radical, either produced by the radiolysis of a hydroxy group of MT or by the decomposition of a hydroperoxide in an oxidized form of MT.

The proposed structure for the adducts observed after irradiation of representative model compounds involves the reactivity of hydroxyl and cinnamyl functions of the unsaturated aromatic alcohol. This supports the occurrence of similar reactions in the blends of starch with industrial lignins [15.27].

From a quantitative point of view, the amount of converted CA in blends with starch or Glucidex G19 maltodextrine has been assessed by ^{1}H-NMR. The decrease of olefinic proton integration compared with aromatic proton integration allows the accurate evaluation of the amount of reacted cinnamic unsaturation. Conversion degrees as high as 45% were measured in blends initially containing about 0.5 mol/kg, after 400 kGy EB irradiation.

The resulting degree of conversion for CA does not correspond strictly to the grafting yield since other phenomena should be taken into account. The formation of adducts without reaction of the cinnamyl C=C bond (Fig. 15.15), by a mechanism resembling the one observed in BA-maltodextrine blends, has been mentioned above. Some reaction of CA without coupling to MT can be anticipated, but with consumption of some olefinic functions.

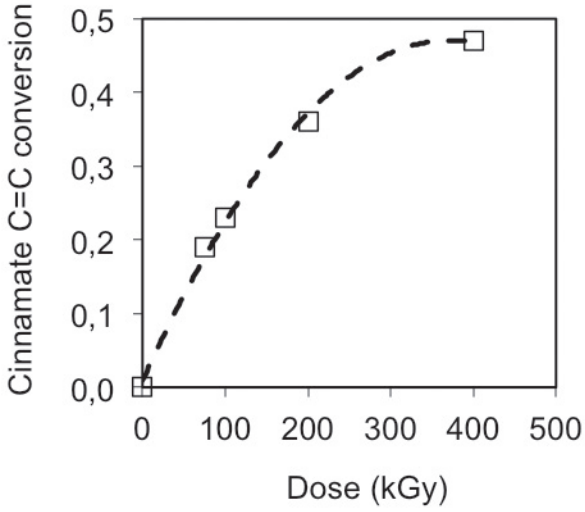

FIG. 15.15. Dose dependence of the mol fraction of reacted cinnamic C=C bonds in CA–starch blends after EB irradiation.

15.5. LATEST DEVELOPMENTS AND PERSPECTIVES

15.5.1. Influence of glycerol

The studies carried out by various authors so far on the presence of glycerol as a plasticizer in thermoplastic starch have shown it to have an impact on the mechanical properties of starch and the overall water absorption of the final blend. The amount of glycerol below 12 wt% in thermoplastic starch leads to an anti-plasticization phenomenon [15.32], while a higher glycerol content leads to plasticization but with an increased sensitivity to water sorption and eventual phase separation [15.33]. The presence of glycerol is also found to counterbalance the positive effects of the amylose content on the elongation and TS seen in unplasticized starch [15.34]. The typical amount of glycerol reported in studies devoted to thermoplastic starch varies between 20 and 30 wt% of the dry starch content.

Glycerol has been studied as a plasticizer because of its preferred interactions with the amorphous regions of starch over the crystalline domains [15.35, 15.36]. These interactions between glycerol and the amorphous regions of starch lead to the partial immobilization of glycerol [15.37]. The strong glycerol−polysaccharide interactions were found to be reversed by the addition of water, suggesting that water disrupts these interactions. It was also reported that application of heat to glycerol–amylopectin mixtures further increases the

immobilization of the plasticizer [15.35]. It is unclear, however, whether the reason for these effects is the result only of the amorphization process of starch or if the possibility of interchain interactions is affected by the presence of glycerol. The resulting physical modification of starch was found to allow improvements in the mechanical properties of the blends after irradiation.

The above results emphasize the importance of physicochemical interactions between the polymer chains with the additives and their impact on the final properties of the blend after irradiation. Such a phenomenon was shown to affect the reactivity under radiation of thermoplastic starch blends, where glycerol is a conventional plasticizer that is present together with aromatic additives such as CA, cinnamic acid and their derivatives or other lignin compounds that can be used for upgrading the properties of the materials.

Despite the various limitations imposed by the physical and chemical complexity of the blends on various analytical techniques, this chapter reports on the use of different complementary techniques for understanding the radiation induced processes. The presence of CA mainly limits chain scission, which is important in preventing the loss of mechanical properties of the actual thermoplastic starch blends [15.38]. It has also been established that glycerol limits — if not impedes — gel formation without inhibiting the grafting process [15.39]. Thus, by varying the amount of water content or glycerol and aromatic additive, the properties of the final blend after irradiation can be finely tuned. Work is still under way to gain a deeper understanding of the specific interactions between various aromatic compounds with lignin type substituents and polysaccharides within the blends, along with improved quantification of the grafting degree of CA in different polysaccharide blends.

15.5.2. Protective effects against radiation of lignin and lignin-like monomers

It has been observed that the presence of aromatic additives induced important structural modifications in the $\bar{M}_w$ of starch and maltodextrines, together with positively altered physical properties, as a result of radiation induced chain scission, grafting and interchain bridging. In particular, the study of starch-derived maltodextrin blends containing cinnamyl alcohol showed that the grafting of CA limits chain scission. It was also established from the study of these model blends that the type of aromatic additive, blend composition, presence of glycerol and applied dose affect the final characteristics and properties of the blend. An interesting consequence of glycerol presence in the blend was the absence of any gel formation resulting from the grafting of CA in the irradiated maltodextrin blends. Attempts have been made to understand whether the absence of gel in the presence of glycerol was a result of some

attenuation in the radiation induced grafting of CA or changes in the interactions between CA and maltodextrin. Glycerol can indeed behave as an $HO^{\bullet}$ scavenger and affect free radical reactions [15.40].

Glycerol can also associate with the polysaccharide by hydrogen bonding and can influence the maltodextrin–CA interactions, thus changing the distribution of reactants involved in the grafting process. Either of these effects or a combination of both is conceivable. In an ongoing study, the radiochemical yields for scission and cross-linking have been studied for a model blend system based on the polysaccharide pullulan, which is an α glucan like starch and cellulose, when subjected to EB radiation [15.41]. The $G(s)$ and $G(x)$ values have been calculated for the aqueous pullulan blends containing relatively trace amounts of an aromatic additive, cinnamyl alcohol, as a lignin-like compound suspected to exert a radio-protective effect and to act as a grafting agent onto glucose polymers. The emphasis in Ref. [15.41] has been laid on the understanding of the influence of: (a) the concentration of CA required to achieve the desired structural modifications in the pullulan chains, i.e. radio-protection against chain scission and increase in molecular mass through grafting and cross-linking, and (b) the physicochemical interactions between pullulan and CA in the absence and presence of glycerol (a commonly used plasticizer in thermoplastic starch) on the $G(s)$ and $G(x)$.

The combined information obtained from the use of the Saito method, based on $\bar{M}_w$ evolution before the gel point, and the Charlesby–Pinner model, based on gel fraction measurements, gave an insight into the influence of the amount of the aromatic additive required for achieving the desired degree of radio-protection and chain cross-linking in the EB irradiated pullulan. The study also showed the presence of glycerol to affect $G(x)$ arising mainly from its role in physicochemical interactions rather than its capacity to act as an $HO^{\bullet}$ radical scavenger. The presence of CA was found to decrease both the $G(s)$ and $G(x)$, the decrease in $G(s)$ being greater than that observed in $G(x)$. The presence of glycerol in the blends was found to affect only the $G(x)$ values, suggesting that physicochemical interactions involving glycerol affect only the degree of cross-linking between the chains and not the degree of scission under radiation. For all formulations, the $G(s)$ values always remained greater than the $G(x)$ values [15.42].

These findings will allow the design of radiation processable formulations minimizing the degradation of the starch substrate, while allowing for the hydrophobization and structural modifications limiting retrogradation of thermoplastic material. Particularly the simultaneous enhancement of the elongation and load at break of the starch based materials is the key issue. Efforts are currently being undertaken in this direction.

15.6. CONCLUSION

The studies reported in this chapter clearly demonstrate the potential of radiation grafting for adjusting the properties of starch based thermoplastic materials. The study of model blends allowed the quantitative assessment of the conversion degree of the reactive additives added to amorphized polysaccharides. It is clearly established by MALDI-TOF mass spectrometry that grafting reactions take place and increase as a function of dose and of additive content. The proposed structure for the observed adducts after irradiation of representative model compounds involves the reactivity of hydroxyl and cinnamyl functions of the unsaturated aromatic alcohol. This supports the occurrence of similar reactions in the blends of starch with industrial lignins. The effect at the surface of starch with industrial lignin can be interpreted in terms of exomigration and grafting at the film surface. In addition, the radiation grafting of organic additives onto starch is shown to impede retrogradation efficiently, whereas aromatic compounds resembling lignin monomers exert a protective effect against radiation, by limiting the extent of chain scission.

ACKNOWLEDGEMENTS

This work was funded in part by the French National Research Agency's LignoStarch programme. The authors express their thanks to the European Union's European Fund for Economic and Regional Development, the Region de Champagne-Ardenne and Conseil general de la Marne for their financial support to the Programme PlAneT. The IAEA is acknowledged for financial support through its CRP on Development of Radiation Processed Products of Natural Polymers for Applications in Agriculture, Healthcare, Industry and Environment.

REFERENCES TO CHAPTER 15

[15.1] STEVENS, E.S., Green Plastics: An Introduction to the New Science of Biodegradable Plastics, Princeton University Press, Princeton, NJ (2001) 238 pp.

[15.2] EUROPEAN BIOPLASTICS European Bioplastics (2016), http://docs.european-bioplastics.org/2016/publications/md/EUBP_share_of_material_types_2014_en.jpg

[15.3] SHEN, L., HAUFE, J., PATEL, M.K., Product Overview and Market Projection of Emerging Bio-based Plastics, Utrecht University, Utrecht, Netherlands (2009) 227 pp.

[15.4] JANSSEN, L., MOSCICKI, L., Thermoplastic Starch, Wiley-VCH, Weinheim, Germany (2009) 242 pp.

[15.5] BELLO-PEREZ, L.A., ROGER, P., BAUD, B., COLONNA, P., Macromolecular features of starches determined by aqueous high-performance size exclusion chromatography, J. Cereal Sci. **27** (1998) 267–278.
[15.6] PARKER, R., RING, S.G., Starch structure and properties, Carbohydr. Europ. **15** (1996) 6–10.
[15.7] CHEETHAM, N.W.H., TAO, L., Variation in crystalline type with amylose content in maize starch granules: an X-ray powder diffraction study, Carbohydr. Polym. **36** (1998) 277–284.
[15.8] ZEEMAN, S.C., KOSSMANN, J., SMITH, A.M., Starch: Its metabolism, evolution, and biotechnological modification in plants, Annu. Rev. Plant Biol. **61** (2010) 209–234.
[15.9] WANG, T.L., BOGRACHEVA, T.Y., HEDLEY, C.L., Starch: as simple as A, B, C, J. Ex. Bot. **49** (1998) 481–502.
[15.10] BEMILLER, J., WHISTLER, R., Starch: Chemistry and Technology, Elsevier, Amsterdam (2009) 879 pp.
[15.11] BULÉON, A., COLONNA, P., PLANCHOT, V., BALL, S., Starch granules: structure and biosynthesis, Int. J. Biol. Macromol. **23** (1998) 85–112.
[15.12] SAGAR, A.D., VILLAR, M.A., THOMAS, E.L., ARMSTRONG, R.C., MERRILL, E.W., Irradiation-modification of starch-containing thermoplastic blends. I. Modification of properties and microstructure, J. Appl. Polym. Sci. **61** (1996) 139–155.
[15.13] SAGAR, A.D., VILLAR, M.A., THOMAS, E.L., ARMSTRONG, R.C., MERRILL, E.W., Irradiation-modification of starch-containing thermoplastic blends. II. Rheological studies, J. Appl. Polym. Sci. **61** (1996) 157–162.
[15.14] WONGSUBAN, B., KHARIDAH, M., GHAZALI, Z., HASHIM, K., HASSAN, M.A., The effect of electron beam irradiation on preparation of sago starch/polyvinyl alcohol foams, Nucl. Instrum. Meth. Phys. Res. Sect. B **11** (2003) 244–250.
[15.15] LOURDIN, D., BIZOT, H., COLONNA, P., Correlation between static mechanical properties of starch glycerol materials and low temperature relaxation, Macromol. Symp. **114** (1997) 179–185.
[15.16] RÖPER, H., KOCH, H., The role of starch in biodegradable thermoplastic materials, Starch/Staerke **42** (1990) 123–130.
[15.17] POUTANEN, K., FORSSELL, P., Modification of starch properties with plasticizers, TRIP **4** (1990) 128–132.
[15.18] RUCKERT, D., CAZAUX, F., COQUERET, X., Electron-beam processing of destructurized allylurea–starch blends: Immobilization of plasticizer by grafting, J. Appl. Polym. Sci. **73** (1999) 409–417.
[15.19] OLIVIER, A., GORS, C., CAZAUX, F., COQUERET, X., Physical stabilization of starch–allylurea blends by EB-grafting: a compositional and structural study, Biomacromol. **1**, 2000, 282–289.
[15.20] OLIVIER, A., CAZAUX, F., COQUERET, X., Compatibilization of starch-allylurea blends by electron beam irradiation: spectroscopic monitoring and assessment of grafting efficiency, Biomacromol. **2** (2001) 1260–1266.

[15.21] GLASSER, W., NORTHEY, R., SCHULTZ, T., Lignin: Historical, Biological and Materials Perspectives, ACS Symposium Series No. 742, American Chemical Society, Washington, DC (2000).
[15.22] BAUMBERGER, S., "Starch-ligin films", Chemical Modification, Properties, and Usages of Lignin (HU, T.Q., Ed.), Kluwer Academic Publishers, Plenum Publishers, New York (2002) Ch. 1–19.
[15.23] BAUMBERGER, S., LAPIERRE, C., MONTIES, B., LOURDIN, D., COLONNA, P., Preparation and properties of thermally moulded and cast lignosulfonates starch blends, Ind. Crops Prod. **6** (2004) 253–258.
[15.24] GIERER, J., WÄNNSTRÖM, S., Formation of ether bonds between lignins and carbohydrates during alkaline pulping processes, Holzforschung **40** (1986) 347–352.
[15.25] TOIKKA, M., SIPILÄ, J., TELEMAN, A., BRUNOW, G., Lignin–carbohydrate model compounds. Formation of lignin–methyl arabinoside and lignin–methyl galactoside benzyl ethers via quinone methide intermediates, J. Chem. Soc. Perkin Trans. **22** (1998) 3813–3818.
[15.26] LUNZALUNGA, O., BIETTI, M., Photo- and radiation chemical induced degradation of lignin model compounds, J. Photochem. Photobiol. B. **56** 2–3 (2000) 85–108.
[15.27] LEPIFRE, S., et al., Reactivity of sulphur-free alkali lignins within starch films, Industr. Crops Res. **20** (2004) 219–230.
[15.28] ZHENG, D., Modification des propriétés de surface de matériaux lignifiés: impact d'un greffage par voie physique, PhD dissertation, AgroParisTech, Paris (2011).
[15.29] DOANE, W.M., USDA research on starch based biodegradable plastics, Starch/Stärke **44** (1992) 293–295.
[15.30] LEPIFRE, S., et al., Lignin incorporation combined with electron-beam irradiation improves the surface water resistance of starch films, Biomacromol. **5** (2004) 1678–1686.
[15.31] IVANOV, V.S., Radiation Chemistry of Polymers, VSP, Utrecht, Netherlands (1992).
[15.32] GARCIA, V., et al., Thermal transitions of cassava starch at intermediate water contents, J. Therm. Anal. **47** (1996) 1213–1228.
[15.33] MALI, S., SAKANAKA, L.S., YAMASHITA, F., GROSSMANN, M.V.E., Water sorption and mechanical properties of cassava starch films and their relation to plasticizing effect, Carbohyd. Polym. **60** (2005) 283–289.
[15.34] LOURDIN, D., DELLA VALLE, G., COLONNA, P., Influence of amylose content on starch films and foams, Carbohydr. Polym. **27** (1995) 261–270.
[15.35] KRUISKAMP, P.H., SMITS, A.L.M., VAN SOEST, J.J.G., FEIL, H., VLIEGENTHART, J.F.G., The influence of plasticizer on molecular organization in dry amylopectine measured by DSC and solid state NMR spectroscopy, J. Ind. Microbol. Biot. **26** (2001) 90–94.
[15.36] SMITS, A.L.M., KRUISKAMP, P.H., VAN SOEST, J.J.G., VLIEGENTHART, J.F.G., Interaction between dry starch and plasticizers glycerol or ethylene glycol measured by DSC and solid state NMR spectroscopy, Carbohydr. Polym. **53** (2003) 409–416.
[15.37] SMITS, A.L.M., HULLEMAN, S.H.D., VAN SOEST, J.J.G., FEIL, H., VLIEGENTHART, J.F.G., The influence of polyols on the molecular organization in starch based plastic, Polym. Adv. Technol. **10** (1999) 570–574.

[15.38] KHANDAL, D., et al., Tailoring the properties of thermoplastic starch by blending with cinnamyl alcohol and radiation processing: An insight into the competitive grafting and scission reactions, Radiat. Phys. Chem. **81** (2012) 986–990.
[15.39] KHANDAL, D., MIKUS, P.Y., DOLE, P., COQUERET, X., Radiation processing of thermoplastic starch by blending aromatic additives: Effect of blend composition and radiation parameters, Radiat. Phys. Chem. **84** (2013) 218–222.
[15.40] BAUGH, P.J., et al., "The radiolysis of glycerol in aqueous solutions", Proc. of the Fifth Tihany Symposium on Radiation Chemistry (Proc. Mtg Siofok, Hungary, 1982) Adadémiai Kiadó, Budapest (1983) 249–256.
[15.41] KHANDAL, D., AGGARWAL, M., SURI, G., COQUERET, X., Electron beam irradiation of maltodextrin and cinnamyl alcohol mixtures: Influence of glycerol on cross-linking, Carbohydr. Polym. **117** (2015) 150–159.
[15.42] KHANDAL, D., COQUERET, X., Radiochemical yields of scission and crosslinking in pullulan blends containing cinnamyl alcohol (in preparation).

Chapter 16

BIODEGRADABLE AND BIOACTIVE POLYMERIC COATINGS AND FILMS FOR FOOD PACKAGING: PREPARATION, CHARACTERIZATION AND APPLICATION

R.A. KHAN, K.D. VU, M. LACROIX
Institute Armand-Frappier,
Canadian Irradiation Center, University of Quebec,
Laval, Canada

16.1. INTRODUCTION

Petroleum based synthetic polymers have become a major class of materials since their development during World War II. Packaging is one application area that was revolutionized by synthetic polymers such as PE, polypropylene, polystyrene, poly(ethylene terephtalate) and poly(vinyl chloride). These polymers quickly found wide acceptance in different packaging applications owing to attractive properties such as their flexibility, toughness, low weight, processability and reasonable price [16.1–16.3]. Almost all foods, whether fresh or processed, are enclosed in some form of packaging at the various stages of their preparation, during handling and storage and on their way to the consumer. The main function of packaging is to protect food from the outside environment. However, the growing dependence on synthetic polymers has raised a number of environmental concerns. Most plastic materials are not biodegradable and are derived from non-renewable resources. The property of durability which makes these materials so useful for various applications also favours their persistence in the environment, thus generating difficulties for their disposal. The three main strategies available for the management of plastic wastes are incineration, recycling and landfill. Various drawbacks associated with these three end-of-life options drive the plastics industry to search for other solutions [16.4–16.5]. The increasing need for food quality while reducing packaging waste has encouraged the exploration of new packaging materials, such as edible and biodegradable films from renewable resources. The use of such materials with their reduced environmental impact is expected to reduce the waste problem by exploiting the potential of cheap renewable biomass feedstock (crops) and agro-industrial by-products [16.6–16.8].

16.2. BIODEGRADABLE POLYMERS

By definition, biodegradable polymers have the capacity to be broken down into small molecules (such as carbon dioxide, water and methane) or converted into biomass by microorganisms (bacteria or fungi) and/or by enzymes when placed in a suitable environment [16.9–16.10]. Biodegradable polymers are generally classified either as natural polymers (bio-polymers), which are derived from renewable or natural resources, or as synthetic biodegradable polymers (fossil or non-renewable), which are made synthetically from petroleum. Bio-polymers can in turn be divided into three main categories based on their origin and production [16.11]: (a) polymers derived from bio-polymers e.g. polysaccharides such as starch and modified cellulose and proteins such as casein and gluten; (b) polymers produced by classical chemical synthesis using renewable bio-based monomers, such as PLA, and (c) polymers produced by microorganisms or genetically modified bacteria. To date, this last group of bio-based polymers consists mainly of the poly(hydroxyalkanoates), but developments with bacterial cellulose are in progress.

The basic materials investigated for their potential use as edible and biodegradable films and coatings in food packaging are those directly extracted from biomass (marine, agricultural animals and plants). The principal polysaccharides of interest for material production are cellulose, starch and chitosan [16.11]. Proteins have functional side chains that are highly suitable for chemical modification and tailoring properties required for packaging material. Owing to this molecular diversity, proteins have considerable potential for the formation of linkages that differ with respect to their position, nature and energy. Proteins can be divided into proteins of plant origin (e.g. gluten, soy, pea and potato) and proteins of animal origin (e.g. casein, whey, collagen and keratin). All these bio-polymers are hydrophilic by nature and somewhat crystalline, which are factors that cause problems, especially in relation to the packaging of moist products. The excess of disulphide cross-linking and thermal degradation of these polymers are also two main problems in their processing and performance. On the other hand, these polymers produce materials with excellent gas barriers [16.12].

The films described in this chapter are prepared from polysaccharides, essentially chitosan, alginate, starch and cellulose derivatives, as well as from two biodegradable synthetic polyesters, PLA and PCL.

16.2.1. Edible films and coatings for food applications

People have been covering food products since ancient times. Wax has been used to delay the dehydration of citrus fruits in China since the twelfth

century [16.13]. The application of coatings to meat to prevent shrinkage has been a usual practice since the sixteenth century at the latest, when meat cuts began to be coated with fats [16.14]. Vegetable and milk proteins were used to obtain edible films to preserve fruits and vegetables, as well as eggs and fish [16.15, 16.16]. In the 19th century, sucrose was initially applied as an edible protective coating for nuts such as almonds and hazelnuts to prevent oxidation and rancidness during storage. An important discovery was an edible coating that is an aqueous emulsion of oil and different waxes, which, when fruits are coated with it, improves their shine and colour, prevents softening and the onset of mealiness, and is able to control water loss and ripening. Polysaccharides such as alginates, collagen, carrageenan, cellulose ethers, pectin and starch derivatives have also been used extensively for the preparation of coatings in order to improve the quality of stored meat. Such edible films and coatings developed during the past 40 years are described in many scientific papers and patents [16.15–16.17].

Coatings are either applied to or made directly on foods whereas films are independent structures that can wrap food after its manufacture. They are located on the food surface or are thin layers between several parts within the product, for example, between the fruits and the dough in a pie. Questions can be raised as to whether edible packaging should be considered a food ingredient or whether we should be more cautious and qualify it as a food additive. There is currently no regulation in the European Community to specify how edible packaging has to be classified. Foods are defined in the Codex Alimentarius as: "all raw, partially treated or treated substances used for human nutrition and feeding". This includes drinks, chewing gum and all components used in the formulation, preparation, making and treatment of foods, but does not include substances used as drugs and cosmetics, or tobacco. According to this definition, edible coatings would qualify as food. On the other hand, since they do not provide significant nutritional value, edible coatings are more properly classified as food additives. In cases when an edible coating is used in order to improve the quality of food, it could be regarded as an ingredient. In such a case, the coating should be tasteless and not detectable, or if this is not possible, the taste of the edible coating should be compatible with the food. Although many functions of edible packaging are identical to those of plastic films, particularly their barrier properties to gas, vapours and solutes, their use strictly requires an over packaging, notably for handling and hygienic reasons [16.18, 16.19]. Edible packaging and coating, being both food packaging and a food ingredient, has to fulfil requirements for both of these two roles: good mechanical and barrier properties; free of toxins; good physicochemical and microbiological stability; good sensory qualities, made from low-cost materials by a simple and environmentally friendly technology [16.15, 16.17, 16.18, 16.20, 16.21].

Edible packaging must have some functional and specific properties. Indeed, first of all it has to be selective towards mass transfers, but in some cases it has active properties, or it can be both selective and active. In most cases, the water barrier efficiency of films is desirable to retard the surface dehydration of both fresh (meat, fruits and vegetables) and frozen products. The water absorption that induces caking in food powder or the loss of crispness in dried cakes, for example, could be delayed by coatings. The control of gas exchanges, particularly of oxygen, allows better control of the ripening of fruits or a significant reduction in the oxidation of oxygen sensitive foods and the rancidity of polyunsaturated fats, for example. Organic vapour transfers have to be diminished with the aim of retaining aroma compounds in the product during storage or to prevent solvent penetration in foods, which can introduce toxicity or off-flavors. The penetration of oil during frying and of sucrose or sodium chloride during osmotic dehydration can be limited by an edible film.

One of the more interesting applications of edible films and coatings is their use inside a composite food to control mass transfers between the different compartments of the product, for example, in order to reduce water migration in a pie. The effect of light and the effect of UV light that lead to free radical reactions in foods could be reduced. In the latter case, the efficiency of the film at preventing light effects can be improved by the addition of pigments or light absorbers. Thus, when films are carriers or used for encapsulation of food additives or ingredients, they are active.

Edible packaging can improve the mechanical properties of food to facilitate handling and transportation. Sensorial characteristics such as colour, shininess, transparency, roughness and sticking can be improved. Edible films and coatings enable the protection or separation of small pieces or food portions for individual consumption, or the isolation of pre-dosed quantities of food additives or ingredients with the aim of facilitating the formulation and the preparation of food in industrial plants. Functional efficiency strongly depends on the nature of the components and the film's composition and structure. The choice of film forming substance and/or active additive is a function of the objective, of the nature of the food product and of the application method. So lipids or hydrophobic substances such as resins, waxes and some non-soluble proteins are the most efficient for moisture transfer retardation [16.15, 16.22]. On the contrary, water soluble hydrocolloids, such as polysaccharides and proteins, are not efficient barriers against water transfer; however, their permeability to permanent gases is often lower than those of plastic films. Moreover, hydrocolloids usually provide higher mechanical properties to edible packaging than do lipids and hydrophobic substances. Therefore, the advantages of all substances can be used in composite films made from both hydrocolloids and lipids.

Natural film forming substances, particularly proteins, require the use of film additives, such as plasticizers, to improve film resistance and elasticity and emulsifiers to increase the hydrophobic globule distribution in composite emulsion based edible films. Different types of edible packaging can be obtained as a function of the composition and manufacturing technique. Indeed, homogeneous films with a smooth surface are obtained from homogeneous solutions of polysaccharides or proteins, or from molten lipids. Their appearance depends on the nature of the main component; for example, water soluble cellulose derivatives give transparent and shiny films whereas gluten or casein based films are coloured and unpolished. Some mixtures of proteins and polysaccharides make homogeneous edible packaging if all components are completely soluble in water or in a hydro alcoholic solution.

Composite packaging is defined as films or coatings whose structure is heterogeneous, that is, composed of a continuous matrix with some inclusions, such as lipid globules in the case of an emulsion, or solid particles in the case of non-soluble substances (e.g. fibres or hydrophobic proteins), or composed of several layers. Usually, multilayered films have better mechanical and barrier efficiencies than emulsion based films and coatings, but their manufacturing requires one step of spreading or lamination and drying for each layer. Therefore, their use industrially does not seem very interesting because there are too many steps in their making; emulsion based edible films provide nearly the same properties but only require one operation in their preparation [16.23].

16.2.2. Biodegradable films for packaging

The purpose of developing biodegradable polymer films is to offer commercially interesting replacement alternatives to existing synthetic, non-biodegradable products for food packaging applications. Despite the number of investigations under way relating to modified bio-polymers and blends, still further research and development is needed before they become competitive to the commonly used synthetic polymers [16.3]. Biodegradable packaging has the advantage of being produced from renewable resources, being non-toxic and degrading into non-polluting substances. Edible packaging is consumed with the product, and therefore no disposal is required. At the same time, these materials, like their synthetic counterparts, offer the possibility of layering, incorporating additives (flavouring, colouring and sweeteners) and supplementing the nutritional value of food.

Films can regulate the transfer of moisture, oxygen, carbon dioxide, lipid and aroma and flavour compounds in food systems to increase product shelf life and improve quality. The most common materials used to form edible films are polysaccharides, proteins and lipid compounds. Many of these materials have

good film forming properties. Films formed from polysaccharides are hydrophilic and provide efficient barriers to oils and lipids, but their moisture barrier properties are poor. Protein based films are highly interesting, as they confer more potential functional properties. Many lipid compounds such as animal and vegetable fats have been used to make edible films and coatings. Lipid films have excellent moisture barrier properties but they can cause textural and organoleptic problems due to their oxidation and waxy taste [16.5]. The properties of bio-polymers and biodegradable polymer films depend on the raw material that they are based on, the additives used and on the (chemical) modifications that take place during production. Water vapour, oxygen permeability and tensile test are the most frequently used methods to determinate film characteristics for food packaging films [16.1–16.3].

16.3. BIOACTIVE FILMS FOR PACKAGING

Antimicrobial agents incorporated into edible films or coatings are released onto the surface of food to control microbial growth. Such coatings can also serve as a barrier to moisture and oxygen. The main cause of spoilage of many foods is microbial growth on the product surface. The application of antimicrobial agents to packaging can create an environment inside the package that may delay or even prevent the growth of microorganisms on the product surface and thereby lead to an extension of the shelf life and/or the improved safety of the product. To control undesirable microorganisms in foods during storage and distribution, antimicrobial substances can be either incorporated into food packaging materials or coated onto the surface of food. Based on how effectively they influence the food, antimicrobial films can be divided into two types. The first category comprises films that contain an antimicrobial agent that migrates to the surface of the food. The second category comprises films that are effective against surface growth without any migration of the active agents to the food.

Both synthetic and naturally occurring compounds have been tested for antimicrobial activity in packaging. Antimicrobial enzymes may be bound to the inner surfaces of food contact films. Enzymes may be released into foods from packaging materials where they would produce microbial toxins. Glucose oxidase has exerted antimicrobial effects due to the production of hydrogen peroxides [16.24]. Benzoate, sorbate, bacteriocins, essential oils and lysozymes are also used as natural antimicrobial compounds [16.15, 16.25, 16.26]. Antimicrobial absorbent food pads are used in trays for meat packaged for retail to soak up meat juice. Absorbent food pads that inhibit foodborne pathogens contain an antimicrobial element comprising an anionic surfactant in the form of

alkyl sulphonate salts, alkyl sulphate salts and one or more acids, such as citric or malic acid.

Another possibility for antimicrobial films is to incorporate radiation emitting materials into them. Japanese researchers have developed a material that emits long wavelength infrared radiation on exposure to water or water vapour. This is thought to be effective against microorganisms without any of the risks associated with high energy radiation [16.27]. Future work in antimicrobial films may focus on the use of biologically derived antimicrobial materials that are either bound or incorporated into films and do not need to migrate to the food to be effective. For example, a group of substances known as bacteriocins, which are proteins derived from microorganisms such as nisin, has been approved for food use [16.15, 16.24, 16.25]. Fresh foods may contain microorganisms both on their surfaces and within. These microorganisms, if not destroyed, lead to food spoilage. The prevention of food spoilage by inhibiting or destroying microorganisms is the basis of food preservation. Different types of antimicrobial agents are used in food packaging. Examples are essential oils, chitosan, bacteriocins, weak organic acids, fungicides, enzymes and grapefruit seed extract. A brief discussion is given below.

16.3.1. Essential oils

Essential oils and their components are becoming increasingly popular as naturally occurring antimicrobial agents. The antimicrobial properties of thyme essential oils are mainly related to their high phenolic content. The essential oil of Sardinian *Thymus* [16.28] contains substances such as carvacrol and thymol. *Melaleuca alternifolia* [16.29], *Pelargonium* and *Cultivas* [16.30], *Senecio graveolens* (Compositae) [16.31], *Picea excels* [16.32] and *Ocimum gratissimum* leaf [16.33] are showing popularity as sources of naturally occurring antimicrobial agents. Ouattara et al. [16.34] evaluated the combined effect of low dose gamma irradiation and protein based coatings with thyme oil and trans-cinnamaldehyde to extend the shelf life of precooked shrimp. The product shelf life was significantly extended without altering the appearance and taste of shrimp for thymol treatment concentrations of up to 0.9%.

16.3.2. Chitosan

Chitosan is inherently antimicrobial and has been used in films and coatings. Chitosan, a cationic polymer, promotes cell adhesion, as charged amines interact with negative charges on the cell membrane causing leakage of intracellular constituents [16.35]. Chitosan has been used as a coating and appears to protect fresh vegetables and fruits from fungal degradation. Chitosan has two functions.

It produces antifungal activity and acts as a barrier between the produce and microorganisms [16.36]. Rhoades and Roller studied [16.37] the antimicrobial activity of degraded and native chitosan against spoilage microorganisms. Mild hydrolysis of chitosan resulted in improved inhibitory activity in saline and greater inhibition of the growth of spoilage yeasts, whereas highly degraded products of chitosan exhibited no antimicrobial activity.

16.3.3. Bacteriocin

The bacteriocin nisin has been used as an antimicrobial agent in foods since the 1960s. Nisin, produced by the lactic acid bacterium, *Lactococcus lactis*, is most effective in its antimicrobial activity against lactic acid bacteria and other gram-positive organisms, notably the *Clostridia* species [16.38]. Recently, the use of nisin in packaging materials has been attracting intense interest [16.39–16.45]. Pediocin is another bacteriocin that was found to be effective against *L. monocytogenes*. Ming et al. [16.46] applied nisin and pediocin to cellulose casings to reduce levels of *Listeria monocytogenes* in meats and poultry. Pediocin coated bags completely inhibited the growth of inoculated *L. monocytogenes* during 12 weeks storage at 4°C.

16.4. NANOCOMPOSITE FILMS FOR PACKAGING

Recent advances in nanoscience and nanotechnology make it possible to manipulate packaging materials at the level of atoms and molecules in order to improve the products, particularly from the viewpoints of physical properties and biological activity. Polymer nanocomposites traditionally include mineral fillers in the range of 10–50% by weight (clay, silica or talc), incorporated into the film during preparation. The properties of the nanocomposite film that can be improved this way as compared with conventional polymer or composite films include increased modulus, strength, solvent and heat resistance, and decreased gas permeability and flammability [16.47].

However, the mechanical strength of the films in general decreases when fillers are present [16.48]. Inclusion of nanocrystalline cellulose, carbon nanotubes (CNTs), and chitin/chitosan nanofibres was shown to bring about other improvements [16.49–16.52].

16.5. PREPARATION AND CHARACTERIZATION OF BIODEGRADABLE FILMS

Typically, for the preparation of biodegradable films, solution casting is widely used, whereby solutions are cast on a support, allowed to dry, and the formed film is then detached from the support. Compression moulding is also used for the fabrication of thermoplastic biodegradable films. Examples of bio-polymers (chitosan, methylcellulose and alginate) films were prepared by solution casting from its 1% aqueous solution. The mechanical and some barrier properties of these bio-polymer films are presented in Table 16.1. All the bio-polymers are strongly hydrophilic in nature, so the water vapour permeability (WVP) of bio-polymers is higher than that of synthetic polymers. The mechanical properties of the films vary depending of the film composition and treatments applied on film formulations [16.1, 16.53, 16.54].

TABLE 16.1. MECHANICAL AND BARRIER PROPERTIES OF BIO-POLYMERS

Polymer	Tensile strength (MPa)	Tensile modulus (MPa)	Elongation at break (%)	WVP (g·mm ·m^{-2} ·d^{-1} ·kPa^{-1})	Oxygen transmission rate (cm^{3}· / mm^{2}·day)
Chitosan	65–80	1590–2000	6–10	4.0–4.0	0.8–1.4
MC	48–56	1200–1400	12–15	6.0–7.0	20–25
Alginate	57–80	2000–2200	10–12	5.0–6.0	1.0–1.5
PET [a]	75	2800	60	0.2	1
PE [16.1, 16.8, 16.53–16.55]	18	300	600	0.12	300

[a] PET: Poly(ethylene terephthalate);

16.5.1. Effect of gamma radiation on chitosan films

All bio-polymer films are very susceptible to gamma radiation. It is reported [16.53] that chitosan films lose 36.66% of their TS after exposure to 25 kGy of gamma radiation. At a 5 kGy dose, the TS of chitosan films improved by 10%. At a low dose, some cross-links could have been formed between chitosan

molecules and thus improved the TS of the films but at a higher dose, chitosan molecules might be broken down and show lower strength. Similarly, the tensile modulus (TM) of the chitosan films was reported to rise slightly from 450 MPa to 478 MPa upon irradiation at 5 kGy, but decreased significantly at higher doses (343 MPa at 25 kGy).

16.5.1.1. Effect of gamma radiation on alginate films

For alginate films, it was found that at lower absorbed doses (0.1–0.5 kGy), the puncture strength (PS) and puncture deformation (PD) values increased significantly ($p \leq 0.05$). The increase of mechanical properties of alginate based films at low absorbed doses (0.1–0.5 kGy) may be attributed to the generation of free radicals and cross-linking of alginate molecules. However, at doses higher than 1 kGy, both PS and PD values decreased significantly ($p \leq 0.05$). The decrease in PS and PD values may be due to chain scission when alginate is exposed to gamma irradiation, as previously reported [16.54].

16.5.1.2. Effect of gamma radiation on methylcellulose based films

MC based films were exposed to γ radiation (^{60}Co source) from 0.5–50 kGy doses and PS, PD, viscoelasticity coefficient and WVP values of the films were measured. The results are presented in Table 16.2.

TABLE 16.2. EFFECT OF GAMMA RADIATION ON THE MECHANICAL PROPERTIES OF MC BASED FILMS [16.1, 16.55]

Dose (kGy)	Puncture strength (N/mm)	Puncture deformation (mm)	Viscoelasticity coefficient (%)	WVP ($g \cdot mm \cdot m^{-2} \cdot d^{-1} \cdot kPa^{-1}$)
0	146 ± 6	4.5 ± 0.2	41.2 ± 2.0	6.3 ± 0.2
0.5	144 ± 9	4.4 ± 0.2	40.2 ± 1.2	6.6 ± 0.3
1	145 ± 10	4.50 ± 0.1	41.0 ± 1.8	6.3 ± 0.2
5	146 ± 4	4.6 ± 0.1	38.9 ± 2.2	6.3 ± 0.1
10	140 ± 12	4.6 ± 0.1	35.4 ± 1.1	6.0 ± 0.3
25	132 ± 3	4.6 ± 0.1	34.4 ± 0.6	5.9 ± 0.1
50	124 ± 5	4.7 ± 0.1	32.2 ±1.2	5.8 ± 0.2

The results show that up to a 10 kGy dose, no significant changes ($p > 0.05$) were observed in PS and PD values. However, WVP and the viscoelasticity coefficient decreased significantly ($p \leq 0.05$) at doses ≥1 kGy and ≥5 kGy, respectively. At a dose of 50 kGy, films lost 15% PS, 9% viscoelasticity coefficient and 9% WVP, whereas a significant ($p \leq 0.005$) increase of PD (6%) was observed. Indeed, irradiation treatment may have affected the internal structure of cellulose leading to a reduction of mechanical strength of the films but improving the barrier and deformation properties significantly. In this context, it is suggested that the action of gamma irradiation induced a decrease in molecular weight that leads to a loss in film strength. The improvement in barrier properties may be attributed to rearrangements and hydrogen bonding that involves the new additional chain ends [16.1, 16.55].

16.6. PREPARATION OF BIODEGRADABLE FILMS BY COMPRESSION MOULDING

Compression moulding is one of the main techniques for the preparation of films. In this section, examples are shown of how to prepare biodegradable films and how mechanical and other properties can be further enhanced. Additionally, applications of monomers, grafting and irradiation on various films are discussed together with the resultant properties.

16.6.1. MC reinforced PCL based biodegradable films

16.6.1.1. Mechanical properties

Compression moulding was used to prepare films from methylcellulose and MC reinforced polycaprolactone. The MC content in the composite was 10–50% by weight. The PS of PCL and MC based films was found to be 94 N/mm and 147 N/mm, respectively. Figure 16.1 shows the effect of MC content on the PS of PCL based biodegradable films.

The incorporation of MC in a PCL matrix caused a significant increase of PS ($p \leq 0.05$). With 10% MC reinforcement, the PS of the films increased by 8.3% compared with PCL films (control). On the other hand, 20%, 30%, 40% and 50% MC contents raised the PS of the films by 19%, 25%, 32% and 32%, respectively. It is clear that PS values reach a plateau after 40% MC content in PCL based films. Therefore, MC films acted as a reinforcing agent in a PCL matrix. The PS values of the PCL based films were increased because of the higher PS values of MC (147 N/mm) compared with the PS of PCL (94 N/mm).

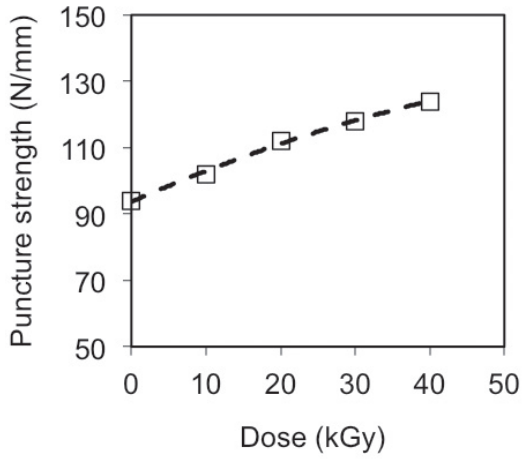

FIG. 16.1. Changes in puncture strength of composite films with absorbed dose [16.8].

No significant changes in PS values were observed after 40% MC addition, which indicated saturation of the strength of the PCL/MC/PCL based films.

The PD values of PCL and MC based films were measured and were found to be 7.84 mm and 4.46 mm, respectively. Figure 16.2 shows the effect of MC content on the PD of PCL based composite films. A monotonous decrease of PD values was observed with an increase of MC percentage in the PCL based films. The incorporation of MC films caused a significant decrease of PD ($p \leq 0.05$). For

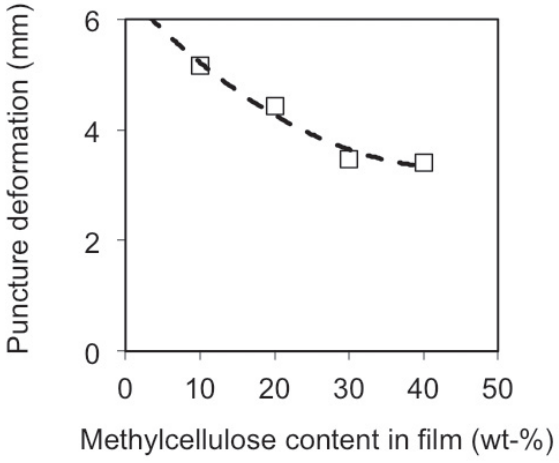

FIG. 16.2. PD of the composite films [16.8].

the addition of 10% MC film in the PCL matrix, the PD value of the composite decreased to 34%. For the 50% MC content composite, it reached 4.23%, which indicated a 59% decrease of PD values compared with PCL films. This is caused by the low PD values of MC films compared with PCL films. It is clear that the MC films had lower PD values than the PCL films did. At a higher content of MC, which acts as a reinforcing material, the film tends to become somewhat more rigid. This is a common observation in conventional composite materials. Here, MC is acting as a reinforcing agent in PCL based composite films, so a higher amount of MC can make the composites stiffer. The decreased PD values may be related to the increased stiffness of the composite films caused by the addition of MC films. The visco-elasticity (*Y*) coefficient values of PCL and MC based films were found to be 19% and 41%, respectively [16.8].

Figure 16.3 shows the effect of MC content on the viscoelasticity coefficient (*Y*) of the PCL based films. A continuous increase of *Y* coefficient values was observed with an increase of MC percentage in the PCL based composite films. For 50% MC content films, the *Y* coefficient value reached 31%, which is 63% higher than PCL films but still lower than MC based films. Since MC films have higher *Y* coefficient values, with increasing MC concentration, the *Y* coefficient values of the films increased. The increase of *Y* coefficient values indicates the flexibile nature of biodegradable films and seemed to increase proportionally with MC content. This is a promising result because the PS of the films was also improved. This is a rare combination in composite films. Generally, with a rise in strength, the flexibility of the composite films decreases [16.8].

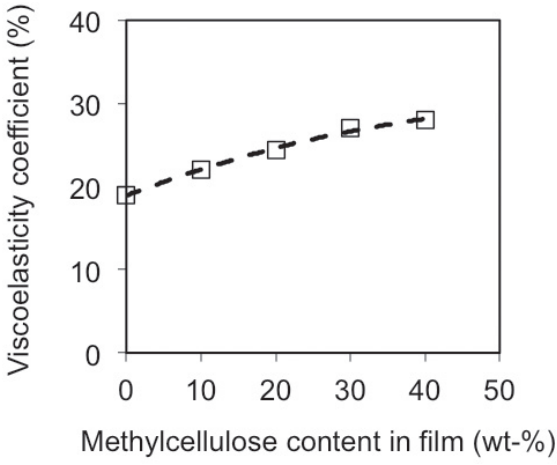

FIG. 16.3. Viscoelasticity coefficient of the composite films [16.8].

16.6.1.2. Water vapour permeability

The water vapour permeability (WVP) of PCL and MC based films was measured. The values of WVP for PCL and MC based films were found to be 1.51 $g \cdot mm \cdot m^{-2} \cdot day^{-1} \cdot kPa^{-1}$ and 6.34 $g \cdot mm \cdot m^{-2} \cdot day^{-1} \cdot kPa^{-1}$, respectively. Figure 16.4 shows the effect of MC content on the WVP of the PCL based biodegradable films.

The WVP values increased continuously with increased MC content in PCL based films. The WVP of 10% MC content films was 1.6 $g \cdot mm \cdot m^{-2} \cdot day^{-1} \cdot kPa^{-1}$ and reached 2.6 $g \cdot mm \cdot m^{-2} \cdot day^{-1} \cdot kPa^{-1}$ for 50% MC composites, which is an 82% increase compared with PCL films. This can be explained by the higher WVP of MC based films. Owing to the large amount of hydrogen bonds, most bio-polymeric films are strongly hydrophilic, i.e. they are poor barriers to water vapour. The presence of MC films in PCL based composites is responsible for slightly higher WVP values compared with MC based films. But the important finding is the drastic decrease in the WVP values of the composite films compared with the MC based films. The 50% MC containing PCL based films gained much higher (144%) barrier properties than MC based films. The fabricated composite films consist of three layers. The upper layer is PCL, which is protective against water vapour penetration, and this caused drastic reductions of WVP. The WVP values indicated that the biodegradable PCL based films are excellent barriers.

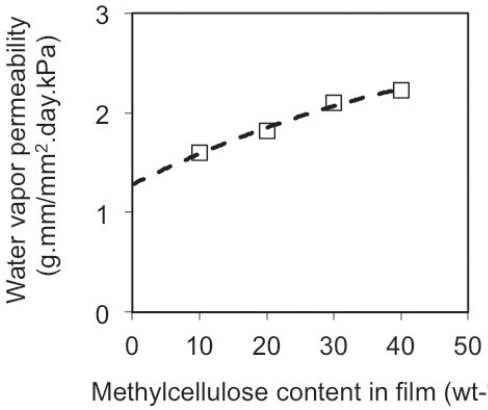

FIG. 16.4. WVP of the composite films as a function of MC content [16.8].

16.6.1.3. Oxygen transmission rate

The oxygen transmission rate (OTR) is defined as the quantity of oxygen gas passing through a unit area of the parallel surface of a film per unit time under a predefined partial pressure of oxygen, temperature and relative humidity. The transfer of oxygen from the environment to food has an important effect on food quality and shelf life. Oxygen causes food deterioration such as lipid and vitamin oxidation, leading to sensory and nutrient changes. OTR is very important since oxygen gas influences the rates of oxidation and respiration in the enclosed food, which may be, for example, fruits and vegetables. Figure 16.5 represents the OTR of PCL, MC based films and composite (50% MC based film content). It is clear that PCL based films displayed a much higher OTR than did the native PCL and MC based films. Generally, synthetic polymers (PCL, polypropylene, PE, etc.) have higher OTR values than bio-polymers (chitosan, MC, whey protein, alginate, etc.). Owing to their large amount of hydrogen bonds, bio-polymer films are hydrophilic, which makes them excellent barriers to non-polar substances, such as oxygen. Biodegradable composite films fabricated using PCL and MC showed very promising results. It is clear that composite film has an even lower OTR than MC based films, which indicates a better interface between MC and PCL. This interface, as well as the use of MC film within the composite, decreases the OTR of composite films compared with PCL or bio-polymeric films (MC based films) when they are used as a reinforcing agent.

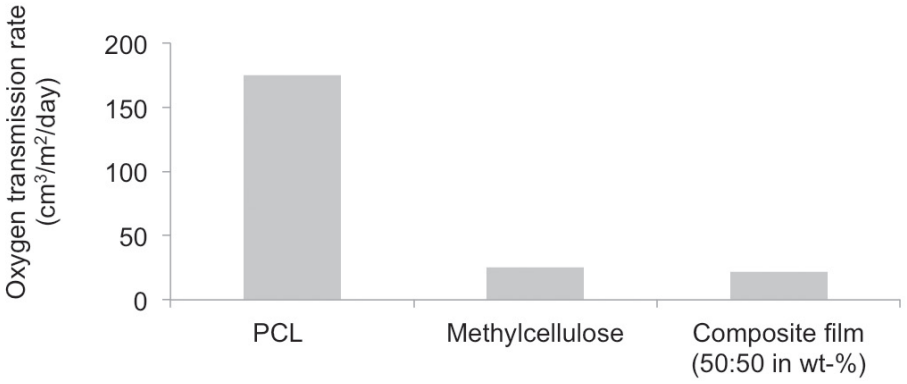

FIG. 16.5. OTR of the constitutive composite films [16.8].

16.6.1.4. Degradation tests of the composite films

Degradation tests performed on the composite films (50% MC content) were carried out in a static water bath at room temperature (25°C) for different time periods. After certain periods of time, samples were taken out from the bath and wiped using tissue paper, and their mechanical properties were then measured. Figure 16.6 shows the loss of PS of the films after degradation in aqueous medium.

It seems that the PS of the films declined continuously with time during aqueous degradation. After two weeks, the PS of the films had decreased to 8%, while after 4 and 6 weeks, the films had lost 11% and 12%, respectively. The reduction of strength occurred because of the presence of MC based films; MC is strongly hydrophilic and rapidly degradable in nature. Water diffused at the cutting edges of the composite samples and the MC films started to swell out very slowly. Hydroxyl (–OH) is one of the important functional groups in MC, and causes the formation of a large amount of hydrogen bonds in the presence of water and induces their swelling. After six weeks of aqueous degradation, the PS of the composite reached 109.4 MPa, which is still higher than the PS of PCL. This is a very good sign that the composites retained a major fraction of their strength after six weeks, which is likely to be due to the use of MC films as they are readily soluble in water. The PD, *Y* coefficient and WVP of the degraded samples were also investigated. After six weeks, the PD values of the composite films reached 5.40 mm, which is 67% higher than the PD of the non-degraded samples.

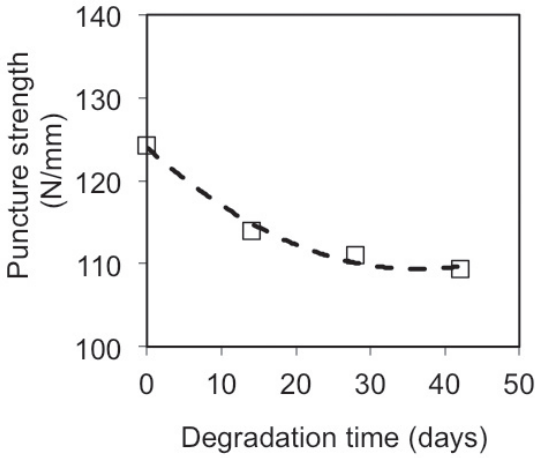

FIG. 16.6. The loss of PS of the composite films after degradation in deionized water at 25°C [16.8].

On the contrary, the *Y* coefficient values were reduced to 17% from 31%. This is caused by the degradation of the MC based films included in the composites. The values of PD and Y coefficient of the degraded composite samples were found to be close to the PCL films. After six weeks of aqueous degradation, the films were shown to lose mass. The results are shown in Fig. 16.7 [16.8]. After 2, 4 and 6 weeks, composite films lost 5.5%, 8.9% and 14.4% of their original mass (i.e. weight), respectively. The WVP values of the degraded samples increased to 26%, which indicates reduced barrier properties compared with non-degraded composite films. The MC based films, which are used as the reinforcing agent, is responsible for the weight loss of the composite samples.

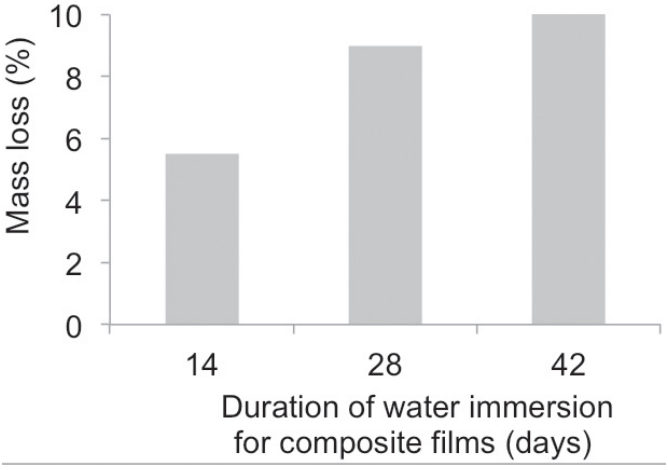

FIG. 16.7. Mass loss of the composite films after degradation in deionized water at 25°C [16.8].

16.6.2. Modification of bio-polymeric films using monomers and gamma radiation

16.6.2.1. Effect of silane monomer on the mechanical properties of chitosan films and PCL based composites

Figure 16.8 represents the effect of gamma radiation on the TS values of chitosan films (without silane) and silane (0.25% w/w) grafted chitosan films (with silane). For chitosan films (control), the TS was found to be 30 MPa. When chitosan films were exposed to gamma radiation, the strength of the films improved significantly up to 5 kGy (33 MPa at 5 kGy) and then decreased (19 MPa at 25 kGy). But all the silane grafted films showed significantly higher TS values than the control sample [16.56].

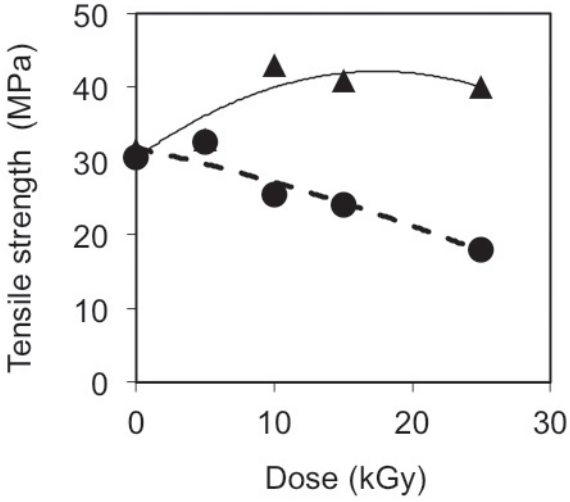

FIG. 16.8. The TS of unmodified chitosan (●) and silane grafted chitosan (▲) films as a function of gamma radiation dose [16.56].

The highest TS value (44 MPa) was observed at 10 kGy. At 25 kGy, the TS of the films reached 41 MPa, which is still significantly higher than the TS of the control sample. Thus, it is clearly observed that the TS of the silane grafted chitosan films was improved significantly by gamma radiation. The silane undergoes a condensation reaction with the naturally occurring hydroxyl group on the chitosan, which improved the TS values. Cross-linking and chain scission occurred when polymers are irradiated using gamma radiation. Thus, with higher radiation dose, there are more possibilities of grafting between silane and chitosan. As a result, the TS values of the silane containing films increased. Higher radiation doses were responsible for the degradation of the films and hence a decrease of the TS values was observed. Figure 16.9 showed the effect of gamma radiation on TM values of chitosan and silane grafted chitosan films. The TM of the chitosan films was found to be 450 MPa [16.56].

The irradiated chitosan films reached 478 MPa at 5 kGy dose and were then found to decline, but silane coupled chitosan films gained significantly higher TM values compared with the control sample. The highest TM values were 590 MPa at 10 kGy for silane grafted chitosan films, which were then found to slightly decrease with further radiation dose. Improvement in the TM values of the silane composite films is due to the increased cross-linking between the hydroxyl group of chitosan and the amino group of silane with the applied radiation dose.

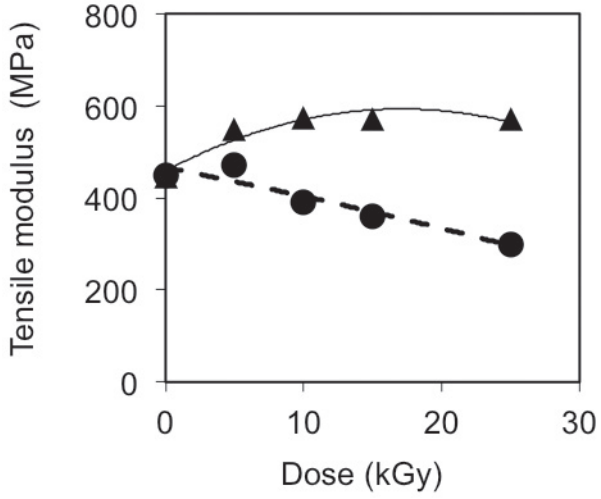

FIG. 16.9. Effect of gamma radiation dose on the TM of unmodified chitosan (●) and silane grafted chitosan (▲) films [16.56].

16.6.2.2. Mechanical properties of the PCL based insoluble composite films

Figure 16.10 shows the effect of silane on PCL based composites. The silane-containing chitosan film reinforced PCL based composites (the silane content is 0.25% w/w, at 10 kGy) was compared with chitosan film reinforced PCL based composites. It was found that the composites that included silane underwent a significantly higher increase in TS values than did the composites that did not include silane. At 20% (w/w) chitosan content, the TS value of the PCL based composite was found to be 18 MPa but a value of 22 MPa was observed for the silane composites. The highest TS values were observed at 20% chitosan content. With the increase of chitosan content, the TS values of the composite films showed significant improvement. Improvement in the TS values of the composite films is due to the higher TS value of chitosan (30 MPa) compared with PCL (12 MPa). Chitosan therefore acts as a reinforcement agent in the composite films. Again, chitosan is strongly hydrophilic and PCL is strongly hydrophobic, which attributes to the poor interfacial adhesion between them. However, when a silane coupling agent was added, the surface of chitosan films were covered by a silane network through oxane bonds with the chitosan surface. This silane bridge improves the adhesion between chitosan and PCL in the silane composite. Thus, silane improves the interfacial adhesion between PCL and chitosan and enhances the strength of films significantly [16.56].

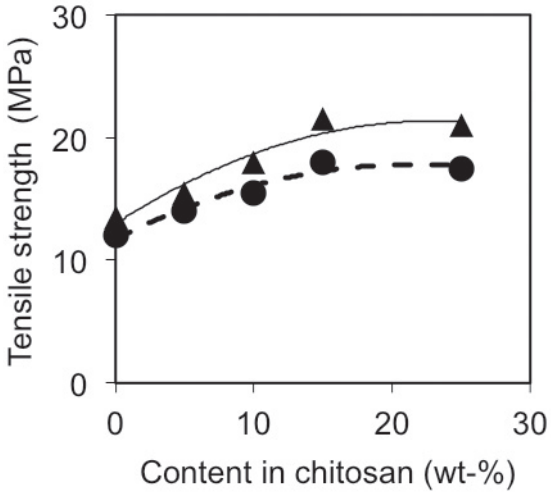

FIG. 16.10. Effect of chitosan content on the TS of two series of PCL based composite materials, one without silane content (●) and the other including silane (▲) modification (0.25 % w/w in aqueous media); both were subject to irradiation at 10 kGy [16.56].

16.6.3. Nano biocomposite films

16.6.3.1. Mechanical and barrier properties of PCL based composite films reinforced with CNTs and the effects of gamma radiation

(a) The effect of CNT on the mechanical properties of PCL based biodegradable films

CNTs were mixed by blending with melted PCL and films were then formed by compression moulding. The TS of PCL was found to be 16 MPa. The addition of a minute amount of CNT significantly ($p \leq 0.05$) improved the TS values of PCL films. Figure 16.11 shows the effect of the addition of CNT on the TS of PCL films. With 0.05%, 0.1%, 0.2% and 0.5% (by wt) incorporation of CNT, the TS values reached 20 MPa, 29 MPa, 37 MPa and 41 MPa, respectively. A mere 0.2% wt addition of CNT caused a 131% improvement in the TS of PCL films. The drastic improvement of strength of PCL occurred owing to the addition of CNT, which has a very high strength (1−2 GPa). The reinforcing effect of CNTs was due to the strong interfacial interaction between the polymer matrix and the CNTs.

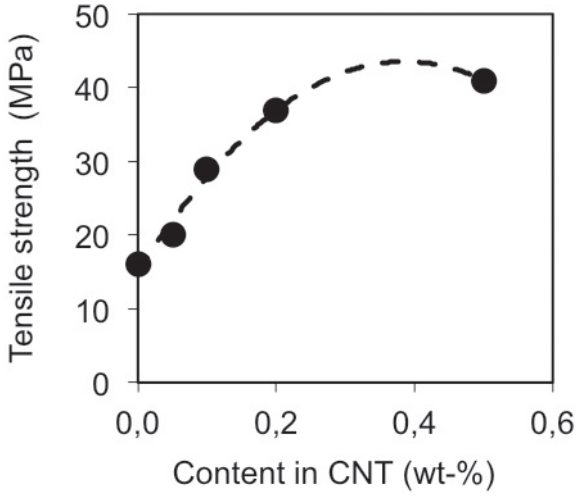

FIG. 16.11. TS of the composite films [16.57].

Similarly, the TM of PCL films was also improved by the incorporation of CNT. Figure 16.12 shows the effect of CNT content on the TM values of PCL films. The TM of PCL film was found to be 156 MPa. The incorporation of CNT into PCL films caused a significant ($p \leq 0.05$) enhancement of the modulus. At 0.05%, 0.1%, 0.2% and 0.5% (by weight) CNT content PCL films, the TM values were found to be 173 MPa, 181 MPa, 193 MPa and 206 MPa, respectively. Thus, by incorporating only 0.2% CNT, the PCL films underwent a 24.71% increase of TM values. The increased TM values of the CNT reinforced PCL films may be attributed to the increased stiffness of the films caused by the addition of CNT. Moreover, the increased TM values indicated a better dispersion of the CNTs in PCL matrix. The 'elongation at break' (Eb) of PCL was found to be 555%. With the incorporation of CNT, the Eb values of PCL films were also significantly enhanced ($p \leq 0.05$). Figure 16.13 illustrates the effect of CNT on the Eb (%) values of PCL films. With 0.05%, 0.1%, 0.2% and 0.5% (by weight) incorporation of CNT, the Eb values reached 760%, 910%, 1047% and 1215%, respectively. This investigation clearly reveals that CNTs caused a significant increase in the mechanical properties of PCL films. This is a rare combination in that all of the tensile properties (TS, TM and Eb) of the PCL films significantly improved with the addition of CNT. During the melt blending process, the CNTs were dispersed homogeneously within the matrix PCL and, as a result, strong interfacial interaction ocurred between CNTs and PCL and improved the mechanical properties of the film [16.57].

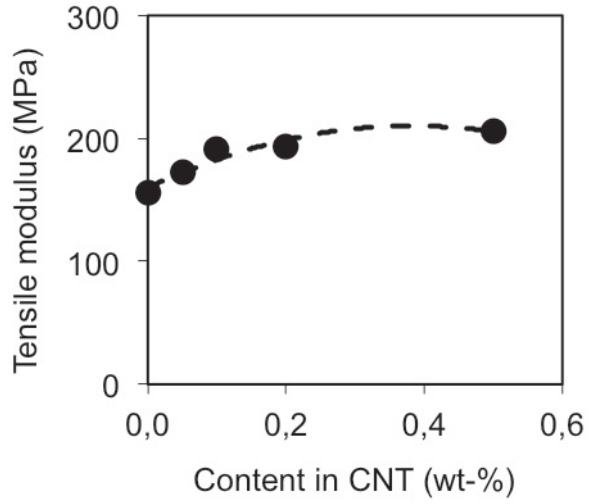

FIG. 16.12. Tensile modulus of the composite films [16.57].

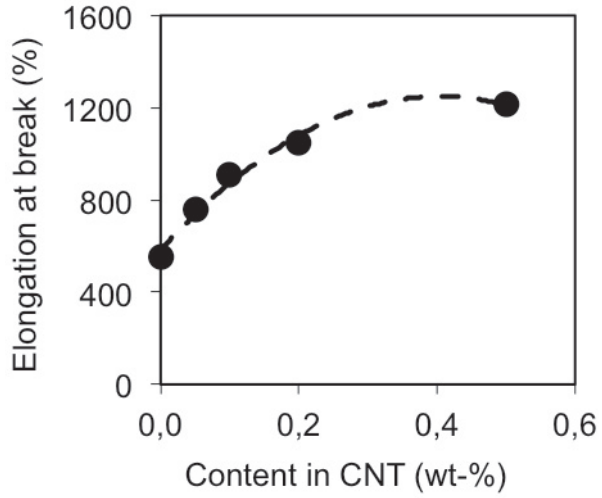

FIG. 16.13. Eb (%) of the composite films [16.57].

(b) Water vapour permeability (WVP)

The WVP of PCL films and CNT reinforced PCL based composites were measured. The WVP for PCL films was 1.51 g·mm·m^2·day^{-1}·kPa^{-1}. Figure 16.14 shows the effect of CNT content on the WVP of the PCL based composites.

The values of WVP decreased continuously with the increase of CNT in PCL based films. The WVP values of 0.05%, 0.1%, 0.2% and 0.5% (by wt) CNT reinforced PCL films were 1.40, 1.22, 1.08 and 0.92 $g \cdot mm \cdot m^{-2} \cdot day^{-1} \cdot kPa^{-1}$, respectively (Fig. 16.14). With a 0.2% CNT addition to PCL films, the WVP decreased to 39%, which indicates improved barrier properties. The presence of nanotubes in CNT is thought to increase the tortuosity in PCL based composite films leading to slower diffusion processes and hence to a lower permeability [16.57]. The barrier properties are enhanced if the filler is less permeable and has a good dispersion into the matrix. In the present study, the interactions of CNT with PCL may have enhanced the water vapour barrier. This can also be explained by the strong hydrophobic character of CNTs. Owing to the higher amount of hydrogen bonds, most of the biodegradable polymeric films are hydrophilic, and this is why they are poor barriers to water vapour. The presence of CNTs in PCL based composites is responsible for lower WVP values compared to control PCL films. The WVP values of the composites indicated that they form excellent barriers to water vapour.

(c) OTR of PCL and composites

The OTR of PCL and CNT reinforced composite films was measured. Figure 16.15 shows the OTR of PCL, and CNT incorporated PCL films. Composite films containing CNTs showed much lower OTR values than PCL films. The OTR value of PCL film was found to be 175 $cm^3 \cdot m^{-2} \cdot day^{-1}$.

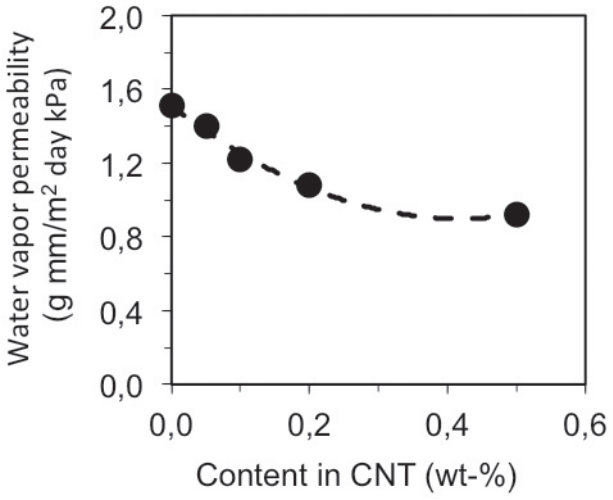

FIG. 16.14. Effect of CNT on WVP of PCL [16.57].

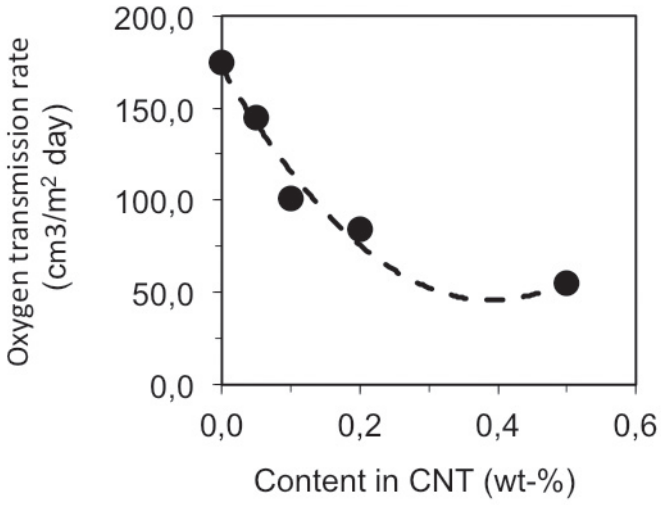

FIG. 16.15. Effect of CNT on OTR of PCL [16.57].

Incorporation of 0.05%, 0.1%, 0.2% and 0.5% (by wt) CNTs in PCL films decreased OTR values to 145%, 101%, 84% and 55 $cm^3 \cdot m^{-2} \cdot day^{-1}$, respectively. Therefore, 0.2% CNT reinforced PCL based composites showed a 68% reduction in OTR. OTR is explained in Section 16.6.1.3. The addition of CNT to PCL created a barrier to non-polar substances, such as oxygen, and as a result, the OTR values decreased [16.57].

(d) Effect of CNT on carbon dioxide transmission rate (CO^2TR)

The carbon dioxide transmission rate (CO_2TR) value of PCL film was 1170 $cm^3 \cdot m^{-2} \cdot day^{-1}$. The composite films containing 0.1%, 0.2% and 0.5% CNTs showed 1430 $cm^3 \cdot m^{-2} \cdot day^{-1}$, 2300 $cm^3 \cdot m^{-2} \cdot day^{-1}$ and 2734 $cm^3 \cdot m^{-2} \cdot day^{-1}$. Figure 16.16 shows the CO_2TR of PCL and CNT reinforced composite films. It is clear that CNT containing composite films showed higher CO_2TR values than did the PCL films. The addition of only 0.2% CNT to PCL caused a 49% increase in CO_2TR values. It is to be noted here that modified atmosphere packaging has gained considerable popularity over the last decades as a modern non-thermal method of food preservation. The proper combination of gases (carbon dioxide, nitrogen and oxygen) in the headspace of food packs results in suppression of the microbial flora of perishable foods developed under aerobic conditions and with retention of their sensorial attributes. Therefore, CO_2TR is as important as OTR. The CO_2TR of bio-polymers is low because of its strong hydrophilic nature, but the CO_2TR of synthetic polymers is very high. The CO_2TR of high density

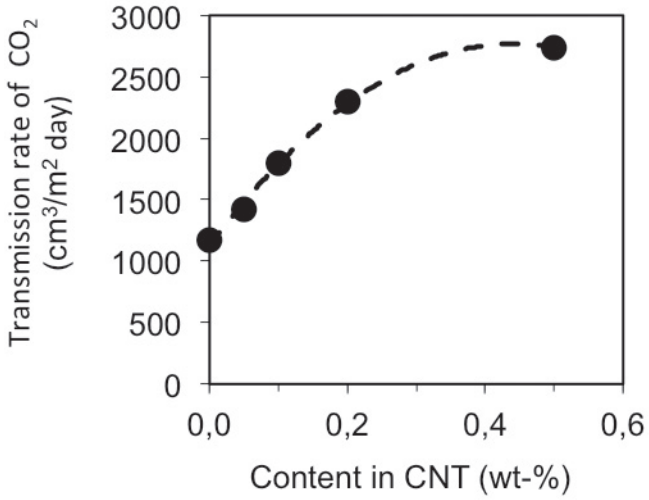

FIG. 16.16. Effect of CNT on CO_2TR of PCL [16.57].

PE is 17 470 $cm^3 \cdot m^{-2} \cdot day^{-1}$. This is because synthetic polymers are strongly hydrophobic and are therefore less of a barrier to non-polar gases such as carbon dioxide. When CNT was added to PCL, the CO_2TR was improved because the composite was more hydrophobic in nature and thus the CO_2TR was enhanced [16.57].

(e) Effect of gamma radiation on PCL and composite films

The PCL films and CNT (0.2%) reinforced PCL based composites were exposed to gamma radiation at 2–25 kGy. The TS, TM and Eb of PCL and composite films were measured. The results are presented in Figs 16.17–16.19. It was found that gamma radiation had a significant influence on the strength of PCL and composites (Fig. 16.17). The TS of PCL film was found to be 16 MPa but 10 kGy irradiated films reached 28 MPa, which is 75% higher than the control sample. After the 10 kGy dose, the TS values decreased and reached 22 MPa at 25 kGy dose, which is still higher than the control sample. The TS of composite (0.2% CNT reinforced) film was 37 MPa but the strength of the films improved significantly (41 MPa) after irradiation at 15 kGy. The TS value of the irradiated film improved to 11% which is much less than that PCL films (75%). Similarly, the TM values of PCL films improved significantly due to exposure of irradiation. The results are depicted in Fig. 16.18. The highest TM value was observed at 10 kGy. The TM values of composites improved up to a 15 kGy dose, then slightly decreased and reached 270 MPa at 25 kGy. The irradiated PCL films gained 76%

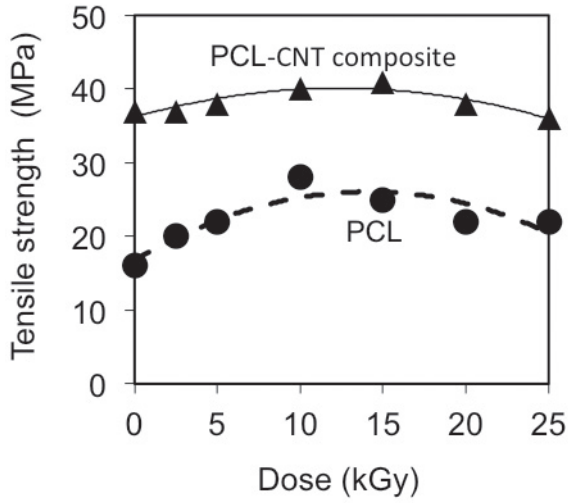

FIG. 16.17. Effect of gamma radiation on TS of PCL and composites [16.57].

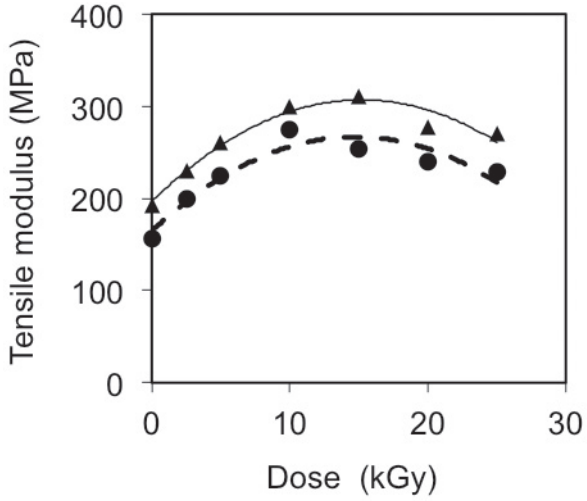

FIG. 16.18. Effect of gamma radiation on TM of PCL (▲) and composites (●) [16.57].

higher TM values at 10 kGy than did the control PCL films. On the other hand, composites gained 61% higher TM values at 15 kGy dose than their counterpart control composite. An unexpected result was observed for Eb (%) values. With the rise of TS and TM values, the Eb values of the PCL films and composites also increased with the increase in radiation dose. The effect of gamma radiation

on Eb values of PCL and composites are presented in Fig. 16.19. Both PCL and composites achieved higher Eb values than their control counterpart samples. The maximum Eb values were obtained at 15 kGy dose for PCL and composites [16.57].

From this investigation, it is clear that gamma radiation has a strong role in the improvement of the mechanical properties of PCL films. The CNT reinforced composites showed a positive trend of enhancement of mechanical properties but the intensity is much lower than that of PCL. The nanotubes from CNT may hinder the cross-linking of PCL and thus reduce the strong influence of irradiation for CNT reinforced composites. It is reported that when polymeric materials are subjected to gamma radiation, radicals are produced on the main chain by hydrogen and hydroxyl abstraction. Gamma radiation also breaks some carbon–carbon bonds and produces radicals. Chain scission may also take place to form other radicals.

Gamma radiation produces various types of reactive species in polymers during irradiation treatment. Peroxides are produced when polymers are irradiated in the presence of oxygen. In this investigation, irradiation was carried out in presence of oxygen. Therefore, the peroxides produced may react with PCL and could produce PCL diperoxides and PCL hydroperoxides by a radical chain reaction process. The reaction occurs in three steps: activation, propagation and termination. It is also reported that the effect of gamma radiation on polymers (such as PCL) produces ionization and excitation, and as a result some free radicals are produced. The polymers may undergo cleavage or scission

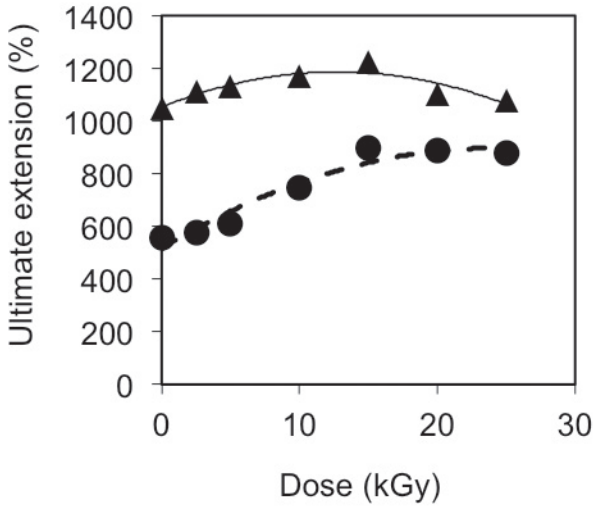

FIG. 16.19. Effect of gamma radiation on Eb of PCL (▲) and composites (●) [16.57].

(i.e. the polymer molecules may be broken into smaller fragments). Subsequent rupture of chemical bonds yields fragments of the large polymer molecules. The free radicals thus produced may react to change the structure of the polymer and also the physical properties of the materials. Cross-linking may also occur (i.e. the molecules may be linked together into large molecules) [16.57].

Gamma irradiation also affects the polymeric structure and can produce active sites. Gamma irradiation of PCL may result in cross-linking which produces higher mechanical properties up to a certain dose. Active sites inside the polymer might be also produced by the application of gamma radiation. However, at higher doses of gamma radiation, chain scission may dominate over cross-linking reactions, resulting in a decrease of mechanical properties after a certain dose. The barrier properties of non-irradiated and irradiated (10 kGy) PCL and composites (0.2% CNT reinforced) were also measured. The WVP of PCL film was found to be 1.51 $g \cdot mm \cdot m^{-2} \cdot d^{-1} \cdot kPa^{-1}$, but the WVP of irradiated PCL decreased to 1.32 $g \cdot mm \cdot m^{-2} \cdot day^{-1} \cdot kPa^{-1}$, which is 13% less than that of control PCL film. Similarly, the WVP of 0.2% CNT reinforced PCL based composites showed 9% lower values following irradiation at 10 kGy. The values of WVP for unirradiated and irradiated composites were 1.08 and 0.98 $g \cdot mm \cdot m^{-2} \cdot d^{-1} \cdot kPa^{-1}$. So, gamma radiation improved the water vapour barrier properties by reducing the WVP values. It is expected that during irradiation of PCL and composites, cross-linking of PCL molecules can happen and thus improve the water vapour barriers. It is reported that active sites inside the polymeric matrix might be produced by the application of gamma radiation and, as a result, more cross-linked structures may form and thus improve the mechanical and barrier properties [16.57]. A dramatic result was observed for OTR. The OTR of the irradiated (10 kGy) PCL increased to 224 $cm^3 \cdot m^{-2} \cdot day^{-1}$ from 175 $cm^{-3} \cdot m^{-2} \cdot day$. On the other hand, the OTR of the irradiated (10 kGy) PCL based composite (0.2% CNT) increased to 152 $cm^3 \cdot m^{-2} \cdot day^{-1}$ from 136 $cm^3 \cdot m^{-2} \cdot day^{-1}$. Similarly, the CO_2TR of irradiated PCL and composites were also improved. The CO_2TR of the irradiated PCL (10 kGy) increased to 1440 $cm^3 \cdot m^{-2} \cdot day^{-1}$ from 1170 $cm^3 \cdot m^{-2} \cdot day^{-1}$, and the CO_2TR of the irradiated (10 kGy) composite increased to 1830 $cm^3 \cdot m^{-2} \cdot day^{-1}$ from 1710 $cm^3 \cdot m^{-2} \cdot day^{-1}$. PCL is partly crystalline, and during irradiation treatment structural changes may occur within it. Both oxygen and carbon dioxide are non-polar in nature but PCL is polar. Active sites can form in PCL during gamma radiation and chain scission may also occur. As a result, crystallinity can decrease and the amorphous nature of PCL may improve [16.57], which may help the passage of more oxygen and carbon dioxide.

Mechanical and barrier properties of modified methylcellulose (MC) films containing cellulose nanocrystals (CNC). A preliminary study showed that the utilization of 0.1% trimethylolpropane trimethacrylate (TMPTMA) (as a monomer that function as a cross-linking agent) in methylcellulose (MC)

based films and the application of an irradiation dose of 5 kGy were effective for producing films with the highest TS and TM. Thus, cellulose nanocrystals (CNC) at different concentrations (0%, 0.025%, 0.25% and 1.0%, w/w in aqueous solution) were incorporated into MC based films containing 0.1% TMPTMA. The impacts on mechanical and barrier properties on the films were evaluated. The effect of the irradiation dose (0.1 kGy, 0.5 kGy, 1.0 kGy, 5.0 kGy and 10 kGy) on MC based films was also considered since radiation is required for the initiation of the polymerization reaction between TMPTMA and MC.

(a) The impact of CNC incorporation on TS and TM of MC based films

The impact of CNC at different irradiation doses on the TS of MC based films is presented in Fig. 16.20.

It can be observed that without CNC (0%, w/w), increasing irradiation doses from 0.1 to 5 kGy caused an increase in the TS of the MC based films from 37.9 MPa (at 0.1 kGy) to the maximum value of 48.2 MPa (at 5 kGy). There was a slight decrease in the TS (46.2 MPa) of MC based films when applying an irradiation of 10 kGy, which could be due to the degradation and or deformation of the bio-polymer caused by the high dose treatment. In fact, Shahabi-Ghahfarrokhi et al. [16.58] also observed that irradiation at a high dose of 9 kGy could destroy

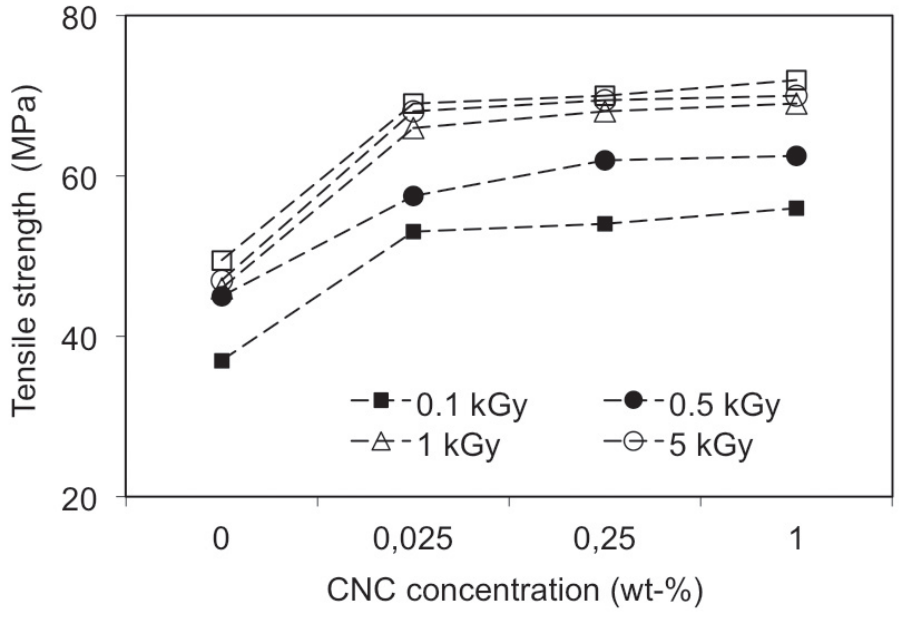

FIG. 16.20. Impact of incorporation of CNCs on TS of the MC based films [16.2].

the crystalline structure of kefiran bio-polymer and produce a mixture of oligo-, di- and monosaccharides. It is known that the decrease in the crystallinity of the polymer leads to a decrease in the TS of the film [16.59].

It is of interest to see that increasing CNC concentration in MC based films caused an increase in the TS of the films. For example, at a low irradiation dose of 0.1 kGy, the addition of 0.025% CNC caused a significant increase ($p \leq 0.05$) in the TS of the films, from 37.9 MPa (without CNC) to 52.45 MPa, which is equal to an increase of 38.4% in the TS. The incorporation of 0.25% CNC into MC based films only caused a slight increase in the TS value (55.3 MPa) as compared with that of 0.025% CNC. A further increase of CNC at 1.0% did not cause a significant increase ($p > 0.05$) in TS compared with that caused by 0.25% CNC. The reason for this may be the aggregation of CNC particles after a certain concentration is reached, which results in a lack of further improvement of the TS value [16.60].

Similar patterns of TS were observed at higher irradiation doses of 0.5 kGy, 1.0 kGy, 5.0 kGy and 10.0 kGy. There was a significant increase in the TS of the films when 0.025% CNC was incorporated, and the TS further increased slightly at 0.25% CNC and finally reached a plateau thereafter (Fig. 16.20). It can be observed that there were no significant differences among the TS values of the films irradiated at 1.0 kGy, 5.0 kGy and 10.0 kGy when CNC was incorporated into MC based films at concentrations of 0.25% or 1%. Thus, incorporation of 0.25% CNC and irradiation at 1 kGy can be considered suitable conditions to produce film with a high TS (69 MPa). Under this condition, the TS value was increased by 81% compared with that of MC based film without CNC that was irradiated at 0.1 kGy. CNC has an important role as a reinforcing agent, which has been demonstrated by several studies. For example, Dhar et al. [16.61] incorporated 1% CNC with different polymorphs (CNC I, CNC II and CNC: 1 → 2) into PLA films and found that CNC I, CNC II and CNC: 1 → 2 could improve the TS of the films by 34%, 72% and 74%, respectively, compared with PLA film alone. Khan et al. [16.60] also observed that the incorporation of CNC into chitosan improved the TS of the films. The authors found that incorporation of 1%, 3%, 5% and 10% CNC into chitosan film improved the TS of the films by 8.8%, 16.5%, 25.3% and 24%, respectively, compared with the control.

In the case of TM (Young modulus), a similar pattern to TS was obtained. Without CNC incorporation in MC based films, increasing the irradiation dose from 0.1 kGy to 5 kGy caused an increase in TM from 1446 MPa to 1791 MPa. A further increase in the irradiation dose to 10 kGy caused a decrease in the TM of the films. As mentioned above, the decrease in the TM of the MC based film (1522 MPa) at 10 kGy could be due to the degradation or deformation of the bio-polymer caused by the high dose of radiation [16.58].

Similar to TS, increase the concentration of CNC in MC based films caused an increase in the TM of the film. However, irrespective of irradiation doses, there was no significant difference ($p > 0.05$) in TM values between 0.25% and 1.0% CNC added to the MC based films. Similar to the values found for TS above, the incorporation of 0.25% CNC into MC based film is a suitable concentration. With 0.25% CNC added, the TM values of films irradiated at 0.1 kGy, 0.5 kGy, 1.0 kGy, 5.0 kGy and 10 kGy were 1978 MPa, 2071 MPa, 2149 MPa, 2202 MPa and 2132 MPa. The increase in TM values was also observed in the study of Khan et al. in which CNC was incorporated into chitosan film [16.60]. Thus, the results confirm that the incorporation of CNC could improve the mechanical properties of the MC based films.

(b) Impact of CNC incorporation on Eb of MC based films

Profiles of Eb of the MC based films at different CNC concentrations are presented in Fig. 16.21. Without incorporated CNC, the Eb value was increased from 14.4%, when MC based films were irradiated at 0.1 kGy, to 24.7%, when irradiated at 5 kGy; however, at 10 kGy, the Eb value was reduced to 18%. This fact is similar to the observations made of the TS and TM of the film which

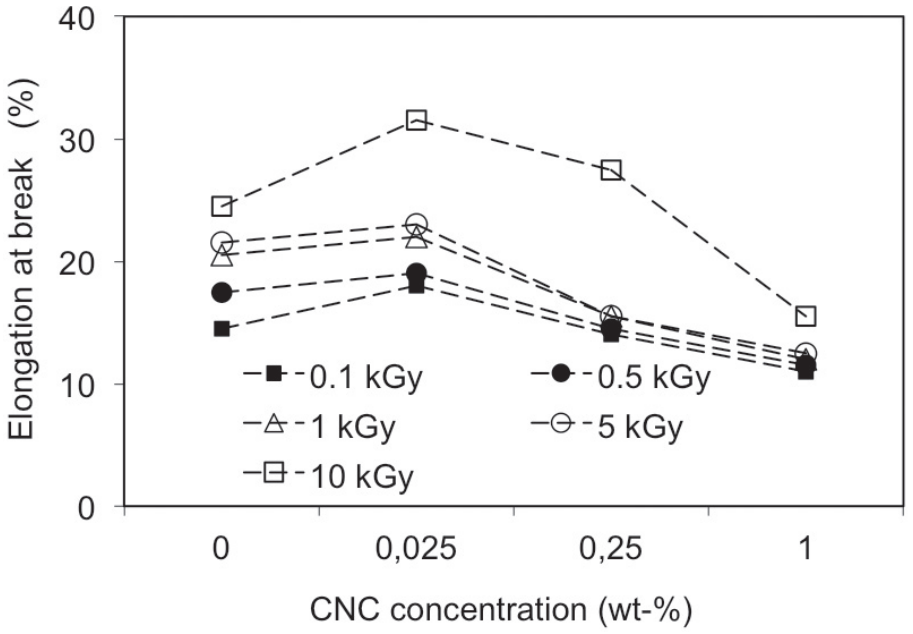

FIG. 16.21. Impact of incorporation of CNC on elongation at break of the MC based films [16.2].

might be related to degradation and/or deformation of the bio-polymer at high irradiation dose.

Higher Eb values were obtained when 0.025% CNC was incorporated into the MC based films and irradiated at all doses, except at 5 kGy there was a decrease in the Eb value compared with that of the film without CNC; however, the difference was not significant (Fig. 16.21). It is of interest to find that the highest Eb value (32%) was obtained in MC based film containing 0.025% CNC and irradiated at 0.5 kGy. This means that at low concentrations of CNC and under low dose irradiation, a better network might be created among the CNC, methylcellulose and cross-linking agent (TMPTMA) which would help to improve the elongation properties of the film.

However, it can be observed that increasing CNC concentration to 0.25% and 1.0% in the MC based films caused a significant decrease in Eb values, irrespective of irradiation dose (Fig. 16.21). The possible reason could be that at high concentrations of CNC, the films become more brittle and stiff, reducing their elasticity. Or there may be a strong intermolecular force between CNC and methylcellulose which prevents the motion of the polymer [16.62]. Future study may need to evaluate the impact of concentration of plasticizers (glycerol or polyols) required to improve the Eb of the films containing 0.25% CNC concentration since at this concentration, films have good properties in TS and TM, as presented above.

(c) Impact of CNC incorporation on WVP of MC based films

The impact of CNC at different irradiation doses on the WVP of MC based films is presented in Fig. 16.22. Without CNC incorporation, the WVP of the MC based films was from 5.3 to 5.9 $g \cdot mm \cdot m^{-2} \cdot d^{-1} \cdot kPa^{-1}$. Incorporation of 0.025% CNC into the film caused an increase in the WVP of the films that were irradiated at 1 kGy, 5 kGy and 10 kGy; however, in cases of irradiation at low doses (0.1 kGy and 0.5 kGy), there were no significant changes in the WVP of the films (Fig. 16.22). The exact reason for this is not known. It is possible that at high irradiation doses, the structure of the bio-polymer might be changed (decreasing the level of crystallity) and with CNC added at a low concentration (0.025%), it was not able to improve the barrier properties of the films.

However, it is of interest to observe that, irrespective of irradiation dose, increasing the CNC concentration in the MC based films improves the barrier properties of the films (lower WVP values compared with CNC at 0.025%) (Fig. 16.22). The lowest WVP values were obtained with MC based films containing 1% CNC and irradiated at 0.5 kGy. The results confirm that CNC functioned as a reinforcing agent to improve the prevention of the diffusion of water through vapour. The results are also in accordance with other studies that

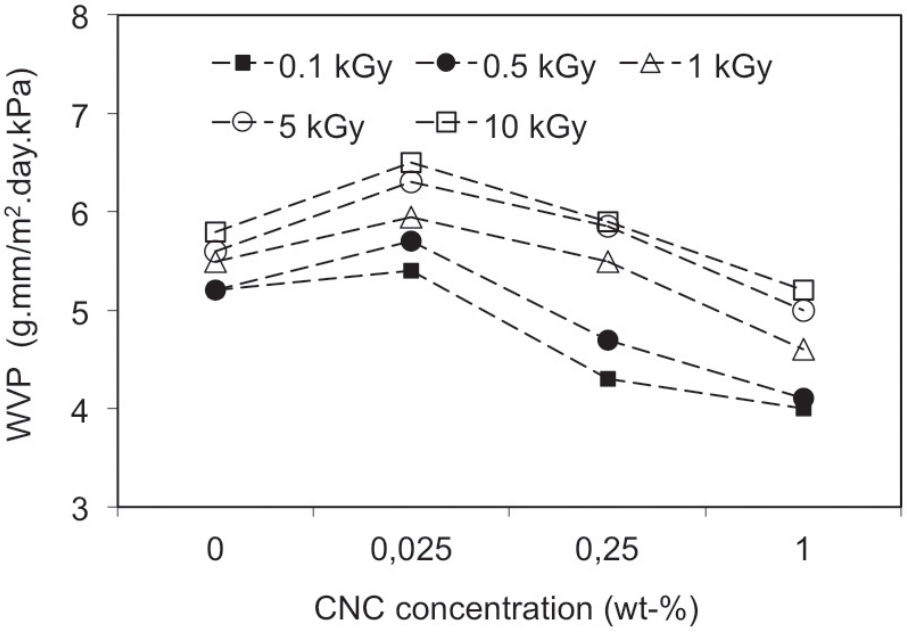

FIG. 16.22. Impact of incorporation of CNC on WVP of the MC based films [16.2].

demonstrated that the incorporation of CNC could improve the barrier properties of bio-polymeric films [16.60–16.62].

16.7. APPLICATION OF COMBINED TREATMENT OF IRRADIATION AND ANTIMICROBIAL COATINGS FOR REDUCTION OF FOOD PATHOGENS IN BROCCOLI FLORETS

The effect of combined treatment of antimicrobial coatings and irradiation on the sensitivity of *Listeria monocytogenes* has been studied [16.63]. D_{10} values for *L. monocytogenes* in control samples and in samples coated with film without antimicrobial agents (FWA) were 0.40 kGy and 0.42 kGy, respectively (Table 16.3). The coating of broccoli florets with organic acids plus lactic acid bacteria (LAB) metabolites (A-LAB), organic acids and citrus extract (A-C), organic acids, citrus extract and spice mixture (A-C-S), and organic acids and rosemary extract (A-R) caused a decrease in the D_{10} values of *L. monocytogenes* (Table 16.3). The lower D_{10} values indicate the higher sensitivity of *L. monocytogenes* to irradiation treatment (or increasing radiosensitivity). The relative sensitivities (D_{10} value of control/D_{10} value of treatment) of 1.36, 1.31,

1.45 and 1.34 were obtained for the antimicrobial coatings containing A-LAB, A-C, A-C-S and A-R formulations. The results demonstrated that antimicrobial coatings can be used to improve antibacterial effect against *L. monocytogenes*.

TABLE 16.3. D_{10} VALUES FOR SELECTED FOODBORNE PATHOGENS ON BROCCOLI FLORETS COATED WITH VARIOUS ANTIMICROBIAL FORMULATIONS [16.63]

	D_{10} (kGy)					
Bacteria	Control	FWA	A-LAB	A-C	A-C-S	A-R
L. monocytogenes	0.40 ± 0.05	0.42 ± 0.03	0.29 ± 0.09	0.30 ± 0.03	0.27 ± 0.10	0.30 ± 0.06
E.coli	0.38 ± 0.06	0.34 ± 0.11	0.20 ± 0.04	0.16 ± 0.10	0.24 ± 0.03	0.23 ± 0.10
S. Typhimurium	0.50 ± 0.10	0.60 ± 0.01	0.21 ± 0.12	0.29 ± 0.01	0.28 ± 0.07	0.25 ± 0.03

Note: Values are means ± standard deviations.

D_{10} values of 0.38 kGy and 0.34 kGy were observed for *Escherichia coli* in control samples and for samples coated with FWA, respectively (Table 16.3). All the bioactive coatings caused either a decrease in the D_{10} value of *E. coli* to irradiation treatment or an increase in the radiosensitivity of *E. coli*. The D_{10} values of *E. coli* in the samples coated with A-C-S, A-R, A-LAB and A-C corresponded to the increase in sensitivity of *E. coli* to irradiation by 1.60, 1.64, 1.95 and 2.39 times compared with the control without antimicrobial coating. It is of interest to observe that coating of the broccoli sample with a mixture of organic acid and citrus extract (A-C) was the most effective way to reduce the growth of *E. coli*. It was also found that *E. coli* was more sensitive than *L. monocytogenes* towards combined irradiation and antimicrobial coatings.

D_{10} values were observed for *Salmonella* Typhimurium and are shown in Table 16.3. It is not known why the coating of broccoli samples with FWA caused an increase in the D_{10} value of *S.* Typhimurium (or a decrease in the sensitivity of *S.* Typhimurium to irradiation treatment). It is possible that coating components might protect *S.* Typhimurium during γ irradiation treatment. D_{10} values of *S.* Typhimurium corresponded to the increase in sensitivity of *S.* Typhimurium to irradiation by 1.73, 1.77, 1.96 and 2.40 times. The antimicrobial coating

containing A-LAB was the most efficient formulation for eliminating *S.* Typhimurium from broccoli florets.

16.8. ADDITIONAL COMMENTS

Bio-polymeric (chitosan, methylcellulose and alginate) films were prepared by solution casting and their mechanical and barrier properties were evaluated. The TS and TM of the bio-polymeric films are higher than the corresponding values for synthetic non-biodegradable polymeric films. On the other hand, the Eb of synthetic polymers is higher than that of bio-polymeric films. All of the bio-polymers are strongly hydrophilic in nature, so the WVP of the bio-polymers is higher. But the OTR of the bio-polymeric films is very promising as it was much lower than that of synthetic polymers.

When irradiated at low gamma absorbed doses, bio-polymers become cross-linked and their mechanical properties improve slightly. But at higher doses, bio-polymeric films lose their strength. At a 5 kGy dose, the TS of chitosan films improved to about 10% but at 25 kGy, the TS values were reduced significantly (Fig. 16.8). At a low dose, chitosan molecules could cross-link and thus improve the TS of the films but at a higher dose, chitosan molecules are broken down and the films therefore showed lower strength. All of the irradiated bio-polymeric films (up to 25 kGy) had better barrier properties than the unirradiated ones. Vinyl monomers were grafted with these bio-polymers using gamma radiation. A significant increase in the mechanical properties was observed after grafting. Simultaneously, the barrier properties were also developed. The study on radio-sensitization demonstrated that there were different levels of radiosensitization of bacteria depending on the bioactive coating that was applied to the broccoli florets. The A-C coating was the most effective for increasing the radiosensitivity of *E. coli*, whereas the A-LAB coating was the most effective for increasing the radiosensitivity of *S.* Typhimurium. All coatings (A-LAB, A-C, A-C-S and A-R) had similar radio-sensitizing effects ($p \leq 0.05$) on *L. monocytogenes*. These results suggest that the use of bioactive MC based coatings containing A-LAB and A-C mixtures could be a useful technology for controlling the level of microbes on broccoli before γ irradiation because these coating significantly radiosensitize various bacteria. These formulations could be applied to other vegetables in combination with γ irradiation and offer a promising and feasible industrial technology for eliminating foodborne pathogens.

16.9. FUTURE TRENDS IN BIOACTIVE COATINGS AND FILMS FOR FOOD PACKAGING

Biodegradable packaging based on bio-polymers represent a new generation of materials emerging on the packaging market with an expanding range of potential applications. This type of packaging is environmentally friendly and its use is predicted to increase. Synthetic polymer based products are starting to be replaced by bio-polymer based materials. However, bio-based packaging materials have some drawbacks, such as lower mechanical strength and lower water resistance than their petroleum based non-degradable polymer counterparts. As a result, bio-polymer based packaging has not been widely used in the food packaging industry. Many on-going studies are currently investigating means of improving the mechanical strength and water resistance of the bio-polymer materials by using various physicochemical treatments such as radiation grafting, cross-linking and thermal or UV-curing.

Bio-nanocomposites have a high potential, but currently are not widely produced and are too expensive to be used in many applications. In spite of improvements in the mechanical and water barrier properties of several natural bio-polymers through nanotechnology, these improvements are not sufficient to compete with and replace petroleum based plastics. In particular, the water resistance of bio-nanocomposites is too poor to utilize them as packaging materials, especially in wet environmental conditions. Therefore, the most important factors for the development of new packaging materials using natural bio-polymer based nanocomposites include the development of the optimum formulation for the individual polymer and processing method to obtain the desired properties to meet a wide range of applications as well as achieving a cost reduction of the bio-nanocomposites.

In nano-active packaging, a much lower amount of material would be required to exert a specific effect which is particularly useful when dealing with expensive bioactive agents. A timely and targeted release may improve the effectiveness of micronutrients, broaden the application range of food ingredients and ensure optimal dosage, thereby improving the cost effectiveness of the product. Bio-polymers need to be modified to make them suitable as matrix polymers for nanofibers and crystals. The optimum formulation for each polymer must be developed through a combination of ingredients such as polymers, nanofibers, plasticizers, compatibilizers or coupling agents. Blends of more than two natural bio-polymers or of one natural bio-polymer with another synthetic biodegradable polymer such as PLA or PCL can also provide a good opportunity for improving the properties of the bio-nanocomposite materials. For reducing the processing cost of bio-nanocomposites, a melt intercalation method using extrusion or injection moulding is inevitable. It is essential to minimize

the thermal degradation of the main polymer matrix during processing. It also appears necessary to develop a thermally stable plasticizer or compatibilizer that could improve the elongation properties of the films. Natural polymer based nanocomposites can increase the barrier properties of packaging materials with antimicrobial activity. They could also be used for active food packaging with bio-functional properties and to address environmental concerns. However, they are at an early stage of development and further research is needed.

The focus of packaging in the past has been on the appearance, the level of physical protection of the product conferred and the size and integrity of the package. A greater emphasis on the safety features associated with the addition of antimicrobial agents may be the next area for development in packaging technology. Many of the antimicrobial compounds that have been studied are not permitted for food application, as they need to migrate to the food to be effective. Technical challenges exist in incorporating appropriate antimicrobial agents into packaging systems. The choice of an antimicrobial compound may be limited by not only its compatibility with the type of packaging material used, but also to the heat liability of the component during extrusion. Current trends suggest that packaging will generally incorporate antimicrobial agents, and sealing systems will continue to improve. Researchers have primarily focused their interest on developing new approaches and on testing new methods with model systems, but not quite as much on applications in real food products. Antimicrobial packaging technology must focus on the technical feasibility, consumer acceptance and food safety aspects of antimicrobial agents, in addition to their chemical, microbiological and physiological effects.

Edible coatings are promising systems for the future improvement of food quality and preservation during processes and storage. Indeed, they could be used where plastic packaging cannot be applied, that is, they can separate several compartments within a complex food product. Edible packaging can be described as intelligent packaging because it is both active and selective and has infinite potential uses. Edible films and coatings are natural polymers obtained from agricultural productions such as animal and vegetable proteins, gums and lipids and are perfectly biodegradable, and therefore perfectly safe for the environment. Their cost is comparatively higher than those of synthetic polymeric films, but is of the same order as complex, multilayered and active plastic films. However, the cost of edible films is not a handicap to their development because the quantities used are very low, and they are especially applied for very specific goals in value added food products. Thus, the knowledge of edible polymers and that of plastic materials should be used synergistically for the development of new applications, new biodegradable materials and new environmental approaches. Consequently, both plastic and edible packaging potentiality appears to be a successful key for tomorrow's food packaging. The commercialization of biodegradable packaging

films faces numerous challenges, but also offers many opportunities. The raw materials are abundantly available from replenishable resources and the capital investments for mass production do not seem exorbitant. Multicomponent coatings and films are gaining increased attention. Such materials exhibit cooperative functional attributes. Another major requirement of such biodegradable materials for packaging films is that they should comply with food legislation; more specifically, they should not interact with food components during extended storage. All these characteristics together should result in no compromise on food quality and environmental friendliness. Though expensive, bio packaging is needed for packaging, especially for value added products, and it offers an alternative route for waste management. Biodegradable packaging and coatings offer the potential for a clean, pollution-free environment in the future.

ACKNOWLEDGEMENTS

The authors thank Nordion Inc. for gamma radiation processing and Winpak Division Ltd for providing packaging material used for irradiated samples. The IAEA is acknowledged for its financial support through its CRP on the Development of Radiation Processed Products of Natural Polymers for Applications in Agriculture, Healthcare, Industry and Environment. The authors sincerely thank the Natural Sciences and Engineering Research Council of Canada for financial support through the discovery and Collaborative Research and Development grant programmes.

REFERENCES TO CHAPTER 16

[16.1] KHAN, R.A., et al., Production and properties of nanocellulose reinforced methylcellulose based biodegradable films, J. Agric. Food Chem. **58** (2010) 7878–7885.

[16.2] SHARMIN, N., et al., Modification and characterization of biodegradable methylcellulose films with trimethylolpropane trimethacrylate (TMPTMA) by gamma radiation: Effect of nanocrystalline cellulose, J. Agric. Food Chem. **60** 2 (2012) 623–629.

[16.3] HUANG, S.J., Polymer waste management–biodegradation, incineration and recycling, J. Macromol. Sci. Part A **32** 4 (1995) 593–597.

[16.4] TRZNADEL, M., Biodegradable polymer materials, Int. J. Polym. Sci. Technol. **22** 12 (1995) 58–65.

[16.5] GUILBERT, S., CUQ, B., GONTARD, N., Recent innovations in edible and/or biodegradable packaging materials, Food Addit. Contam. **14** 6 (1997) 741–751.

[16.6] SCOTT, G., Green polymers. Polym. Degrad. Stabil. **68** (2000) 1–7.
[16.7] SWIFFT, G., Opportunities for environmentally degradable polymers, J. Macromol. Sci. Part A **32** 4 (1995) 641–651.
[16.8] KHAN, R.A., SALMIERI, S., DUSSAULT, D., SHARMIN, N., LACROIX, M., Mechanical, barrier and interfacial properties of biodegradable composite films made of methylcellulose and PCL, J. Appl. Polym. Sci. **123** 3 (2012) 1690–1697.
[16.9] ALBERTSSON, A.C., KARLSSON, S., "Chemistry and biochemistry of polymer biodegradation", Chemistry and Technology of Biodegradable Polymers (GRIFFIN, E.G.J.L., Ed.), Blackie Academic and Professional, London (1994) 7–17.
[16.10] KARLSSON, S., ALBERTSSON, A.C., Biodegradable polymers and environmental interaction, Polym. Eng. Sci. **38** 8 (1994) 1251–1254.
[16.11] WEBER, C.J., HAUGAARD, V., FESTERSEN, R., BERTELSEN, G., Production and applications of biobased packaging materials for the food industry, Food Addit. Contam. **19** 1 (2002) 172–177.
[16.12] KROCHTA, J.M., JOHNSTON, C.D., Edible and biodegradable polymer films: challenges and opportunities, J. Food Technol. **51** (1997) 61–74.
[16.13] GUILBERT, S., BIQUET, B., "Technology and application of edible protective films", Food Packaging and Preservation (MATHLOUTHI, M., Ed.), Elsevier Applied Science Publishers, London (1986) 371–394.
[16.14] KESTER, J.J., FENNEMA, O.R., Edible films and coatings: a review, J. Food Technol. **48** (1986) 47–58.
[16.15] CAGRI, A., USTUNOL, Z., RYSER, E.T., Antimicrobial edible films and coatings, J. Food Prot. **67** 4 (2004) 833–848.
[16.16] GENNADIOS, A., WELLER, C.L., TESTIN, R.F., Property modification of edible wheat, gluten-based films, Trans. Am. Soc. Agric. Eng. **36** 2 (1993) 465–478.
[16.17] BIQUET, B., LABUZA, T.P., Evaluation of the moisture permeability of chocolate films as an edible moisture barrier, J. Food Sci. **53** 4 (1988) 989–998.
[16.18] TORRES, J.A., "Edible films and coatings from proteins", Protein Functionality in Food Systems (HETTIARACHCHY, N.S., ZIEGLER, G.R., Eds), Marcel Dekker, New York (1994).
[16.19] BALDWIN, E., "Edible coatings for fresh fruits and vegetables: Past, present and future", Edible Coatings and Films to Improve Food Quality (KROCHTA, J.M., BALDWIN, E.A., NISPEROS-CARRIEDO, M.O., Eds) Technomic Publishing Co. Inc., Basel, (1994) 25 pp.
[16.20] SAKELLARIOU, P., ROWE, R.C., WHITE, E.F.T., An evaluation of the interaction and plasticizing efficiency of the polyethylene glycols in ethyl cellulose and hydroxypropylmethylcellulose films using the torsional braid pendulum, Int. J. Pharm. **31** (1986) 55–66.
[16.21] McHUGH, T.H., KROCHTA, J.M., Milk-protein-based edible films and coatings, Food Technol. **48** 1 (1994) 97–112.
[16.22] GONTARD, N., GUILBERT, S., "Biopackaging technology and properties of edible and/or biodegradable material of agricultural origin", Food Packaging and Preservation (MATHLOUTHI, M., Ed.), Blackie Academic and Professional, London (1994).

[16.23] DEBEAUFORT, F., VOILLEY, A., Effect of surfactants and drying rate on barrier properties of emulsified edible films, Int. J. Food Sci. Technol. **30** 2 (1995) 183–192.
[16.24] FIELD, C.E., PIVARNIK, L.F., BARNETT, S.M., RAND, J.R.A.G., Utilization of glucose oxidase for extending the shelf-life of fish, J. Food Sci. **51** 1 (1996) 66–70.
[16.25] VOJDANI, F., TORRES, J.A., Potassium sorbate permeability of methylcellulose and hydroxypropyl methylcellulose multi-layer films, J. Food Proc. Preserv. **13** (1989) 417–430.
[16.26] CAGRI, A., USTUNOL, Z., RYSER, E.T., Antimicrobial, mechanical, and moisture barrier properties of low pH whey protein-based edible films containing p-aminobenzoic or sorbic acids, J. Food Sci. **66** 6 (2001) 865–870.
[16.27] BRODY, A.L., STRUPINSKY, E.R., KLINE, L.R., "Antimicrobial packaging", Active Packaging for Food Applications (BRODY, A.L., STRUPINSKY, E.R., KLINE, L.R., Eds), Technomic Publishing, Lancaster, PA (2001) 131–194.
[16.28] COSENTINO, S., et al., In-vitro antimicrobial activity and chemical composition of Sardinian Thumus essential oils, Lett. Appl. Microbiol. **29** (1999) 130–135.
[16.29] CARSON, C.F., RILEY, T.V., Antimicrobial activity of the major components of the essential oil of *Melaleuca alternifolia*, J. Appl. Bacteriol. **78** 13 (1995) 264–269.
[16.30] LIS-BALCHIN, M., BUCHBAUER, M., RIBISCH, G., WENGER, M.T., Comparative antibacterial effects of novel *Pelargonium* essential oils and solvent extracts, Lett. Appl. Microbiol. **27** 3 (1998) 135–141.
[16.31] PEREZ, C., AGNESE, A.M., CABRERA, J.L., The essential oil of *Senecio graveolens (Compositae):* Chemical composition and antimicrobial activity tests, J. Ethnopharmacol. **66** (1999) 91–96.
[16.32] CANILLAC, N., MOUREY, A., Antibacterial activity of the essential oil of *Picea excelsa* on *Listeria*, *Staphylococcus aureus* and coliform bacteria, Food Microbiol. **18** (2001) 261–268.
[16.33] ORAFIDIYA, L.O., OYEDELE, A.O., SHITTU, A.O., ELUJOBA, A.A., The formulation of an effective topical antibacterial product containing *Ocimum gratissimum* leaf essential oil, Int. J. Pharm. **224** (2001) 177–184.
[16.34] OUATTARA, B., SABATO, S.F., LACROIX, M., Combined effect of antimicrobial coating and gamma irradiation on shelf life extension of pre-cooked shrimp (*Penaeus spp*.), Int. J. Food Microbiol. **68** (2001) 1–9.
[16.35] GOLDBERG, S., DOYLE, R., ROSENBERG, M., Mechanism of enhancement of microbial cell hydrophobicity by cationic polymers, J. Bacteriol. **172** 10 (1990) 5650–5654.
[16.36] CUQ, B., CONTARD, N., GUILBERT, S., "Edible films and coatings as active layers", Active Food Packaging (ROONEY, M.L., Ed.), Blackie Academic and Professional, Chapman and Hall, Glasgow, UK (1995) 111–142.
[16.37] RHOADES, J., ROLLER, S., Antimicrobial actions of degraded and native chitosan against spoilage organisms in laboratory media and foods, Appl. Environ. Microbiol. **66** 1 (2000) 80–86.
[16.38] SCHILLINGER, U., GEISEN, R., HOLZAPFEL, W.H., Potential of antagonistic microorganisms and bacteriocins for the biological preservation of foods, Trends Food Sci. Tech. **7** (1996)158–164.

[16.39] SCANNELL, A.G.M., HILL, C., ROSS, R.P., MARX, S., HARTMEIER, W., ARENDT, K.E., Development of bioactive food packaging materials using immobilized bacteriocins Lacticin 3147 and Nisaplin, Int. J. Food Microbiol. **60** (2000) 241–249.

[16.40] DAESCHEL, M.A., McGUIRE, J., AL-MAKHLAFI, H., Antimicrobial activity of nisin adsorbed to hydrophilic and hydrophobic silicon surfaces, J. Food Prot. **55** (1992) 731–735.

[16.41] CUTTER, C.N., SIRAGUSA, G.R., Incorporation of nisin into a meat binding system to inhibit bacteria on beef surfaces, Lett. Appl. Microbiol. **27** (1998) 19–24.

[16.42] SIRAGUSA, G.R., CUTTER, C.N., WILLETT, J.L., Incorporation of bacteriocin in plastic retains activity and inhibits surface growth of bacteria on meat, Food Microbiol. **16** (1999) 229–235.

[16.43] CUTTER, C.N., WILLETT, J.L., SIRAGUSA, G.R., Improved antimicrobial activity of nisin-incorporated polymer films by formulation change and addition of food grade chelator, Lett. Appl. Microbiol. **33** (2001) 325–328.

[16.44] NATRAJAN, N., SHELDON, B.W., Efficacy of nisin-coated polymer films to inactivate Salmonella Typhimurium on fresh broiler skin, J. Food Prot. **63** (2000) 1189–1196.

[16.45] KO, S., JAMES, M.E., HETTIARACHCHY, N.S., JOHNSON, M.G., Physical and chemical properties of edible films containing nisin and their action against *Listeria monocytogenes*, J. Food Sci. **66** 7 (2001) 1006–1011.

[16.46] MING, X., WEBER, G.H., AYRES, J.W., SANDINE, W.E., Bacteriocins applied to food packaging materials to inhibit *Listeria monocytogenes* on meats, J. Food Sci. **62** (1997) 413–415.

[16.47] GIANNELIS, E.P., Polymer-layered silicate nanocomposites: synthesis, properties and applications, Appl. Organometal. Chem. **12** (1998) 675–680.

[16.48] HERNANDEZ, R.J., "Additives and compounding in plastics packaging", Plastics Packaging: Properties, Processing, Applications, and Regulations (SELKE, S., CULTER, J., HERNANDEZ, R., Eds), Hanser Publishers, Munich, Germany (2000) 135–156.

[16.49] YING, H.U., CHEN, W., LU, L., LIU, J., CHANG, C., Electromechanical actuation with controllable motion based on a single-walled carbon nanotube and natural biopolymer composite, ACS Nano **6** 4 (2011) 3498–3502.

[16.50] KHAN, R.A., et al., Production and properties of nanocellulose reinforced methylcellulose-based biodegradable films, J. Agric. Food Chem. **58** (2010) 7878–7885.

[16.51] CHIU, W.-M., CHANG, Y.-A., KUO, H., LIN, M., WEN, W.C., A study of carbon nanotubes/biodegradable plastic polylactic acid composites, J. Appl. Polym. Sci. **108** (2008) 3024–3030.

[16.52] AZEREDO, H.M.C., MATTOSO, L.H.C., WOOD, D., WILLIAMS, T.G., BUSTILLOS, R.J.A., McHUGH, T.H., Nanocomposite edible films from mango puree reinforced with cellulose nanofibers, J. Food Sci. **74** 5 (2009) 31–35.

[16.53] KHAN, A., et al., Effect of γ-irradiation on the mechanical and barrier properties of HEMA grafted chitosan-based films, Radiat. Phys. Chem. **81** (2012) 941–944.

[16.54] HUQ, T., et al., Effect of gamma radiation on the physico-chemical properties of alginate-based films and beads, Radiat. Phys. Chem. **81** (2012) 945–948.
[16.55] KHAN, R.A., et al., Preparation, gamma-irradiation and thermo-mechanical characterization of chitosan-loaded methylcellulose films, Polym. Environ. **20** (2012) 43–52.
[16.56] SHARMIN, N., et al., Effectiveness of silane monomer and gamma radiation on chitosan films and PCL-based composites, Radiat. Phys. Chem. **81** (2011) 932–935.
[16.57] KHAN, R., DUSSAULT, D., SALMIERI, S., SAFRANY, A., LACROIX, M., Production and properties of carbon nanotube reinforced PCL-based composite films: Effect of gamma radiation, J. Appl. Polym. Sci. **127** (2012) 3962–3969.
[16.58] SHAHABI-GHAHFARROKHI, I., KHODAIVAN, F., MOUSAVI, M., YOUSEFI, H., Effect of ɣ-irradiation on the physical and mechanical properties of kefiran biopolymer film, Int. J. Biol. Macromol. **74** (2015) 343–350.
[16.59] BANGYEKAN, C., AHT-ONG, D., SRIKULKIT, K., Preparation and properties evaluation of chitosan-coated cassava starch films, Carbohydr. Polym. **63** (2006) 61–71.
[16.60] KHAN, A., et al., Mechanical and barrier properties of nanocrystalline cellulose reinforced chitosan based nanocomposite films, Carbohydr. Polym. **90** (2012) 1601–1608.
[16.61] DHAR, P., TARAFDER, D., KUMAR, A., KATIYAR, V., Effect of cellulose nanocrystal polymorphs on mechanical, barrier and thermal properties of poly(lactic acid) based bionanocomposites, RSC Adv. **5** (2015) 60426–60440.
[16.62] AZEREDO, H.M., et al., Nanocellulose reinforced chitosan composite films as affected by nanofiller loading and plasticizer content, J. Food Sci **75** (2010) 19–28.
[16.63] TAKALA, P., VU, K.D., SALMIERI, S., LACROIX, M., Effect of antimicrobial coatings on the radiosensitization of *Escherichia coli, Salmonella* Typhimurium and *Listeria monocytogenes* in fresh broccoli, J. Food Prot. **74** 7 (2011) 1065–1069.

ABBREVIATIONS

AAc	acrylic acid
AAcNa	acrylic acid sodium salt
AFM	atomic force microscopy
AU	allylurea
BA	para-methoxy benzyl
C	number of intermolecular cross-linking events
CA	cinnamyl alcohol
CM	carboxy methyl
CMC	carboxy methyl cellulose
CNC	cellulose nanocrystals
CNT	carbon nanotube
CO_2TR	carbon dioxide transmission rate
CRP	coordinated research programme
DD	degree of deacetylation
DLS	dynamic light scattering
DN	degree of neutralization
DPPH	1,1-diphenyl-2-picrylhydrazyl
DS	degree of substitution
Eb	elongation at break
EB	electron beam
EDS	equilibrium degree of swelling
EFB	empty fruit bunch
FTIR	Fourier transform infrared spectroscopy
FW	fresh weight
FWA	film without anti-microbial agents
GA	gum arabic
GBR	guided bone regeneration
GG	guar gum
GlcN	D-glucosamine hydrochloride
GlcNAc	N acetyl glucosamine
GPC	gel permeation chromatography
h	hour
HEMA	hydroxyethyl methacrylate
LAB	lactic acid bacteria
LBG	locust bean gum
LCST	lower critical solution temperature
M/G	mannose–galactose ratio
MALLS	multi angle laser light scattering

MC	Methylcellulose
NaAlg	sodium alginate
NMR	nuclear magnetic resonance
OTR	oxygen transmission rate
PAAc	poly(acrylic acid)
PCL	poly(caprolactone)
PD	puncture deformation
PE	polyethylene
PLA	poly(lactic acid)
PMMA	poly(methyl methacrylate)
PNIPAAm	poly-N-isopropyl acrylamide
ppm	part per million
PS	puncture strength
PVA	poly(vinyl alcohol)
PVP	polyvinyl pyrrolidone
SAP	superabsorbent polymer
SPAD	soil plant analysis development
TAIC	triallylisocyanurate
TG	tara gum
TM	tensile modulus
TMPTMA	trimethylolpropane trimethacrylate
TS	tensile strength
UV	ultraviolet
UV-Vis	ultraviolet-visible
VUR	vesicoureteral reflux
wt	weight
WVP	water vapour permeability

NOTATION

a	parameter of polymer conformation
A	initial unit area
A_2	second virial coefficient
B	weight of an insoluble portion after extraction with water
c	concentration
c^*	critical concentration
C	weight after drying
CF	cellulose fraction
$C[\eta]$	coil overlap parameter
d	slope of a curve
D	absorbed dose
D_D	dose absorbed in dosimeter
D_g	gelation dose
D_M	dose absorbed in the material
dn/dc	refractive index increment
D_v	virtual dose
D_{10}	absorbed dose reducing the amount of pathogen to 10%
$[d\dot{\gamma} / dt]$	change in shear rate with time
E	energy
$E°$	standard electrode potential
e_{aq}^-	hydrated electron
F	force
$g^2(\boldsymbol{q};\tau)$	autocorrelation function at wave vector $\boldsymbol{q}$
G	radiation-chemical yield
G^*	complex modulus
G'	storage modulus
G''	loss modulus
G_m	shear modulus
G_R	elastic modulus
$G(s)$	radiation-chemical yield of chain scission
$G(x)$	radiation-chemical yield of cross-linking
h	height
I	radiation intensity
I_0	incident radiation intensity
k	rate constant
k′	Huggins constant
k″	Kraemer constant
K*	optical constant

K_{SEC}	equilibrium constant
l	carbon–carbon length
L	length
m	mass
$\bar{M}_n$	number-average molecular weight
$\bar{M}_{n0}$	initial number-average molecular weight
m_s	total sample mass (solution mass if the sample is a solution)
M	molecular weight
$(\bar{M}_c)_m$	average molecular weight of network chains
$\bar{M}_w$	weight-average molecular weight
$\bar{M}_w/\bar{M}_n$	polydispersity index
$\bar{M}_{w0}$	initial weight-average molecular weight
n_{cb}	number of chain break events
n_0	refractive index of the solvent
n_x	number of intermolecular cross-linking events
N_A	Avogadro's number
N_A	concentration of HCl
N_B	concentration of NaOH
p	average number of breaks of each chain
p_0	degradation density (average number of breaks of each chain per monomer unit and unit dose)
$P(\theta)$	form factor or scattering function
pK_a	(logarithmic) acid dissociation constant
pH_c	critical pH of soluble complex
pH_d	critical pH value for dissociation of insoluble complex
pH_φ	critical pH of insoluble complex
q_0	cross-linking density (the proportion of monomer units cross-linked per unit dose)
R	radius of gyration
R_g	mean square radius of a particle
R_θ	Rayleigh ratio (excess scattered intensity ratio)
R_H	hydrodynamic diameter or Stokes radius
s	sol fraction
t	time
$t_{solution}$	flow time of a solution
$t_{solvent}$	flow time of a solvent
$\tan \delta$	phase angle
V	volume
V_A	volume of HCl
V_e	volume at end point
V_e	elution volume

V_i	interstitial volume
V_p	pore volume
W	weight
W_d	weight of the dry sample
W_i	weight of the initial sample
W_s	weight of the swollen sample
x	thickness of material
Y	viscoelasticity coefficient
β	correction function
γ	shear strain
	shear rate
δL	amount of linear displacement
Γ	decay rate
η	viscosity
$[\eta]$	intrinsic viscosity (limiting viscosity number)
η^*	complex viscosity
η_0	zero shear viscosity
η_∞	viscosity at an infinite shear rate
η_{inh}	inherent viscosity
η_{rel}	relative viscosity
η_{red}	reduced viscosity
η_{sp}	specific viscosity
θ	angle of a detector with respect to a sample cell
κ	linear attenuation coefficients for positron electron pair production
μ	total linear attenuation coefficient
$\mu_{2,0}$	initial weight-average degree of polymerization
$(\mu/\rho)_D$	mass energy absorption coefficient of the dosimeter
$(\mu/\rho)_M$	mass energy absorption coefficient of the material sample
ξ	Flory characteristic ratio or rigidity factor
λ	incident laser wavelength
λ_0	wavelength in vacuo of the incident beam
ρ	density
σ	linear attenuation coefficients for Compton scattering
τ	shear stress
ω	angular frequency

CONTRIBUTORS TO DRAFTING AND REVIEW

Abad, L.V.	Philippine Nuclear Research Institute, Philippines
Al-Assaf, S.	University of Chester, United Kingdom
Coqueret, X.	The University of Reims Champagne-Ardenne, France
Duarte, C.L.	Energetic and Nuclear Research Institute-IPEN, Brazil
Kume, T.	Centre for Applications of Nuclear Technique in Industry, Viet Nam
Lacroix, M.	University of Quebec, Canada
Khairul Zaman, H.M.D.	Polycomposite Sdn. Bhd., Malaysia
Safrany, A.	International Atomic Energy Agency
Sen, M.	Hacettepe University, Turkey
Tahtat, D.	Nuclear Research Center, Algeria
Ulanski, P.	Lodz University of Technology, Poland

IAEA
International Atomic Energy Agency

No. 24

ORDERING LOCALLY

In the following countries, IAEA priced publications may be purchased from the sources listed below or from major local booksellers.

Orders for unpriced publications should be made directly to the IAEA. The contact details are given at the end of this list.

BELGIUM

Jean de Lannoy
Avenue du Roi 202, 1190 Brussels, BELGIUM
Telephone: +32 2 5384 308 • Fax: +32 2 5380 841
Email: jean.de.lannoy@euronet.be • Web site: http://www.jean-de-lannoy.be

CANADA

Renouf Publishing Co. Ltd.
22-1010 Polytek Street, Ottawa, ON K1J 9J1, CANADA
Telephone: +1 613 745 2665 • Fax: +1 643 745 7660
Email: order@renoufbooks.com • Web site: http://www.renoufbooks.com

Bernan Associates
4501 Forbes Blvd., Suite 200, Lanham, MD 20706-4391, USA
Telephone: +1 800 865 3457 • Fax: +1 800 865 3450
Email: orders@bernan.com • Web site: http://www.bernan.com

CZECH REPUBLIC

Suweco CZ, s.r.o.
SESTUPNÁ 153/11, 162 00 Prague 6, CZECH REPUBLIC
Telephone: +420 242 459 205 • Fax: +420 284 821 646
Email: nakup@suweco.cz • Web site: http://www.suweco.cz

FRANCE

Form-Edit
5 rue Janssen, PO Box 25, 75921 Paris CEDEX, FRANCE
Telephone: +33 1 42 01 49 49 • Fax: +33 1 42 01 90 90
Email: fabien.boucard@formedit.fr • Web site: http://www.formedit.fr

Lavoisier SAS
14 rue de Provigny, 94236 Cachan CEDEX, FRANCE
Telephone: +33 1 47 40 67 00 • Fax: +33 1 47 40 67 02
Email: livres@lavoisier.fr • Web site: http://www.lavoisier.fr

L'Appel du livre
99 rue de Charonne, 75011 Paris, FRANCE
Telephone: +33 1 43 07 43 43 • Fax: +33 1 43 07 50 80
Email: livres@appeldulivre.fr • Web site: http://www.appeldulivre.fr

GERMANY

Goethe Buchhandlung Teubig GmbH
Schweitzer Fachinformationen
Willstätterstrasse 15, 40549 Düsseldorf, GERMANY
Telephone: +49 (0) 211 49 874 015 • Fax: +49 (0) 211 49 874 28
Email: kundenbetreuung.goethe@schweitzer-online.de • Web site: http://www.goethebuch.de

HUNGARY

Librotrade Ltd., Book Import
Pesti ut 237. 1173 Budapest, HUNGARY
Telephone: +36 1 254-0-269 • Fax: +36 1 254-0-274
Email: books@librotrade.hu • Web site: http://www.librotrade.hu

INDIA

Allied Publishers
1st Floor, Dubash House, 15, J.N. Heredi Marg, Ballard Estate, Mumbai 400001, INDIA
Telephone: +91 22 4212 6930/31/69 • Fax: +91 22 2261 7928
Email: alliedpl@vsnl.com • Web site: http://www.alliedpublishers.com

Bookwell
3/79 Nirankari, Delhi 110009, INDIA
Telephone: +91 11 2760 1283/4536
Email: bkwell@nde.vsnl.net.in • Web site: http://www.bookwellindia.com

ITALY

Libreria Scientifica "AEIOU"
Via Vincenzo Maria Coronelli 6, 20146 Milan, ITALY
Telephone: +39 02 48 95 45 52 • Fax: +39 02 48 95 45 48
Email: info@libreriaaeiou.eu • Web site: http://www.libreriaaeiou.eu

JAPAN

Maruzen-Yushodo Co., Ltd.
10-10, Yotsuyasakamachi, Shinjuku-ku, Tokyo 160-0002, JAPAN
Telephone: +81 3 4335 9312 • Fax: +81 3 4335 9364
Email: bookimport@maruzen.co.jp • Web site: http://maruzen.co.jp

RUSSIAN FEDERATION

Scientific and Engineering Centre for Nuclear and Radiation Safety
107140, Moscow, Malaya Krasnoselskaya st. 2/8, bld. 5, RUSSIAN FEDERATION
Telephone: +7 499 264 00 03 • Fax: +7 499 264 28 59
Email: secnrs@secnrs.ru • Web site: http://www.secnrs.ru

UNITED STATES OF AMERICA

Bernan Associates
4501 Forbes Blvd., Suite 200, Lanham, MD 20706-4391, USA
Telephone: +1 800 865 3457 • Fax: +1 800 865 3450
Email: orders@bernan.com • Web site: http://www.bernan.com

Renouf Publishing Co. Ltd.
812 Proctor Avenue, Ogdensburg, NY 13669-2205, USA
Telephone: +1 888 551 7470 • Fax: +1 888 551 7471
Email: orders@renoufbooks.com • Web site: http://www.renoufbooks.com

Orders for both priced and unpriced publications may be addressed directly to:

IAEA Publishing Section, Marketing and Sales Unit
International Atomic Energy Agency
Vienna International Centre, PO Box 100, 1400 Vienna, Austria
Telephone: +43 1 2600 22529 or 22530 • Fax: +43 1 2600 29302
Email: sales.publications@iaea.org • Web site: http://www.iaea.org/books

16-15211

INTERNATIONAL ATOMIC
ENERGY AGENCY
VIENNA
ISBN 978-92-0-101516-7